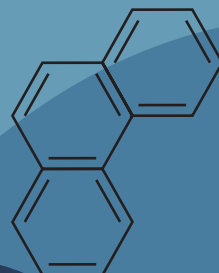
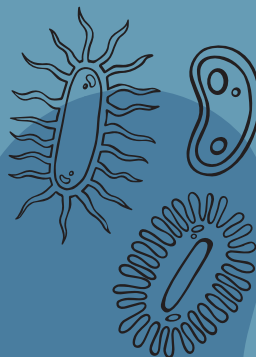
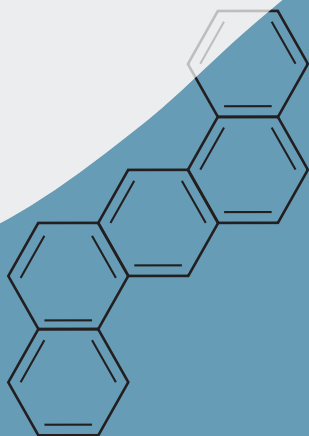


# Biodegradation of polycyclic aromatic hydrocarbons in the surface ocean

**Alicia Martínez Varela**





# Biodegradation of polycyclic aromatic hydrocarbons in the surface ocean

Alicia Martinez Varela

Doctoral thesis by compendium of publications  
Ph.D. program in Marine Sciences

Supervised by  
Dr. Maria Vila Costa and  
Dr Benjamí Piña

Department of Environmental Chemistry  
Institute of Environmental Assessment and  
Water Research (IDAEA-CSIC)

Figueró-Montmany and Erinyà, 2022





# TABLE OF CONTENTS

List of figures

List of tables

Abstract

*Resum*

---

## **PART I - GENERAL INTRODUCTION** 25

Introduction 27

Thesis objectives 55

Methodology summary 61

---

## **PART II - MAIN CHAPTERS** 75

### **Chapter 1**

Biodegradation as an important sink of aromatic hydrocarbons in the oceans 77

### **Chapter 2**

Contrasted responses to background concentrations of PAH of bacterial communities from Mediterranean and Antarctic coastal waters 97

### **Chapter 3**

Large enrichment of anthropogenic organic matter begrading bacteria in the sea-surface microlayer at coastal Livingston Island (Antarctica) 117

### **Chapter 4**

PAH degradation in the sea-surface microlayer at coastal Antarctica 141

## **Chapter 5**

Bacterial responses to background organic pollutants in the northeast subarctic Pacific Ocean	167
---	-----

## **PART III - GENERAL DISCUSSION AND CONCLUSIONS**

---

General discussion	195
General conclusions	208
Fundamental gaps of knowledge	210
Recommendations for future research	210
Future research perspectives	211

## **PART IV - ANNEX**

---

Supporting information of Chapter 1	218
Supporting information of Chapter 2	246
Supporting information of Chapter 3	262
Supporting information of Chapter 4	274
Supporting information of Chapter 5	292
Aknowledgements	314

# LIST OF FIGURES

## PART I - GENERAL INTRODUCTION

---

Figure 1. The nine planetary boundaries.	28
Figure 2. Bioaccumulation and biomagnification.	31
Figure 3. Hypothetical chemical transportation modes for organic chemicals.	33
Figure 4. OP entry modes to the ocean.	34
Figure 5. Heptane chemical representation.	39
Figure 6. Generic structure for triester OPEs targeted in this thesis.	40
Figure 7. Perfluorosulfonic acids and Perfluorinated organic acids.	40
Figure 8. Average relative abundances of marine phyla across oceanic biomes.	45
Figure 9. Interaction between ADOC and marine microbial communities.	47
Figure 10. Initial ring hydroxylation for Naphthalene.	48
Figure 11. Map of the experimental locations.	57

## PART II - MAIN CHAPTERS

---

### Chapter 1

Figure 1. Global distribution of PAHs in the oceans.	86
Figure 2. PAH profiles in the oceans.	88
Figure 3. Cplankton relationships with biomass versus $K_{ow}$ .	89
Figure 4. Cplankton relationships with biomass versus $K_{ow}$ .	90
Figure 5. Frequencies of PAH degradation genes in the global oceans.	91

### Chapter 2

Figure 1. PAH removal rates in the Antarctica and the Mediterranean.	106
Figure 2. Fold changes in the contribution of functional categories.	107
Figure 3. Free living bacterial response.	110

### Chapter 3

Figure 1. Location of the sampling stations.	122
Figure 2. Bacterial abundance for SML and SSL.	126



Figure 3. Relative abundances in the SML vs. SSL for selected taxa.	127
Figure 4. Fold change in relative abundances of specific taxa.	129
Figure 5. Correlation map between nutrients, PFAS and bacterial abundances.	131
Figure 6. Low abundance and abundant taxa.	132
<b>Chapter 4</b>	
Figure 1. PAH removal rates in the SML and SSL.	151
Figure 2. Characterization of community structure after 24 h.	154
Figure 3. Total number of differently expressed transcripts.	156
Figure 4. Fold-change in PAH degradation genes.	157
<b>Chapter 5</b>	
Figure 1. Sampling sites in NESAP region.	171
Figure 2. Characterization of community structure after 24 h.	179
Figure 3. Characterization of bacterial activities after 24 h.	180
Figure 4. Taxa-specific contributions to the metatranscriptome.	182
Figure 5. Changes in the contribution of functional categories.	184

### **PART III - GENERAL DISCUSSION AND CONCLUSIONS**

---

Figure 1   Half-lives of several PAH compounds.	199
Figure 2   Fold changes of PAH-degrading pfam profiles.	200
Figure 3   Composition of HCB strains.	204
Figure 4   Transcript expression trends of selected functionalities.	207

### **PART IV - ANNEX**

---

#### **Supplemental information Chapter 1**

Figure S1. Relative abundance of PAHs in the particulate phase per subbasin.	236
Figure S2. Particulate phase measured PAHs concentrations map.	236
Figure S3. Correlation between measured and estimated $C_p$ .	237
Figure S4. Median concentrations of PAHs in the plankton phase.	239
Figure S5. Relative occurrence of individual PAHs in plankton per subbasin.	240

Figure S6. Ratios for PAHs sources in plankton samples per subbasin.	240
Figure S7. Biological pump fluxes; phytoplankton and fecal fluxes maps.	241
Figure S8. Surface Ocean Entrance/Exit fluxes ratio versus $K_{ow}$ .	242
Figure S9. Methyl anthracene/Methyl phenanthrene ratios in dissolved samples.	242
Figure S10. Relative abundance of alpha and beta subunits of RHD.	243
Figure S11. Relative abundance of alpha and beta subunits of RHD over depth.	243
<b>Supplemental information Chapter 2</b>	
Figure S1. Taxonomical composition of free living bacteria.	254
Figure S2. Metatranscripts taxonomical assignation 3 h.	255
Figure S3. Metatranscriptomes taxonomic affiliation fold changes.	256
Figure S4. Fold-change in expression of genes involved in PAH degradation.	257
Figure S5. Fold change 16S HCB at time 48.	258
Figure S6. Contribution of ASV corresponding to HCB.	259
<b>Supplemental information Chapter 3</b>	
Figure S1. Nutrient and PFOS concentrations in the SML and SSL.	268
Figure S2. Relative abundances of the dominant taxonomical groups.	269
Figure S3. Relative abundance of the dominant taxonomical groups.	270
Figure S4. ADOC degraders relative abundance.	271
<b>Supplemental information Chapter 4</b>	
Figure S1. Map of the sampled sea water.	285
Figure S2. PAH degradation rates.	285
Figure S3. Comparison of relative abundance of genes and transcripts.	286
Figure S4. PCA plot.	287
Figure S5. Relative abundances of HCB.	287
Figure S6. Relative contributions of taxa to the community composition and transcripts pool.	288
Figure S7. Fold-change in expression of genes involved in PAH degradation.	289
Figure S8. Fold change of the relative abundance of transcripts.	290
<b>Supplemental information Chapter 5</b>	
Figure S1. 16S rRNA gene ASV sequences dendrogram at initial conditions.	306

Figure S2. Contribution of the dominant groups.	306
Figure S3. 16S rRNA gene ASV sequences dendrogram at initial conditions.	307
Figure S4. 16S rRNA gene ASV sequences dendrogram at initial conditions.	308
Figure S5. Contribution of dominant groups to the pool of transcripts.	309
Figure S6. Significant taxonomy-specific changes in transcriptome regulation.	310

# LIST OF TABLES

## PART I - GENERAL INTRODUCTION

---

Table 1. Listing of POPs targeted by the Stockholm Convention.	30
Table 2. Reported PAH levels.	37
Table 3. 16 priority PAH issued by the EPA.	38
Table 4. Different types of omics (or metaOmics) approaches.	42
Table 5. Metabolism table.	44

## PART III - GENERAL DISCUSSION AND CONCLUSIONS

---

Table 1. Summary of potential factors influencing PAH-microorganisms interactions studied in this thesis.	196
---	-----

## PART IV - ANNEX

---

### Supplemental information Chapter 1

Table S1. Sampling: Ancillary data for water sample's transects.	219
Table S2. Sampling: Ancillary data for plankton samples .	221
Table S3. Blanks and surrogate recoveries (%) for particulate phase samples.	224
Table S4. Blanks, breakthroughs and surrogate recoveries (%) for plankton samples.	225
Table S5. Particulate organic carbon (POC, $\mu\text{M}$ ) at surface (3 m depth).	226
Table S6. Carbon, Nitrogen and estimated trophic position for plankton samples.	227
Table S7. Organic carbon export from the surface mixed layer	228
Table S8. Particulate phase average PAHs concentrations in $\text{ng gdw}^{-1}$ .	229
Table S9. Particulate phase average PAHs concentrations in $\text{ng gC}^{-1}$ .	230
Table S10. Plankton phase measured PAHs concentrations.	231
Table S11. Biological pump fluxes.	232

Table S12. Slopes fitted to the field data of $C_{\text{Plankton}}$ versus Biomass.	234
Table S13. Relative abundance of alpha and beta subunits of RHD per ocean basin.	235
<b>Supplemental information Chapter 2</b>	
Table S1. Biotic and abiotic features at initial conditions.	247
Table S2. Community composition of microbial communities at initial time point (T3).	248
Table S3. PAH dissolved and particulate phase concentrations time course.	249
Table S4. Pfam profiles of proteins involved in PAH degradation and horizontal gene transfer.	251
Table S5. Community composition of microbial communities at final time point (T48).	252
Table S6. Subset of genera including previously reported hydrocarbonoclastic bacterial strains.	253
<b>Supplemental information Chapter 3</b>	
Table S1. Coordinates of the sampling stations from South Bay, Livingston Island.	263
Table S2. Ancillary data for the seawater sampling sites.	263
Table S3. Meteorological conditions for each sampling event.	264
Table S4. Inorganic nutrient concentrations and PFOS concentrations.	265
Table S5. Subset of taxa, previously reported as bacterial ADOC degraders (AD).	266
<b>Supplemental information Chapter 4</b>	
Table S1. Abiotic and meteorological parameters at initial conditions.	275
Table S2. PAH dissolved phase concentrations time course in each condition.	275
Table S3. Summary of experimental conditions and analyses performed.	277
Table S4. Sequencing depths for the 16S rDNA amplicon sequences.	278
Table S5. Metatranscriptome library sizes.	279
Table S6. Pfam profiles of proteins involved in PAH degradation.	280
Table S7. Subset of genera including previously reported hydrocarbonoclastic bacterial strains.	281

Table S8. Inorganic nutrient concentrations and bacterial abundance measurements.	282
Table S9. Community composition of microbial communities at initial time point.	283
Table S10. Community composition of microbial communities at final time point (24 h).	284

### **Supplemental information Chapter 5**

Table S1. Coordinates and physical variables of the sampling sites.	293
Table S2. Biological parameters of the three sampled sites at initial conditions.	293
Table S3. ADOC environmental concentrations at the three sites.	294
Table S4. Subset of taxa, previously reported as being associated to the presence of ADOC.	296
Table S5. Relative abundances of taxonomical groups associated to ADOC.	297
Table S6. ADOC amendment enrichment factors in the experiment.	298
Table S7. Relative abundances of ADOC associated taxa.	299
Table S8. List of ADOC model families, degradation pathway genes and half-life times.	301
Table S9. Sequencing depth for each library.	302
Table S10. Average identity match of ASVs from our data set assigned to ADOC-A genera.	303



## LIST OF ABBREVIATIONS

AD	ADOC degrading strains
ADOC	Anthropogenic Dissolved organic carbon
ADOC-A	ADOC associated strains
AHA	non-canonical amino acid L-azidohomolanine
ASV	sequence variant
BCF	Bioaccumulation factor
CBzs	Chlorobenzenes
CEC	Contaminants of emerging concern (CEC).
CSIC	Consejo Superior de Investigaciones Científicas (Spanish National Research Council)
DCIM	Dichlormethane
DMS	Dimethyl sulfide, with the formula CH <sub>3</sub> SCH <sub>3</sub>
DMSP	Dimethylsulfoniopropionate, with the formula (CH <sub>3</sub> ) <sub>2</sub> S+CH <sub>2</sub> CH <sub>2</sub> COO <sup>-</sup>
DNA	Deoxyribonucleic acid
DOC	Dissolved organic carbon
DOM	Dissolved organic matter
EPA	American Environmental Protection Agency
EPA	Environmental Protection Agency
EU	European Union
FL	Fliers
FL	Free-living bacteria
FOSEs	Perfluorooctane sulfonamidoethanol
FTOHs	Fluorotelomer alcohols
GC	Gas chromatography
GC-MS	Gas-chromatography coupled to mass spectrometry
H	Henry's law constant
H'	Dimensionless Henry's law constant
HAD	Haloalkylphosphorus hydrolase
HCB	Hydrocarbonoclastic bacteria
HCB	Hexachlorobenzene
Hex	Hexane
HMM	Hidden Markov models
HMW	High-molecular-weight (referring to PAH with more than 3 fused aromatic rings)
HPLC	High-performance liquid chromatography
IDAEA	Institut de diagnostic ambiental I estudis de l'aigua (Environmental Assessment and Water research Institute)
IPBES	The Intergovernmental Science-Policy Platform on Biodiversity and Ecosystem Services
IPCC	International Panel on Climate Change
K <sub>aw</sub>	Air-water partition coefficient
KEGG	Kyoto encyclopedia of genes and genomes
K <sub>ow</sub>	Octanol-water partition coefficient
LC-MS	Liquid-chromatography coupled to mass spectrometry
LMW	Low-molecular-weight (referring to PAH with up to 3 fused aromatic rings)
MAG	Metagenome assembled genome
MeOH	Methanol
MM	Multimedia multiple hopper
MO	Multiple hopper exchanging with the oceans
mRNA	Messenger RNA



MT	Multiple hopper exchanging with terrestrial surfaces
NCBI	National Center for Biotechnology Information
NESAP	North east subarctic pacific
OHCB	Obligate Hydrocarbonoclastic bacteria
OP	Organic Pollutants
OPE	Organophosphate Esters
OPE-FRP	OPE Flame Retardants and Plasticizers
ORF	Open Reading Frame
PA	Particle-associated bacteria
PAH	Polycyclic aromatic hydrocarbons
PBDEs	Polybrominated diphenyl ethers
PCB	Polychlorinated biphenyls substances
PCBs	Polychlorinated biphenyls
PCBs	Lighter polychlorinated biphenyls
PCDD/Fs	Polychlorinated dioxins and furans
PCR	Polymerase chain reaction
PDE	Phosphodiesterase
PFAM	Protein Families Database
PFASs	Per- and polyfluoroalkyl substances
PFCAs	Perfluorocarboxylates
PFCAs	Perfluoroalkyl carboxylates
PFOA	Perfluorinated organic acids
PFOS	Perfluorosulfonic acids
PFSAs	Perfluoroalkane sulfonates
PME	Phosphomonoesterases
POM	Particulate organic matter
POP	Persistent organic pollutants
PTE	Phosphotriesterases
QS	Quorum sensing
RHD	Ring Hydroxylating dioxygenases
RNA	Ribonucleic acid
SAGs	Single-cell genomics
SALCS	Semivolatile aromatic like compounds
SC	Scintillation counter
SH	Single hoppers
SML	Sea surface microlayer
SSL	Subsurface layer
SW	Swimmers
TCA	Trichloroacetic acid
TEA	Terminal electron acceptor
TEP	Transparent exopolymer particles
TFA	Trifluoroacetic acid
UCM	Unresolved complex mixture
UNEP	United Nations Environmental Program
US	United States (of America)
UTC	Universal Time Coordinated



## ABSTRACT

Increasing quantities of organic pollutants (OP) are being released to the environment, posing a threat to Earth's life system. In the marine environment, OP pollution caused by oil spill accidents receives a lot of academic and societal attention. However, the magnitude of semi-volatiles OP introduced by atmospheric deposition and by maritime currents, that are persistent enough to undergo long-range distances and be deposited in polar environments and in the middle of the big oceanic gyres (far from source points), is orders of magnitude larger. Little is known, however, about the cycling of these background OP in the oceans and their effects to marine ecosystems. It is believed that an important sink of OP in the marine environment must be microbial biodegradation, since it is widely recognized their capacity to consume many OPs. However, neither the magnitude of biodegradation nor the identity of the main degraders nor OP effects to microorganisms, is known.

Polycyclic aromatic hydrocarbons (PAH) and other semi-volatile hydrocarbons are among the most abundant OP in the marine environment. Their wide spectrum of physicochemical properties make PAH family an ideal surrogate to study the biogeochemistry of OP in seawater. This thesis focuses on the biodegradation activities under background concentrations of PAH in the upper ocean, and the co-occurring microbial responses to this exposure. The goals of this work are: 1) to get insights into microbial PAH biodegradation under realistic conditions in different upper ocean environments by means of biogeochemical, molecular and genomic approaches, 2) identify the main players and describe the main metabolisms co-occurring along with biodegradation in the interaction between PAH and microorganisms by means of physiological measurements and metatranscriptomic approaches, and 3) localize marine hot spots of PAH biodegradation and describe some of the main physicochemical influencing factors of biodegradation. For this purposes we did short term incubations with background concentrations of PAH, mimicking those conditions found in the surface ocean in several oceanic provinces with contrasted physicochemical conditions. In particular, the field work was developed in the Maritime Antarctica, the NE Subarctic Pacific and the NW Mediterranean. GC-MS was used to measure PAH biodegradation rates in mass balance models, 16S rRNA gene amplicon sequencing and metatranscriptomics were used to assess the changes in the composition and gene expression profiles of PAH-consuming microbial communities, bioinformatic approaches were used to quantify PAH degrading genes in public metagenomic datasets and to annotate sequencing data, and multivariate statistical tools were applied to detect signifi-

cant differences in taxa and transcripts between PAH exposed communities and controls.

We found that PAH microbial metabolic capacity is a widespread trait in the global upper ocean although PAH biodegradation rates span a wide range of values. These findings strongly suggest a fundamental role of microbial degradation as a relevant driver of PAH fate in the upper ocean. We observed that PAH at background concentrations after short term exposure (24-48 hrs) had an impact on microbial communities compositions and functionality. Biodegradation rates varied according to site, although in general, PAH pre-exposed communities responded faster to PAH exposure. We found that particle associated (PA) cohorts from the sea-surface microlayer (SML) in Antarctic coastal waters were particularly suited to biodegrade heavy-molecular weight (HMW) PAHs at background concentration. The main taxa responsible for PAH biodegradation at background concentrations varied depending on the site and the habitat, and included many different groups. Hydrocarbonoclastic bacteria (HCB), that is, bacteria specialized in the use of hydrocarbons as a source of carbon and energy, appeared as important key players in the short exposure experiments, consistent with previously observed HCB responses under high PAH concentrations such as in oil spill conditions. Similarly, community successional dynamics similar to those found under higher levels of PAH exposure were observed in all sites, but the response time differed in each site. The battery of genes expressed during PAH exposure included PAH degrading genes plus genes involved in stress response and detoxifying strategies among others. Comparison of results from the different sites identified new environmental drivers affecting the efficiency of PAH biodegradation in the upper ocean beyond those already described and those that are commonly overlooked: bacterial life-style (PA vs free-living), microbial community pre-exposure history to organic pollutants and the habitat (specially the SML).

Overall, this thesis adds new information and field-based evidence regarding the microbial controls over the fate and transport of the background PAH concentrations in the surface ocean. In a context of increasing emissions and global change, it becomes crucial to be able to forecast the fate of OP once in the ocean. This requires understanding at a mechanistic level how do microbial metabolic processes and the pool of OP in the ocean intertwine, in order to elucidate a more updated, and always evolving, global carbon cycle.

## RESUM

*Quantitats creixents de contaminants orgànics (CO) s'alliberen al medi ambient, cosa que suposa una amenaça per al sistema de vida de la Terra. En el medi marí, la contaminació causada per vessaments de petroli accidentals rep molta atenció tant acadèmica com social. No obstant això, la magnitud de la contaminació per CO semi-volàtils que arriba als oceans de manera difusa és ordres de magnitud més gran en comparació als vessaments accidentals. Els CO semi-volàtils arriben als oceans per deposició atmosfèrica i pels corrents marítims, i alguns d'ells són prou persistents com per traslladar-se distàncies de llarg abast i dipositar-se en ambients polars i enmig dels grans girs oceànics (allunyat dels punts d'emissió). Actualment hi ha poca informació sobre el cicle d'aquests CO a la columna d'aigua i sobre quins són els efectes que causen sobre els ecosistemes marins. Es creu que un destí important dels CO al medi marí són els processos de biodegradació per part dels microorganismes, ja que és àmpliament reconeguda la seva capacitat per consumir molts CO. Tanmateix, no es coneix ni la magnitud de la biodegradació ni la identitat dels principals degradadors, ni tampoc els efectes dels CO als microorganismes.*

*Els hidrocarburs aromàtics policíclics (HAP) i altres hidrocarburs semi-volàtils es troben entre els CO més abundants en el medi marí. L'àmpli espectre de propietats fisicoquímiques dels HAP els converteixen en un model ideal per estudiar la biogeoquímica dels CO a l'aigua de mar. Aquesta tesi es centra en les activitats de biodegradació sota concentracions ambientals realistes de HAP a les aigües marines superficials i les respostes microbianes concomitants a aquesta exposició. Els objectius d'aquest treball són: 1) explorar la biodegradació microbiana de HAP en condicions realistes en diferents entorns d'aigües superficials marines mitjançant tècniques biogeoquímiques, moleculars i genòmiques, 2) identificar els principals actors de la degradació i descriure els principals metabolismes que coexisteixen juntament amb la biodegradació mitjançant mesures fisiològiques i tècniques metatranscriptòmiques i 3) localitzar "punts calents" de biodegradació de HAP en hàbitats marins i descriure alguns dels principals factors fisicoquímics que influeixen en la biodegradació.*

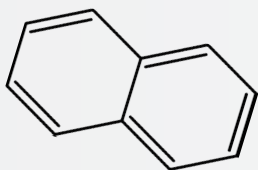
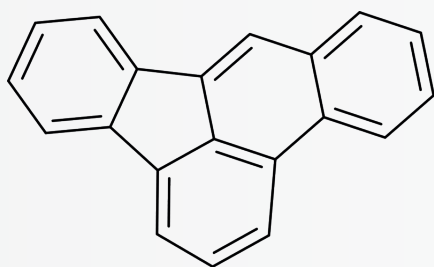
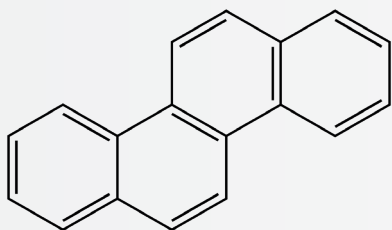
*Per tal d'assolir els objectius, hem realitzat incubacions de curta durada amb aigua superficial marina amb concentracions de HAP ambientals, imitant les concentracions que es troben a l'oceà superficial en diverses províncies oceàniques i amb condicions fisicoquímiques contrastades. En particular, el treball de camp es va desenvolupar a l'Antàrtida Marítima, al NE del Pacífic subàrtic i al NO del*

*Mediterrani. Es va utilitzar la cromatografia de gasos i l'espectrometria de masses per mesurar les taxes de biodegradació de HAP a través de models de balanç de masses. Fent ús d'eines de seqüenciació del gen rRNA 16S i la metatranscriptòmica es van avaluar els canvis en la composició i els perfils d'expressió gènica de les comunitats microbianes exposades a nivells ambientals de HAP. Mitjançant eines bioinformàtiques es van quantificar els gens de degradació de HAP, i aplicant mètodes d'estadística multivariant es van detectar diferències significatives en tàxons, transcriptomes,..etc. entre comunitats exposades a HAP i els controls.*

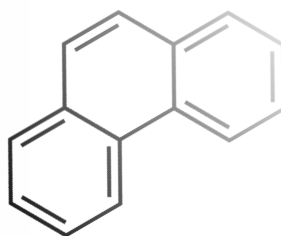
*Els resultats indiquen que la capacitat microbiana de biodegradació dels HAP és un tret estès a l'oceà superficial a escala global, tot i que les taxes de biodegradació dels HAP tenen una gran variabilitat. Aquestes troballes suggereixen el paper fonamental de la biodegradació microbiana com a un dels principals processos que modulen el destí dels HAP a l'oceà superficial. En els experiments d'incubació vam observar que les exposicions a curt termini (24-48 hores) amb concentracions ambientals de HAP tenen un impacte en la composició i la funcionalitat de les comunitats microbianes. Les taxes de biodegradació variaven segons el lloc, tot i que, en general, les comunitats pre-exposades als HAP o al altres CO van respondre més ràpidament. Vam trobar que les cohorts associades a partícules que habiten la microcapa de la superfície del mar en les aigües costaneres antàrtiques eren especialment adequades per biodegradar HAP d'alt pes molecular a concentracions ambientals. Els principals tàxons responsables de la biodegradació dels HAP a concentracions ambientals variaven segons el lloc i l'hàbitat, i inclouen molts grups diferents. Durant els experiments de curta exposició les poblacions de bacteris hidrocarbonoclàstics (HCB), és a dir, els bacteris especialitzats en l'ús d'hidrocarburs com a font de carboni i energia, van esdevenir actors clau en la biodegradació. Aquestes observacions estan en consonància amb els resultats previs d'altres autors, on s'ha observat respostes similars per part de les poblacions de HCB sota concentracions elevades de HAP, com per exemple en vessaments de petroli. A més a més, durant les incubacions vam observar dinàmiques de successió de les comunitats microbianes similars a les que s'han observat en comunitats exposades a nivells més alts d' HAP, tot i que el temps de resposta de les poblacions ha estat diferent a cada ubicació experimental. La bateria de gens expressats durant l'exposició als HAP inclou gens de degradació de HAP, a banda d'altres gens implicats en donar resposta a l'estrès i altres estratègies de desintoxicació. Mitjançant la comparació dels resultats dels diferents experiments hem identificat nous factors ambientals que afecten l'eficiència de la biodegradació dels HAP a l'oceà superficial, més enllà dels ja descrits. Aquests factors són: estil de vida bacterià (bacteris associats a partícules vs. bacteris de vida lliure), l'histo-*

*rial d'exposició als CO de la comunitat microbiana i l'hàbitat (diferents capes de la columna d'aigua).*

*En general, aquesta tesi aporta nova informació i evidències experimentals pel que fa als controls microbians sobre el destí i el transport de la contaminació de HAP a nivells ambientals a les aigües superficials marines. En un context d'emissions contaminants creixements i de canvi global, esdevé important ser capaços de fer un pronòstic del destí dels contaminants orgànics un cop arriben als oceans. Això requereix comprendre a nivell mecanicista com s'entrellacen els processos metabòlics microbians i el conjunt de contaminants orgànics a l'oceà, per tal d'actualitzar el cicle global del carboni.*

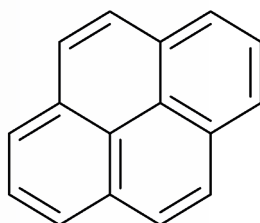






# PART I

## GENERAL INTRODUCTION





## INTRODUCTION

### *The Anthropocene and the global change scenario*

The climate stability of the last 11.500 years laid out the conditions that supported human development, giving birth to the modern world as we understand it today. The Holocene interglacial epoch (11.500 yr to the present days) granted stable ice caps and sea level, and predictable weather seasons, with an extended provision of natural resources to sustain the life system of planet Earth, to which humans are intrinsically dependent. Inevitably, human activities have shaped landscape and altered the surrounding environments since the beginning of times. However, it was not until the burst of the industrial era that the steep increase in intensity and magnitude of the alterations began to significantly influence climate (IPCC, 2014) and ecosystems (IPBES, 2019) at a global scale, threatening the planetary conditions that sustain life itself. Many authors refer to this period as the **Anthropocene**, that is, the era in which humans have become a relevant driver of change for the Earth processes, cycles, and interactions between its constituent biophysical media (atmosphere, hydrosphere, cryosphere, biosphere, geosphere and anthroposphere) (Steffen et al., 2007; Waters et al., 2016; Zalasiewicz et al., 2020). All these anthropogenic changes, occurring at the planetary scale and with irreversible and potentially devastating consequences, place the biosphere in a global change scenario.

But... can we, humans, reverse this scenario somehow? Realistic and quantitative estimations of the critical thresholds at which key Earth System processes or critical planet elements should not be surpassed have been proposed by different authors (Lenton et al., 2008; Rockstrom et al., 2009; Steffen et al., 2015). Rockstrom and colleagues (2009) presented the “**planetary boundaries**” concept. The authors identified nine key global processes and estimated the threshold levels that should not be transgressed in order to avoid undesired and irreversible global environmental changes (Figure 1). According to Rockstrom and colleagues, some of the boundaries have already been transgressed, whereas others remain inaccurately quantified. This is the case for the **chemical pollution** planetary boundary. The ubiquitous spread of single chemicals with known adverse-

ly effects, ultimately affecting human health and the functioning of ecosystems, and the influence of some of these chemicals interfering with other planetary boundaries, are evidences to support the relevance of chemical pollution as a planetary boundary itself. However, global analyses on the presence and fate of the cooccurring chemical pollutants are still lacking, and the large-scale effects remain largely unknown, challenging the estimation of a quantitative threshold.

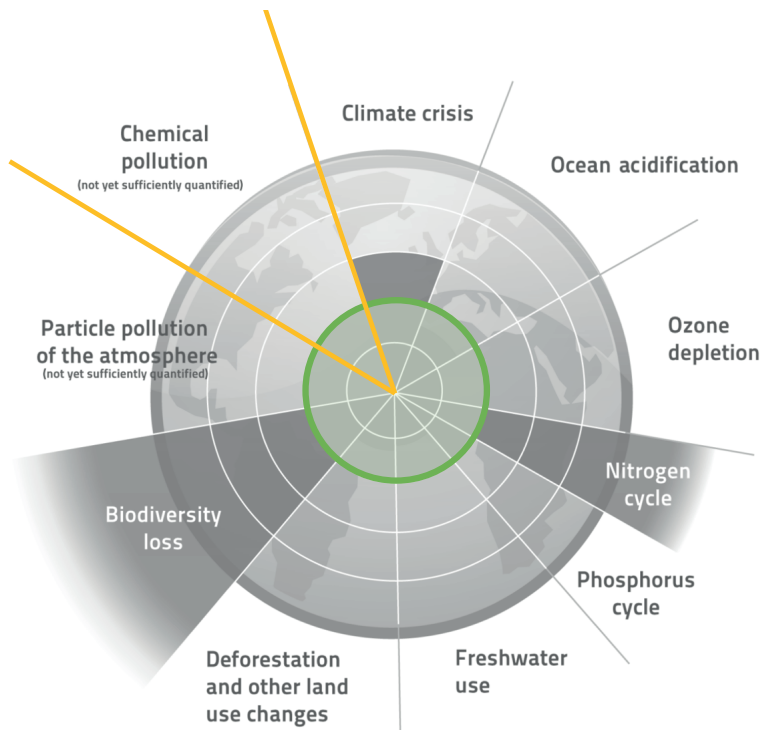


**FIGURE 1** | “The nine planetary boundaries”, adapted from Rockstrom et al., 2009. The safe operating space is depicted with the concentric green zone. Dark gray color represents an estimate of the current position for each boundary. Yellow lines indicate the chemical pollution boundary, object of this study.

This thesis focuses in the **chemical pollution boundary**, by addressing the interaction between this pollution and the microbial life in the oceans.

### ***Anthropogenic chemical pollution***

Hundreds of thousands of chemicals, either naturally originated or industrially synthesized, surround us throughout our lives in a daily basis (Muir and Howard, 2006, Wang et al., 2020). Some of these chemicals, even being undeniably advantageous and helpful in our lives, are considered pollutants for their known undesired effects to humans or the ecosystems health and sustainability. The intentional or unintentional release of such multitude of pollutants into the environment, and the cooccurrence with

their degradation products, represents a planetary harmful stress that remains inadequately quantified yet.

The seminal Rachel Carson's "Silent Spring" publication in 1962 triggered a global concern about the adverse impact of polluting chemicals on both the environment and human health. Since then, regional and international regulations have banned the production and commercialization of a number of pollutants due to their toxicity hazard. In spite of these regulations, some of the theoretically phased out pollutants can still be found in the environment today, due to their intrinsic persistence. These **legacy pollutants** include polychlorinated biphenyls (PCBs), flame-retardant polybrominated diphenyl ethers (PBDEs), organochlorine pesticides or their metabolites, like DDT or DDE, and others, and they are still causing detrimental effects in the environment years after their banning (Sharkey et al., 2020). In addition, there are thousands of non-regulated pollutants detected in the environment with poorly understood fates and biological impacts, the so-called **contaminants of emerging concern (CEC)**. The limitation of current chemical analytical methods, the great number of potentially hazardous pollutants, and the low concentrations for some of them, represent formidable challenges for a broad assessment of the actual risk of chemical pollution for the both environmental and human health.























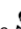















### ***Organic pollutants***

Organic pollutants (OP) comprise a wide range of chemicals, from tens to hundreds thousands of them, with multiple sources, life-cycles, and properties. Although some of these OPs are also synthesized naturally (i.e. some hydrocarbons), most are, or have been in the past, produced for industrial or commercial use as pesticides, solvents, pharmaceuticals, and industrial bulk chemicals, or unintentionally released from the use of fossil fuels or combustion processes.

OP resistant to environmental degradation are classified as Persistent Organic Pollutants (POPs). The United Nations Stockholm Convention on POPs, with participation of dozens of parties including the European Union (EU), signed an unprecedented environmental treaty aiming to eliminate or restrict the production and use of 12 POPs ("The dirty dozen"). Today the convention's treaty is signed by 181 parties who have agreed to reduce or ban the production, use or emission of an ever-growing list of key POPs. In 2021 this list (Table 1), which is under ongoing revision and allows the addition of new substances to the convention, includes a total of 35 chemicals, and a list of OP that are under review for their future inclusion (UNEP, 2019).

Similarly to the Stockholm convention, other regulations apply to these or other groups of OP and hazardous chemicals at regional and global scales. Examples of these are the United States (US) Environmental Protection Act (EPA) (the first one dating from 1970) aiming to prevent pollution and environmental damage, the Seveso directive

**TABLE 1** | Listing of POPs targeted by the Stockholm Convention (UNEP, 2021), classified in three annexes.

<p><b>Annex A</b> - Parties must implement measures to eliminate the production and usage of chemicals listed under Annex A .</p>		
<p>Aldrin </p> <p>Decabromodiphenyl ether (commercial mixture, c-decaBDE) </p> <p>Endrin </p> <p>Hexabromocyclododecane (HBCDD) </p> <p>Hexachlorobutadiene </p> <p>Lindane </p> <p>Pentachlorophenol and its salts and esters </p> <p>Perfluorooctanoic acid (PFOA), its salts and PFOA-related compounds </p> <p>Tetrabromodiphenyl ether and pentabromodiphenyl ether </p>	<p>Chlordane </p> <p>Dicofol </p> <p>Heptachlor </p> <p>Hexabromodiphenyl ether and heptabromodiphenyl ether </p> <p>Alpha hexachlorocyclohexane </p> <p>Mirex </p> <p>Polychlorinated biphenyls (PCB) </p> <p>Toxaphene </p> <p>Short-chain chlorinated paraffins (SCCPs) </p>	<p>Chlordecone </p> <p>Dieldrin </p> <p>Hexabromobiphenyl </p> <p>Hexachlorobenzene (HCB) </p> <p>Beta hexachlorocyclohexane </p> <p>Pentachlorobenzene </p> <p>Polychlorinated naphthalenes </p> <p>Technical endosulfan and its related isomers </p>
<p><b>Annex B</b> - Parties must take measures to restrict the production and usage of chemicals listed under this annex, but in light of any applicable acceptable purposes and/or specific exemptions listed under Annex B.</p>		
<p>DDT </p>	<p>Perfluorooctane sulfonic acid and its salts, perfluorooctane sulfonyl fluoride </p>	
<p><b>Annex C</b> - Parties must take measures to reduce the unintentional release of chemicals listed under Annex C.</p>		
<p>Hexachlorobenzene (HCB) </p> <p>Polychlorinated biphenyls (PCB) </p>	<p>Hexachlorobutadiene (HCBd) </p> <p>Polychlorinated dibenzo-<i>p</i>-dioxins (PCDD) </p> <p>Polychlorinated naphthalenes </p>	<p>Pentachlorobenzene </p> <p>Polychlorinated dibenzofurans (PCDF) </p>
<p>Keys: Pesticide  ; Industrial Chemical  ; Unintentional Production </p>		

(1982) at improving the safety of sites containing large quantities of dangerous substances, the Basel convention (1992) on improving the hazardous waste management, the Registration, Evaluation, Authorisation and Restriction of Chemicals (REACH) adopted in the EU to improve the protection of human health and the environment from the risks posed by chemicals and the EU Marine Strategy Framework Directive, putting the stress in the protection of Oceans and Seas (2008).

The screening criteria for chemicals to be identified as a priority OP in these regulations are defined by the compound's chemical and physical properties, and its ecotoxicology which ultimately determine their transport and fate once released into the environment and ultimate impact.

These criteria are summarized below:

**Adverse effects.** Chemicals with tested toxicity or ecotoxicity causing adverse effects to human health or to the environment.

**Bioaccumulation.** Hydrophobic chemicals are prone to attach to fatty tissue, bioaccumulating in biota with concentrations reaching several orders of magnitude higher than those found in the water media, and biomagnifying along trophic chains (Figure 2).

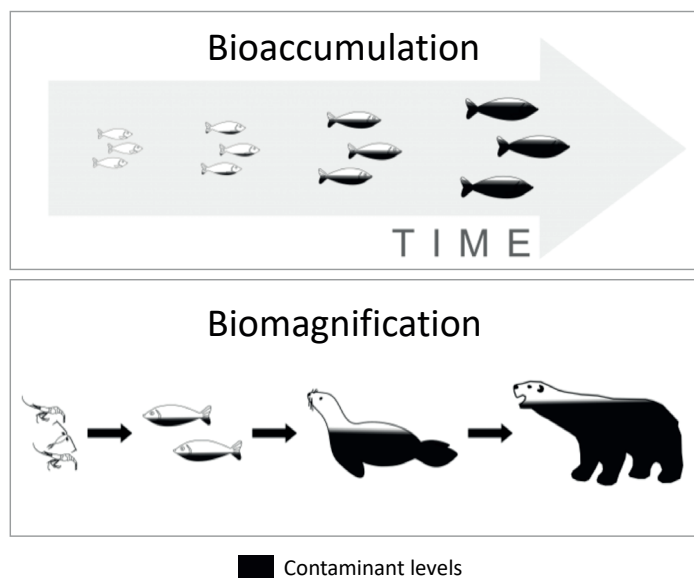


**FIGURE 2** | Bioaccumulation and biomagnification (Image adapted from ©WWF)

o **Biomagnification.** Progressive increase in contaminant concentrations along trophic chains.

o **Bioaccumulation.** Increase of contaminants in biota due to increasing exposure time in a contaminated environment.

Evidence of bioaccumulation is determined by the following parameters:

i) The Bioconcentration factor (BCF), which measures how enriched is a chemical in biota over the water media.

$$BCF = \frac{C_B}{C_W} \quad [1]$$

where  $C_B$  and  $C_W$  are the chemical concentrations in the biota and water, respectively.

ii) The octanol-water partition constant ( $K_{ow}$ ), which measures how hydrophobic a compound is:

$$K_{ow} = \frac{C_o}{C_w} \quad [2]$$

where  $C_o$  concentration of a chemical in the octanol phase and  $C_w$  is the concentration of a chemical in the aqueous phase.  $K_{ow}$  is usually expressed as  $\log K_{ow}$ .

**Persistence.** Chemicals with stable structure resistant to environmental degradation through chemical, biological and photolytic processes (Buccini, 2003). The more resistant compounds will remain in the environment for long periods of time, being the ocean one of the major reservoirs of persistent OP (Jurado et al., 2004).

**Long range transport potential.** Chemicals with the potential to be transported far from their emission sources by atmospheric or oceanic currents. Long-range transport can be determined by the tendency of a chemical to remain in the water or organic phase or its migration to the air phase at equilibrium. This partitioning behaviour between the different environmental matrices is expressed by the partition coefficients  $K_{AW}$  (air-water) and  $K_{OA}$  (octanol-water, being octanol usually used as a surrogate of the organic and lipid-like phases).

Thus, once in the environment, environmental temperature and the chemical and physical profile of each compound will determine the transportation modes and their fate. OP with high  $K_{AW}$  and low  $K_{OA}$  will volatilize to the atmosphere and remain in



the gas phase, being transported by atmospheric currents. These chemicals are known as “fliers”. Oppositely, the chemicals called the “swimmers” are those with low  $K_{AW}$  and  $K_{OA}$  values. These will stay in the water bodies and be mobilized mainly by oceanic currents. The chemicals with intermediate  $K_{AW}$  and  $K_{OA}$  values are transported by a process called “grasshopping”, partitioning between the hydrosphere and the atmosphere, and being transported at regional and global scale through successive cycles of volatilization, atmospheric transport and atmospheric deposition into the ocean (Wania and Mackay, 1996; Gouin and Wania, 2007; McConnell et al., 2013) (Figure 3).

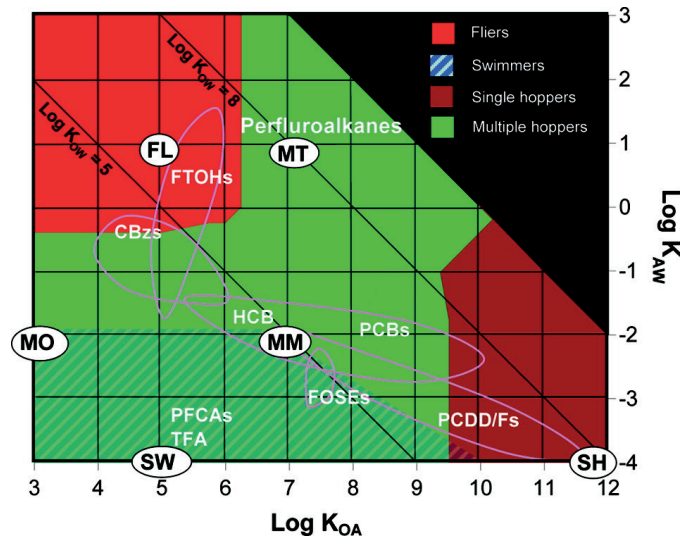


**FIGURE 3** | Hypothetical chemical transportation modes for organic chemicals, based on their partitioning properties  $\log K_{AW}$  and  $\log K_{OA}$  (Gouin and Wania, 2007). Single hoppers (SH), swimmers (SW), multiple hopper exchanging with the oceans (MO), multimedia multiple hopper (MM), multiple hopper exchanging with terrestrial surfaces (MT), and fliers (FL). In white examples of OP placed within their hypothetical transport modes: polychlorinated dioxins and furans (PCDD/Fs); perfluorocarbox-ylates (PFCAs); trifluoroacetic acid (TFA); lighter polychlorinated biphenyls (PCBs); hexachlorobenzene (HCB); fluorotelomer alcohols (FTOHs); perfluorooctane sulfon-amidoethanol (FOSEs); chlorobenzenes (CBzs).

The scenario depicted in Figure 3 shows the major media and transport routes when fugacity-driven partitioning between phases is considered. Lately, it has been shown that there are amplification processes that modify this scenario. For example, wet deposition by rain and snow enhance the deposition of chemicals to ocean and land, irrespective of their  $K_{AW}$  (Casal et al., 2019; Casas et al., 2021).

The resistant grass-hopping OP will even reach polar regions, where low temperatures and the high biomass in the southern ocean will limit the re-volatilization, generating chronic OP pollution in marine areas far from the pollution emission sources (Wania and Mackay, 1996; Jurado and Dachs, 2008).

## OP in the Ocean

Marine coastal environments are direct collectors of OP via continental riverine and run-off inflows. The most labile and volatile OP (low  $K_{AW}$  values) are removed upstream, considerably decreasing the total OP concentrations finally reaching the marine ecosystems (Gioia and Dachs, 2012). Coastal sites close to populated areas show high concentrations of OP as well as other pollutants compared to the open ocean (Dachs and Méjanelle, 2010; Jiang et al., 2014). The major entry of semi-volatile OP to the seawater occurs by passive diffusive exchange between the atmosphere and the ocean (absorption and volatilization processes), as well as by wet and dry depositions (Wania and Mackay, 1996; Dachs et al., 2002; González-Gaya et al., 2016) (Figure 4). This so-called airborne diffusive pollution results in widespread background concentrations of multitude of OPs. Thus, in the open ocean, swimmer and semi-volatile individual OP compounds are found at concentrations from the pico- to the nano- molar range, but the cooccurrence of thousands of different anthropogenic compounds increases up to micromolar concentrations.

Once in the ocean, OPs partition between the dissolved, particulate and colloidal phases, depending on sorption processes, partitioning coefficients and the amount of suspended particulate material in the water (Galbán-Malagón et al., 2012a). Dissolved OPs constitute the **anthropogenic dissolved organic carbon (ADOC)** pool, and its cycling dynamics is inevitably linked to the carbon oceanic cycle and to the marine food-webs (Vila-Costa et al., 2020). The exact chemical composition of ADOC remains unknown, as a significant part of the compounds have not been identified or characterized. As part of this complex mixture, there is the unresolved complex mixture (UCM), which is a commonly observed feature in crude oil when analyzed by gas chromatography, where resolved peaks corresponding to characterized chemicals lay above a hump-shaped background signal of unresolved peaks.

The highly hydrophobic nature of ADOC compounds facilitates the passive uptake or sorption into organic matter,

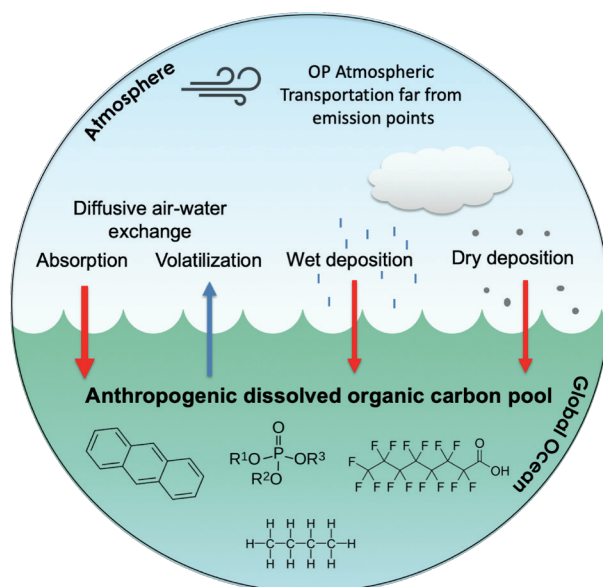


**FIGURE 4** | OP entry modes to the ocean, once in the ocean they become part of the ADOC pool.

either to suspended particles or living cells. ADOC enters marine food webs by bioaccumulating in marine primary producers and biomagnifying towards higher trophic levels (Goerke et al., 2004; Berrojalbiz et al., 2009; Jamieson et al., 2017; Krasnobaev et al., 2020). Part of the most persistent ADOC is exported to the ocean floor by the so-called biological pump (Galbán-Malagón et al., 2012b), an ensemble of processes comprising primary production, vertical transport, and sedimentation by which organic carbon from the ocean surface is sequestered in the oceans depths (Lutz et al., 2007). These vertical fluxes limit the re-volatilization of the compounds into the atmosphere (Scheringer et al., 2004), influencing the air-water diffusive exchange and atmospheric deposition by modifying the ADOC air-water equilibrium phases when ADOC compounds are transported into the deep sea (Dachs et al. 2002, Dachs and Méjanelle, 2010). The less persistent fraction of ADOC is susceptible to be transformed in the upper ocean through other removal processes such as photo-degradation processes or the mineralization to CO<sub>2</sub> by heterotrophic microorganism's respiration (Antonioni et al., 2016; Vila-Costa et al., 2019, 2020).

Thus, oceans play an important role in controlling the transport, fate and sink of swimmers and semi-volatile OPs at regional and global scales (Dachs et al., 2002). However, the total amount of OPs arriving to the ocean and the distribution along the water column are still unknown, since very scarce experimental data exists in order to validate the ADOC fates model in the global Ocean. Biotic and abiotic potential of the ocean have been understudied and addressing these processes is needed to constrain the fate of the large reservoirs of OPs in the ocean.

## ***Polycyclic Aromatic Hydrocarbons in the oceans***

### **Chemical structure and physico-chemical properties**

**Polycyclic Aromatic Hydrocarbons (PAH)** are cyclic hydrocarbons formed by two or more fused benzene rings, starting with two (naphthalene) up to ten (ovalene). Low-molecular-weight PAHs (LMW) are those presenting up to three fused rings, while those with more than three rings are High-molecular-weight PAH (HMW). PAH molecular weights correlate to their octanol-water partition coefficients (usually expressed as log K<sub>ow</sub>) and to a higher resistance to transformation processes. In addition, high K<sub>ow</sub> values generally suggest low aqueous solubility and a high bioaccumulation factor. Thus, the molecular weight appears as the major determinant of the behavior and bioavailability of individual PAH.

The wide spectrum of physicochemical properties, and the fact that PAHs and other semi-volatile hydrocarbons are among the most abundant anthropogenic chemicals in the environment, makes PAH family of pollutants a well suited surrogate to study ADOC biodegradation.

### Sources and fate

There are three major PAH sources into the environment. Petrogenic PAH pollution is caused by direct oil spills and natural oil seeps, whereas pyrogenic ones originate during the incomplete combustion of fossil fuels and organic matter. Although considered a minor fraction of the total, biogenic PAH can be synthesized by certain plants and cyanobacteria (Abdel-Shafy and Mansour, 2016a; Duran and Cravo-Laureau, 2016). Although PAHs have been present in marine environments for billions of years, human activities have triggered a large increase of the level of PAHs in marine ecosystems, becoming the major sinks for these compounds today (Henner et al., 1997; Nizzetto et al., 2008). Coastline ecosystems close to urban and industrial areas generally present higher PAHs levels in seawater and in marine sediments compared to open seas (Guitart et al., 2007; Christiansen et al., 2013). Marine currents and mixing dynamics make these high PAH concentrations drop through dilution into the open ocean, where individual PAH compounds are found at the nano to the pico molar concentration range (Table 2). The major input source of PAH into the global ocean is atmospheric deposition, comprising passive exchange between the atmosphere and the ocean, as well as wet and dry deposition. In the ocean, PAH are globally ubiquitously distributed through cycles of atmospheric transport, deposition and volatilization, owing to their semivolatile nature. Today, PAH are found in all marine basins, even in remote marine polar regions such as the Arctic and the Southern Ocean (Friedman and Selin, 2012; Cabrerizo et al., 2014; Casal et al., 2018). In terms of global carbon fluxes, the input of  $\Sigma 64$  PAH and semi-volatile aromatic like compounds (SALCs) entering the global ocean from the atmosphere is estimated to represent  $\sim 1 \text{ Tg C yr}^{-1}$  and  $400 \text{ Tg C yr}^{-1}$ , respectively (Gonzalez-Gaya et al., 2016). Thus, the sea surface microlayer (SML), the thin interface layer between the ocean and the atmosphere, is a direct recipient of atmospherically deposited PAH in the ocean under calm wind conditions. In fact, PAH enrichments at the SML have been reported in different marine regions (Wurl and Obbard, 2004; Cincinelli et al., 2005; Fuoco et al., 2005; Stortini et al., 2009; Casas et al., 2020). However, SML PAH enrichments, as well as the enrichment of other organic and surface-active substances, are possibly driven by rising bubbles accumulated at the air-water interface or by the attachment of these organic substances to buoyant particles from subsurface waters (Hasse, 2009; Hunter, 2009)

The PAH partitioning dynamics and their fate in the water column will depend on the way PAH enter the ocean, their molecular weight, and to several environmental factors such as the amount of suspended particulate matter and temperature. Due to their hydrophobic nature and low aqueous solubility, PAH tend to sorb into organic particles, including black carbon. However, labile particulate PAH are removed before sinking by both abiotic, such as sunlight photo-oxidation occurring in the surface photic zone (King et al., 2014; Bacosa et al., 2015) and biotic processes such as degradation mediated by microorganism (Head et al., 2006; Ghosal et al., 2016). Nevertheless, to date, most PAH biodegradation studies have been done with concentrations orders of magnitude higher than the ones found in the environment, mimicking oil spill scenarios. The most refrac-

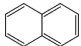
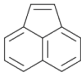
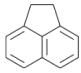
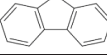
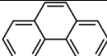
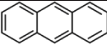
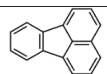
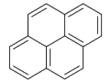
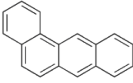
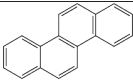
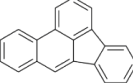
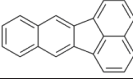
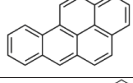
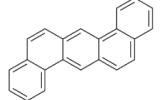
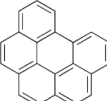
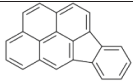
tory PAH are vertically transported to the depths, accumulating in deep-sea sediments (Louvado et al., 2015) or biodegraded by microbial communities adapted to deep-sea low temperatures and hydrostatic high pressure conditions (Yuan et al., 2015).

PAH also accumulate in marine biota entering food webs via both passive and active uptake by microorganisms. Due to their PAH hydrophobicity PAH bioaccumulate in a long list of marine wildlife, from invertebrates to marine mammals (Romero et al., 2020; Lourenço et al., 2021; Berrojalbiz et al., 2011; Yu et al., 2019).

**TABLE 2** | Reported PAH levels in the different oceanic regions and sea layers.

Region	PAH compounds	Matrix	Concentration range	Reference
Central Mediterranean (Sarno river outlet, Gulf of Naples, Tyrrhenian Sea)	$\Sigma_{16}$ PAHs	Surface sea water	23.1 to 2670.4 ng L <sup>-1</sup>	Montuori & Triassi, 2012
SE Mediterranean Sea (Alexandria's coastal water, Egypt)	$\Sigma_{16}$ PAHs	Surface sea water	13.4 and 6076 ng L <sup>-1</sup>	El-Naggar et al., 2018
Eastern Mediterranean Sea	$\Sigma_{19}$ PAH	Surface sea water	0.161 to 8.797 ng L <sup>-1</sup> (dissolved) and 0.033 to 0.319 ng L <sup>-1</sup> (particulate)	Berrojalbiz et al., 2011
Western Mediterranean Sea	$\Sigma_{19}$ PAH	Surface sea water	0.158 to 0.808 ng L <sup>-1</sup> (dissolved) and 0.033 to 0.369 ng L <sup>-1</sup> (particulate)	Berrojalbiz et al., 2011
NW Mediterranean Sea (French coast)	$\Sigma_{17}$ PAH	Surface sea water	4.7 · 10 <sup>3</sup> -1.5 · 10 <sup>5</sup> pg L <sup>-1</sup>	Guigue et al., 2011
Terra Nova Bay, Antarctica	$\Sigma_{13}$ PAH	Surface sea water	2.24 to 4.01 ng L <sup>-1</sup> (dissolved) 1.65 to 3.65 ng L <sup>-1</sup> (particulate)	Cincinelli et al., 2005
Gerlache Inlet Sea, Antarctica	$\Sigma_{13}$ PAH	Surface sea water	5.27–9.43 ng L <sup>-1</sup>	Stortini et al., 2009
Gerlache Inlet Sea, Antarctica	$\Sigma_{14}$ PAH	Surface sea water	331 pg L <sup>-1</sup> (dissolved)	Fuoco et al., 2005
South Shetland Islands, Antarctica	$\Sigma_{25}$ PAH	Suspended particulate matter	30–82 ng L <sup>-1</sup> dw	Curtosi et al., 2009
NW Mediterranean Sea	$\Sigma_{15}$ PAH	Surface sea water	3.6-3.1 ng L <sup>-1</sup>	Guitart et al., 2007
NW Mediterranean Sea	$\Sigma_{17}$ PAH	Surface sea water	4.7-1.5 ng L <sup>-1</sup>	Guitart et al., 2010
North-South Atlantic ocean transect	$\Sigma_{10}$ PAH	Surface sea water	58-1.1. ng L <sup>-1</sup>	Nizzetto et al., 2008
Mediterranean Sea Leghorn, Italy	$\Sigma_{13}$ PAH	Sea surface microlayer	20-1520 ng L <sup>-1</sup> (dissolved) 80-15400 ng L <sup>-1</sup> (particulate)	Cincinelli et al., 2001

TABLE 3 | 16 priority PAH issued by the EPA

Compound	Chemical structure	List	MW G mol <sup>-1</sup>	Log Kow
Naphthalene		EPA	128.1	3.29
Acenaphthylene		EPA	152.1	4.0
Acenaphthene		EPA	154.2	3.92
Fluorene		EPA	166.2	4.18
Phenanthrene		EPA	178.2	4.57
Anthracene		EPA	178.2	4.54
Fluoranthene		EPA	202.3	5.22
Pyrene		EPA	202.3	5.18
Benzo(a)anthracene		EPA, SCF, EU	228.3	5.91
Crysene		EPA, SCF, EU	228.3	5.65
Benzo(b)fluoranthene		EPA, SCF, EU	252.3	5.80
Benzo(k)fluoranthene		EPA, SCF, EU	252.3	6.0
Benzo(a)pyrene		EPA, SCF, EU	252.3	6.04
Dibenzo(a,h)anthracene		EPA, SCF, EU	276.3	6.50
Benzo(g,h,i)perylene		EPA, SCF, EU	278.4	6.75
Indeno(1,2,3-cd)pyrene		EPA, SCF, EU	276.3	7.66

## Toxicity and monitoring

PAH are known to cause acute health effects upon living organisms. Marine oil spills and other PAH polluted aquatic environments revealed that PAH cause immunotoxicity, embryonic abnormalities, and cardiotoxicity in fish, benthic organisms, and marine vertebrates (Romero et al., 2018; Barron, 2012). PAH hydrophobic nature grants access to living cells, interfering in the enzymatic cellular activity and causing mutagenic and carcinogenic effects (Jacob, 2008). Further toxicological research has described other types of toxicities for individual PAH such as developmental toxicity, genotoxicity, oxidative stress, and endocrine disruption (Bekki et al., 2009; Cherr et al., 2017; Lee et al., 2011).

PAH are currently not subjected to the international convention on POPs, due to their potential degradability. However, their potential for long-range transport, ubiquity and concerning toxicity to human health and the environment make them relevant to OP environmental surveys and regular monitoring. The list of 16 priority PAH issued by the US EPA in 1976 (Keith and Telliard, 1979; ATSDR, 1995) has become a standardized proxy of PAH pollution and risk assessment. In Europe, a list of 15 HMW PAHs (+1 methylated PAH) issued by the EU Scientific Committee for Food (SCF) and the EU Commission (Regulation No 835/2011) is regularly monitored in different environmental matrices and consumers' goods (Table 3).

## Other ADOC compounds used in this thesis

### n-Alkanes

#### Chemical structure and physico-chemical properties

n-Alkanes are saturated acyclic hydrocarbons formed exclusively by hydrogen and carbon atoms and constitute the major fraction in crude oil complex mixtures (Figure 5). With the chemical formula  $C_nH_{2n+2}$ , alkanes range from the simplest methane ( $n = 1$ ) to very large chains, either branched or unbranched. Considering their MW, they can be classified as short-chain alkanes (SC,  $< C_{12}$ ), medium-chain alkanes (MC,  $C_{12}$ - $C_{20}$ ) and long-chain alkanes (LC,  $C_{21}$ - $C_{35}$ ). The longer the chain the less soluble and bioavailable the compounds are.

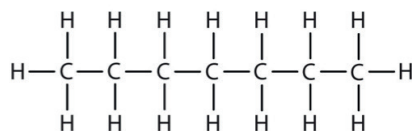


FIGURE 5 | Heptane chemical representation

### Sources and fate

Oil pollution and incomplete combustion are the main anthropogenic sources to marine alkane ubiquitous occurrence. n-Alkanes are also biosynthesized by living organisms as a result of enzymatic transformations of fatty acid molecules (Wang and Shao, 2013; Abbasian et al., 2015; Love et al., 2021).

## Organophosphate Esters

### Chemical structure and physico-chemical properties

Organophosphate esters (OPEs) are synthetically produced phosphoric acid derivatives widely commercialized for many applications. They are considered emergent pollutants, since they have only been considered for regulation recently (Reemtsma et al., 2008). In this thesis we focus in triesters (Figure 6), high-production-volume compounds used to protect or to potentiate the properties of plastics, textiles and other materials as plasticizers and flame retardants (OPE-FRP) (Van Der Veen and De Boer, 2012).

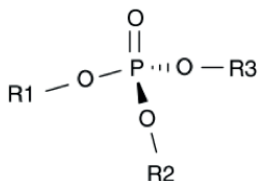


FIGURE 6 | Generic structure for triester OPEs targeted in this thesis. (Singh and Walker, 2006)

### Sources and fate

The intense production, confirmed persistence, and widespread usage, fueled by the recent ban on brominated diphenylethers flame retardants, lead to the ubiquitous occurrence of OPE-FRP in many environmental compartments (Bollmann et al., 2012; Su et al., 2016; Li et al., 2017). In the oceans, the main known input source of OPE-FRPs is through atmospheric deposition (Castro-Jiménez et al., 2014), although riverine inflows haven't been quantified accurately yet. Nevertheless, concentrations of OPE-FRPs in coastal water are very low even in highly polluted areas, suggesting these compounds might be naturally processed either physicochemically (Su et al., 2016) or by microorganisms (Yamaguchi et al., 2016).

## Per- and polyfluoroalkyl substances

### Chemical structure and physico-chemical properties

Per- and poly- fluorinated alkyl substances (PFASs) are a group of manmade aliphatic organofluorine compounds containing only carbon-fluorine bonds (no C-H bonds) and C-C bonds (Buck et al., 2011) (Figure 7). These chemicals, have been synthesized for more than 60 years but only recently have been considered as emergent pollutants. They are used in the industry as waxes and coating materials due to their surfactant properties.

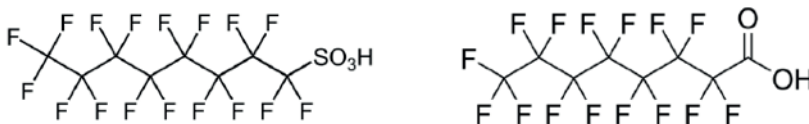


FIGURE 7 | Perfluorosulfonic acids (PFOS) and Perfluorinated organic acids (PFOA) included in the Stockholm Convention on Persistent Organic Pollutants as an Annex B substances (UNEP, 2009). C8-based PFASs such as perfluorosulfonic acids (PFOS) and perfluorinated organic acids (PFOA) are the most persistent, bioaccumulative and biologically active compounds



## Sources and fate

Today, most of the PFASs used in industry are ubiquitously distributed in the different environmental matrices, known to undergo long range transport and be subject to partitioning processes, by which short-chain PFASs and PFCAs are mainly distributed in the water phase (Ahrens et al., 2009). Oceanic occurrence of PFAS has been reported in the SML, in the underlying surface waters and in the marine depths, as well as attached to plankton cells from the open ocean and coastal waters (Gonzalez-Gaya et al., 2014; Yamashita et al., 2005; Casal et al., 2017; Casas et al., 2020). Once in the water column, PFASs could undergo transformation processes towards more persistent degradation products (Yamashita et al., 2005; Wania, 2007; Dreyer et al., 2009; Liu and Mejia Avenadoño, 2013; Ahrens and Bundschuh, 2014), as observed in a mesocosms experiment mimicking realistic environmental conditions (Cerro-Gálvez et al., 2020)

## Life at microscale

The microscopic world was described for the first time by Antonie van Leeuwenhoek in the 17<sup>th</sup> century after the newly developed first single-lens microscope. However, it was not until the 19<sup>th</sup> century when higher-magnification microscopes and the onset of modern Microbiology by Pasteur and Koch, among others, allowed the understanding of microbial life forms and the importance of microorganisms in everyday life: from the first vaccines to the successful isolation and cultivation of bacteria. These discoveries facilitated the basic techniques and instruments used in microbiology still today. It was not until the last decades of the 20<sup>th</sup> century that the rise of molecular techniques allowed the study of the composition of complex microbial communities. The term microbial loop was coined, referring to the carbon cycle process by which dissolved organic carbon (DOC) is incorporated as microbial biomass (making it available towards higher trophic levels) or respired to CO<sub>2</sub>, underpinning the key role of microbial communities in the global biogeochemical cycles. Massive amplicon sequencing of specific genes (16S rDNA genes for prokaryotes and 18S rDNA and mitochondrial COX genes for eukaryotes) from environmental samples provided the first realistic profiles of microbial diversity and phylogeny in nature. Nowadays, high throughput sequencing technology allows the sequencing of thousands to millions of 16S or 18S rDNA genes, improving phylogenies and giving insights into new lineages. Those methodologies that take advantage of high-throughput analytical technologies to massively analyze the biological constituents (including the genetic material) of a given sample are known as omic approaches. When omic analyses are applied to complex microbiome from an environmental sample, these techniques are referred as metaOmics. The different omic and metaOmic approaches can be classified depending on the cellular part subject of the study (Table 4). Metagenomic studies recovering the genetic material directly from environmental samples, revealed to which extent microbial biodiversity had been missed by cultivation dependant techniques, since only a minor share (1-10%) of microorganisms appear to be culturable. While meta-genomic techniques grant the access to functional and metabolic diversity of microbial commu-

TABLE 4 | Different types of omics (or metaOmics) approaches

	From bacterial isolates or single species: Omics	From complex microbiomes: MetaOmics
<b>DNA</b>	<b>Genomics</b> Study of the genome (genetic material) of a particular organism.	<b>MetaGenomics</b> Study of the genetic material from complex microbiomes.
<b>RNA (mRNA)</b>	<b>Transcriptomics</b> mRNA captures a snapshot in time of the total transcripts present in a cell, thus transcriptomics study the gene expression of a particular organism.	<b>MetaTranscriptomics</b> Study of the gene expression and regulation from complex microbiomes.
<b>Proteins</b>	<b>Proteomics</b> Study of the entire set of proteins (proteome) produced or modified by an organism	<b>MetaProteomics</b> Study of the proteome from complex microbiomes
<b>Metabolites</b>	<b>Metabolomics</b> Study of the unique chemical fingerprints that specific cellular processes leave behind (metabolites) revealing the physiology of a cell. The complete set of metabolites resulting from cellular functions is referred as metabolome.	<b>MetaMetabolomics</b> Study of the metabolome from complex microbiomes

nities, other approaches are required in today's global change context for assessing the community metabolic responses and resilience in front of environmental disturbances. Methodologies analyzing the gene expression (mRNA), the proteome and the metabolome from environmental samples may provide the required information on the metabolically active cells and processes (Moran et al., 2013).

Overall, metaOmics techniques provide thorough information not only on the microbial community structural shifts, but also on the mechanisms of adaptation and the responses which allow microorganisms survive adverse and fluctuating conditions in their immediate surroundings.

### ***Marine microbiome***

Viruses, bacteria, archaea, fungi, protist, algae and animals sizing between 0.2 and 100µm living in the oceans constitute the marine microbiome. Taxonomically, phylogenetically and metabolically widely diverse, marine microorganisms occur in all the habitats found in the oceans, even those with harsh environmental conditions (Poli et al., 2017). While individually small in size, the marine microbiome is estimated to constitute around 70% of the total biomass in the sea (Bar-On et al., 2018). They are known to participate and maintain key biogeochemical processes at a planetary scale (primary production, respiration, etc), to which the other forms of life depend on (Azam and Malfatti, 2007).

Marine microorganisms can be classified depending on their metabolic preferences (Table 5). This classification sorts organisms based on the energy and carbon sources they use, as well as the electron or hydrogen atom donor. Those organisms relying on CO<sub>2</sub> as carbon source to build biomass (fix CO<sub>2</sub>) are known as **autotrophs** or primary producers, those that use alternative carbon sources are known as **heterotrophs** or secondary producers. However, many lineages have very flexible nutritional preferences, known as mixotrophs, and can shift from one metabolic strategy to another as the environmental conditions change. Table 5 includes a classification of organisms depending on the nature of their preferred metabolism.

Marine bacteria constitute a large domain of prokaryotic microorganisms. This thesis focuses on the **marine heterotrophic bacteria** (Yilmaz et al., 2016) (Figure 8).

The metabolism of heterotrophic bacteria consists in the consumption of dissolved or particulate organic matter (OM), which is incorporated as bacterial biomass, respired to CO<sub>2</sub> (remineralized) or transformed to more refractory OM. In the oceans, bacterial production is the key process of the microbial loop, the pathway which transfers organic matter and energy towards higher trophic levels in the food chain (Jiao and Zheng, 2011; Jiao et al., 2011). However, not all organic matter molecules are equally

TABLE 5 | Metabolism table (Adapted from Munn, 2019).

Energy source	Hydrogen-atom or electron source	Carbon source	Name	Representative examples
Sun Light (photo-)	Organic (organo-)	Organic (heterotroph)	Photoorganoheterotroph	<i>Rhodobacter</i> and green non-sulfur bacteria
	Inorganic (litho-)	CO <sub>2</sub> (autotroph)	Photoorganoautotroph	Some archaea (Halobarchaea)
Breaking chemical compounds (chemo-)	Organic (organo-)	Organic (heterotroph)	Photolithoheterotroph	Purple non-sulfur bacteria
		CO <sub>2</sub> (autotroph)	Photolithoautotroph	Cyanobacteria
	Inorganic (litho-)	Organic (heterotroph)	Chemoorganoheterotroph	Animals and fungi
Breaking chemical compounds (chemo-)	Organic (organo-)	CO <sub>2</sub> (autotroph)	Chemoorganautotroph	Anaerobic methanotrophic archaea
		Organic (heterotroph)	Chemolithoheterotroph	Some bacteria from genus <i>Oceanithermus</i>
	Inorganic (litho-)	CO <sub>2</sub> (autotroph)	Chemolithoautotroph	<i>Nitrobacter</i> and archaea such as <i>Methanobacteria</i>

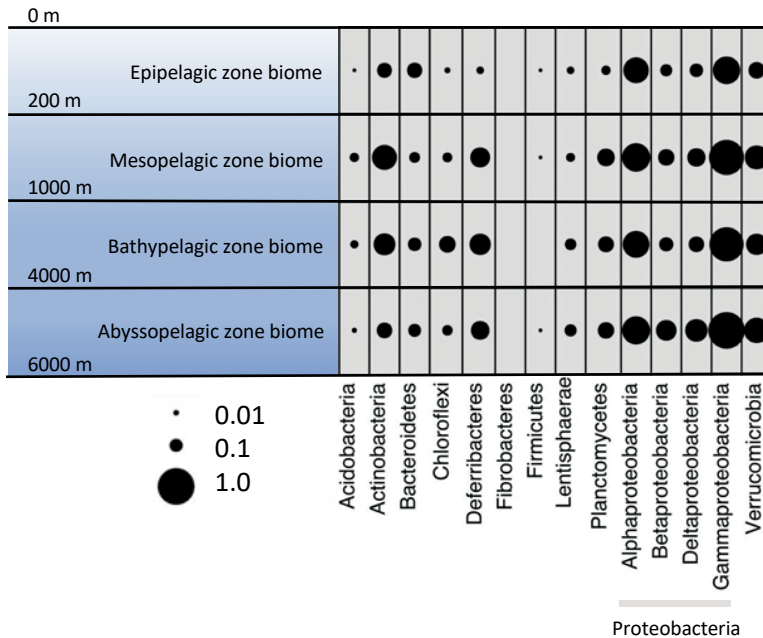


**FIGURE 8** | Bubble plot showing the average relative abundances of marine phyla across oceanic biomes. The scale for bubbles are indicated in the plot, and values were scaled from 0 to 1, with 0 representing the minimum average relative abundance, and 1 representing the maximum relative abundance. (Adapted from Yilmaz et al., 2016)

bioavailable to heterotrophic bacteria. The efficiency of the carbon flux depends on the amount and quality of the OM, as well as the composition of the bacterial community.

Moreover, bacteria can be classified as free-living (FL), particle-associated (PA) and bacteria that shift between these two lifestyles (Grossart, 2010). PA bacteria can sense, colonize, metabolize organic particles, releasing dissolved OM into the surrounding environment making it available for their FL counterparts. As an example, the term “marine snow” refers to organic aggregates that concentrate high levels of organic substrate, becoming hot spots of PA microbial activity and OM transformations.

### ***Interactions between OP and marine microbiomes***

Microorganisms are sensitive to the alterations in their immediate surrounding environment. Changes in the availability, composition and concentration of the ocean’s dissolved organic carbon (DOC) and other key nutrients are known to trigger changes in microbial community structures and in the succession of different functional groups (Hutchins et al., 2017, Mason et al., 2012). However, the microbial responses linked to the changes in concentration and composition of the anthropogenic fraction of DOC (ADOC) under realistic conditions are largely unknown. Despite ADOC concentrations are two orders of magnitude lower than DOC, ADOC bioaccumulation increases its intracellular

concentrations to the micromolar range, concentration at which it becomes relevant (Vila-Costa et al., 2020).

The majority of the current research on the interaction of microbial communities and OP focus on the responses under acute pollution events, such as oil leakage accidents or waste water treatment plants. The microbial responses are measured and assessed under high concentrations of ADOC, and the focus of the studies generally revolves around the capacity of microorganisms to degrade these compounds, ultimately for bioremediation purposes in acute polluted sites (Head, 2006; Gallego et al., 2014; Crisafi et al., 2016; Atashgahi et al., 2018, Dombrowski et al., 2016, Gutierrez et al., 2013). These studies have set the grounds of the genetic and biogeochemical basis for the microbially-mediated degradation processes of some OP, but many mechanistical questions remain unanswered. Bacterial and fungal culturable isolates capable of transforming certain OP have provided knowledge on the OP biodegradation pathways, the enzymes involved and the resulting metabolites (Cerniglia, 1992; Ghosal et al., 2013; Takahashi et al., 2013; Zacharia, 2019). While some of the degrading strains metabolically benefit from ADOC as nutrient and energy supply (Head et al., 2006), ADOC compounds can also be transformed fortuitously by promiscuous enzymes, subsequently entering into different catabolic pathways, a process termed **cometabolism** (Gonzalez-Gil et al., 2017, Nzila, 2013). Furthermore, OP molecular biotransformation do not always conclude in the complete compound's mineralization, and in some cases it results in derivatives more harmful and resistant than the original compound, a process known as **bioactivation** (Gerba et al., 2019). The study of transformation products has become popular in today's environmental chemistry research field (Kotthoff et al., 2019). Unfortunately, very scarce information exists on biodegradation and bioactivation rates under the realistic ADOC concentrations that are found in the oceans, and even less on the consequences of the microbial metabolic capacity as a significant modulator of the total oceanic ADOC pool.

A long list of OP's proven to cause adverse effects on living organisms and ecosystems (Pignatello et al., 2010). Hydrophobic OP can penetrate biological membranes causing non-specific baseline toxicity by narcosis. Cellular narcosis occurs when the structure and functioning of the membranes is affected by OPs, leading to a decrease in biological activity and ultimately threatening the organism viability (Van Wezel and Opperhuizen, 1995; Escher et al., 2002). Known adverse effects of OPs in marine phytoplankton and bacteria include loss of viability, reduction of cell abundance and efficiency, and alterations in respiration and photosynthesis (Echeveste et al., 2016, Gilde and Pinckney, 2012; Johnston et al., 2015; Echeveste et al., 2010; Fernandez-Pinos et al., 2017)m. However, most of OP toxicity assessments are done under non-realistic environmental conditions, neglecting abiotic influencing factors, the interconnection between different components of the ecosystems, and using OP concentrations orders of magnitude above environmental concentrations. This notwithstanding, recent studies reported the activation of anti-toxic and cell repair mechanisms in naturally-occurring upper ocean micro-

organisms exposed to low and environmentally relevant concentrations of OP mixtures (Cerro-Gálvez et al., 2019; Cerro-Gálvez et al., 2020, 2021).

Therefore, the interaction between the OP, found at nano and pico molar concentrations of ADOC in the ocean, and the naturally occurring microbial communities is bidirectional. On one side, ADOC impacts the ecology of the microbial communities, both compositionally and functionally. In fact, ADOC can represent simultaneously a nutrient supply and energy source for some microbes, and a toxic agent compromising the viability of cells and triggering cell repair and detoxifying mechanisms. On the other side, microbial metabolism can modulate the ocean's ADOC concentration pool and its biogeochemical cycle (Figure 9).

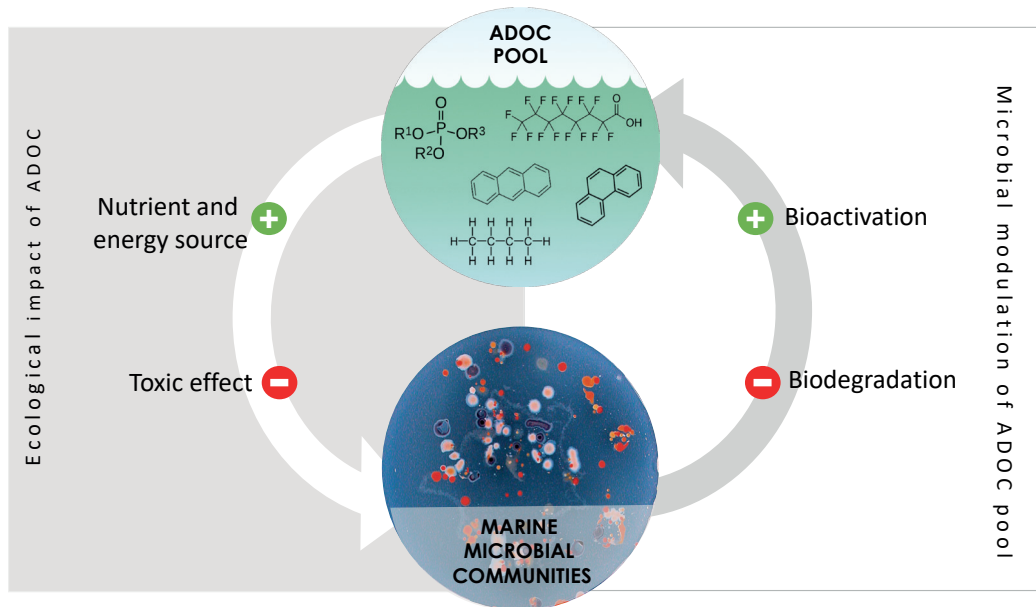


**FIGURE 9** | Two-sided interaction between the global ocean ADOC pool and the naturally occurring marine microbial communities.

## Marine microbiomes and PAH, a story of love and hate

The different microbial responses to PAH exposure in marine environments are modulated by the concentration and the compositional nature of the PAH and SALCs mixture, the local environmental conditions, and the dynamics affecting and regulating the physiology of the naturally occurring microbial community. This has been mostly studied in oil spill scenarios. The sequencing surveys from marine oil polluted sites provided insights into the marine microorganisms associated to the presence of hydrocarbons and into the phylogeny of those capable of coping and/or degrading PAH and SALC mixtures in the different marine ecosystems (Gallego et al., 2014; Lozada et al., 2014; Dombrowski et al., 2016; Karthikeyan et al., 2020; Rodríguez-Salazar et al., 2021). Marine microorganisms associated to PAH are very diverse and possess multiple strategies to cope with PAH, in order to facilitate PAH assimilation and/or to quench PAH inherent toxicity.

### PAH biodegradation pathways and PAH-degrading bacterial players

The isolation of a number of PAH-degrading strains from different polluted sites revealed the different metabolic pathways and key enzymes for the biodegradation of individual PAH compounds under aerobic and anaerobic conditions (Cerniglia, 1992; Kweon et al., 2008; Carmo et al., 2009; Kanaly and Harayama, 2010; Ghosal et al., 2016; Wang et al., 2018). Today, PAH biodegradation is in the spotlight for its potential biotechnological uses. In fact, bioremediation techniques (this is exploiting microbes metabolic capacities to remove pollutants in a polluted media) have become the most commonly used and effective strategies for cleaning up PAH-polluted sites (Abdel-Shafy and Mansour, 2016b; Ghosal et al., 2016).

Oxygen-dependent bacterial PAH degradation pathways involve cascades of many different metabolic reactions (Leahy and Colwell, 1990; Cerniglia, 1992; Seo et al., 2009; Peng et al., 2010; Mallick et al., 2011; Ghosal et al., 2016). The common initiating catalyzing step is the incorporation of oxygen to the PAH closed ring structures through hydroxylation, converting the aromatic compounds into a cis-dihydrodiol. This step is catalyzed by ring hydroxylating dioxygenases (RHD), a multicomponent complex which includes a hydroxylase and electron transfer components (Figure 10). The hydroxylase component encompasses an alpha subunit hosting the RHD active catalytic site (Cerniglia, 1992; Ferraro et al., 2006; Seo et al., 2009; Mallick et al., 2011; Cai et al., 2016). From the cis-dihydrodiol, dehydrogenases and ring-cleaving

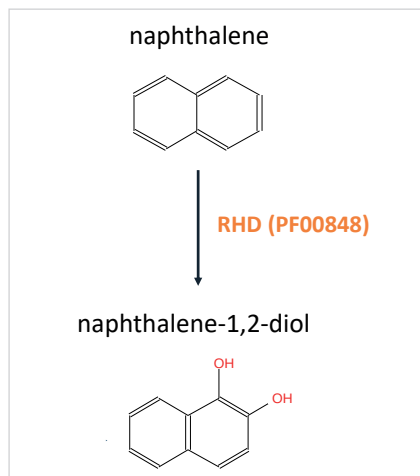


**FIGURE 10** | Initial ring hydroxylation for Naphthalene aerobic degradation pathway mediated by RHD, PFAM profile PF00848.



dioxygenases oxidize the substrate towards intermediate molecules such as catechols which are ultimately transformed into tricarboxylic acid (TCA) cycle intermediates. Aerobic PAH degradation can be also carried out by monooxygenases from the cytochrome P450 enzyme family (Brezna et al., 2006).

For the anaerobic catabolism, two different activation steps have been described: 1) carboxylation and 2) methylation followed by fumarate addition (Foght, 2008; Carmona et al., 2009).

Hydrocarbon degrading bacteria are known as hydrocarbonoclastic bacteria (HCB). HCB include obligate (specialists bacteria with a tightly narrow range of carbon substrates) and facultative bacterial strains (Yakimov et al., 2007). Many of them are known to use PAH as substrate, either as carbon or energy source. PAH mixtures can be also degraded fortuitously as a non-growth-substrate through cometabolism (Nzila, 2013, Yuan et al., 2015, Vila et al., 2015). HCB appear to be ubiquitous, as they are present in remote and non-polluted marine environments such as polar sea-ice or deep seawater (Garneau et al., 2016; Yuan et al., 2015; McFarlin et al., 2018, Yakimov et al., 2021). Interestingly, HCB are naturally found in low numbers, but they can become predominant shortly after a pulse of PAH or other hydrocarbons (Head et al., 2006; Lozada et al., 2014; Teramoto et al., 2013, Cafaro et al., 2013).

Studies with hydrocarbon-degrading consortia cultures from marine polluted sites showed that the PAH degrading capabilities of the microbial community exceed those of the isolated individual strains (Dombrowski et al, 2016). These findings suggest that the removal of PAH and other SALCs complex mixtures requires the combine non-redundant enzymatic capabilities of the microbial community. The characterization of the different HCB groups present in areas impacted by marine oil spills revealed microbial succession patterns based on the bacterial nutritional preferences following hydrocarbon supplies (Camilli et al., 2010; Hazen et al., 2010; Dubinsky et al., 2013; King et al., 2015; Rodriguez-R et al., 2015). As an example, some gammaproteobacteria, such as Pseudomonadaceae, are known to be rapid responders, and exponentially grow at the initial stages of PAH exposure. Oppositely, alphaproteobacterial HCB become predominant once the most labile PAH and SALCs compounds have already been removed.

Beyond the composition of the microbial community, other factors such as temperature, the pre-exposure history of the community or nutrient availability influence the efficiency and rate of PAH biodegradation (Leahy and Colwell, 1990; Bagi et al., 2013; Hazen et al., 2016). Furthermore, not all PAH compounds are equally bioavailable by bacteria. PAH become less bioavailable with increasing molecular weight since tend to partition to the particulate organic matter pools, with a high affinity to black carbon. Similarly, in the water column, petrogenic PAH are more bioavailable than pyrogenic ones, since these later have higher MW and are more hydrophobic, thus are particle-bound, with an ultimate fate bound to black carbon present in sediments.

PAH biodegradation rates with varying substrate PAH mixtures and environmental conditions have been reported by isolated marine HCB strains, by marine consortia culture enrichments and by naturally occurring microbial communities in different marine ecosystems (Table 6). However, in all cases, PAH mixture concentrations are orders of magnitude above those found in the oceanic water column. Consequently, the real implications of the microbial metabolic capabilities upon PAH marine chronic pollution and PAH fates remain unknown. Measurements of in situ biodegradation rates, the incidence of naturally occurring microbial PAH networks and their metabolic capacity under realistic conditions at background concentrations need to be further explored.

### **Microbial strategies and cellular mechanism to cope with PAH exposure**

Beyond biodegradation, marine oil spills have shown a wide variety of marine microbial strategies to cope with PAH exposure. These are very diverse: from cell protection and detoxifying mechanisms to exuding substances to facilitate PAH availability. Again, most of these microbial strategies in front of PAH exposure have been observed under high concentrations of PAH (Joye et al., 2016), and few studies have tackled the microbial mechanisms coping with environmentally relevant concentrations of PAH (Cerro-Gálvez et al., 2019).

### **Chemosensing and motility**

Some bacteria can perceive subtle variations of background concentrations of chemicals in their surroundings through sensory mechanisms consisting of transmembrane chemoreceptors that recognize chemoeffectors (chemical signals, including attractants and repellents). Chemoreceptors can consist of one or two-component systems (Matilla and Krell, 2017) and transmit the environmental information through chemosensory-signalling pathways (Wadhams and Armitage, 2004; Ortega et al., 2017). Response regulator proteins act as transcription factors interpreting this information and activating or inhibiting the expression of wide arrays of genes. These strategies facilitate PAH biodegradation by sensing and bringing bacteria into contact with degradation substrates (chemoattraction) (Parales and Harwood, 2002; Parales et al., 2008), or, in the contrary, getting away from the toxic compounds (chemorepulsion) (Lacal et al., 2013). Chemotaxis is the biasing movement which facilitates the migration of bacteria following a given chemical concentration gradient. For example, a direct motility mode is achieved by flagellum-dependent chemotaxis. Flagella are filamentous organelles that drive bacterial locomotion towards or away from the chemical. In this case the signalling cascade either activates or suppresses the activity of a transmembrane histidine kinase protein, by which the direction of flagellar motor rotation is controlled. Enhanced expression of genes for bacterial chemotaxis and flagella motility have been observed in HCB strains after oil spills (Mason et al., 2012), and different studies suggest that chemoattraction increases

the bioavailability of heterogeneously distributed aromatic substrates (reviewed by Lecal et al., 2013).

### **Quorum sensing**

Quorum sensing (QS) is an intercellular communication mechanism which allows gene expression regulation of certain genes as a response to the fluctuating cell-population density. QS is thought to enhance biodegradation of hydrocarbons by regulating the expression of genes involved in processes such as biofilm formation or horizontal gene transfer. In fact, QS genes involved in biofilm formation from a marine isolated bacterium exposed to PAH increased along with biofilm development and PAH degradation rates (Mangwani et al., 2015).

### **Production of biosurfactants**

Biosurfactants are surface active molecules synthesised and secreted by bacteria. Biosurfactants can be divided into LMW surfactants (glycolipids, lipopeptides, fatty acids and phospholipids) and HMW surfactants (extracellular polymeric substances), differing in physiology and surface active properties (Matvyeyeva et al., 2014). According to their properties, some biosurfactants increase the bioavailability of hydrophobic substrates such as PAH by increasing their solubility, increasing dispersion and reducing their surface tension (Perfumo et al 2018). Others have the ability to form emulsions that facilitate the adhesion of bacteria to the hydrophobic substrate-water interface. In addition, biosurfactants can form gel-like aggregated matrices known as biofilms, which can serve as a habitat for HCB to grow. The capacity to produce biosurfactants has been demonstrated for many HCB strains and for bacteria isolated from hydrocarbon contaminated marine environments (Gutierrez et al., 2013, 2018; Antoniou et al. 2015; Patowary et al., 2017).

### **Modification of cell structure**

Modifications of the membrane composition and properties can respond to a cell defence mechanism against toxic compounds (i.e. PAH). Such stressors can alter the membrane fluidity/rigidity by modifying the membrane phospholipids composition, compromising the cell viability (Kallimanis et al., 2007). For bacteria to survive, these changes need to be counteracted by changes in the length of the fatty acids, in their saturation degree, and in the cis/trans configuration of the unsaturated fatty acids (Ortega et al., 2017). In turn, this affects permeability of the membrane, possibly influencing the passive diffusion of PAH into the cell, as observed under ADOC mix exposure at low concentrations (Cerro-Gálvez et al., 2019).

### Getting past the membrane

The intracellular localization of PAH-degrading enzymes requires the passage of substrate compounds through the cell membrane. Bacterial hydrocarbon uptake is influenced on one side by the hydrocarbon's size and polarity, and by the permeability of the cell membrane on the other. Some hydrophobic substrates can be internalized by the cell through passive diffusion via membrane pores, whereas others make use of outer membrane proteins implicated in the active trans-membrane transport, as observed by Hearn et al., 2008 for aromatic hydrocarbons.

### Pumping out the cell

In the opposite direction, toxicants such as OP can be extruded from the cell by transport protein systems known as efflux pumps. Efflux pumps can be substrate-specific or can transport a range of structurally different compounds, the later known as multi-drug efflux pumps (Martinez et al., 2009, Blanco et al., 2016). Yao and colleagues (2017) unravelled the positive role of efflux pumps from a HCB strain in the biodegrading of PAH by pumping out metabolized toxic substances.

### Horizontal gene transfer

Mobile Genetic Elements (MGE) are DNA sequences encoding for enzymes and proteins that mediate the transfer of DNA sequences within the genome or between bacterial or archaeal cells. The dissemination of genes between cells, known as Horizontal gene transfer (HGT), is considered a key adaptation strategy of microbial communities to specific environmental changes, such as contaminated environments or the presence of a toxicant (Wright et al., 2008; Sobczyk and Hazen, 2009; Y. Wang et al., 2017; Lekunberri et al., 2018). Catabolic or resistance genes are often either harboured or flanked by MGE, consisting of transposon and integron genes, and, in many cases, encoded in extrachromosomal, self-replicating elements, called plasmids, which successfully spread catabolic or resistance traits to cooccurring phylogenetically diverse bacteria (Top et al., 2002; Nojiri et al., 2004; Yuanqi Wang et al., 2017). Moreover, the microbial community history of exposure to con-taminants such as ADOC can also determine the microbial adaptive strategies to these perturbations. These pre-adaptative mechanisms and their evolutionary ecological consequences have been largely studied as linked to the spreading of antibiotic re-sistance among pathogenic bacteria, but they are also operating in the dissemination of resistance genes to other selective agents such as heavy metals or disinfectants (Gillings, 2013). The pre-history of marine microbial communities under chronic ADOC pollution levels could also determine microbial adaptations to these selective agents. Tests with marine bacterial isolates have shown correlation between MGE (in this case plasmid DNA conferring resistance to toxic chemicals) and the levels of in situ

chemical pollution (Baya et al., 1986). Also, riverine water affected by industrial chemical pollution has shown higher gene transfer potential compared to a non-polluted reference community (Wright et al., 2008). Unfortunately very few field studies exist in order to verify how long-term exposure to ADOC at environmentally relevant concentrations can promote higher gene plasticity within a microbial community, conferring the capacity to respond faster to ADOC pulses when compared to non-pre-adapted microbial communities (i.e. pristine marine ecosystems) (Cerro-Gálvez et al., 2021).



## THESIS OBJECTIVES

This thesis investigates the interaction between marine microbial communities in the upper ocean and PAH pollution at background concentrations, focusing on biodegradation processes and the concurrent microbial strategies to cope with PAH perturbations.

We aimed to investigate whether or not PAH biodegradation is a relevant process modulating PAH concentrations in the upper ocean, evaluate the relative influence of other factors such as climate region, bacterial lifestyle or pollutant pre-exposure history on microbial biodegradation of PAH at environmentally relevant concentrations and describe the anti-toxic strategies that occur in parallel to PAH biodegradation. The general working hypothesis of this thesis is that background concentrations of PAH in the upper ocean have significant effects over the composition and the functioning of marine microbial communities. While microbially mediated ecosystem functions might be affected by PAH global oceanic occurrence, the PAH pool concentrations are also susceptible to be modified by microbially-mediated transformations. These two-sided effect interaction affecting the cycling dynamics of PAH is not characterized, neither included in today's modeling approaches.

We tested the following **hypotheses**:

**H1** The global ocean microbiome harbors the metabolic potential to degrade PAH, becoming a key modulator of the PAH oceanic pool.

**H2** Community PAH pre-exposure history influences the response strategy and response time in front of a PAH exposure.

**H3** Naturally occurring microbial communities from the least polluted marine environments, such as polar and sub-polar regions, can also actively degrade PAH at environmental relevant concentrations.

**H4** Bacterial lifestyles (particle-associated and free living) have differentiated responses to PAHs.

**H5** The sea surface microlayer is a microhabitat for HCB and a hotspot of PAH biodegradation.

The **main goals** of this thesis are to assess the magnitude of PAH chronic pollution biodegradation potential in the global ocean and test how microbial indigenous communities from different contrasting environments responded at structural and functional level to PAH at environmentally relevant concentrations, as well as assessing the consequences of microbial-PAH interaction over the PAH pool.

The **specific objectives** of this thesis were:

**1** To determine the global ocean capacity to metabolize a model family of ADOC, PAH, and explore whether or not microbial degradation is a neglected modulating vector of the PAH pool. (**Chapter 1**)

**2** To determine the impact of PAH exposure in microbial communities from environments with contrasted pollution levels (i.e. Polluted vs pristine site). (**Chapter 2**)

**3** To compare the abundances of HCB and different ADOC families concentrations in the different upper ocean habitats. (**Chapter 3**)

**4** To determine the biodegradation rates under realistic nominal concentrations of PAH in environments with contrasted pollution levels and in adjacent marine habitats. (**Chapter 2 and Chapter 4**)

**5** To determine how microbial interaction with PAH changes when other ADOC compounds are also present (**Chapter 5**)

The **long term objectives** of this thesis are to provide new insights on the role played by marine microorganism modulating the global concentrations of PAH in the upper ocean in different marine habitats (i.e. polluted vs. pristine, temperate vs. polar, sub-surface seawater vs sea surface microlayer) and bacterial lifestyles (i.e. particle associated vs. free living, HCB vs dominant non-HCB).

We have addressed the objectives and tested the hypotheses by combining omics, mo-



lecular, analytical chemistry and bioinformatics methodologies, in exposure experiments from contrasted environments and making use of global genomic and ADOC databases (Figure 11). All incubation experiments were performed using close-to-realistic concentrations of OP compounds (taking primarily PAH as a model family of ADOC) in order to simulate the microbial-ADOC pool interactions occurring in the oceans today.

The different experimental designs and sampling sites are described below for each chapter:

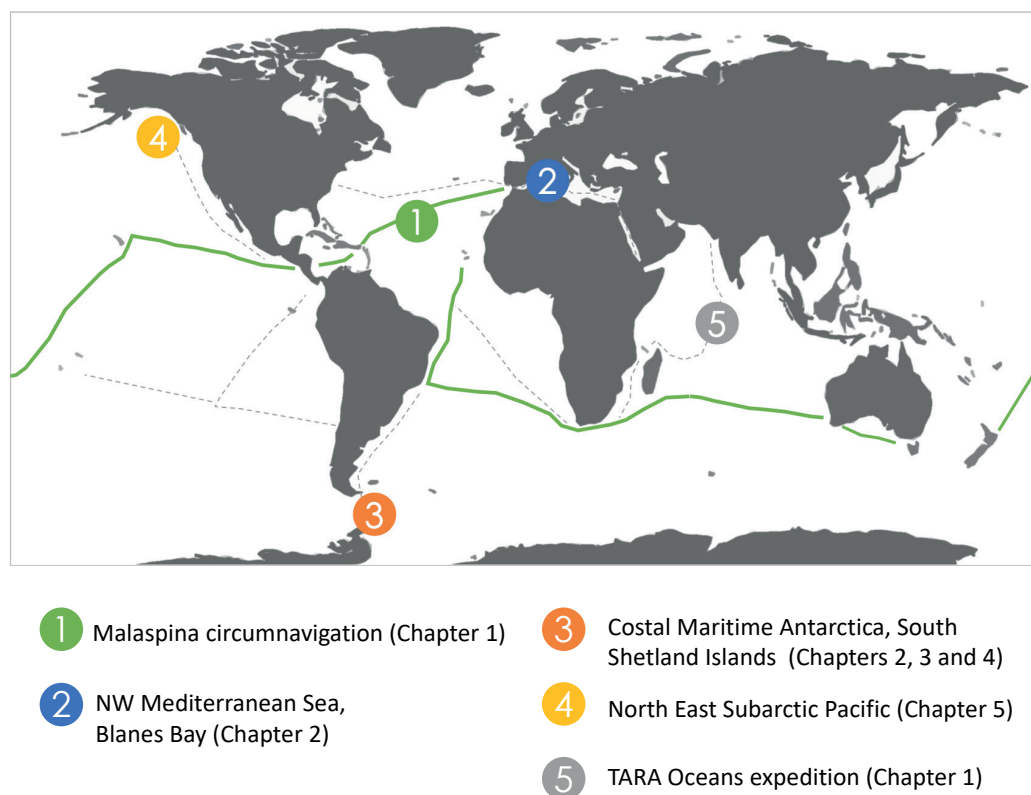


**FIGURE 11** | Map of the experimental locations and oceanographic expeditions.

In **Chapter 1** we combine an available database of worldwide genetic repertoires (Tara Oceans, (Sunagawa et al., 2015)) and our own PAH global concentrations databases (Malaspina circumnavigation Figure 11) to search for genetic evidence of PAH microbial degradation as a neglected PAH pool modulator at global scale.

**Chapter 2** explores the differentiated microbial responses at structural and functional levels to PAH, as well as the biogeochemical consequences of microbial-PAH inter-

action over the PAH pool between polluted and pristine marine microbial communities. Incubation experiments doped with realistic concentrations of PAH were performed with Antarctic coastal water (Livingston Island) and NW Mediterranean Sea (Blanes Bay) (Figure 11), corresponding to the two contrasting habitats with differentiated community pre-exposure adaptations to in situ ADOC levels.

**Chapter 3** explores and compares the naturally occurring microbial bacterial genera capable to degrade ADOC and the correlation with in situ ADOC concentrations from two contrasting adjacent marine habitats, the sea surface microlayer (SML) and the sub-surface layer (SSL) in Antarctic waters (Figure 11). In **Chapter 4**, an incubation experiment with PAH was performed with water from the SML and SSL in Antarctic coastal waters, in order to assess PAH biodegradation rates under realistic conditions in each habitat, as well as structural and functional responses characteristic of each layer and microorganisms' lifestyle.

Finally, in **Chapter 5** we analyze the community structure and functional responses of three differentiated naturally occurring communities over a gradient of ADOC pollution at the north-east Subarctic Pacific (NESAP) (Figure 11). The different community responses were studied in exposure experiments with three model families of ADOC (OPE-FRP, n-alkanes and PAHs) at two different nominal concentrations.





## METHODOLOGY SUMMARY

The different methodological approaches adopted in this thesis are summarized below:

### Analytical chemistry methodology

The identification and quantification of the OP selected families was done with gas-chromatography coupled to mass spectrometry (GC-MS). The gas chromatograph is the chemical analytical instrument that allows separating the chemical components from a complex sample. The mass spectrometer is the detector which identifies the different analytes from the chromatogram by their mass spectrum.

### Genomic and molecular

The following techniques were used to determine microbial community composition and community functionality:

#### Community composition

##### **Amplicon sequencing of the 16S rRNA gene**

16S rRNA gene is used for the identification, classification and quantification of prokaryotes of an environmental sample. This gene is the most commonly used genetic marker to study bacterial phylogeny and taxonomy, owing to its conserved regions being present in almost all bacteria (Janda and Abbott, 2007).

**Flow Cytometry** is a technique used to quantify bacterial population abundances, as well as sorting between high and low nucleic acid bacterial subpopulations (HNA and LNA respectively) (Falcioni et al., 2008).

## Community functionality

### **Metatranscriptomics**

This omics technique focuses on the study of the gene expression of an environmental sample by extracting the RNA and sequencing it on a next generation sequencing platform. The resulting sequences are assigned to taxonomical and functional reference databases.

### **Boncat (Bioorthogonal non-canonical amino acid tagging)**

This technique is based on the in vivo incorporation of the non-canonical amino acid L-azidohomocysteine (AHA), a surrogate for L-methionine, followed by fluorescent labelling of AHA-translationally active cells within complex environmental samples (Leizeaga et al., 2017).

### **DMSP cycling rates**

Dimethylsulfoniopropionate (DMSP) is an organic molecule that is used as a sulfur and carbon source by marine bacteria. DMSP turnover rates usually correlate to leucine incorporation rates thus it can be taken as a proxy of microbial activity (Vila-Costa et al 2007).

## **Bioinformatic tools and pipelines**

This approach was used to process sequencing data, data analysis and data visualization.

## Sequencing data processing

**DADA2 package and workflow** were used to process the 16S rRNA raw amplicon sequencing data into exact amplicon sequence variants (ASV) (Callahan et al., 2016). Briefly, the workflow takes the demultiplexed fastq files and outputs the ASV and the abundances for each sample. Taxonomic assignment to 16S rRNA gene fragments is performed with reference taxonomic databases.

**Different software packages were used to process the metatranscriptomic raw illumina reads into transcripts**, which are assigned to functional and taxonomical classifications. In brief, MEGAHIT assembler was used for the high-quality reads de novo assembly, which provides longer and expressed genome segments offering a reference set of genes (Li et al., 2016).

Functional annotation can be read-based or assembled-based. Read-based tools require predicted open reading frames as input (performed in our case with PRODIGAL). Assembly based gene annotation performs a functional assignment

based on similarity of searches using aligning specific tools such as DIAMOD, which searches against functional databases like the Kyoto Encyclopedia of Genes and Genomes (known as KEGG) or the National Center for Biotechnology Information (NCBI) RefSeq.

### Data analysis, visualization and statistics

#### **R software**

R is a programming language and free software used for statistical analysis. R environment was used to prepare and normalize the omics data, as well as performing statistical analyses and plotting the results (R Core Team, 2019).

**HMMER** is a bioanalysis tool that uses hidden Markov Models profiles (HMM). HMM are probabilistic model profiles that comprise the evolutionary changes that might have occurred in a set of related sequences. HMMER was used to search for specific gene profiles against metatranscriptome data (Eddy and Wheeler, 2015).

## REFERENCES

- Abbasian, F., Lockington, R., Mallavarapu, M., and Naidu, R. (2015) A Comprehensive Review of Aliphatic Hydrocarbon Biodegradation by Bacteria. *Appl Biochem Biotechnol* 176: 670–699.
- Abdel-Shafy, H.I. and Mansour, M.S.M. (2016a) A review on polycyclic aromatic hydrocarbons: Source, environmental impact, effect on human health and remediation. *Egypt J Pet* 25: 107–123.
- Abdel-Shafy, H.I. and Mansour, M.S.M. (2016b) A review on polycyclic aromatic hydrocarbons: Source, environmental impact, effect on human health and remediation. *Egypt J Pet* 25: 107–123.
- Ahrens, L., Barber, J.L., Xie, Z., and Ebinghaus, R. (2009) Longitudinal and Latitudinal Distribution of Per-fluoroalkyl Compounds in the Surface Water of the Atlantic Ocean. *Environ Sci Technol* 43: 3122–3127.
- Ahrens, L. and Bundschuh, M. (2014) Fate and effects of poly- and perfluoroalkyl substances in the aquatic environment: A review. *Environ Toxicol Chem* 33: 1921–1929.
- Antoniou, E., Fodelianakis, S., Korkakaki, E., and Kalogerakis, N. (2015) Biosurfactant production from marine hydrocarbon-degrading consortia and pure bacterial strains using crude oil as carbon source. *Front Microbiol* 6: .
- Antoniou, M.G., Zhao, Cen, O’Shea, K.E., Zhang, G., Dionysiou, D.D., Zhao, Chun, et al. (2016) CHAPTER 1 Photocatalytic Degradation of Organic Contaminants in Water: Process Optimization and Degradation Pathways. In *RSC Energy and Environment Series*. Antoniou, M.G., Zhao, Cen, O’Shea, K.E., Zhang, G., Dionysiou, D.D., Zhao, Chun, et al. (eds). Royal Society of Chemistry, pp. 1–34.
- Atashgahi, S., Hornung, B., van der Waals, M.J., da Rocha, U.N., Hugenholtz, F., Nijse, B., et al. (2018) A benzene-degrading nitrate-reducing microbial consortium displays aerobic and anaerobic benzene degradation pathways. *Sci Rep* 8: 4490.
- ATSDR (1995) TOXICOLOGICAL PROFILE FOR POLYCYCLIC AROMATIC HYDROCARBONS.
- Azam, F. and Malfatti, F. (2007) Microbial structuring of marine ecosystems. *Nat Rev Microbiol* 2007 510 5: 782–791.
- Bacosa, H.P., Erdner, D.L., and Liu, Z. (2015) Differentiating the roles of photooxidation and biodegradation in the weathering of Light Louisiana Sweet crude oil in surface water from the Deepwater Horizon site. *Mar Pollut Bull* 95: 265–272.
- Bagi, A., Pampanin, D.M., Brakstad, O.G., and Kommedal, R. (2013) Estimation of hydrocarbon biodegradation rates in marine environments: A critical review of the Q10 approach. *Mar Environ Res* 89: 83–90.
- Bagi, A., Pampanin, D.M., Lanzén, A., Bilstad, T., and Kommedal, R. (2014) Naphthalene biodegradation in temperate and arctic marine microcosms. *Biodegradation* 25: 111–125.
- Bar-On, Y.M., Phillips, R., and Milo, R. (2018) The biomass distribution on Earth. *Proc Natl Acad Sci* 201711842.
- Barron, M. (2012) Ecological impacts of the deepwater horizon oil spill: implications for immunotoxicity. *Toxicol Pathol* 40: 315–320.
- Baya, A.M., Brayton, P.R., Brown, V.L., Grimes, D.J., Russek-Cohen, E., and Colwell, R.R. (1986) Coincident plasmids and antimicrobial resistance in marine bacteria isolated from polluted and unpolluted Atlantic Ocean samples. *Appl Environ Microbiol* 51: 1285–1292.
- Bekki, K., Takigami, H., Suzuki, G., Tang, N., and Hayakawa, K. (2009) Evaluation of Toxic Activities of Polycyclic Aromatic Hydrocarbon Derivatives Using In Vitro Bioassays. *J Heal Sci* 55: 601–610.
- Berrojalbiz, N., Dachs, J., Ojeda, M.J., Valle, M.C., Castro-Jiménez, J., Wollgast, J., et al. (2011) Biogeochemical and physical controls on concentrations of polycyclic aromatic hydrocarbons in water and plankton of the Mediterranean and Black Seas. *Global Biogeochem Cycles* 25: .
- Berrojalbiz, N., Lacorte, S., Calbet, A., Saiz, E., Barata, C., and Dachs, J. (2009) Accumulation and Cycling of Polycyclic Aromatic Hydrocarbons in Zooplankton Accumulation and Cycling of Polycyclic Aromatic Hydrocarbons in Zooplankton. *Environ Sci Technol* 43: 2295–2301.
- Blanco, P., Hernando-Amado, S., Reales-Calderon, J.A., Corona, F., Lira, F., Alcalde-Rico, M., et al. (2016) Bacterial Multidrug Efflux Pumps: Much More Than Antibiotic Resistance Determinants. *Microorg* 2016, Vol 4, Page 14 4: 14.
- Bollmann, U.E., Möller, A., Xie, Z., Ebinghaus, R., and Einax, J.W. (2012) Occurrence and fate of organophosphorus flame retardants and plasticizers in coastal and marine surface waters. *Water Res* 46: 531–538.



- Brakstad, O.G., Davies, E.J., Ribicic, D., Winkler, A., Brønner, U., and Netzer, R. (2018) Biodegradation of dispersed oil in natural seawaters from Western Greenland and a Norwegian fjord. *Polar Biol* 41: 2435–2450.
- Brezna, B., Kweon, O., Stingley, R.L., Freeman, J.P., Khan, A.A., Polek, B., et al. (2006) Molecular characterization of cytochrome P450 genes in the polycyclic aromatic hydrocarbon degrading *Mycobacterium vanbaalenii* PYR-1. *Appl Microbiol Biotechnol* 71: 522–532.
- Buccini, J. (2003) The development of a global treaty on persistent organic pollutants (POPs). The Hand Book of Environmental Chemistry, Persistent Organic POLLutants, Fiedler H (Springer-Verlag, Berlin/Heidelberg).
- Buck, R.C., Franklin, J., Berger, U., Conder, J.M., Cousins, I.T., de Voogt, P., et al. (2011) Perfluoroalkyl and polyfluoroalkyl substances in the environment: terminology, classification, and origins. *Integr Environ Assess Manag* 7: 513–41.
- Cabrerizo, A., Galbán-Malagón, C., Del Vento, S., and Dachs, J. (2014) Sources and fate of polycyclic aromatic hydrocarbons in the Antarctic and Southern Ocean atmosphere. *Global Biogeochem Cycles* 28: 1424–1436.
- Cafaro, V., Izzo, V., Notomista, E., and Di Donato, A. (2013) Marine hydrocarbonoclastic bacteria. *Mar Enzym Biocatal Sources, Biocatal Charact Bioprocesses Mar Enzym* 373–402.
- Cai, Minggang, Liu, M., Hong, Q., Lin, J., Huang, P., Hong, J., et al. (2016) Fate of polycyclic aromatic hydrocarbons in seawater from the western Pacific to the Southern Ocean (17.5°N to 69.2°S) and their inventories on the antarctic shelf. *Environ Sci Technol* 50: 9161–9168.
- Callahan, B.J., McMurdie, P.J., Rosen, M.J., Han, A.W., Johnson, A.J.A., and Holmes, S.P. (2016) DADA2: High-resolution sample inference from Illumina amplicon data. *Nat Methods* 13: 581–583.
- Camilli, R., Reddy, C.M., Yoerger, D.R., Van Mooy, B.A.S., Jakuba, M. V., Kinsey, J.C., et al. (2010) Tracking hydrocarbon plume transport and biodegradation at deepwater horizon. *Science* (80- ) 330: 201–204.
- Carmona, M., Zamarro, M.T., Blazquez, B., Durante-Rodriguez, G., Juarez, J.F., Valderrama, J.A., et al. (2009) Anaerobic Catabolism of Aromatic Compounds: a Genetic and Genomic View. *Microbiol Mol Biol Rev* 73: 71–133.
- Carson, R. (1962) *Silent spring*.
- Casal, P., Cabrerizo, A., Vila-Costa, M., Pizarro, M., Jiménez, B., and Dachs, J. (2018) Pivotal Role of Snow Deposition and Melting Driving Fluxes of Polycyclic Aromatic Hydrocarbons at Coastal Livingston Island (Antarctica). *Environ Sci Technol* 52: 12327–12337.
- Casal, P., Casas, G., Vila-Costa, M., Cabrerizo, A., Pizarro, M., Jiménez, B., and Dachs, J. (2019) Snow amplification of persistent organic pollutants at coastal antarctica. *Environ Sci Technol* 53: 8872–8882.
- Casal, P., Zhang, Y., Martin, J.W., Pizarro, M., Jiménez, B., and Dachs, J. (2017) Role of Snow Deposition of Perfluoroalkylated Substances at Coastal Livingston Island (Maritime Antarctica). *Environ Sci Technol* 51: 8460–8470.
- Casas, G., Martinez-Varela, A., Roscales, J.L., Pizarro, M., Vila-Costa, M., Jimenez, B., and Dachs, J. (2020) Enrichment of Perfluoroalkyl Substances in the Surface Microlayer and Sea-Spray Aerosols in the Southern Ocean. *Environ Pollut* 267:.
- Casas, G., Martinez-Varela, A., Vila-Costa, M., Jiménez, B., and Dachs, J. (2021) Rain Amplification of Persistent Organic Pollutants. *Environ Sci Technol* 55: 12961–12972.
- Castro-Jiménez, J., Berrojalbiz, N., Pizarro, M., and Dachs, J. (2014) Organophosphate Ester (OPE) Flame Retardants and Plasticizers in the Open Mediterranean and Black Seas Atmosphere. *Environ Sci Technol* 48: 3203–3209.
- Cerniglia, C.E. (1992) Biodegradation of polycyclic aromatic hydrocarbons. *Biodegradation* 3: 351–368.
- Cerro-Gálvez, E., Dachs, J., Lundin, D., Fernández-Pinos, M.-C., Sebastián, M., and Vila-Costa, M. (2021) Responses of Coastal Marine Microbiomes Exposed to Anthropogenic Dissolved Organic Carbon. *Environ Sci Technol* 55: 9609–9621.
- Cerro-Gálvez, E., Roscales, J.L., Jiménez, B., Sala, M.M., Dachs, J., and Vila-Costa, M. (2020) Microbial responses to perfluoroalkyl substances and perfluorooctanesulfonate (PFOS) desulfurization in the Antarctic marine environment. *Water Res* 171:.
- Cerro-Gálvez, E., Casal, P., Lundin, D., Piña, B., Pinhassi, J., Dachs, J., and Vila-Costa, M. (2019) Microbial responses to anthropogenic dissolved organic carbon in the Arctic and Antarctic coastal seawaters. *Environ Microbiol* 21: 1466–1481.

Cherr, G.N., Fairbairn, E., and Whitehead, A. (2017) Impacts of Petroleum-Derived Pollutants on Fish Development. <https://doi.org/101146/annurev-animal-022516-022928> 5: 185–203.

Christiansen, C., Leipe, T., Witt, G., Christoffersen, P.L., and Lund-Hansen, L.C. (2013) Selected elements, PCBs, and PAHs in sediments of the North Sea—Baltic Sea transition zone: Sources and transport as derived from the distribution pattern. <http://dx.doi.org/101080/00167223200910649597> 109: 81–94.

Cincinelli, A., Stortini, A.M., Checchini, L., Martellini, T., Del Bubba, M., and Lepri, L. (2005) Enrichment of organic pollutants in the sea surface microlayer (SML) at Terra Nova Bay, Antarctica: Influence of SML on superficial snow composition. *J Environ Monit* 7: 1305–1312.

Cincinelli, A., Stortini, A.M., Perugini, M., Checchini, L., and Lepri, L. (2001) Organic pollutants in sea-surface microlayer and aerosol in the coastal environment of Leghorn-Tyrrhenian Sea.

Crisafi, F., Giuliano, L., Yakimov, M.M., Azzaro, M., and Denaro, R. (2016) Isolation and degradation potential of a cold-adapted oil/PAH-degrading marine bacterial consortium from Kongsfjorden (Arctic region). *Rend Lincei* 27: 261–270.

Curtosi, A., Pelletier, E., Vodopivec, C.L., and Mac Cormack, W.P. (2009) Distribution of PAHs in the water column, sediments and biota of potter cove, south Shetland Islands, antarctica. *Antarct Sci* 21: 329–339.

Dachs, J., Lohmann, R., Ockenden, W. end. A., Méjanelle, L., Eisenreich, S.J., and Jones, K.C. (2002) Oceanic Biogeochemical Controls. *Environ Sci Technol* 36: 4229–4237.

Dachs, J. and Méjanelle, L. (2010) Organic Pollutants in Coastal Waters, Sediments, and Biota: A Relevant Driver for Ecosystems During the Anthropocene? *Estuaries and Coasts* 33: 1–14.

Dombrowski, N., Donaho, J.A., Gutierrez, T., Seitz, K.W., Teske, A.P., and Baker, B.J. (2016a) Reconstructing metabolic pathways of hydrocarbon-degrading bacteria from the Deepwater Horizon oil spill. *Nat Microbiol* 1: 16057.

Dombrowski, N., Donaho, J.A., Gutierrez, T., Seitz, K.W., Teske, A.P., and Baker, B.J. (2016b) Reconstructing metabolic pathways of hydrocarbon-degrading bacteria from the Deepwater Horizon oil spill. *Nat Microbiol* 1: 16057.

Dreyer, A., Weinberg, I., Temme, C., and Ebinghaus, R. (2009) Polyfluorinated Compounds in the Atmosphere of the Atlantic and Southern Oceans: Evidence for a Global Distribution. *Environ Sci Technol* 43: 6507–6514.

Dubinsky, E.A., Conrad, M.E., Chakraborty, R., Bill, M., Borglin, S.E., Hollibaugh, J.T., et al. (2013) Succession of Hydrocarbon-Degrading Bacteria in the Aftermath of the Deepwater Horizon Oil Spill in the Gulf of Mexico. *Environ Sci Technol* 47: 10860–10867.

Duran, R. and Cravo-Laureau, C. (2016) Role of environmental factors and microorganisms in determining the fate of polycyclic aromatic hydrocarbons in the marine environment. *FEMS Microbiol Rev* 40: 814–830.

Echeveste, P., Agustí, S., and Dachs, J. (2010) Cell size dependent toxicity thresholds of polycyclic aromatic hydrocarbons to natural and cultured phytoplankton populations. *Environ Pollut* 158: 299–307.

Echeveste, P., Galbán-Malagón, C., Dachs, J., Berrojalbiz, N., and Agustí, S. (2016) Toxicity of natural mixtures of organic pollutants in temperate and polar marine phytoplankton. *Sci Total Environ* 571: 34–41.

Eddy, S.R. and Wheeler, T.J. (2015) HMMER User's Guide Biological sequence analysis using profile hidden Markov models.

El-Naggar, N.A., Emara, H.I., Moawad, M.N., Soliman, Y.A., and El-Sayed, A.A.M. (2018) Detection of polycyclic aromatic hydrocarbons along Alexandria's coastal water, Egyptian Mediterranean Sea. *Egypt J Aquat Res* 44: 9–14.

Escher, B.I., Eggen, R.I.L., Schreiber, U., Schreiber, Z., Vye, E., Wisner, B., and Schwarzenbach, R.P. (2002) Baseline toxicity (narcosis) of organic chemicals determined by in vitro membrane potential measurements in energy-transducing membranes. *Environ Sci Technol* 36: 1971–1979.

Falcioni, T., Papa, S., and Gasol, J.M. (2008) Evaluating the flow-cytometric nucleic acid double-staining protocol in realistic situations of planktonic bacterial death. *Appl Environ Microbiol* 74: 1767–1779.

Fernández-Pinos, M.-C., Vila-Costa, M., Arrieta, J.M., Morales, L., González-Gaya, B., Piña, B., and Dachs, J. (2017) Dysregulation of photosynthetic genes in oceanic *Prochlorococcus* populations exposed to organic pollutants. *Sci Rep* 7:.

Ferraro, D.J., Okerlund, A.L., Mowers, J.C., and Ramaswamy, S. (2006) Structural basis for regioselectivity and stereoselectivity of product formation by naphthalene 1,2-dioxygenase. *J Bacteriol* 188: 6986–6994.

Foght, J. (2008) Anaerobic biodegradation of aromatic hydrocarbons: Pathways and prospects. *J Mol Microbiol Biotechnol* 15: 93–120.

Friedman, C.L. and Selin, N.E. (2012) Long-range atmospheric transport of polycyclic aromatic hydrocarbons: A global 3-D model analysis including evaluation of arctic sources. *Environ Sci Technol* 46: 9501–9510.

Fuoco, R., Giannarelli, S., Wei, Y., Abete, C., Francesconi, S., and Termine, M. (2005) Polychlorobiphenyls and polycyclic aromatic hydrocarbons in the sea-surface micro-layer and the water column at Gerlache Inlet, Antarctica. *J Environ Monit* 7: 1313.

Galbán-Malagón, C., Berrojalbiz, N., Ojeda, M.-J., and Dachs, J. (2012a) The oceanic biological pump modulates the atmospheric transport of persistent organic pollutants to the Arctic. *Nat Commun* 3: 862.

Galbán-Malagón, C., Berrojalbiz, N., Ojeda, M.-J., and Dachs, J. (2012b) The oceanic biological pump modulates the atmospheric transport of persistent organic pollutants to the Arctic. *Nat Commun* 3: 862.

Gallego, S., Vila, J., Tauler, M., Springael, D., and Grifoll, M. (2014) Community structure and PAH ring-hydroxylating dioxygenase genes of a marine pyrene-degrading microbial consortium. 543–556.

Garneau, M.É., Michel, C., Meisterhans, G., Fortin, N., King, T.L., Greer, C.W., and Lee, K. (2016) Hydrocarbon biodegradation by Arctic sea-ice and sub-ice microbial communities during microcosm experiments, Northwest Passage (Nunavut, Canada). *FEMS Microbiol Ecol* 92:.

Gerba, C.P. (2019) Chapter 28 - Environmental Toxicology. In *Environmental and Pollution Science (Third Edition)*. Elsevier Inc., pp. 511–540.

Ghosal, D., Dutta, A., Chakraborty, J., Basu, S., and Dutta, T.K. (2013) Characterization of the metabolic pathway involved in assimilation of acenaphthene in *Acinetobacter* sp. strain AGAT-W. *Res Microbiol* 164: 155–163.

Ghosal, D., Ghosh, S., Dutta, T.K., and Ahn, Y. (2016) Current state of knowledge in microbial degradation of polycyclic aromatic hydrocarbons (PAHs): A review. *Front Microbiol* 7:.

Gifford, S.M., Sharma, S., Booth, M., and Moran, M.A. (2013) Expression patterns reveal niche diversification in a marine microbial assemblage. *ISME J* 7: 281–298.

Gilde, K. and Pinckney, J.L. (2012) Sublethal Effects of Crude Oil on the Community Structure of Estuarine Phytoplankton. *Estuaries and Coasts* 35: 853–861.

Gillings, M.R. (2013) Evolutionary consequences of antibiotic use for the resistome, mobilome, and microbial pangenome. *Front Microbiol* 4:.

Gioia, R. and Dachs, J. (2012) The riverine input-output paradox for organic pollutants. *Front Ecol Environ* 10: 405–406.

Goerke, H., Weber, K., Bornemann, H., Ramdohr, S., and Plötz, J. (2004) Increasing levels and biomagnification of persistent organic pollutants (POPs) in Antarctic biota. *Mar Pollut Bull* 48: 295–302.

González-Gaya, B., Dachs, J., Roscales, J.L., Caballero, G., and Jiménez, B. (2014) Perfluoroalkylated Substances in the Global Tropical and Subtropical Surface Oceans. *Environ Sci Technol* 48: 13076–13084.

González-Gaya, B., Fernández-Pinos, M.-C., Morales, L., Méjanelle, L., Abad, E., Piña, B., et al. (2016) High atmosphere–ocean exchange of semivolatile aromatic hydrocarbons. *Nat Geosci* 9: 438–442.

Gonzalez-Gil, L., Carballa, M., and Lema, J.M. (2017) Cometabolic Enzymatic Transformation of Organic Micropollutants under Methanogenic Conditions. *Environ Sci Technol* 51: 2963–2971.

Gouin, T. and Wania, F. (2007) Time Trends of Arctic Contamination in Relation to Emission History and Chemical Persistence and Partitioning Properties. *Environ Sci Technol* 41: 5986–5992.

Grossart, H.P. (2010) Ecological consequences of bacterioplankton lifestyles: changes in concepts are needed. *Environ Microbiol Rep* 2: 706–714.

Guigue, C., Tedetti, M., Giorgi, S., and Goutx, M. (2011) Occurrence and distribution of hydrocarbons in the surface microlayer and subsurface water from the urban coastal marine area off Marseilles, Northwestern Mediterranean Sea. *Mar Pollut Bull* 62: 2741–2752.

Guitart, C., García-Flor, N., Bayona, J.M., and Albaigés, J. (2007a) Occurrence and fate of polycyclic aromatic hydrocarbons in the coastal surface microlayer. *Mar Pollut Bull* 54: 186–194.

Guitart, C., García-Flor, N., Bayona, J.M., and Albaigés, J. (2007b) Occurrence and fate of polycyclic aromatic hydrocarbons in the coastal surface microlayer. *Mar Pollut Bull* 54: 186–194.

Guitart, C., García-Flor, N., Miquel, J.C., Fowler, S.W., and Albaigés, J. (2010) Effect of the accumulation of polycyclic aromatic hydrocarbons in the sea surface microlayer on their coastal air-sea exchanges. *J Mar Syst*

79: 210–217.

Gutierrez, T., Berry, D., Yang, T., Mishamandani, S., McKay, L., Teske, A., and Aitken, M.D. (2013) Role of Bacterial Exopolysaccharides (EPS) in the Fate of the Oil Released during the Deepwater Horizon Oil Spill. *PLoS One* 8: :e67717.

Gutierrez, T., Morris, G., Ellis, D., Bowler, B., Jones, M., Salek, K., et al. (2018) Hydrocarbon-degradation and MOS-formation capabilities of the dominant bacteria enriched in sea surface oil slicks during the Deepwater Horizon oil spill. *Mar Pollut Bull* 135: 205–215.

Gutierrez, T., Singleton, D.R., Berry, D., Yang, T., Aitken, M.D., and Teske, A. (2013) Hydrocarbon-degrading bacteria enriched by the Deepwater Horizon oil spill identified by cultivation and DNA-SIP. *ISME J* 7: 2091–2104.

Hasse, L. (2009) Transport processes in the sea-surface microlayer. In *The Sea Surface and Global Change*. Cambridge University Press, pp. 93–120.

Hazen, T.C., Dubinsky, E.A., DeSantis, T.Z., Andersen, G.L., Piceno, Y.M., Singh, N., et al. (2010) Deep-sea oil plume enriches indigenous oil-degrading bacteria. *Science* (80- ) 330: 204–208.

Hazen, T.C., Prince, R.C., and Mahmoudi, N. (2016) Marine Oil Biodegradation. *Environ Sci Technol* 50: 2121–2129.

Head, I.M., Jones, D.M., and Röling, W.F.M. (2006) Marine microorganisms make a meal of oil. *Nat Rev Microbiol* 4: 173–182.

Hearn, E.M., Patel, D.R., and Berg, B. van den (2008) Outer-membrane transport of aromatic hydrocarbons as a first step in biodegradation. *Proc Natl Acad Sci* 105: 8601–8606.

Henner, P., Schiavon, M., Morel, J.-L., and Lichtfouse, E. (1997) Polycyclic aromatic hydrocarbon (PAH) occurrence and remediation methods Polycyclic aromatic hydrocarbons (PAH) occurrence and remediation methods. *Analisis, EDP Sci* 25: 56–59.

HJ, L., WJ, S., J, L., and GB, K. (2011) Temporal and geographical trends in the genotoxic effects of marine sediments after accidental oil spill on the blood cells of striped beakperch (*Oplegnathus fasciatus*). *Mar Pollut Bull* 62: 2264–2268.

Hunter, K.A. (2009) Chemistry of the sea-surface microlayer. In *The Sea Surface and Global Change*. Cambridge University Press, pp. 287–320.

Hutchins, D.A. and Fu, F. (2017) Microorganisms and ocean global change. *Nat Microbiol* 2:.

IPBES secretariat (2019) Global Assessment Report on Biodiversity and Ecosystem Services | IPBES secretariat, Bonn, Germany.

IPCC (2014) AR5 Synthesis Report: Climate Change .

Jacob, J. (2008) The significance of polycyclic aromatic hydrocarbons as environmental carcinogens. 35 years research on PAH-a retrospective. *Polycycl Aromat Compd* 28: 242–272.

Jamieson, A.J., Malkocs, T., Piertney, S.B., Fujii, T., and Zhang, Z. (2017) Bioaccumulation of persistent organic pollutants in the deepest ocean fauna. *Nat Ecol Evol* 2017 13 1: 1–4.

Janda, J.M. and Abbott, S.L. (2007) 16S rRNA Gene Sequencing for Bacterial Identification in the Diagnostic Laboratory: Pluses, Perils, and Pitfalls. *J Clin Microbiol* 45: 2761–2764.

Jiang, J.J., Lee, C.L., and Fang, M. Der (2014) Emerging organic contaminants in coastal waters: Anthropogenic impact, environmental release and ecological risk. *Mar Pollut Bull* 85: 391–399.

Jiao, N., Farooq, A., and Sean, S. (2011) Microbial Carbon Pump in the Ocean.

Jiao, N. and Zheng, Q. (2011) The Microbial Carbon Pump: from Genes to Ecosystems. *Appl Environ Microbiol* 77: 7439–7444.

Johnston, E.L., Mayer-Pinto, M., and Crowe, T.P. (2015) REVIEW: Chemical contaminant effects on marine ecosystem functioning. *J Appl Ecol* 52: 140–149.

Joye, S., Kleindienst, S., Gilbert, J., Handley, K., Weisenhorn, P., Overholt, W., and Kostka, J. (2016) Responses of Microbial Communities to Hydrocarbon Exposures. *Oceanography* 29: 136–149.

Jurado, E. and Dachs, J. (2008) Seasonality in the “grasshopping” and atmospheric residence times of persistent organic pollutants over the oceans.

Jurado, E., Jaward, F.M., Lohmann, R., Jones, K.C., Simó, R., and Dachs, J. (2004) Atmospheric dry deposition of persistent organic pollutants to the atlantic and inferences for the global oceans. *Environ Sci Technol* 38: 5505–5513.

- Kanally, R.A. and Harayama, S. (2010) Review article Advances in the field of high-molecular-weight polycyclic aromatic hydrocarbon biodegradation. 3: 136–164.
- Karthikeyan, S., Rodriguez-R, L.M., Heritier-Robbins, P., Hatt, J.K., Huettel, M., Kostka, J.E., and Konstantinidis, K.T. (2020) Genome repository of oil systems: An interactive and searchable database that expands the catalogued diversity of crude oil-associated microbes. *Environ Microbiol* 22: 2094–2106.
- Keith, L. and Telliard, W. (1979) ES&T Special Report: Priority pollutants: I-a perspective view. *Environ Sci Technol* 13: 416–423.
- King, G.M., Kostka, J.E., Hazen, T.C., and Sobocky, P.A. (2015) Microbial Responses to the Deepwater Horizon Oil Spill: From Coastal Wetlands to the Deep Sea. *Ann Rev Mar Sci* 7: 377–401.
- King, S.M., Leaf, P.A., Olson, A.C., Ray, P.Z., and Tarr, M.A. (2014) Photolytic and photocatalytic degradation of surface oil from the Deepwater Horizon spill. *Chemosphere* 95: 415–22.
- Kotthoff, L., Keller, J., Lörchner, D., Mekonnen, T.F., and Koch, M. (2019) Transformation Products of Organic Contaminants and Residues—Overview of Current Simulation Methods. *Molecules* 24:.
- Krasnobaev, A., Dam, G. ten, Boerrigter-Eenling, R., Peng, F., Leeuwen, S.P.J. van, Morley, S.A., et al. (2020) Legacy and Emerging Persistent Organic Pollutants in Antarctic Benthic Invertebrates near Rothera Point, Western Antarctic Peninsula. *Environ Sci Technol* 54: 2763–2771.
- Kweon, O., Kim, S.-J., Baek, S., Chae, J.-C., Adjei, M.D., Baek, D.-H., et al. (2008) A new classification system for bacterial Rieske non-heme iron aromatic ring-hydroxylating oxygenases. *BMC Biochem* 9: 11.
- Lacal, J., Reyes-Darias, J.A., García-Fontana, C., Ramos, J.L., and Krell, T. (2013) Tactic responses to pollutants and their potential to increase biodegradation efficiency. *J Appl Microbiol* 114: 923–933.
- Leahy, J.G. and Colwell, R.R. (1990) Microbial degradation of hydrocarbons in the environment. *Microbiol Rev* 54: 305–315.
- Leizeaga, A., Estrany, M., Forn, I., and Sebastián, M. (2017) Using Click-Chemistry for Visualizing in Situ Changes of Translational Activity in Planktonic Marine Bacteria. *Front Microbiol* 8:.
- Lekunberri, I., Balcázar, J.L., and Borrego, C.M. (2018) Metagenomic exploration reveals a marked change in the river resistome and mobilome after treated wastewater discharges. *Environ Pollut* 234: 538–542.
- Lenton, T.M., Held, H., Kriegler, E., Hall, J.W., Lucht, W., Rahmstorf, S., and Schellnhuber, H.J. (2008) Tipping elements in the Earth's climate system. *Proc Natl Acad Sci* 105: 1786–1793.
- Li, D., Luo, R., Liu, C., Leung, C., Ting, H., Sadakane, K., et al. (2016) MEGAHIT v1.0: A fast and scalable metagenome assembler driven by advanced methodologies and community practices. *Methods* 102: 3–11.
- Li, J., Xie, Z., Mi, W., Lai, S., Tian, C., Emeis, K.-C., and Ebinghaus, R. (2017) Organophosphate Esters in Air, Snow, and Seawater in the North Atlantic and the Arctic. *Environ Sci Technol* 51: 6887–6896.
- Liu, J. and Mejia Avendaño, S. (2013) Microbial degradation of polyfluoroalkyl chemicals in the environment: A review. *Environ Int* 61: 98–114.
- Lofthus, S., Bakke, I., Tremblay, J., Greer, C.W., and Brakstad, O.G. (2020) Biodegradation of weathered crude oil in seawater with frazil ice. *Mar Pollut Bull* 154: 111090.
- Lourenço, R.A., Taniguchi, S., da Silva, J., Gallotta, F.D.C., and Bicego, M.C. (2021) Polycyclic aromatic hydrocarbons in marine mammals: A review and synthesis. *Mar Pollut Bull* 171: 112699.
- Louvado, A., Gomes, N.C.M., Simões, M.M.Q., Almeida, A., Cleary, D.F.R., and Cunha, A. (2015) Polycyclic aromatic hydrocarbons in deep sea sediments: Microbe-pollutant interactions in a remote environment. *Sci Total Environ* 526: 312–328.
- Love, C.R., Arrington, E.C., Gosselin, K.M., Reddy, C.M., Van Mooy, B.A.S., Nelson, R.K., and Valentine, D.L. (2021) Microbial production and consumption of hydrocarbons in the global ocean. *Nat Microbiol* 2021 64 6: 489–498.
- Lozada, M., Marcos, M.S., Commendatore, M.G., Gil, M.N., and Dionisi, H.M. (2014) The bacterial community structure of hydrocarbon-polluted marine environments as the basis for the definition of an ecological index of hydrocarbon exposure. *Microbes Environ* 29: 269–76.
- Lutz, M.J., Caldeira, K., Dunbar, R.B., and Behrenfeld, M.J. (2007) Seasonal rhythms of net primary production and particulate organic carbon flux to depth describe the efficiency of biological pump in the global ocean. *J Geophys Res Ocean* 112: 10011.
- Mallick, S., Chakraborty, J., and Dutta, T.K. (2011) Role of oxygenases in guiding diverse metabolic pathways in the bacterial degradation of low-molecular-weight polycyclic aromatic hydrocarbons : A review Role

of oxygenases in guiding diverse metabolic pathways in the bacterial degradation of low-molecular weight compounds. *Environ Microbiol* 7: 7828.

Martinez, J.L., Sánchez, M.B., Martínez-Solano, L., Hernandez, A., Garmendia, L., Fajardo, A., and Alvarez-Ortega, C. (2009) Functional role of bacterial multidrug efflux pumps in microbial natural ecosystems. *FEMS Microbiol Rev* 33: 430–449.

Mason, O.U., Hazen, T.C., Borglin, S., Chain, P.S.G., Dubinsky, E.A., Fortney, J.L., et al. (2012) Metagenome, metatranscriptome and single-cell sequencing reveal microbial response to Deepwater Horizon oil spill. *ISME J* 6: 1715–1727.

Matilla, M.A. and Krell, T. (2017) Chemoreceptor-based signal sensing. *Curr Opin Biotechnol* 45: 8–14.

Matvyeyeva, O.L., Vasylychenko, O.A., and Aliieva, O.R. (2014) Microbial Biosurfactants Role in Oil Products Biodegradation. *Int J Environ Bioremediation Biodegrad* 2: 69–74.

McConnell, L.L., Dachs, J., Hapeman, C.J., and American Chemical Society. Division of Agrochemicals (2013) Occurrence, fate and impact of atmospheric pollutants on environmental and human health.

McFarlin, K.M., Perkins, M.J., Field, J.A., and Leigh, M.B. (2018) Biodegradation of crude oil and Corexit 9500 in Arctic seawater. *Front Microbiol* 9.

Montuori, P. and Triassi, M. (2012) Polycyclic aromatic hydrocarbons loads into the Mediterranean Sea: Estimate of Sarno River inputs. *Mar Pollut Bull* 64: 512–520.

Moran, M.A., Satinsky, B., Gifford, S.M., Luo, H., Rivers, A., Chan, L.K., et al. (2013) Sizing up metatranscriptomics. *ISME J* 7: 237–243.

Muir, D.C.G. and Howard, P.H. (2006) Are there other persistent organic pollutants? A challenge for environmental chemists. *Environ Sci Technol* 40: 7157–7166.

Nizzetto, L., Lohmann, R., Gioia, R., Jahnke, A., Temme, C., Dachs, J., et al. (2008) PAHs in air and seawater along a North-South Atlantic transect: trends, processes and possible sources. *Environ Sci Technol* 42: 1580–5.

Nojiri, H., Shintani, M., and Omori, T. (2004) Divergence of mobile genetic elements involved in the distribution of xenobiotic-catabolic capacity. *Appl Microbiol Biotechnol* 64: 154–174.

Nzila, A. (2013) Update on the cometabolism of organic pollutants by bacteria. *Environ Pollut* 178: 474–482.

Ortega, Á., Zhulin, I.B., and Krell, T. (2017) Sensory Repertoire of Bacterial Chemoreceptors. *Microbiol Mol Biol Rev* 81.

Parales, R.E. and Harwood, C.S. (2002) Bacterial chemotaxis to pollutants and plant-derived aromatic molecules. *Curr Opin Microbiol* 5: 266–273.

Parales, R.E., Ju, K.-S., Rollefson, J., and Ditty, J. (2008) Bioavailability, transport and chemotaxis of organic pollutants. *Microb Bioremediation Caister Ac*: 145–187.

Patowary, K., Patowary, R., Kalita, M.C., and Deka, S. (2017) Characterization of Biosurfactant Produced during Degradation of Hydrocarbons Using Crude Oil As Sole Source of Carbon. *Front Microbiol* 8: 279.

Peng, J.-J., Cai, C., Qiao, M., Li, H., and Zhu, Y.-G. (2010) Dynamic changes in functional gene copy numbers and microbial communities during degradation of pyrene in soils. *Environ Pollut* 158: 2872–2879.

Perfumo, A., Rudden, M., Marchant, R., and Banat, I.M. (2018) Biodiversity of Biosurfactants and Roles in Enhancing the (Bio)availability of Hydrophobic Substrates. *Cell Ecophysiol Microbe Hydrocarb Lipid Interact* 75–103.

Pignatello, J.J., Katz, B.G., and Li, H. (2010) Sources, Interactions, and Ecological Impacts of Organic Contaminants in Water, Soil, and Sediment: An Introduction to the Special Series. *J Environ Qual* 39: 1133–1138.

Poli, A., Finore, I., Romano, I., Gioiello, A., Lama, L., and Nicolaus, B. (2017) Microbial Diversity in Extreme Marine Habitats and Their Biomolecules. *Microorganisms* 5.

R Core Team (2019) R: A Language and Environment for Statistical Computing.

Reemtsma, T., Quintana, J.B., Rodil, R., Garcí'a-López, M., and Rodr'íguez, I. (2008) Organophosphorus flame retardants and plasticizers in water and air I. Occurrence and fate. *TrAC Trends Anal Chem* 27: 727–737.

Ribicic, D., Netzer, R., Winkler, A., and Brakstad, O.G. (2018) Microbial communities in seawater from an Arctic and a temperate Norwegian fjord and their potentials for biodegradation of chemically dispersed oil at low seawater temperatures. *Mar Pollut Bull* 129: 308–317.

Rockström, J., Steffen, W., Noone, K., Persson, Å., Chapin, F.S., Lambin, E.F., et al. (2009) A safe operating space for humanity. *Nature* 461: 472–475.

Rodriguez-R, L.M., Overholt, W.A., Hagan, C., Huettel, M., Kostka, J.E., and Konstantinidis, K.T. (2015) Microbial community successional patterns in beach sands impacted by the Deepwater Horizon oil spill. *ISME J* 9: 1928–1940.

Rodríguez-Salazar, J., Loza, A., Ornelas-Ocampo, K., Gutierrez-Rios, R.M., and Pardo-López, L. (2021) Bacteria From the Southern Gulf of Mexico: Baseline, Diversity, Hydrocarbon-Degrading Potential and Future Applications. *Front Mar Sci* 0: 232.

Romero, I.C., Judkins, H., and Vecchione, M. (2020) Temporal Variability of Polycyclic Aromatic Hydrocarbons in Deep-Sea Cephalopods of the Northern Gulf of Mexico. *Front Mar Sci* 0: 54.

Romero, I.C., Sutton, T., Carr, B., Quintana-Rizzo, E., Ross, S.W., Hollander, D.J., and Torres, J.J. (2018) Decadal Assessment of Polycyclic Aromatic Hydrocarbons in Mesopelagic Fishes from the Gulf of Mexico Reveals Exposure to Oil-Derived Sources. *Environ Sci Technol* 52: 10985–10996.

Scheringer, M., Salzmann, M., Stroebe, M., Wegmann, F., Fenner, K., and Hungerbühler, K. (2004) Long-range transport and global fractionation of POPs: insights from multimedia modeling studies. *Environ Pollut* 128: 177–188.

Seo, J.S., Keum, Y.S., and Li, Q.X. (2009) Bacterial degradation of aromatic compounds.

Sharkey, M., Harrad, S., Abou-Elwafa Abdallah, M., Drage, D.S., and Berresheim, H. (2020) Phasing-out of legacy brominated flame retardants: The UNEP Stockholm Convention and other legislative action worldwide. *Environ Int* 144: 106041.

Singh, B.K. and Walker, A. (2006) Microbial degradation of organophosphorus compounds. *FEMS Microbiol Rev* 30: 428–471.

Sobecky, P.A. and Hazen, T.H. (2009) Horizontal Gene Transfer and Mobile Genetic Elements in Marine Systems. *Methods Mol Biol* 532: 435–453.

Steffen, W., Crutzen, P.J., and McNeill, J.R. (2007) The Anthropocene: Are Humans Now Overwhelming the Great Forces of Nature. *AMBIO A J Hum Environ* 36: 614–621.

Steffen, W., Richardson, K., Rockström, J., Cornell, S.E., Fetzer, I., Bennett, E.M., et al. (2015) Planetary boundaries: Guiding human development on a changing planet. *Science* (80-) 347:.

Stortini, A.M., Martellini, T., Del Bubba, M., Lepri, L., Capodaglio, G., and Cincinelli, A. (2009) n-Alkanes, PAHs and surfactants in the sea surface microlayer and sea water samples of the Gerlache Inlet sea (Antarctica). *Microchem J* 92: 37–43.

Su, G., Letcher, R.J., and Yu, H. (2016) Organophosphate Flame Retardants and Plasticizers in Aqueous Solution: pH-Dependent Hydrolysis, Kinetics, and Pathways. *Environ Sci Technol* 50: 8103–8111.

Sunagawa, S., Coelho, L.P., Chaffron, S., Kultima, J.R., Labadie, K., Salazar, G., et al. (2015) Ocean plankton. Structure and function of the global ocean microbiome. *Science* 348: 1261359.

Takahashi, S., Abe, K., and Ker, Y. (2013) Microbial Degradation of Persistent Organophosphorus Flame Retardants. In *Environmental Biotechnology - New Approaches and Prospective Applications*. InTech.

Teramoto, M., Queck, S.Y., and Ohnishi, K. (2013) Specialized Hydrocarbonoclastic Bacteria Prevailing in Seawater around a Port in the Strait of Malacca. *PLoS One* 8: e66594.

Top, E.M., Springael, D., and Boon, N. (2002) Catabolic mobile genetic elements and their potential use in bioaugmentation of polluted soils and waters. *FEMS Microbiol Ecol* 42: 199–208.

United Nations Environmental Programme (2009) SC-4 / 17 : Listing of perfluorooctane sulfonic acid , its salts and perfluorooctane sulfonyl fluoride.

Van Der Veen, I. and De Boer, J. (2012) Phosphorus flame retardants: Properties, production, environmental occurrence, toxicity and analysis. *Chemosphere* 88: 1119–1153.

Vergeynst, L., Christensen, J.H., Kjeldsen, K.U., Meire, L., Boone, W., Malmquist, L.M.V., and Rysgaard, S. (2019) In situ biodegradation, photooxidation and dissolution of petroleum compounds in Arctic seawater and sea ice. *Water Res* 148: 459–468.

Vila-Costa, M., Cerro-Gálvez, E., Martínez-Varela, A., Casas, G., and Dachs, J. (2020a) Anthropogenic dissolved organic carbon and marine microbiomes. *ISME J* 14: 2646–2648.

Vila-Costa, M., Cerro-Gálvez, E., Martínez-Varela, A., Casas, G., and Dachs, J. (2020b) Anthropogenic dissolved organic carbon and marine microbiomes. *ISME J* 14: 2646–2648.

Vila-Costa, M., Pinhassi, J., Alonso, C., Perenthaler, J., and Simó, R. (2007) An annual cycle of dimethylsulfoniopropionate-sulfur and leucine assimilating bacterioplankton in the coastal NW Mediterranean.

Vila-Costa, M., Sebastián, M., Pizarro, M., Cerro-Gálvez, E., Lundin, D., Gasol, J.M., and Dachs, J. (2019) Microbial consumption of organophosphate esters in seawater under phosphorus limited conditions. *Sci Rep* 9: 233.

Vila, J., Tauler, M., and Grifoll, M. (2015) Bacterial PAH degradation in marine and terrestrial habitats. *Curr Opin Biotechnol* 33: 95–102.

Wadhams, G.H. and Armitage, J.P. (2004) Making sense of it all: bacterial chemotaxis. *Nat Rev Mol Cell Biol* 5: 1024–1037.

Wang, W. and Shao, Z. (2013) Enzymes and genes involved in aerobic alkane degradation. *Front Microbiol* 4: 1–7.

Wang, W., Wang, L., and Shao, Z. (2018) Polycyclic aromatic hydrocarbon (PAH) degradation pathways of the obligate marine PAH degrader *Cycloclasticus* sp. strain P1. *Appl Environ Microbiol* 84:.

Wang, Y., Hatt, J.K., Tsementzi, D., Rodriguez-R, L.M., Ruiz-Pérez, C.A., Weigand, M.R., et al. (2017) Quantifying the importance of the rare biosphere for microbial community response to organic pollutants in a freshwater ecosystem. *Appl Environ Microbiol* 83:.

Wang, Yuanqi, Hatt, J.K., Tsementzi, D., Rodriguez-R, L.M., Ruiz-Pérez, C.A., Weigand, M.R., et al. (2017) Quantifying the importance of the rare biosphere for microbial community response to organic pollutants in a freshwater ecosystem. *Appl Environ Microbiol* 83:.

Wang, Z., Walker, G.W., Muir, D.C.G., and Nagatani-Yoshida, K. (2020) Toward a Global Understanding of Chemical Pollution: A First Comprehensive Analysis of National and Regional Chemical Inventories. *Environ Sci Technol*.

Wania, F. (2007) A Global Mass Balance Analysis of the Source of Perfluorocarboxylic Acids in the Arctic Ocean. *Environ Sci Technol* 41: 4529–4535.

Wania, F. and Mackay, D. (1996) Tracking the Distribution of Persistent Organic Pollutants.

Waters, C.N., Zalasiewicz, J., Summerhayes, C., Barnosky, A.D., Poirier, C., Gałuszka, A., et al. (2016) The Anthropocene is functionally and stratigraphically distinct from the Holocene. *Science* (80- ) 351:.

Van Wezel, A.P. and Opperhuizen, A. (1995) Narcosis due to environmental pollutants in aquatic organisms: Residue-based toxicity, mechanisms, and membrane burdens. *Crit Rev Toxicol* 25: 255–279.

Wright, M.S., Baker-Austin, C., Lindell, A.H., Stepanauskas, R., Stokes, H.W., and McArthur, J.V. (2008) Influence of industrial contamination on mobile genetic elements: class 1 integron abundance and gene cassette structure in aquatic bacterial communities. *ISME J* 2008 24 2: 417–428.

Wurl, O. and Obbard, J.P. (2004) A review of pollutants in the sea-surface microlayer (SML): A unique habitat for marine organisms. *Mar Pollut Bull* 48: 1016–1030.

Yakimov, M.M., Bargiela, R., and Golyshin, P.N. (2021) Calm and Frenzy: marine obligate hydrocarbonoclastic bacteria sustain ocean wellness. *Curr Opin Biotechnol* 73: 337–345.

Yakimov, M.M., Timmis, K.N., and Golyshin, P.N. (2007) Obligate oil-degrading marine bacteria.

Yamaguchi, H., Arisaka, H., Seki, M., Adachi, M., Kimura, K., and Tomaru, Y. (2016) Phosphotriesterase activity in marine bacteria of the genera *Phaeobacter*, *Ruegeria*, and *Thalassospira*. *Int Biodeterior Biodegrad* 115: 186–191.

Yamashita, N., Kannan, K., Taniyasu, S., Horii, Y., Petrick, G., and Gamo, T. (2005) A global survey of perfluorinated acids in oceans. *Mar Pollut Bull* 51: 658–668.

Yao, X., Tao, F., Zhang, K., Tang, H., and Xu, P. (2017) Multiple roles for two efflux pumps in the polycyclic aromatic hydrocarbon-degrading *Pseudomonas putida* strain B6-2 (DSM 28064). *Appl Environ Microbiol* 83:.

Yilmaz, P., Yarza, P., Rapp, J.Z., and Glöckner, F.O. (2016) Expanding the World of Marine Bacterial and Archaeal Clades. *Front Microbiol* 0: 1524.

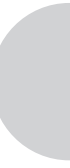
Yu, Z., Lin, Q., Gu, Y., Du, F., Wang, X., Shi, F., et al. (2019) Bioaccumulation of polycyclic aromatic hydrocarbons (PAHs) in wild marine fish from the coastal waters of the northern South China Sea: Risk assessment for human health. *Ecotoxicol Environ Saf* 180: 742–748.

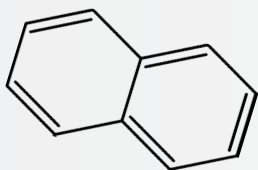
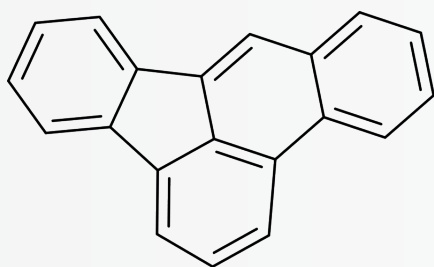
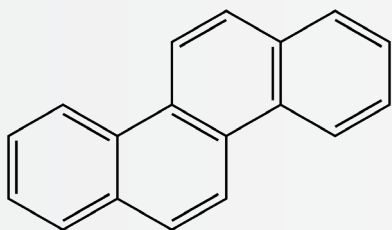
Yuan, J., Lai, Q., Sun, F., Zheng, T., and Shao, Z. (2015) The diversity of PAH-degrading bacteria in a deep-sea water column above the Southwest Indian Ridge. *Front Microbiol* 6:.

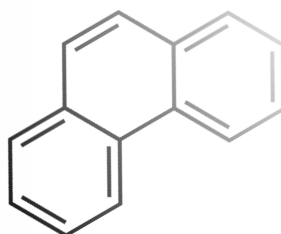
Zacharia, J.T. (2019) Degradation Pathways of Persistent Organic Pollutants (POPs) in the Environment. *Persistent Org Pollut*.

Zalasiewicz, J., Waters, C., and Williams, M. (2020) The Anthropocene. *Geol Time Scale* 2020 1257–1280.



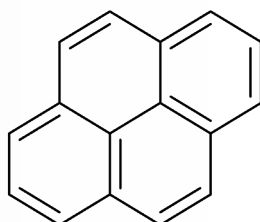






# PART II

## MAIN CHAPTERS





# 1

## **Biodegradation as an important sink of aromatic hydrocarbons in the oceans**

Belen González-Gaya, **Alicia Martínez-Varela**,  
Maria Vila-Costa, Paulo Casal, Elena Cerro-Gálvez,  
Naiara Berrojalbiz, Daniel Lundin, Montserrat Vidal,  
Carmen Mompeán, Antonio Bode,  
Begoña Jiménez and Jordi Dachs

Nature Geoscience, 2019

Atmospheric deposition of semivolatile aromatic hydrocarbons accounts for an important input of organic matter to the surface ocean. Nevertheless, the biogeochemical cycling and sinks of semivolatile aromatic hydrocarbons in the ocean remain largely uncharacterized. Here we present measurements of 64 polycyclic aromatic hydrocarbons in plankton and seawater from the Atlantic, Pacific, Indian and Southern Oceans, as well an assessment of their microbial degradation genes. Concentrations of the more hydrophobic compounds decreased when the plankton biomass was higher, consistent with the relevance of the biological pump. The mass balance for the global oceans showed that the settling fluxes of aromatic hydrocarbons in the water column were two orders of magnitude lower than the atmospheric deposition fluxes. This imbalance was high for low molecular weight hydrocarbons, such as phenanthrene and methylphenanthrenes, highly abundant in the dissolved phase. Parent polycyclic aromatic hydrocarbons were depleted to a higher degree than alkylated polycyclic aromatic hydrocarbons, and the degradation genes for polycyclic aromatic hydrocarbons were found to be ubiquitous in oceanic metagenomes. These observations point to a key role of biodegradation in depleting the bioavailable dissolved hydrocarbons and to the microbial degradation of atmospheric inputs of organic matter as a relevant process for the marine carbon cycle.

## INTRODUCTION

Polycyclic aromatic hydrocarbons (PAHs) and other semivolatile aromatic-like compounds (SALCs) are ubiquitous in the environment, and at relatively high concentrations and some of them cause carcinogenic and toxic effects to biota, being thus harmful for ecosystems (Zhang and Tao., 2009; Wilcke 2007; Reddy et al., 2012; Harvey 1991; Douben 2003; Hylland 2006; Fernandez-Pinos et al., 2017). PAH and SALCs enter the oceanic water column by atmospheric deposition (Gonzalez-gaya et al., 2016; Ferrington and Quinn, 2015; Ma et al., 2013; Castro-Jimenez et al., 2012). This diffuse but ubiquitous input of PAHs is quantitatively of larger magnitude than the direct inputs due to oil spills and natural seeps (Gonzalez-gaya et al., 2016; Castro-Jimenez et al., 2012). The atmospheric input of SALCs is also a relevant contribution of organic carbon to the oceans, and has been quantified as 400 Tg yr<sup>-1</sup>, equivalent to 15% of the global carbon input due to air–water diffusive CO<sub>2</sub> exchange (Gonzalez-gaya et al., 2016). The global fate of PAHs remains unquantified despite previous assessments in the marine environment (Ferrington and Takada, 2014; Dachs et al., 1996; Deyme et al., 2011; Halsall et al., 2001; Nizzeto et al., 2008; Lohmann et al., 2009; Lohmann et al., 2013; Dachs et al., 1997; Berrojalbiz et al., 2011), and the identification of the settling of organic-carbon-bound PAHs as a sink of PAHs (Dachs et al., 1996; Deyme et al., 2011; Bouloubassi et al., 2006; Adhikari et al., 2015).

Biological and photodegradation are other potential sinks of PAHs and SALCs in the photic zone (Dachs et al., 1997; Berrojalbiz et al., 2011; Head et al., 2006). The initial step in the biodegradation of PAH is commonly catalysed by ring hydroxylating dioxygenases (RHDs) (Mallick et al., 2011; Kimes et al., 2014), mostly characterized in naphthalene and phenanthrene degradation (Mallick et al., 2011; Cerniglia 1992; Peng et al., 2008, Seo et al., 2009), but with a broad range specificity to aromatic substrates (Moody et al., 2001; Iwai et al., 2011; Brezna et al., 2003; Kanaly and Harayama, 2010). Field studies have been limited exclusively to highly impacted seawater by oil spills (Maxon et al., 2012; Gallego et al., 2014; Dombrowski et al., 2016; Liu et al., 2017; Rivers et al., 2013), but not for airborne aromatic hydrocarbon degradation in the oceans.

The objectives of this work are (1) to report the largest data set available for PAH concentrations in the particulate phase (CP) and plankton (Cplankton) from the global oceans and (2) to elucidate the role of the biological pump and biodegradation as competing sinks of PAHs in the ocean.

## MATERIALS AND METHODS

### *Sampling strategy*

All samples were gathered during the Malaspina 2010 circumnavigation cruise between December 2010 and July 2011 on board of the Research Vessel Hespérides, and from coastal Livingston Island (South Shetland archipelago, Antarctica) between December 2014 and February 2015 (Figure 1 and Tables S1 and S2, SI). The Malaspina sampling campaign crossed the Atlantic, Pacific and Indian oceans between 35°N and 40°S, covering all the tropical and subtropical oceanic gyres (Figure 1). Water samples (n=69) were taken from the subsurface (4 m), using the continuous water sampling systems of the boat, during one-day long transects in alternate days (Table S1, SI). The mean volume was 239 L (ranging from 69 to 391 L). Particles were retained over pre-combusted GF/F filters (142 mm diameter, 0.7 µm pore size, Whatman). The hydrophobic pollutants in the dissolved phase were concentrated in XAD-2 resin placed on stainless columns after the filtration, and have been reported in a companion study.<sup>8</sup> Filters were kept at -20°C and XAD columns were kept refrigerated until their further treatment in the laboratory after the cruise. Plankton samples (n=71 for the Malaspina cruise and n=26 for Livingston Island) were gathered from vertical trawls with a 50 µm mesh size net. During the Malaspina cruise, samples were taken from 20 m deeper than the deep chlorophyll maximum depth (DCM) to surface (depths ranging from 20 to 160), and were immediately filtered (GF/D, 2.7 µm pore size, Whatman) and kept at -20°C until their analysis in the laboratory. At Livingston Island, the vertical trawl depth was of 14 and 30 m depth for the Johnsons and Raquelias sampling sites, respectively.

Concurrently with the surface particles and plankton, the dissolved, gas and aerosol phases were sampled and the diffusive fluxes, dry and wet deposition were measured during the Malaspina cruise and Antarctic campaign. The methods and results for the dissolved phase and the fluxes have been reported elsewhere (Gonzalez-Gaya et al., 2016), and are used in this work when needed. All together, they account for the largest available dataset of PAHs concentrations for the oceanic environment, comprising the concentrations of 64 individual PAHs in over 500 samples.

### *PAH analysis and quantification*

Particulate phase and plankton samples were analyzed following a slightly modified protocol (Berrojalbiz et al., 2011). Prior to the extraction, a mix of deuterated PAHs (Acenaphthene-D<sub>10</sub>, Phenanthrene-D<sub>10</sub>, Chrysene-D<sub>12</sub>, and Perylene-D<sub>12</sub>) was added as recovery standard. Filters containing the particulate and plankton samples were freeze-dried and Soxhlet extracted overnight with a mixture of dichloromethane and methanol (DCIM:MeOH 2:1) and DCIM:Hexane (1:1), respectively. Particulate phase samples were



further purified and fractionated on an alumina column. Plankton samples were purified and fractionated on a combined silica and alumina column. Further details are provided in Supplementary Text 1.

The aromatic fractions underwent the instrumental analysis for 64 individual PAHs on an Agilent 6890 Series gas chromatograph coupled with a mass spectrometer Agilent 5973 (GS-MS) operating in selected ion monitoring (SIM) and electron impact mode as described elsewhere (Gonzalez-Gaya et al., 2016). The quantification followed the internal standard procedure, using a mix of labelled standards Anthracene-D<sub>10</sub>, Pyrene-D<sub>10</sub>, P-therpenyl-D<sub>14</sub> and Benzo[b]fluoranthene-D<sub>12</sub> added to the samples prior to injection.

The 64 target PAHs identified and quantified were: naphthalene, methyl-naphthalenes (sum of 2 isomers), dimethyl-naphthalenes (sum of 6 isomers), acenaphthylene, acenaphthene, fluorene, dibenzothiophene, methyl-dibenzothiophenes (sum of 3 isomers), dimethyl-dibenzothiophenes (sum of 5 isomers), phenanthrene, methyl-phenanthrenes (sum of 4 isomers), dimethyl-phenanthrenes (sum of 7 isomers), anthracene, fluoranthene, pyrene, methyl-pyrenes and methyl-fluoranthenes (sum of 5 isomers), dimethyl-pyrenes and dimethyl-fluoranthenes (sum of 8 isomers), benzo[g,h,i]fluoranthene, benzo[a]anthracene, chrysene, methyl-chrysenes (sum of 3 isomers), benzo[b+k]fluoranthene (sum of 2 isomers), benzo[e]pyrene, benzo[a]pyrene, perylene, indeno[1,2,3-cd]pyrene, dibenzo[a,h]anthracene, benzo[g,h,i]perylene. The 64 target PAHs are represented in tables and figures as 19 parental PAHs and 9 groups of alkylated PAHs.

### **Quality Assurance and Quality Control**

Particulate phase blanks (4 field blanks and 7 laboratory blanks) were concurrently extracted and analyzed with the field samples. The average total pg found per blank was always, at least, one order of magnitude lower than the PAHs measured at the field samples. The average sample recovery was 76% for Perylene-D<sub>12</sub>, for which all given concentrations have been its own surrogate recovery corrected (Supplementary Table S3). Nine field blanks (4 from the tropical oceans and 5 from Southern ocean) and 7 laboratory blanks were concurrently extracted and analyzed with the field plankton samples. The average total pg found per blank was as well one order of magnitude lower than the measured in field samples. Moreover, the efficiency of extraction of plankton samples was evaluated by doing a second extraction of five random samples, and between 81% and 100% of each single PAH was extracted in the first batch. Recoveries of the deuterated PAHs ranged between 25% for Acenaphthene-D<sub>10</sub> and 102% for Perylene-D<sub>12</sub>. All concentrations have been surrogate recovery corrected (Table S4, SI). The detection limit (DL) was set as the inferior limit of the calibration curve (0.02 ng for all compounds). The quantification limit (QL) corresponds to the mean blank level of each sample phase.

Organic Carbon in particles and plankton. The surface particulate organic carbon (POC) was measured during the Malaspina 2010 circumnavigation concurrently with the water phase sampling. Two to eight liters of seawater taken with a Niskin bottle from a depth of 3 m were filtered onto GF/F filters (0.7 μm pore size, Whatman), dried overnight (60°C) and kept frozen (-20°C) until further treatment. Previous to analysis, the filters were dried for 24 h at 60°C, exposed to HCl (35%) vapors to remove carbonates, and re-dried. Com-

bustion catalyzed with V2O5 was performed with an elemental analyzer (Carlo Erba 1108) and quantification of OC was done through gas chromatography coupled with a thermal conductivity detector (complete data set in Table S5, SI).

The spatial variability of biomass and stable isotopes in plankton size fractions was studied in concurrent samples to the plankton phase to determine nitrogen and carbon sources. Samples for isotopes analysis were collected by 40  $\mu\text{m}$  mesh size vertical tows along the upper 200 m of the water column. Sampling was always performed right after the plankton phase collection used for PAH analysis. Filtrate was separated into five size fractions (40 - 200, 200 - 500, 500 - 1000, 1000 - 2000 and 2000 - 5000  $\mu\text{m}$  mesh size) by filtration over nylon sieves and removing the large gelatinous organisms found. Aliquots for each size fraction were collected on glass-fiber filters, dried (60°C, 48 h) and stored in a desiccator. The determination of biomass (dry weight), carbon and nitrogen content and natural abundance of stable carbon and nitrogen isotopes was performed after the circumnavigation at the Servicios de Apoyo á Investigación (Universidade da Coruña, Spain). Isotope analysis was accomplished with an elemental analyzer (Carlo Erba CHNSO 1108) coupled to an isotope-ratio mass spectrometer (Finnigan Mat Delta Plus). Further analytical details can be consulted elsewhere (Mompeán et al., 2016; Morales et al., 2015) Total carbon and nitrogen data (computed as the sum of the biomass of all size fractions from 40 to 5000  $\mu\text{m}$ ), biomass-weighted average  $\delta^{13}\text{C}$  and  $\delta^{15}\text{N}$  values and estimated trophic position of the 500-1000 $\mu\text{m}$  size-class are included in Table S6 in the SI.

### **$C_p^*$ and PAHs biological pump fluxes calculations**

By assuming air-water-particle equilibria, it is possible to predict a  $C_p^*$  value (concentrations in particles equilibrated with the gas phase) from the measured CG by,

$$C_p^* = \frac{C_G K_{OC}}{H'} \quad [1]$$

where the organic carbon-water partition coefficients (KOC) were estimated as the ratio between the concentrations in the particulate and dissolved phases of the surface water, and  $H'$  is Henry's Law constant temperature and salinity corrected as explained elsewhere.<sup>8</sup> With these assumptions:

$$\frac{C_p^*}{C_p} = \frac{C_G}{C_W H'} = \frac{f_A}{f_W} \quad [2]$$

Biological pump calculations were done by using Siegel and coworker's global climatology of organic carbon export from the surface mixed layer ( $F_{OC}$ ) (Siegel 2014). The reported monthly averaged FOC during the sampling was used to estimate the organic matter flux ( $F_{OM'}$  assuming that it is 1.8 times  $F_{OC}$ ) (Dachs et al., 2002), due to phytoplankton ( $F_{Phyto}$ ) (gC

$\text{m}^2\text{day}^{-1}$ ) and to zooplankton associated pellets ( $F_{\text{fecal}}$  ( $\text{gC m}^{-2}\text{day}^{-1}$ )) separately (Table S11, SI). Therefore, the biological pump fluxes ( $F_{\text{Settling}}$  ( $\text{ng m}^{-2}\text{day}^{-1}$ )) are given by:

$$F_{\text{Settling}} = -F_{\text{OM}} C_{\text{plankton}} = -(F_{\text{phyto}} + F_{\text{fecal}}) C_{\text{plankton}} \quad [3]$$

where  $C_{\text{plankton}}$  ( $\text{ng g C}^{-1}$ ) is the concentration of PAHs measured in plankton normalized by organic carbon content. We assume that the concentrations in plankton are representative of the concentrations in phytoplankton and fecal pellets. For the Malaspina cruise, plankton biomass was correlated with net primary production ( $p < 0.01$ ). The calculated biological pump fluxes shape the biggest database reported for PAHs at a global scale and moreover, this is the first time that phytoplankton and fecal contribution to PAH settling fluxes are estimated separately.

However, the estimation method for the PAH fluxes associated with the biological pump may underestimate the settling flux of black-carbon-bound PAHs, especially for the high molecular weight PAHs abundant in aerosols. PAHs adsorbed on black carbon may not be bioavailable (Dachs et al., 2000) and thus not degraded in the water column. Furthermore, it is unlikely that the vertical tows with plankton nets captured completely the submicrometre black carbon particles. Finally, the biological pump fluxes for SALCs were estimated from the biological pump fluxes of PAHs and the ratio SALCs/PAHs measured for seawater. SALC fluxes in Figure 5 are given as carbon equivalents ( $\text{Tg C yr}^{-1}$ ) assuming 80% content of carbon.

### **Bioinformatics**

Hidden Markov Models (HMMs) are sensitive tools for the identification of protein and protein domain sequences. HMMs corresponding to the alpha ("Ring hydroxylating alpha subunit (catalytic domain)", PF00848) and beta ("Ring hydroxylating beta subunit", PF00866) subunits of the RHD multicomponent complex were downloaded from Pfam (Finn et al., 2015). Similarly, HMMs corresponding to 40 single-copy marker genes were downloaded from the specl website (Mende et al., 2013). The HMMs were used to search all protein sequences from metagenomes from the Tara Oceans expedition (2009-2013) (Pesant et al., 2015) using HMMER (Eddy, 2011) with score thresholds built into the Pfam profiles (20.20 and 20.50 respectively for PF00848 and PF00866) and 20 for the specl single-copy HMMs. The identified proteins were subsequently quantified in surface and DCM samples of the free-living bacterial fraction (cells collected on an  $0.22 \mu\text{m}$  filter after pre-filtration through a  $3 \mu\text{m}$  filter). The abundances of alpha and beta RHD subunits were normalized by division with the mean abundance of the 40 single-copy genes (Mano and Borenstein, 2015)

### **Statistical analysis**

Statistical analysis was performed using SPSS Statistics (21.0 IBM Corp.). Kolmogorov–Smirnov tests were run to assure normality of the data, which was found for most compounds (24 and 20 out of 28 in the water and particulate phases, respectively) ( $P >$

0.05). PAH concentrations in the plankton were not normally distributed. Nevertheless, a logarithmic transformation of the data gave a statistically normalized distribution ( $P > 0.05$ ). Parametric statistics were thus applied for the comparisons and correlations within the data set. We used analysis of variance, paired t-tests and linear correlations for interoceanic basins and between-matrix comparisons, and analysis of variance and Tukey's HSD post hoc test to determine whether the relative abundances of alpha and beta subunits exhibited a significant variation between layers and between basins.

## RESULTS AND DISCUSSION

### ***PAH concentrations in particles from surface waters***

The  $C_p$  of  $\Sigma_{64}$  PAHs ranged between 7.7 and 4,700 ng g dw<sup>-1</sup> (global mean 270 ng g dw<sup>-1</sup> (dw, dry weight)). The most abundant compounds were dibenzothiophene (DBT), naphthalene and phenanthrene and its methylated forms (Figs. 1 and 2 and Supplementary Table 8). These concentrations are in the range of those reported for the North and South Atlantic Ocean (Nizzeto et al., 2008; Lohmann et al., 2009; Lohmann et al., 2013), but lower than those reported for the Mediterranean Sea (Berrojalbiz et al., 2020). The relative abundance of individual PAHs in the different oceanic sub-basins was not significantly different (Supplementary Figure 1). However, the sum of the particle phase concentrations of all the PAHs was significantly higher ( $P < 0.05$ ) in the Indian Ocean than in the rest of the oceanic basins, which reflects the large dry deposition of aerosol-bound PAHs in this region (Gonzalez-Gaya et al., 2016), probably associated with higher black-carbon aerosol concentrations. The normalization of  $C_p$  (ng g C<sup>-1</sup>) by particulate organic carbon decreased the variability of  $C_p$  between regions near the continents and the open ocean (Supplementary Figure 2 and Supplementary Table 9).

As air–water diffusive exchange is the major input of PAHs for most 2–5 ring PAHs (Gonzalez-Gaya et al., 2016), it is reasonable that PAH concentrations in the particulate phase were influenced by the levels of PAHs in the gas phase. We predicted the surface seawater particle phase PAH concentrations ( $C_p^*$ ) assuming that the gas and dissolved phases were at equilibrium (Materials & Methods). The predicted  $C_p^*$  for individual PAHs were significantly correlated ( $P < 0.01$ ) with the measured  $C_p$  (Supplementary Figure 3), although predicted values were significantly higher than the measured  $C_p$  for most 2–4 ring PAHs. This is consistent with degradation and sinking depleting concentrations of most PAHs at surface at a faster rate than the atmospheric inputs Supplementary Text 2 and Supplementary Figure 3).

### ***PAH in oceanic plankton and the biological pump***

Phenanthrene and its methylated forms (methylphenanthrene and dimethylphenanthrene) were the most abundant PAHs in all the oceans (Figure 2, Supplementary Figure 4 and Supplementary Table 10). The plankton phase PAH profiles were similar to those found in the dissolved phase (Figure 2) with a high predominance of low molecular weight PAHs and a low abundance of high molecular weight PAHs. The ratios of parent

to methylated PAHs were lower in the plankton samples than in the dissolved phase. The relative abundances of the individual PAHs were not significantly different among the oceanic sub-basins (Supplementary Figure 5), and the diagnostic ratios (Supplementary Figure 6) suggested a mixture of pyrolytic and petrogenic sources. There was a remarkable variability in PAH plankton concentrations, with the highest in the proximities of the Brazilian and West African coasts (Figure 1 and Supplementary Table 10) and the lowest concentrations in the Indian and Southern Oceans, as well as large regions of the Pacific Ocean. No statistical correlation was found between  $C_{\text{plankton}}$  and  $\delta^{15}\text{N}$ , which suggests that the trophic level of plankton (from 1.2 to 1.9 (Supplementary Table 6)) did not influence significantly the occurrence of PAHs.  $C_{\text{plankton}}$  for the ocean reported here are generally between one and two orders of magnitude lower than those in the Mediterranean Sea (Berrojalbiz et al., 2011). The biological pump fluxes of PAHs associated with settling particles were calculated for all the sampling stations and targeted PAHs (Supplementary Figure 7 and Supplementary Table 11) by multiplying the organic carbon normalized  $C_{\text{plankton}}$  by the vertical settling fluxes of organic carbon reported previously in an oceanic climatology (Siegel, 2014) (Supplementary Table 7). The average settling flux for the  $\Sigma$  64PAHs was  $82.5 \text{ ng m}^{-2} \text{ day}^{-1}$ , with the maximum fluxes in the eastern part of the North Atlantic basin and near South African coasts (Supplementary Figure 7). Sinking fluxes reported for the Mediterranean Sea (Ma et al., 2013; Dachs et al., 1996; Deyme, 2011; Tsapakis et al., 2006) are comparable to the highest rates reported here for the open ocean.

Settling fluxes are an effective mechanism for the sequestration of the more hydrophobic organic compounds (higher  $K_{\text{ow}}$ ) (Berrojalbiz et al., 2011; Galbán-Malagón et al., 2012). The biological pump flux of settling organic-matter-bound PAHs reduces their water column concentrations, as these cannot be replenished by diffusive air–water exchange (Galbán-Malagón et al., 2012). This process is reflected in the plankton phase concentrations of the more hydrophobic PAHs, which decreased at sites with a higher plankton biomass (B) following a power law (Figure 3, top panel). The more hydrophobic PAHs (higher  $K_{\text{ow}}$ ) corresponded to higher slopes for the correlations between  $C_{\text{plankton}}$  and B (Supplementary Table 12), consistent with a higher export at a higher biomass and especially affecting the more hydrophobic compounds.

### **Mass balance of PAHs in the surface ocean**

Atmospheric deposition is the main input of most PAHs to the open ocean and accounts for an input of  $1.09 \text{ Tg yr}^{-1}$ , as quantified in a companion work (Gonzalez-Gaya et al., 2016). The settling flux of  $\Sigma$  64PAHs due to the biological pump integrated for the Atlantic, Pacific and Indian Oceans was of  $0.008 \text{ Tg yr}^{-1}$  (Figure 4). The global atmospheric deposition and settling flux of PAHs may be higher than these figures because upwelling zones near continental margins and the Arctic and Southern Oceans have not been accounted. The integrated sinking flux of the biological pump was two orders of magnitude lower than the sum of the atmospheric inputs of PAHs through air–water diffusive exchange and dry deposition (Figure 4). Similar imbalances were reported for the Mediterranean and Black Seas (Tsapakis et al., 2006; Ma et al., 2013). This imbalance was

maximum for the more abundant dissolved phase PAHs, such as phenanthrene and its methyl derivatives (Supplementary Figure 8), and decreased as the hydrophobicity of the PAH increased (higher  $K_{ow}$ ). The fact that 99% of the atmospheric inputs of PAHs do not settle to the deep ocean suggests that degradation is a key process that drives the fate of PAHs in the photic zone of the ocean. High molecular weight PAHs may not be available for degradation due to the strong sorption to organic carbon, and especially atmospherically deposited black carbon (Dachs & Eisenreich, 2000). Photodegradation induces a selective decrease of some PAHs. For example, benzo[a]pyrene is more reactive than benzo[e]pyrene. The benzo[a]pyrene/benzo[e]pyrene ratio in the dissolved phase was lower (median 0.5) than in the gas phase (median 1) with significant differences ( $P < 0.5$ ), which

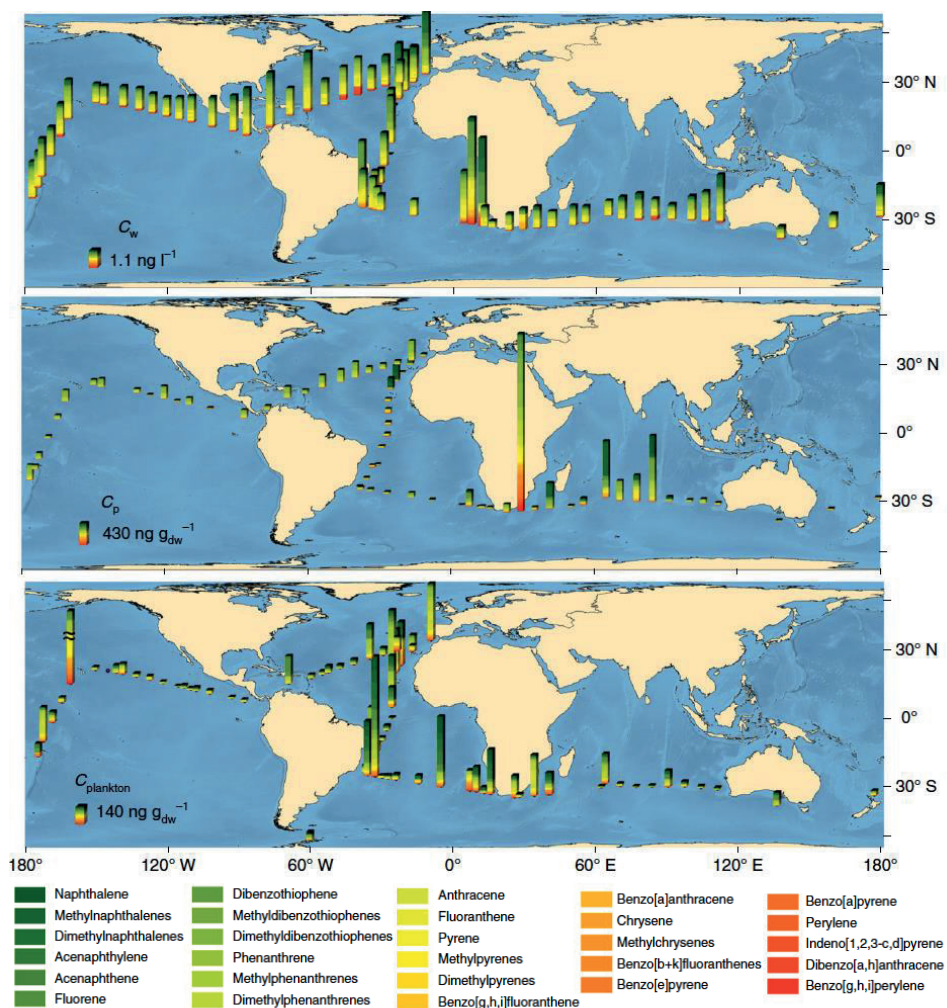


**FIGURE 1** | Global distribution of PAHs in the oceans. PAH concentration in the dissolved phase (upper panel), particulate phase (middle panel) and plankton (bottom panel). The column marked sample with a '≈' is reduced tenfold to adjust the bar size. The numbers in the scale of each panel correspond to the sum concentrations for the 64 targeted PAHs.

suggests photodegradation of PAHs close to the air–water interface. Conversely, the benzo[a]pyrene/benzo[e]pyrene ratios in plankton samples (median 0.6), which reflect the concentrations in deeper water (Methods), were not significantly lower than those in the dissolved phase at the surface, which suggests a lack of direct photodegradation at deeper waters. In plankton samples, the ratios phenanthrene/(methylphenanthrene + dimethylphenanthrene), DBT/(methyl-DBT + dimethyl-DBT) and pyrene/(methylpyrene + dimethylpyrene) were significantly lower ( $P < 0.05$ ) than in the dissolved phase. These differences suggest that microbial degradation dominates photodegradation for the top 200 m of the water column, as biodegradation is faster for parent PAHs (Bagby et al., 2017), and direct photodegradation is faster for alkylated PAHs (Radović et al., 2014). Furthermore, the three ratios in plankton showed significant correlations among them, consistent with a unique driver (biodegradation). Indirect photodegradation could not be estimated. Whereas the PAH-degrading capacity of microorganisms has been studied in marine isolates, quantification in the field-based experiments has been hampered by the relatively large half-life of these compounds, usually in the order of tens of days (Supplementary Text 2). For example, microcosm experiments performed during a Malaspina expedition (Methods) did not show a significant decrease of PAH concentrations after 24 hours of in situ incubation with native microbial cultures (Fernandez-Pinós et al., 2017), probably because such a short time period cannot induce a measurable reduction of PAH concentrations. The field-derived mass balance performed here integrates longer time periods, which provides an appropriate approach to estimate the magnitude of the degradation of PAHs in the ocean.

### ***Microbial degradation of aromatic hydrocarbons***

The depletion of PAH concentrations by degradation is also reflected in the concentrations at different depths. Organic-carbon normalized  $\Sigma_{64}$  PAH concentrations in surface particulates ranged from 1,100 ng g C<sup>-1</sup> to 210,000 ng g C<sup>-1</sup>, higher than those in plankton (which ranged from 16 to 13,000 ng g C<sup>-1</sup>), which integrate the photic water column. Furthermore, organic-carbon-normalized  $C_p$  values were not correlated with organic-carbon-normalized  $C_{\text{plankton}}$ . This suggests that higher organic-carbon-normalized concentrations are supported at surface due to atmospheric deposition inputs and heavy fuel sources, as reflected by the high abundances of sulfur-containing PAHs (DBT and methyl-DBTs) and 2-methylantracene (Supplementary Figure 9), but concentrations are reduced at depth due to biodegradation. Concentrations in plankton for the tropical/sub-tropical oceans and the Southern Ocean also showed relatively more pronounced decreasing concentrations at a high plankton biomass for the less hydrophobic compounds (Figure 3).

The plankton biomass was significantly correlated with the water column bacterial abundance ( $P < 0.01$ ). Microbial degradation is a plausible process that favours the faster decrease of low molecular weight PAHs with increasing biomass (Figure 3). This is consistent with other observations of the microbial consumption of PAHs with 2–4 rings (Berojalbiz et al., 2009, 2011; Bagby et al., 2017). Furthermore, the reported degradation

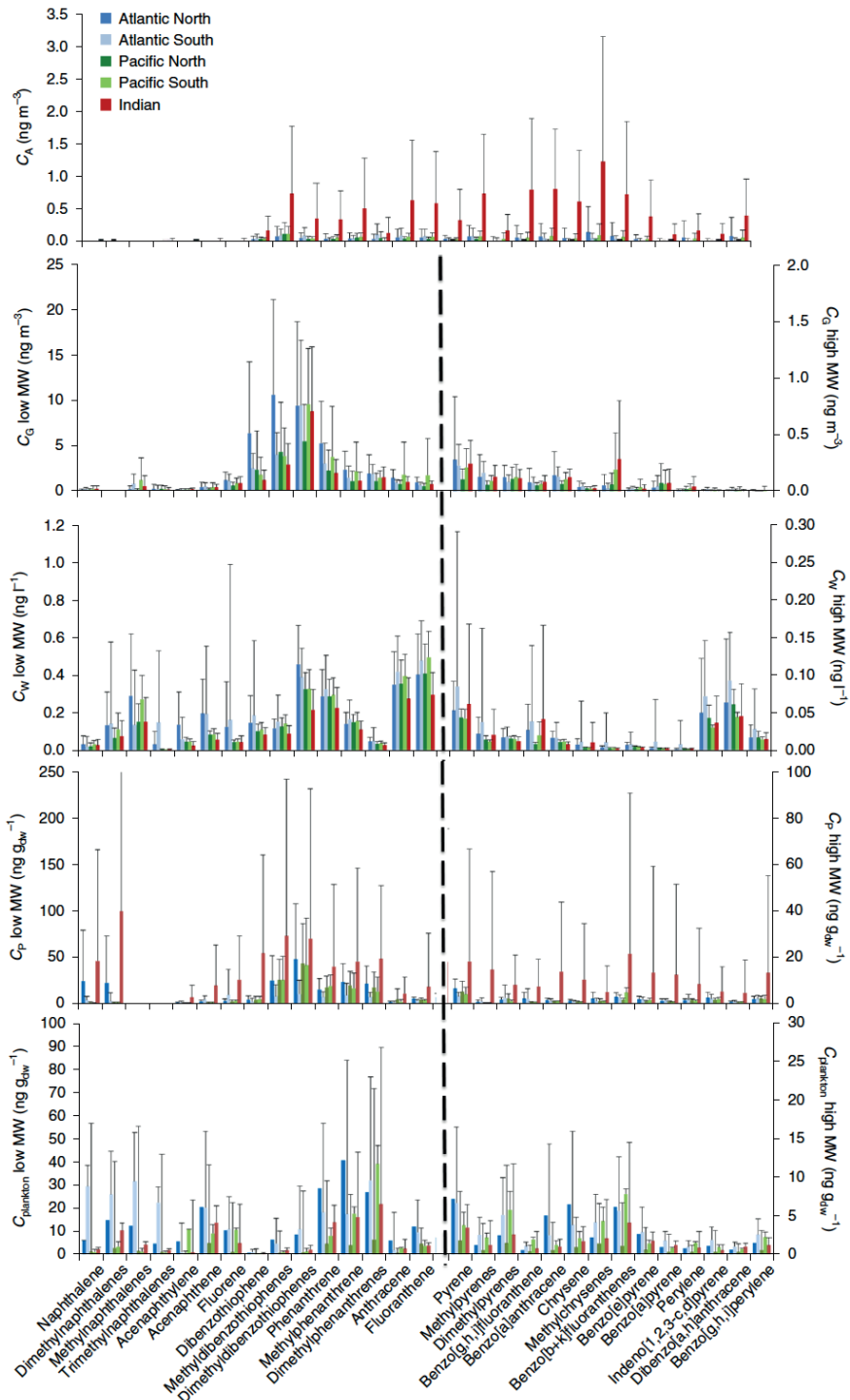


**FIGURE 2** | PAH profiles in the oceans. Mean concentrations and s.d. of PAHs in the aerosol (CA), gas (CG), dissolved (CW), CP and Cplankton phases for the different oceanic basins. MW, molecular weight.



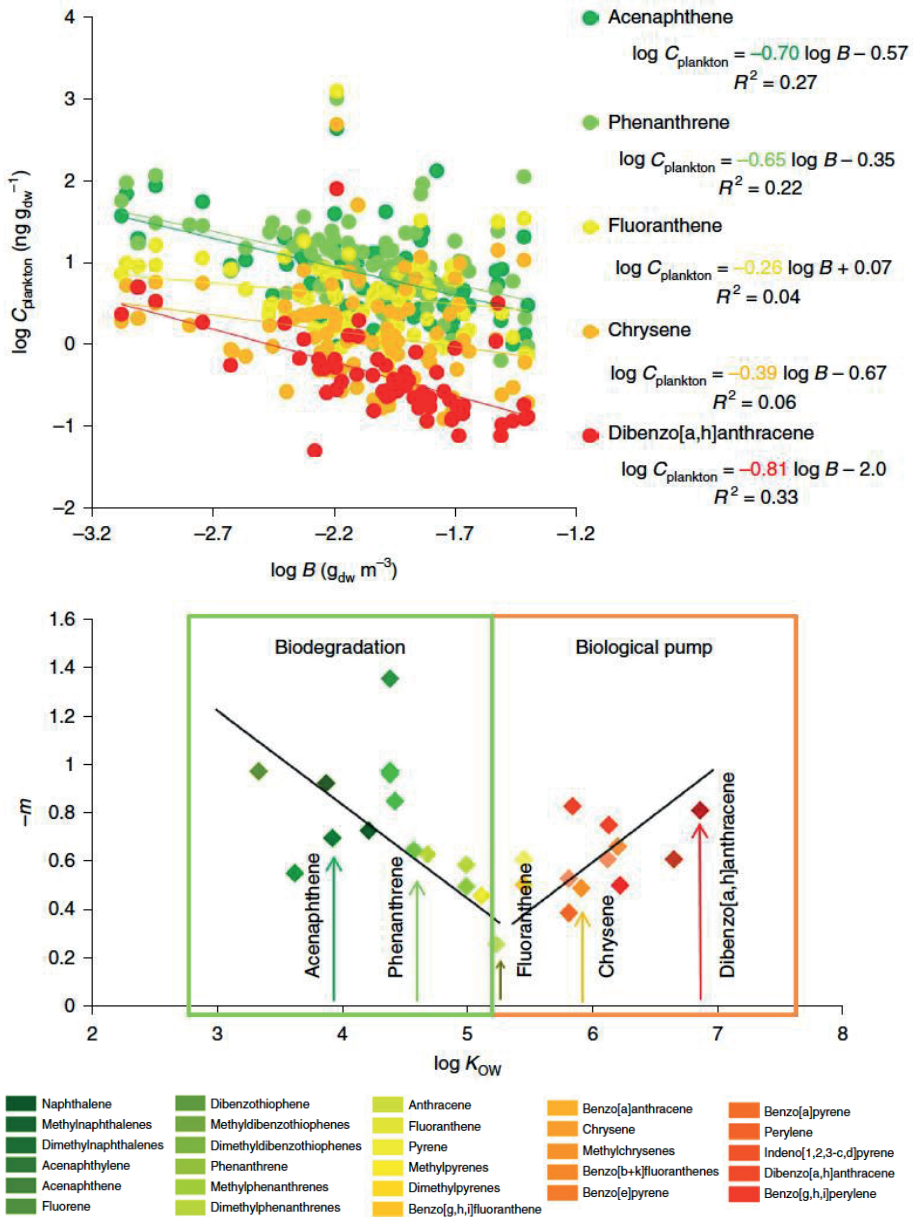


**FIGURE 3** | Cplankton relationships with biomass (B) and the fitted slope versus KOW.  $C_{\text{plankton}}$  for the Pacific, Atlantic, Indian and Southern Oceans versus B fitted to a power law ( $\log C_{\text{plankton}} = m \log B + a$ ) (top panel). Slopes (m) from the relationship between PAH concentrations in plankton and biomass versus KOW of the individual compounds (bottom panel).

kinetics of such PAHs is not only faster than their settling fluxes in the oligotrophic ocean, but also fast enough to induce a depletion of dissolved phase concentrations that drives an air–water diffusive flux of PAHs (Supplementary Text 2). The lower concentrations at high plankton biomass further suggest that photodegradation, even if it occurred, was of significantly lower magnitude than microbial degradation for the top 200 m. A large measured biomass from the plankton nets indicates a large zooplankton community. Zooplankton is known to have a degradation capability for low molecular weight PAHs (Berrojalbiz et al., 2009), and both zooplankton and bacteria can contribute to the biodegradation of PAHs. Note that the correlations shown in Figure 3 were derived from the concentrations from all oceans, and thus, biodegradation and the biological pump are major drivers of the fate of PAHs in the global ocean. There was not a correlation between  $C_{\text{plankton}}$  and distance to continents, which shows that biogeochemical controls on the concentrations dominate over the distance to potential continental sources as drivers of water column concentrations.

The analyses of the presence of essential PAH-degrading genes in metagenomes from the global oceans allowed confirmation of the potential for the microbial degradation of PAHs. We quantified the relative abundance of PAH-degrading genes in the water

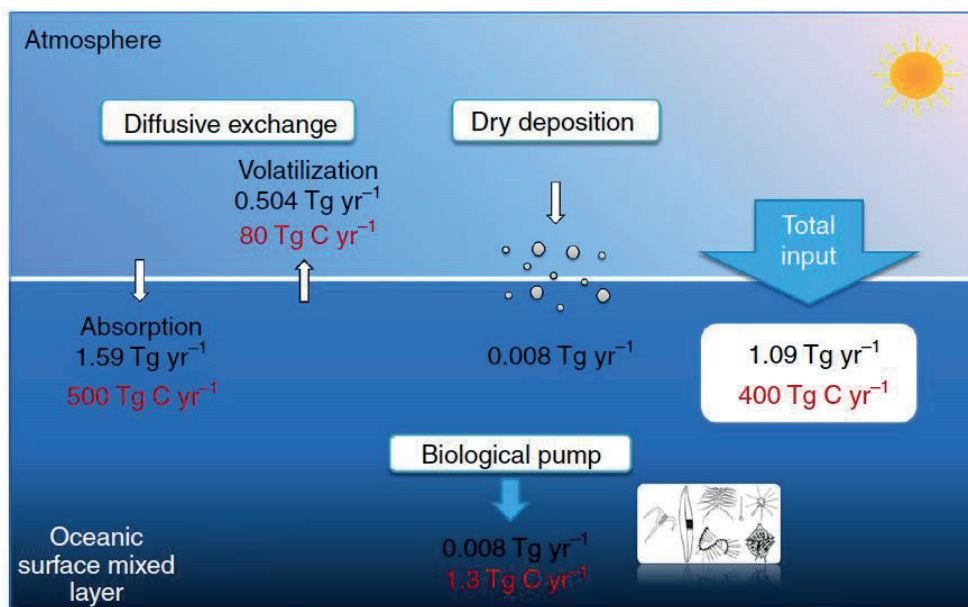


**FIGURE 4 |**  $C_{\text{plankton}}$  relationships with biomass (B) and the fitted slope versus KOW.  $C_{\text{plankton}}$  for the Pacific, Atlantic, Indian and Southern Oceans versus B fitted to a power law ( $\log C_{\text{plankton}} = m \log B + a$ ) (top panel). Slopes (m) from the relationship between PAH concentrations in plankton and biomass versus KOW of the individual compounds (bottom panel).

column by analysing the frequency of the alpha and beta subunits of RHD in the public metagenomic database of the oceanographic research expedition Tara Oceans (2009–2013). To proxy the frequency of genes per genome (o cell), we corrected the abundance of the alpha and beta subunits by the mean abundance of single-copy marker genes per station (Mende et al., 2013). The relative abundance of the alpha and beta subunits in marine genomes was 0.78 genes cell<sup>-1</sup> (0.38–1.3 global range) and 0.03 genes cell<sup>-1</sup> (0.009–1.7 global range), respectively (Figure 5). The alpha subunit contains the RHD active catalytic sites (hydroxylase) (Ferraro et al., 2006). In some cases, there is a beta subunit, which is suggested to stabilize the alpha subunit (Ferraro et al., 2005) or to be related to enzymes that significantly contribute to substrate specificity (Gibson & Perales, 2000; Kauppi et al., 1998). PAH degradation subunits were found to be ubiquitous in the global surface waters (Figure 5). Such ubiquity is a necessary condition to confirm the feasibility of microbial degradation as a relevant process that lowers the water column concentrations of PAHs at a global scale.

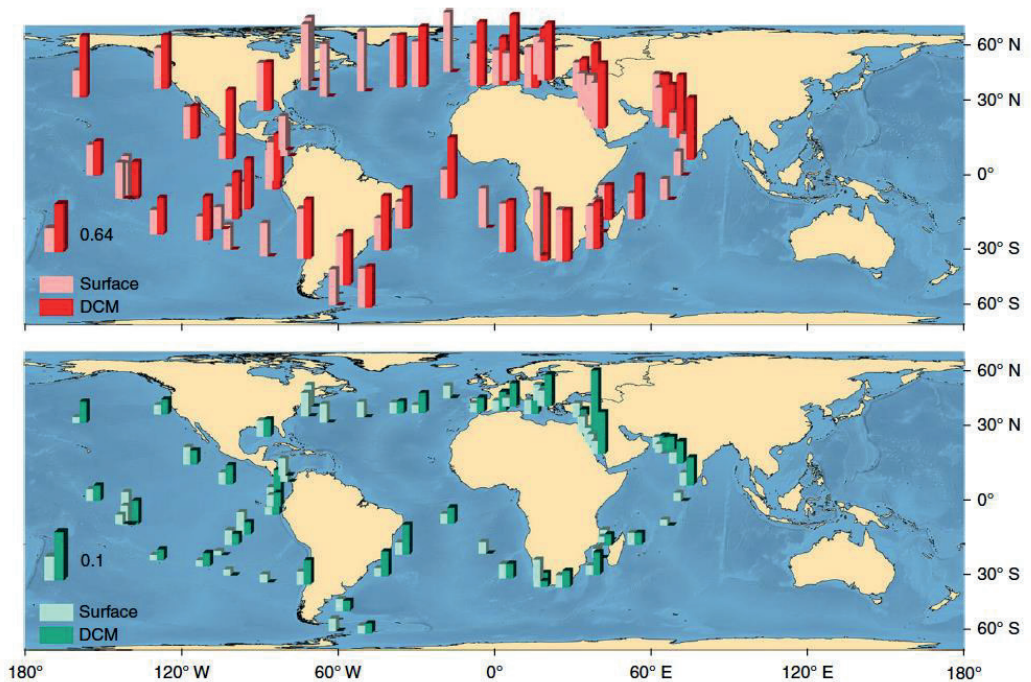


**FIGURE 5** | Frequencies of PAH degradation genes in the global oceans. Relative abundances of the RHD alpha subunit (upper panel) and the RHD beta subunit (lower panel) normalized to the averaged single-copy genes per station. Units are genes per cell.

The highest average relative abundance of the alpha subunit was observed in the North Atlantic Ocean (Supplementary Figure 10), and the lowest in the Southern Ocean, although a large variability was observed in each oceanic region (Supplementary Figure 10 and Supplementary Table 13). Significant differences were observed between depths ( $P < 0.05$ , Supplementary Figure 11 and Supplementary Table 13). Surface waters had a significantly lower relative abundance of the alpha subunit than that of the deep chlorophyll maximum depth (DCM), consistent with the maximum PAH concentrations (on a biomass basis) at the DCM (Dachs et al., 1997), and the occurrence of biogenic aromatic compounds.

Although photodegradation plays a role close to the air–water interface, microbial degradation seems to be the dominating depleting mechanism for the more abundant PAHs in the top 200 m of the water column. The same processes may be relevant for the largest SALC organic carbon pool (Figure 4), and thus be quantitatively relevant for the marine carbon cycle. Future work should delimitate whether the microbial carbon pump transforms SALCs into refractory dissolved organic carbon or there is a complete respiration of allochthonous airborne SALCs to  $\text{CO}_2$ , which could help explain the observed heterotrophy of the oligotrophic oceans (Duarte et al., 2013).

## AUTHOR CONTRIBUTIONS

B.G.-G., M.V.-C. and J.D. designed the work and wrote the manuscript. B.G.-G., P.C., B.J. and J.D. participated in the sampling campaigns. B.G.-G. and P.C. analysed the PAHs. B.G.-G., A.M.-V., M.V.-C., P.C., E.C.-G., N.B., B.J. and J.D. performed the fate assessment. A.M.-V., M.V.-C., E.C.-G. and D.L. did the bioinformatics work. C.M. and A.B. measured the carbon and nitrogen composition of the plankton samples. M.V. measured the organic carbon in the surface particulates. All the authors commented on the discussion and final version of the manuscript.

## REFERENCES

- Adhikari, P.L., Maiti, K., and Overton, E.B. (2015) Vertical fluxes of polycyclic aromatic hydrocarbons in the northern Gulf of Mexico. *Mar Chem* 168: 60–68.
- Bagby, S.C., Reddy, C.M., Aeppli, C., Fisher, G.B., and Valentinea, D.L. (2017) Persistence and biodegradation of oil at the ocean floor following Deepwater Horizon. *Proc Natl Acad Sci U S A* 114: E9–E18.
- Berrojalbiz, N., Dachs, J., Ojeda, M.J., Valle, M.C., Castro-Jiménez, J., Wollgast, J., et al. (2011) Biogeochemical and physical controls on concentrations of polycyclic aromatic hydrocarbons in water and plankton of the Mediterranean and Black Seas. *Global Biogeochem Cycles* 25: 1–14.
- Berrojalbiz, N., Lacorte, S., Calbet, A., Saiz, E., Barata, C., and Dachs, J. (2009) Accumulation and Cycling of Polycyclic Aromatic Hydrocarbons in Zooplankton Accumulation and Cycling of Polycyclic Aromatic Hydrocarbons in Zooplankton. *Environ Sci Technol* 43: 2295–2301.
- Bouloubassi, I., Méjanelle, L., Pete, R., Fillaux, J., Lorre, A., and Point, V. (2006) PAH transport by sinking particles in the open Mediterranean Sea: a 1 year sediment trap study. *Mar Pollut Bull* 52: 560–571.
- Brezna, B., Khan, A.A., and Cerniglia, C.E. (2003) Molecular characterization of dioxygenases from polycyclic aromatic hydrocarbon-degrading *Mycobacterium* spp. *FEMS Microbiol Lett* 223: 177–83.
- Castro-Jiménez, J., Berrojalbiz, N., Wollgast, J., Dachs, J., and Dachs Polycyclic, J. (2012) Polycyclic aromatic hydrocarbons (PAHs) in the Mediterranean Sea: Atmospheric occurrence, deposition and decoupling with

settling fluxes in the water column. *Environ Pollut* 166: 40–47.

Cerniglia, C.E. in *Microorganisms to Combat Pollution*, ed. Rosenb.

Dachs, J., Bayona, J.M., Fowler, S.W., Miquel, J.-C., and Albaigés, J. (1996) Vertical fluxes of polycyclic aromatic hydrocarbons and organochlorine compounds in the western Alboran Sea (southwestern Mediterranean). *Mar Chem* 52: 75–78.

Dachs, J., Bayona, J.M., Raoux, C., and Albaigés, J. (1997) Spatial, vertical distribution and budget of polycyclic aromatic hydrocarbons in the western Mediterranean seawater. *Environ Sci Technol* 31: 682–688.

Dachs, J. and Eisenreich, S.J. (2000) Adsorption onto aerosol soot carbon dominates gas-particle partitioning of polycyclic aromatic hydrocarbons. *Environ Sci Technol* | Request PDF. *Environ Sci Technol* 34: 3690–3697.

Deyme, R., Bouloubassi, I., Taphanel-Valt, M.H., Miquel, J.C., Lorre, A., Marty, J.C., and Méjanelle, L. (2011) Vertical fluxes of aromatic and aliphatic hydrocarbons in the Northwestern Mediterranean Sea. *Environ Pollut* 159: 3681–3691.

Dombrowski, N., Donaho, J.A., Gutierrez, T., Seitz, K.W., Teske, A.P., and Baker, B.J. (2016) Reconstructing metabolic pathways of hydrocarbon-degrading bacteria from the Deepwater Horizon oil spill. *Nat Microbiol* 1: 16057.

Douben, P.E.T. (2003) *PAHs : an ecotoxicological perspective*, Chichester: John Wiley & Sons,).

Duarte, C.M., Regaudie-De-Gioux, A., Arrieta, J.M., Delgado-Huertas, A., and Agustí, S. (2013) The oligotrophic ocean is heterotrophic. *Ann Rev Mar Sci* 5: 551–569.

Farrington, J.W. and Quinn, J.G. (2015) “Unresolved Complex Mixture” (UCM): A brief history of the term and moving beyond it. *Mar Pollut Bull* 96: 29–31.

Farrington, J.W. and Takada, H. (2014) Persistent organic pollutants (POPs), polycyclic aromatic hydrocarbons (PAHs), and plastics: Examples of the status, trend, and cycling of organic chemicals of environmental concern in the ocean. *Oceanography* 27: 196–213.

Fernández-Pinos, M.-C., Vila-Costa, M., Arrieta, J.M., Morales, L., González-Gaya, B., Piña, B., and Dachs, J. (2017) Dysregulation of photosynthetic genes in oceanic *Prochlorococcus* populations exposed to organic pollutants. *Sci Rep* 7:.

Ferraro, D.J., Gakhar, L., and Ramaswamy, S. (2005) Rieske business: Structure-function of Rieske non-heme oxygenases. *Biochem Biophys Res Commun* 338: 175–190.

Ferraro, D.J., Okerlund, A.L., Mowers, J.C., and Ramaswamy, S. (2006) Structural basis for regioselectivity and stereoselectivity of product formation by naphthalene 1,2-dioxygenase. *J Bacteriol* 188: 6986–6994.

Galbán-Malagón, C., Berrojalbiz, N., Ojeda, M.-J., and Dachs, J. (2012) The oceanic biological pump modulates the atmospheric transport of persistent organic pollutants to the Arctic. *Nat Commun* 3: 862.

Gallego, S., Vila, J., Tauler, M., Springael, D., and Grifoll, M. (2014) Community structure and PAH ring-hydroxylating dioxygenase genes of a marine pyrene-degrading microbial consortium. 543–556.

Gibson, D.T. and Parales, R.E. (2000) Aromatic hydrocarbon dioxygenases in environmental biotechnology. *Curr Opin Biotechnol* 11: 236–243.

González-Gaya, B., Fernández-Pinos, M.-C., Morales, L., Méjanelle, L., Abad, E., Piña, B., et al. (2016) High atmosphere–ocean exchange of semivolatile aromatic hydrocarbons. *Nat Geosci* 9: 438–442.

Halsall, C.J., Sweetman, A.J., Barrie, L.A., and Jones, K.C. (2001) Modelling the behaviour of PAHs during atmospheric transport from the UK to the Arctic. *Atmos Environ* 35: 255–267.

Harvey, R.G. (1991) *Polycyclic Aromatic Hydrocarbons: Chemistry and Carcinogenicity* - Ronald G. Harvey - Google Llibres, Cambridge.

Head, I.M., Jones, D.M., and Röling, W.F.M. (2006) Marine microorganisms make a meal of oil. *Nat Rev Microbiol* 4: 173–182.

Hylland, K. (2006) Polycyclic aromatic hydrocarbon (PAH) ecotoxicology in marine ecosystems. *J Toxicol Environ Health A* 69: 109–123.

Iwai, S., Johnson, T.A., Chai, B., Hashsham, S.A., and Tiedje, J.M. (2011) Comparison of the specificities and efficacies of primers for aromatic dioxygenase gene analysis of environmental samples. *Appl Environ Microbiol* 77: 3551–3557.

Kanaly, R.A. and Harayama, S. (2010) Review article Advances in the field of high-molecular-weight polycyclic aromatic hydrocarbon biodegradation. 3: 136–164.

- Kimes, N.E., Callaghan, A. V., Suflita, J.M., and Morris, P.J. (2014) Microbial transformation of the deepwater horizon oil spill-past, present, and future perspectives. *Front Microbiol* 5: 1–11.
- Liu, J., Techtmann, S.M., Woo, H.L., Ning, D., Fortney, J.L., and Hazen, T.C. (2017) Rapid Response of Eastern Mediterranean Deep Sea Microbial Communities to Oil. *Sci Rep* 7: 5762.
- Lohmann, R., Gioia, R., Jones, K.C., Nizzetto, L., Temme, C., Xie, Z., et al. (2009) Organochlorine pesticides and PAHs in the surface water and atmosphere of the North Atlantic and Arctic Ocean. *Environ Sci Technol* 43: 5633–5639.
- Lohmann, R., Klanova, J., Pribylova, P., Liskova, H., Yonis, S., and Bollinger, K. (2013) PAHs on a west-to-east transect across the tropical Atlantic Ocean. *Environ Sci Technol* 47: 2570–2578.
- Ma, Y., Xie, Z., Yang, H., Möller, A., Halsall, C., Cai, M., et al. (2013) Deposition of polycyclic aromatic hydrocarbons in the North Pacific and the Arctic. *J Geophys Res Atmos* 118: 5822–5829.
- Mallick, S., Chakraborty, J., and Dutta, T.K. (2011) Role of oxygenases in guiding diverse metabolic pathways in the bacterial degradation of low-molecular-weight polycyclic aromatic hydrocarbons : A review Role of oxygenases in guiding diverse metabolic pathways in the bacterial degradation of low-molecular-weight polycyclic aromatic hydrocarbons. *Environ Sci Technol* 45: 7828–7838.
- Mason, O.U., Hazen, T.C., Borglin, S., Chain, P.S.G., Dubinsky, E.A., Fortney, J.L., et al. (2012) Metagenome, metatranscriptome and single-cell sequencing reveal microbial response to Deepwater Horizon oil spill. *ISME J* 6: 1715–1727.
- Mende, D.R., Sunagawa, S., Zeller, G., and Bork, P. (2013) Accurate and universal delineation of prokaryotic species. *Nat Methods* 10: 881–884.
- Moody, J.D., Freeman, J.P., Doerge, D.R., and Cerniglia, C.E. (2001) Degradation of phenanthrene and anthracene by cell suspensions of *Mycobacterium* sp. strain PYR-1. *Appl Environ Microbiol* 67: 1476–1483.
- Nizzetto, L., Gioia, R., Li, J., Borgå, K., Pomati, F., Bettinetti, R., et al. (2012) Biological pump control of the fate and distribution of hydrophobic organic pollutants in water and plankton. *Environ Sci Technol* 46: 3204–3211.
- Peng, R.H., Xiong, A.S., Xue, Y., Fu, X.Y., Gao, F., Zhao, W., et al. (2008) Microbial biodegradation of polycyclic aromatic hydrocarbons. *FEMS Microbiol Rev* 32: 927–955.
- Radović, J.R., Aeppli, C., Nelson, R.K., Jimenez, N., Reddy, C.M., Bayona, J.M., and Albaigés, J. (2014) Assessment of photochemical processes in marine oil spill fingerprinting. *Mar Pollut Bull* 79: 268–277.
- Reddy, C.M., Arey, J.S., Seewald, J.S., Sylva, S.P., Lemkau, K.L., Nelson, R.K., et al. (2012) Composition and fate of gas and oil released to the water column during the Deepwater Horizon oil spill. *Proc Natl Acad Sci U S A* 109: 20229–34.
- Rivers, A.R., Sharma, S., Tringe, S.G., Martin, J., Joye, S.B., and Moran, M.A. (2013) Transcriptional response of bathypelagic marine bacterioplankton to the Deepwater Horizon oil spill. *ISME J* 7: 2315–2329.
- Seo, J.S., Keum, Y.S., and Li, Q.X. (2009) Bacterial degradation of aromatic compounds.
- Siegel, D.A., Buesseler, K.O., Doney, S.C., Sailley, S.F., Behrenfeld, M.J., and Boyd, P.W. (2014) Global assessment of ocean carbon export by combining satellite observations and food-web models. *Global Biogeochem Cycles* 28: 181–196.
- Tsapakis, M., Apostolaki, M., Eisenreich, S., and Stephanou, E.G. (2006) Atmospheric deposition and marine sedimentation fluxes of polycyclic aromatic hydrocarbons in the Eastern Mediterranean Basin. *Environ Sci Technol* 40: 4922–4927.
- Wilcke, W. (2007) Global patterns of polycyclic aromatic hydrocarbons (PAHs) in soil. *Geoderma* 141: 157–166.
- Zhang, Y. and Tao, S. (2009) Global atmospheric emission inventory of polycyclic aromatic hydrocarbons (PAHs) for 2004. *Atmos Environ* 43: 812–819.







# 2

## **Contrasted responses to background concentrations of PAH of bacterial communities from Mediterranean and Antarctic coastal waters**

**Alícia Martínez-Varela**, Gemma Casas, Naiara Berrojalbiz, Benjamin Piña, Jordi Dachs and Maria Vila-Costa

Large quantities of polycyclic aromatic hydrocarbons (PAH) and other semi-volatile aromatic-like compounds (SALCs) are deposited into the global ocean every year. Microbial degradation is a key sink that modulates the occurrence and fate of these airborne pollutants in the upper ocean. However, little is known on the geographical variability of this process under realistic field conditions. Microbial communities from two contrasting habitats, at coastal sites in the Mediterranean and the Maritime Antarctica, were incubated with environmentally relevant concentrations of PAHs for 48h to assess both PAH degradation rates and the impacts of PAHs on microbial communities at the compositional and functional levels. A minimal response was observed in Antarctic waters, either in terms of PAH degradation or changes in microbial composition. In contrast, Mediterranean bacteria readily degraded the less hydrophobic PAHs, with rates averaging  $4.72 \pm 0.5 \text{ ng L h}^{-1}$ . Metatranscriptomic analyses of Mediterranean communities after three hours of incubation showed significant enrichments of genes associated to horizontal gene transfer, stress response and PAH degradation, mainly harbored by Alphaproteobacteria. In contrast, 16S amplicon sequencing analyses revealed a decrease in relative abundance of hydrocarbonoclastic strains after 48 hours. Considering the large differences in pollution levels, nutrients availability and temperatures between the two sites, these results provide experimental evidence of the divergences in biodegradation modulating PAH concentrations and the effects of PAH on microbial communities in the global upper ocean.

## INTRODUCTION

Large quantities of polycyclic aromatic hydrocarbons (PAH) and other semi-volatile aromatic-like compounds (SALCs) are released to the environment and can distribute globally by long-range atmospheric transport and deposition (González-Gaya et al., 2016). The dissolved complex mixture of PAH and SALCs enters the oceanic water column mainly by atmospheric air-water diffusive exchange, with an estimated global input of 400 Tg yr<sup>-1</sup> (González-Gaya et al., 2016, 2019). Once in the ocean, they represent a major fraction of the anthropogenic dissolved organic carbon (ADOC) (Vila-Costa et al., 2020, Trilla-Prieto et al. 2021). While PAHs occur in relatively low abundances in the marine water column, their hydrophobicity with potential for bioconcentrating in marine organisms, toxicity, recalcitrance, co-occurrence and the possibility of generation of secondary reactive metabolites pose a threat to ecosystems (Hylland, 2006). Surprisingly, the biological pump sinking fluxes of PAH and SALCS is estimated to represent only 1% of the total input estimations, suggesting the largest share is transformed in the upper ocean, mainly by biodegradation (Ghosal et al., 2016; González-Gaya et al., 2019). Unfortunately, the scarcity of experimental biodegradation data in field studies hampers the assessment of the magnitude of this microbial pump and how this process impacts microbial communities.

The metabolic pathways for the microbial transformation of PAH under aerobic conditions, from primary biodegradation to their total breakdown to CO<sub>2</sub>, are well known for isolated bacteria, and typically start with the hydroxylation of an aromatic ring via a ring hydroxylating dioxygenase (RHD) (Mallick et al., 2011; Ghosal et al., 2016). Many bacterial strains capable of metabolizing these compounds have been identified and successfully isolated from oil spills (Mittal and Singh, 2009; Gutierrez, David R Singleton, et al., 2013; Lamendella et al., 2014; Mason et al., 2014). These so-called hydrocarbonclastic bacteria (HCB), including facultative and obligate hydrocarbon degraders, possess a large arsenal of genes related to PAH catabolism and assimilation. These include genes for sensing hydrocarbon presence, positive PAH chemotaxis, PAH-specific detoxifying mechanisms, facilitators of gene transfer of PAH catabolic genes between the microbial com-

munity, or the production of biosurfactants to increase hydrocarbons bioavailability (Top and Springael, 2003; Joye et al., 2016). Genomics and transcriptomics, and their environmental counterpart, metagenomics and metatranscriptomics, have revealed some of the multiple strategies employed to cope against PAH toxicities and the metabolisms used for PAH biodegradation under lab and field conditions (Rivers et al., 2013; Cerro-Gálvez et al., 2021). The degree of biodegradation of PAH is influenced not only by the composition of the naturally occurring microbial community, but also by the environmental factors directly influencing kinetics such as temperature, PAH concentrations and water-particle-cell partitioning, and others directly influencing the microbial consortia functioning. Among them, nutrient limitation and the level of pre-exposure and acclimation to ADOC pollution levels have recently been identified as relevant (Cerro-Gálvez et al., 2021). It has been suggested that environmental exposure to ADOC may trigger the horizontal dissemination within the community of the genes required to cope with or metabolize ADOC, via mobile genetic elements (MGE) as it has been observed after antibiotics exposures in riverine bacterial communities (Top and Springael, 2003; Gillings, 2013; Lekunberri et al., 2018). Unfortunately, most previous studies on bacteria exposure to PAHs focused in the microbial responses after accidental oil discharges, with high concentrations of PAH, and punctual occurrence (Head et al., 2006; Gutierrez, David R. Singleton, et al., 2013; Gallego et al., 2014; Crisafi et al., 2016; Dombrowski et al., 2016; Atashgahi et al., 2018). The microbial responses to the ubiquitous, chronic and background concentrations of PAH pollution found in the oceans have been much less studied, and this dearth of data hampers correct assessment of biodegradation, as well its inclusion in biogeochemical models.

The marine environment is a good site to determine the variability of PAH biodegradation and PAH influences on microbial communities since it offers different contrasting environments in terms of pollution, nutrient limitations and temperatures. For instance, the semi-enclosed Mediterranean basin contains temperate waters encircled by highly populated areas, being the Gibraltar strait the only significant entrance of seawater from the Atlantic Ocean. Thus, riverine run-off and atmospheric inputs are the most relevant PAH inputs (Lipiatou et al., 1997; Berrojalbiz et al., 2011; Castro-Jiménez et al., 2012). Oppositely, the Southern Ocean is a polar environment connected to all major oceanic basins and far from any major pollution emission source. In these conditions, diffusive atmospheric and snow and glacier meltdown represent the main PAH entry to the water column (Cabrerizo et al., 2014; Casal et al., 2019).

The goals of this study are to quantify PAH biodegradation rates and describe microbial responses to the exposure of environmentally relevant concentrations of PAH in two contrasting marine environments by means of biogeochemical measurements, changes in community composition using 16S amplicon sequencing, and changes in gene expression profiles by metatranscriptomics. The two contrasting sites are Mediterranean

Sea, representing a polluted site with a pre-adapted microbiome expectedly harbouring high gene plasticity; and the Maritime Antarctica, representing a pristine site without microbial pre-adaptation traits towards ADOC pollution.

## MATERIALS AND METHODS

### *Description of the experiments*

The same experimental design was implemented at two different locations, Blanes Bay, North-Western Mediterranean Sea (41°40'13''N, 02°48'01''E, August 8, 2017), and South Bay at Livingston Island (South Shetlands Islands, Antarctica, 62°39'26.3''S 60°23'18.4''W, February 27, 2018). The experiment consisted in 48 hours incubation of surface sea water challenged with environmentally relevant concentrations of individual PAH (300ng L<sup>-1</sup>). Three hours prior to the surface seawater sampling, PAH mix (PAH-Mix 9 from Dr Ehrenstorfer GmbH) or solvent alone without PAH spike for the bottles run as controls, was added to 2L and 1L pre-cleaned and 400°C baked glass bottles, allowing the solvent (cyclohexane) evaporation to avoid any toxic effects derived from solvents presence. Each experimental condition consisted in duplicates. At each experiment location, surface seawater (5m depth) was collected using 20L metal carboys. Abiotic samples were run with HPLC water at both locations. The 48h incubations took place in the dark and at in situ monitored constant temperature.

### *PAH analysis*

Briefly, 1L of seawater was filtered through pre-combusted GF/F glass fibre filter (Whatman) to collect the particulate-phase PAHs by using a vacuum pumping system. Filters were stored at -20°C until the extraction procedure. Once in the laboratory, each filter was freeze-dried, weighed and spiked with 50 ng of a mix containing five recovery standards (Naphthalene-d<sub>8</sub>, Acenaphthene-d<sub>10</sub>, Phenanthrene-d<sub>10</sub>, Chrysene-d<sub>12</sub> and perylene-d<sub>12</sub>; Sigma-Aldrich). PAHs were extracted with a mixture of hexane-acetone (1:1 v/v) solution by ultrasonication three times. The supernatant containing PAHs was collected in a pre-combusted pear-shaped glass flask, concentrated using a rotary evaporator and solvent exchanged to hexane. The extracts were then purified using a glass column filled with 100mg of anhydrous sodium sulphate over 1 g of neutral alumina (aluminium oxide 90, activated at 450°C for 12h) and eluted with 15 ml of hexane/dichloromethane (3:1, v/v). The extracts were further concentrated under a gentle stream of purified N<sub>2</sub> to a final volume of 100 µL and transferred to an injection amber glass vial.

Dissolved-phase PAHs were collected using solid phase extraction C18 cartridges (Agilent, 6ml, 1g). Cartridges were pre-conditioned with 6 ml of hexane, 6ml of propanol and 6ml of HPLC-grade water with 2% of propanol. Filtered seawater samples were loaded on the cartridges by using a vacuum pumping system. This extraction of dissolved PAHs was performed on the field immediately after filtration. Each cartridge was spiked with 50 ng of the same recovery standard mix. After extraction, the cartridges were kept under vacuum for 30 min to remove any residual water and stored at -20°C until further treat-

ment in the laboratory. PAHs were eluted from the cartridges with 12ml of a mixture of hexane:dichloromethane (1:1, v/v). The extracts were solvent exchanged to isoctane and concentrated under a gentle stream of purified N<sub>2</sub> to a final volume of 100 µL.

PAHs analysis were conducted by gas chromatography coupled with a mass spectrometer Agilent 5973 (GC-MS) based on an established method with minor modifications (Casas et al., 2021). The system was operated in electron impact mode (EI, 70 eV) and with the splitless injection mode. The separation was achieved with a 30 m x 0.25 mm i.d. x 0.25 µm DB5 capillary column (Agilent). Compounds were quantified by the internal standard procedure for which the final sample eluents were spiked with 50 ng of three internal standards prior injection (Anthracene-d<sub>10</sub>, Pyrene-d<sub>10</sub>, Benzo(b)fluoranthene-d<sub>12</sub>). MassHunter (Agilent) was used for the quantification. The analytical procedure for both matrices was validated by determining the recovery rates of the surrogates for each sample. Analytical blanks were analysed in parallel to all samples. The following 13 PAHs were analysed in the seawater samples: Fluorene, Anthracene, Phenanthrene, Pyrene, Fluoranthene, Crysene, Benzo(a)anthracene, Benzo(b)fluoranthene, Benzo(k)fluoranthene, Benzo(a)pyrene, Dibenzo(a,h)anthracene, Indeno(1,2,3-cd)pyrene and Benzo(ghi)perylene. Naphtalene, Acenaphthene and Acenaphthilene results were excluded from the study due to poor results in the quality control process of the data. PAH concentrations were determined at initial time and after 48 hours from the start of the incubation.

### ***Nucleic acid extraction and sequencing***

Samples for RNA and 16S rDNA library construction were collected after 3 hours and 48 hours of PAH addition, respectively. After incubation, seawater samples were prefiltered through a 20 µm nylon mesh onto 0.2 µm pore-size 47 mm polytetrafluoroethylene filters, in order to capture the free-living bacterial cells fraction, all under low vacuum pressure. After 3 hours of incubation, 1.2L from each bottle were dedicated to RNA, for which the duration of the filtration step was no longer than 15 min for RNA, to minimize RNA degradation. Filters were placed into 1 ml RNeasy (Sigma-Aldrich, Saint Louis, MO). After 48 h, from the same bottles, the 0.4L left in each bottle were dedicated to DNA. Each filter was placed in 1 ml lysis buffer (50 mM Tris HCl, 40 mM EDTA, 0.75 M sucrose). All filters were stored at -20 °C.

Amplified RNA were sequenced at the National Center for Genomic Analysis (CNAG, Barcelona, Spain) using Illumina high output model HS200 2 x 100 bp v4.

DNA extraction for 16S rDNA sequencing was performed as described in Vila-Costa et al. 2018. For metatranscriptomic analyses, total RNA was extracted, DNA removed, rRNA depleted, and mRNA amplified as previously described (Poretsky et al. 2014), with the only modification that total RNA was extracted with mirVana isolation kit (Ambion), after removing the storage reagent by centrifugation. Partial amplification of the 16S rRNA gene (245 bp fragments) was done in 50 µl reactions using primers 515F-Y (5'-GTGYCAG-CMGCCGCGGTAA) and 926R (5'-CCGYCAATTYMTTTRAGTTT) (Parada et al., 2016), each at

0.2  $\mu\text{M}$  final concentration PCR conditions were as follows: an initial denaturation step at 95°C for 5 min and 35 cycles at 95°C (30 s), 58°C (30 s), 72°C (40 s) and a final elongation step at 72°C for 10 min. Sequencing was performed in an Illumina MiSeq sequencer (2 x 250 bp, Research and Testing Laboratory; <http://rtlgenomics.com/>).

### ***Prokaryotic cell abundance***

Prokaryotic cell abundance was estimated by flow cytometry as described elsewhere (Falcioni et al., 2008). Briefly, samples (0.4 ml) for heterotrophic non-pigmented total bacteria enumeration were stained with 4  $\mu\text{l}$  of a 10 SG1 (Molecular Probes) solution (final dilution, 1:1000 [vol/vol]) for 10 min and run through the FACSCalibur flow cytometer at a low speed (15  $\mu\text{l min}^{-1}$ ), with fluorescent microspheres as an internal standard [yellow-green 0.92- $\mu\text{m}$  Polysciences latex beads ( $10^6 \text{ ml}^{-1}$ )]. Bacteria were detected in a dot plot of side scatter versus green fluorescence (FL1) and population concentration was estimated with CellQuest and PaintAGate software (Becton Dickinson, Palo Alto, CA).

### ***Nutrient analysis***

Analytical procedures for nutrients Sub-samples (15 ml) for dissolved inorganic nutrient (nitrate( $\text{NO}_3^-$ ), nitrite ( $\text{NO}_2^-$ ), ammonium ( $\text{NH}_4^+$ ) and phosphate ( $\text{PO}_4^{3-}$ )) were kept at -20°C until analysis by standard segmented flow with colorimetric detection (Grasshoff et al., 2009) using a SEAL Analyzer AA3 HR. Phosphoric acid was added to acidify the sample to pH 2 and the ampoules were heat-sealed and stored in the dark at 4°C until analysis. Samples were measured with a SHIMADZU TOC-5000 analyzer, following the high-temperature catalytic oxidation (HTCO) technique (Cauwet, 1994). Detection limits for inorganic nutrient analysis, defined as three times the standard deviation of ten replicates at 50% diluted samples, were 0.006  $\mu\text{M}$  for  $\text{NO}_3^-$ , 0.003  $\mu\text{M}$  for  $\text{NO}_2^-$ , 0.003  $\mu\text{M}$  for  $\text{NH}_4^+$ , and 0.01  $\mu\text{M}$  for  $\text{PO}_4^{3-}$ .

### ***Bioinformatics***

For 16S amplicon reads, spurious sequences and primers were trimmed using Cutadapt v.1.16 (Martin, 2011). The cutoff before a base would be trimmed from either end of the read was set to a minimum phred quality score of 20 (1% error rate), and primers and illumina adapters were removed with a minimum overlap of 10 base pairs. DADA2 v1.4 was used to differentiate the 16S V4-5 amplicon sequence variants (ASVs) and remove chimeras (parameters: maxN = 0, maxEE = 2,4, truncLen = 220,180; Callahan et al., 2016). DADA2 resolves ASVs by modeling the errors in Illumina-sequenced amplicon reads. The approach is threshold-free, inferring exact variants up to 1 nucleotide difference using the quality score distribution in a probability model. Taxonomic assignment of the ASVs was performed with the SILVA algorithm classifier against SILVA database release 138 (Quast et al., 2013). ASVs classified as Mitochondria or Chloroplast were removed. The dataset accounted for a total of 2326 unique ASV and the minimum sequencing depth was 24550. Rarefaction to the minimum sequencing depths was done with rrarefy() function from vegan v1.4-4 package in R (Oksanen et al., 2020). Archaea accounted for <1% of the

total pool of reads and were discarded from the analyses.

For the metatranscriptomes, cDNA sequences were quality trimmed with Cutadapt (Martin, 2011) and Sickle (<https://github.com/najoshi/sickle>) and internal standards and any remaining rRNA and tRNA sequences were quantified and removed using the Bowtie2 mapping program (Langmead and Salzberg, 2012) against the internal standard sequences and an in-house database of marine bacterial stable RNA sequences. Subsequently, high quality reads were de-novo assembled using the MEGAHIT program (v1.1.2) (Li et al., 2016) with default parameters. Open reading frame (ORFs) prediction was done using Prodigal. (Hyatt et al 2010). Contigs were then aligned to the NCBI RefSeq database (downloaded October 2016) using the Diamond aligner, v0.9.24, (Buchfink et al., 2015) in blastx mode with default parameters. Functional SEED classification and taxonomic affiliation were assigned with MEGAN 6.7.3 (Huson et al., 2016). Transcripts were mapped to the open reading frames (ORFs) using bowtie2 (v2.3.5.1) and quantified using Samtools (v1.9). Data was then exported for further analysis in R/tidyverse. Relative raw gene counts were normalized to library sizes.

Search for specific PAH degrading and transposases genes within the metatranscriptomes was performed using Hmmersearch with default parameters against the specific Pfam hmmer profiles. The list of the specific Pfam profiles used is listed in Figure S4 and Table S4 and were downloaded from “Pfam” database (Mistry et al., 2021).

### ***Identification of hydrocarbonoclastic bacterial genera***

A list of hydrocarbonoclastic bacterial (HCB) genera was retrieved from the literature (Lozada et al., 2014; Karthikeyan et al., 2020), comprising genera either collected from hydrocarbon polluted environments, observed to have stimulated growth following hydrocarbon exposure, or showing hydrocarbon catabolic activity, both from isolates and from marine environments, after MAGS reconstruction. The detection of specific HCB genera (see Table S6 and Figure S6) was performed by filtering at genus level all those ASVs and transcripts with taxonomical affiliation matching to those targeted HCB groups. All HCB-ASV and transcripts within the same genus were assumed to share similar metabolism. Additionally, a subset of ASV assigned to HCB genera were compared with BLAST against a relevant isolate from the same genus known to degrade PAH or retrieved from an oil polluted sites. Those ASVs with >97% of similarity were taken as true match. All HCB-ASV within the same genus were assumed to share similar metabolism.

### ***Statistical analyses***

The significance of the difference in community composition between locations and treatments was tested with a permutation analysis of variance (PERMANOVA, with function Adonis, from “vegan v1.4-4” package in R). Fold changes were calculated for the relative values between treatments (control vs PAH), using the function foldchange from “gtools” package (R Core Team, 2019). Significant differences between treatments and controls were tested using the “t.test” function from R package “stats”, with a threshold for the



significance set at  $p < 0.05$ . Further graphs were plotted using the “ggplot2” package, also in R environment (Wickham, 2009).

## RESULTS AND DISCUSSION

### *Initial conditions*

Antarctica's austral summer was characterized by cold ( $1.5^{\circ}\text{C}$ ) and nutrient-rich waters, hosting an initial bacterial community dominated by Bacteroidota ( $54.3 \pm 1.1\%$ ) and Proteobacteria, mostly Gammaproteobacteria ( $26.6 \pm 0.1\%$ ) and a minor contribution of Alphaproteobacteria (Table S1, Table S2 and Figure S1). In contrast, a warm ( $26.4^{\circ}\text{C}$ ) and oligotrophic system characterized the Mediterranean coastal sampling site. This site was dominated by SAR11 clade and other Alphaproteobacteria ( $49.28 \pm 0.5\%$ ) (Table S1, Table S2 and Figure S1). Diversity indexes based on 16S rDNA amplicon sequencing showed that the Mediterranean microbiome was significantly more diverse than the Antarctic microbiome ( $H'$ :  $4.61 \pm 0.10$  and  $1.56 \pm 0.30$  respectively, Table S1). Abundances of heterotrophic cells quantified by flow cytometry were 1.8-fold to 4.4-fold higher in the Mediterranean compared to Antarctica (Table S1). The Antarctica heterotrophic bacterial community was dominated by HNA cells, whereas in the Mediterranean the share was evenly distributed between HNA and LNA cells.

### *PAH biodegradation*

PAH compounds were analysed and quantified at time 0 and after 48h of PAH exposure. In both Mediterranean and Antarctic sites, 96-97% of LMW PAH were found in the dissolved phase, whereas HMW PAH were evenly partitioned between phases in Antarctica (47 % particulate, 53 % dissolved) and mostly found in the dissolved phase in the Mediterranean (85% on average). No significant PAH degradation was observed in the Antarctica experiments. In the Mediterranean, a  $29.9 \pm 1.3\%$  decrease in the concentration of the total 13 PAH ( $\sum_{13} \text{PAH}$ ) from the dissolved and the particulate phases after 48 h of incubation was observed. This decrease was due to the fast degradation of the less hydrophobic PAHs (Anthracene, Phenanthrene, Pyrene and Fluoranthene,  $\log K_{ow} < 5.5$ ) (Figure 1, Table S3). In fact, the less hydrophobic individual PAH removal rates in the Mediterranean, calculated as the difference of the total PAH concentrations between time 0 and 48 hours, ranges from  $1.7 \pm 0.2 \text{ ng h}^{-1}$  to  $6.2 \pm 0.1 \text{ ng h}^{-1}$ , averaging  $4.72 \pm 0.5 \text{ ng h}^{-1}$ , whereas concentrations of the heavier, more hydrophobic PAHs showed essentially no changes during the experiment. We consider that the observed removal rates reflect biodegradation, since experiments were run in the dark and, therefore, no direct photo-degradation could occur.

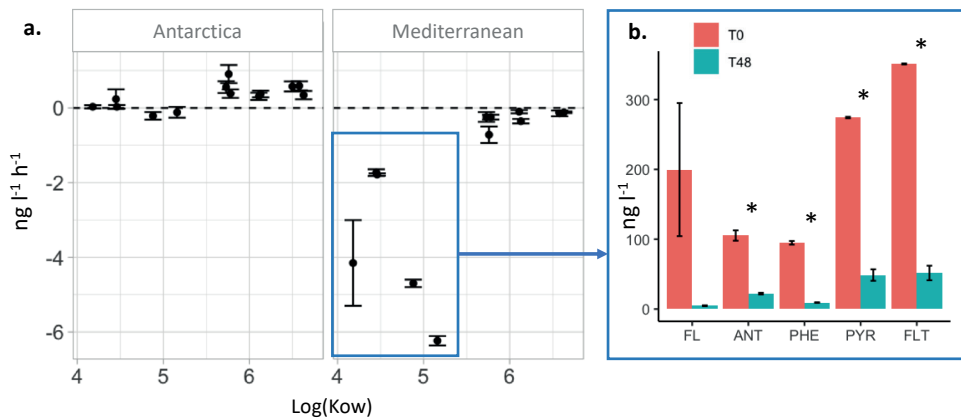


**FIGURE 1** | (a) PAH removal rates for the PAH amended samples in the Antarctica and the Mediterranean, calculated as the difference of concentrations between time 0 and 48 hours (units in  $\text{ng L}^{-1} \text{h}^{-1}$ ). (b) Concentrations of the PAH compounds with fastest removal rates in the Mediterranean (units in  $\text{ng L}^{-1}$ ). Significant differences between initial and final exposure time are indicated with \*, based on t-test p-value < 0.01. (FL: Fluorene, ANT: Anthracene, PHE: Phenanthrene, PYR: Pyrene, FLT: Fluoranthene, Kow : Octanol – Water constant)

Numerous abiotic and biotic factors can influence the biodegradation processes (Ghosal et al., 2016). For example, PAH solubility and bioavailability increase with decreasing logKow and, therefore, PAH with low logKow tend to be removed faster by microorganisms than more hydrophobic ones (Froehner et al., 2012), which is consistent with our observations in the Mediterranean. In addition, higher temperatures increase the solubility of PAH molecules, making them more bioavailable for microbial organisms uptake and metabolism. Although our results show no significant removal of PAH in the Antarctica samples, biodegradation of PAH and other petroleum hydrocarbons by marine microorganisms have been reported in a number of studies in similarly cold regions (Crisafi et al., 2016b; Garneau et al., 2016; Ribicic et al., 2018), although with longer exposure times (15 – 30 days). These results suggest that the Antarctica's system responded to PAH presence much slower than the Mediterranean system, in which 48 h of incubation was sufficient for the naturally occurring microbial community to remove the less hydrophobic PAH.

### ***Metatranscriptomic responses to PAH exposure***

Both communities were exposed to the same nominal concentrations of PAH. Gene expression levels were captured after 3 h of PAH exposure by means of metatranscriptomic analysis. Overall, Mediterranean metatranscriptome showed a higher number of PAH-related transcripts enriched in the PAH exposed community in comparison to that of the Antarctica, consistent with PAH biodegradation rates (Figure 2).



In the Mediterranean, SAR11 clade, Rhodobacterales and other Alphaproteobacteria accumulated the highest number of significant increases in the relative transcript contribution to the total transcripts pool at the PAH exposed water compared to controls (t-test,  $P < 0.05$ ), suggesting that this Alphaproteobacterial community was well adapted to PAH disturbance (Figure 2). This result contrasts with the general common bloom of HC Gammaproteobacteria following pulses of PAH in oil spills scenarios (King, Kostka, Hazen, & Sobecky, 2015; Mason et al., 2012), but it is in agreement with other observations under low concentrations of ADOC compounds (Martinez-Varela et al., 2021).

To widen the understanding of bacterial HGT functioning under PAH exposure at low concentrations, specific transposon families were searched within the metatranscriptomes. Transcripts identified as phage integrases and transposon-related genes DDE\_Tnp\_1, rve, Y1 and Y2 Tnp and TnpB showed significant enrichments in the PAH exposed Mediterranean samples (Figure 2). The increased expression of these genetic elements, which are associated to HGT-related functions, in the PAH exposed Mediterranean community suggests that: 1) PAH exposure triggered immediate HGT events, which are known to confer a selective advantage in front of other toxicant exposures at high concentrations such as antibiotics, metals and other synthetic pollutants (Lekunberri et al., 2018; Wright et al., 2008), and 2) that the naturally occurring microbial population showed a high gene plasticity, harbouring the genetic potential for gene transfer. In fact, MGE-mediated HGT is considered the main adaptive trait in freshwater and soil ecosystems acutely contaminated by industrial pollutants (Sobecky & Hazen, 2009; Wright et al., 2008). MGE trigger the activation of degradation metabolic pathways within the community, favouring the removal of toxicants in the media, or biosurfactant production to facilitate the bioavailability of the compounds (Joye et al., 2016). This study provides preliminary experimental data on the role played by ADOC as an environmental stressor promoting local adaptation of microbial communities to background pollution in seawater.

Furthermore, transcripts assigned to membrane transport and stress response showed 1.5 and 2.1 fold increases respectively at the PAH exposed Mediterranean metatranscriptome compared to controls. In particular, these transcripts were significantly enriched for Alphaproteobacteria clades not included in the SAR11 and Rhodobacterales groups. These results are consistent with previous reports showing that functions related to the activation of stress responses, membrane transportation, and HGT constitute microbial responses to ADOC exposure at environmentally relevant concentrations (Cerro-Gálvez et al., 2019; Martinez-Varela et al., 2021).

In the Antarctica, the taxonomic transcripts affiliation remained mostly unchanged after PAH incubation (Figure S2 and Figure S3), which induced fewer changes in relative transcript contribution than the ones observed in the Mediterranean experiments. The only significant changes in transcript abundance in PAH-incubated samples relative to controls corresponded to an enrichment of phosphorus metabolism-related

transcripts from the Pseudomonadales group, and a depletion of transcripts related to either Nitrogen metabolism affiliated to Rhodobacterales or to Cofactors, Vitamins and Prosthetic groups and Regulation and cell Signalling affiliated to Sphingobacterales. Transcripts related to gene transfer remained unaltered by the PAH exposure (Figure 2).

Specific search for PAH degradation-related genes showed that the relative abundance of most of them increased at the PAH exposed community in the Mediterranean, but it was reduced in the Antarctica PAH-incubated samples, consistent with the measured PAH biodegradation rates (Figure 2 and Figure S4). The ring hydroxylating dioxygenase (RHD), catalyser complex of the ring-opening PAH dihydroxylation (PF00848), was found significantly enriched at the Mediterranean PAH exposed community for those transcripts affiliated to Rhodobacterales and to Proteobacteria other than Alpha- and Gammaproteobacteria groups. At the same site, different taxa showed significantly higher transcription levels for transcripts involved in the steps following the ring hydroxylation towards catechol and protocatechuate pathway (Figure S4). The immediate enrichments of PAH degrading genes in the Mediterranean, combined with the degradation rates observed at this site, suggest the naturally occurring community must have taken part in the biodegradation of the less hydrophobic PAH.

### ***Changes in Community composition***

Significant changes in community composition between controls and PAH treatments were observed in the Mediterranean microbiomes after 48h of exposure (PERMANOVA,  $p = 0.03$ , Figure 3 and Figure S1). Non-HC gammaproteobacterial groups significantly decreased their contribution to the 16S pool from the PAH treated samples, whereas other dominant groups (Bacteroidota, Flavobacterales and Chitinophagales) significantly increased (Figure 3 and Table S4). In Antarctica, no statistically significant changes were observed between control and PAH exposed communities (Figure 3).

In the Mediterranean, HC alphaproteobacterial and HC Alteromonadales relative abundances significantly decreased in the PAH treated samples (Figure 3 and Figure S5 and Figure S6). In fact, PAH exposed communities showed a general decline (1.8-fold to 4.7-fold) for different genera of HC bacterial strains, including the HC Actinobacteria genera *Arthrobacter*, HC Gammaproteobacteria genera *Glaciecola*, *Thalassotalea*, *Bermanella*, *Oleiphilulus* and *Alteromonas*, and HC Alphaproteobacteria genera *Sulfitobacter*, *Jannaschia* and *Tropicibacter* (Figure S5). The opposite occurred in Antarctica, where HCB low abundant taxa belonging to the rare biosphere (relative abundance < 0.03 %) clearly increased their relative contribution to the total pool of ASV (Figure S6). For instance, the copiotroph HC Gammaproteobacteria genera *Pseudoalteromonas* showed a 5.9-fold increase at the PAH exposed community compared to controls (Figure S5). Some of these copiotrophic HCB strains, such as HCB belonging to Alteromonadales (*Glaciecola*, *Alteromonas*, *Pseudoalteromonas* and *Thalassotalea*) are found ubiquitously at low

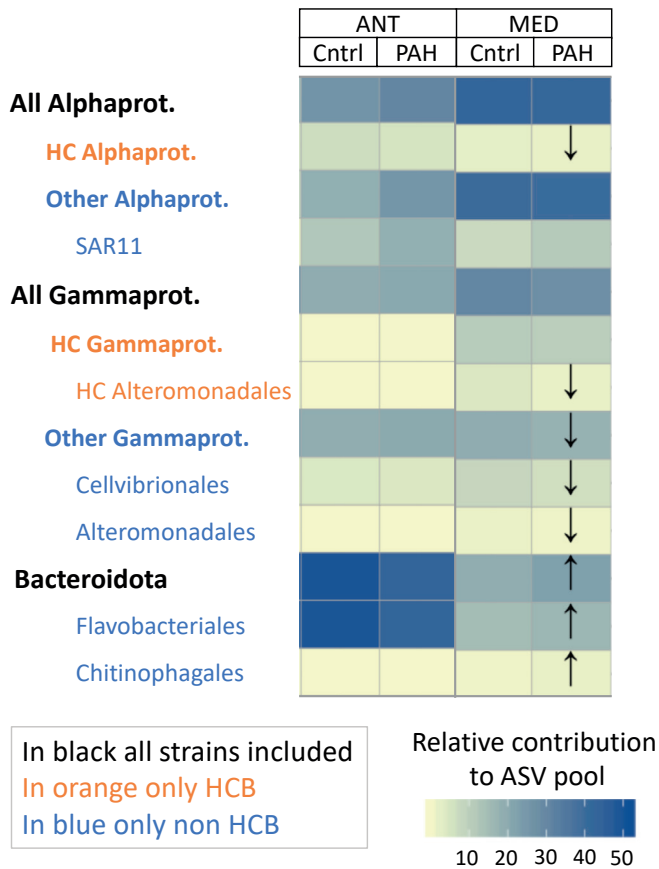


**FIGURE 3** | Free living bacterial response based on 16S rRNA gene analysis. Arrows indicate significant changes in the relative values after 48 h between control and PAH exposed communities based on t test,  $p < 0.05$ .

abundances, but exponentially increase their populations in the immediate aftermath of marine oil spills (Kleindienst et al., 2016), becoming key players at the initial stages of the microbial succession of hydrocarbon degradation (Kostka et al., 2011; Dubinsky et al., 2013). These results contrast with other experimental observations in polar and subpolar marine systems, where significant microbial community shifts were observed after shorter exposure times under ADOC background concentrations (24 h) (Cerro-Gálvez et al., 2019; Martínez-Varela et al., 2021). This could be due to the fact that microbial PAH removal and HCB succession is conditioned by multiple factors such as the concentrations of other available carbon sources in the environment, nutrient availability or the temperature (Ghosal et al., 2016; Cerro-Gálvez et al., 2019). Also, these contrasting trends between sites suggest that the pace at which microbial communities respond to low concentrations of PAH is site specific. In the Mediterranean, copiotroph HCB sub population

is already retreating after 48 h, suggesting a faster microbial response in front of PAH perturbation in comparison to Antarctica's microbiome.

## Conclusions

Overall, our results show that the Mediterranean microbiome responded faster than that of the Antarctica to the PAH exposure at environmentally relevant concentration. In the Mediterranean, we observed the immediate activation of transcripts related to stress response mechanisms in front of PAH toxicity, horizontal gene transfer events and PAH metabolism. Following this immediate response, significant changes in the community composition after 48 h from the initial PAH exposure were also observed. At this site, the Alphaproteobacterial community seemed to be well adapted to ADOC perturbation, showing the highest number of transcript significant enrichments after 3 h. Aligned to these compositional and functional responses, the concentrations of the less hydrophobic LMW PAH were significantly reduced after 48 h in the Mediterranean, indicating that these compounds are readily biodegraded by this natural community.

This paper provides initial data on PAH biodegradation rates along with a description of the impacts of PAH on microbial communities in two contrasting sites of the upper ocean, temperate Mediterranean vs polar Antarctic coastal waters. Results show a wide divergence of rates and bacterial responses to PAH background concentrations, pointing to the importance of environmental drivers when assessing the magnitude of the microbial biodegradation pump to modulate PAH concentrations in the global oceans.

## AUTHOR CONTRIBUTIONS

A.M.-V., M.V.-C. designed the experiments. A.M.-V., M.V.-C. and G.C. collected the water and performed the incubation experiments. A.M.-V. performed the molecular and analytical laboratory work. N.B. quantified the PAH compounds, and B.P. performed statistical analyses. All the authors commented on the discussion and final version of the manuscript.

## REFERENCES

- Atashgahi, S., Hornung, B., van der Waals, M.J., da Rocha, U.N., Hugenholtz, F., Nijse, B., et al. (2018) A benzene-degrading nitrate-reducing microbial consortium displays aerobic and anaerobic benzene degradation pathways. *Sci Rep* 8: 4490.
- Berrojalbiz, N., Dachs, J., Ojeda, M.J., Valle, M.C., Castro-Jiménez, J., Wollgast, J., et al. (2011) Biogeochemical and physical controls on concentrations of polycyclic aromatic hydrocarbons in water and plankton of the Mediterranean and Black Seas. *Global Biogeochem Cycles* 25: n/a-n/a.
- Buchfink, B., Xie, C., and Huson, D.H. (2015) Fast and sensitive protein alignment using DIAMOND. *Nat Methods* 12: 59–60.
- Cabrerizo, A., Galbán-Malagón, C., Del Vento, S., and Dachs, J. (2014) Sources and fate of polycyclic aromatic hydrocarbons in the Antarctic and Southern Ocean atmosphere. *Global Biogeochem Cycles* 28: 1424–1436.
- Casal, P., Casas, G., Vila-Costa, M., Cabrerizo, A., Pizarro, M., Jiménez, B., and Dachs, J. (2019) Snow amplification of persistent organic pollutants at coastal Antarctica. *Environ Sci Technol* 53: 8872–8882.

Casas, G., Martínez-Varela, A., Vila-Costa, M., Jiménez, B., and Dachs, J. (2021) Rain Amplification of Persistent Organic Pollutants. *Environ Sci Technol* 55: 12961–12972.

Castro-Jiménez, J., Berrojalbiz, N., Wollgast, J., and Dachs, J. (2012) Polycyclic aromatic hydrocarbons (PAHs) in the Mediterranean Sea: Atmospheric occurrence, deposition and decoupling with settling fluxes in the water column. *Environ Pollut* 166: 40–47.

Cauwet, G. (1994) HTO method for dissolved organic carbon analysis in seawater: influence of catalyst on blank estimation. *Mar Chem* 47: 55–64.

Cerro-Gálvez, E., Dachs, J., Lundin, D., Fernández-Pinos, M.-C., Sebastián, M., and Vila-Costa, M. (2021) Responses of Coastal Marine Microbiomes Exposed to Anthropogenic Dissolved Organic Carbon. *Environ Sci Technol* 55: 9609–9621.

Cerro-Gálvez, E., Casal, P., Lundin, D., Piña, B., Pinhassi, J., Dachs, J., and Vila-Costa, M. (2019) Microbial responses to anthropogenic dissolved organic carbon in the Arctic and Antarctic coastal seawaters. *Environ Microbiol* 21: 1466–1481.

Crisafi, F., Giuliano, L., Yakimov, M.M., Azzaro, M., and Denaro, R. (2016a) Isolation and degradation potential of a cold-adapted oil/PAH-degrading marine bacterial consortium from Kongsfjorden (Arctic region). *Rend Lincei* 27: 261–270.

Crisafi, F., Giuliano, L., Yakimov, M.M., Azzaro, M., and Denaro, R. (2016b) Isolation and degradation potential of a cold-adapted oil/PAH-degrading marine bacterial consortium from Kongsfjorden (Arctic region). *Rend Lincei* 27: 261–270.

Dombrowski, N., Donaho, J.A., Gutierrez, T., Seitz, K.W., Teske, A.P., and Baker, B.J. (2016) Reconstructing metabolic pathways of hydrocarbon-degrading bacteria from the Deepwater Horizon oil spill. *Nat Microbiol* 1: 16057.

Dubinsky, E.A., Conrad, M.E., Chakraborty, R., Bill, M., Borglin, S.E., Hollibaugh, J.T., et al. (2013) Succession of Hydrocarbon-Degrading Bacteria in the Aftermath of the Deepwater Horizon Oil Spill in the Gulf of Mexico. *Environ Sci Technol* 47: 10860–10867.

Falcioni, T., Papa, S., and Gasol, J.M. (2008) Evaluating the flow-cytometric nucleic acid double-staining protocol in realistic situations of planktonic bacterial death. *Appl Environ Microbiol* 74: 1767–1779.

Froehner, S., Dombroski, L.F., Machado, K.S., Scapulatempo Fernandes, C., and Bessa, M. (2012) Estimation of bioavailability of polycyclic aromatic hydrocarbons in river sediments. *Int J Environ Sci Technol* 9: 409–416.

Gallego, S., Vila, J., Tauler, M., Springael, D., and Grifoll, M. (2014) Community structure and PAH ring-hydroxylating dioxygenase genes of a marine pyrene-degrading microbial consortium. 543–556.

Garneau, M.-È., Michel, C., Meisterhans, G., Fortin, N., King, T.L., Greer, C.W., and Lee, K. (2016) Hydrocarbon biodegradation by Arctic sea-ice and sub-ice microbial communities during microcosm experiments, Northwest Passage (Nunavut, Canada). *FEMS Microbiol Ecol* 92:.

Ghosal, D., Ghosh, S., Dutta, T.K., and Ahn, Y. (2016) Current state of knowledge in microbial degradation of polycyclic aromatic hydrocarbons (PAHs): A review. *Front Microbiol* 7:.

Gillings, M.R. (2013) Evolutionary consequences of antibiotic use for the resistome, mobilome, and microbial pangenome. *Front Microbiol* 4:.

González-Gaya, B., Fernández-Pinos, M.-C., Morales, L., Méjanelle, L., Abad, E., Piña, B., et al. (2016) High atmosphere–ocean exchange of semivolatile aromatic hydrocarbons. *Nat Geosci* 9: 438–442.

González-Gaya, B., Martínez-Varela, A., Vila-Costa, M., Casal, P., Cerro-Gálvez, E., Berrojalbiz, N., et al. (2019) Biodegradation as an important sink of aromatic hydrocarbons in the oceans. *Nat Geosci* 12: 119–125.

Grasshoff, K., Kremling, K., and Ehrhardt, M. (2009) *Methods of Seawater Analysis*, 3rd ed. Kiel: Wiley - VCH.

Gutierrez, T., Singleton, David R., Berry, D., Yang, T., Aitken, M.D., and Teske, A. (2013) Hydrocarbon-degrading bacteria enriched by the Deepwater Horizon oil spill identified by cultivation and DNA-SIP. *ISME J* 7: 2091–2104.

Gutierrez, T., Singleton, David R., Berry, D., Yang, T., Aitken, M.D., and Teske, A. (2013) Hydrocarbon-degrading bacteria enriched by the Deepwater Horizon oil spill identified by cultivation and DNA-SIP. *ISME J* 7: 2091–2104.

Head, I.M., Jones, D.M., and Röling, W.F.M. (2006) Marine microorganisms make a meal of oil. *Nat Rev Microbiol* 4: 173–182.



Huson, D.H., Beier, S., Flade, I., Górska, A., El-Hadidi, M., Mitra, S., et al. (2016) MEGAN Community Edition - Interactive Exploration and Analysis of Large-Scale Microbiome Sequencing Data. *PLOS Comput Biol* 12: e1004957.

Hylland, K. (2006) Polycyclic aromatic hydrocarbon (PAH) ecotoxicology in marine ecosystems. *J Toxicol Environ Health A* 69: 109–123.

Joye, S., Kleindienst, S., Gilbert, J., Handley, K., Weisenhorn, P., Overholt, W., and Kostka, J. (2016) Responses of Microbial Communities to Hydrocarbon Exposures. *Oceanography* 29: 136–149.

King, G.M., Kostka, J.E., Hazen, T.C., and Sobczyk, P.A. (2015) Microbial Responses to the Deepwater Horizon Oil Spill: From Coastal Wetlands to the Deep Sea. *Ann Rev Mar Sci* 7: 377–401.

Kleindienst, S., Grim, S., Sogin, M., Bracco, A., Crespo-Medina, M., and Joye, S.B. (2016) Diverse, rare microbial taxa responded to the Deepwater Horizon deep-sea hydrocarbon plume. *ISME J* 10: 400–415.

Kostka, J.E., Prakash, O., Overholt, W.A., Green, S.J., Freyer, G., Canion, A., et al. (2011) Hydrocarbon-degrading bacteria and the bacterial community response in Gulf of Mexico beach sands impacted by the deepwater horizon oil spill. *Appl Environ Microbiol* 77: 7962–7974.

Lamendella, R., Strutt, S., Borglin, S., Chakraborty, R., Tas, N., Mason, O.U., et al. (2014) Assessment of the Deepwater Horizon oil spill impact on Gulf coast microbial communities. *Front Microbiol* 5: 1–10.

Langmead, B. and Salzberg, S.L. (2012) Fast gapped-read alignment with Bowtie 2. *Nat Methods* 2012 949: 357–359.

Lekunberri, I., Balcázar, J.L., and Borrego, C.M. (2018) Metagenomic exploration reveals a marked change in the river resistome and mobilome after treated wastewater discharges. *Environ Pollut* 234: 538–542.

Lipiatou, E., Tolosa, I., Simó, R., Bouloubassi, I., Dachs, J., Marti, S., et al. (1997) Mass budget and dynamics of polycyclic aromatic hydrocarbons in the Mediterranean Sea. *Deep Sea Res Part II Top Stud Oceanogr* 44: 881–905.

Mallick, S., Chakraborty, J., and Dutta, T.K. (2011) Role of oxygenases in guiding diverse metabolic pathways in the bacterial degradation of low-molecular-weight polycyclic aromatic hydrocarbons : A review Role of oxygenases in guiding diverse metabolic pathways in the bacterial degradation of low-molecula. 7828: 1–10.

Martin, M. (2011) Cutadapt removes adapter sequences from high-throughput sequencing reads. *EMBnet.journal* 17: 10.

Martinez-Varela, A., Cerro-Gálvez, E., Auladell, A., Sharma, S., Moran, M.A., Kiene, R.P., et al. (2021) Bacterial responses to background organic pollutants in the northeast subarctic Pacific Ocean. *Environ Microbiol* 1462-2920.15646.

Mason, O.U., Hazen, T.C., Borglin, S., Chain, P.S.G., Dubinsky, E.A., Fortney, J.L., et al. (2012) Metagenome, metatranscriptome and single-cell sequencing reveal microbial response to Deepwater Horizon oil spill. *ISME J* 6: 1715–1727.

Mason, O.U., Scott, N.M., Gonzalez, A., Robbins-Pianka, A., Bælum, J., Kimbrel, J., et al. (2014) Metagenomics reveals sediment microbial community response to Deepwater Horizon oil spill. *ISME J* 8: 1464–1475.

Mistry, J., Chuguransky, S., Williams, L., Qureshi, M., Salazar, G.A., Sonnhammer, E.L.L., et al. (2021) Pfam: The protein families database in 2021. *Nucleic Acids Res* 49: D412–D419.

Mittal, A. and Singh, P. (2009) Isolation of hydrocarbon degrading bacteria from soils contaminated with crude oil spills | Request PDF. *Indian J Exp Biol* 47: 760–765.

Oksanen, J., Blanchet, G.F., Friendly, M., Kindt, R., Legendre, P., McGlinn, D., et al. (2020) Vegan: Community Ecology Package.

Parada, A.E., Needham, D.M., and Fuhrman, J.A. (2016) Every base matters: assessing small subunit rRNA primers for marine microbiomes with mock communities, time series and global field samples. *Environ Microbiol* 18: 1403–1414.

Poretsky, R., Rodriguez-R, L.M., Luo, C., Tsementzi, D., and Konstantinidis, K.T. (2014) Strengths and Limitations of 16S rRNA Gene Amplicon Sequencing in Revealing Temporal Microbial Community Dynamics. *PLoS One* 9: e93827.

Quast, C., Pruesse, E., Yilmaz, P., Gerken, J., Schweer, T., Yarza, P., et al. (2013) The SILVA ribosomal RNA gene database project: Improved data processing and web-based tools. *Nucleic Acids Res* 41: D590.

R Core Team (2019) R: A Language and Environment for Statistical Computing.

Ribicic, D., Netzer, R., Winkler, A., and Brakstad, O.G. (2018) Microbial communities in seawater from an

Arctic and a temperate Norwegian fjord and their potentials for biodegradation of chemically dispersed oil at low seawater temperatures. *Mar Pollut Bull* 129: 308–317.

Rivers, A.R., Sharma, S., Tringe, S.G., Martin, J., Joye, S.B., and Moran, M.A. (2013) Transcriptional response of bathypelagic marine bacterioplankton to the Deepwater Horizon oil spill. *ISME J* 7: 2315–2329.

Sobecky, P.A. and Hazen, T.H. (2009) Horizontal Gene Transfer and Mobile Genetic Elements in Marine Systems. *Methods Mol Biol* 532: 435–453.

Top, E.M. and Springael, D. (2003) The role of mobile genetic elements in bacterial adaptation to xenobiotic organic compounds. *Curr Opin Biotechnol* 14: 262–269.

Trilla-Prieto, N., Vila-Costa, M., Casas, G., Jiménez, B., and Dachs, J. (2021) Dissolved Black Carbon and Semivolatile Aromatic Hydrocarbons in the Ocean: Two Entangled Biogeochemical Cycles? *Environ Sci Technol Lett* 8: 918–923.

Vila-Costa, M., Cerro-Gálvez, E., Martínez-Varela, A., Casas, G., and Dachs, J. (2020) Anthropogenic dissolved organic carbon and marine microbiomes. *ISME J* 14: 2646–2648.

Wickham, H. (2009) *Ggplot2: Elegant Graphics for Data Analysis.*, 2nd ed. Springer New York.

Wright, M.S., Baker-Austin, C., Lindell, A.H., Stepanauskas, R., Stokes, H.W., and McArthur, J.V. (2008) Influence of industrial contamination on mobile genetic elements: class 1 integron abundance and gene cassette structure in aquatic bacterial communities. *ISME J* 2008 24 2: 417–428.





# 3

## **Large enrichment of anthropogenic organic matter degrading bacteria in the sea-surface microlayer at coastal Livingston Island (Antarctica)**

**Alícia Martínez-Varela**, Gemma Casas, Benjamin Piña, Jordi Dachs and Maria Vila-Costa

Frontiers in Microbiology, 2020

The composition of bacteria inhabiting the sea-surface microlayer (SML) is poorly characterized globally and yet undescribed for the Southern Ocean, despite their relevance for the biogeochemistry of the surface ocean. We report the abundances and diversity of bacteria inhabiting the SML and the subsurface waters (SSL) determined from a unique sample set from a polar coastal ecosystem (Livingston Island, Antarctica). From early to late austral summer (January–March 2018), we consistently found a higher abundance of bacteria in the SML than in the SSL. The SML was enriched in some Gammaproteobacteria genus such as *Pseudoalteromonas*, *Pseudomonas*, and *Colwellia*, known to degrade a wide range of semivolatile, hydrophobic, and surfactant-like organic pollutants. Hydrocarbons and other synthetic chemicals including surfactants, such as perfluoroalkyl substances (PFAS), reach remote marine environments by atmospheric transport and deposition and by oceanic currents, and are known to accumulate in the SML. Relative abundances of specific SML enriched bacterial groups were significantly correlated to concentrations of PFASs, taken as a proxy of hydrophobic anthropogenic pollutants present in the SML and its stability. Our observations provide evidence for an important pollutant-bacteria interaction in the marine SML. Given that pollutant emissions have increased during the Anthropocene, our results point to the need to assess chemical pollution as a factor modulating marine microbiomes in the contemporaneous and future oceans.

## INTRODUCTION

The sea surface microlayer (SML) is the uppermost top layer of the marine water column and constitutes the boundary layer where gases and particles exchange between the sea and the atmosphere (Garbe et al., 2014). As a microenvironment thinner than 1000 mm, the SML exhibits distinct, extreme and variable physicochemical and biological features compared to those in the underlying bulk water. The structure and function of SML bacterial residents, known as bacterioneuston (Naumann, 1917), have been poorly characterized, probably due to logistical limitations and the difficulties for sampling the SML. However, the bacterioneuston is thought to play a central role in the mediation of many air-sea exchange interactions and biogeochemical and climate-related processes at regional and global scales (Kuznetsova and Lee, 2001; Brooks et al., 2009; Nakajima et al., 2013). Far from being a benevolent habitat for microbial life, bacterioneuston withstand intense environmental stressors such as harsh ultra-violet (UV) radiation, wind speed driven turbulences, temperature and salinity gradients, as well as the enrichment of toxic persistent compounds such as heavy metals or hydrophobic organic pollutants (OP) (Guerin, 1989; Wurl and Obbard, 2004; Agogu  et al., 2005; Cincinelli et al., 2005; Garc a-Flor et al., 2005; Ju et al., 2008; Wurl and Holmes, 2008; Stolle et al., 2011; Cunliffe et al., 2013; Engel et al., 2018; Rahlff et al., 2019). In the SML, in addition to an accumulation of hydrophobic organic compounds, there is an enrichment of organic matter (OM) with surfactant properties, both anthropogenic and biogenic. The accumulation of these pools of OM in the SML, which under calm meteorological conditions can even form visible aggregates or surface slicks, can promote bacterial growth (Stolle et al., 2011; Cunliffe et al., 2013; Kurata et al., 2016; Sabbaghzadeh et al., 2017; Engel et al., 2018; Parks et al., 2020). For instance, fast peptide turnovers (Kuznetsova and Lee, 2001) or degradation of hydrocarbons (Coelho et al., 2011) have been observed in the SML.

In terms of community composition, high similarity between subsurface layer (SSL) and SML bacterial community structure have been observed in a number of oceanic regions (Agogu  et al., 2005; Obernosterer et al., 2005; Fan et al., 2018; Z ncker et al., 2018), possibly caused by disruption of the SML and mixing with underlying waters. Uncoupling between bacterioplankton and bacterioneuston community compositions have been observed under low wind speeds conditions and visible surface slicks (Stolle et al.,

2010). As bacterioneuston communities can be transferred from the SML into the atmosphere through sea-spray aerosol, then subject to atmospheric transport, the composition of the SML is a key factor for the regional and global microbial dispersion (Aller et al., 2005; Hervas and Casamayor, 2009; Mayol et al., 2014, 2017; Michaud et al., 2018). The SML is also a direct recipient of atmospherically deposited aerosols, which have been shown to trigger community dissimilarities between SML and SSL bacterial populations in other regions, due to effects of nutrient inputs (Vila-Costa et al., 2013; Astrahan et al., 2016; Marín-Beltrán et al., 2019) and pollination events (Södergren, 1987) on bacterioneuston. The diffusive atmosphere-ocean exchange and snow deposition are the main sources of not only semivolatile OP, such as Polycyclic Aromatic Hydrocarbons (PAH) and polychlorinated biphenyls (Galbán-Malagón et al., 2013; Casal et al., 2018, 2019), but also other hydrophobic and surfactant-like OPs such as perfluoroalkylsubstances (Casal et al., 2017). All these OP become part of the anthropogenic dissolved organic carbon (ADOC) (Vila-Costa et al., 2020) pool, which due to its hydrophobic and surfactant-like properties is enriched in the SML (Cincinelli et al., 2005; Stortini et al., 2009; Casas et al., 2020). The accumulation of ADOC and other surfactant-like organic matter is driven by rising bubbles with chemicals accumulated at the airwater interface and by ADOC attachment to buoyant particles from subsurface waters (Hunter, 2009). Removal processes of ADOC in the SML are volatilization and sea-spray aerosolization (Ehrenhauser et al., 2014), photodegradation (King et al., 2014; Yuan et al., 2019), settling of particulate matter, and microbial degradation (Coelho et al., 2011, 2013).

Ocean microbiomes harbor a subset of bacteria known to play a central role in the biodegradation of ADOC (Head et al., 2006; Berry and Gutierrez, 2017). Acute pollution events, as well as research with isolates, have revealed the genetic battery required for degradation of various families of ADOC constituents by specific taxa, as well as some of the degradation pathways mediated by these strains (Head et al., 2006; Takahashi et al., 2013; Dombrowski et al., 2016). A key microbial strategy that influences the bioavailability of ADOC is the bacterial production of biosurfactants, amphiphilic biomolecules encompassing a large spectrum of chemical families, that facilitate the solubilization and emulsification of ADOC compounds, mostly hydrophobic, or by changing the properties of the bacterial cell wall (Matvyeyeva et al., 2014; Andualem Bezza and Chirwa, 2015; Wittgens et al., 2017). The accumulation of amphiphilic and hydrophobic compounds in the SML modifies its surface tension, thus modifying the rate of air-water diffusive exchange of gases (Salter et al., 2009; Kurata et al., 2016) and atmospheric deposition of aerosols (Del Vento and Dachs, 2007). All these processes depict the SML as a highly dynamic system for interactions between organic matter and bacterioneuston (Wurl and Obbard, 2004), which has not yet been studied in depth, and never addressed for the Southern Ocean.



The goal of this study was to better understand the temporal dynamics and main environmental drivers of bacterial abundance and community composition in the SML in the maritime Antarctica. This was done by comparing, for the first time, SML and SSL community taxonomical structure during the nutrient-rich upwelling summer season in South Bay (Livingston Island, Antarctica). We characterized microbial communities by flow cytometry and 16S rRNA gene sequencing, and correlated the data with different water and air physicochemical variables, as well as perfluoroalkyl substances, taken as surrogates of hydrophobic and surfactant organic matter, as well as the SML stability.

## MATERIALS AND METHODS

### *Site Description and Sampling*

Samples were collected during austral summertime 2018, from January 8th to March 1st, at the South Bay of Livingston Island (South Shetland, Antarctica, 62°39' S, 60°23' W). SML and SSL sampling was conducted from a rigid inflatable boat at five different locations (Figure 1 and Supplementary Table S1). Physicochemical parameters were measured at each sampling station with a CTD probe. The SML was sampled with a glass plate SML sampler. This method was first described by Harvey and Burzell (1972) and has been used in a number of studies for sampling organic matter, microorganisms, surfactants, and organic pollutants related to SML investigations (Knulst et al., 2003; García-Flor et al., 2005; Ju et al., 2008). The pre rinsed plate (40 × 30 cm) was inserted vertically into the water, and then withdrawn slowly allowing the SML adhere onto the glass plate. The glass plate containing the SML sample was then wiped between two polypropylene (PP) plates draining the sample into PP bottles. This process was repeated until obtaining a volume of 1.5 L of SML water. Subsurface layer seawater samples were collected in 2 L PP bottles by submerging the bottles and opening it at 0.5 m depth.

### *Meteorological Data*

The meteorological parameters were provided by the Spanish Meteorological Agency (AEMET) and measured at the meteorological station at Livingston Island (62°39'46.2''S 60°23'24.6''W). The values were averaged coinciding, roughly, with the sampling hours (From 9 am to 11.30 am).

### *Prokaryotic Cell Abundance*

Subsamples of 1.8 mL for quantification of abundances of prokaryotes were fixed with 1% buffered paraformaldehyde solution (pH 7.0) plus 0.05% glutaraldehyde, left at room temperature in the dark for 10 min, and frozen and stored at -80°C until further processing. Prokaryotic cell abundance was estimated by flow cytometry as described elsewhere (Gasol and Morán, 2015).

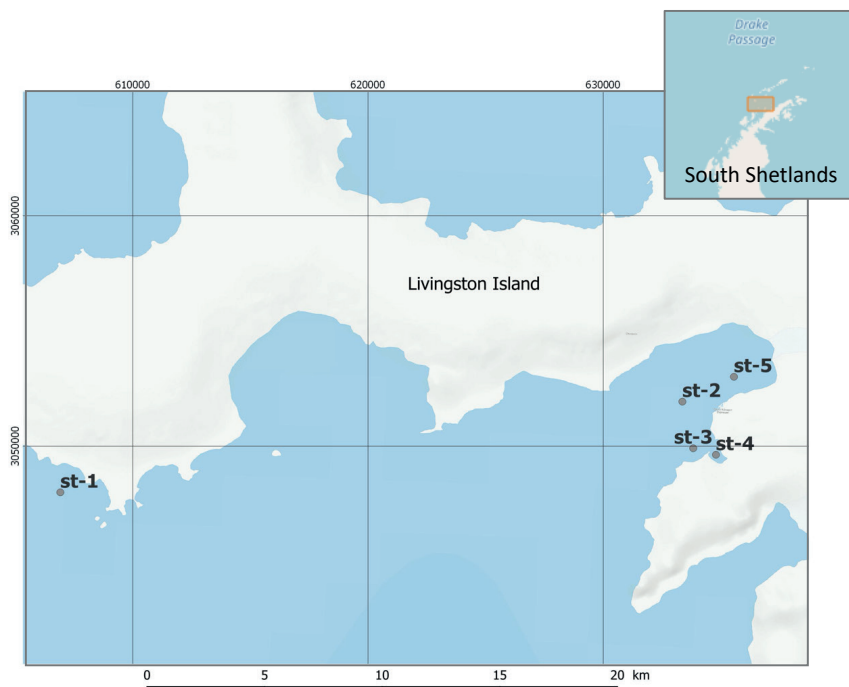


**FIGURE 1** | Location of the sampling stations for the SML and SSL at South Bay of Livingston Island (South Shetlands, Antarctica).

### ***Perfluoroalkyl Compounds Extraction and Detection***

SML and SSL samples were taken simultaneously to the samples used for bacterial analysis. Seawater was analyzed as reported previously (Casal et al., 2017). Briefly, samples were filtered through pre-combusted glass fiber filters (47 mm, GF/F Whatman). The analytes were extracted using solid phase extraction (SPE) with OASIS WAX cartridges (Waters). After loading 500 mL of SML water and 2 L of SSL water through the cartridges, these were stored at -20°C in sealed bags until their elution with methanol, followed by methanol containing 0.1% ammonia in an ultraclean laboratory. PFAS analysis was performed by Ultra Performance Liquid Chromatography tandem triple quadrupole mass spectrometry (UPLC-MS/MS) based on an established method with minor modifications (González-Gaya et al., 2014). Details of methods and results of PFAS in the SML and SSL are reported and discussed elsewhere (Casas et al., 2020) and used here when needed.

### ***Nutrients***

Sub-samples (15 mL) were taken and kept at -20°C for analyzing dissolved inorganic nutrients, nitrate C nitrite ( $\text{NO}_3^- + \text{NO}_2^-$ ), ammonium ( $\text{NH}_4^-$ ) and Phosphate ( $\text{PO}_4^{3-}$ ). Analyses were done by standard segmented flow with colorimetric detection (Grasshoff et al.,

1999) using a SEAL Analyzer AA3 HR. H<sub>3</sub>PO<sub>4</sub> was added to acidify the sample to pH 2 and the ampoules were heat-sealed and stored in the dark at 4°C until analysis. Samples were measured with a SHIMADZU TOC- 5000 analyzer, following the high-temperature catalytic oxidation (HTCO) technique (Cauwet, 1994). For the inorganic nutrients analysis, detection limits (defined as three times the standard deviation of 10 replicates at 50% diluted samples) were 0.006 mM for NO<sub>3</sub><sup>-</sup>, 0.003 mM for NO<sub>2</sub><sup>-</sup>, 0.003 mM for NH<sub>4</sub><sup>+</sup>, and 0.01 mM for PO<sub>4</sub><sup>3-</sup>.

### ***DNA Extraction, Library Preparation, and Taxonomical Identification of 16S rDNA Amplicons***

Samples for 16S rDNA library construction were collected from SML and SSL. 400 mL of each sample were prefiltered through 3 mm pore-size 47 mm diameter polytetrafluoroethylene filters (Millipore, Billerica, MA) to remove grazers and the particle-attached living fraction, and sequentially onto 0.2 mm pore-size 47 mm PTFE (Millipore, Billerica, MA) under filters to capture the free-living bacteria cells fraction, using a peristaltic pump with a flow of <50 mL min<sup>-1</sup>. Each filter was placed in 1 mL lysis buffer (50 mM Tris HCl, 40 mM EDTA, 0.75 M sucrose). All filters were stored at -20°C until further processing. After unthawing samples were incubated with lysozyme, proteinase K and sodium dodecylsulfate (SDS), and nucleic acids were extracted simultaneously with phenol/chloroform/isoamyl alcohol (25: 24: 1 vol: vol: vol) and with chloroform/isoamyl alcohol (24: 1, vol: vol) as described in Vila-Costa et al. (2013). The resulting solution was concentrated to 200 mL using an Amicon Ultra 10-kDa filter unit (Millipore). Partial bacterial 16S gene fragments of both DNA were amplified using primers 515f/926r (Parada et al., 2016) plus adaptors for Illumina MiSeq sequencing. The PCR reaction mixture was thermocycled at 95°C for 3 min, 30 cycles at 95°C for 45 s, 50°C for 45 s, and 68°C for 90 s, followed by a final extension of 5 min at 68°C. PCR amplicon sizes were checked in tris-acetate-EDTA (TAE) agarose gels. Illumina MiSeq sequencing was conducted at the Pompeu Fabra University Sequencing Service.

### ***Bioinformatics***

DADA2 v1.4 was used to differentiate the 16S V4-5 amplicon sequence variants (ASVs) and remove chimeras (parameters: maxN = 0, maxEE = 2.4, truncLen = 227,210; Callahan et al., 2016). DADA2 resolves ASVs by modeling the errors in Illumina-sequenced amplicon reads. The approach is threshold-free, inferring exact variants up to one nucleotide difference using the quality score distribution in a probability model. Previously, spurious sequences and primers were trimmed using cutadapt v.1.16 (Martin, 2011). Taxonomic assignment of the ASVs was performed with the RDP algorithm classifier against RDP database release 11.5 (Cole et al., 2014). ASVs classified as Mitochondria or Chloroplast were removed. The final ASV table contained 46 samples, obtaining for the entire sample set 549,256 amplicon sequence variants (ASV) from 16S rRNA gene V4-5 fragments, from which 12,769 were unique. Unique bacterial ASV averaged 291 and 267 per sample in SML and SSL, respectively.

### **Statistical Analyses**

Statistically significant differences between layers of abiotic and biotic parameters were assessed by Wilcoxon signed-rank test ( $p < 0.05$ ) using the `wilcox.test()` function from “dplyr” package in R. Package “ggpubr” was used for spearman correlations significance ( $p < 0.05$ ) and the bivariate plots from the spearman significant correlations. Shannon Diversity indexes were calculated with `diversity()` function from “vegan v1.4-4” package. Further graphs were carried out using the “ggplot2” package, also in R environment (Wickham, 2009). Enrichment factors in the SML were calculated as the ratio between absolute values in the SML respect to the SSL. Absolute values were calculated multiplying the 16S relative values of each group by the absolute counts of total bacteria obtained by flow cytometry. Fold changes were calculated similarly using the 16S relative values with function `foldchange()` from “gtools” package (R Core Team, 2014).

## **RESULTS AND DISCUSSION**

### **Characterization of the Sampling Domain**

The SML and SSL samples were collected during the Austral summer, from early January to early March in 2018, at five sampling sites of South Bay, Livingston Island (South Shetlands), representative of the maritime Antarctica (Figure 1 and Supplementary Table S1). Over the sampling period, sea surface temperature (SST) averaged  $1.7 \pm 0.4\text{C}$ , and atmospheric temperature and solar radiation were  $2.6 \pm 1.07\text{C}$  and  $62.9 \pm 47.46 \text{Wm}^{-2}$ , respectively (Supplementary Tables S2, S3). Surface seawater from the three most coastal sites (St-3, St-4, and St-5), influenced by terrestrial inputs such as glacial meltdown runoff during the summer season, averaged  $33.5 \pm 0.2$  PSU for salinity,  $7.7 \pm 2$  FTU for turbidity and  $1.6 \pm 0.2\text{C}$  for SST. These values were statistically different ( $p < 0.05$ , Student's t-test) than those from the most off-shore sites (St-1 and St-2) which averaged in surface waters  $34.0 \pm 0.4$  PSU for salinity,  $4.4 \pm 1.4$  FTU for turbidity, and  $2.1 \pm 0.5\text{C}$  for SST. During summer months, strong upwelling events are caused by the Antarctic divergence and westerly winds inducing nutrient rich waters. Dissolved inorganic nitrogen and phosphate measures were within the range of those previously reported in Antarctic surface waters (<10 m) during summer months (Garcia et al., 2013), confirming a non-limited nutrient system. Averaged phosphate ( $\text{PO}_4^{3-}$ ) concentrations showed a significant enrichment in the SML ( $1.7 \pm 0.2 \text{mmolL}^{-1}$  at SML and  $1.4 \pm 0.3 \text{mmolL}^{-1}$  at SSL,  $P = 0.027$ , Paired Wilcoxon test). Conversely, Nitrate C nitrite ( $\text{NO}_3 + \text{NO}_2$ ) concentrations in the SML were not significantly different than in the SSL (averaged  $22 \pm 4.1 \text{mmolL}^{-1}$  at SML and  $19.1 \pm 5.4 \text{mmolL}^{-1}$  at SSL), and ammonium ( $\text{NH}_4^+$ ) showed a large variability across the dataset (averaged  $4.3 \pm 3.7 \text{mmolL}^{-1}$  at SML and  $6.3 \pm 7 \text{mmolL}^{-1}$  at SSL) (Supplementary Table S4 and Supplementary Figure S1).

The level of pollution by anthropogenic dissolved organic carbon was tracked by taking the concentrations of perfluoroalkyl substances (PFASs) as a proxy of ADOC. PFAS are organic synthetic compounds globally distributed by oceanic currents and by atmospheric transport through marine aerosols and deposition (Casal et al., 2017). PFAS

were measured for the same set of samples than bacterioplankton (Casas et al., 2020). Thanks to their amphiphilic nature, PFAS have surfactant properties. In addition, PFAS have been shown to accumulate in planktonic organisms (Casal et al., 2017) due to their hydrophobicity. PFAS also accumulate in the SML (Casas et al., 2020). Surfactants have often been used as surrogates of the occurrence of the SML and its stability (Biffinger et al., 2004; Ju et al., 2008), thus we took PFAS as proxy of a developed SML enriched in ADOC. Specifically, we take the common perfluorooctanesulfonic acid (PFOS) as proxy of a surfactant and anthropogenic chemical. Recently, this compound has also been found to be partially degradable by Antarctic bacteria through desulfurization (Cerro-Gálvez et al., 2020). PFOS concentrations were significantly higher in the SML than in the SSL ( $50.3 \pm 50.8 \text{ pgL}^{-1}$  and  $16.5 \pm 8.7 \text{ pgL}^{-1}$  respectively, paired Wilcoxon test,  $p = 0.009$ ). The concentrations in the SSL are comparable to those reported for this region previously (Casal et al., 2017), and in some regions of the Atlantic, Pacific and Indian Oceans (González-Gaya et al., 2014).

Enrichment factors (EF), defined as the ratio of PFOS concentration in the SML over the SSL, fluctuated from 1.2 up to 26.3 along the time series. PFOS concentration peaked on 27/01/2018 at  $230 \text{ pgL}^{-1}$  at the SML, indicating a very high stable event at the SML over the period 22/01/2018 – 03/02/2018, coinciding with a peak of SST ( $2.47\text{--}1.87\text{C}$ ), atmospheric temperature ( $2.7\text{--}5.6\text{C}$ ) and solar radiation ( $153.8\text{--}136.6 \text{ Wm}^{-2}$ ) on the 27/01/2018 and 28/01/2018. Contrasting with these conditions, on 20/01/2018, 08/02/2018 and 16/02/2018 minor differences between PFOS concentration at both layers were found, consistent with disruption of the SML, possibly caused by wind speed ( $>5 \text{ ms}^{-1}$ ), yielding low SML stability and a breakdown of surface stratification (Supplementary Table S4 and Supplementary Figure S1).

### **Structure of Bacterioplankton and Bacterioplankton Communities**

Pairs of SML and SSL samples showed a significant higher bacterial abundance for bacterioplankton compared to bacterioplankton in all samples (Paired Wilcoxon test,  $P = 0.004$ ), consistent with observations from other oceanic regions and freshwaters (Cunliffe et al., 2013). Enrichment factors averaged  $9.1 \pm 5.8$  for total bacterial abundance. For high and low nucleic acid bacteria (HNA and LNA), the average abundances were  $7.6 \times 10^5 \pm 2.8 \times 10^5 \text{ cells ml}^{-1}$  and  $6.4 \times 10^5 \pm 1.5 \times 10^5 \text{ cells ml}^{-1}$  for SML, and  $1.4 \times 10^5 \pm 6.7 \times 10^4 \text{ cells ml}^{-1}$  and  $4.8 \times 10^4 \pm 2 \times 10^4 \text{ cells ml}^{-1}$  for SSL (**Figure 2**), respectively. Significantly higher enrichment factors were observed for LNA cells compared to HNA cells, with an average  $16.8 \pm 10.6$  for LNA, and  $6.7 \pm 5.1$  for HNA. LNA bacteria, with smaller cell size and lower DNA content, have usually been regarded as the inactive fraction of the microbial community, with observed lower LNA specific growth rates and lower production of cell numbers in enrichment cultures compared to HNA (Wang et al., 2009; Vila-Costa et al., 2012). Higher LNA enrichment in the SML could be explained by the smaller cell size of this bacterial fraction, which becomes an advantageous trait for vertical transportation from subsurface waters and accumulation at the top surface layer (Michaud et al., 2018).

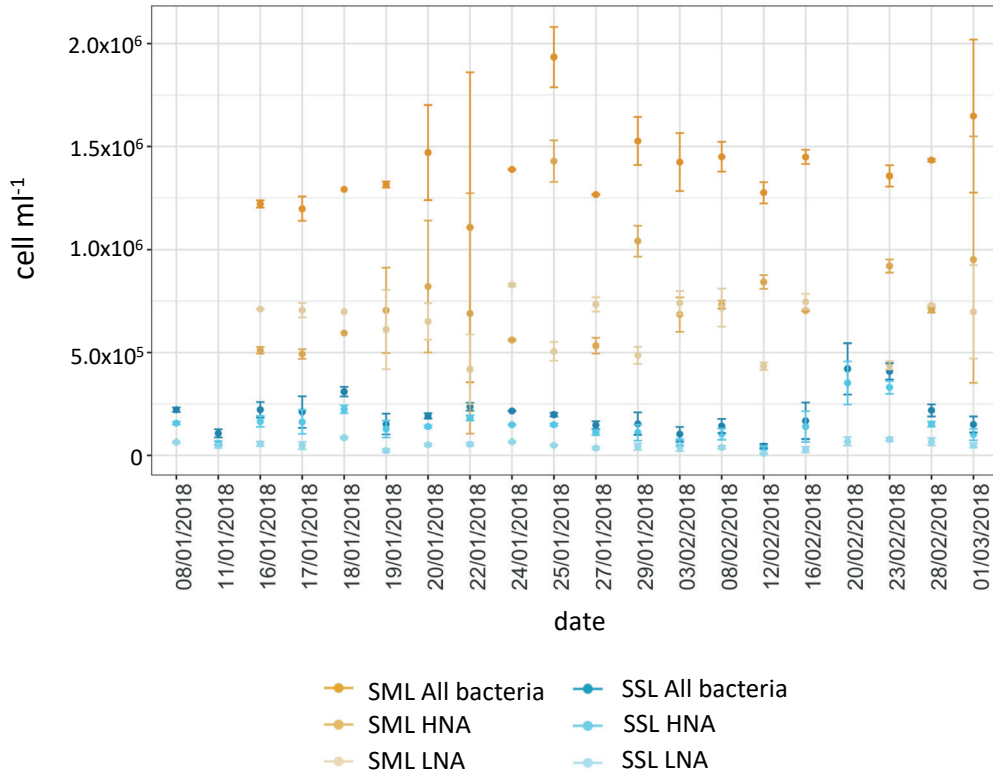


**FIGURE 2 |** Bacterial abundance of LNA, HNA, and total heterotrophic bacteria for SML and SSL during the austral summer. Values are means of duplicates. Error bars show standard deviations.

Significant differences of 16S amplicon sequence variants (ASVs) distribution were observed between sampling stations consistent with the pattern observed with physical and chemical parameters (Permanova test,  $p = 0.001$ , Supplementary Figure S2). While Layer (SML vs. SSL) appeared as a modest, yet significant, source of variability ( $P = 0.044$ ), the interaction of both, sampling Station and Layer, accounted for a significant principal factor of variation ( $P = 0.001$ ). Concerning the biodiversity, the Shannon index averaged  $3.7 \pm 0.7$  at the SML, and  $3.6 \pm 0.6$  at the SSL. Cell abundances were not significantly correlated to 16S diversity indices as it has been observed for the SML at other sites (Zäncker et al., 2018). This suggests a common core microbiome, enriched in the SML, and a limited number of taxa differentiating between layers and sites.

Bacterial assemblages were dominated by Flavobacteriia ( $30.5 \pm 9.5\%$  at SML and  $30.1 \pm 10.1\%$  at SSL), Gammaproteobacteria ( $26.8 \pm 15\%$  at SML and  $26.2 \pm 16.6\%$  at SSL), SAR11 clade ( $17.2 \pm 7.9\%$  at SML and  $16.1 \pm 9.2\%$  at SSL) and Rhodobacterales ( $15.5 \pm 8.1\%$  at SML and  $13.1 \pm 5\%$  at SSL) (Supplementary Figure S3). The bacterial composition of SSL was similar to those described previously in this region (Wilkins et al., 2013; Cavicchioli, 2015).

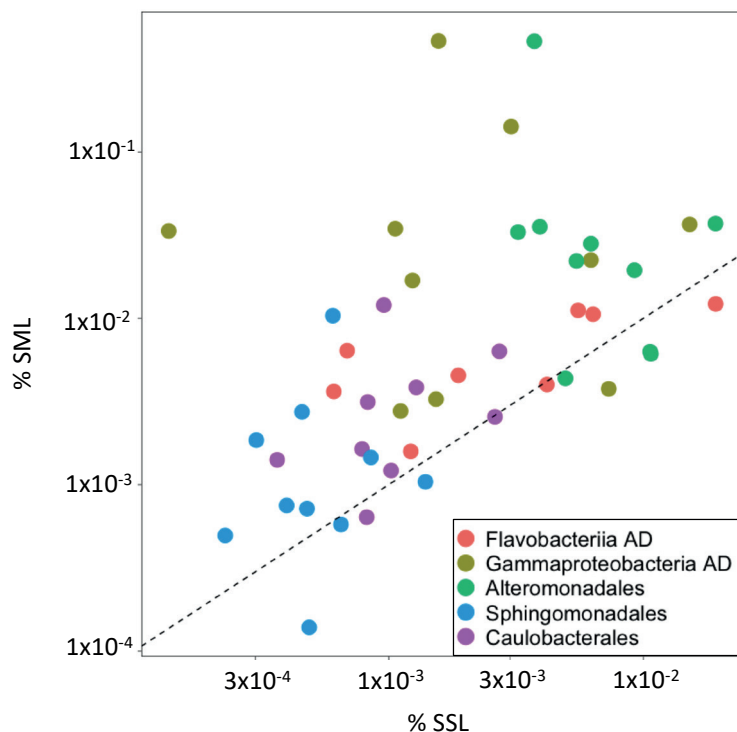


**FIGURE 3** | Relative abundances in the SML vs. SSL for selected taxa. Flavobacteriia AD and Gammaproteobacteria AD were significantly enriched in the SML, while Alteromonadales, Sphingomonadales and Caulobacteriales presented high positive fold changes in the SML ( $FC > 2$ ). Notice the logarithmic scale of the axes. Data points on the 1:1 dashed line indicate equal contribution to the 16S ASV pool.

Both the SML and SSL microbiomes included genera with known facultative and obligate ADOC degraders (AD) strains, some of them also associated with biosurfactant production (see Supplementary Table S5 for details). Relative to the total bacterial community, AD averaged  $12.3 \pm 10.2\%$  at SML and  $10.3 \pm 7.6\%$  at SSL (for relative abundances of AD within their taxonomical group see Supplementary Figure S4). At a finer taxonomic resolution, higher relative abundances of specific AD bacteria, known to be stimulated under high ADOC concentrations, were observed at the SML. The fold change of these groups in the SML vs. the SSL ranged from 1.5 to 50 (**Figures 3, 4**). Specifically, on average, significant higher relative abundances were observed for Gammaproteobacteria AD ( $FC = 10.26$ ) and Flavobacteriia AD ( $FC = 1.68$ ) (Wilcoxon paired data test  $p < 0.05$ ). Other ADOC associated taxonomical groups with  $>2$ -fold increase in relative abundances at the SML for the overall data set were Alteromonadales ( $FC = 6.4$ ), Caulobacteriales ( $FC = 2.5$ ), and Sphingomonadales ( $FC = 2.16$ ) (**Figure 3**). Further, in a day-by-day basis, some gammaproteobacterial groups were systematically highly enriched at SML during the austral summer (**Figure 4**). Gammaproteobacteria AD and the ADOC-associated orders Alteromonadales and Pseudomonadales, taken separately, showed fold changes from  $>5$  to  $>50$  over various sampling days at the SML, and *Pseudoalteromonas*, *Colwellia*, *Pseudomonas*

bloomed at the SML from 24th January onward. *Colwellia*, *Pseudomonas*, and *Pseudoalteromonas* are generalist strains with rapid facultative degrading capabilities toward ADOC, but also prompt to degrade other dissolved organic matter compounds. *Colwellia* have been described as abundant and fast responder following ADOC background concentration exposures in polar environments (Cerro-Gálvez et al., 2019), and to oil spills in marine environments (Gutierrez et al., 2013; Dombrowski et al., 2016; Lofthus et al., 2018; Vergeynst et al., 2018). In fact, *Colwellia* single cell assembled genomes (SAGs) retrieved from contaminated marine sites have revealed a more specific metabolic activity toward aromatic hydrocarbons, as well as a full set of genes involved with chemotaxis, motility and adaptations to cold environments such as Antarctica (Mason et al., 2014).

As some of these taxa are not obligate ADOC consumers, it is relevant to address whether the SML is enriched in dissolved organic carbon (DOC) or only in ADOC and bio-surfactants. Previous works have shown that DOC in seawater from this region had values of  $62 \pm 7$  mmol C L<sup>-1</sup>, while DOC concentrations in the SML were of  $69 \pm 11$  mmol C L<sup>-1</sup> (Calleja et al., 2009; Ruiz-Halpern et al., 2014). So the differences in concentrations are small in terms of bulk DOC. In Antarctica, several works have reported the enrichment of hydrophobic pollutants in the Southern Ocean SML, such as for n-alkanes, PAHs, PCBs, PFAS and phthalates (Cincinelli et al., 2005; Stortini et al., 2009; Casas et al., 2020). A recent work for the Arctic ocean (Chance et al., 2018), did find a specific enrichment of surfactant-like substances in the SML, but not of the total pool of DOC. These reports suggest that the moderate reported enrichment of DOC in the SML, when occurring, may be mostly driven by the fractions of hydrophobic and surfactant-like DOC, but probably not other pools of DOC.

### ***Environmental Drivers of Community Compositions. Can Anthropogenic and Surfactant-Like Organic Compounds Modulate Bacterioneuston Communities?***

Bacterioneuston community composition is controlled by physicochemical and biological parameters, including nutrient concentrations, phytoplankton assemblages and their exudates (Taylor et al., 2014). Bivariate correlations between environmental and bacterial composition variables, considering all measures in the SML and SSL, show that phosphate concentrations were positively correlated to most of the taxonomical groups, and significantly to specific Flavobacteriia AD, while ammonia concentrations were negatively correlated to Bacteroidetes phyla, Flavobacteriia, Alphaproteobacteria, SAR11 Clade and Actinobacteria, pointing to the pivotal role of nutrients as key drivers of microbial compositions (**Figure 5**; Allen et al., 2012; Cavicchioli, 2015). Further, relative abundances of Alteromonadales and Gammaproteobacteria AD were positively correlated to concentrations of PFOS and other PFAS (Spearman correlation,  $p < 0.05$ , Figure 5). Also, Perfluorohexanoic acid (PFHXA) correlated negatively to dominant Rhodobacterales and alphaproteobacterial AD, suggesting toxic consequences of part of ADOC toward these taxa. These correlations are consistent with ADOC modulating the structure of community composition and is aligns with the dual effect of ADOC compounds on marine microor-



ganisms (Head et al., 2006; Rodríguez et al., 2018). From one side, ADOC can be a source of nutrients and organic carbon, and on the contrary, ADOC compounds can induce toxicity to bacteria (see e.g., Cerro-Gálvez et al., 2019, 2020; Vila-Costa et al., 2019). Our observations are consistent with previously documented microbial responses triggered by ADOC pollution events and in chronically polluted marine environments (Head et al., 2006; Hazen et al., 2010; Rivers et al., 2013; Joye et al., 2016).

The specific SML highly enriched taxa, Gammaproteobacteria AD and Flavobacteriia AD, but also ADOC-associated orders such as Alteromonadales and Pseudomonadales, coincide with those taxonomical groups not only known to be capable of degrading ADOC (such as hydrocarbons) or Bacteriomeuston community composition is controlled by physicochemical and biological parameters, including nutrient concentrations, phytoplankton assemblages and their exudates (Taylor et al., 2014). Bivariate correlations between environmental and bacterial composition variables, considering all measures in the SML and SSL, show that phosphate concentrations were positively correlated to most of the taxonomical groups, and significantly to specific Flavobacteriia AD, while ammonia concentrations were negatively correlated to Bacteroidetes phyla, Flavobacteriia, Alphaproteobacteria, SAR11 Clade and Actinobacteria, pointing to the pivotal role of nutrients as key drivers of microbial compositions (Figure 5; Allen et al., 2012; Cavicchioli, 2015).

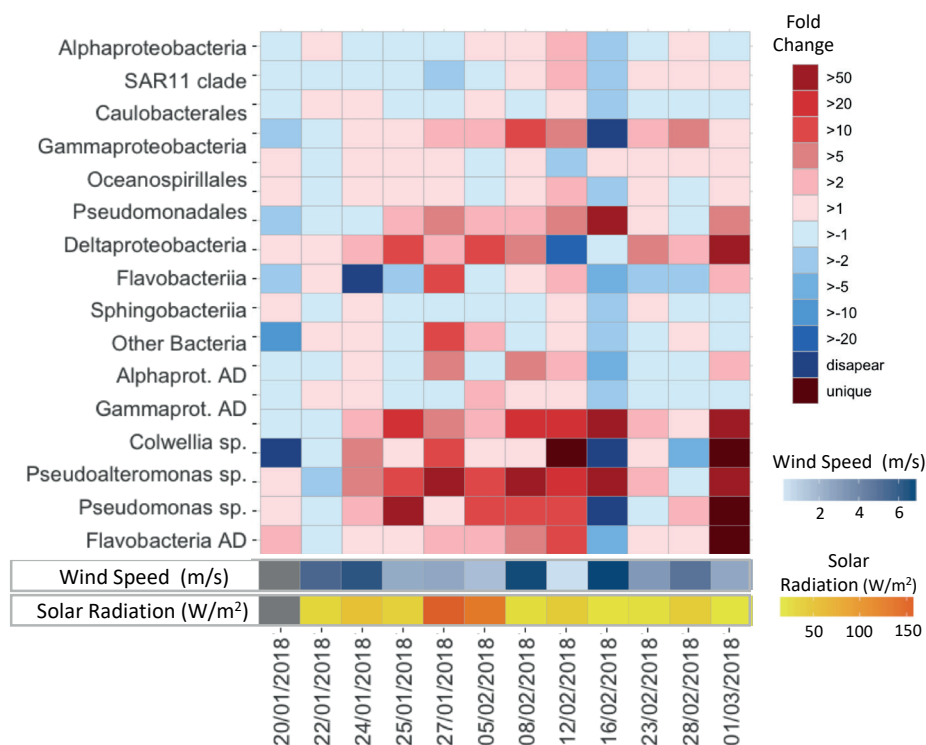


**FIGURE 4 |** Fold change values in relative abundances of specific taxa in the SML vs. SSL during the austral summer.

Further, relative abundances of Alteromonadales and Gammaproteobacteria AD were positively correlated to concentrations of PFOS and other PFAS (Spearman correlation,  $p < 0.05$ , Figure 5). Also, Perfluorohexanoic acid (PFHXA) correlated negatively to dominant Rhodobacterales and alphaproteobacterial AD, suggesting toxic consequences of part of ADOC toward these taxa. These correlations are consistent with ADOC modulating the structure of community composition and is aligns with the dual effect of ADOC compounds on marine microorganisms (Head et al., 2006; Rodríguez et al., 2018). From one side, ADOC can be a source of nutrients and organic carbon, and on the contrary, ADOC compounds can induce toxicity to bacteria (see e.g., Cerro-Gálvez et al., 2019, 2020; Vila-Costa et al., 2019). Our observations are consistent with previously documented microbial responses triggered by ADOC pollution events and in chronically polluted marine environments (Head et al., 2006; Hazen et al., 2010; Rivers et al., 2013; Joye et al., 2016).

The specific SML highly enriched taxa, Gammaproteobacteria AD and Flavobacteriia AD, but also ADOC-associated orders such as Alteromonadales and Pseudomonadales, coincide with those taxonomical groups not only known to be capable of degrading ADOC (such as hydrocarbons) or that have been observed to be stimulated by the presence of oil (Hazen et al., 2010; Neethu et al., 2019) but also with a described resistance to oxidative stress situations such as those originated by UV radiation (Alonso-Sáez et al., 2006; Ruiz-González et al., 2013; Svenningsen et al., 2015). The presence of ROS-resistant ADOC-degrading bacterioneuston have been reported in other studies in aquatic environments, proving ADOC metabolism at the SML (Guerin, 1989; Coelho et al., 2011). To our knowledge, this is the first report of their occurrence in polar regions.

The consistently significant higher enrichment of taxonspecific ADOC degraders at the SML than other taxa in a day-by-day basis coincides with the taxa found at low relative abundances (<3%) in the underlying SSL (examples of these are: on the 25/01/2018 *Pseudomonas* accounted for 6.3% at SML and 0.1% at the SSL; on the 16/02/2018 *Pseudomonas* accounted for 46.2% at SML and 0.03% at SSL, among others). This is consistent with the observed growth of ADOC stimulated rare biosphere after oil spills and under ADOC exposure at environmental levels (Wang et al., 2017; Cerro-Gálvez et al., 2019). This large repository of dormant and low abundance bacterial taxa are part of a local seed bank which specially benefits from ecosystem variations such as sudden growth substrate availability or environmental advantageous conditions (Galand and Logez, 2019). The large temporal and spatial variability of the SML may favor the occasional or opportunistic growth of these taxa. In our data set, low abundant taxa (<3%) represented a pool of 2433 and 2546 unique ASVs at the SML and SSL respectively, with 718 ASV shared between both low abundance ASV pools (Figure 6). On the other side, abundant ASVs pools included 18 unique ASV for both layers, and all of them were also present at the low abundance ASV pools. These results point to a rapid growth of opportunist or specialist species at the SML, possibly recruited and transported vertically from the underlying bulk water low abundance biosphere, and with the required resistance traits or fast UV-repair mechanism to withstand SML extreme environmental conditions.

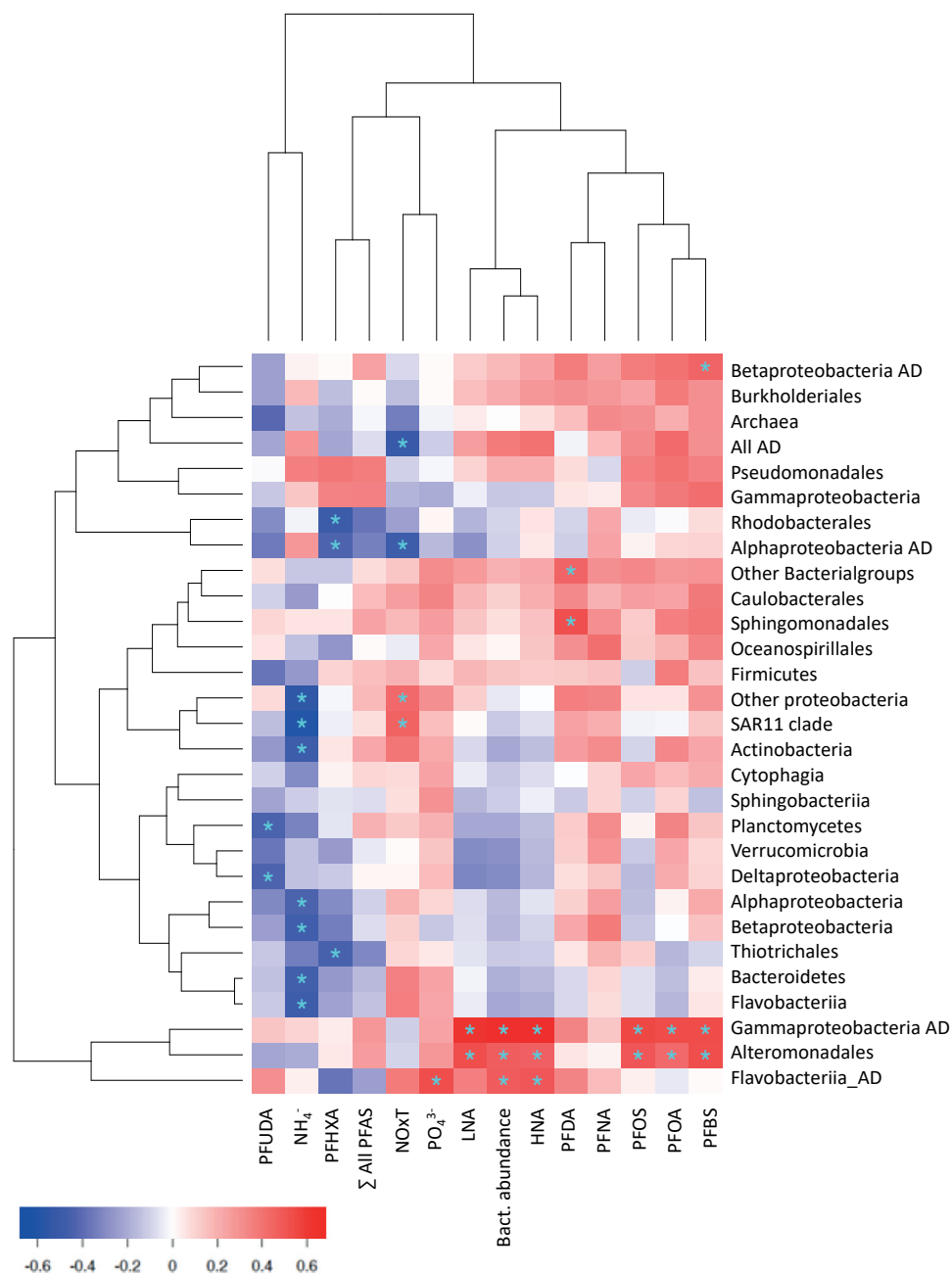


**FIGURE 5 |** Correlation map between nutrients, PFAS and bacterial abundances and prevalence of bacterial groups. Red and blue sectors represent positive and negative correlations, asterisks indicate significant correlations (Spearman correlation,  $p < 0.05$ ). In the x axis: PFUDA, Perfluoroundecanoic acid; PFHXA, Perfluorohexanoic acid; PFDA, Perfluorodecanoic acid; PFNA, Perfluorononanoic acid; PFOS, Perfluorooctane sulfonate; PFOA, Perfluorooctanoic Acid; PFBS, Perfluorobutane sulfonate; LNA, Low Nucleic Acid; HNA, High Nucleic Acid.

Many of the taxa described as ADOC degraders have also been reported to be biosurfactant producers (Supplementary Table S5). Biosurfactants play a role by both promoting ADOC degradation and their detoxification. On the other hand, their amphiphilic properties favor their accumulation in the surface microlayer. The observation of large enrichments of ADOC degrading taxa may lead to a dynamic synergistic interaction between bacteria, pollutants and surfactants. The latter may also have contributions from other planktonic groups (Zutic et al., 1981; Wurl et al., 2009). All these processes may show a synergy favoring the fast turnover of ADOC in the marine environment, and future work is required to elucidate its relevance.

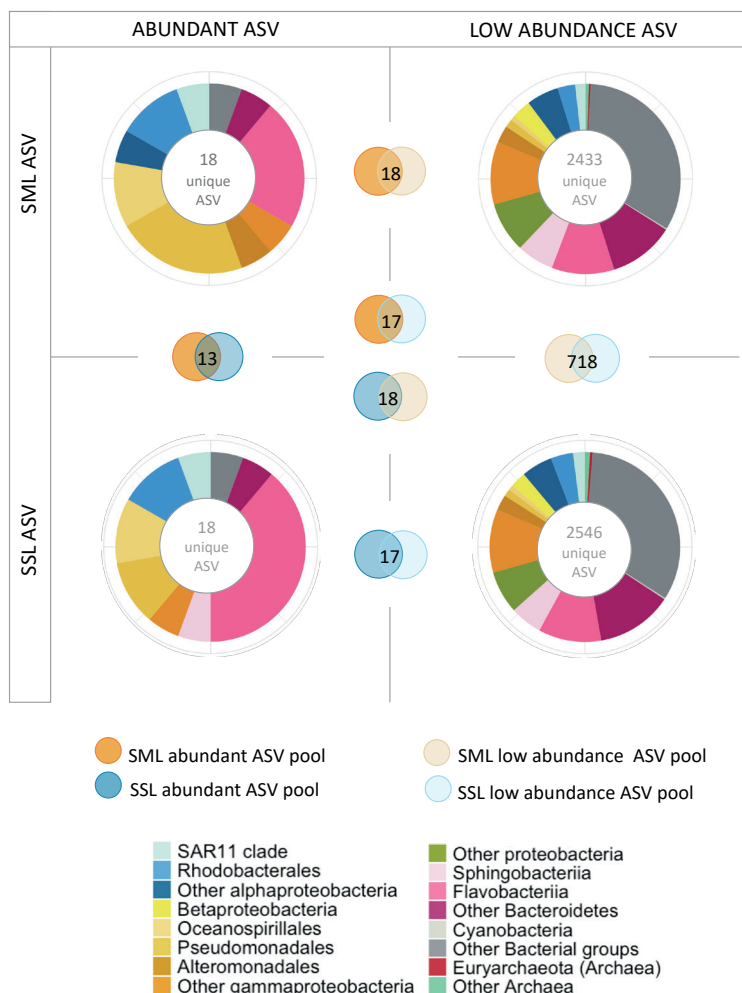


**FIGURE 6** | Low abundance and abundant taxa analysis based on 16S rDNA ASV counts. Taxonomical distribution of main taxonomical groups assigned to ASVs with high abundances (>3%) and low abundances (<3%). Overlapping circles indicate the number of unique ASVs shared in the different abundance pools.

## CONCLUSIONS

We analyzed the bacterial community composition and abundance in paired SML and SSL samples over the austral summer in coastal seawater of Livingston Island (South Shetlands, Antarctica), together with chemical and physical measurements. Whereas total bacterial abundances were higher in the SML than in the SSL, both layers shared a similar taxa composition, which varied spatially among sampling sites. The main significant differences between SML and SSL samples from the same site corresponded to higher relative abundances at the SML of taxa reported to be ADOC degraders, such as Gammaproteobacteria AD and Flavobacteriia AD, and ADOC-associated orders Alteromonadales, Caulobacterales and Sphingomonadales. These taxa showed remarkably higher SML enrichments than the rest of the microbiome. In a day-by-day analysis, we observed that specific gammaproteobacteria taxa were systematically enriched at the SML, while the same taxa were found at low relative abundances in the underlying bulk water, supporting the hypothesis that bacterioneuston composition might be directly sourced from differing adjacent environments indigenous bacterial communities belonging to a low abundant or even rare biosphere. We found significant positive correlations between the relative abundances of Alteromonadales, Gammaproteobacteria AD and Sphingomonadales and the concentrations of PFOS, used as a proxy of hydrophobic and surfactant-like ADOC. These results suggested that ADOC is a vector modulating bacterial compositions in the SML. While UV radiation, wind speed and organic matter have been proposed as the main influences determining bacterioneuston community composition (Agogué et al., 2005; Stolle et al., 2011; Rahlff et al., 2019), our findings provide field evidence that ADOC accumulation at the SML could also be another, although neglected, community composition driver. ADOC, as a double-edged sword, can become potential growth substrate for microorganisms, but also act as a toxic agent and hamper bacterial growth of other taxa. Our results suggest that, due to its unique interphase position, SML will respond sensitively to an increasing arrival and accumulation of anthropogenic organic pollution to the oceans. While bacterioneuston plays a central role in mediating biogeochemical processes at global scale, chronic ADOC pollution SML enrichments might modify the bacterioneuston's bioreactor functioning, with a relevant biogeochemical role in the surface ocean.

## ACKNOWLEDGEMENTS

We thank the staff of the Marine Technology Unit (UTM-CSIC for their logistical support during the sampling campaign at Livingston Island. Special thanks to TERNUA for their non-profit collaboration by sponsoring with technical eco-friendly clothing and gear equipment for Antarctic campaigns and for increasing our project visibility.

## AUTHOR CONTRIBUTION

A.M.-V., M.V.-C. and J.D. designed the sampling strategy and wrote the manuscript. A.M.-V., G.C., and J.D. conducted the field sampling. A.M.-V. performed the molecular work and data analyses. G.C. quantified the PFAS concentrations. B.P. and A.M.-V. performed the statistical analyses. All authors discussed the results and implications and commented on the final version of the manuscript.

## REFERENCES

- Agogué, H., Casamayor, E. O., Bourrain, M., Obernosterer, I., Joux, F., Herndl, G. J., et al. (2005). A survey on bacteria inhabiting the sea surface microlayer of coastal ecosystems. *FEMS Microbiol. Ecol.* 54, 269–280. doi: 10.1016/j.femsec. 2005.04.002
- Allen, L. Z., Allen, E. E., Badger, J. H., McCrow, J. P., Paulsen, I. T., Elbourne, L. D., et al. (2012). Influence of nutrients and currents on the genomic composition of microbes across an upwelling mosaic. *ISME J.* 6, 1403–1414. doi: 10.1038/ismej.2011.201
- Aller, J. Y., Kuznetsova, M. R., Jahns, C. J., and Kemp, P. F. (2005). The sea surface microlayer as a source of viral and bacterial enrichment in marine aerosols. *J. Aerosol Sci.* 36, 801–812. doi: 10.1016/j.jaerosci.2004.10.012
- Alonso-Sáez, L., Gasol, J. M., Lefort, T., Hofer, J., and Sommaruga, R. (2006). Effect of natural sunlight on bacterial activity and differential sensitivity of natural bacterioplankton groups in Northwestern Mediterranean coastal waters. *Appl. Environ. Microbiol.* 72, 5806–5813. doi: 10.1128/aem.00597-06
- Andualem Bezza, F., and Chirwa, E. M. N. (2015). Biosurfactant-enhanced bioremediation of aged polycyclic aromatic hydrocarbons (PAHs) in creosote contaminated soil. *Chemosphere* 144, 635–644. doi: 10.1016/j.chemosphere. 2015.08.027
- Astrahan, P., Herut, B., Paytan, A., and Rahav, E. (2016). The impact of dry atmospheric deposition on the sea-surface microlayer in the SE Mediterranean sea: an experimental approach. *Front. Mar. Sci.* 3:222. doi: 10.3389/fmars.2016. 00222
- Berry, D., and Gutierrez, T. (2017). Evaluating the detection of hydrocarbon-degrading bacteria in 16S rRNA gene sequencing surveys. *Front. Microbiol.* 8:896.
- Biffinger, J. C., Kim, H. W., and DiMugno, S. G. (2004). The polar hydrophobicity of fluorinated compounds. *Chembiochem* 5, 622–627. doi: 10.1002/cbic. 200300910
- Brooks, I. M., Yelland, M. J., Upstill-Goddard, R. C., Nightingale, P. D., Archer, S., d’Asaro, E., et al. (2009). Supplement to physical exchanges at the air-sea interface: UK-SOLAS field measurements. *Bull. Am. Meteorol. Soc.* 90, 629–644.
- Callahan, B. J., McMurdie, P. J., Rosen, M. J., Han, A. W., Johnson, A. J. A., and Holmes, S. P. (2016). DADA2: high-resolution sample inference from Illumina amplicon data. *Nat. Methods* 13, 581–583. doi: 10.1038/nmeth.3869
- Calleja, M. L., Duarte, C. M., Prairie, Y. T., Agustí, S., and Herndl, G. J. (2009). Evidence for surface organic matter modulation of air-sea CO<sub>2</sub> gas exchange. *Biogeosciences* 6, 1105–1114. doi: 10.5194/bg-6-1105-2009
- Casal, P., Cabrerizo, A., Vila-Costa, M., Jiménez, B., and Dachs, J. (2018). Pivotal role of snow deposition and melting driving fluxes of polycyclic aromatic hydrocarbons at coastal Livingston Island (Antarctica). *Environ. Sci. Technol.* 52, 12327–12337.

Casal, P., Casas, G., Vila-Costa, M., Cabrerizo, A., Pizarro, M., Jiménez, B., et al. (2019). Snow amplification of persistent organic pollutants at coastal Antarctica. *Environ. Sci. Technol.* 53, 8872–8882. doi: 10.1021/acs.est.9b03006

Casal, P., Zhang, Y., Martin, J. W., Pizarro, M., Jiménez, B., and Dachs, J. (2017). Role of snow deposition of perfluoroalkylated substances in the surface microlayer at coastal Livingston Island (Maritime Antarctica). *Environ. Sci. Technol.* 51, 8460–8470. doi: 10.1021/acs.est.7b02521

Casas, G., Martínez-Varela, A., Roscales, J. L., Vila-Costa, M., Dachs, J., and Jimenez, B. (2020). Enrichment of perfluoroalkyl substances in the surface microlayer and sea-spray aerosols in the Southern Ocean. *Environ. Pollut.* doi: 10.1016/j.envpol.2020.115512

Cavicholi, R. (2015). Microbial ecology of Antarctic aquatic systems. *Nat. Rev. Microbiol.* 13, 691–706.

Cauwet, G. (1994). HTO method for dissolved organic carbon analysis in seawater: influence of catalyst on blank estimation. *Mar. Chem.* 47, 55–64.

Cerro-Gálvez, E., Casal, P., Lundin, D., Piña, B., Pinhassi, J., Dachs, J., et al. (2019). Microbial responses to anthropogenic dissolved organic carbon in the Arctic and Antarctic coastal seawaters. *Environ. Microbiol.* 21, 1466–1481. doi: 10.1111/1462-2920.14580

Cerro-Gálvez, E., Roscales, J. L., Jiménez, B., Sala, M. M., Dachs, J., and Vila-Costa, M. (2020). Microbial responses to perfluoroalkyl substances and perfluorooctanesulfonate (PFOS) desulfurization in the Antarctic marine environment. *Water Res.* 171:115434. doi: 10.1016/j.watres.2019.115434

Chance, R. J., Hamilton, J. F., Carpenter, L. J., Hackenberg, S. C., Andrews, S. J., and Wilson, T. W. (2018). Water-soluble organic composition of the Arctic Sea surface microlayer and association with ice nucleation ability. *Environ. Sci. Technol.* 52, 1817–1826. doi: 10.1021/acs.est.7b04072

Cincinelli, A., Stortini, A. M., Checchini, L., Martellini, T., Del Bubba, M., and Lepri, L. (2005). Enrichment of organic pollutants in the sea surface microlayer (SML) at Terra Nova Bay, Antarctica: influence of SML on superficial snow composition. *J. Environ. Monit.* 7, 1305–1312. doi: 10.1039/b507321a

Coelho, F., Sousa, S., Santos, L., Santos, A., Almeida, A., Gomes, N., et al. (2011). Exploring hydrocarbon-oclastic bacterial communities in the estuarine surface microlayer. *Aquat. Microb. Ecol.* 64, 185–195. doi: 10.3354/ame01526

Coelho, F. J. R. C., Santos, A. L., Coimbra, J., Almeida, A., Cunha, Â., Cleary, D. F. R., et al. (2013). Interactive effects of global climate change and pollution on marine microbes: the way ahead. *Ecol. Evol.* 3, 1808–1818. doi: 10.1002/ece3.565

Cole, J. R., Wang, Q., Fish, J. A., Chai, B., Mcgarrell, D. M., Sun, Y., et al. (2014). Ribosomal Database Project: data and tools for high throughput rRNA analysis. *Nucleic Acids Res.* 42, D633–D642.

Cunliffe, M., Engel, A., Frka, S., Gašparovič, B. Ž., Guitart, C., Murrell, J. C., et al. (2013). Sea surface microlayers: a unified physicochemical and biological perspective of the air-ocean interface. *Prog. Oceanogr.* 109, 104–116. doi: 10.1016/j.pocean.2012.08.004

Del Vento, S., and Dachs, J. (2007). Influence of the surface microlayer on atmospheric deposition of aerosols and polycyclic aromatic hydrocarbons. *Atmos. Environ.* 41, 4920–4930. doi: 10.1016/j.atmosenv.2007.01.062

Dombrowski, N., Donaho, J. A., Gutierrez, T., Seitz, K. W., Teske, A. P., and Baker, B. J. (2016). Reconstructing metabolic pathways of hydrocarbon-degrading bacteria from the Deepwater Horizon oil spill. *Nat. Microbiol.* 1:16057.

Ehrenhauser, F. S., Avij, P., Shu, X., Dugas, V., Woodson, I., Liyana-Arachchi, T., et al. (2014). Bubble bursting as an aerosol generation mechanism during an oil spill in the deep-sea environment: laboratory experimental demonstration of the transport pathway. *Environ. Sci. Process. Impacts* 16, 65–73. doi: 10.1039/c3em00390f

Engel, A., Sperling, M., Sun, C., Grosse, J., and Friedrichs, G. (2018). Organic matter in the surface microlayer: insights from a wind wave channel experiment. *Front. Mar. Sci.* 5:182. doi: 10.3389/fmars.2018.00182

Fan, J., Li, H., Chang, Y., Wang, X., Ming, H., Su, J., et al. (2018). Spatial analysis of bacteriouneston and bacterioplankton diversity in the north China Sea. *Aquat. Ecosyst. Health Manag.* 21, 1–9. doi: 10.1080/14634988.2017.1400360

Galand, P. E., and Logares, R. (2019). “Ecology of rare microorganisms,” in *Encyclopedia of Microbiology*, ed. T. Schmidt (Amsterdam: Elsevier), 90–96.

Galbán-Malagón, C. J., Del Vento, S., Berrojalbiz, N., Ojeda, M.-J., and Dachs, J. (2013). Polychlorinated biphenyls, hexachlorocyclohexanes and hexachlorobenzene in seawater and phytoplankton from the Southern

Ocean (Weddell, South Scotia, and Bellingshausen Seas). *Environ. Sci. Technol.* 47, 5578–5587. doi: 10.1021/es400030q

Garbe, C., Rutgersson, A., Boutin, J., Leeuw, G., and Delille, B. (2014). “Transfer across the air-sea interface,” in *Ocean-Atmosphere Interactions of Gases and Particles*, eds P. Liss and M. Johnson (Berlin: Springer), 55–112.

Garcia, H. E., Locarnini, R. A., Boyer, T. P., Antonov, J. I., Baranova, O. K., Zweng, M. M., et al. (2013). “Dissolved inorganic nutrients (phosphate, nitrate, silicate),” in *World Ocean Atlas 2013*, Vol. 76, eds S. Levitus and A. Mishonov (Silver Spring, MD: NESDIS), 25.

García-Flor, N., Guitart, C., Ábalos, M., Dachs, J., Bayona, J. M., and Albaigés, J. (2005). Enrichment of organochlorine contaminants in the sea surface microlayer: an organic carbon-driven process. *Mar. Chem.* 96, 331–345. doi: 10.1016/j.marchem.2005.01.005

Gasol, J. M., and Morán, X. A. G. (2015). “Flow cytometric determination of microbial abundances and its use to obtain indices of community structure and relative activity,” in *Hydrocarbon and Lipid Microbiology Protocols*, eds T.

McGenity, K. Timmis, and B. Nogales (Berlin: Springer), 159–187. doi: 10.1007/8623\_2015\_139

González-Gaya, B., Dachs, J., Roscales, J. L., Caballero, G., and Jiménez, B. (2014). Perfluoroalkylated substances in the global tropical and subtropical surface oceans. *Environ. Sci. Technol.* 48, 13076–13084. doi: 10.1021/es503490z

Grasshoff, K., Kremling, K., and Ehrhardt, M. (1999). *Methods of Seawater Analysis*, 3rd Edn. Weinheim:Wiley-VCH.

Guerin, W. F. (1989). Phenanthrene degradation by estuarine surface microlayer and bulk water microbial populations. *Microb. Ecol.* 17, 89–104. doi: 10.1007/bf02025596

Gutierrez, T., Singleton, D. R., Berry, D., Yang, T., Aitken, M. D., and Teske, A. (2013). Hydrocarbon-degrading bacteria enriched by the Deepwater Horizon oil spill identified by cultivation and DNA-SIP. *ISME J.* 7, 2091–2104. doi: 10.1038/ismej.2013.98

Harvey, G. W., and Burzell, L. A. (1972). A simple microlayer method for small samples. *Limnol. Oceanogr.* 17, 156–157. doi: 10.4319/lo.1972.17.1.0156

Hazen, T. C., Dubinsky, E. A., Desantis, T. Z., Andersen, G. L., Piceno, Y. M., Singh, N., et al. (2010). Deep-sea oil plume enriches indigenous oil-degrading bacteria. *Science* 330, 204–208. doi: 10.1126/science.1195979

Head, I. M., Jones, D. M., and Röling, W. F. M. (2006). Marine microorganisms make a meal of oil. *Nat. Rev. Microbiol.* 4, 173–182. doi: 10.1038/nrmicro1348

Hervas, A., and Casamayor, E. O. (2009). High similarity between bacterioneuston and airborne bacterial community compositions in a high mountain lake area. *FEMS Microbiol. Ecol.* 67, 219–228. doi: 10.1111/j.1574-6941.2008.00617.x

Hunter, K. A. (2009). “Chemistry of the sea-surface microlayer,” in *The Sea Surface and Global Change*, eds P. S. Liss and R. A. Duce (Cambridge: Cambridge University Press), 287–320. doi: 10.1017/cbo9780511525025.010

Joye, S., Kleindienst, S., Gilbert, J., Handley, K., Weisenhorn, P., Overholt, W., et al. (2016). Responses of microbial communities to hydrocarbon exposures. *Oceanography* 29, 136–149. doi: 10.5670/oceanog.2016.78

Ju, X., Jin, Y., Sasaki, K., and Saito, N. (2008). Perfluorinated surfactants in surface, subsurface water and microlayer from dalian coastal waters in China. *Environ. Sci. Technol.* 42, 3538–3542. doi: 10.1021/es703006d

King, S. M., Leaf, P. A., Olson, A. C., Ray, P. Z., and Tarr, M. A. (2014). Photolytic and photocatalytic degradation of surface oil from the Deepwater Horizon spill. *Chemosphere* 95, 415–422. doi: 10.1016/j.chemosphere.2013.09.060

Knulst, J. C., Rosenberger, D., Thompson, B., and Paatero, J. (2003). Intensive sea surface microlayer investigations of open leads in the pack ice during Arctic Ocean 2001 expedition. *Langmuir* 19, 10194–10199. doi: 10.1021/la035069%2B

Kurata, N., Vella, K., Hamilton, B., Shivji, M., Soloviev, A., Matt, S., et al. (2016). Surfactant-associated bacteria in the near-surface layer of the ocean. *Sci. Rep.* 6:19123.

Kuznetsova, M., and Lee, C. (2001). Enhanced extracellular enzymatic peptide hydrolysis in the sea-surface microlayer. *Mar. Chem.* 73, 319–332. doi: 10.1016/s0304-4203(00)00116-x



Lofthus, S., Netzer, R., Lewin, A. S., Heggset, T. M. B., Haugen, T., and Brakstad, O. G. (2018). Biodegradation of n-alkanes on oil–seawater interfaces at different temperatures and microbial communities associated with the degradation. *Biodegradation* 29, 141–157. doi: 10.1007/s10532-018-9819-z

Marín-Beltrán, I., Logue, J. B., Andersson, A. F., and Peters, F. (2019). Atmospheric deposition impact on bacterial community composition in the NW Mediterranean. *Front. Microbiol.* 10:858. doi: 10.3389/fmicb.2019.00858

Martin, M. (2011). Cutadapt removes adapter sequences from high-throughput sequencing reads. *EMBnet J.* 17:10. doi: 10.14806/ej.17.1.200

Mason, O. U., Han, J., Woyke, T., and Jansson, J. K. (2014). Single-cell genomics reveals features of a *Colwellia* species that was dominant during the Deepwater Horizon oil spill. *Front. Microbiol.* 5:332. doi: 10.3389/fmicb.2014.00332

Matvyeyeva, O. L., Vasylychenko, Î. À., and Aliievà, O. R. (2014). Microbial biosurfactants role in oil products biodegradation. *Int. J. Environ. Bioremediat. Biodegrad.* 2, 69–74.

Mayol, E., Arrieta, J. M., Jiménez, M. A., Martínez-Asensio, A., Garcias-Bonet, N., Dachs, J., et al. (2017). Long-range transport of airborne microbes over the global tropical and subtropical ocean. *Nat. Commun.* 8:201.

Mayol, E., Jiménez, M. A., Herndl, G. J., Duarte, C. M., and Arrieta, J. M. (2014). Resolving the abundance and air–sea fluxes of airborne microorganisms in the North Atlantic Ocean. *Front. Microbiol.* 5:557. doi: 10.3389/fmicb.2014.00557

Michaud, J. M., Thompson, L. R., Kaul, D., Espinoza, J. L., Richter, R. A., Xu, Z. Z., et al. (2018). Taxon-specific aerosolization of bacteria and viruses in an experimental ocean-atmosphere mesocosm. *Nat. Commun.* 9:2017.

Nakajima, R., Tsuchiya, K., Nakatomi, N., Yoshida, T., Tada, Y., Konno, F., et al. (2013). Enrichment of microbial abundance in the sea-surface microlayer over a coral reef: implications for biogeochemical cycles in reef ecosystems. *Mar. Ecol. Prog. Ser.* 490, 11–22.

Naumann, E. (1917). Beiträge zur kenntnis des teichnannoplanktons, I. I. Über das neuston des süßwassers. *Biol. Cent* 37, 98–106.

Neethu, C. S., Saravanakumar, C., Purvaja, R., Robin, R. S., and Ramesh, R. (2019). Oil-spill triggered shift in indigenous microbial structure and functional dynamics in different marine environmental matrices. *Sci. Rep.* 9:1354.

Obernosterer, I., Catala, P., Reinthaler, T., Herndl, G. J., and Lebaron, P. (2005). Enhanced heterotrophic activity in the surface microlayer of the Mediterranean Sea. *Aquat. Microb. Ecol.* 39, 293–302.

Parada, A. E., Needham, D. M., and Fuhrman, J. A. (2016). Every base matters: assessing small subunit rRNA primers for marine microbiomes with mock communities, time series and global field samples. *Environ. Microbiol.* 18, 1403–1414.

Parks, G., Dean, C. W., Kluge, J. A., Soloviev, A. V., Shivji, M., Tartar, A., et al. (2020). Analysis of surfactant-associated bacteria in the sea surface microlayer using deoxyribonucleic acid sequencing and synthetic aperture radar. *Int. J. Remote Sens.* 41, 3886–3901.

R Core Team (2014). *R: A Language and Environment for Statistical Computing*. Vienna: R Foundation for Statistical Computing

Rahlf, J., Stolle, C., Giebel, H.-A., Ribas-Ribas, M., Damgaard, L. R., and Wurl, O. (2019). Oxygen profiles across the sea-surface microlayer—effects of diffusion and biological activity. *Front. Mar. Sci.* 6:11. doi: 10.3389/fmars.2019.00011

Rivers, A. R., Sharma, S., Tringe, S. G., Martin, J., Joye, S. B., and Moran, M. A. (2013). Transcriptional response of bathypelagic marine bacterioplankton to the Deepwater Horizon oil spill. *ISME J.* 7, 2315–2329.

Rodríguez, J., Gallampois, C. M. J., Timonen, S., Andersson, A., Sinkko, H., Haglund, P., et al. (2018). Effects of organic pollutants on bacterial communities under future climate change scenarios. *Front. Microbiol.* 9:2926. doi: 10.3389/fmicb.2018.02926

Ruiz-González, C., Simó, R., Sommaruga, R., and Gasol, J. M. (2013). Away from darkness: a review on the effects of solar radiation on heterotrophic bacterioplankton activity. *Front. Microbiol.* 4:131. doi: 10.3389/fmicb.2013.00131

Ruiz-Halpern, S., Ll Calleja, M., Dachs, J., Del Vento, S., Pastor, M., Palmer, M., et al. (2014). Ocean-at-

mosphere exchange of organic carbon and CO<sub>2</sub> surrounding the Antarctic Peninsula. *Biogeosciences* 11, 2755–2770.

Sabbaghzadeh, B., Upstill-Goddard, R. C., Beale, R., Pereira, R., and Nightingale, P. D. (2017). The Atlantic Ocean surface microlayer from 50° N to 50° S is ubiquitously enriched in surfactants at wind speeds up to 13 m s<sup>-1</sup>. *Geophys. Res. Lett.* 44, 2852–2858.

Salter, I., Zubkov, M. V., Warwick, P. E., and Burkill, P. H. (2009). Marine bacterioplankton can increase evaporation and gas transfer by metabolizing insoluble surfactants from the air-seawater interface. *FEMSMicrobiol. Lett.* 294, 225–231.

Södergren, A. (1987). Origin and composition of surface slicks in lakes of differing trophic status<sup>1</sup>. *Limnol. Oceanogr.* 32, 1307–1316.

Stolle, C., Labrenz, M., Meeske, C., and Jürgens, K. (2011). Bacterioneuston community structure in the southern Baltic sea and its dependence on meteorological conditions. *Appl. Environ. Microbiol.* 77, 3726–3733.

Stolle, C., Nagel, K., Labrenz, M., and Jürgens, K. (2010). Bacterial activity in the sea-surface microlayer: in situ investigations in the Baltic Sea and the influence of sampling devices. *Aquat. Microb. Ecol.* 58, 67–78.

Stortini, A. M., Martellini, T., Del Bubba, M., Lepri, L., Capodaglio, G., and Cincinelli, A. (2009). n-Alkanes, PAHs and surfactants in the sea surface microlayer and sea water samples of the Gerlache Inlet sea (Antarctica). *Microchem. J.* 92, 37–43.

Svenningsen, N. B., Pérez-Pantoja, D., Nikel, P. I., Nicolaisen, M. H., De Lorenzo, V., and Nybroe, O. (2015). *Pseudomonas putida* mt-2 tolerates reactive oxygen species generated during matrix stress by inducing a major oxidative defense response. *BMC Microbiol.* 15:202. doi: 10.1186/s12866-015-0542-1

Takahashi, S., Abe, K., and Ker, Y. (2013). “Microbial degradation of persistent organophosphorus flame retardants,” in *Environmental Biotechnology - New Approaches and Prospective Applications*, ed. M. Petre (London: InTech), 91.

Taylor, J. D., Cottingham, S. D., Billinge, J., and Cunliffe, M. (2014). Seasonal microbial community dynamics correlate with phytoplankton-derived polysaccharides in surface coastal waters. *ISME J.* 8, 245–248.

Vergeynst, L., Wegeberg, S., Aamand, J., Lassen, P., Gosewinkel, U., Fritt-Rasmussen, J., et al. (2018). Biodegradation of marine oil spills in the Arctic with a Greenland perspective. *Sci. Total Environ.* 626, 1243–1258.

Vila-Costa, M., Barberan, A., Auguet, J.-C., Sharma, S., Moran, M. A., and Casamayor, E. O. (2013). Bacterial and archaeal community structure in the surface microlayer of high mountain lakes examined under two atmospheric aerosol loading scenarios. *FEMS Microbiol. Ecol.* 84, 387–397.

Vila-Costa, M., Cerro-Gálvez, E., Martínez-Varela, A., Casas, G., and Dachs, J. (2020). Anthropogenic dissolved organic carbon and marine microbiomes. *ISME J.* 1–3.

Vila-Costa, M., Gasol, J. M., Sharma, S., and Moran, M. A. (2012). Community analysis of high-and low-nucleic acid-containing bacteria in NW Mediterranean coastal waters using 16S rDNA pyrosequencing. *Environ. Microbiol.* 14, 1390–1402.

Vila-Costa, M., Sebastián, M., Pizarro, M., Cerro-Gálvez, E., Lundin, D., Gasol, J. M., et al. (2019). Microbial consumption of organophosphate esters in seawater under phosphorus limited conditions. *Sci. Rep.* 9:233.

Wang, Y., Hammes, F., Boon, N., Chami, M., and Egli, T. (2009). Isolation and characterization of low nucleic acid (LNA)-content bacteria. *ISME J.* 3, 889–902.

Wang, Y., Hatt, J. K., Tsementzi, D., Rodríguez-R, L. M., Ruiz-Pérez, C. A., Weigand, M. R., et al. (2017). Quantifying the importance of the rare biosphere for microbial community response to organic pollutants in a freshwater ecosystem. *Appl. Environ. Microbiol.* 83, 3321–3337.

Wickham, H. (2009). *Ggplot2: Elegant Graphics for Data Analysis*, 2nd Edn. New York, NY: Springer.

Wilkins, D., Yau, S., Williams, T. J., Allen, M. A., Brown, M. V., Demaere, M. Z., et al. (2013). Key microbial drivers in Antarctic aquatic environments. *FEMS Microbiol. Rev.* 37, 303–335.

Wittgens, A., Kovacic, F., Müller, M. M., Gerlitzki, M., Santiago-Schübel, B., Hofmann, D., et al. (2017). Novel insights into biosynthesis and uptake of rhamnolipids and their precursors. *Appl. Microbiol. Biotechnol.* 101, 2865–2878.

Wurl, O., and Holmes, M. (2008). The gelatinous nature of the sea-surface microlayer. *Mar. Chem.* 110, 89–97.

Wurl, O., Miller, L., Röttgers, R., and Vagle, S. (2009). The distribution and fate of surface-active substances in the sea-surface microlayer and water column. *Mar. Chem.* 115, 1–9.

Wurl, O., and Obbard, J. P. (2004). A review of pollutants in the sea-surface microlayer (SML): a unique habitat for marine organisms. *Mar. Pollut. Bull.* 48, 1016–1030.

Yuan, X., Floresyona, D., Aubert, P. H., Bui, T. T., Remita, S., Ghosh, S., et al. (2019). Photocatalytic degradation of organic pollutant with polypyrrole nanostructures under UV and visible light. *Appl. Catal. B Environ.* 242, 284–292.

Zäncker, B., Cunliffe, M., and Engel, A. (2018). Bacterial community composition in the sea surface microlayer off the peruvian coast. *Front. Microbiol.* 9:2699. doi: 10.3389/fmicb.2018.02699

Zutic, V., Cosovic, B., Marcenko, E., Bihari, N., and Kršinic, F. (1981). Surfactant production by marine phytoplankton. *Mar. Chem.* 10,505–520.



# 4

## **PAH degradation in the sea-surface microlayer at coastal Antarctica**

**Alícia Martínez-Varela**, Gemma Casas, Naiara Berrojalbiz, Benjamin Piña, Jordi Dachs and Maria Vila-Costa

As much as 400 Tg of carbon from airborne semivolatile aromatic hydrocarbons are deposited to the oceans every year, the largest identified source of anthropogenic organic carbon to the ocean. Microbial degradation is a key sink of these pollutants in surface waters, but has received little attention in polar environments. We have challenged Antarctic microbial communities from the sea-surface microlayer (SML) and the sub-surface layer (SSL) to polycyclic aromatic hydrocarbons (PAH) at environmentally relevant concentrations. PAH degradation as well as the microbial responses at compositional and functional level were assessed. Significantly faster removal rates were observed in the SML, with rates 2.6-fold higher than in the SSL. In the SML, the highest removal rates were observed for the more hydrophobic, and particle-bound PAH. After 24 hours of PAH exposure, particle-associated bacteria in the SML showed the highest number of significant changes in their composition. These included significant enrichments of several hydrocarbonoclastic bacteria, especially the fast-growing genera *Pseudoalteromonas*, which increased their relative abundances by 8-fold. Simultaneous metatranscriptomic analysis showed that the free living fraction of SML was the most active fraction, especially for members of the order Alteromonadales, that includes *Pseudoalteromonas*. Their key role on PAH biodegradation in polar environments should be elucidated in further studies. This study highlights the relevant role of bacterial populations inhabiting the sea surface microlayer, especially the particle-associated habitat, as relevant bioreactors for removal of aromatic hydrocarbons in the oceans.

## INTRODUCTION

Polycyclic aromatic hydrocarbons (PAHs) and other semivolatile aromatic-like compounds originate from incomplete combustion of fossil fuels, oil spills, and natural processes such as oil seepage and biomass burning (Hylland, 2006; Duran and Cravo-Lau-reau, 2016). Semivolatile aromatic-like compounds are hydrophobic, bioaccumulative, and toxic, affecting marine organisms and posing a threat to ecosystems (Hylland, 2006; Ball and Truskewycz, 2013). Their semi-volatile nature allows them to be atmospherically transported and deposited, and in consequence, they are ubiquitous in the global ocean, even reaching remote polar regions far from their emission sources (Lohmann et al., 2009; Cabrerizo et al., 2014; Abdel-Shafy and Mansour, 2016; Cai et al., 2016; González-Gaya et al., 2016; Balmer et al., 2019; Casal et al., 2019). Quantification of atmospherically deposited PAHs into the global ocean reveals a global monthly entry of 0.09Tg C (1 Tg a year)(González-Gaya et al., 2016), which would equal 4 Deepwater Horizon oil spills every month (Reddy et al., 2012; González-Gaya et al., 2016). Surprisingly, only 1% of the total airborne PAHs are sequestered to the depths by the biological pump (González-Gaya et al., 2019). This and other evidences suggest that a major fraction of airborne aromatic hydrocarbons is removed at the surface ocean by microbial degradation and, to a lesser extent, by photo-degradation (de Bruyn et al., 2012; González-Gaya et al., 2019).

In oil-contaminated environments, microbial degradation is the major PAH removal process, mediated by hydrocarbonoclastic bacteria (HCB, specialist and facultative hydrocarbon degraders)(Head et al., 2006; Dong et al., 2015; Crisafi et al., 2016; Berry and Gutierrez, 2017; Gontikaki et al., 2018). Highly polluted sites, such as oil spill affected areas from temperate and polar regions, have provided the current knowledge of the biogeochemical and molecular basis for the biodegradation of PAHs (Lors et al., 2012; Dombrowski et al., 2016; Ghosal et al., 2016; Gupte et al., 2016; Joye et al., 2018). Physiological and transcriptomic data show that the spectrum of bacterial responses to PAH expands from anti-toxic stress responses and cellular repair (Heipieper and Martínez, 2010) to mechanisms increasing PAH bioavailability and facilitating their biodegradation (Head et al., 2006; Redmond and Valentine, 2012; Gutierrez, Singleton, et al., 2013; Joye et al., 2018). In situ measurements of PAH degradation rates are comparatively scarce, and only few studies have focused on the microbial responses to airborne PAHs, semivol-

atile aromatic-like compounds and other organic pollutants at environmentally relevant concentrations (Cerro-Gálvez et al., 2019; González-Gaya et al., 2019; Vila-Costa et al., 2019; Martínez-Varela et al., 2021).

The SML is the thin interface between the ocean and the atmosphere, operationally defined as the top 100-1000  $\mu\text{m}$  of the marine water column (Liss et al., 2005). Under favorable meteorological conditions, SML physicochemical and biological features can largely differ from those at the subsurface layer (SSL) (Stolle et al., 2010; Astrahan et al., 2016; Marín-Beltrán et al., 2019). However, rising bubbles or wind and current driven turbulences lead to temporal disruptions and mixing events, making the SML an extremely variable microenvironment. The active air-sea exchange and mixing dynamics of particles, gases and water through the SML contributes to the enrichment of amphiphilic, hydrophobic, surfactant-like compounds, and an array of miscellaneous organic molecules at the SML (Calace et al., 2004; Sabbaghzadeh et al., 2017; Uning et al., 2018), including atmospherically deposited PAHs (Wurl and Obbard, 2004; Cincinelli et al., 2005; Stortini et al., 2009) and other organic pollutants such as polychlorinated biphenyls (Fuoco et al., 2005; García-Flor, Guitart, Ábalos, Dachs, J. M. Bayona, et al., 2005) and perfluoroalkyl substances (Ju et al., 2008; Casas et al., 2020). Bacteria inhabiting the SML are known as bacterioneuston (Naumann, 1917), and are exposed to unique physicochemical properties and harsh environmental stressors. Bacterioneuston participate in air-sea interactions influencing key biogeochemical and climate related processes (Kuznetsova and Lee, 2001; Brooks et al., 2009; Nakajima et al., 2013). However, very few works addressed the interaction of bacterioneuston and pollution by PAHs and other airborne organic contaminants at low concentrations. For instance, Coelho et al (2011) explored the potential of bacterioneuston strains to degrade PAH by isolating HCB from the SML of a chronically oil polluted estuarine (Coelho et al., 2011). Martínez-Varela et al. (2020) found strong correlations between the enrichment of perfluoroalkyl substances (one of the ubiquitous constituents within anthropogenic dissolved organic carbon (ADOC)) and ADOC degrading strains at the Antarctic SML (Martínez-Varela et al., 2020). Unfortunately, analyses of responses to PAH and other ADOC compounds are still scarce for the marine environment, and absent in some compartments such as the SML.

In the Southern Ocean, atmospheric diffusive loadings and snow deposition represent the major source of PAHs into the ocean (Cabrerizo et al., 2014; Casal et al., 2019). Several field measurements from Antarctica (Cincinelli et al., 2001; Guitart et al., 2004; Fuoco et al., 2005; Stortini et al., 2009) and other marine regions (Guitart et al., 2007; Lim et al., 2007; Huang et al., 2020) showed that PAHs accumulate at the SML due to their hydrophobic nature, reporting enrichment factors up to eight-fold (Cincinelli et al., 2005; Fuoco et al., 2005; Stortini et al., 2009). Stortini et al. (2009) observed a positive correlation between organic acids and PAH enrichments at the SML in Antarctica, suggesting organic acids might act as amphiphilic surfactants, facilitating PAH enrichment at the surface (Stortini et al., 2009). Furthermore, the low temperatures in the polar marine environments modify the physicochemical properties of PAH by increasing their partitioning to organic films, such as those occurring at the SML (Tremblay et al., 2005).



Previous studies have shown that particle-associated bacteria (PA) differ from the free living fraction (FL), both at taxonomical and functional level (Smith et al., 2013; Hu et al., 2020). Whether or not high concentrations of PAH sorbed onto/into particles stimulates those bacterial communities better suited for PAH degradation remains unknown.

The goal of this study was to characterize and compare the PAH degradation capacity of two fractions (PA and FL) of the bacterial communities present in the two adjacent habitats of the surface ocean (SML and SSL) in coastal Antarctica. We exposed each Antarctic bacterial community to environmental concentrations of PAH for 24 hours and measured PAH degradation rates, and assessed the responses at taxonomical and functional level by means of 16S rRNA amplicon sequencing and metatranscriptomics. This approach allowed to answer whether or not SML is a neglected hot spot of PAH degradation in Antarctic waters and elucidate the main players in biodegradation.

## MATERIALS AND METHODS

### *Site Description and Sampling*

Seawater from the SML and SSL was collected over the mid austral summertime (21st of February 2018) at the South Bay of Livingston Island (South Shetlands, Antarctica). SML and SSL sampling was conducted from a rigid inflatable boat at 62°38.346' S, 60°23.912' W (Figure S1). The SML was sampled with a glass plate SML sampler. This sampling method was first described by Harvey and Burzell (Harvey and Burzell, 1972) (1972) and has been used in a number of studies for sampling organic matter, microorganisms, surfactants, and organic pollutants in the SML (Knulst et al., 2003; García-Flor, Guitart, Ábalos, Dachs, J.M. Bayona, et al., 2005; Ju et al., 2008; Casas et al., 2020; Martínez-Varela et al., 2020). The pre-rinsed plate (40x30 cm) was inserted vertically into the water, and then withdrawn slowly allowing the SML adhering onto the glass plate. The glass plate containing the SML sample was then wiped between two teflon (PTFE) plates draining the sample into 1 L 400°C pre-baked glass bottles. This process was repeated until obtaining a volume of 6 L of SML water. Subsurface layer seawater samples were collected in 2 L PP bottles by submerging the bottles and opening it at 0.5m depth. Simultaneously, physico-chemical parameters were measured at the sampling station with a CTD probe (Table S1).

### *Experimental set up with natural communities from the SSL and the SML*

Three hours prior to the surface seawater sampling, a mixture of PAHs (PAH-mix 9, Dr. Ehrenstorfer) was added to 1L pre-cleaned and 400°C pre-baked empty glass bottles. The same process was followed in the control bottles, where the same volume of solvent without PAH spike was added. Then, the solvent (Cyclohexane) was allowed to evaporate in treatment and control bottles to avoid any toxic effects derived from the presence of solvent. Nominal individual PAH concentrations in the treatments were 200 ng L<sup>-1</sup>. 0.7 L of seawater from SML and SSL were dispensed into the experimental bottles. Two replicates were performed for each unique experimental condition. Abiotic controls were run with HPLC-grade water with two replicates and were incubated, sampled and ana-

lyzed following the same sample procedure than the alive treatments. The experiment incubations were carried out at an outdoors deck of the Spanish Antarctic Base facilities in Livingston Island (62° 39' 43" S, 60° 23' 17" W). Experiment bottles were incubated during 24h in the dark, at an in situ temperature between 1C and 2C.

### ***Bacterial abundance***

Prokaryotic cell abundance was estimated by flow cytometry as described elsewhere (Falcioni et al., 2008). Briefly, fixed samples (0.4 ml) for heterotrophic non-pigmented total bacteria enumeration were stained with 4 µl of a 10× SG1 (Molecular Probes) solution (final dilution, 1:1,000 [vol/vol]) for 10 min and run through the FACSCalibur flow cytometer at a low speed (15 µl min<sup>-1</sup>), with fluorescent microspheres as an internal standard (yellow-green 0.92-µm Polysciences latex beads [106 ml<sup>-1</sup>]). Bacteria were detected in a dot plot of side scatter versus green fluorescence (FL1) and population concentration was estimated with CellQuest and PaintAGate software (Becton Dickinson, Palo Alto, CA).

### ***Nucleic acids extraction and sequencing***

At the beginning of the experiment and after 24h of PAH addition, 0.69 L of seawater of each layer were pre-filtered through a 3 µm pore-size 47 mm diameter poly-tetrafluoroethylene filter to collect the particle-associated bacteria (PA; >3.0 µm). Cells in the filtrate were then collected on 0.2 µm pore-size 47 mm polytetrafluoroethylene to obtain the free living fraction (FL; 0.2–3.0 µm), using a peristaltic pump with a flow of < 50 mL min<sup>-1</sup>. The duration of the filtration step was no longer than 15 min to minimize RNA degradation. Each filter was cut in two halves, one was placed in 1 ml RNAlater (Sigma-Aldrich, Saint Louis, MO) and the other one into 1 ml lysis buffer (50 mM Tris HCl, 40 mM EDTA, 0.75 M sucrose) and stored at -20C to preserve RNA and DNA respectively. DNA extraction was performed as described in Vila-Costa et al. (2019). Total RNA was extracted, DNA removed, rRNA depleted and mRNA enriched by amplification as described in Poretsky et al. (2010) with the only modification that total RNA was extracted with mirVana isolation kit (Ambion), after removing the storage reagent by centrifugation.

Partial bacterial 16S gene fragments of both DNA were amplified using primers 515F-Y (5'-GTGYCAGCMGCCGCGTAA) and 926R (5'-CCGYCAATTYMTTTRAGTTT) (Parada et al., 2016) plus adaptors for Illumina MiSeq sequencing. The PCR reaction mixture was thermocycled at 95C for 3 minutes, 30 cycles at 95C for 45s, 50C for 45s, and 68C for 90s, followed by a final extension of 5 min at 68C. PCR amplicon sizes were checked in tris-acetate-EDTA (TAE) agarose gels. Illumina MiSeq sequencing was conducted at the Pompeu Fabra University Sequencing Service.

### ***Dissolved phase concentrations of PAHs***

Concentrations of PAHs were measured in the dissolved phase at the beginning (T0) of the experiment and at the end of the incubation (T24) using the filtrate obtained after sampling DNA/RNA material (Table S2), using the same filtration procedure for treatments and controls. SSL and SML water in treatments and controls, and HPLC water from

abiotic controls, were concentrated on Bond Elut C18 cartridges (500 mg, Agilent), after filtration, using a Baker vacuum system, adapting a previously described methodology (Berrojalbiz et al., 2009). After drying the cartridges under vacuum, these were air-tight wrapped and kept at -20C until their further analysis in the laboratory. Once in the ultra-clean lab in Barcelona, PAHs were extracted with hexane:dichloromethane (1:1, v/v). Then, the extract was concentrated to 0.5 mL by vacuum rotary evaporation and transferred to vials and further evaporated to 400  $\mu$ L under a gentle nitrogen stream. Before quantification, per-deuterated internal standards were added to vials. PAHs analysis were conducted by gas chromatography coupled with a mass spectrometer (GC-MS). The targeted PAHs were Fluorene, Anthracene, Phenanthrene, Pyrene, Fluoranthene, Crysene, Benzo(a)anthracene, Benzo(b)fluoranthene, Benzo(k)fluoranthene, Benzo(a)pyrene, Dibenzo(a,h)anthracene, Indeno(1,2,3-cd)pyrene and Benzo(ghi)perylene. Naphthalene, Acenaphthene, Acenaphthylene even though they were present in the PAHs mix used, they were excluded of the study since our analytical procedure is not appropriate for a quantitative analysis of these volatile PAHs. Surrogate standards were added before extraction to calculate the target analyte recoveries to ensure the quality of the analytical procedure. Internal standard procedure was used to quantify the samples.

The PAH removal rates were calculated by the difference between initial and final time point concentrations. In all treatments, concentrations were above limits of quantification. During the time-course of the incubations, the PAHs added in seawater undergo partitioning to the organic matter pools due to their hydrophobicity. Then, it is possible that part of the apparent decrease of concentrations is due to partitioning to cells (bacteria and phytoplankton). The extent of this potential artifact of the removal rates estimates was assessed assuming that the microorganism-water bioconcentration factor was proportional to the hydrophobicity of the chemical, as given by the octanol-water partition constant ( $K_{ow}$ ).

$$BCF = \frac{C_M}{C_W} = f_{OM} \frac{K_{ow}}{\delta} \quad [1]$$

Where  $C_M$  and  $C_W$  are the PAH concentrations in the microorganism and water, respectively,  $f_{OM}$  is the fraction of organic matter, and  $\delta$  is the density of octanol. Such dependence of BCF on  $K_{ow}$  has been reported before for phytoplankton and bacteria (Del Vento and Dachs, 2002; Berrojalbiz et al., 2009; Wang and Kelly, 2018). This allowed to estimate the concentration of individual PAHs in microorganism (bacteria and phytoplankton). The biomass of bacteria was estimated from the cell counts obtained from flow cytometry and assuming a carbon content of 20 fgC cell<sup>-1</sup> (Lee and Fuhrman, 1987). The biomass of phytoplankton was obtained by concurrent plankton sampling with vertical tows of a 50  $\mu$ m mesh net as explained elsewhere (Casal et al., 2018). Similarly, sorption to DOC was estimated by assuming that the DOC-water partition coefficient was 0.1 $K_{ow}$ , as commonly done (González-Gaya et al., 2016), and considering a DOC content of 60  $\mu$ M which is the

average value in Antarctic seawater(Doval et al., 2002).

Benchmarking approach (Mclachlan et al., 2016) was performed using phenanthrene as normalizing chemical because it did not show significant differences in removal rates between layers. Benchmarking approach is commonly used to correct for artifacts in chemical concentrations when working with low volumes of water and glass bottles(Cerro-Gálvez et al., 2020).

### ***Bioinformatics***

Spurious sequences and primers were trimmed using Cutadapt v.1.16 (Martin, 2011). The cutoff before a base would be trimmed from either end of the read was set with a minimum phred quality score of 20 (1% error rate), and primers and illumina adapters were removed with a minimum overlap of 10 base pairs. DADA2 v1.4 was used to differentiate the 16S V4-5 amplicon sequence variants (ASVs) and remove chimeras (parameters: maxN = 0, maxEE = 2,4, truncLen = 220,200)(Callahan et al., 2016). DADA2 resolves ASVs by modeling the errors in Illumina-sequenced amplicon reads. The approach is threshold-free, inferring exact variants up to 1 nucleotide difference using the quality score distribution in a probability model. Taxonomic assignment of the ASVs was performed with the SILVA algorithm classifier against SILVA database release 138 (Quast et al., 2013). ASVs classified as Mitochondria or Chloroplast were removed. The final ASV table contained 23 samples (see details in Table S4).The entire sample set yielded a total of unique 1096 amplicon sequence variants (ASV) from 16S rRNA gene V4-5 fragments. The average number of sequences per samples was  $56215.08 \pm 34382.35$  and  $30024 \pm 9982.27$  for FL and PA fraction respectively, with a minimum sequencing depth of 11664 sequences. Maximum and minimum number of unique ASVs per sample was 253 and 71, respectively, averaging  $147.39 \pm 45.75$  of unique bacterial ASV per sample. Rarefaction was done to the minimum sequencing depth with `rarefy()` function from package `vegan v1.4-4"` in R environment (Oksanen et al., 2020). Archaea accounted for <1% of the total pool of reads and were discarded from the analyses.

For the metatranscriptomes, cDNA sequences were quality trimmed with Cutadapt(Martin, 2011) (and Sickle (<https://github.com/najoshi/sickle>) and internal standards and any remaining stable RNA was quantified and removed using the Bowtie2 mapping program against the internal standard sequences and an in-house database of marine bacterial stable RNA sequences (rRNA and tRNA) respectively . Subsequently, high quality reads were de-novo assembled using the MEGAHIT program (v1.1.2) (Li et al., 2016) with default parameters. Open reading frame (ORFs) prediction was done using Prodigal (Hyatt et al., 2010). Contigs were then aligned to the NCBI RefSeq database (downloaded October 2016) using the Diamond aligner (v0.9.24)(Buchfink et al., 2015) in blastx mode with default parameters. Functional SEED classification and taxonomic affiliation were assigned with MEGAN 6.7.3 (Huson et al., 2016). Transcripts were mapped to the open reading frames (ORFs) using `bowtie2 (v2.3.5.1)` and quantified using `Samtools (v1.9)`. Data was then exported for further analysis in R/`tidyverse`. Relative raw gene counts were normalized to library sizes (Table S5).

Search for expression of specific PAH degrading genes within the metatranscriptomes was performed using Hmmersearch against Pfam hmmer PAH degradation profiles. The list of the specific Pfam profiles used is listed in Figure 4 and Table S6 and was obtained from “MetaCyc” (Caspi et al., 2020) and downloaded from “Pfam” database (Mistry et al., 2021).

### ***Identification of hydrocarbonoclastic bacterial genera***

A list of hydrocarbonoclastic bacterial (HCB) genera was retrieved from the literature, including genera either collected from hydrocarbon polluted environments, observed to have stimulated growth following hydrocarbon exposure or showing hydrocarbon catabolic activity, both from isolates and marine environments (after metagenome-assembled genome (MAGS) reconstruction) (Lozada et al., 2014; Karthikeyan et al., 2020). The detection of specific HCB genera was performed by filtering at genus level all those ASVs and transcripts with taxonomical affiliation matching to those targeted HCB groups (see Table S7). Although in some cases it might not be hold, HCB-ASV and transcripts within the same genus were assumed to share similar metabolism as it has been observed for most HCB taxa by Gutierrez et al 2013 (Gutierrez, Singleton, et al., 2013).

3

### ***Statistical analyses***

R software was used to perform the different statistical analyses. Significant differences in removal rates between layers were tested with non-parametric Mann-Whitney test (unpaired Wilcoxon rank test, from package stats v. 3.6.2,  $P \leq 0.05$ ). Community composition significant differences between layers was tested with a permutation analysis of variance (PERMANOVA, with function Adonis from package vegan v1.4-4). Fold changes of specific taxa were calculated for the relative values between layers (SML vs SSL) and between treatments (PAH exposed vs controls) using the function foldchange (package gtools v. 3.9.2) (R Core Team, 2019). Significant differences of specific taxa between treatments were tested with a paired two sample t-test (using the “t.test” function from package stats v. 3.6.2,  $P \leq 0.05$ ). Analysis of differentially expressed genes was performed with the “EdgeR” package v. 3.36.0 (Robinson et al., 2009) In brief, metatranscriptomic data and the design matrix of the experiment were fitted into a negative binomial generalized linear model, and dispersion estimates from the read counts across all samples were obtained. Differentially expressed genes between experimental groups were determined by using likelihood ratio test. Significance is tested through data randomizations with threshold set by the False Discovery Rate correction,  $FDR \leq 0.05$ . Further graphs were plotted using the package ggplot v. 3.3.5, also in R environment (version 4.1.1.) (Wickham, 2009).

## RESULTS AND DISCUSSION

### ***Characterization of initial conditions at the SML and SSL***

Initial seawater physicochemical and meteorological conditions are summarized in Table S1. Sea surface temperature, wind speed and radiation conditions (1.9°C, 2.4 ms<sup>-1</sup> and 5.7 Wm<sup>2</sup>, respectively) were favorable for the formation of SML (Table S1). The concentrations of nutrients confirm a non-nutrient limited system, consistent with the prevalent upwelling in the region during the austral summer (Garcia et al., 2013) (Table S8). Total dissolved phase PAH concentrations were 0.74 ± 0.14 ng L<sup>-1</sup> in the SML, and 3.63 ± 0.19 ng L<sup>-1</sup> in SSL (Table S2), in agreement with previous studies carried out in South Bay (Casal et al., 2018).

Analysis of bacterial composition by 16S rRNA gene amplicon sequencing showed similar initial bacterial populations in both layers, although Pseudomonadales was significantly enriched at the SML (t-test, P < 0.02, Figure S3) Microbial community composition in the FL fraction was significantly different than in the PA fraction (PERMANOVA P=0.03, Figure S4, Table S9), consistent with observations from other studies (Eloe et al., 2011; Rieck et al., 2015; Roth Rosenberg et al., 2021). The SAR11 clade, Rhodobacterales and Oceanospirillales, while dominant in both habitats, showed a significant preference for the FL life style (t-test, P < 0.03, Table S9).

The PAH degrading potential of each community was estimated by quantifying the relative abundance of HCB at the initial conditions. The contribution of HCB to the total pool of 16S rRNA gene was significantly higher in the PA than in the FL fractions in both layers (t-test, P < 0.04 for the SML and P < 0.01 for the SSL, Table S7, Table S9 and Figure S5). *Sulfitobacter* was dominant within the HCB pool at initial conditions, accounting for an averaged 4.4 ± 0.9% of total 16S rRNA genes. Some strains were almost specific of each layer: *Pseudoalteromonas* and *Psychrobacter* strains, known to be highly resistant to solar radiation (Agogué et al., 2005; Santos et al., 2012), were abundant within the HCB pool in the SML and almost absent in the SSL, while *Colwellia* predominated only at the PA from the SSL. A previous work has shown an enrichment of pollutant degraders in the surface microlayer from South Bay (Martinez-Varela et al., 2020) for the same austral summer, even though with an important day-to-day variability.

### ***PAH degradation rates at the SML and SSL***

The degradation of PAH in the SML and SSL was measured in a short-term experiment (24h) with treatments spiked with PAHs, while with in-situ concentrations in the controls. PAH concentrations measured in PAH treatments and in both biotic and abiotic controls at time 0 and 24 hrs are shown in Table S2. The PAH spiked concentrations are in the range of the natural variability of PAH in the marine environment, and are below the concentrations of total semivolatile aromatic-like compounds concentrations in the open ocean (González-Gaya et al., 2019). Thus, the assessment of PAH removal and changes in bacterial composition and activity were measured under environmentally relevant conditions.

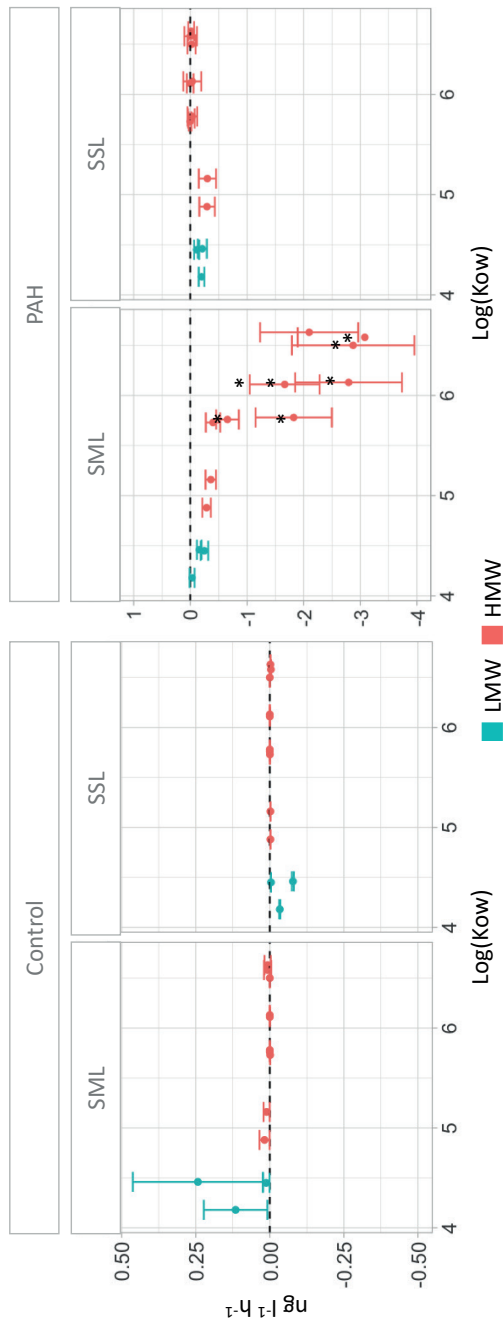


**FIGURE 1** | PAH removal rates in the sea surface microlayer (SML) and the subsurface layer (SSL) for treatments and controls calculated as the difference of concentrations between time 0 and 24 hours (units in ng L<sup>-1</sup> h<sup>-1</sup>). Significant differences between layers (Mann-Whitney test, p < 0.05) are labeled with an asterisk.

Significantly higher PAH removal rates were measured in the SML than in the SSL for Crysene, Benzo(a)anthracene, Benzo(a)pyrene, Benzo(k)fluoranthene, Benzo(b)fluoranthene, Dibenzo(a,h)anthracene, Indeno(1,2,3-cd)pyrene and the sum of HMW (Figure 1, Mann-whitney test,  $P < 0.04$ ). At the SML, removal rates of individual high molecular weight PAH compounds (HMW, PAH with four or more fused rings) ranged from  $0.29 \pm 0.08 \text{ ng L}^{-1} \text{ h}^{-1}$  to  $3.08 \pm 1.2 \text{ ng L}^{-1} \text{ h}^{-1}$ , averaging  $1.6 \text{ ng L}^{-1} \text{ h}^{-1}$ . Low molecular weight (LMW) PAH at the SML showed significantly lower biodegradation rates than HMW PAHs, ranging from  $0.03 \pm 0.04 \text{ ng L}^{-1} \text{ h}^{-1}$  to  $0.25 \pm 0.07 \text{ ng L}^{-1} \text{ h}^{-1}$ , averaging  $0.14 \text{ ng L}^{-1} \text{ h}^{-1}$  (Mann-Whitney test,  $P < 0.04$ ). These removal rates contrast with those at the SSL, where HMW PAH remained mostly unchanged, while LMW PAH were removed at an average rate of  $0.17 \pm 0.03 \text{ ng L}^{-1} \text{ h}^{-1}$ , comparable to the observed in the SML (Figure 1) Differences in removal rates for concentrations corrected by benchmarking (see M&M) confirmed that were significant for Benzo(a)anthracene, Benzo(a)pyrene, Benzo(b)fluoranthene, Benzo(ghi)perylene, Benzo(k)fluoranthene, Crysene, Dibenzo(a,h)anthracene, Indeno(1,2,3-cd)pyrene and the sum of all HMW (Figure S2).

Removal rates of PAHs at the SML showed an inverse correlation to the  $K_{ow}$  values for the different PAHs, a trend not observed in the SSL (Figure 1). These rates were measured in the dissolved phase concentrations, so the removal of PAH could potentially be caused either by the abiotic process of diffusive partitioning of PAHs to the particulate organic carbon pool (POC, that is mostly bacteria and phytoplankton), or due to biodegradation. To distinguish between both processes, partitioning was modeled from field data (see M&M for details). The more hydrophobic the PAH is, the more the chemical bioconcentrates in the cells (Del Vento and Dachs, 2002). There is the possibility, then, that the decrease of HMW PAHs at SML simply reflected their sorption to the POC pool. However, the fraction of PAHs retained in bacteria and phytoplankton was estimated to range between 0.1% for LMW PAHs and up to 9% for the most hydrophobic HMW PAHs. Similar estimates were found due to sorption to DOC. Both microorganism abundance and DOC cannot vary remarkably over a 24-hour period, thus cannot account for the strong decrease of HMW PAHs. In any case, the potential decrease to sorption to changing organic matter pools are remarkably lower than the average decrease of  $52.2 \pm 1 \%$  for HMW PAHs at the SML, strongly suggesting that biodegradation was the main removal process. Direct photo-degradation could not occur as experiments were run in dark conditions.

The fact that the removal rates were significantly higher for HMW PAHs than for LMW PAHs (t-test,  $P = 0.04$ ), suggests that biodegradation mostly occurred in the particle phase, that is, in the PA habitat. This is consistent with the proposed fast water-bacteria partitioning model (Axelman et al., 1997; Del Vento and Dachs, 2002), in which diffusion of PAHs from the dissolved phase is much higher than their rate of degradation either inside or at the vicinity of the cell surface. In fact, in the environment, BCF values are kept constant (close to steady state), and this explains the fact that the removal of hydrophobic PAHs was mirrored by the dissolved phase concentrations of PAHs. HMW PAHs are highly hydrophobic and thus are mainly present in the particulate organic carbon, mainly bacteria, phytoplankton and detritus.



Our results are at variance with previous experimental data using cultures of HCB retrieved from polluted environments, which showed similar 24h-biodegradation rates for LWM and HMW PAH, although they were performed under different conditions from those present in the maritime Antarctica (Kanaly and Harayama, 2010; Huang et al., 2016; Umar et al., 2017; Khattoon and Malik, 2019; Medić et al., 2020). In a polar environment, sub-ice bacterial communities have the capacity to remove up to 95% of LMW and HMW PAH from a mesocosm, but after a longer period (15 days) (Garneau et al., 2016) than in our experiment (1 day). Taken together, these data illustrate the remarkable capacity of SML communities to quickly degrade PAHs at low temperatures.

### **Changes in community composition due to exposure to PAHs.**

Exposure to PAHs for 24 hours resulted in significant changes in the SML bacterial community, particularly for the PA bacterial fraction, whereas the SSL populations remained relatively unaltered (Figure 2). HCB genera appeared particularly enriched in the PAH exposed SML populations, especially in the PA fraction, consistently with HMW PAH hydrophobicity facilitating the adsorption to the POC present in the SML (Figure 2). More specifically, the facultative HCB *Pseudoalteromonas* showed the highest increase in relative abundance between control and PAH treatment from 3.7 % to  $25.6 \pm 0.3$  % (for the PA) and from  $0.8 \pm 0.2$  % to  $5.8 \pm 0.9$  % (for the FL) after 24 hours of exposure (Table S9). This increase suggests that even subtle PAH concentrations can trigger the exponential growth of low abundant taxa, becoming key players for PAH-microbiome interaction, as observed both in polar and in temperate seas (Sauret et al., 2014; Cerro-Gálvez et al., 2019; Martínez-Varela et al., 2021). *Pseudoalteromonas* species are early responders following marine oil spills (Dubinsky et al., 2013; Krolicka et al., 2017; Gutierrez et al., 2018), as well as in PAH enriched mesocosms experiments at low temperatures (Dong et al., 2015; Krolicka et al., 2017). Their nutritional preference towards PAH have been described in several studies (Hedlund and Staley, 2006; Hazen et al., 2010; Jin et al., 2016). *Pseudoalteromonas* and other Alteromonadales strains such as *Glaciecola*, *Colwellia* and *Alteromonas*, produce exopolymeric polysaccharide substances (EPS) with amphiphilic properties (Gutierrez, Berry, et al., 2013; Dang et al., 2016; Roca et al., 2016; Mapelli et al., 2017) (Table S7) which may increase PAH solubility and bioavailability by increasing the interfacial surface between hydrophobic substrates and bacteria (Gutierrez, Berry, et al., 2013; Quigg et al., 2016). EPS also provide a physical structure facilitating faster transformation steps in PA communities, as observed with marine oil snow (Hatcher et al., 2018). Other than the direct responses of bacteria to PAH consumption and exposure, enrichments or depletions of some taxa after PAH addition might result from indirect negative effects of PAH on phytoplankton and grazers, thus affecting the mortality of certain groups (Barata et al., 2005; Fernández-Pinos et al., 2017).

Other HCB groups such as HC Bacteroidia, and the cold-adapted hydrocarbon degrading genus *Colwellia*, showed fold changes above 2 in the SML when exposed to PAHs (Table S10). Simultaneously, at the SML PA fraction, significant decreases in their relative abundances were observed for Oceanospirillales, Pseudomonadales, All Bacteroidota, Flavobacteriales (as a whole class) and the HCB *Psychrobacter*. This suggests not all taxa

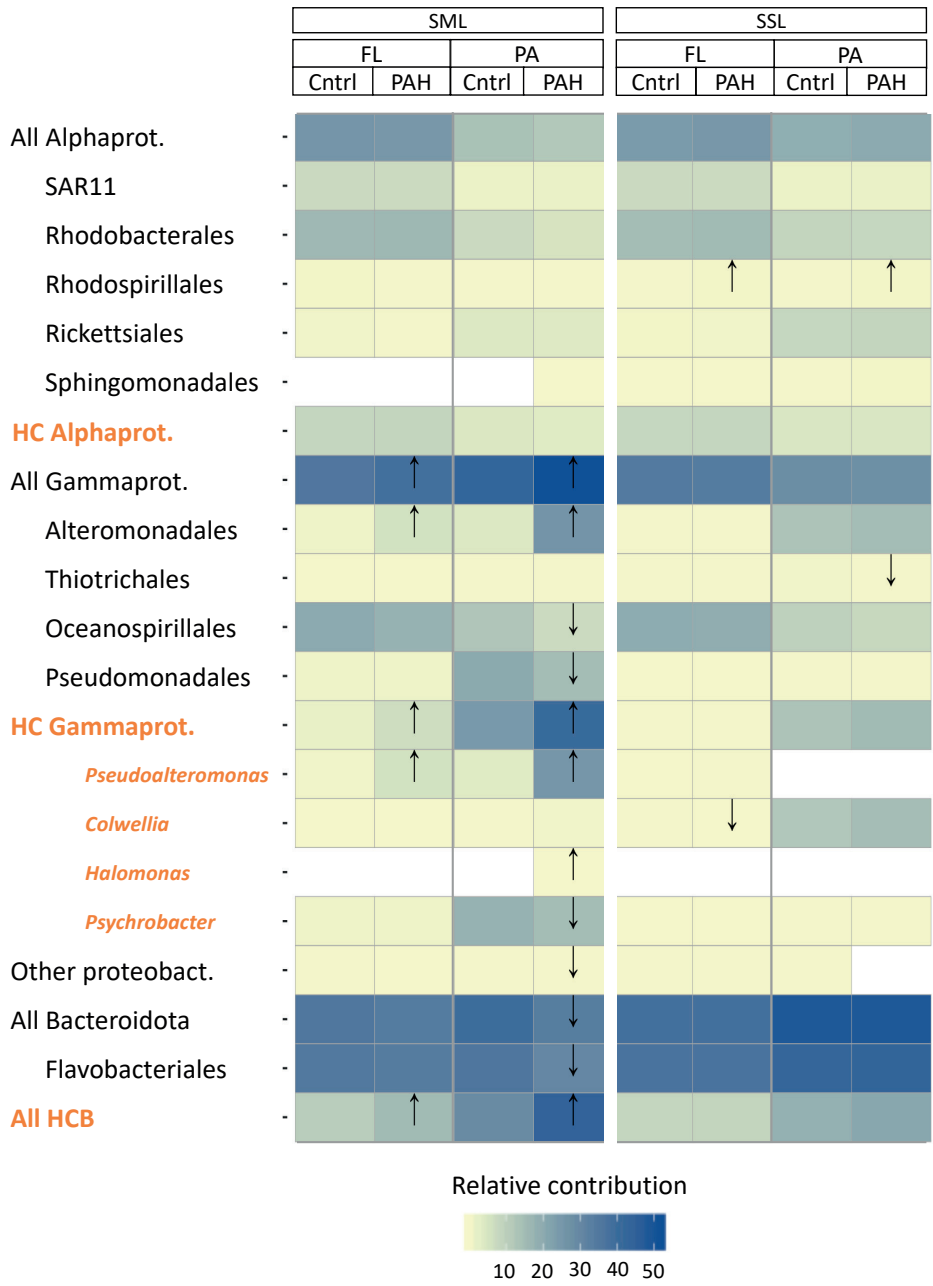


**FIGURE 2 |** Characterization of community structure after 24 h of PAH exposure in the sea surface microlayer (SML) and subsurface layer (SSL) for particle-associated (PA) and free living (FL) bacterial fractions based on 16S rRNA gene amplicon sequencing. Statistical differences between controls and PAH treatments were detected by t-test and labeled with an arrow in the figure. In orange, hydrocarbonoclastic bacteria (HCB) as listed in Table S5. Notice that general taxonomical groups (in black) include HCB.

were favored by PAH exposure.

At the SSL, Rhodospirillales, including different marine strains from genera *Thalassospira*, capable of degrading PAHs (Kodama et al., 2008; Kim and Kwon, 2010; Zhao et al., 2010), increased significantly their relative contribution in both fractions after PAH exposure. Conversely, *Colwellia sp.* and *Thiotrichales* decreased their relative abundance at the PAH exposed community at FL and PA, respectively.

### **Changes in gene expression profiles after 24 h of PAH exposure**

The snapshot of activities of the different groups of bacteria 24 h after PAH exposure was assessed analyzing gene expression profiles by metatranscriptomic approaches. Overall, the highest number of significant changes at the PAH exposed communities was observed at the FL SML (Figure 3, EdgeR (Robinson et al., 2009) FDR<0.05). In this fraction, most of the functional enrichments of differentially expressed genes (DEG) were mainly associated to Alteromonadales, but also to Rhodobacterales, Cellvibrionales and other gammaproteobacterial (Figure 3). Notably, Alteromonadales showed significant increases of expression levels at the PAH exposed community for all functional categories, including metabolism of aromatic compounds, supporting its pivotal key role in PAH degradation. This was consistent with the *Pseudoalteromonas* major role in explaining 16S community shift responses in the SML.

PAH degradation genes were tracked based on the pfam profiles integrated in the degradation pathway of the model PAH naphthalene (Figure 4). The ring hydroxylating dioxygenase (RHD), catalyzer complex of the initiating PAH dihydroxylation step (PF00848), was found enriched in all PAH exposed communities except for the SML PA (Figure 4). However, when looking into the transcripts taxonomical affiliation, all PAH-degrading transcript assigned to Alteromonadales were found enriched at the FL and PA cohorts of the SML, suggesting this group played a relevant role in biodegradation processes in this layer (Figure S7). At the SSL PA, the whole battery of PAH degrading genes were enriched, being homogenously distributed across phylogenetically distinct taxa (Figure 4 and Figure S7). At the SSL FL fraction the genes from the upper-pathway of PAH degradation were enriched (from the RHD to the prior steps towards catechol or protocatechuate), but later steps (PF00561 and PF07836) towards tricarboxylic acid (TCA) cycle were found depleted. Thus, the metatranscriptomic profiles after 24 hours captured different stages of the degradation of PAHs, steered by different taxa, at both layers (SML and SSL) and for both fractions (PA and FL). After 24 hours, PA Alteromonadales in the SML had already degraded a significant fraction of HMW PAHs adsorbed to POC, then biodegradation was occurring mainly in the SML FL and SSL PA fractions. The more pronounced decrease of HMW PAHs than LMW PAHs is consistent with these different kinetic in bacterial degradation for both fractions.

Importantly, PAH biodegradation does not occur in a nutshell. It requires of other metabolisms involving strategies to chemically sense hydrocarbons, to move towards them, to produce substances modifying their bioavailability, and to deploy an array of cell detoxification strategies to cope with PAH toxicity (Joye et al., 2016, 2018). Consistently, genes related to chemotaxis and to motility on one side, and to stress response regu-

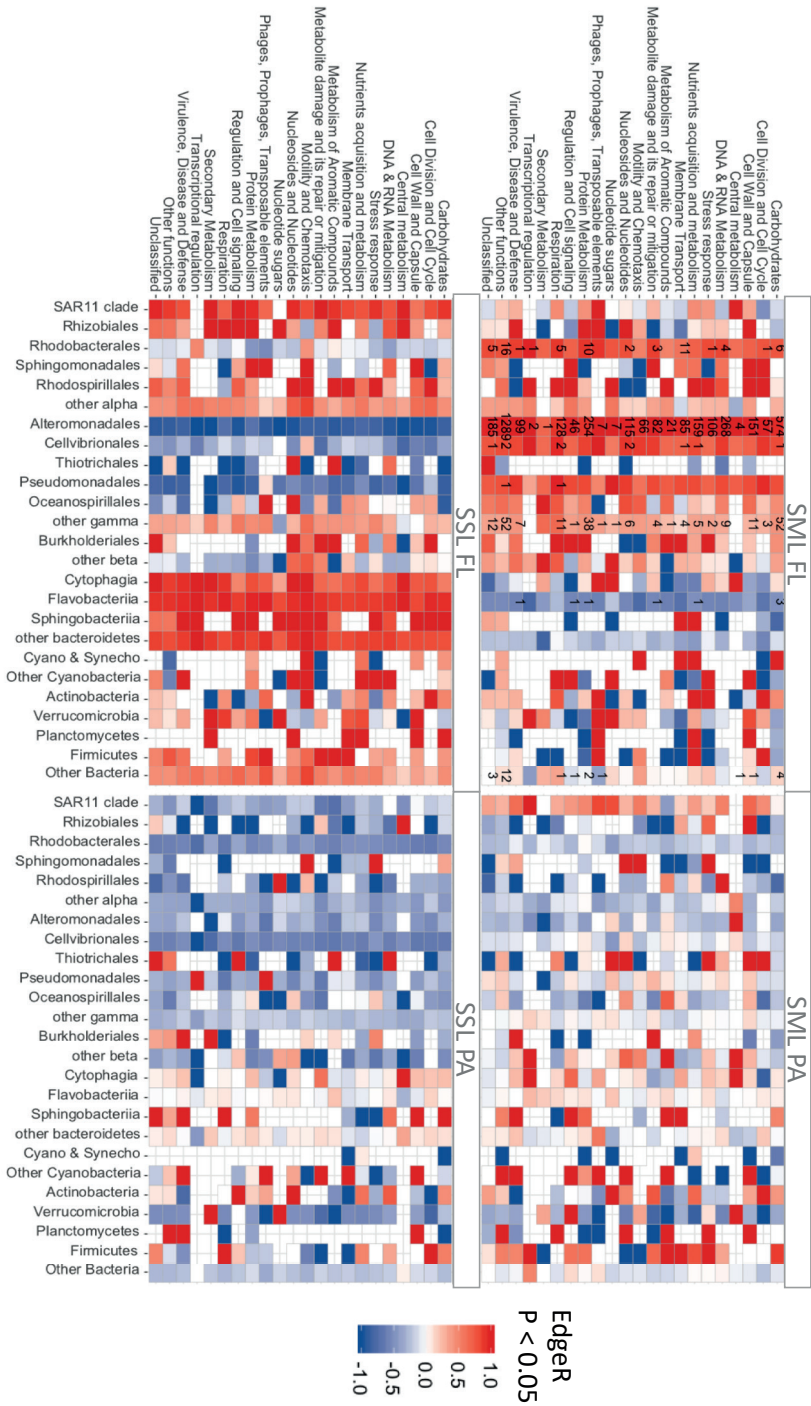


**FIGURE 3 |** Total number of significantly enriched (in red) or depleted (in blue) transcripts detected by edgeR (FDR < 0.05) between PAH treatments and controls metatranscriptomes. Counts are indicated inside each tile. Rows correspond to SEED categories. (SML: sea surface microlayer; SSL: subsurface layer; PA: Particle-associated; FL: Free living)

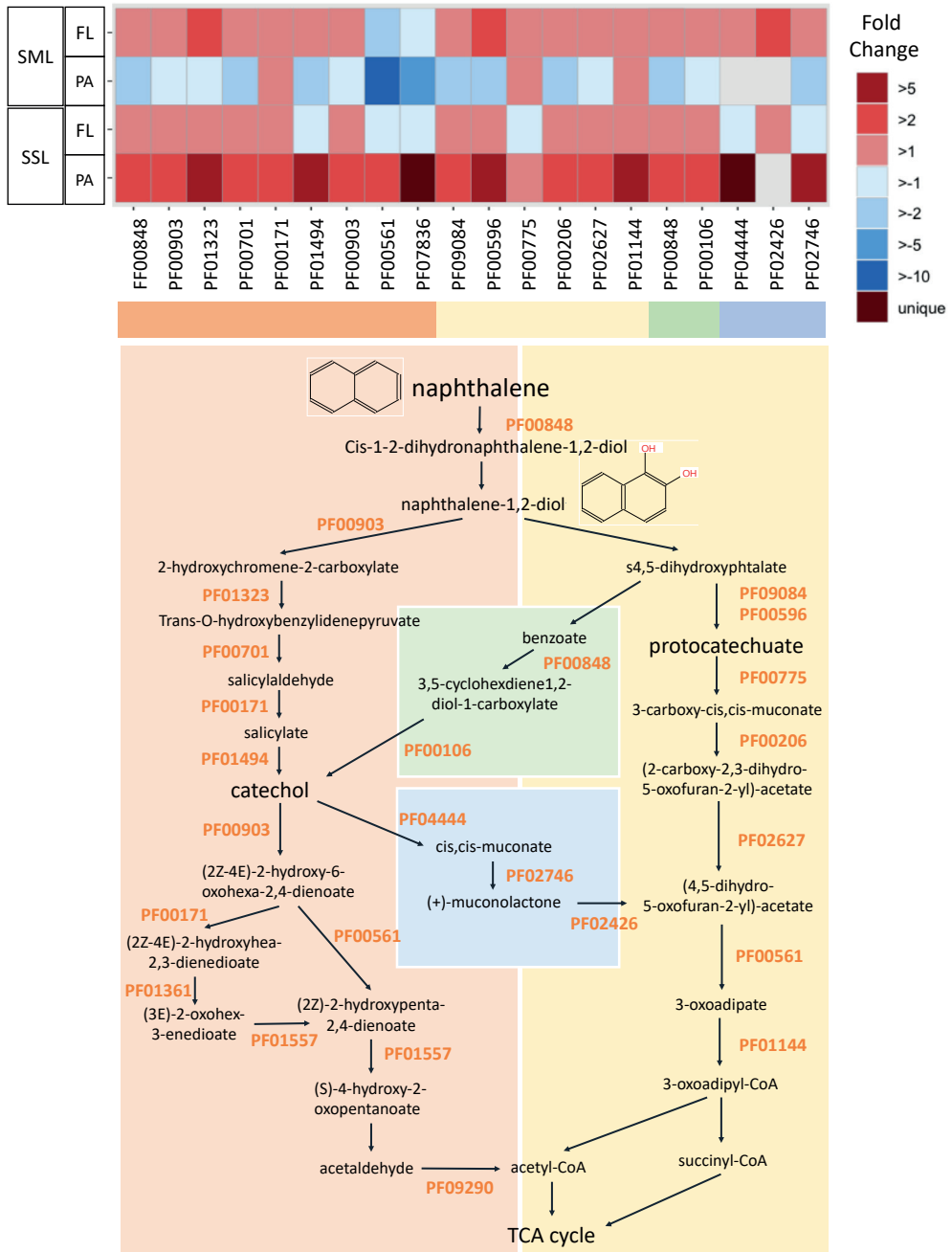


**FIGURE 4 |** Fold-change in expression of genes involved in PAH degradation between PAH treatments and controls measured by metatranscriptomics. PAH degradation pathway is represented for the naphthalene (model and simplest PAH compound). The list of the specific Pfam profiles involved in PAH degradation is listed in Table S4. (SML: sea surface microlayer; SSL: subsurface layer; PA: Particle-associated; FL: Free living)

lation and detoxifying multidrug efflux pumps on the other were found enriched in FL SML community exposed to PAH (t-test,  $P < 0.05$ , Figure S8). Similarly, at the PA cohort, a significant increase was observed for transcripts associated to the functional categories of “Flagellar Biosynthesis protein FliS” and “Widespread colonization island”, the later category being involved in biofilm formation and surface colonization (Planet et al., 2003; Caruso, 2020) (t-test,  $P < 0.05$ ). At SSL significant changes were observed uniquely for the FL fraction (Figure S8).

All together, these results support SML as a hotspot habitat for PAH degradation in Antarctic coastal waters. The surprising fact that fast PAH degradation is observed for the HMW PAH at the SML might be related to the synergistic combination of several factors: (1) traditionally, HMW PAH have been considered to be more persistent than LMW PAH due to strong sorption of HMW PAH to black carbon. However, black carbon concentrations are extremely low in Antarctica and thus it does not lower the bioavailable concentrations. The higher hydrophobicity of HMW PAHs drive their partitioning to microorganisms and detritus, which are the major organic matter pools, facilitating their biodegradation by particle associated bacteria (2) organic pollutants are enriched at the SML (Casas et al.; Cincinelli et al., 2005; Stortini et al., 2009) , (3) enrichment of hydrocarbonoclastic and organic pollutant degrading bacterial communities in the SML compared to subsurface waters (Coelho et al., 2011; Martinez-Varela et al., 2020). These findings need deeper characterization in further studies, that will elucidate the potential Antarctic ecosystem vulnerability to anthropogenic stressors such as semivolatile organic pollutants.

## ACKNOWLEDGEMENTS

We thank the staff of the Marine Technology Unit (UTM-CSIC) for their logistical support during the sampling campaign at Livingston Island. We also thank Dr Daniel Lundin for unconditional bioinformatic support. Special thanks to TERNUA for their nonprofit collaboration by sponsoring with technical ecofriendly clothing and gear equipment for Antarctic campaigns and for increasing our project visibility.

## AUTHOR CONTRIBUTION

A.M.-V., M.V.-C. and J.D. designed the sampling strategy and wrote the manuscript. A.M.-V., G.C., and J.D. conducted the field sampling. A.M.-V. performed the molecular work and data analyses. G.C. quantified the PFAS concentrations. B.P. and A.M.-V. performed the statistical analyses. All authors discussed the results and implications and commented on the final version of the manuscript.

A.M.-V., M.V.-C. and J.D. designed the experimental setup and wrote the manuscript. A.M.-V. and G.C. conducted the field sampling and the experiment. A.M.-V., and N.B. analyzed and quantified the PAH concentrations. A.M.-V., M.V.-C. and B.P. performed the molecular work and data analyses. All authors discussed the results and implications and commented on the final version of the manuscript.

## REFERENCES

- Abdel-Shafy, H.I. and Mansour, M.S.M. (2016) A review on polycyclic aromatic hydrocarbons: Source, environmental impact, effect on human health and remediation. *Egypt J Pet* 25: 107–123.
- Agogué, H., Joux, F., Obernosterer, I., and Lebaron, P. (2005) Resistance of marine bacterioneuston to solar radiation. *Appl Environ Microbiol* 71: 5282–5289.
- Astrahan, P., Herut, B., Paytan, A., and Rahav, E. (2016) The Impact of Dry Atmospheric Deposition on the Sea-Surface Microlayer in the SE Mediterranean Sea: An Experimental Approach. *Front Mar Sci* 3: 222.
- Axelman, J., Broman, D., and Näf, C. (1997) Field measurements of PCB partitioning between water and planktonic organisms: Influence of growth, particle size, and solute-solvent interactions. *Environ Sci Technol* 31: 665–669.
- Ball, A. and Truskewycz, A. (2013) Polyaromatic hydrocarbon exposure: An ecological impact ambiguity. *Environ Sci Pollut Res* 20: 4311–4326.
- Balmer, J.E., Hung, H., Yu, Y., Letcher, R.J., and Muir, D.C.G. (2019) Sources and environmental fate of pyrogenic polycyclic aromatic hydrocarbons (PAHs) in the Arctic. *Emerg Contam* 5: 128–142.
- Barata, C., Calbet, A., Saiz, E., Ortiz, L., and Bayona, J.M. (2005) Predicting single and mixture toxicity of petrogenic polycyclic aromatic hydrocarbons to the copepod *Oithona davisae*. *Environ Toxicol Chem* 24: 2992–2999.
- Berrojalbiz, N., Lacorte, S., Calbet, A., Saiz, E., Barata, C., and Dachs, J. (2009) Accumulation and Cycling of Polycyclic Aromatic Hydrocarbons in Zooplankton Accumulation and Cycling of Polycyclic Aromatic Hydrocarbons in Zooplankton. *Environ Sci Technol* 43: 2295–2301.
- Berry, D. and Gutierrez, T. (2017) Evaluating the Detection of Hydrocarbon-Degrading Bacteria in 16S rRNA Gene Sequencing Surveys. *Front Microbiol* 8: 896.
- Brooks, I.M., Yelland, M.J., Upstill-Goddard, R.C., Nightingale, P.D., Archer, S., d'Asaro, E., et al. (2009) Physical exchanges at the air-sea interface: UK-SOLAS field measurements. *Bull Am Meteorol Soc* 90: 629–644.
- de Bruyn, W.J., Clark, C.D., Ottelle, K., and Aiona, P. (2012) Photochemical degradation of phenanthrene as a function of natural water variables modeling freshwater to marine environments. *Mar Pollut Bull* 64: 532–538.
- Buchfink, B., Xie, C., and Huson, D.H. (2015) Fast and sensitive protein alignment using DIAMOND. *Nat Methods* 12: 59–60.

- Cabrerizo, A., Galbán-Malagón, C., Del Vento, S., and Dachs, J. (2014) Sources and fate of polycyclic aromatic hydrocarbons in the Antarctic and Southern Ocean atmosphere. *Global Biogeochem Cycles* 28: 1424–1436.
- Cai, Minggang, Liu, M., Hong, Q., Lin, J., Huang, P., Hong, J., et al. (2016) Fate of Polycyclic Aromatic Hydrocarbons in Seawater from the Western Pacific to the Southern Ocean (17.5°N to 69.2°S) and Their Inventories on the Antarctic Shelf. *Environ Sci Technol* 50: 9161–9168.
- Calace, N., Mirante, S., Petronio, B.M., Pietroletti, M., and Rugo, C. (2004) Fulvic acid enrichment in the microlayer of the Gerlache Inlet sea (Antarctica): Preliminary results. In *International Journal of Environmental Analytical Chemistry*. Taylor & Francis Group, pp. 413–421.
- Callahan, B.J., McMurdie, P.J., Rosen, M.J., Han, A.W., Johnson, A.J.A., and Holmes, S.P. (2016) DADA2: High-resolution sample inference from Illumina amplicon data. *Nat Methods* 13: 581–583.
- Caruso, G. (2020) Microbial Colonization in Marine Environments: Overview of Current Knowledge and Emerging Research Topics. *J Mar Sci Eng* 8: 78.
- Casal, P., Cabrerizo, A., Vila-Costa, M., Pizarro, M., Jiménez, B., and Dachs, J. (2018) Pivotal Role of Snow Deposition and Melting Driving Fluxes of Polycyclic Aromatic Hydrocarbons at Coastal Livingston Island (Antarctica). *Environ Sci Technol* 52: 12327–12337.
- Casal, P., Casas, G., Vila-Costa, M., Cabrerizo, A., Pizarro, M., Jiménez, B., and Dachs, J. (2019) Snow amplification of persistent organic pollutants at coastal antarctica. *Environ Sci Technol* 53: 8872–8882.
- Casas, G., Dachs, J., Martínez-Varela, A., Roscales, J.L., Pizarro, M., Vila-Costa, M., and Jimenez, B. Enrichment of Perfluoroalkyl Substances in the Surface Microlayer and Sea-Spray Aerosols in the Southern Ocean. *Environ Pollut*.
- Casas, G., Martínez-Varela, A., Roscales, J.L., Pizarro, M., Vila-Costa, M., Jimenez, B., and Dachs, J. (2020) Enrichment of Perfluoroalkyl Substances in the Surface Microlayer and Sea-Spray Aerosols in the Southern Ocean. *Environ Pollut* 267:.
- Caspi, R., Billington, R., Keseler, I.M., Kothari, A., Krummenacker, M., Midford, P.E., et al. (2020) The MetaCyc database of metabolic pathways and enzymes—a 2019 update. *Nucleic Acids Res* 48: D455–D453.
- Cerro-Gálvez, E., Roscales, J.L., Jiménez, B., Sala, M.M., Dachs, J., and Vila-Costa, M. (2020) Microbial responses to perfluoroalkyl substances and perfluorooctanesulfonate (PFOS) desulfurization in the Antarctic marine environment. *Water Res* 171:.
- Cerro-Gálvez, E., Casal, P., Lundin, D., Piña, B., Pinhassi, J., Dachs, J., and Vila-Costa, M. (2019) Microbial responses to anthropogenic dissolved organic carbon in the Arctic and Antarctic coastal seawaters. *Environ Microbiol* 21: 1466–1481.
- Cincinelli, A., Stortini, A.M., Checchini, L., Martellini, T., Del Bubba, M., and Lepri, L. (2005) Enrichment of organic pollutants in the sea surface microlayer (SML) at Terra Nova Bay, Antarctica: Influence of SML on superficial snow composition. *J Environ Monit* 7: 1305–1312.
- Cincinelli, A., Stortini, A.M., Perugini, M., Checchini, L., and Lepri, L. (2001) Organic pollutants in sea-surface microlayer and aerosol in the coastal environment of Leghorn-Tyrrhenian Sea.
- Coelho, F., Sousa, S., Santos, L., Santos, A., Almeida, A., Gomes, N., and Cunha, Â. (2011) Exploring hydrocarbonoclastic bacterial communities in the estuarine surface microlayer. *Aquat Microb Ecol* 64: 185–195.
- Crisafi, F., Giuliano, L., Yakimov, M.M., Azzaro, M., and Denaro, R. (2016) Isolation and degradation potential of a cold-adapted oil/PAH-degrading marine bacterial consortium from Kongsfjorden (Arctic region). *Rend Lincei* 27: 261–270.
- Dang, N.P., Landfald, B., and Willassen, N.P. (2016) Biological surface-active compounds from marine bacteria. *Environ Technol (United Kingdom)* 37: 1151–1158.
- Dombrowski, N., Donaho, J.A., Gutierrez, T., Seitz, K.W., Teske, A.P., and Baker, B.J. (2016) Reconstructing metabolic pathways of hydrocarbon-degrading bacteria from the Deepwater Horizon oil spill. *Nat Microbiol* 1: 16057.
- Dong, C., Bai, X., Sheng, H., Jiao, L., Zhou, H., and Shao, Z. (2015) Distribution of PAHs and the PAH-degrading bacteria in the deep-sea sediments of the high-latitude Arctic Ocean. *Biogeosciences* 12: 2163–2177.
- Doval, M.D., Álvarez-Salgado, X.A., Castro, C.G., and Pérez, F.F. (2002) Dissolved organic carbon distributions in the Bransfield and Gerlache Straits, Antarctica. *Deep Res Part II Top Stud Oceanogr* 49: 663–674.
- Dubinsky, E.A., Conrad, M.E., Chakraborty, R., Bill, M., Borglin, S.E., Hollibaugh, J.T., et al. (2013) Succession of Hydrocarbon-Degrading Bacteria in the Aftermath of the Deepwater Horizon Oil Spill in the Gulf of Mexico.



Environ Sci Technol 47: 10860–10867.

Duran, R. and Cravo-Laureau, C. (2016) Role of environmental factors and microorganisms in determining the fate of polycyclic aromatic hydrocarbons in the marine environment. *FEMS Microbiol Rev* 40: 814–830.

Eloe, E.A., Shulse, C.N., Fadrosch, D.W., Williamson, S.J., Allen, E.E., and Bartlett, D.H. (2011) Compositional differences in particle-associated and free-living microbial assemblages from an extreme deep-ocean environment. *Environ Microbiol Rep* 3: 449–458.

Falcioni, T., Papa, S., and Gasol, J.M. (2008) Evaluating the flow-cytometric nucleic acid double-staining protocol in realistic situations of planktonic bacterial death. *Appl Environ Microbiol* 74: 1767–1779.

Fernández-Pinos, M.-C., Vila-Costa, M., Arrieta, J.M., Morales, L., González-Gaya, B., Piña, B., and Dachs, J. (2017) Dysregulation of photosynthetic genes in oceanic *Prochlorococcus* populations exposed to organic pollutants. *Sci Rep* 7:.

Fuoco, R., Giannarelli, S., Wei, Y., Abete, C., Francesconi, S., and Termine, M. (2005) Polychlorobiphenyls and polycyclic aromatic hydrocarbons in the sea-surface micro-layer and the water column at Gerlache Inlet, Antarctica. *J Environ Monit* 7: 1313.

García-Flor, N., Guitart, C., Ábalos, M., Dachs, J., Bayona, J. M., and Albaigés, J. (2005) Enrichment of organochlorine contaminants in the sea surface microlayer: An organic carbon-driven process. *Mar Chem* 96: 331–345.

García-Flor, N., Guitart, C., Ábalos, M., Dachs, J., Bayona, J.M., and Albaigés, J. (2005) Enrichment of organochlorine contaminants in the sea surface microlayer: An organic carbon-driven process. *Mar Chem* 96: 331–345.

Garcia, H.E., Locarnini, R.A., Boyer, T.P., Antonov, J.I., Baranova, O.K., Zweng, M.M., et al. (2013) Dissolved Inorganic Nutrients (phosphate, nitrate, silicate). In *World Ocean Atlas 2013*. Levitus, S. and Mishonov, A. (eds). NESDIS, NOAA Atlas, pp. 76, 25.

Garneau, M.É., Michel, C., Meisterhans, G., Fortin, N., King, T.L., Greer, C.W., and Lee, K. (2016) Hydrocarbon biodegradation by Arctic sea-ice and sub-ice microbial communities during microcosm experiments, Northwest Passage (Nunavut, Canada). *FEMS Microbiol Ecol* 92:.

Ghosal, D., Ghosh, S., Dutta, T.K., and Ahn, Y. (2016) Current state of knowledge in microbial degradation of polycyclic aromatic hydrocarbons (PAHs): A review. *Front Microbiol* 7:.

Gontikaki, E., Potts, L.D., Anderson, J.A., and Witte, U. (2018) Hydrocarbon-degrading bacteria in deep-water subarctic sediments (Faroe-Shetland Channel). *J Appl Microbiol* 125: 1040–1053.

González-Gaya, B., Fernández-Pinos, M.C., Morales, L., Méjanelle, L., Abad, E., Piña, B., et al. (2016) High atmosphere-ocean exchange of semivolatile aromatic hydrocarbons. *Nat Geosci* 9: 438–442.

González-Gaya, B., Martínez-Varela, A., Vila-Costa, M., Casal, P., Cerro-Gálvez, E., Berrojalbiz, N., et al. (2019) Biodegradation as an important sink of aromatic hydrocarbons in the oceans. *Nat Geosci* 12: 119–125.

Guitart, C., García-Flor, N., Bayona, J.M., and Albaigés, J. (2007) Occurrence and fate of polycyclic aromatic hydrocarbons in the coastal surface microlayer. *Mar Pollut Bull* 54: 186–194.

Guitart, C., García-Flor, N., Dachs, J., Bayona, J.M., and Albaigés, J. (2004) Evaluation of sampling devices for the determination of polycyclic aromatic hydrocarbons in surface microlayer coastal waters. *Mar Pollut Bull* 48: 961–968.

Gupte, A., Tripathi, A., Patel, H., Rudakiya, D., and Gupte, S. (2016) Bioremediation of Polycyclic Aromatic Hydrocarbon (PAHs): A Perspective. *Open Biotechnol J* 10: 363–378.

Gutierrez, T., Berry, D., Yang, T., Mishamandani, S., McKay, L., Teske, A., and Aitken, M.D. (2013) Role of Bacterial Exopolysaccharides (EPS) in the Fate of the Oil Released during the Deepwater Horizon Oil Spill. *PLoS One* 8: :e67717.

Gutierrez, T., Morris, G., Ellis, D., Bowler, B., Jones, M., Salek, K., et al. (2018) Hydrocarbon-degradation and MOS-formation capabilities of the dominant bacteria enriched in sea surface oil slicks during the Deepwater Horizon oil spill. *Mar Pollut Bull* 135: 205–215.

Gutierrez, T., Singleton, D.R., Berry, D., Yang, T., Aitken, M.D., and Teske, A. (2013) Hydrocarbon-degrading bacteria enriched by the Deepwater Horizon oil spill identified by cultivation and DNA-SIP. *ISME J* 7: 2091–2104.

Harvey, G.W. and Burzell, L.A. (1972) A SIMPLE MICROLAYER METHOD FOR SMALL SAMPLES<sup>1</sup>. *Limnol Oceanogr* 17: 156–157.

- Hatcher, P.G., Obeid, W., Wozniak, A.S., Xu, C., Zhang, S., Santschi, P.H., and Quigg, A. (2018) Identifying oil/marine snow associations in mesocosm simulations of the Deepwater Horizon oil spill event using solid-state <sup>13</sup>C NMR spectroscopy. *Mar Pollut Bull* 126: 159–165.
- Hazen, T.C., Dubinsky, E.A., DeSantis, T.Z., Andersen, G.L., Piceno, Y.M., Singh, N., et al. (2010) Deep-sea oil plume enriches indigenous oil-degrading bacteria. *Science* (80- ) 330: 204–208.
- Head, I.M., Jones, D.M., and Röling, W.F.M. (2006) Marine microorganisms make a meal of oil. *Nat Rev Microbiol* 4: 173–182.
- Hedlund, B.P. and Staley, J.T. (2006) Isolation and characterization of *Pseudoalteromonas* strains with divergent polycyclic aromatic hydrocarbon catabolic properties. *Environ Microbiol* 8: 178–182.
- Heipieper, H.J. and Martínez, P.M. (2010) Toxicity of Hydrocarbons to Microorganisms. In *Handbook of Hydrocarbon and Lipid Microbiology*. Springer Berlin Heidelberg, pp. 1563–1573.
- Hu, Y., Xie, G., Jiang, X., Shao, K., Tang, X., and Gao, G. (2020) The Relationships Between the Free-Living and Particle-Attached Bacterial Communities in Response to Elevated Eutrophication. *Front Microbiol* 423.
- Huang, X., Shi, J., Cui, C., Yin, H., Zhang, R., Ma, X., and Zhang, X. (2016) Biodegradation of phenanthrene by *Rhizobium petrolearium* SL-1. *J Appl Microbiol* 121: 1616–1626.
- Huang, Y.J., Lin, B.S., Lee, C.L., and Brimblecombe, P. (2020) Enrichment behavior of contemporary PAHs and legacy PCBs at the sea-surface microlayer in harbor water. *Chemosphere* 245: 125647.
- Huson, D.H., Beier, S., Flade, I., Górška, A., El-Hadidi, M., Mitra, S., et al. (2016) MEGAN Community Edition - Interactive Exploration and Analysis of Large-Scale Microbiome Sequencing Data. *PLOS Comput Biol* 12: e1004957.
- Hyatt, D., Chen, G.-L., LoCascio, P.F., Land, M.L., Larimer, F.W., and Hauser, L.J. (2010) Prodigal: prokaryotic gene recognition and translation initiation site identification. *BMC Bioinformatics* 11: 119.
- Hylland, K. (2006) Polycyclic aromatic hydrocarbon (PAH) ecotoxicology in marine ecosystems. *J Toxicol Environ Health A* 69: 109–123.
- Jin, J., Yao, J., Zhang, Q., and Liu, J. (2016) Biodegradation of pyrene by *Pseudomonas* sp. JPN2 and its initial degrading mechanism study by combining the catabolic *nahAc* gene and structure-based analyses. *Chemosphere* 164: 379–386.
- Joye, S., Kleindienst, S., Gilbert, J., Handley, K., Weisenhorn, P., Overholt, W., and Kostka, J. (2016) Responses of Microbial Communities to Hydrocarbon Exposures. *Oceanography* 29: 136–149.
- Joye, S., Kleindienst, S., and Peña-Montenegro, T.D. (2018) SnapShot: Microbial Hydrocarbon Bioremediation. *Cell* 172: 1336-1336.e1.
- Ju, X., Jin, Y., Sasaki, K., and Saito, N. (2008) Perfluorinated surfactants in surface, subsurface water and microlayer from Dalian coastal waters in China. *Environ Sci Technol* 42: 3538–3542.
- Kanaly, R.A. and Harayama, S. (2010) Review article Advances in the field of high-molecular-weight polycyclic aromatic hydrocarbon biodegradation. 3: 136–164.
- Karthikeyan, S., Rodriguez-R, L.M., Heritier-Robbins, P., Hatt, J.K., Huettel, M., Kostka, J.E., and Konstantinidis, K.T. (2020) Genome repository of oil systems: An interactive and searchable database that expands the catalogued diversity of crude oil-associated microbes. *Environ Microbiol* 22: 2094–2106.
- Khatoun, K. and Malik, A. (2019) Screening of polycyclic aromatic hydrocarbon degrading bacterial isolates from oil refinery wastewater and detection of conjugative plasmids in polycyclic aromatic hydrocarbon tolerant and multi-metal resistant bacteria. *Heliyon* 5:.
- Kim, S.-J. and Kwon, K.K. (2010) Marine, Hydrocarbon-Degrading Alphaproteobacteria. In *Handbook of Hydrocarbon and Lipid Microbiology*. Springer Berlin Heidelberg, pp. 1707–1714.
- Knulst, J.C., Rosenberger, D., Brian Thompson, A., and Paatero, J. (2003) Intensive Sea Surface Microlayer Investigations of Open Leads in the Pack Ice during Arctic Ocean 2001 Expedition. 19: 10194–10199.
- Kodama, Y., Stiknowati, L.I., Ueki, A., Ueki, K., and Watanabe, K. (2008) *Thalassospira tepidiphila* sp. nov., a polycyclic aromatic hydrocarbon-degrading bacterium isolated from seawater. *Int J Syst Evol Microbiol* 58: 711–715.
- Krolicka, A., Boccadoro, C., Nilsen, M.M., and Baussant, T. (2017) Capturing Early Changes in the Marine Bacterial Community as a Result of Crude Oil Pollution in a Mesocosm Experiment. *Microbes Environ* 32: 358–366.
- Kuznetsova, M. and Lee, C. (2001) Enhanced extracellular enzymatic peptide hydrolysis in the sea-surface

microlayer. *Mar Chem* 73: 319–332.

Lee, S. and Fuhrman, J.A. (1987) Relationships between Biovolume and Biomass of Naturally Derived Marine Bacterioplankton. *Appl Environ Microbiol* 53: 1298–1303.

Li, D., Luo, R., Liu, C., Leung, C., Ting, H., Sadakane, K., et al. (2016) MEGAHIT v1.0: A fast and scalable metagenome assembler driven by advanced methodologies and community practices. *Methods* 102: 3–11.

Lim, L., Wurl, O., Karuppiyah, S., and Obbard, J.P. (2007) Atmospheric wet deposition of PAHs to the sea-surface microlayer. *Mar Pollut Bull* 54: 1212–1219.

Liss, P.S., Watson, A.J., Bock, J., Jaehne, B., Asher, W.E., Frew, N.M., et al. (2005) Sea surface and global change | Oceanography and marine science | Cambridge University Press, Liss, Peter S and Duce, Robert A (eds) Cambridge University Press.

Lohmann, R., Gioia, R., Jones, K.C., Nizzetto, L., Temme, C., Xie, Z., et al. (2009) Organochlorine pesticides and PAHs in the surface water and atmosphere of the North Atlantic and Arctic Ocean. *Environ Sci Technol* 43: 5633–5639.

Lors, C., Damidot, D., Ponge, J.-F., and Périé, F. (2012) Comparison of a bioremediation process of PAHs in a PAH-contaminated soil at field and laboratory scales Comparison of a bioremediation process of PAHs in a PAH-1 contaminated soil at field and laboratory scales 2 3. 165: 11–17.

Lozada, M., Marcos, M.S., Commendatore, M.G., Gil, M.N., and Dionisi, H.M. (2014) The bacterial community structure of hydrocarbon-polluted marine environments as the basis for the definition of an ecological index of hydrocarbon exposure. *Microbes Environ* 29: 269–76.

Mapelli, F., Scoma, A., Michoud, G., Aulenta, F., Boon, N., Borin, S., et al. (2017) Biotechnologies for Marine Oil Spill Cleanup: Indissoluble Ties with Microorganisms. *Trends Biotechnol* 35: 860–870.

Marín-Beltrán, I., Logue, J.B., Andersson, A.F., and Peters, F. (2019) Atmospheric Deposition Impact on Bacterial Community Composition in the NW Mediterranean. *Front Microbiol* 10: 858.

Martin, M. (2011) Cutadapt removes adapter sequences from high-throughput sequencing reads. *EMBnet.journal* 17: 10.

Martinez-Varela, A., Casas, G., Piña, B., Dachs, J., and Vila-Costa, M. (2020) Large Enrichment of Anthropogenic Organic Matter Degrading Bacteria in the Sea-Surface Microlayer at Coastal Livingston Island (Antarctica). *Front Microbiol* 11: 2153.

Martinez-Varela, A., Cerro-Gálvez, E., Auladell, A., Sharma, S., Moran, M.A., Kiene, R.P., et al. (2021) Bacterial responses to background organic pollutants in the northeast subarctic Pacific Ocean. *Environ Microbiol* 1462-2920.15646.

Mclachlan, M.S., Zou, H., and Gouin, T. (2016) Using Benchmarking To Strengthen the Assessment of Persistence.

Medić, A., Lješević, M., Inui, H., Beškoski, V., Kojić, I., Stojanović, K., and Karadžić, I. (2020) Efficient biodegradation of petroleum: N-alkanes and polycyclic aromatic hydrocarbons by polyextremophilic *Pseudomonas aeruginosa* strain with multidegradative capacity. *RSC Adv* 10: 14060–14070.

Mistry, J., Chuguransky, S., Williams, L., Qureshi, M., Salazar, G.A., Sonnhammer, E.L.L., et al. (2021) Pfam: The protein families database in 2021. *Nucleic Acids Res* 49: D412–D419.

Nakajima, R., Tsuchiya, K., Nakatomi, N., Yoshida, T., Tada, Y., Konno, F., et al. (2013) Enrichment of microbial abundance in the sea-surface microlayer over a coral reef: Implications for biogeochemical cycles in reef ecosystems. *Mar Ecol Prog Ser* 490: 11–22.

Naumann, E. (1917) Über das Neuston des Süßwassers. *Biol Cent* 37: 98–106.

Oksanen, J., Blanchet, G.F., Friendly, M., Kindt, R., Legendre, P., McGlenn, D., et al. (2020) Vegan: Community Ecology Package.

Parada, A.E., Needham, D.M., and Fuhrman, J.A. (2016) Every base matters: assessing small subunit rRNA primers for marine microbiomes with mock communities, time series and global field samples. *Environ Microbiol* 18: 1403–1414.

Planet, P.J., Kachlany, S.C., Fine, D.H., DeSalle, R., and Figurski, D.H. (2003) The widespread colonization island of *Actinobacillus actinomycetemcomitans*. *Nat Genet* 34: 193–198.

Poretsky, R.S., Sun, S., Mou, X., and Moran, M.A. (2010) Transporter genes expressed by coastal bacterioplankton in response to dissolved organic carbon. *Environ Microbiol* 12: 616–627.

Quast, C., Pruesse, E., Yilmaz, P., Gerken, J., Schweer, T., Yarza, P., et al. (2013) The SILVA ribosomal RNA

gene database project: Improved data processing and web-based tools. *Nucleic Acids Res* 41: D590.

Quigg, A., Passow, U., Chin, W.-C., Xu, C., Doyle, S., Bretherton, L., et al. (2016) The role of microbial exopolymers in determining the fate of oil and chemical dispersants in the ocean Scientific Significance Statement. *Limnol Oceanogr Lett* 1: 3–26.

R Core Team (2019) R: A Language and Environment for Statistical Computing.

Reddy, C.M., Arey, J.S., Seewald, J.S., Sylva, S.P., Lemkau, K.L., Nelson, R.K., et al. (2012) Composition and fate of gas and oil released to the water column during the Deepwater Horizon oil spill. *Proc Natl Acad Sci U S A* 109: 20229–34.

Redmond, M.C. and Valentine, D.L. (2012) Natural gas and temperature structured a microbial community response to the Deepwater Horizon oil spill. *Proc Natl Acad Sci U S A* 109: 20292–20297.

Rieck, A., Herlemann, D.P.R., Jürgens, K., and Grossart, H.P. (2015) Particle-associated differ from free-living bacteria in surface waters of the baltic sea. *Front Microbiol* 6: 1297.

Robinson, M.D., McCarthy, D.J., and Smyth, G.K. (2009) edgeR: A Bioconductor package for differential expression analysis of digital gene expression data. *Bioinformatics* 26: 139–140.

Roca, C., Lehmann, M., Torres, C.A.V., Baptista, S., Gaudêncio, S.P., Freitas, F., and Reis, M.A.M. (2016) Exopolysaccharide production by a marine *Pseudoalteromonas* sp. strain isolated from Madeira Archipelago ocean sediments. *N Biotechnol* 33: 460–466.

Roth Rosenberg, D., Haber, M., Goldford, J., Lalzar, M., Aharonovich, D., Al-Ashhab, A., et al. (2021) Particle-associated and free-living bacterial communities in an oligotrophic sea are affected by different environmental factors. *Environ Microbiol* 1462-2920.15611.

Sabbaghzadeh, B., Upstill-Goddard, R.C., Beale, R., Pereira, R., and Nightingale, P.D. (2017) The Atlantic Ocean surface microlayer from 50°N to 50°S is ubiquitously enriched in surfactants at wind speeds up to 13 m s<sup>-1</sup>. *Geophys Res Lett* 44: 2852–2858.

Santos, A.L., Baptista, I., Lopes, S., Henriques, I., Gomes, N.C.M., Almeida, A., et al. (2012) The UV responses of bacterioneuston and bacterioplankton isolates depend on the physiological condition and involve a metabolic shift. *FEMS Microbiol Ecol* 80: 646–658.

Sauret, C., Séverin, T., Vétiou, G., Guigue, C., Goutx, M., Pujo-Pay, M., et al. (2014) “Rare biosphere” bacteria as key phenanthrene degraders in coastal seawaters. *Environ Pollut* 194: 246–253.

Smith, M.W., Zeigler Allen, L., Allen, A.E., Herfort, L., and Simon, H.M. (2013) Contrasting genomic properties of free-living and particle-attached microbial assemblages within a coastal ecosystem. *Front Microbiol* 4: 120.

Stolle, C., Nagel, K., Labrenz, M., and Jürgens, K. (2010) Bacterial activity in the sea-surface microlayer: In situ investigations in the Baltic Sea and the influence of sampling devices. *Aquat Microb Ecol* 58: 67–78.

Stortini, A.M., Martellini, T., Del Bubba, M., Lepri, L., Capodaglio, G., and Cincinelli, A. (2009) n-Alkanes, PAHs and surfactants in the sea surface microlayer and sea water samples of the Gerlache Inlet sea (Antarctica). *Microchem J* 92: 37–43.

Tremblay, L., Kohl, S.D., Rice, J.A., and Gagné, J.P. (2005) Effects of temperature, salinity, and dissolved humic substances on the sorption of polycyclic aromatic hydrocarbons to estuarine particles. *Mar Chem* 96: 21–34.

Umar, Z.D., Aziz, N.A.A., Zulkifli, S.Z., and Mustafa, M. (2017) Rapid biodegradation of polycyclic aromatic hydrocarbons (PAHs) using effective *Cronobacter sakazakii* MM045 (KT933253). *MethodsX* 4: 104–117.

Uning, R., Latif, M.T., Yu, K.L., Cheng, S.Y., Ahamad, F., Khan, M.F., et al. (2018) Surfactants in the Sea Surface Microlayer, Underlying Water and Atmospheric Particles of Tropical Coastal Ecosystems. *Water Air Soil Pollut* 229:.

Del Vento, S. and Dachs, J. (2002) Prediction of uptake dynamics of persistent organic pollutants by bacteria and phytoplankton. *Environ Toxicol Chem* 21: 2099–2107.

Vila-Costa, M., Sebastián, M., Pizarro, M., Cerro-Gálvez, E., Lundin, D., Gasol, J.M., and Dachs, J. (2019) Microbial consumption of organophosphate esters in seawater under phosphorus limited conditions. *Sci Rep* 9: 233.

Wang, Q. and Kelly, B.C. (2018) Assessing bioaccumulation behaviour of hydrophobic organic contaminants in a tropical urban catchment. *J Hazard Mater* 358: 366–375.

Wickham, H. (2009) *Ggplot2: Elegant Graphics for Data Analysis.*, 2nd ed. Springer New York.

Wurl, O. and Obbard, J.P. (2004) A review of pollutants in the sea-surface microlayer (SML): a unique habitat for marine organisms. *Mar Pollut Bull* 48: 1016–1030.

Zhao, B., Wang, H., Li, R., and Mao, X. (2010) *Thalassospira xianhensis* sp. nov., a polycyclic aromatic hydrocarbon-degrading marine bacterium. *Int J Syst Evol Microbiol* 60: 1125–1129.



# 5

## **Bacterial responses to background organic pollutants in the northeast subarctic Pacific Ocean**

**Alícia Martínez-Varela**, Elena Cerro-Gálvez, Adrià Auladell, Shalabh Sharma, Mary Ann Moran, Ronald P. Kiene, Benjamin Piña, Jordi Dachs and Maria Vila-Costa

Environmental Microbiology, 2021

Thousands of man-made synthetic chemicals are released to oceans and compose the anthropogenic dissolved organic carbon (ADOC). Little is known about the effects of this chronic pollution on marine microbiome activities. In this study, we measured the pollution level at three sites in the Northeast Subarctic Pacific Ocean (NESAP) and investigated how mixtures of three model families of ADOC at different environmentally relevant concentrations affected naturally occurring marine bacterioplankton communities' structure and metabolic functioning. The offshore northernmost site (North) had the lowest concentrations of hydrocarbons, as well as organophosphate ester plasticizers, contrasting with the two other continental shelf sites, the southern coastal site (South) being the most contaminated. At North, ADOC stimulated bacterial growth and promoted an increase in the contribution of some Gammaproteobacteria groups (e.g. Alteromonadales) to the 16 rRNA pool. These groups are described as fast responders after oil spills. In contrast, minor changes in South microbiome activities were observed. Gene expression profiles at Central showed the co-existence of ADOC degradation and stress-response strategies to cope with ADOC toxicities. These results show that marine microbial communities at three distinct domains in NESAP are influenced by background concentrations of ADOC, expanding previous assessments for polar and temperate waters.



## INTRODUCTION

Increasingly large amounts of semi-volatile and hydrophobic organic pollutants (OP) are globally transported and atmospherically deposited to the open ocean, leading to chronic diffuse pollution (Lohmann et al., 2007; Dachs and Méjanelle, 2010; González-Gaya et al., 2016). These thousands of synthetic organic compounds and hydrocarbons compose the anthropogenic dissolved organic carbon (ADOC) (Vila-Costa et al., 2020). Individual ADOC compounds are found at concentrations from the pico- to the nano- molar range, but the combined co-occurrence of thousands of different anthropogenic compounds can reach micromolar concentrations (Dachs and Méjanelle, 2010; González-Gaya et al., 2016; Vila-Costa et al., 2020). ADOC contributes to oceanic dissolved organic matter budgets. However, knowledge regarding its impact on resident plankton activities and diversity remains unknown. Most studies on the toxicity and bioaccumulation of some families of ADOC constituents have focused on large oceanic fauna occupying the apex of food webs (Krahn et al., 2007; Cullon et al., 2009; Desforges et al., 2018). Yet the effects of ADOC exposure to microorganisms at realistic environmental levels remain largely unexplored, as well ADOC implications to the major biogeochemical cycles driven by microorganisms.

Recent quantifications of ADOC flux indicate that polycyclic aromatic hydrocarbons (PAH), a representative ADOC family, are reaching the marine environment in remarkably higher quantities than seen in past assessments of atmospheric inputs (Jurado et al., 2008; Kanakidou et al., 2012; González-Gaya et al., 2016). Only a minor share (1%) of PAHs entering the oceans is removed from surface waters through settling particles within the water column (i.e. by the biological pump), until eventually sinking into the deep ocean (González-Gaya et al., 2019). It has been suggested that a major fraction of airborne PAHs is removed from the upper sea layers through biodegradation, and abiotic removal processes such as photodegradation accounts for only a minor portion (King et al., 2014; González-Gaya et al., 2016). Thus, microbial degradation plays a key role in modulating ADOC fate in the upper ocean but remains unquantified in sub-Arctic waters. While at low temperatures biodegradation rates are generally lower, the adaptation to cold temperatures of Arctic bacteria allow them to eventually degrade ADOC compounds at metabolic rates similar than those at warmer environments (Bagi et al., 2013).

Microbial responses to ADOC are diverse, ranging from metabolically advantageous to eliciting lethal and sub-lethal toxic effects (Head et al., 2006; Heipieper and Martínez, 2010). Most of the different microbial strategies to cope with ADOC have been described in both cultures and in naturally occurring communities, but at high concentrations, much above the environmental levels (e.g. Abbasian et al., 2016; Joye et al., 2016). As most ADOC compounds are hydrophobic, they become strongly sorbed onto the cell membranes, altering their physicochemical properties, potentially promoting harmful effects by narcosis that can inhibit key functions of planktonic cells. This process may lead to contrasting taxonspecific responses on heterotrophic bacteria (Van Wezel and Opperhuizen, 1995; Echeveste et al., 2010; Fernández-Pinos et al., 2017; Mitchell and Silhavy, 2019; Cerro-Gálvez et al., 2019a, 2019b). Acute pollution events, such as oil spills, and long-term exposed areas, have improved our understanding of microbial successions and taxonomical preferences in highly polluted environments (Mason et al., 2012; Dombrowski et al., 2016; Liu et al., 2017; Vergeynst et al., 2018). Biodegradation is one strategy that co-exists with other microbial responses, such as detoxification metabolisms, to cope with labile and semi-labile ADOC compounds (Wang and Shao, 2013; Gupta et al., 2015; Habe and Omori, 2017; Vergeynst et al., 2019; Vila-Costa et al., 2020). Facultative and obligate ADOC microbial consumers, as well as ADOC-tolerant organisms, have been characterized, and a number of hydrocarbonoclastic bacteria (HCB, this is facultative and obligate hydrocarbon-degrading bacteria) species have been proposed as taxonomic microbial indicators of hydrocarbon pollution (Kostka et al., 2011; Parmar et al., 2016; Krollicka et al., 2017, 2019). Beyond taxonomical markers, functional gene expression can describe the transcriptomic fingerprint of the different co-occurring interactions between ADOC and microorganisms in acute environmental contamination events (DeBry et al., 2007; Reunamo et al., 2017). As an example, in an oil challenged mesocosms experiment, Valencia-Agami et al., 2019, tracked bacterial hydrocarbon degradation activity based on the copy number of the Alkane 1-monooxygenase (*alkB* gene), in combination with the detected culturable HCB bacteria. Contrastingly, the microbial responses to the baseline ADOC present in the oceans are less known. Initial data show that despite low in situ concentrations, the ADOC pool has an effect on the marine microorganisms requiring further research (Echeveste et al., 2010; Fernández-Pinos et al., 2017; Vergeynst et al., 2019; Cerro-Gálvez et al., 2019a, 2021).

This work aims to expand our knowledge of the pollution level in subpolar regions to better understand the role played by environmental parameters in modulating the microbial response to ADOC in surface seawater. Experiments were performed at three different sites representative of the spatial heterogeneity of the northeast subarctic Pacific (NESAP). Microbiomes were challenged with three representative families of ADOC; polycyclic aromatic hydrocarbons (PAHs), n-alkanes, and the emerging pollutants organophosphate ester flame retardants and plasticizers (OPE) at background concentrations for 24 h. Sites and microbial responses were characterized at chemical, structural and functional level by means of gas chromatography–mass spectrometry, by sequencing the small sub-unit ribosomal RNA gene (*rRNA* gene, hereafter *rDNA*) and *rRNA* molecules

(rRNA) of Bacteria and by metatranscriptomics. As far as we know, this is the first study addressing baseline ADOC effects on marine microbial communities in a sub-polar region.

## MATERIALS AND METHODS

### Experiment sites

Experiments were conducted on board of the University–National Oceanographic Laboratory System (UNOLS) vessel R/V Oceanus during July 2016. The cruise track and the three experiments sites were designed to cover the heterogenic regimes along the spatial gradients in surface water of the NESAP (Figure 1; Supporting Information Table S1). The first experiment was conducted at an iron depleted offshore station with a HNLC regime (Experiment 1: North, located at 55.00 N, 138.59 W). The second and third experiments were located closer to the coast on the British Columbia continental shelf at two different latitudes and distinct hygrometric domains (Experiment 2: Central, Hecate Strait, located at 52.58 N, 130.32 W, and Experiment 3: South, La Perouse Bank, located at 48.65 N, 126.67 W).

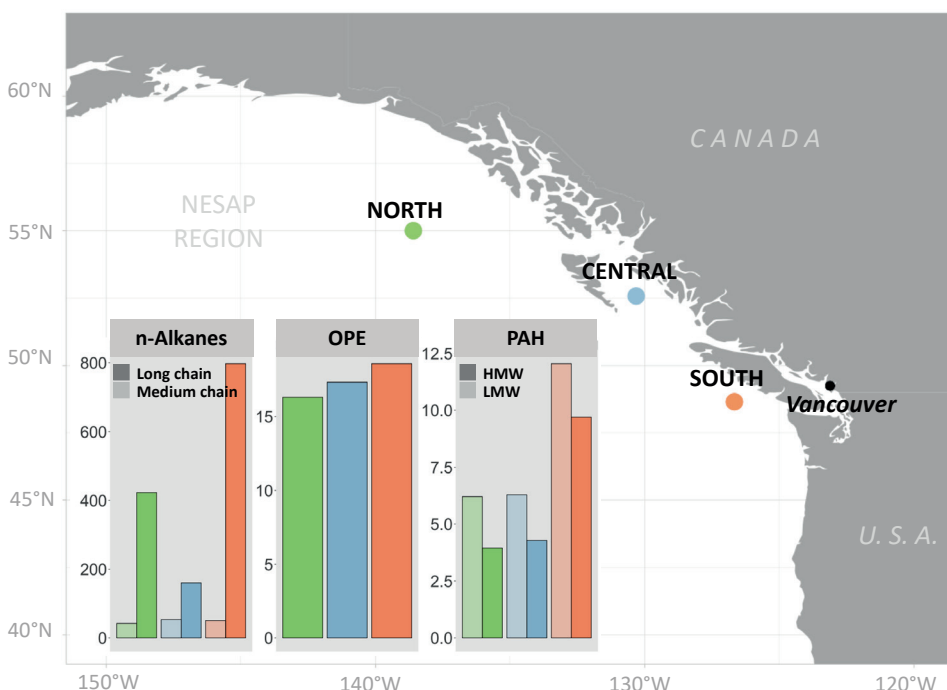


**FIGURE 1** | Sampling sites in three distinct trophic domains in NESAP region and in situ concentrations of three model families of ADOC (in ng L<sup>-1</sup>). OPE: organophosphate esters, PAH: polycyclic aromatic hydrocarbons. HMW: high-molecular weight (PAH composed of four or more rings). LMW: low-molecular weight (PAH composed of less than four fused rings). Medium chain n-Alkanes: C12–C20. Long chain n-Alkanes: C21–C35.

### ***Experimental set up with natural communities***

Three hours prior to the surface seawater sampling, ADOC mixtures at two concentration levels (low and high) were added to 2 l pre-cleaned and 400C baked glass bottles, allowing solvents (alkanes: toluene, PAHs: cyclohexane and OPE: acetone) evaporation to avoid any toxic effects derived from solvents presence (for ADOC composition amendments, see Supporting Information Table S6). The relative concentrations of the ADOC families present in the seawater (control/treatment ratio) varied at each station, as the pollutant concentrations were different at each experiment site (Supporting Information Tables S3 and S6). At each station surface seawater (1–2 m depth) was collected using Niskin bottles attached to a Seabird CTD probe (Seabird 911plus unit). Depth profiles of hygrometric features were measured and seawater was dispensed into the experimental bottles. Seawater without ADOC spike were run as controls, but solvents were also spiked and let to evaporate before water addition as done with treatments. Experiment bottles were incubated during 24 h in the dark and at in situ temperature (13–15 °C, see Supporting Information Table S1).

### ***Dissolved phase concentrations of PAH, n-alkanes and OPE***

Concentrations of PAHs, OPEs and n-alkanes, chosen as model molecules present in ADOC, were measured in the dissolved phase at the beginning of each experiment. The 20 l of surface seawater (1–2 m depth) was collected using metallic carboys. The water was pre-filtered on a pre-combusted glass fibre filter (GF/F, Whatmann) and then eluted and concentrated on a XAD-2 (polystyrene copolymer resin) absorbent column. Analyses were performed following the procedures described elsewhere (Berrojalbiz et al., 2009; Fernández-Pinos et al., 2017; González-Gaya et al., 2019; Vila-Costa et al., 2020).

### ***Bacterial abundance***

Prokaryotic cell abundance was estimated by flow cytometry as described elsewhere (Falcioni et al., 2008). Briefly samples (0.4 ml) for heterotrophic non-pigmented total bacteria enumeration were stained with 4 µl of a 10<sup>6</sup> SG1 (molecular probes) solution (final dilution, 1:1000 [vol/vol]) for 10 min and run through the FACSCalibur flow cytometer at a low speed (15 µl min<sup>-1</sup>), with fluorescent microspheres as an internal standard [yellow-green 0.92-µm Polysciences latex beads (10<sup>6</sup> ml<sup>-1</sup>)]. Bacteria were detected in a dot plot of side scatter versus green fluorescence (FL1) and population concentration was estimated with CellQuest and PaintAGate software (Becton Dickinson, Palo Alto, CA). Abundance yields were calculated following the equation:  $\mu = (N2-N1)/24$  (N1 and N2 are bacterial abundances at T0 and T24 respectively). High and low nucleic acid content cells (HNA and LNA, respectively) were counted separately.

### ***DMSP measurements***

DMS loss and DMSP consumption rates were measured using the radio-labelled <sup>35</sup>S methods outlined by Kiene et al. (2000). Briefly, <sup>35</sup>S-labelled DMSPd or DMS were added to samples at non-perturbing concentrations (<1% of ambient levels). Samples were incu-

bated in the dark at surface water temperatures for <1 h (35S-DMSP) or < 7 h (35S-DMS). The rate constant  $30 \text{ d}^{-1}$  for DMSPd turnover was determined by measuring the disappearance of 35SDMSP from the dissolved (< 0.2  $\mu\text{m}$ ) pool. Consumption rates ( $\text{nmol L}^{-1}$ ) were calculated by multiplying in situ DMSPd concentrations by the measured rate constant (kDMSPd).

### ***Bioorthogonal non-canonical amino acid tagging***

After 24 h of ADOC exposure, subsamples of 45 ml of each sample were incubated at room temperature for 2 h in the dark with sterile-filtered bioorthogonal amino acid L-homopropargylglycine (HPG, used as surrogate of L-methionine) at a final concentration of 0.5  $\mu\text{M}$ . HPG targets proteins that have been newly synthesized in reaction to an experimental condition such as ADOC exposure. Cell fixation was done by adding 5 ml of 0.2  $\mu\text{m}$  pre-filtered paraformaldehyde overnight 4°C. Killed controls were also performed in parallel, by fixing the biomass with 5 ml of 0.2  $\mu\text{m}$  prefiltered paraformaldehyde prior to the initial HPG incubation. The fixed samples were gently filtered through 0.2  $\mu\text{m}$  pore size polycarbonate filters under low vacuum pressure. Filters were left to dry and stored at  $-20^\circ\text{C}$  until further processing. After thawing, cell wall permeabilization and click-reaction, filter pieces were counterstained with 4',6-diamidino-2-phenylindole (DAPI, 10  $\mu\text{g/ml}$  final concentration) Percentages of the hybridized cells to DAPI stained cells were analysed through epifluorescence microscopy (Olympus BX61) under blue light and UV excitation. Images were acquired using a digital camera (Zeiss camera AxioCam MRm, Carl Zeiss Microimaging, S.L., Barcelona, Spain) at 630 $\times$  magnification through the Axiovision software and analysed using the automated image analysis software ACMETool. All images (at least 10 fields/filter) were acquired using 20 ms as exposure time (Leizeaga et al., 2017).

### ***Nucleic acids extraction and sequencing***

After 24 h of ADOC addition, 2 l seawater was pre-filtered through a 3  $\mu\text{m}$  pore-size 47 mm diameter poly-tetrafluoroethylene filter to exclude grazers and the particle-attached bacteria and free-living bacterial cells were collected on 0.2  $\mu\text{m}$  pore-size 47 mm polytetrafluoroethylene filters under low vacuum pressure. The duration of the first filtration was no longer than 15 min to minimize RNA degradation. The filter was placed in 1 ml RNAlater (Sigma-Aldrich, Saint Louis, MO) and the water left was filtered for DNA collection, and placed into 1 ml lysis buffer (50 mM Tris HCl, 40 mM EDTA, 0.75 M sucrose) and stored at  $-20^\circ\text{C}$  to preserve RNA and DNA respectively. DNA extraction was performed as described in the study by Vila-Costa et al. (2020). Total RNA was extracted, DNA removed, rRNA depleted and mRNA enriched by amplification as described in the study by Poretsky et al. (2014) with the only modification that total RNA was extracted with mirVana isolation kit (Ambion), after removing the storage reagent by centrifugation. Three mRNA standards were synthesized (Gifford et al., 2011) by in vitro transcription from plasmids with restriction enzyme: pTXB1 vector (New England Biolabs, Ipswich, MA) with NcoI restriction enzyme (Promega, Madison, WI), pFN18K Halotag T7 Flexi vector

(Promega) with BamHI restriction enzyme (Promega) and pGEM-4Z (Promega) with Scal restriction enzyme (Promega). This artificial mRNA was added after RNA extraction but before mRNA enrichment as in the study by Rinta-Kanto et al. (2012) and used as an internal standard to calculate absolute transcript abundances (Moran et al., 2013; Satinsky et al., 2013). See Supporting Information for details. Final DNA and amplified RNA were sequenced at the National Center for Genomic Analysis (CNAG, Barcelona, Spain) using Illumina high output model HS200 2 × 100 bp v4. Partial amplification of the 16S rRNA gene (~245 bp fragments) was done in 50 µl reactions using primers 515F-Y (5'-GTGYCAG-CMGCCGCGGTAA) and 926R (5'-CCGYCAATTYMTTTRAGTTT) (Parada et al., 2016), each at 0.2 µM final concentration. The final concentration of MgCl<sub>2</sub> was 2 mM. PCR conditions were as follows: an initial denaturation step at 95°C for 5 min and 35 cycles at 95°C (30 s), 58°C (30 s), 72°C (40 s) and a final elongation step at 72°C for 10 min. Sequencing was performed in an Illumina MiSeq sequencer (2 × 250 bp, Research and Testing Laboratory; <http://rtlgenomics.com/>). The complete nucleotide and transcript sequence dataset generated and analysed in this study was deposited in the sequence read archive (SRA) under the bioproject accession no. PRJNA656679 and PRJNA656681.

### ***Bioinformatics***

DADA2 v1.4 was used to differentiate the 16S V4-5 amplicon sequence variants (ASVs) and remove chimeras (parameters: maxN = 0, maxEE = 2,4, truncLen = 227 210; Callahan et al., 2016). DADA2 resolves ASVs by modelling the errors in Illumina-sequenced amplicon reads. The approach is threshold-free, inferring exact variants up to one nucleotide difference using the quality score distribution in a probability model. Previously, spurious sequences and primers were trimmed using cutadapt v.1.16 (Martin, 2011). Taxonomic assignment of the ASVs was performed with the SILVA algorithm classifier against SILVA database release 138 (Quast et al., 2013). ASVs classified as Mitochondria or Chloroplast were removed. The final ASV table contained 48 samples, with a pool of 15262 ASV, accounting for 324.7 ASV on average per sample and the minimum sequencing depth was 22 035. Rarefaction was done with rrarefy() function from 'vegan v1.4-4' package in R (Oksanen et al., 2020). Archaea accounted for <3% of the total pool of reads and were discarded from the analyses. For the metatranscript data, the FASTX toolkit was used for quality control of 195.6 million 100-bp reads, imposing a minimum quality score of 20 over 80% of read length. Reads from all the libraries were aligned to an in-house rRNA database assembled with representative rRNAs and internal standard sequences as previously described (Gifford et al., 2011, 2013). Reads with a bit score ≥ 50 in Blastn analysis were removed from further analysis, and a check of the removed and retained reads confirmed efficient separation. The remaining potential protein encoding reads were annotated against NCBI's RefSeq and COG databases using Blastx. Specific hydrocarbon and OPE degrading genes retrieved from the literature (see Supporting Information Table S8) were searched within the metatranscriptome by keyword and based on FOAM annotation hydrocarbon degradation transcript assignment (Prestat et al., 2014).

### ***Identification of ADOC associated genera***

ADOC-A genera were retrieved from the literature (Takahashi et al., 2013; Lozada et al., 2014; Karthikeyan et al., 2020). The genera strains comprised in this group have been retrieved from ADOC polluted environments, observed to have stimulated growth following ADOC exposure, or with the capacity to metabolically participate in different steps of ADOC degradation processes.

The detection of specific ADOC-A bacterial genera (see Supporting Information Table S4) was performed by filtering at genus level all those ASVs and transcripts with taxonomical affiliation matching to those targeted ADOC-A groups. Additionally, the subset of ASV assigned to ADOC-A genera were compared with BLAST against a relevant isolate from the same genus known to degrade ADOC or retrieved from ADOC polluted sites. Those ASVs with >97% of similarity were taken as true match (Supporting Information Tables S10 and S11). All ADOC-A-ASV within the same genus were assumed to share similar metabolism.

### ***Statistical analyses***

The significance of the difference in community composition between locations was tested with a permutation analysis of variance (PERMANOVA, with function `Adonis()`) from 'vegan v1.4-4' package in R. Fold changes were calculated for the relative values between treatments (low and high) and controls computed as: treatment/control if treatment > control, and as control/treatment otherwise, using the function `foldchange()` from 'gtools' package (R Core Team, 2019). Significant differences between treatments were tested using the 'HSD.test()' function with a threshold for the significance set at  $P < 0.05$  from R package 'agricolae'. Analysis of differentially expressed genes was performed with the 'EdgeR' package (Robinson et al., 2009). Further graphs were plotted using the 'ggplot2' package, also in R environment (Wickham, 2009).

## **RESULTS AND DISCUSSION**

### ***Characterization of NESAP sampling sites and microbiomes***

Three sites from the northeast subarctic Pacific (NESAP) region were chosen to perform the experiments. The three sites draw a gradient from offshore colder and more pristine waters at higher latitudes (Experiment 1: North), to coastal warmer southern waters on the British Columbia continental shelf, to the wide but shallow Hecate strait (Experiment 2: Central) reaching La Perouse Bank (Experiment 3: South) (**Figure 1**; Supporting Information - Table S1). The percentage of seawater optical transparency, taken as a proxy of low trophic state and productivity of the ecosystem (Williamson et al., 2011), was higher at South (96.9%), compared to those at Central and North (averaging 90.8%). The opposite pattern was observed for most biological variables. Chlorophyll concentration, bacterial abundance, proportion of active heterotrophic cells and bacterial production rates were highest at Central ( $1.7 \mu\text{g L}^{-1}$ ,  $1.3 \times 10^5 \pm 2.1 \times 10^3 \text{ cells ml}^{-1}$ ,  $12.1 \pm 6.94\%$

and 1.5 nM Leu d<sup>-1</sup>), followed closely by North (1.7 µg L<sup>-1</sup>, 6.8 × 10<sup>4</sup> ± 1.7 × 10<sup>3</sup> cells ml<sup>-1</sup>, 8.1% and 1.3 nM Leu d<sup>-1</sup>), and lowest at South (0.2 µg L<sup>-1</sup>, 9.8 × 10<sup>4</sup> ± 1.3 × 10<sup>3</sup> cells ml<sup>-1</sup>, 7.45 ± 2.81 and 0.7 nM Leu d<sup>-1</sup>) (Supporting Information Table S2). Dimethylsulfoniopropionate (DMSP) turnover rates followed the same pattern, with higher values in Central compared to North and South (Supporting Information Table S2). These results suggest Central and North harboured the most active microbiomes.

The taxonomic affiliation of the members of the community and the active groups were characterized by 16S rDNA and rRNA amplicon sequencing, respectively. Community composition of both coastal sites (Central and South) was more similar to each other compared to the open ocean site (North) (Supporting Information Figure S1). From the same set of samples, Herr et al. (2019) observed a phytoplankton community composition shift between offshore North waters (dominated by nanophytoplankton) and on-shelf waters

(Central and South, dominated by microphytoplankton). Community composition, dominated by SAR11 and Flavobacteriales, was similar to those reported previously in surface waters of the same oceanic regions (Wright et al., 2012; Muck et al., 2019). The dominant active groups were detected based on their 16S rRNA pool contribution, taking into a count that non-growing cells also contribute to this pool (Blazewicz et al., 2013). Comparing their relative abundances, Flavobacteriales and Rhodobacteriales dominated the contribution to the rRNA pool at North with average relative abundances of 15.1 ± 0.3% and 20.7 ± 1.4%, respectively, significantly higher than their onshelf sites contributions (P < 0.01). The dominant SAR11 clade showed markedly different activity levels among the three sites, accounting for a large percentage of the total 16S rRNA pool at South site (26 ± 2.7%), but decreasing at higher latitudes (20.8 ± 2.7% in Central and 22 ± 1.9% in North) (Supporting Information Figure S2).

### ***Pollutant concentrations***

Concentrations of PAHs, OPEs and n-alkanes, chosen as model molecules covering the wide range of physicochemical properties present in ADOC, were measured in the dissolved phase at the beginning of each experiment. After extraction and fractionation, dissolved ADOC were concentrated on a polymeric adsorbent column (XAD-2), and analysed by gas chromatography coupled to mass spectrometry (GC-MS). The highest concentrations for the three model families of ADOC were recorded at the South site, which corresponded to the most anthropogenic influenced site at a 270 km distance from Vancouver (**Figure 1**; Supporting Information Table S3). Analogous north-south gradients of PAH and alkane abundances have been reported for coastal sediments (Yunker et al., 2015). However, this is the first report of dissolved phase concentrations of organic pollutants for the NESAP, as previous work focused on the Arctic (Ma et al., 2013) or coastal sites such as the Georgia strait (Frouin et al., 2013). The sum of 64 PAHs concentrations was 21.47 ng L<sup>-1</sup> at the South site, double the concentrations found at sites North and Central (10.15 and 10.56 ng L<sup>-1</sup>, respectively). Concentrations of individual PAHs, such as phenanthrene and pyrene, were comparable to those found at similar latitudes in the



North Atlantic seawater (Nizzetto et al., 2008). At all stations, the low-molecular weight (LMW) fraction of PAHs, such as phenanthrene and methylphenanthrenes, were found at higher concentrations than the high-molecular weight (HMW) fraction, consistent with the dissolved phase enriched with the more soluble PAHs, as reported in other regions (Ma et al., 2013; Ganzález-Gaya et al., 2016). A similar latitudinal pattern was observed for n-alkane (C12–C35) with highest concentrations at South (847.98 ng L<sup>-1</sup>), followed by North (464.95 ng L<sup>-1</sup>) and Central (213.25 ng L<sup>-1</sup>). The concentrations of n-alkanes fell within the range of previously observed concentrations in oceanic surface waters (Stortini et al., 2009; Guigue et al., 2011; Fourati et al., 2018). Similarly, as described by Stortini et al. (2009) in Antarctic waters, long chain alkanes (>C20–C35) were predominant at the three sites, while medium chain alkanes (C12–C19) contributed minimally to the total budget of n-alkanes. Alkanes are highly hydrophobic chemicals, and thus alkanes tend to be sorbed to organic matter pools such as particles and DOC. The adsorbent used to retain ADOC, can also retain partly the most hydrophobic DOC. Therefore, from the high octanol–water partition coefficients of alkanes, it is predicted that most apparently dissolved phase alkanes are sorbed to colloidal DOC. Therefore, alkanes concentrations correspond to the apparently dissolved phase, including both the dissolved and colloidal phases. OPE concentrations were similar at the three sites, with the lowest concentration of 16.31 ng L<sup>-1</sup> at site North, 17.33 ng L<sup>-1</sup> at Central and 18.58 ng L<sup>-1</sup> at South. Highest concentrations were found for TCEP, with concentrations above 6 ng L<sup>-1</sup>, while EHDPP and TEHP were only detected at South. The OPE concentrations detected in the NESAP region were at similar levels as in Canadian Arctic surface water (McDonough et al., 2018). However, mean concentrations from North Atlantic waters at comparable latitudes are one order of magnitude lower (Li et al., 2017). Still, OPE levels measured in the open waters of NESAP are far below the concentrations found at anthropogenically affected waters around the world, which can range from 92 to 1392 ng L<sup>-1</sup> (Hu et al., 2014).

### ***ADOC degrading microorganisms***

Specific bacterial genera reported so far in the literature to be associated and stimulated by ADOC presence, or with known capabilities for degrading organic pollutants, including strict specialists and general consumers, were retrieved in our sample sets at initial conditions (see Supporting Information Table S4 and Experimental procedures section for detailed information). This group will be henceforth referred to as ADOC-associated (ADOCA). ADOC-A genera accounted for an average of  $0.18 \pm 0.02\%$  of total 16S rDNA pool in all samples at the initial conditions (Supporting Information Table S5). These low abundances are similar to those encountered in polar environments (Garneau et al., 2016; Cerro-Gálvez et al., 2019b) and are consistent with microorganisms contributing to the rare biosphere (Kleindienst et al., 2016; Karthikeyan et al., 2020). It is worthy to notice that the diversity of ADOC-A is continuously growing in the literature, so ADOC-A genera in this study is limited to the current knowledge. Significant differences were observed between sites (Supporting Information Table S5) for specific ADOC-A genera and taxonomic orders including strains known to be stimulated by the presence of oil (Hazen et al., 2010;

Kostka et al., 2011; Joye et al., 2016; Neethu et al., 2019). For example, some Alphaproteobacteria ADOC-A genera such as Sphingobium, Sphingomonas and Sulfitobacter were found at the North site at abundances that were an order of magnitude higher compared to those at the other two sites (significance  $P < 0.05$ ). In contrast, Gammaproteobacteria ADOC-A genera, including hydrocarbon degrader specialists Alcanivorax, Oleibacter, Oleispira and Colwellia (among others), were found significantly less abundant at North compared to the other two sites ( $P < 0.01$ ). The ADOC-A active genera averaged at 0.43–0.07% of the total rRNA pool in all samples at initial conditions. Interestingly, among ADOC-A genera, Gammaproteobacteria ADOC-A were observed to be the most active group at Central and South (0.15–0.03% and 0.85–0.1% respectively, Supporting Information Table S5).

### ***Microbial responses to ADOC exposure at high and low concentrations after 24 h***

Microbial communities were challenged with known concentrations of PAH, n-alkanes and OPE at concentrations representative of the marine environment. Concentrations in the treatments were 100 ng L<sup>-1</sup> and 3000 ng L<sup>-1</sup> for n-alkanes, 30 ng L<sup>-1</sup> and 900 ng L<sup>-1</sup> for PAHs, and 30 ng L<sup>-1</sup> and 900 ng L<sup>-1</sup> for OPE, for the lower and upper levels respectively. The lowest levels are comparable to the measured levels in oceanic waters elsewhere (Vila-Costa et al., 2020), including this work for NESAP. The upper levels correspond to concentrations of total alkanes, PAHs and OPEs reported in coastal waters (Valavanidis et al., 2008; El-Naggar et al., 2018; Schmidt et al., 2021). In addition to the targeted alkanes and PAHs considered in this study, there are other hydrocarbons in seawater. When hydrocarbons are analysed chromatographically, these appear as a wide signal in the chromatogram, not as resolved peaks, defined as the unresolved complex mixture (UCM), with a concentration that is one to three orders of magnitude larger than those of the targeted PAHs or alkanes present in the mixture added to the incubations (González-Gaya et al., 2016). Therefore, both the high and low doses correspond to environmentally relevant concentrations of organic pollutants found in the marine environment (Supporting Information Table S6).

After 24 h, low and high additions of ADOC significantly decreased the abundance yield of the heterotrophic non-pigmented bacterial fraction of the microbial communities, measured by flow cytometry. The contrasting trophic strategies of bacteria with different DNA content and therefore different cytometric signatures (Vila-Costa et al., 2012) motivated an analysis separating abundance yield of high nucleic acid (HNA) and low nucleic acid (LNA) content bacteria in this experiment. LNA bacteria specially decreased in North and South, and HNA bacteria in Central ( $P < 0.05$ ) (Figure 2; Supporting Information Figure S3). At North, relative abundances of dominant Gammaproteobacteria and Rhodospirillales increased in ADOC exposed mesocosms,  $P < 0.05$  whereas total Bacteroidota, Cyanobacteria and Rickettsiales significantly decreased ( $P < 0.05$ ) (Figure 2; Supporting Information Table S7 and Figure S4). Similarly, in Central, dominant Gammaproteobacteria, and specially Cellvibrionales and SAR86 clade, increased significant-

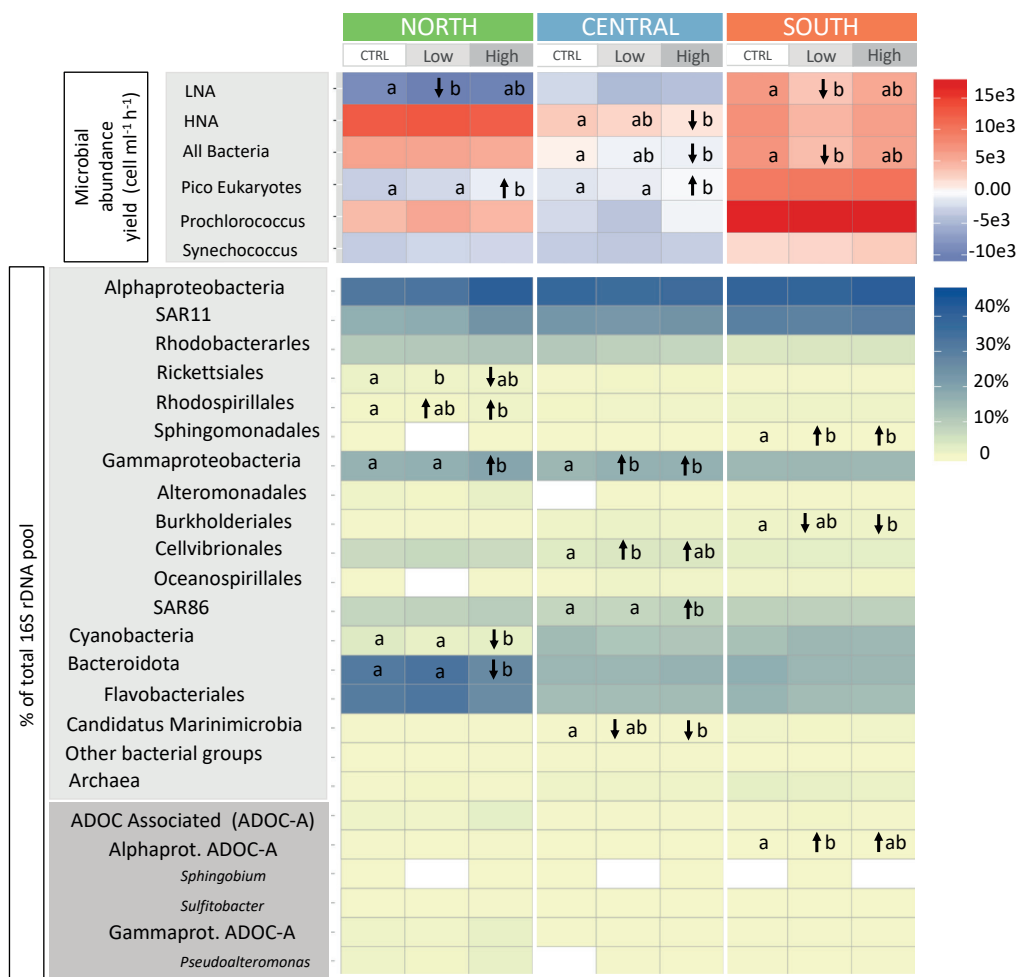


**FIGURE 2 |** Characterization of community structure after 24 h of exposure to ADOC at control, low and high concentrations by flow cytometry and 16S rDNA amplicon sequencing. Statistical differences between control and ADOC treatments were determined by ANOVA followed by a post-hoc Tukey test (treatments without overlapping letters are statistically different). ADOC-A: ADOC-associated bacteria.

ly in relative abundances in the ADOC exposed treatments ( $P < 0.05$ ), while *Candidatus Marinimicrobia* decreased in the high dose treatment ( $P < 0.03$ ). Oppositely, in South, Sphingomonadales and Alphaproteobacteria ADOC-A group increased significantly compared to controls ( $P < 0.05$ ), whereas Burkholderiales decreased (Supporting Information - Table S7). Our observations show taxon-specific responses, affecting both low abundance and dominant groups, independent of the pre-adaptation of the communities to the in situ pollution level. This suggests that subtle increases of ADOC concentrations in seawater can promote or inhibit the growth of specific fractions of the community, as observed in polar environments for high hydrocarbon concentrations and over longer periods of time (Garneau et al., 2016).

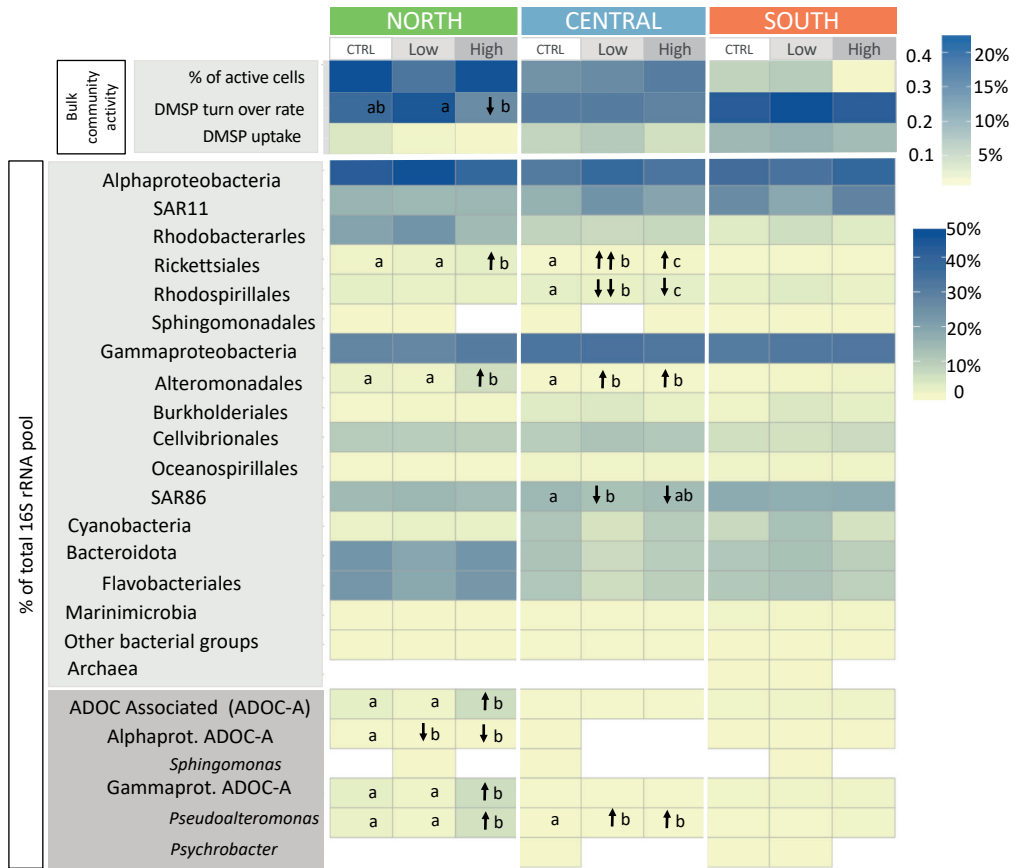


**FIGURE 3** | Characterization of bacterial activities after 24 h of exposure to ADOC at low and high concentrations. Statistical differences between control and ADOC treatments were detected by ANOVA (labelled with letters) followed by a post hoc Tukey test.

The percentage of active cells (i.e., the percentage of cells assimilating L-homopropargylglycine measured following Bioorthogonal non-canonical amino-acid tagging approach (BONCAT) ) and DMSP cycling rates remained unaltered at all sites after treatments except for a decrease in DMSP transformation at North under high ADOC concentrations (**Figure 3**). The 16S rRNA pool was dominated by Alphaproteobacteria, Gammaproteobacteria and Flavobacteriales at all samples. In Central, members belonging to Alteromonadales (and specially *Pseudoalteromonas*) and Rickettsiales groups increased significantly their relative contribution in the ADOC exposed treatments compared to controls ( $P < 0.01$  and  $P < 0.05$ , respectively). SAR86 clade and Rhodospirillales were significantly depleted at the low concentration treatments ( $P < 0.05$ ). Similarly, at North, a significant increase of relative abundances of Alteromonadales, Rickettsiales, Gammaproteobacteria ADOC-A and total ADOC-A were observed in the high ADOC exposed communities ( $P < 0.01$ ,  $P < 0.03$ ,  $P < 0.02$ ,  $P < 0.01$ , respectively). Specifically, *Pseudoalteromonas* played a

dominant active role increasing from a relative abundance of  $1.19 \pm 0.6\%$  in the controls, to  $5.2 \pm 0.5\%$  in the high-dose ADOC-treated water ( $P < 0.01$ ), consistent with previously reported growth of the rare biosphere after oil spills and under background levels of ADOC exposure (Kleindienst et al., 2016; Wang et al., 2017; Cerro-Gálvez et al., 2019b). Our data indicate ADOC exposure promoted the activity of members of the rare or very low abundant biosphere in North, suggesting the existence of a seedbank of inactive and low abundance taxa which can bloom under specific and advantageous ecosystem variations (Galand and Logares, 2019), such as the presence of ADOC as growth substrate.

Moreover, our data confirm the heterogeneity of ADOC coping responses after 24 h of exposure in microbial populations. While specialized and facultative bacteria can profit metabolically from ADOC and secondary products by using it as growth substrate (Head et al., 2006), the chemicals' toxic nature can inhibit bacterial growth, hamper bacterial viability or even cause lethal effects for which physiological anti-toxic mechanisms are activated (Van Wezel and Opperhuizen, 1995; Fernández-Pinos et al., 2017; Mitchell and Silhavy, 2019; Cerro-Gálvez et al., 2019a, 2019b). These effects were explored at Central site by metatranscriptomics.

### **Gene expression profile of ADOC exposed communities at Central site**

Gene expression profiles of the microbial communities were analysed through metatranscriptomics at Central (Poretsky et al., 2014). The taxonomical affiliation of the transcripts enriched in the ADOC treatments corresponded to Rhodobacterales and Alphaproteobacteria ADOC-A *Roseobacter*, *Jannaschia* and *Sulfitobacter*, as well as Betaproteobacteria ADOC-A *Comamonas* and *Polaromonas*. The taxonomical affiliation of the depleted transcripts corresponded to the dominant groups SAR11, Flavobacteriales and Cyanobacteria, as well as specific ADOC-A Gammaproteobacteria such as Oceanospirillales, Alteromonadales, Thiotrichales and Cellvibrionales, known to be rapid responders to oil stimuli (**Figure 4**; Supporting Information Figure S5). These observations are consistent with a sequential succession of ADOC-degrading players within the community. We observed in Central that after 24 h of ADOC exposure, some Gammaproteobacteria taxa (e.g. Cellvibrionales) increased in relative abundance (**Figure 2**) and their contribution to the transcript pool was co-dominated with alphaproteobacterial ADOC-A strains such as *Sulfitobacter* and *Jannaschia* (**Figure 4**). This succession and co-existence of taxa is similar to what has been observed in oil spill accidents (Kostka et al., 2011; Redmond and Valentine, 2012). For instance, Mason et al. (2012) and King et al. (2015) observed that early and opportunistic taxonomic groups corresponded to Gammaproteobacteria (i.e. Oceanospirillales, Alteromonadales and Pseudomonadales), that were succeeded by Alphaproteobacteria taxa (i.e. Rhodobacteraceae) that seemed to benefit from secondary or intermediate degradation products or more recalcitrant chemicals (Kostka et al., 2011). This shift to rapid ADOC responders has also been observed recently for communities exposed to background concentrations of ADOC compounds, both in temperate and polar environments (Wang et al., 2017; Cerro-Gálvez et al., 2019b). Our metatranscrip-

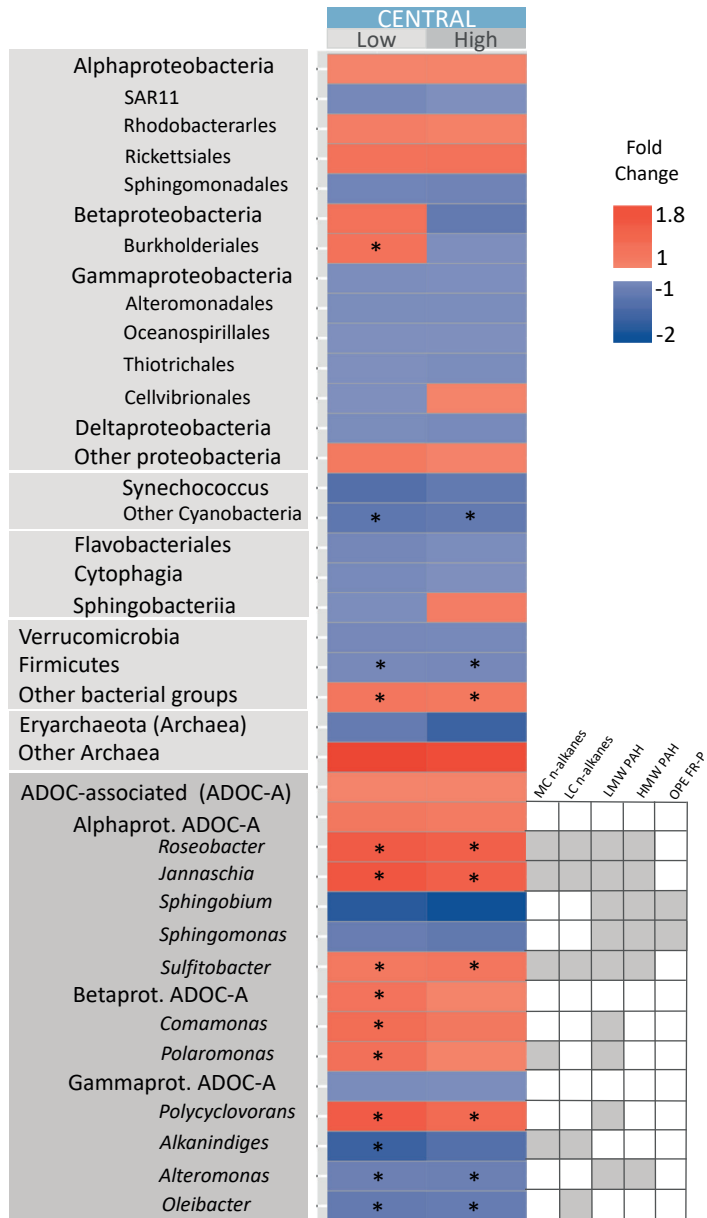


**FIGURE 4** | Changes of taxa-specific contributions to the metatranscriptomic pool in treatments versus controls after 24 h of ADOC exposure at Central station. Statistical significant differences are labelled with an \*. Secondary box in grey shows capabilities of ADOC degradation according to the literature (Supporting Information Table S4).

Some data suggest that we captured the later succession stage of ADOC consumption in Central after 24 h of ADOC exposure. Overall, a total of 86 transcripts got significantly enriched in the ADOC treatments whereas 659 transcripts got depleted (FDR < 0.05). Transcripts significantly enriched in the amended treatments corresponded to genes categorized in the COG classification for involvement in lipid transport and metabolism and in intracellular trafficking, secretion and vesicular transport in low dose treatments, and posttranslational modification, protein turnover, chaperones and transcription at high-dose treatment ( $P < 0.05$ , **Figure 5** and Supporting Information Figure S6). In contrast, depletion was observed for the transposase category and for inorganic ion transport and metabolism in high and low-dose treatments, and for cell wall/membrane/envelope biogenesis and translation, ribosomal structure and biogenesis at high-dose treatments. The lower transcript expenditure on biogenesis processes suggests narcosis. Cellular narcosis occurs when ADOC environmental baseline toxicity disrupts the structure and functioning of cell membranes, causing a decrease in biological activity (Escher et al., 2017; **Figure 5** and Supporting Information Figure S6) and prompting the activation of anti-toxin and cell repair mechanisms (Cerro-Gálvez et al., 2019b). Transcripts devoted to cell detoxification, cell repair and anti-stress mechanisms increased in relative contribution to the total rRNA pool (**Figure 5**). Examples of this are the chaperones that assist in proper protein folding and functioning, and the intracellular trafficking, secretion and vesicular transport transcripts that are involved in production of outer membrane vesicles formation through blebbing (Toyofuku et al., 2019) which can eject toxic agents when bacteria are grown on ADOC-rich or other hydrophobic compound-rich media (Borneleit et al., 1988; Kobayashi et al., 2000).

We used marker genes to assess ADOC microbial degradation stages (Supporting Information Table S8). Initial degradation steps of alkanes, PAH and OPEs, carried out by medium chain alkane degrading gene (alkB), aromatic ring hydroxylating dioxygenases (RHD) and the phosphotriesterases respectively, showed significant depletion after 24 h of ADOC exposure (**Figure 5**). Conversely, enzymes involving later stages of ADOC removal were found significantly enriched (protocatechuate dioxygenases alpha and beta subunits). This finding, along with the decline of transcripts from Gammaproteobacteria ADOC-A rapid responders (**Figure 4**), suggests that peak degradation activity was surpassed after 24 h of ADOC addition. Together, these results suggest the coexistence of stress, detoxifying and degradation responses following ADOC exposure, even at the low concentrations as observed in polar marine environments (Cerro-Gálvez et al., 2019b). On one hand, the significant decreases in relative abundance of transcripts assigned to cell biogenesis in the amendments indicates that ADOC toxicity obstructed the normal functioning of the bacterial cells. In parallel, we observed enrichment of an array of detoxifying and cell protection strategies. On the other hand, the significant enrichment of protocatechuate dioxygenases after 24 h suggests that late stage ADOC degradation was carried out primarily by ADOC-A genera belonging to Alphaproteobacteria.

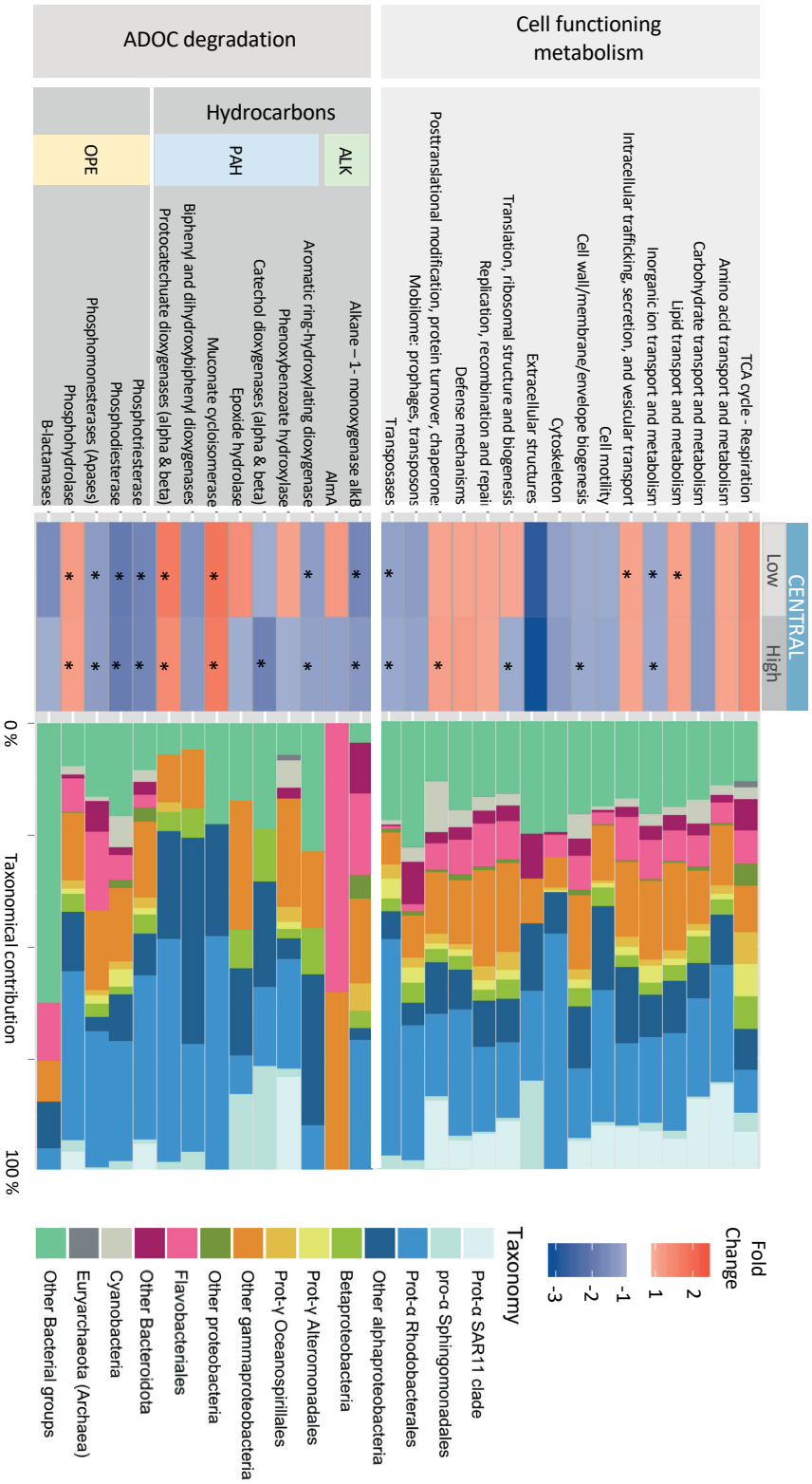


**FIGURE 5** | Changes in the contribution of functional categories to the metatranscriptomic pool in treatments versus controls after 24 h of ADOC exposure at Central station. Statistical significant differences are labelled with an \*. Contribution of different taxa to each functional category is shown in the right panel.



## CONCLUSIONS

The results presented here provide new information on the concentrations and microbial responses to ADOC pollution in surface waters of three different NESAP oceanic regions. The concentrations for the three model families of ADOCs (PAHs, n-alkanes and OPEs) were similar to or lower than those measured in other oceanic regions, with a decreasing gradient from the most anthropogenic influenced site (South) to the most pristine (North). ADOC additions within the range of environmental background concentrations in 24 h incubations modified the composition and function of the microbial communities. South microbiomes exhibited the most resilience, with minor community changes, while North communities exhibited the greatest changes after exposure to ADOC. Some of the ADOC-related bacterial groups, reported previously to become dominant in marine oil spills (Nogales et al., 2011), such as Alteromonadales and Gammaproteobacteria ADOC-A, were found to significantly increase in abundance and contribution to the total pool of 16S rRNA in the ADOC treated communities at North. Simultaneously, we observed that dominant taxonomic groups such as Bacteroidota significantly decreased their contribution to the 16S rDNA pool after the ADOC exposure at the North site, consistent with toxic effects due to exposure to ADOC. Gene expression profiles of ADOC amended at Central site shed light onto the delicate balance between ADOC metabolizing processes and stress-response and detoxifying strategies for bacteria coping with ADOC toxicities. These results expand our current knowledge on the concentrations and responses of marine microorganisms to background anthropogenic pollution in the upper ocean in the poorly studied NESAP region.

## ACKNOWLEDGEMENTS

This publication is dedicated to the memory of our missed friend, mentor and colleague, Prof. Ronald P. Kiene. The authors thank the Capitan and crew of the R/V Oceanus.

## AUTHOR CONTRIBUTION

E.C.-G., M.V.-C. and J.D. designed the experiments. E.C.-G. and R.K. participated in the sampling campaign and performed the experiments and the in situ measurements. E.C.-G. analyzed the PAHs, OPE and alkanes, and extracted the DNA and RNA. A.M.-V. performed the bacterial abundance and BON-CAT analyses. A.M.-V., A.A. and S.S. did the bioinformatics work. A.M.-V. analysed the data and wrote the manuscript. All the authors commented on the discussion and final version of the manuscript.

## REFERENCES

- Abbasian, F., Lockington, R., Megharaj, M., and Naidu, R. (2016) A review on the genetics of aliphatic and aromatic hydrocarbon degradation. *Appl Biochem Biotechnol* 178: 224–250.
- Bagi, A., Pampanin, D.M., Brakstad, O.G., and Kommedal, R. (2013) Estimation of hydrocarbon biodegradation rates in marine environments: a critical review of the Q10 approach. *Mar Environ Res* 89: 83–90.
- Berrojálbiz, N., Lacorte, S., Calbet, A., Saiz, E., Barata, C., and Dachs, J. (2009) Accumulation and cycling of polycyclic aromatic hydrocarbons in zooplankton. *Environ Sci Technol* 43: 2295–2301.
- Blazewicz, S.J., Barnard, R.L., Daly, R.A., and Firestone, M. K. (2013) Evaluating rRNA as an indicator of microbial activity in environmental communities: limitations and uses. *ISME J* 7: 2061–2068.
- Borneleit, P., Hermsdorf, T., Claus, R., Walther, P., and Kleber, H.P. (1988) Effect of hexadecane-induced vesiculation on the outer membrane of *Acinetobacter calcoaceticus*. *J Gen Microbiol* 134: 1983–1992.
- Callahan, B.J., McMurdie, P.J., Rosen, M.J., Han, A.W., Johnson, A.J.A., and Holmes, S.P. (2016) DADA2: high-resolution sample inference from Illumina amplicon data. *Nat Methods* 13: 581–583.
- Cerro-Gálvez, E., Dachs, J., Lundin, D., Fernández-Pinos, M.- C., Sebastián, M., and Vila-Costa, M. (2021) Responses of coastal marine microbiomes exposed to anthropogenic dissolved organic carbon. *Environ Sci Technol*. <https://pubs.acs.org/doi/10.1021/acs.est.0c07262>.
- Cerro-Gálvez, E., Sala, M.M., Marrasé, C., Gasol, J.M., Dachs, J., and Vila-Costa, M. (2019a) Modulation of microbial growth and enzymatic activities in the marine environment due to exposure to organic contaminants of emerging concern and hydrocarbons. *Sci Total Environ* 678: 486–498.
- Cerro-Gálvez, E., Casal, P., Lundin, D., Piña, B., Pinhassi, J., Dachs, J., and Vila-Costa, M. (2019b) Microbial responses to anthropogenic dissolved organic carbon in the Arctic and Antarctic coastal seawaters. *Environ-Microbiol* 21: 1466–1481.
- Cullon, D.L., Yunker, M.B., Alleyne, C., Dangerfield, N.J., O’neill, S., Whitticar, M.J., and Ross, P.S. (2009) Persistent organic pollutants in Chinook salmon (*Oncorhynchus tshawytscha*): implications for resident killer whales of British Columbia and adjacent waters. *Environ Toxicol Chem* 28: 148–161.
- Dachs, J., and Méjanelle, L. (2010) Organic pollutants in coastal waters, sediments, and biota: a relevant driver for ecosystems during the Anthropocene? *Estuaries Coasts* 33: 1–14.
- DeBruyn, J.M., Chewing, C.S., and Sayler, G.S. (2007) Comparative quantitative prevalence of mycobacteria and functionally abundant *nidA*, *nahAc*, and *nagAc* Dioxigenase genes in coal tar contaminated sediments. *Environ Sci Technol* 41: 5426–5432.
- Desforges, J.P., Hall, A., McConnell, B., Rosing-Asvid, A., Barber, J.L., Brownlow, A., et al. (2018) Predicting global killer whale population collapse from PCB pollution. *Science* (80-) 361: 1373–1376.
- Dombrowski, N., Donaho, J.A., Gutierrez, T., Seitz, K.W., Teske, A.P., and Baker, B.J. (2016) Reconstructing metabolic pathways of hydrocarbon-degrading bacteria from the Deepwater horizon oil spill. *Nat Microbiol* 1: 16057.

Echeveste, P., Dachs, J., Berrojalbiz, N., and Agustí, S. (2010) Decrease in the abundance and viability of oceanic phytoplankton due to trace levels of complex mixtures of organic pollutants. *Chemosphere* 81: 161–168.

El-Naggar, N.A., Emara, H.I., Moawad, M.N., Soliman, Y.A., and El-Sayed, A.A.M. (2018) Detection of polycyclic aromatic hydrocarbons along Alexandria's coastal water, Egyptian Mediterranean Sea. *Egypt J Aquat Res* 44: 9–14.

Escher, B.I., Baumer, A., Bittermann, K., Henneberger, L., König, M., Kühnert, C., and Klüver, N. (2017) General baseline toxicity QSAR for nonpolar, polar and ionisable chemicals and their mixtures in the bioluminescence inhibition assay with *Allivibrio fischeri*. *Environ Sci Process Impacts* 19: 414–428.

Falcioni, T., Papa, S., and Gasol, J.M. (2008) Evaluating the flow-cytometric nucleic acid double-staining protocol in realistic situations of planktonic bacterial death. *Appl Environ Microbiol* 74: 1767–1779.

Fernández-Pinos, M.-C., Vila-Costa, M., Arrieta, J.M., Morales, L., González-Gaya, B., Piña, B., and Dachs, J. (2017) Dysregulation of photosynthetic genes in oceanic *Prochlorococcus* populations exposed to organic pollutants. *Sci Rep* 7: 8029.

Fourati, R., Tedetti, M., Guigue, C., Goutx, M., Zaghdien, H., Sayadi, S., and Elleuch, B. (2018) Natural and anthropogenic particulate-bound aliphatic and polycyclic aromatic hydrocarbons in surface waters of the Gulf of Gabes (Tunisia, southern Mediterranean Sea). *Environ Sci Pollut Res* 25: 2476–2494.

Frouin, H., Dangerfield, N., Macdonald, R.W., Galbraith, M., Crewe, N., Shaw, P., et al. (2013) Partitioning and bioaccumulation of PCBs and PBDEs in marine plankton from the strait of Georgia, British Columbia, Canada. *Prog Oceanogr* 115: 65–75.

Galand, P.E., and Logares, R. (2019) Ecology of rare microorganisms. In *Encyclopedia of Microbiology*: Amsterdam, NL: Elsevier, pp. 90–96.

Garneau, M.-È., Michel, C., Meisterhans, G., Fortin, N., King, T.L., Greer, C.W., and Lee, K. (2016) Hydrocarbon biodegradation by Arctic Sea-ice and sub-ice microbial communities during microcosm experiments, Northwest Passage (Nunavut, Canada). *FEMS Microbiol Ecol* 92: fiw130.

Gifford, S.M., Sharma, S., Booth, M., and Moran, M.A. (2013) Expression patterns reveal niche diversification in a marine microbial assemblage. *ISME J* 7: 281–298.

Gifford, S.M., Sharma, S., Rinta-Kanto, J.M., and Moran, M. A. (2011) Quantitative analysis of a deeply sequenced marine microbial metatranscriptome. *ISME J* 5: 461–472.

González-Gaya, B., Fernández-Pinos, M.-C., Morales, L., Méjanelle, L., Abad, E., Piña, B., et al. (2016) High atmosphere–ocean exchange of semivolatile aromatic hydrocarbons. *Nat Geosci* 9: 438–442.

González-Gaya, B., Martínez-Varela, A., Vila-Costa, M., Casal, P., Cerro-Gálvez, E., Berrojalbiz, N., et al. (2019) Biodegradation as an important sink of aromatic hydrocarbons in the oceans. *Nat Geosci* 12: 119–125.

Guigue, C., Tedetti, M., Giorgi, S., and Goutx, M. (2011) Occurrence and distribution of hydrocarbons in the surface microlayer and subsurface water from the urban coastal marine area off Marseilles, northwestern Mediterranean Sea. *Mar Pollut Bull* 62: 2741–2752.

Gupta, S., Pathak, B., and Fulekar, M.H. (2015) Molecular approaches for biodegradation of polycyclic aromatic hydrocarbon compounds: a review. *Rev Environ Sci Biotechnol* 14: 241–269.

Habe, H., and Omori, T. (2017) Genetics of polycyclic aromatic hydrocarbon metabolism in diverse aerobic bacteria. *Biosci Biotechnol Biochem*: 67(2), 8451.

Hazen, T.C., Dubinsky, E.A., DeSantis, T.Z., Andersen, G. L., Piceno, Y.M., Singh, N., et al. (2010) Deep-sea oil plume enriches indigenous oil-degrading bacteria. *Science* (80-) 330: 204–208.

Head, I.M., Jones, D.M., and Röling, W.F.M. (2006) Marine microorganisms make a meal of oil. *Nat Rev Microbiol* 4: 173–182.

Heipieper, H.J., and Martínez, P.M. (2010) Toxicity of hydrocarbons to microorganisms. In *Handbook of Hydrocarbon and Lipid Microbiology*. Berlin/Heidelberg: Springer, pp. 1563–1573.

Herr, A.E., Kiene, R.P., Dacey, J.W.H., and Tortell, P.D. (2019) Patterns and drivers of dimethylsulfide concentration in the northeast subarctic Pacific across multiple spatial and temporal scales. *Biogeosciences* 16: 1729–1754.

Hu, M., Li, J., Zhang, B., Cui, Q., Wei, S., and Yu, H. (2014) Regional distribution of halogenated organophosphate flame retardants in seawater samples from three coastal cities in China. *Mar Pollut Bull* 86: 569–574.

Joye, S., Kleindienst, S., Gilbert, J., Handley, K., Weisenhorn, P., Overholt, W., and Kostka, J. (2016) Re-

sponses of microbial communities to hydrocarbon exposures. *Oceanography* 29: 136–149.

Jurado, E., Dachs, J., Duarte, C.M., and Simo, R. (2008) Atmospheric deposition of organic and black carbon to the global oceans. *Atmos Environ* 42: 7931–7939.

Kanakidou, M., Duce, R.A., Prospero, J.M., Baker, A.R., Benitez-Nelson, C., Dentener, F.J., et al. (2012) Atmospheric fluxes of organic N and P to the global ocean. *Global Biogeochem Cycles* 26: 3026.

Karthikeyan, S., Rodriguez-R, L.M., Heritier-Robbins, P., Hatt, J.K., Huettel, M., Kostka, J.E., and Konstantinidis, K. T. (2020) Genome repository of oil systems: an interactive and searchable database that expands the catalogued diversity of crude oil-associated microbes. *Environ Microbiol* 22: 2094–2106.

Kiene, R.P., Linn, L.J., and Bruton, J.A. (2000) New and important roles for DMSP in marine microbial communities. *J Sea Res*: 43, 209–224.

King, G.M., Kostka, J.E., Hazen, T.C., and Sobocky, P.A. (2015) Microbial responses to the Deepwater horizon oil spill: from coastal wetlands to the Deep Sea. *Annu Rev Mar Sci* 7: 377–401.

King, S.M., Leaf, P.A., Olson, A.C., Ray, P.Z., and Tarr, M.A. (2014) Photolytic and photocatalytic degradation of surface oil from the Deepwater horizon spill. *Chemosphere*

95: 415–422. Kleindienst, S., Grim, S., Sogin, M., Bracco, A., Crespo-

Medina, M., and Joye, S.B. (2016) Diverse, rare microbial taxa responded to the Deepwater horizon deep-sea hydrocarbon plume. *ISME J* 10: 400–415.

Kobayashi, H., Uematsu, K., Hirayama, H., and Horikoshi, K. (2000) Novel toluene elimination system in a toluenetolerant microorganism. *J Bacteriol* 182: 6451–6455.

Kostka, J.E., Prakash, O., Overholt, W.A., Green, S.J., Freyer, G., Canion, A., et al. (2011) Hydrocarbon-degrading bacteria and the bacterial community response in Gulf of Mexico beach sands impacted by the Deepwater horizon oil spill. *Appl Environ Microbiol* 77: 7962–7974.

Krahn, M.M., Hanson, M.B., Baird, R.W., Boyer, R.H., Burrows, D.G., Emmons, C.K., et al. (2007) Persistent organic pollutants and stable isotopes in biopsy samples (2004/2006) from southern resident killer whales. *Mar Pollut Bull* 54: 1903–1911.

Krolicka, A., Boccadoro, C., Nilsen, M.M., and Baussant, T. (2017) Capturing early changes in the marine bacterial community as a result of crude oil pollution in a Mesocosm experiment. *Microbes Environ* 32: 358–366.

Krolicka, A., Boccadoro, C., Nilsen, M.M., Demir-Hilton, E., Birch, J., Preston, C., et al. (2019) Identification of microbial key-indicators of oil contamination at sea through tracking of oil biotransformation: an Arctic field and laboratory study. *Sci Total Environ* 696: 133715.

Leizeaga, A., Estrany, M., Forn, I., and Sebastian, M. (2017) Using click-chemistry for visualizing in situ changes of translational activity in planktonic marine bacteria. *Front Microbiol* 8: 2360.

Li, J., Xie, Z., Mi, W., Lai, S., Tian, C., Emeis, K.-C., and Ebinghaus, R. (2017) Organophosphate esters in air, snow, and seawater in the North Atlantic and the Arctic. *Environ Sci Technol* 51: 6887–6896.

Liu, J., Techtmann, S.M., Woo, H.L., Ning, D., Fortney, J.L., and Hazen, T.C. (2017) Rapid response of eastern Mediterranean Deep Sea microbial communities to oil. *Sci Rep* 7: 5762.

Lohmann, R., Breivik, K., Dachs, J., and Muir, D. (2007) Global fate of POPs: current and future research directions. *Environ Pollut* 150: 150–165.

Lozada, M., Marcos, M.S., Commendatore, M.G., Gil, M.N., and Dionisi, H.M. (2014) The bacterial community structure of hydrocarbon-polluted marine environments as the basis for the definition of an ecological index of hydrocarbon exposure. *Microbes Environ* 29: 269–276.

Ma, Y., Xie, Z., Yang, H., Möller, A., Halsall, C., Cai, M., et al. (2013) Deposition of polycyclic aromatic hydrocarbons in the North Pacific and the Arctic. *J Geophys Res Atmos* 118: 5822–5829.

Martin, M. (2011) Cutadapt removes adapter sequences from high-throughput sequencing reads. *EMBnet.J* 17: 10. Mason, O.U., Hazen, T.C., Borglin, S., Chain, P.S.G.,

Dubinsky, E.A., Fortney, J.L., et al. (2012) Metagenome, metatranscriptome and single-cell sequencing reveal microbial response to Deepwater horizon oil spill. *ISME J* 6: 1715–1727.

McDonough, C.A., De Silva, A.O., Sun, C., Cabrerizo, A., Adelman, D., Soltwedel, T., et al. (2018) Dissolved organophosphate esters and polybrominated diphenyl ethers in remote marine environments: arctic surface water distributions and net transport through Fram Strait. *Environ Sci Technol* 52: 6208–6216.

Mitchell, A.M., and Silhavy, T.J. (2019) Envelope stress responses: balancing damage repair and toxicity.

Nat Rev Microbiol 17: 417–428.

Moran, M.A., Satinsky, B., Gifford, S.M., Luo, H., Rivers, A., Chan, L.-K., et al. (2013) Sizing up metatranscriptomics. ISME J 7: 237–243.

Muck, S., De Corte, D., Clifford, E.L., Bayer, B., Herndl, G.J., and Sintes, E. (2019) Niche differentiation of aerobic and anaerobic ammonia oxidizers in a high latitude deep oxygen minimum zone. Front Microbiol 10: 2141.

Neethu, C.S., Saravanakumar, C., Purvaja, R., Robin, R.S., and Ramesh, R. (2019) Oil-spill triggered shift in indigenous microbial structure and functional dynamics in different marine environmental matrices. Sci Rep 9: 1354.

Nizzetto, L., Lohmann, R., Gioia, R., Jahnke, A., Temme, C., Dachs, J., et al. (2008) PAHs in air and seawater along a north-South Atlantic transect: trends, processes and possible sources. Environ Sci Technol 42: 1580–1585.

Nogales, B., Lanfranconi, M.P., Piña-Villalonga, J.M., and Bosch, R. (2011) Anthropogenic perturbations in marine microbial communities. FEMS Microbiol Rev 35: 275–298.

Oksanen, J., Blanchet, G.F., Friendly, M., Kindt, R., Legendre, P., McGlinn, D., et al. (2020) Vegan: Community Ecology Package.

Parada, A.E., Needham, D.M., and Fuhrman, J.A. (2016) Every base matters: assessing small subunit rRNA primers for marine microbiomes with mock communities, time series and global field samples. Environ Microbiol 18: 1403–1414.

Parmar, T.K., Rawtani, D., and Agrawal, Y.K. (2016) Bioindicators: the natural indicator of environmental pollution. Front Life Sci 9: 110–118.

Poretzky, R., Rodriguez-R, L.M., Luo, C., Tsementzi, D., and Konstantinidis, K.T. (2014) Strengths and limitations of 16S rRNA gene amplicon sequencing in revealing temporal microbial community dynamics. PLoS One 9: e93827.

Prestat, E., David, M.M., Hultman, J., Tas, N., Lamendella, R., Dvornik, J., et al. (2014) FOAM (functional ontology assignments for Metagenomes): a hidden Markov model (HMM) database with environmental focus. Nucleic Acids Res 42: e145.

Quast, C., Pruesse, E., Yilmaz, P., Gerken, J., Schweer, T., Yarza, P., et al. (2013) The SILVA ribosomal RNA gene database project: improved data processing and webbased tools. Nucleic Acids Res 41: D590. R Core Team. (2019) R: A Language and Environment for Statistical Computing.

Redmond, M.C., and Valentine, D.L. (2012) Natural gas and temperature structured a microbial community response to the Deepwater horizon oil spill. Proc Natl Acad Sci U S A 109: 20292–20297.

Reunamo, A., Yli-Hemminki, P., Nuutinen, J., Lehtoranta, J., and Jørgensen, K.S. (2017) Degradation of crude oil and PAHs in iron–manganese concretions and sediment from the northern Baltic Sea. Geomicrobiol J 34: 385–399.

Rinta-Kanto, J.M., Sun, S., Sharma, S., Kiene, R.P., and Moran, M.A. (2012) Bacterial community transcription patterns during a marine phytoplankton bloom. Environ Microbiol 14: 228–239.

Robinson, M.D., McCarthy, D.J., and Smyth, G.K. (2009) edgeR: a bioconductor package for differential expression analysis of digital gene expression data. Bioinformatics 26: 139–140.

Satinsky, B.M., Gifford, S.M., Crump, B.C., and Moran, M.A. (2013) Use of internal standards for quantitative metatranscriptome and metagenome analysis. In Methods in Enzymology: Cambridge, MA: Academic Press Inc, pp. 237–250.

Schmidt, N., Castro-Jiménez, J., Oursel, B., and Sempéré, R. (2021) Phthalates and organophosphate esters in surface water, sediments and zooplankton of the NW Mediterranean Sea: exploring links with microplastic abundance and accumulation in the marine food web. Environ Pollut 272: 115970.

Stortini, A.M., Martellini, T., Del Bubba, M., Lepri, L., Capodaglio, G., and Cincinelli, A. (2009) N-alkanes, PAHs and surfactants in the sea surface microlayer and sea water samples of the Gerlache Inlet Sea (Antarctica). Microchem J 92: 37–43.

Takahashi, S., Abe, K., and Ker, Y. (2013) Microbial degradation of persistent organophosphorus flame retardants. In Environmental Biotechnology - New Approaches and Prospective Applications: London: InTech.

Toyofuku, M., Nomura, N., and Eberl, L. (2019) Types and origins of bacterial membrane vesicles. Nat Rev Microbiol 17: 13–24.

Valavanidis, A., Vlachogianni, T., Triantafyllaki, S., Dassenakis, M., Androutsos, F., and Scoullou, M. (2008) Polycyclic aromatic hydrocarbons in surface seawater and in indigenous mussels (*Mytilus galloprovincialis*) from coastal areas of the Saronikos gulf (Greece). *Estuar Coast Shelf Sci* 79: 733–739.

Valencia-Agami, S.S., Cerqueda-García, D., Putzeys, S., Uribe-Flores, M.M., García-Cruz, N.U., Pech, D., et al. (2019) Changes in the Bacterioplankton community structure from southern Gulf of Mexico during a simulated crude oil spill at Mesocosm scale. *Microorganisms* 7: 441.

Vergeynst, L., Christensen, J.H., Kjeldsen, K.U., Meire, L., Boone, W., Malmquist, L.M.V., and Rysgaard, S. (2019) In situ biodegradation, photooxidation and dissolution of petroleum compounds in Arctic seawater and sea ice. *Water Res* 148: 459–468.

Vergeynst, L., Kjeldsen, K.U., Lassen, P., and Rysgaard, S. (2018) Bacterial community succession and degradation patterns of hydrocarbons in seawater at low temperature. *J Hazard Mater* 353: 127–134.

Vila-Costa, M., Cerro-Gálvez, E., Martínez-Varela, A., Casas, G., and Dachs, J. (2020) Anthropogenic dissolved organic carbon and marine microbiomes. *ISME J*: 14, 2646–2648.

Vila-Costa, M., Gasol, J.M., Sharma, S., and Moran, M.A. (2012) Community analysis of high- and low-nucleic acid-containing bacteria in NW Mediterranean coastal waters using 16S rDNA pyrosequencing. *Environ Microbiol* 14: 1390–1402.

Vila-costa, M., Sebastián, M., Pizarro, M., and Cerro-Gálvez, E. (2020). Microbial consumption of organophosphate esters in seawater under phosphorus limited conditions. *Sci Rep*: 9, 1–11.

Wang, W., and Shao, Z. (2013) Enzymes and genes involved in aerobic alkane degradation. *Front Microbiol* 4: 1–7.

Wang, Y., Hatt, J.K., Tsementzi, D., Rodriguez-R, L.M., Ruiz-Pérez, C.A., Weigand, M.R., et al. (2017) Quantifying the importance of the rare biosphere for microbial community response to organic pollutants in a freshwater ecosystem. *Appl Environ Microbiol* 83: 3321–3337.

Van Wezel, A.P., and Opperhuizen, A. (1995) Narcosis due to environmental pollutants in aquatic organisms: residue-based toxicity, mechanisms, and membrane burdens. *Crit Rev Toxicol* 25: 255–279.

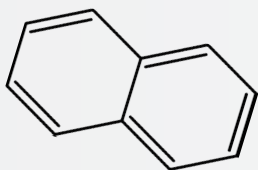
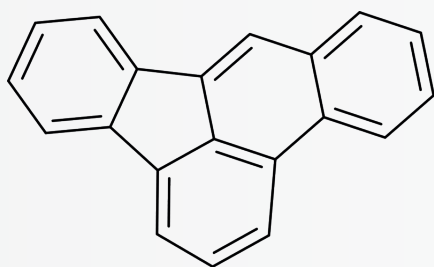
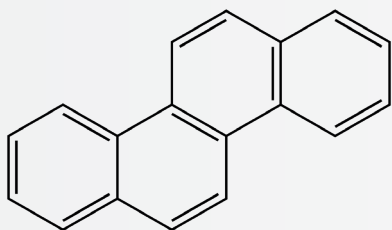
Wickham, H. (2009) *Ggplot2: Elegant Graphics for Data Analysis*, 2nd ed. New York, NY: Springer.

Williamson, C.E., Fischer, J.M., Bollens, S.M., Overholt, E. P., and Breckenridge, J.K. (2011) Toward a more comprehensive theory of zooplankton diel vertical migration: integrating ultraviolet radiation and water transparency into the biotic paradigm. *Limnol Oceanogr* 56: 1603–1623.

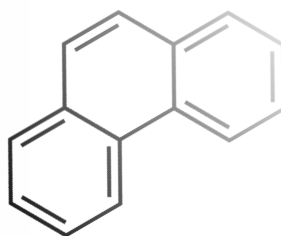
Wright, J.J., Konwar, K.M., and Hallam, S.J. (2012) Microbial ecology of expanding oxygen minimum zones. *Nat Rev Microbiol* 10: 381–394.

Yunker, M.B., Macdonald, R.W., Ross, P.S., Johannessen, S.C., and Dangerfield, N. (2015) Alkane and PAH provenance and potential bioavailability in coastal marine sediments subject to a gradient of anthropogenic sources in British Columbia, Canada. *Org Geochem* 89–90: 80–116.



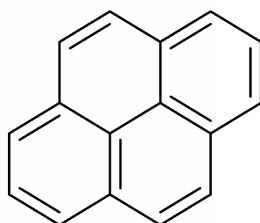






# PART III

## GENERAL DISCUSSION AND CONCLUSIONS





## GENERAL DISCUSSION

The work presented in this thesis adds new information on the interactions between marine microbial communities and airborne PAH, taken as a model family of anthropogenic dissolved organic matter (ADOC, Vila-costa et al., 2020) and the chronic background pollution in the global upper ocean. In particular, we contribute with new insights into PAH microbial biodegradation processes and the cooccurring microbial strategies to cope against PAH toxicities at compositional and transcriptional level under the realistic conditions found in the oceans.

A particular strength of this thesis is that it provides experimental data validating the biodegradation role played by microorganisms in the upper ocean, specially lacking in field studies but urgently required by the scientific community since it is essential for a full assessment of risk and informed prioritization of contaminants (Ottosen et al., 2019). Since biodegradation is determined by microbial and environmental factors, the rate and extent of biodegradation can be different from one environment to the other. Therefore it is important to test biodegradation in experiments performed *in situ* to get representative data closest to realistic conditions. Importantly, PAH-microorganisms interactions promotes changes at different levels: in PAH concentrations, in PAH fate, in microbial metabolisms and in microbial community compositions. In this thesis, we studied PAH biodegradation under realistic conditions from 3 different perspectives:

- (1) Characterizing biodegradation activities
- (2) Identifying players involved in biodegradation
- (3) Identifying the parallel ongoing metabolisms in the interaction between PAH compounds and microorganisms.

In all cases, contrasting habitats, life styles or conditions were included in order to cover a wide spectrum of physiochemical and biological conditions modulating biodegradation in the upper ocean (Table 1).

The dearth of field studies characterizing the impact and biodegradation rates of PAH

at environmental concentrations contrasts with the large body of publications reporting how microbial communities composition and transcription shift in the aftermath of acute OP exposures in the oceans, especially after accidental oil spills with high and unrealistic hydrocarbon concentrations and sporadic occurrence (Kostka et al., 2011; Dubinsky et al., 2013; Dombrowski et al., 2016). This is also reflected in the expanding knowledge of bacterial phylogeny associated to PAH and other hydrocarbons, owing to the growing interest in their functional potentialities for bioremediation (Yakimov et al., 2007, 2021; Crisafi et al., 2016; Mapelli et al., 2017; Pang et al., 2018; Vergeynst et al., 2018). When possible, our results will be compared to this available literature.

**TABLE 1** | Summary of potential factors influencing PAH-microorganisms interactions studied in this thesis. SML: Sea surface microlayer; SSL: Subsurface layer; FL: Free living; PA: Particle associated.

Contrast	Chapter number	Factors influencing PAH-microorganisms interaction
Temperate vs. Polar	1 and 2	Temperature, community composition, pollution level
		Trophic status (or nutrient limitation)
		Pre-exposure history to pollutants
SML vs. SSL	3 and 4	Oxidative stress, community composition
		Physical turbulence and temporal occurrence
		OM content
FL vs. PA	4	Community composition, adaptation strategies
		Metabolic capacities, nutritional preferences
		Microbial life-styles
Unique vs. Mixture spikes	2 to 5	Pollutants synergetic effects
		Toxicity, different carbon and nutrients source from pollutants
		Transformation products

## 1 Characterizing biodegradation activities

Biodegradation potential and activities were characterized through 3 different approaches: **(1)** by quantifying the abundance of PAH-degrading genes in public metagenomic databases **(2)** by measuring degradation rates in mass balance analyses in short term experiments **(3)** by monitoring the expression of PAH-related genes in exposure experiments. A very limited number of field studies report PAH biodegradation by naturally occurring

microbial communities at background concentrations. Most of the studies found in the literature use concentrations of hydrocarbons orders of magnitude above the ones found in the oceans, and the microcosms experiments last longer than our experiments, in the order of >7 days (Scheibye et al., 2017; Brakstad et al., 2018; Kristensen et al., 2015). In this thesis we designed short exposure-time experiments (24-48 hrs) in order to mimic in situ conditions and to assess the immediate response of the naturally occurring microbial community and its potential for biodegradation of PAH at background concentrations.

**1.1. Quantification of the abundance of PAH-degrading genes in public metagenomic databases.** The combined use of chemical and genomic data was not common at the beginning of this thesis since it obligates the interplay of two disconnected fields of research, environmental genomics and analytical chemistry, but more and more these approaches are used in combination to move forward in our understanding of the biogeochemistry of specific DOC or ADOC compounds (González et al., 2019; Song et al., 2020; Kapili and Dekas, 2021; Pierella Karlusich et al., 2021). With the ongoing avalanche of available bacterial MAGs and metagenomic data, genetic data mining has become a very useful technique, allowing for a better description of the regulation and interaction between environmental changes and the naturally occurring microbial communities (Karthikeyan et al., 2020; Love et al., 2021; Royo-Llonch et al., 2021; Yakimov et al., 2021). We reported for the first time the biogeographical abundance of two essential PAH-degrading genes in metagenomes from the global ocean (**Chapter 1**), confirming the widespread genetic potential to degrade airborne PAH by microbial organisms. This evidence, along with the field-derived imbalance between the biological pump sinking flux and the sum of the atmospheric inputs of PAHs, suggest that the fate of native PAH in the upper temperate seawaters is mainly driven by biodegradation processes. Similar results were found by Trilla-Prieto et al (2021), in which the complete set of genes for PAH degradation, from opening the aromatic ring to respiration, were found to be widespread in the global ocean and the microbial genetic potential to remove dissolved black carbon (DBC) from the oceanic water column was assessed (Trilla-Prieto et al., 2021). Likewise, microbially mediated depletion could also be a relevant process modulating the larger pool of SALCS present in the global ocean. Also, our investigation is limited to temperate seawater, so further research is needed to confirm this model and constrain the fate of the large reservoir of SALCs and other OP in both, temperate and polar oceanic regions.

**1.2. Degradation rates measured in short term experiments.** The mass balances from short term PAH exposure experiments under environmental concentrations confirmed that biodegradation rates, even when doped with low concentrations, could substantially vary from one site to another. For instance, in **Chapter 2**, Mediterranean experiment biodegradation rates for the least hydrophobic PAH compounds averaged  $4.72 \pm 0.5 \text{ ng L}^{-1} \text{ h}^{-1}$ , whereas in coastal Antarctica, rates in subsurface layer (0.5m) were close to zero (**Chapter 2 and 4**). This could be explained by a slower community response due to either lower temperatures, as observed in a temperature comparative study with seawater from a temperate location (Ribicic et al., 2018), or the lack of pre-adaptation

history to organic pollutants of Antarctic microbial communities.

Exceptionally, significant HMW PAH degradation rates were observed in Antarctic SML. Very few experiments are performed in the SML, and the PAH exposure experiment in SML of coastal Antarctica is unique (**Chapter 4**). A number of studies report OP enrichments at the SML (Wurl and Obbard, 2004; Cincinelli et al., 2005; Stortini et al., 2008), and few others examine the bacterioneuston compositional traits (Agogué et al., 2005; Stolle et al., 2010; Zäncker et al., 2018). However, experimental or field-based evidences are required to establish the significance and the role played by this interface layer and bacterioneuston communities over the fate of PAH compounds. The lack of experiments conducted with water from the SML is probably explained by the technical challenges of collecting enough quantities of water from this layer, as well as its temporal occurrence and weather dependence. Surprisingly, in the SML experiment from **Chapter 4**, HMW PAH were biodegraded at the SML faster than the SSL, with an average rate of  $1.6 \text{ ng L}^{-1} \text{ h}^{-1}$ . Whether or not this a widespread feature in the oceans or in Antarctica will need to be validated in future studies.

Half-life of PAH measured at background concentrations resulted one order of magnitude lower than those measured at higher concentrations (Figure 1). Although according to kinetics half-lives are independent of PAH concentrations as they are intrinsic properties of the compounds and of the constant rate of the reaction (see supplemental material), experimental evidences show that it is not the case. Results suggest that biodegradation could be a more efficient process at low concentrations. This is possible since high concentrations of PAH have adverse effects to microorganisms that might decrease biodegradation activities (Heipieper and Martínez, 2010). Although interesting, the interaction of toxicity-biodegradation is not addressed in many studies, although this has direct consequences for bioremediation. One of the defense mechanisms to PAH toxicities by microbial cells to avoid PAH accumulation on the membranes is a battery of strategies to change membrane fluidity (remodeling membrane fatty acids, lowering the number of membrane hopanoids, alteration of phospholipid head groups, etc...(Ortega et al., 2017; Joye et al., 2018; Cerro-Gálvez et al., 2019). These changes prevent harm from toxins under high PAH concentrations. However, it might also hinder labile PAH getting past the membrane. PAH uptake for biodegradation also occurs through the membranes. Depending on the size of the PAH, the compound will be directly assimilated by passive uptake, active uptake, or transformed extracellularly. Similarly, the same uptake mechanisms are used for the degradation intermediates. To which degree changes in membrane composition affect the efficiency of biodegradation is not explored in previous studies possibly due to technical challenges that will be solved using new technology, such as single-cell lipidomic approaches that are just now reaching the labs.

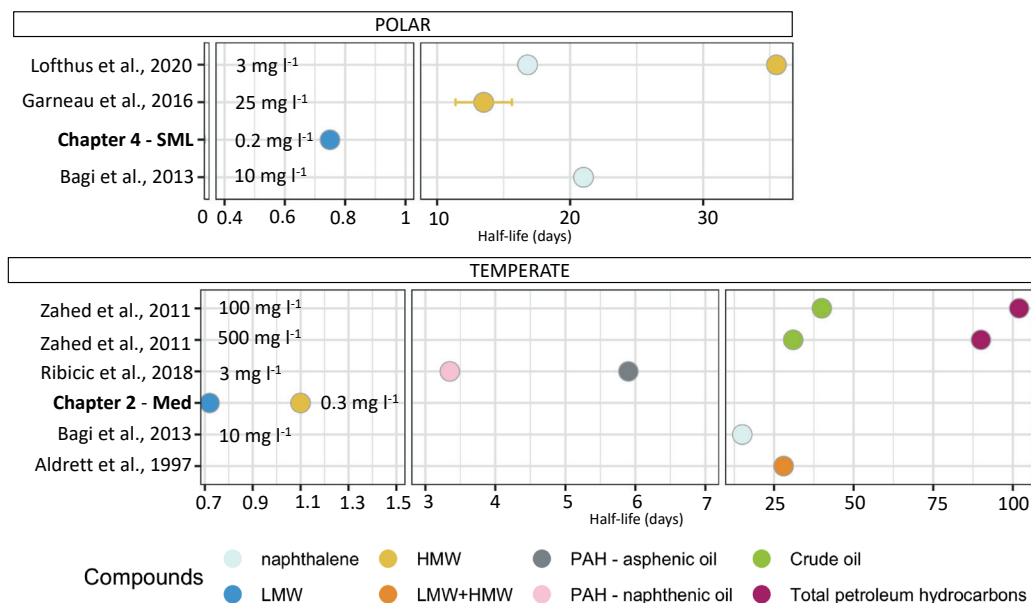


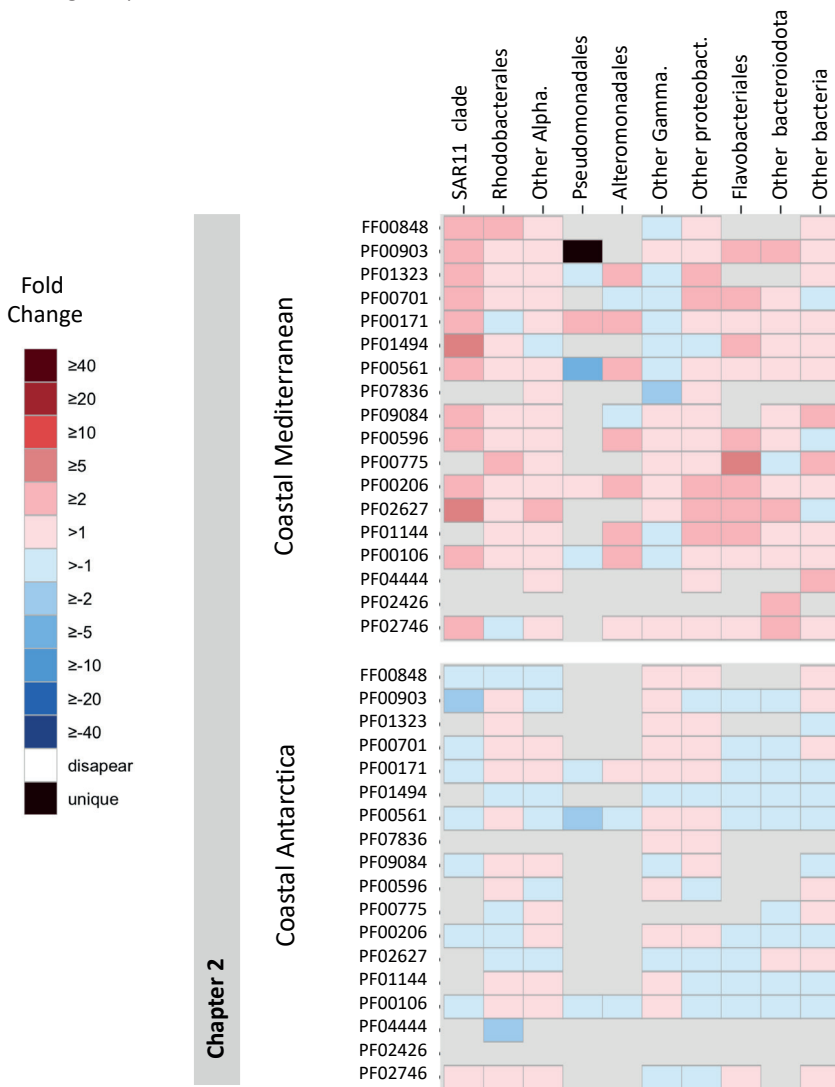
**FIGURE 1** | Half-lives of several PAH compounds from published works and our experiments. HMW: High molecular weight PAH, LMW: Low molecular weight PAH. The biological half-life ( $T_{1/2}$ ) is the time taken for a substance to lose half of its amount. PAH biodegradation half-lives are calculated with equation 1, where  $k$  is the degradation rate constant:

$$t_{1/2} = \frac{\ln(2)}{k} \quad [1]$$

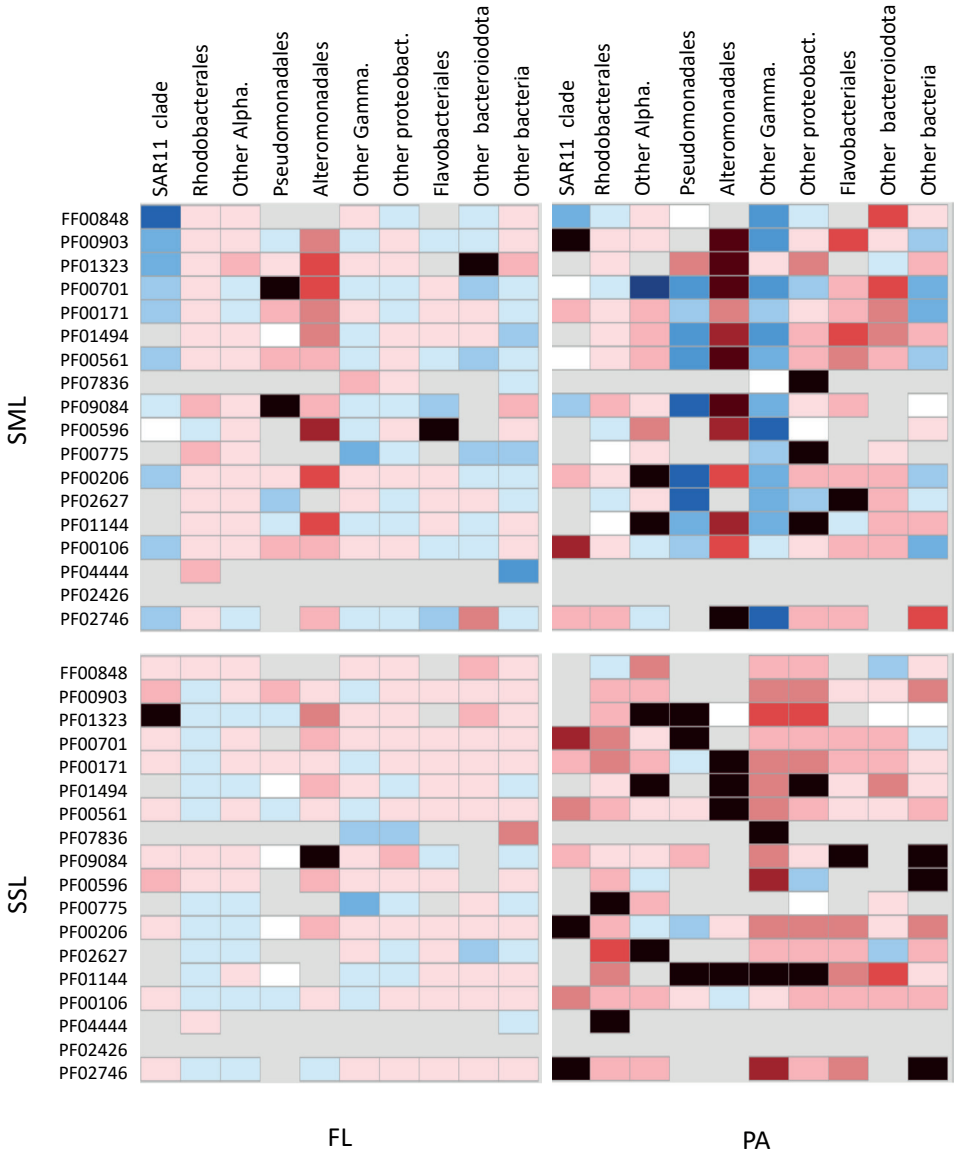
### 1.3. Gene expression of PAH-related genes in short-term exposure experiments.

The genes involved in different stages of PAH degradation were found enriched in most of the PAH exposed communities in manipulated experiments, although with different taxonomic affiliation and response time (Figure 2). In **Chapter 2**, PAH exposed community showed a well adapted and fast responding Alphaproteobacterial community. PAH degradation related transcripts assigned to this group were found enriched 3 h after the PAH exposure, highlighting their role in PAH degradation in the Mediterranean experiment. Interestingly, in **Chapter 4**, in Antarctica, each layer and life-style showed taxa specific enrichments and depletion of PAH-degrading transcripts. The enrichments of PAH-degrading genes affiliated to Alteromonadales at the SML suggested this group played a relevant role in the fast degradation of PAH in the surface layer (Figure 2). This trend was more pronounced at the PA fraction from the SML, which is consistent with previous findings reporting Alteromonadales as one of the main dominant groups in particle associated bacterial metagenomes and metatranscriptomes from the open ocean (Boeuf et al., 2019). Also, SML bacterial composition surveys from different regions have reported Alteromonadales enrichments at the SML to be correlated with transparent exopolymer

**FIGURE 2 |** Fold changes between PAH exposed community compared to controls for the PAH-degrading pfam profiles associated to the different taxonomical groups. Taxonomy of the groups is assessed at order level. See Table 1 to check the contrasting factors in chapter 2 and 4. SML: sea-surface microlayer; SSL: subsurface layer; FL: free living; PA: particle associated.







particles (TEPs) abundances at this layer (Buchan et al., 2014; Taylor et al., 2014; Teeling et al., 2016; Taylor and Cunliffe, 2017). TEPs are biogenic organic matter particles that accumulate at the SML owing to their positive buoyancy (Cunliffe et al., 2009; Wurl et al., 2011; Engel and Galgani, 2016), possibly facilitating the vertical transport of bacteria from the SSL to the SML. This finding, combined with the faster HMW PAH biodegradation rates at the SML, suggest that the biodegradation at the SML mostly occurred at the particle phase, mediated by the PA cohort. This result is consistent with the fact that organic matter reactivity is influenced by the presence of solid-water (eg. POM or ADOC attached to POM - water) or air-water interfaces (SML-atmosphere) (Grossart, 2010).

In **Chapter 5**, the metatranscriptome data of northeast subarctic Pacific Ocean (NESAP) CENTRAL site showed significant transcript enrichments only for the late stages of PAH degradation. The fact that late PAH degrading transcript enrichments were mostly assigned to Rhodobacterales is consistent with the successional patterns observed in advanced stages of oil spills (Hazen et al., 2010; Redmond and Valentine, 2012; Dubinsky et al., 2013), and the analogous observations derived from a laboratory experiment simulating an oil plume (Hu et al., 2017). In all cases, Rhodobacterales became dominant in late stages of degradation, while gammaproteobacterial abundances receded.

Overall, results from **Chapters 1, 2, 4 and 5** indicate that while PAH degradation genetic potential is a widespread trait in all oceanic basins and PAH-degrading genes get expressed at background concentrations of PAH, PAH biodegradation activities are strongly influenced by a wide range of different environmental factors. Our results are in agreement with previous studies, pointing temperature, habitat, pH, nutrients availability, composition of microbial community, chemical nature of PAHs, oxygen and degree of acclimation as relevant environmental drivers of PAH biodegradation (Leahy and Colwell, 1990; Wright et al., 2008; Bagi et al., 2013; Hazen et al., 2016; Ławniczak et al., 2020). This thesis adds new factors influencing efficiency of PAH biodegradation in the upper ocean: bacterial life-style, suggesting that PA bacteria might be more efficient degraders, and the habitat, opening the avenue for a deeper exploration of SML as PAH degrading bioreactor of the sea.

## **2 Changes in microbial communities following PAH exposures at environmental concentrations**

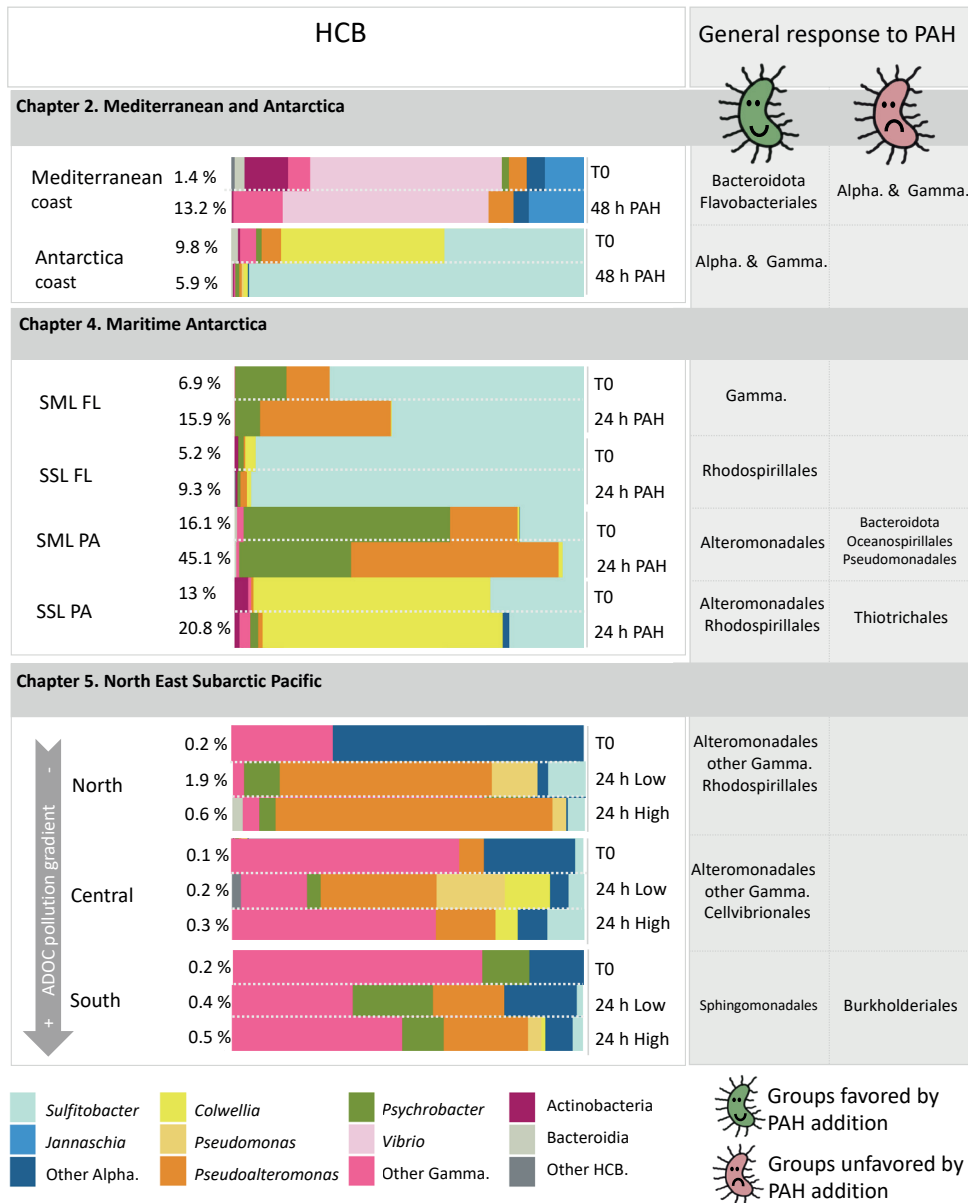
PAH exposures at high concentrations (such in oil-impacted environments) can stimulate the growth of some bacterial groups able to use them as carbon and energy source, and can limit the growth of some others lacking sufficient metabolic strategies to cope with PAH toxicities (Hu et al., 2017; Valencia-Agami et al., 2019). Hydrocarbon-oclastic bacteria (HCB) are specialized bacteria to consume PAH as a carbon or energy source. They have been classically characterized in cultures, but recently also through 16S amplicon sequencing and metagenomic amplified genomes (MAGS) in oil-impacted

environments. (Gauthier et al., 2003; Vila et al., 2010; Karthikeyan et al., 2020; Yakimov et al., 2021). However, very little is known about changes in relative abundances of generalist and specifically HCB after exposures to PAH at background concentrations. In order to retrieve HCB in our 16S amplicon sequencing data, we used an in house database build after compiling taxa from culture works and field-based studies focused on oil impacted marine regions (Lozada et al., 2014; Karthikeyan et al., 2020). For **Chapters 3 and 5** this compendium was expanded to include isolated strains capable of degrading OPE-FRP (Takahashi et al., 2013; Abe et al., 2014; Yamaguchi et al., 2016; Yi et al., 2016; Ravintheran et al., 2019). The dataset was validated manually using blast. In brief, the validation consisted in comparing those ASV from our 16S amplicon sequencing datasets that were assigned to HCB or OPE-degrading genera against relevant isolates from the same genus known to degrade PAH, OPEs or retrieved from an oil polluted site. The ASV's with a similarity score above 97% were taken as true match.

We tracked changes in community composition following short-term PAH exposures by means of 16S amplicon sequencing. Although PAH spike concentrations were in the range of PAH environmental variability, we observed changes in community compositions in all sites tested. Interestingly, each community responded different to the exposure to background concentrations of PAH (**Figure 3**). Overall, Gammaproteobacteria and Alphaproteobacteria groups were the most favoured by the short-time exposure of PAH. However, in the Mediterranean experiment (**Chapter 2**), the most favoured population after 48 h of exposure was Bacteroidota, especially Flavobacteriales.

Our field-based results show HCB communities are not only different at each geographical site, as pointed out in previous studies (Sun and Kostka, 2019), but also specific for each habitat and bacterial life-style (**Figure 3**). Our results showed that an initial higher relative abundance of HCB sub-population does not strictly correlate to a faster or more efficient response to PAH exposure, supporting the fact that microbial responses to PAH are not only determined by the microorganisms exposed to the pulse of PAH (Cerro-Gálvez et al., 2019; Ławniczak et al., 2020). The phylum proteobacteria, and specifically classes alphaproteobacteria and gammaproteobacteria, were the major contributors in all the HCB sub-populations of our dataset (**Figure 3**). The class Gammaproteobacteria is known to harbour the highest diversity of HCB genera (Gutierrez, 2019a; Yakimov et al., 2021), including most obligate hydrocarbonoclastic bacteria (OHCB). OHCB are specialized hydrocarbon degraders with a limited range of growth substrates, that are known to become dominant bacterial players at oil-impacted sites. Examples of PAH degrading specialists are strains belonging to the genera *Cycloclasticus* and *Neptunomonas* (Wang et al., 2018; Gutierrez, 2019b). However, we observed a lack of OHCB dominance following PAH exposures at background concentrations in all sites. Rather, we observed an immediate response at compositional and transcriptional level by generalist HCB bacteria (not OHCB) (**Chapters 2, 4 and 5**). Namely, generalist HCB genera favoured by the presence of PAH at low concentrations. belonged to Alteromonadales, Pseudomonadales, Vibrionales

**FIGURE 3 |** Composition of HCB strains in the different sampled marine system at initial conditions and at the end of the short-term incubations in the PAH exposed community (Left panel titled HCB). The percentage on the left of the bars indicates que relative contribution of HCB sub-population over the total pool of ASVs in that experimental condition. The grey panel on the right indicates the major groups that were favoured or unfavoured by the PAH addition at the end of the incubation. All incubations were performed in the dark, and PAH concentrations were within the range of those found in the oceans. See Table 1 to check the contrasting factors in each chapter. SML: sea-surface microlayer; SSL: subsurface layer; FL: free living; PA: particle associated.



and Rhodobacterales (**Figure 3**). These results are in agreement with microbial successions following oil spills and mesocosm experiments with crude oil, where OHCB are replaced by generalists after oil surface slicks break down into oil droplets dispersed along the water column (Redmond and Valentine, 2012; Chronopoulou et al., 2015). Thus, our results suggest that HCB generalists might be more sensitive and better adapted to cope with low concentrations of growth substrate than OHCB.

Relative abundance of generalist HCB at initial waters ranged from 0.2 to 7% in the free-living fraction. Despite experiments were run over a short period (1-2 days), we observed rapid growth of these generalist HCB bacteria, that reached contributions to the total free-living ASV pool as much as 16%. (Chapter 2, 4 and 5). This is consistent with the previously reported growth of the rare biosphere after oil spills and under background levels of other ADOC compounds exposure (Kleindienst et al., 2016; Wang et al., 2017; Cerro-Gálvez et al., 2019b, Hu et al., 2017). Our findings add evidence to the role played by the very low abundant taxa as a reservoir of inactive bacteria which exponentially grows under specific environmental variations, in this case, stimulated after PAH exposure at background concentration (Wang et al., 2017). The large diversity of low abundance taxa acts as a buffer in front of sudden environmental changes, since these provide a diverse genetic toolbox that could potentially be useful under a particular stressor, such as PAH exposure in our experiments. The fast growing response of low abundant taxa is also associated to a copiotroph life style. Copiotroph bacteria are very sensitive to substrate availability, and rapidly respond to nutrient or other substrate inputs (Ramirez et al., 2012; Ho et al., 2017), outcompeting oligotrophs. In other words: the life-style of feasting and fasting. Thus, HCB with copiotroph life-style might bloom with minimal PAH levels.

The analysis performed in **Chapter 3** confirms a consistent enrichment of HCB strains in the sea surface microlayer in comparison to the underlying waters. **Chapter 4** showed that they are specially abundant in the PA fraction (Figure 3). HCB strains from Gammaproteobacteria and Flavobacteriia and HCB orders Alteromonadales, Caulobacterales and Sphingomonadales were significantly enriched at the SML. Moreover, HCB strains were found correlated with surface-active ADOC compounds concentrations at the SML. These results prove the potential of the SML HCB sub-populations to interact with ADOC, as well as providing field-based evidence that, although neglected, ADOC at background concentrations can be a shaping vector of microbial communities composition at the SML. The potential active role of HCB in pollutants biodegradation at the SML was confirmed in **Chapter 4**, where significant higher PAH degradation rates were observed at the SML than in the SSL. Interestingly, we also observed that specific gammaproteobacteria taxa were systematically enriched at the SML, while the same taxa were found at low abundances in the underlying bulk water, supporting the hypothesis that bacterioneuston composition might be directly sourced from the adjacent environments bacterial communities, belonging to taxa with low abundances or even from the

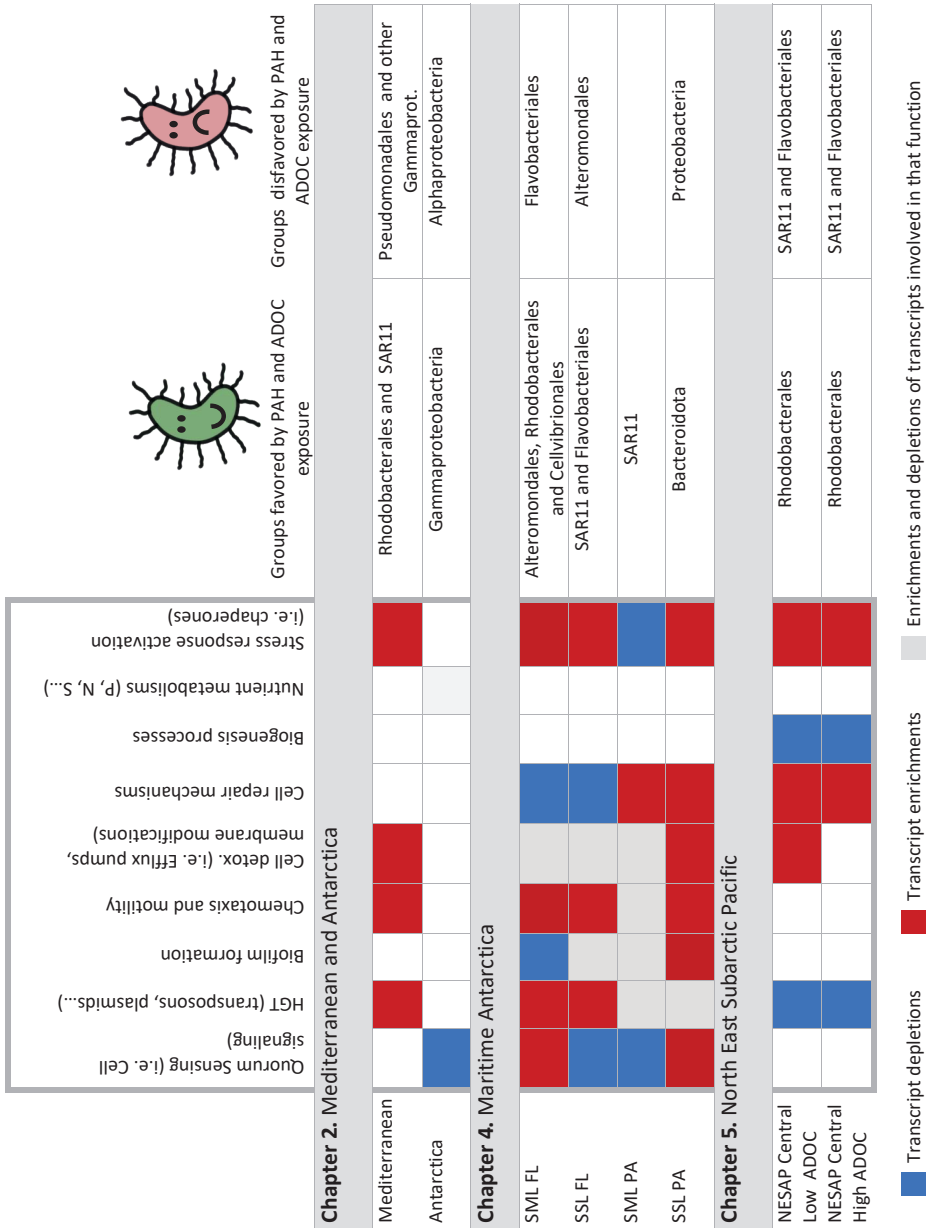
rare biosphere. In a previous report, hydrocarbonoclastic bacterioneuston populations of a chronically polluted oil estuarine were examined for their PAH degrading capacity (Coelho et al., 2011). PAH degrading genes with high homology were found in phylogenetically distinct groups, suggesting the horizontal spread of this genes. In fact, SML higher bacterial abundance and biofilm growing bacteria possibly facilitate the dissemination of genes among bacteria, as well as quorum sensing strategies (Cunliffe & Murrell 2009).

### 3 Gene expression profiles after PAH exposure at background concentrations

The community responses at transcriptional level were tracked by means of metatranscriptomic analysis. This approach allows capturing the immediate response after the exposure of PAH at environmentally relevant concentrations of the whole microbial community. Instead of exclusively snapshotting PAH-degrading genes, we can get the picture of the whole battery of simultaneous ongoing metabolisms of the interaction between PAH and bacteria. In general, our results show that early microbial responses to PAH are habitat specific. However, similar cooccurring strategies devoted to cope against PAH and other ADOC compounds toxicities were detected at the three sites (Mediterranean, Antarctica and sub-Arctic). At functional level, stress response and cell detoxifying mechanisms were transcribed in all experiments after PAH exposure, owing to the known toxic effect on living cells, in spite of the low concentrations amended, and other metabolisms got enriched in some experiments but not all (for instance, those related to cell repair and horizontal gene transfer (HGT)). In general, differentially expressed genes belonged to different taxa (Figure 4). In fact, no clear pattern for the taxonomical transcriptional responses can be deduced from our experiments, since taxonomical groups that were favoured by PAH presence in one experiment, were disfavoured in another. **Figure 4** shows a summary of responses and the main groups involved in the response.

One interesting question that is poorly explored in metagenomic and/or metatranscriptomic data is the presence and expression of genes related to dissemination of genes among the community by HGT as response to environmental stressors (Casacuberta et al., 2013). Regarding pollutants as stressors, only the effects of antibiotics on dissemination of antibiotic resistance genes are explored in field data, whereas there is a dearth of data regarding other organic pollutants (Gillings, 2013). In **Chapter 2**, enrichments of HGT and PAH-degrading genes– related transcripts were observed for the Mediterranean PAH exposed community only three hours after of PAH exposure. Oppositely, the Antarctic pristine community remained unchanged, and so did PAH concentrations over the course of the experiment. These results are consistent with another comparative study performed in two ecoregions (Mediterranean and Patagonia) with different pollution levels and microbial communities with different pre-exposure history. In this study the isolated HCB strains from the polluted site showed higher degradation performance towards alkanes and PAH compared to the less polluted site (Zappalà et al., 2020). Only few

**FIGURE 4 |** Enrichment and depletion transcript trends of selected functionalities after PAH exposure compared to controls. Last two columns summarize the taxonomical groups that were favoured or disfavoured by the exposure at transcriptional level. Communities in Chapters 2 and 4 were amended with PAH, while Chapter 5 was amended with an ADOC-mixture comprising PAH, OPE-FRP and n-alkanes. SML: sea-surface microlayer; SSL: subsurface layer; FL: free living; PA: particle associated.



studies tackle pre-exposure to ADOC contamination as a selective agent for resistance or degradation genes dissemination (Cerro-Galvez et al., 2021, Wright et al., 2008, Nesbo et al., 2011). Our results are in agreement with this few previous data pointing that the history of exposure might determine the immediate transcriptional responses as a result of an adaptive selective trait triggered by PAH, possibly facilitating the dissemination of PAH degrading genes and genes related to stress response or detoxifying strategies such as chemotaxis or antidrug efflux pumps. In other words: What doesn't kill bacteria, makes them stronger. Nevertheless, further experimental comparative research should be conducted to constrain the environmental circumstances that trigger bacterial HGT, PAH biodegradation and the time-response in front of PAH pulses at low concentrations.

## GENERAL CONCLUSIONS

**1** Biodegradation and the biological pump are major drivers of the fate of PAHs in the temperate upper seawater. The presence of PAH-degrading genes (RHD genes) is globally widespread in the upper ocean, pointing to the relevant role of marine microbial communities modulating the pool of PAH in the water column.

**2** PAH biodegradation rates at background concentrations in the surface ocean are very variable and prone to be modulated by multiple biotic and abiotic factors, including: temperature, microbial community composition, cell proximity, nutrient availability, substrate availability, suspended organic matter, etc... Important new environmental factors to take into account include: (1) the habitat, (2) bacteria life-style and (3) the pre-exposure history to PAH

**3** Biodegradation by surface marine bacteria could be a more efficient process at low concentrations than at high concentrations due to PAH toxicities

**4** The main groups favored by PAH exposure at low concentrations are HCB generalist belonging to alphaproteobacteria (Rhodobacterales and Rhodospirillales) and gammaproteobacterial (Alteromonadales).

**5** A succession of taxa and functions can be observed after additions of PAH at low concentrations, similar to what it is observed under oil spill conditions and other high PAH concentrations exposures, although fast and slow responders diverge.

**6** Generalist HCB strains play a key role in the degradation of PAH at low concentrations in the surface ocean.



**7** Sea surface microlayer is a hotspot of HCB strains, and their abundance correlates to a model family of surface active ADOC compounds (PFAS).

**8** SML is a hotspot microhabitat for PAH degradation in Antarctic coastal waters, especially for HMW PAH. HMW PAHs higher hydrophobicity incline their partitioning towards microorganisms and detritus, which are the major organic matter pools, facilitating their biodegradation by particle associated bacteria.

**9** Experimental evidence point that microbial community pre-exposure history to organic pollutants is an influencing factor determining the immediate response after a pulse of PAH.

**10** Horizontal gene transfer via MGE is an adaptive response in front of PAH pulses even at low concentrations, possibly transferring metabolic genes to degrade PAH.

## FUNDAMENTAL GAPS OF KNOWLEDGE

We still lack a fundamental understanding of the interaction between PAH and microorganisms at cellular level. This knowledge would provide clues to understand important questions such as the balance between biodegradation and toxicity, and how this is translated into biodegradation efficiencies. Also, the relative role played by the different environmental and microbial factors modulating PAH biodegradation in the upper ocean needs to be addressed, in order to provide reliable data to feed models of risk assessment for PAHs.

In spite of the growing interest, HCB strains phylogeny and nutritional preferences knowledge is limited by culture isolation techniques and sequencing approaches of the free-living microbiome. Symbiotic associations of HCB strains to other species, or the functioning of HCB consortia under realistic conditions in different habitats such as those initially explored in this thesis are largely unexplored. Complementary research approaches (bioinformatics, field-based, mesocosms experiments...) are needed to investigate HCB strains and their role with PAH fate under realistic conditions.

In **Chapter 5** we investigated the transcription of the degrading genes for other ADOC compounds present at the ADOC mixture beyond PAH (n-alkanes and OPE-FRP). Unlike the well-studied PAH degrading genes, the enzymatic capacity to transform other ADOC manmade compounds such as some contaminants of emerging concern (CEC), with no pre-existing naturally occurring analogues, remains unclear. Further research on the identification of degrading enzymatic capabilities towards ADOC compounds is needed, especially for biotechnological remediation purposes, but also to understand the biological factors that regulate the fate of these compounds once in the water column.

## RECOMMENDATIONS FOR FUTURE RESEARCH

Based on our experimental designs, we recommend to perform both killed and abiotic controls, in order to exclude ADOC losses by abiotic factors such as adsorption to bottle walls or chemical affinity to lipidic particles (for instance, bacterial and algal cells). Killed controls are those that contain killed cells at the same concentrations that the alive treatments. It allows to assess the partitioning between cells and the dissolved phase passively. This accounts for the amount of sorption of ADOC compounds into cells. Abiotic controls (that is, seawater without cells) allow exclusion of any PAH adsorption to organic matter and account for abiotic adsorptions and absorptions to the bottle walls.

Another interesting matter that should be addressed is the role of the SML in the fate of PAH and other ADOC compounds in the marine environment. In spite of the SML fundamental role in the carbon flux and air-sea exchange at a global scale, it remains as a poorly explored habitat. Therefore, more experimental research should be conducted

at the SML, in order to assess the biodegradation of low concentrations of PAH and other ADOC compounds with chemical affinity to the interface habitats, in order to elucidate what are the influencing factors controlling the fate of these compounds in such globally relevant microhabitat.

## **FUTURE RESEARCH PERSPECTIVES**

- Opening the black box of bacteria at single cell level using high-throughput multi-omics approaches. This would allow to explore the effects of PAH at cellular level, such as the effects on cell membranes, improving the predictability of biodegradation estimates. Further, single-cell approaches will allow disentangling the heterogeneity within the communities exposed to PAH and discover the different strategies within the same taxonomical groups at a finer resolution than using metatranscriptomics.

- Characterization of degradation products in non-impacted sites and their effects to the ecosystems. The full degradability of the compounds and the metabolites produced or the entire succession along the substrate transformations are gaps of research that would shed light onto the full toxicity of PAH compounds.

- Combining environmental genomics and analytical chemistry approaches to study ADOC compounds of emerging concern, other than PAH. The complex mixture of OP found in the environment is intractable and new methodological and multidisciplinary approaches are mandatory. The methodologies used in this thesis show that the combination of multidisciplinary techniques yield a wider picture of biodegradation than the use of single techniques (Fenner and Scheringer, 2021).

## REFERENCES

- Abe, K., Yoshida, S., Suzuki, Y., Mori, J., Doi, Y., Takahashi, S., and Kera, Y. (2014) Haloalkylphosphorus hydrolases purified from *Sphingomonas* sp. strain TDK1 and *Sphingobium* sp. strain TCM1. *Appl Environ Microbiol* 80: 5866–73.
- Agogu e, H., Casamayor, E.O., Bourrain, M., Obernosterer, I., Joux, F., Herndl, G.J., and Lebaron, P. (2005) A survey on bacteria inhabiting the sea surface microlayer of coastal ecosystems. *FEMS Microbiol Ecol* 54: 269–280.
- Aldrett, S., Bonner, J.S., Mills, M.A., Autenrieth, R.L., and Frank, L.S. (1997) Microbial degradation of crude oil in marine environments tested in a flask experiment. *Water Res* 31: 2840–2848.
- Bagi, A., Pampanin, D.M., Brakstad, O.G., and Kommedal, R. (2013a) Estimation of hydrocarbon biodegradation rates in marine environments: A critical review of the Q10 approach. *Mar Environ Res* 89: 83–90.
- Bagi, A., Pampanin, D.M., Brakstad, O.G., and Kommedal, R. (2013b) Estimation of hydrocarbon biodegradation rates in marine environments: A critical review of the Q10 approach. *Mar Environ Res* 89: 83–90.
- Boeuf, D., Edwards, B.R., Eppley, J.M., Hu, S.K., Poff, K.E., Romano, A.E., et al. (2019) Biological composition and microbial dynamics of sinking particulate organic matter at abyssal depths in the oligotrophic open ocean. *Proc Natl Acad Sci U S A* 116: 11824–11832.
- Brakstad, O.G., Davies, E.J., Ribicic, D., Winkler, A., Br nner, U., and Netzer, R. (2018) Biodegradation of dispersed oil in natural seawaters from Western Greenland and a Norwegian fjord. *Polar Biol* 41: 2435–2450.
- Buchan, A., LeClerc, G.R., Gulvik, C.A., and Gonz lez, J.M. (2014) Master recyclers: features and functions of bacteria associated with phytoplankton blooms. *Nat Rev Microbiol* 12: 686–698.
- Casacuberta, E. and Gonz lez, J. (2013) The impact of transposable elements in environmental adaptation. *Mol Ecol* 22: 1503–1517.
- Cerro-G lvez, E., Dachs, J., Lundin, D., Fern ndez-Pinos, M.-C., Sebasti n, M., and Vila-Costa, M. (2021) Responses of Coastal Marine Microbiomes Exposed to Anthropogenic Dissolved Organic Carbon. *Environ Sci Technol* 55: 9609–9621.
- Cerro-G lvez, E., Casal, P., Lundin, D., Pi a, B., Pinhassi, J., Dachs, J., and Vila-Costa, M. (2019) Microbial responses to anthropogenic dissolved organic carbon in the Arctic and Antarctic coastal seawaters. *Environ Microbiol* 21: 1466–1481.
- Chronopoulou, P.M., Sanni, G.O., Silas-Olu, D.I., van der Meer, J.R., Timmis, K.N., Brussaard, C.P.D., and McGenity, T.J. (2015) Generalist hydrocarbon-degrading bacterial communities in the oil-polluted water column of the North Sea. *Microb Biotechnol* 8: 434–447.
- Cincinelli, A., Stortini, A.M., Checchini, L., Martellini, T., Del Bubba, M., and Lepri, L. (2005) Enrichment of organic pollutants in the sea surface microlayer (SML) at Terra Nova Bay, Antarctica: Influence of SML on superficial snow composition. *J Environ Monit* 7: 1305–1312.
- Coelho, F., Sousa, S., Santos, L., Santos, A., Almeida, A., Gomes, N., and Cunha,  . (2011) Exploring hydrocarbonoclastic bacterial communities in the estuarine surface microlayer. *Aquat Microb Ecol* 64: 185–195.
- Crisafi, F., Giuliano, L., Yakimov, M.M., Azzaro, M., and Denaro, R. (2016) Isolation and degradation potential of a cold-adapted oil/PAH-degrading marine bacterial consortium from Kongsfjorden (Arctic region). *Rend Lincei* 27: 261–270.
- Cunliffe, M. and Murrell, J.C. (2009) The sea-surface microlayer is a gelatinous biofilm. *ISME J* 1001–1003.
- Cunliffe, M., Salter, M., Mann, P.J., Whiteley, A.S., Upstill-Goddard, R.C., and Murrell, J.C. (2009) Dissolved organic carbon and bacterial populations in the gelatinous surface microlayer of a Norwegian fjord mesocosm. *FEMS Microbiol Lett* 299: 248–254.
- Dombrowski, N., Donaho, J.A., Gutierrez, T., Seitz, K.W., Teske, A.P., and Baker, B.J. (2016) Reconstructing metabolic pathways of hydrocarbon-degrading bacteria from the Deepwater Horizon oil spill. *Nat Microbiol* 1: 16057.
- Dubinsky, E.A., Conrad, M.E., Chakraborty, R., Bill, M., Borglin, S.E., Hollibaugh, J.T., et al. (2013) Succession of Hydrocarbon-Degrading Bacteria in the Aftermath of the Deepwater Horizon Oil Spill in the Gulf of Mexico. *Environ Sci Technol* 47: 10860–10867.
- Engel, A. and Galgani, L. (2016) The organic sea-surface microlayer in the upwelling region off the coast of

- Peru and potential implications for air-sea exchange processes. *Biogeosciences* 13: 989–1007.
- Fenner, K. and Scheringer, M. (2021) The Need for Chemical Simplification As a Logical Consequence of Ever-Increasing Chemical Pollution. *Cite This Environ Sci Technol* 55: 14470–14472.
- Garneau, M.-È., Michel, C., Meisterhans, G., Fortin, N., King, T.L., Greer, C.W., and Lee, K. (2016) Hydrocarbon biodegradation by Arctic sea-ice and sub-ice microbial communities during microcosm experiments, Northwest Passage (Nunavut, Canada). *FEMS Microbiol Ecol* 92:.
- Gauthier, E., Déziel, E., Villemur, R., Juteau, P., Lépine, F., and Beaudet, R. (2003) Initial characterization of new bacteria degrading high-molecular weight polycyclic aromatic hydrocarbons isolated from a 2-year enrichment in a two-liquid-phase culture system. *J Appl Microbiol* 94: 301–311.
- Gillings, M.R. (2013) Evolutionary consequences of antibiotic use for the resistome, mobilome, and microbial pangenome. *Front Microbiol* 4:.
- González, J.M., Hernández, L., Manzano, I., and Pedrós-Alió, C. (2019) Functional annotation of orthologs in metagenomes: a case study of genes for the transformation of oceanic dimethylsulfoniopropionate. *ISME J* 13: 1183.
- Grossart, H.P. (2010) Ecological consequences of bacterioplankton lifestyles: changes in concepts are needed. *Environ Microbiol Rep* 2: 706–714.
- Gutierrez, T. (2019a) Marine, Aerobic Hydrocarbon-Degrading Gammaproteobacteria: Overview. In *Taxonomy, Genomics and Ecophysiology of Hydrocarbon-Degrading Microbes*. Springer, Cham, pp. 143–152.
- Gutierrez, T. (2019b) Marine, Aerobic Hydrocarbon-Degrading Gammaproteobacteria: Overview. *Taxon Genomics Ecophysiol Hydrocarb Microbes* 143–152.
- Hazen, T.C., Dubinsky, E.A., DeSantis, T.Z., Andersen, G.L., Piceno, Y.M., Singh, N., et al. (2010) Deep-sea oil plume enriches indigenous oil-degrading bacteria. *Science* (80- ) 330: 204–208.
- Hazen, T.C., Prince, R.C., and Mahmoudi, N. (2016) Marine Oil Biodegradation. *Environ Sci Technol* 50: 2121–2129.
- Heipieper, H.J. and Martínez, P.M. (2010) Toxicity of Hydrocarbons to Microorganisms. *Handb Hydrocarb Lipid Microbiol* 1563–1573.
- Ho, A., Di Lonardo, D.P., and Bodelier, P.L.E. (2017) Revisiting life strategy concepts in environmental microbial ecology. *FEMS Microbiol Ecol* 93: 6.
- Hu, P., Dubinsky, E.A., Probst, A.J., Wang, J., Sieber, C.M.K., Tom, L.M., et al. (2017) Simulation of Deepwater Horizon oil plume reveals substrate specialization within a complex community of hydrocarbon degraders. *Proc Natl Acad Sci U S A* 114: 7432–7437.
- Joye, S., Kleindienst, S., and Peña-Montenegro, T.D. (2018) SnapShot: Microbial Hydrocarbon Bioremediation. *Cell* 172: 1336-1336.e1.
- Kapili, B.J. and Dekas, A.E. (2021) PPIT: an R package for inferring microbial taxonomy from nifH sequences. *Bioinformatics* 37: 2289–2298.
- Karthikeyan, S., Rodriguez-R, L.M., Heritier-Robbins, P., Hatt, J.K., Huettel, M., Kostka, J.E., and Konstantinidis, K.T. (2020) Genome repository of oil systems: An interactive and searchable database that expands the catalogued diversity of crude oil-associated microbes. *Environ Microbiol* 22: 2094–2106.
- Kleindienst, S., Grim, S., Sogin, M., Bracco, A., Crespo-Medina, M., and Joye, S.B. (2016) Diverse, rare microbial taxa responded to the Deepwater Horizon deep-sea hydrocarbon plume. *ISME J* 10: 400–415.
- Kostka, J.E., Prakash, O., Overholt, W.A., Green, S.J., Freyer, G., Canion, A., et al. (2011) Hydrocarbon-degrading bacteria and the bacterial community response in Gulf of Mexico beach sands impacted by the deep-water horizon oil spill. *Appl Environ Microbiol* 77: 7962–7974.
- Kristensen, M., Johnsen, A.R., and Christensen, J.H. (2015) Marine biodegradation of crude oil in temperate and Arctic water samples. *J Hazard Mater* 300: 75–83.
- Ławniczak, Ł., Woźniak-Karczewska, M., Loibner, A.P., Heipieper, H.J., and Chrzanowski, Ł. (2020) Microbial Degradation of Hydrocarbons—Basic Principles for Bioremediation: A Review. *Mol* 2020, Vol 25, Page 856 25: 856.
- Leahy, J.G. and Colwell, R.R. (1990) Microbial degradation of hydrocarbons in the environment. *Microbiol Rev* 54: 305–315.
- Lofthus, S., Bakke, I., Tremblay, J., Greer, C.W., and Brakstad, O.G. (2020) Biodegradation of weathered crude oil in seawater with frazil ice. *Mar Pollut Bull* 154: 111090.

Love, C.R., Arrington, E.C., Gosselin, K.M., Reddy, C.M., Van Mooy, B.A.S., Nelson, R.K., and Valentine, D.L. (2021) Microbial production and consumption of hydrocarbons in the global ocean. *Nat Microbiol* 2021 64 6: 489–498.

Lozada, M., Marcos, M.S., Commendatore, M.G., Gil, M.N., and Dionisi, H.M. (2014) The bacterial community structure of hydrocarbon-polluted marine environments as the basis for the definition of an ecological index of hydrocarbon exposure. *Microbes Environ* 29: 269–76.

Mapelli, F., Scoma, A., Michoud, G., Aulenta, F., Boon, N., Borin, S., et al. (2017) Biotechnologies for Marine Oil Spill Cleanup: Indissoluble Ties with Microorganisms. *Trends Biotechnol* 35: 860–870.

Nesbø, C.L., Boucher, Y., Dlutek, M., and Doolittle, W.F. (2005) Lateral gene transfer and phylogenetic assignment of environmental fosmid clones. *Environ Microbiol* 7: 2011–2026.

Ortega, Á., Zhulin, I.B., and Krell, T. (2017) Sensory Repertoire of Bacterial Chemoreceptors. *Microbiol Mol Biol Rev* 81:.

Ottosen, C.B., Murray, A.M., Broholm, M.M., and Bjerg, P.L. (2019) In Situ Quantification of Degradation Is Needed for Reliable Risk Assessments and Site-Specific Monitored Natural Attenuation. *Environ Sci Technol* 53: 1–3.

Pang, L., Ge, L., Yang, P., He, H., and Zhang, H. (2018) Degradation of organophosphate esters in sewage sludge: Effects of aerobic/anaerobic treatments and bacterial community compositions. *Bioresour Technol* 255: 16–21.

Pierella Karlusich, J.J., Pelletier, E., Lombard, F., Carsique, M., Dvorak, E., Colin, S., et al. (2021) Global distribution patterns of marine nitrogen-fixers by imaging and molecular methods. *Nat Commun* 2021 121 12: 1–18.

Ramirez, K.S., Craine, J.M., and Fierer, N. (2012) Consistent effects of nitrogen amendments on soil microbial communities and processes across biomes. *Glob Chang Biol* 18: 1918–1927.

Ravintheran, S.K., Sivaprakasam, S., Loke, S., Lee, S.Y., Manickam, R., Yahya, A., et al. (2019) Complete genome sequence of *Sphingomonas paucimobilis* AIMST S2, a xenobiotic-degrading bacterium. *Sci Data* 6: 1–6.

Redmond, M.C. and Valentine, D.L. (2012) Natural gas and temperature structured a microbial community response to the Deepwater Horizon oil spill. *Proc Natl Acad Sci U S A* 109: 20292–20297.

Ribicic, D., McFarlin, K.M., Netzer, R., Brakstad, O.G., Winkler, A., Throne-Holst, M., and Størseth, T.R. (2018) Oil type and temperature dependent biodegradation dynamics - Combining chemical and microbial community data through multivariate analysis. *BMC Microbiol* 18:.

Ribicic, D., Netzer, R., Winkler, A., and Brakstad, O.G. (2018) Microbial communities in seawater from an Arctic and a temperate Norwegian fjord and their potentials for biodegradation of chemically dispersed oil at low seawater temperatures. *Mar Pollut Bull* 129: 308–317.

Royo-Llonch, M., Sánchez, P., Ruiz-González, C., Salazar, G., Pedrós-Alió, C., Sebastián, M., et al. (2021) Compendium of 530 metagenome-assembled bacterial and archaeal genomes from the polar Arctic Ocean. *Nat Microbiol* 6: 1561–1574.

Scheibye, K., Christensen, J.H., and Johnsen, A.R. (2017) Biodegradation of crude oil in Arctic subsurface water from the Disko Bay (Greenland) is limited. *Environ Pollut* 223: 73–80.

Song, D., Zhang, Y., Liu, J., Zhong, H., Zheng, Y., Zhou, S., et al. (2020) Metagenomic Insights Into the Cycling of Dimethylsulfoniopropionate and Related Molecules in the Eastern China Marginal Seas. *Front Microbiol* 11: 157.

Stolle, C., Nagel, K., and Labrenz, M. (2010) Succession of the sea-surface microlayer in the coastal Baltic Sea under natural and experimentally induced low-wind conditions. *Biogeosciences* 7: 2975–2988.

Stortini, A.M., Martellini, T., Del Bubba, M., Lepri, L., Capodaglio, G., and Cincinelli, A. (2008) n-Alkanes, PAHs and surfactants in the sea surface microlayer and sea water samples of the Gerlache Inlet sea (Antarctica).

Sun, X. and Kostka, J.E. (2019) Hydrocarbon-degrading microbial communities are site specific, and their activity is limited by synergies in temperature and nutrient availability in surface ocean waters. *Appl Environ Microbiol* 85:.

Takahashi, S., Abe, K., and Ker, Y. (2013) Microbial Degradation of Persistent Organophosphorus Flame Retardants. In *Environmental Biotechnology - New Approaches and Prospective Applications*. InTech.

Taylor, J.D., Cottingham, S.D., Billinge, J., and Cunliffe, M. (2014) Seasonal microbial community dynamics

correlate with phytoplankton-derived polysaccharides in surface coastal waters. *ISME J* 8: 245–248.

Taylor, J.D. and Cunliffe, M. (2017) Coastal bacterioplankton community response to diatom-derived polysaccharide microgels. *Environ Microbiol Rep* 9: 151–157.

Teeling, H., Fuchs, B.M., Bennke, C.M., Krüger, K., Chafee, M., Kappelmann, L., et al. (2016) Recurring patterns in bacterioplankton dynamics during coastal spring algae blooms.

Trilla-Prieto, N., Vila-Costa, M., Casas, G., Jiménez, B., and Dachs, J. (2021) Dissolved Black Carbon and Semivolatile Aromatic Hydrocarbons in the Ocean: Two Entangled Biogeochemical Cycles? *Environ Sci Technol Lett* 8: 918–923.

Valencia-Agami, S.S., Cerqueda-García, D., Putzeys, S., Uribe-Flores, M.M., García-Cruz, N.U., Pech, D., et al. (2019) Changes in the Bacterioplankton Community Structure from Southern Gulf of Mexico During a Simulated Crude Oil Spill at Mesocosm Scale. *Microorganisms* 7: 441.

Vergeynst, L., Wegeberg, S., Aamand, J., Lassen, P., Gosewinkel, U., Fritt-Rasmussen, J., et al. (2018) Biodegradation of marine oil spills in the Arctic with a Greenland perspective. *Sci Total Environ* 626: 1243–1258.

Vila-Costa, M., Cerro-Gálvez, E., Martínez-Varela, A., Casas, G., and Dachs, J. (2020) Anthropogenic dissolved organic carbon and marine microbiomes. *ISME J* 14: 2646–2648.

Vila, J., Nieto, J.M., Mertens, J., Springael, D., and Grifoll, M. (2010) Microbial community structure of a heavy fuel oil-degrading marine consortium: linking microbial dynamics with polycyclic aromatic hydrocarbon utilization. *FEMS Microbiol Ecol* no-no.

Wang, W., Wang, L., and Shao, Z. (2018) Polycyclic aromatic hydrocarbon (PAH) degradation pathways of the obligate marine PAH degrader *Cycloclasticus* sp. strain P1. *Appl Environ Microbiol* 84.

Wang, Y., Hatt, J.K., Tsementzi, D., Rodríguez-R, L.M., Ruiz-Pérez, C.A., Weigand, M.R., et al. (2017a) Quantifying the importance of the rare biosphere for microbial community response to organic pollutants in a freshwater ecosystem. *Appl Environ Microbiol* 83.

Wang, Y., Hatt, J.K., Tsementzi, D., Rodríguez-R, L.M., Ruiz-Pérez, C.A., Weigand, M.R., et al. (2017b) Quantifying the importance of the rare biosphere for microbial community response to organic pollutants in a freshwater ecosystem. *Appl Environ Microbiol* 83.

Wright, M.S., Baker-Austin, C., Lindell, A.H., Stepanauskas, R., Stokes, H.W., and McArthur, J.V. (2008) Influence of industrial contamination on mobile genetic elements: class 1 integron abundance and gene cassette structure in aquatic bacterial communities. *ISME J* 2008 24 2: 417–428.

Wurl, O. and Obbard, J.P. (2004) A review of pollutants in the sea-surface microlayer (SML): A unique habitat for marine organisms. *Mar Pollut Bull* 48: 1016–1030.

Wurl, O., Wurl, E., Miller, L., Johnson, K., and Vagle, S. (2011) Formation and global distribution of sea-surface microlayers. *Biogeosciences* 8: 121–135.

Yakimov, M.M., Bargiela, R., and Golyshin, P.N. (2021) Calm and Frenzy: marine obligate hydrocarbonoclastic bacteria sustain ocean wellness. *Curr Opin Biotechnol* 73: 337–345.

Yakimov, M.M., Timmis, K.N., and Golyshin, P.N. (2007) Obligate oil-degrading marine bacteria.

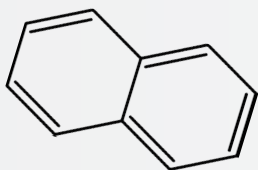
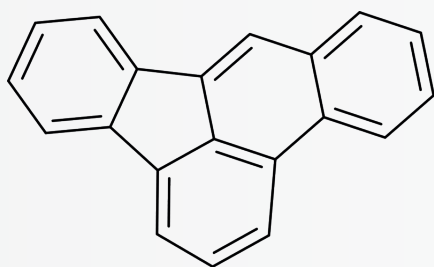
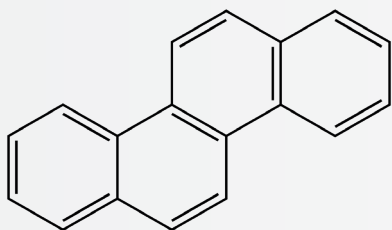
Yamaguchi, H., Arisaka, H., Seki, M., Adachi, M., Kimura, K., and Tomaru, Y. (2016) Phosphotriesterase activity in marine bacteria of the genera *Phaeobacter*, *Ruegeria*, and *Thalassospira*. *Int Biodeterior Biodegrad* 115: 186–191.

Yi, L.B., Chai, L.Y., Xie, Y., Peng, Q.J., and Peng, Q.Z. (2016) Isolation, identification, and degradation performance of a PFOA-degrading strain. *Genet Mol Res* 15: 1–12.

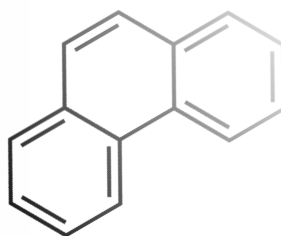
Zahed, M.A., Abdul Aziz, H., Hasnain Isa, M., Mohajeri, L., Mohajeri, S., Rahman, S., and Kutty, M. (2011) Kinetic modeling and half life study on bioremediation of crude oil dispersed by Corexit 9500. *J Hazard Mater* 185: 1027–1031.

Zäncker, B., Cunliffe, M., and Engel, A. (2018) Bacterial community composition in the sea surface microlayer off the peruvian coast. *Front Microbiol* 9.

Zappalà, G., Caruso, G., Denaro, R., Crisafi, F., and Monticelli, L.S. (2020) Ecological and molecular approach to the assessment of oil pollution: A comparative study between two coastal marine (Mediterranean and Patagonian) ecoregions. *WIT Trans Ecol Environ* 242: 85–96.

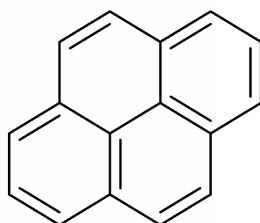






# PART IV

## ANNEX



## **Supporting information of Chapter 1**

**Table S1.** Sampling: Ancillary data for water sample's transects. N and S attend respectively for "north" and "south" basins in the subbasin column. When the station is notated with 0, it means that no static station was performed that day, but the boat was traveling during the sampling.

Station	Subbasin	Volume filtered (L)	Particles dry weight (g)	Initial				Final			
				Date	Time (UTC)	Longitude	Latitude	Date	Time (UTC)	Longitude	Latitude
1	N Atlantic	169.50	0.3626	16/12/10	11:45	-9.564	35.195	16/12/10	21:10	-11.173	34.580
0	N Atlantic	192.00	0.3115	18/12/10	8:50	-15.158	31.823	18/12/10	22:10	-16.600	30.370
4	N Atlantic	165.60	0.3587	20/12/10	10:51	-19.102	28.311	20/12/10	22:13	-20.125	26.452
6	N Atlantic	240.88	0.3154	22/12/10	8:41	-22.247	23.255	22/12/10	21:24	-22.658	22.633
8	N Atlantic	211.11	0.3522	24/12/10	8:55	-24.316	20.260	24/12/10	18:30	-24.974	19.063
10	N Atlantic	345.21	0.6808	26/12/10	8:15	-26.005	14.519	26/12/10	22:08	-25.999	13.660
12	N Atlantic	391.30	0.2067	28/12/10	8:46	-25.994	9.563	28/12/10	21:15	-26.014	8.571
14	N Atlantic	259.26	0.3246	30/12/10	8:35	-26.033	5.012	30/12/10	20:15	-25.998	3.695
16	S Atlantic	277.96	0.4133	01/01/11	9:28	-26.019	0.269	01/01/11	20:05	-26.481	-1.140
18	S Atlantic	237.88	0.3146	03/01/11	9:31	-28.168	-4.780	03/01/11	20:45	-28.709	-5.954
20	S Atlantic	367.50	0.3023	05/01/11	9:00	-30.187	-9.125	05/01/11	18:20	-30.443	-13.443
22	S Atlantic	323.11	0.2686	07/01/11	9:43	-32.378	-13.735	07/01/11	20:40	-32.659	-14.263
24	S Atlantic	272.31	0.2502	09/01/11	9:01	-34.671	-18.399	09/01/11	22:12	-35.114	-19.369
26	S Atlantic	161.56	0.3467	11/01/11	9:45	-36.980	-23.002	11/01/11	20:50	-38.086	-23.374
27	S Atlantic	240.75	0.2512	18/01/11	13:45	-39.661	-23.694	19/01/11	12:28	-37.530	-24.104
28	S Atlantic	317.16	0.2969	19/01/11	14:36	-37.522	-24.105	20/01/11	12:00	-33.485	-24.789
29	S Atlantic	185.79	-	20/01/11	13:00	-33.443	-24.781	20/01/11	21:45	-31.647	-25.155
30	S Atlantic	249.90	0.2746	21/01/11	0:45	-31.070	-25.272	21/01/11	17:45	-30.049	-25.439
34	S Atlantic	170.87	0.3394	24/01/11	15:38	-21.148	-26.999	26/01/11	0:12	-16.224	-27.884
37	S Atlantic	355.70	0.4088	27/01/11	0:45	-10.446	-28.881	28/01/11	16:45	-7.588	-29.374
41	S Atlantic	68.73	0.3001	01/02/11	1:10	2.954	-31.172	01/02/11	19:00	4.913	-31.498
42	S Atlantic	148.18	0.2686	01/02/11	20:45	5.304	-31.555	02/02/11	21:37	8.036	-32.020
43	S Atlantic	147.93	0.401	02/02/11	23:08	8.349	-32.074	04/02/11	2:00	12.440	-32.754
44	S Atlantic	229.95	0.367	04/02/11	2:30	12.520	-32.769	04/02/11	20:00	13.463	-32.919
45	S Atlantic	214.25	0.2988	04/02/11	20:45	13.637	-32.951	05/02/11	18:30	16.751	-33.479
0	Indian	118.67	0.393	12/02/11	7:58	20.976	-35.167	12/02/11	19:50	23.790	-35.099
46	Indian	289.95	0.3184	14/02/11	6:25	27.543	-34.836	14/02/11	18:48	29.637	-34.596
48	Indian	251.18	0.3367	16/02/11	5:30	33.709	-34.176	16/02/11	18:14	35.500	-33.998
50	Indian	358.00	0.3585	18/02/11	5:25	39.880	-33.532	18/02/11	18:14	41.684	-33.369
0	Indian	186.65	0.3491	20/02/11	4:00	54.284	-31.781	20/02/11	17:34	55.536	-31.495
0	Indian	154.38	0.3047	22/02/11	6:00	58.943	-30.852	22/02/11	14:14	61.458	-30.053
53	Indian	213.96	0.3418	25/02/11	3:00	63.247	-27.979	25/02/11	17:00	65.051	-27.899
55	Indian	337.09	0.3422	27/02/11	4:24	69.420	-29.360	27/02/11	16:25	70.811	-29.333
57	Indian	177.53	0.3404	01/03/11	3:03	76.079	-29.904	01/03/11	15:19	77.898	-29.879
59	Indian	226.99	0.3134	03/03/11	3:07	82.624	-29.810	03/03/11	15:22	84.578	-29.777
61	Indian	266.53	0.3278	05/03/11	2:55	89.466	-29.677	05/03/11	16:59	91.679	-29.666
63	Indian	343.13	0.3118	07/03/11	1:36	96.400	-29.579	08/03/11	1:40	99.998	-29.905
65	Indian	216.90	0.2707	09/03/11	2:00	103.311	-30.332	09/03/11	16:05	105.848	-30.635
67	Indian	187.85	0.3392	11/03/11	0:10	110.179	-31.154	11/03/11	13:44	112.038	-31.361
74	Indian	219.69	0.4088	24/03/11	0:25	110.180	-31.154	24/03/11	12:02	137.546	-39.648

PART IV: Supporting information

Station	Subbasin	Volume filtered (L)	Particles dry weight (g)	Initial				Final			
				Date	Time (UTC)	Longitude	Latitude	Date	Time (UTC)	Longitude	Latitude
0	S Pacific	266.09	0.2869	09/04/11	0:30	156.778	-33.911	09/04/11	11:50	159.463	-33.985
80	S Pacific	242.00	0.3548	17/04/11	22:12	177.743	-30.970	18/04/11	8:17	179.143	-28.406
83	S Pacific	222.63	0.2935	21/04/11	19:14	-176.935	-20.602	22/04/11	6:51	-176.364	-19.796
85	S Pacific	256.00	0.3054	23/04/11	20:08	-174.497	-15.889	24/04/11	5:50	-174.102	-15.038
88	S Pacific	269.45	0.309	25/04/11	23:39	-172.736	-11.201	26/04/11	8:25	-172.560	-10.646
92	S Pacific	319.32	0.3518	29/04/11	21:35	-169.462	-3.398	30/04/11	10:32	-168.669	-1.872
95	N Pacific	206.91	0.3427	02/05/11	23:48	-165.403	4.622	03/05/11	9:40	-164.674	6.290
98	N Pacific	242.86	0.3093	05/05/11	22:20	-162.259	11.921	06/05/11	9:40	-161.379	13.758
104	N Pacific	271.17	0.2944	16/05/11	16:00	-150.360	21.066	17/05/11	6:30	-149.556	20.938
106	N Pacific	270.44	0.2942	18/05/11	15:30	-145.208	20.344	19/05/11	4:42	-146.308	20.085
108	N Pacific	207.28	0.2675	20/05/11	15:45	-138.966	19.279	21/05/11	3:11	-138.110	19.079
110	N Pacific	196.26	0.3285	22/05/11	14:55	-133.262	18.053	23/05/11	7:30	-131.486	17.582
112	N Pacific	197.44	0.2908	24/05/11	14:40	-127.569	16.624	25/05/11	4:30	-125.962	16.248
114	N Pacific	300.72	0.2819	26/05/11	14:45	-121.996	15.311	27/05/11	4:37	-120.109	14.845
116	N Pacific	255.68	0.3796	28/05/11	13:30	-115.768	13.771	29/05/11	4:00	-114.664	13.529
118	N Pacific	211.57	0.3135	30/05/11	13:35	-110.393	12.497	31/05/11	3:06	-109.574	12.321
121	N Pacific	283.11	0.3744	02/06/11	12:35	-102.447	10.757	03/06/11	2:10	-100.838	10.428
124	N Pacific	262.15	0.4244	05/06/11	12:50	-93.148	8.760	06/06/11	1:00	-91.917	8.482
126	N Pacific	257.84	0.3702	07/06/11	11:45	-87.960	7.224	08/06/11	1:00	-86.393	6.630
0	N Atlantic	219.00	0.2999	11/06/11	15:15	-78.946	9.779	12/06/11	3:35	-76.588	10.160
129	N Atlantic	224.57	0.3154	22/06/11	10:13	-69.291	15.075	22/06/11	23:36	-68.229	15.325
0	N Atlantic	258.22	0.3278	24/06/11	11:55	-63.363	16.415	25/06/11	1:04	-60.863	17.082
133	N Atlantic	198.50	0.3766	27/06/11	10:20	-55.160	19.020	27/06/11	23:40	-53.689	19.720
136	N Atlantic	244.82	0.3138	30/06/11	9:05	-47.785	21.731	30/06/11	23:40	-45.908	22.374
138	N Atlantic	246.74	0.3178	02/07/11	7:30	-41.908	23.736	02/07/11	22:45	-39.832	24.458
140	N Atlantic	290.41	0.3162	04/07/11	7:35	-35.268	26.111	04/07/11	23:00	-34.037	26.532
142	N Atlantic	251.45	0.2989	06/07/11	6:35	-29.671	27.981	06/07/11	21:43	-28.192	28.455
144	N Atlantic	177.06	0.2584	08/07/11	6:45	-23.691	29.967	08/07/11	21:27	-22.053	30.507
146	N Atlantic	249.09	0.2084	10/07/11	5:43	-17.262	32.083	10/07/11	20:20	-16.101	32.453

**Table S2.** Sampling: Ancillary data for plankton samples . N and S attend respectively for “north” and “south” basins in the subbasin column. \*Southern ocean sampling points are only two and fixed, although they correspond to 13 single samples each. That is the reason why no date or individual dry weight and biomass is indicated here. R and J attend for Raquelias and Johnson, respectively.

Station	Subbasin	Date	Time (UTC)	Longitude	Latitude	Total dry weight (g)	Biomass (g m <sup>-3</sup> )
1	N Atlantic	16/12/10	11:45	-9.530	35.165	1.07	4.73 10 <sup>-3</sup>
3	N Atlantic	19/12/10	8:50	-17.285	29.686	1.11	5.46 10 <sup>-3</sup>
6	N Atlantic	22/12/10	8:41	-22.244	23.256	1.34	7.89 10 <sup>-3</sup>
8	N Atlantic	24/12/10	8:55	-24.304	20.260	1.96	1.45 10 <sup>-2</sup>
10	N Atlantic	26/12/10	8:15	-26.005	14.519	3.48	3.85 10 <sup>-2</sup>
12	N Atlantic	28/12/10	8:46	-25.994	9.564	2.25	1.47 10 <sup>-2</sup>
14	N Atlantic	30/12/10	8:35	-26.033	5.011	3.42	2.08 10 <sup>-2</sup>
16	S Atlantic	01/01/11	9:28	-26.019	0.270	5.42	4.00 10 <sup>-2</sup>
18	S Atlantic	03/01/11	9:31	-28.174	-4.773	1.94	1.04 10 <sup>-2</sup>
20	S Atlantic	05/01/11	9:00	-30.189	-9.110	1.98	6.50 10 <sup>-3</sup>
22	S Atlantic	07/01/11	9:43	-32.378	-13.729	1.57	5.79 10 <sup>-3</sup>
24	S Atlantic	09/01/11	9:01	-34.675	-18.399	3.14	1.23 10 <sup>-2</sup>
26	S Atlantic	11/01/11	9:45	-35.975	-21.090	0.74	2.35 10 <sup>-3</sup>
27	S Atlantic	19/01/11	13:45	-36.223	-24.314	0.28	1.15 10 <sup>-3</sup>
28	S Atlantic	20/01/11	14:36	-33.095	-24.852	0.17	1.15 10 <sup>-3</sup>
29	S Atlantic	21/01/11	13:00	-30.131	-25.400	3.23	2.04 10 <sup>-2</sup>
30	S Atlantic	22/01/11	0:45	-27.589	-25.863	3.11	1.96 10 <sup>-2</sup>
31	S Atlantic	23/01/11	-	-24.243	-26.424	2.10	1.16 10 <sup>-2</sup>
34	S Atlantic	26/01/11	15:38	-14.789	-28.101	1.74	6.40 10 <sup>-3</sup>
37	S Atlantic	30/01/11	0:45	-5.401	-29.687	0.32	1.81 10 <sup>-3</sup>
41	S Atlantic	02/02/11	1:10	6.786	-31.772	3.73	3.00 10 <sup>-2</sup>
42	S Atlantic	03/02/11	20:45	9.417	-32.104	2.19	1.38 10 <sup>-2</sup>
43	S Atlantic	04/02/11	23:08	12.749	-32.791	2.13	1.05 10 <sup>-2</sup>
44	S Atlantic	05/02/11	2:30	15.474	-33.297	0.27	3.93 10 <sup>-3</sup>
45	Indian	13/02/11	-	25.558	-35.139	2.03	2.00 10 <sup>-2</sup>
46	Indian	14/02/11	6:25	27.546	-34.837	4.01	2.15 10 <sup>-2</sup>
48	Indian	16/02/11	5:30	33.724	-34.172	2.32	1.25 10 <sup>-2</sup>
50	Indian	18/02/11	5:25	39.880	-33.532	0.15	9.73 10 <sup>-4</sup>
52	Indian	24/02/11	-	61.458	-30.053	2.21	1.00 10 <sup>-2</sup>
53	Indian	25/02/11	3:00	63.248	-27.976	0.19	8.42 10 <sup>-4</sup>
55	Indian	27/02/11	4:24	69.414	-29.363	0.87	5.51 10 <sup>-3</sup>
57	Indian	01/03/11	3:03	76.086	-29.906	1.80	1.06 10 <sup>-2</sup>
59	Indian	03/03/11	3:07	82.624	-29.810	1.82	1.08 10 <sup>-2</sup>
61	Indian	05/03/11	2:55	89.478	-29.681	0.86	6.32 10 <sup>-3</sup>
63	Indian	07/03/11	1:36	96.395	-29.582	1.71	1.16 10 <sup>-2</sup>
65	Indian	09/03/11	2:00	103.309	-30.333	1.82	1.34 10 <sup>-2</sup>
67	Indian	11/03/11	0:10	110.180	-31.154	3.65	1.79 10 <sup>-2</sup>
74	Indian	24/03/11	0:25	135.224	-39.225	1.00	1.04 10 <sup>-2</sup>

PART IV: Supporting information

Station	Subbasin	Date	Time (UTC)	Longitude	Latitude	Total dry weight (g)	Biomass (g m <sup>-3</sup> )
75	S Pacific	09/04/11	0:30	159.057	-33.976	0.41	7.29 10 <sup>-3</sup>
79	S Pacific	17/04/11	-	176.016	-34.056	1.89	1.12 10 <sup>-2</sup>
83	S Pacific	21/04/11	19:14	-177.417	-21.442	2.40	1.41 10 <sup>-2</sup>
85	S Pacific	23/04/11	20:08	-174.488	-15.903	0.60	3.39 10 <sup>-3</sup>
88	S Pacific	26/04/11	23:39	-172.323	-9.460	0.81	4.54 10 <sup>-3</sup>
92	S Pacific	30/04/11	21:35	-168.357	-1.304	1.47	9.60 10 <sup>-3</sup>
95	S Pacific	03/05/11	23:48	-164.427	6.978	3.24	2.94 10 <sup>-2</sup>
98	N Pacific	06/05/11	22:20	-160.861	15.017	1.43	6.47 10 <sup>-3</sup>
103	N Pacific	16/05/11	16:00	-150.366	21.067	3.36	1.53 10 <sup>-2</sup>
105	N Pacific	18/05/11	15:30	-145.212	20.341	4.41	1.86 10 <sup>-2</sup>
106	N Pacific	19/05/11	-	-141.617	19.902	2.09	9.15 10 <sup>-3</sup>
107	N Pacific	20/05/11	15:45	-138.966	19.279	3.05	1.28 10 <sup>-2</sup>
109	N Pacific	22/05/11	14:55	-133.262	18.057	3.35	1.58 10 <sup>-2</sup>
111	N Pacific	24/05/11	14:40	-127.627	16.617	4.04	1.91 10 <sup>-2</sup>
113	N Pacific	26/05/11	14:45	-121.995	15.311	4.46	1.95 10 <sup>-2</sup>
115	N Pacific	28/05/11	13:30	-115.775	13.760	5.76	3.08 10 <sup>-2</sup>
116	N Pacific	29/05/11	-	-113.270	13.195	3.22	1.52 10 <sup>-2</sup>
117	N Pacific	30/05/11	13:35	-110.392	12.493	2.27	9.25 10 <sup>-3</sup>
118	N Pacific	31/05/11	-	-108.046	11.992	4.23	3.11 10 <sup>-2</sup>
120	N Pacific	02/06/11	12:35	-102.448	10.757	2.23	1.58 10 <sup>-2</sup>
123	N Pacific	05/06/11	12:50	-93.148	8.764	4.41	3.47 10 <sup>-2</sup>
125	N Pacific	07/06/11	11:45	-87.947	7.221	4.61	3.88 10 <sup>-2</sup>
129	N Atlantic	22/06/11	10:13	-69.289	15.073	3.43	1.68 10 <sup>-2</sup>
131	N Atlantic	25/06/11	-	-59.829	17.428	4.07	2.18 10 <sup>-2</sup>
133	N Atlantic	27/06/11	10:20	-55.160	19.020	1.60	5.90 10 <sup>-3</sup>
136	N Atlantic	28/06/11	-	-52.629	20.013	1.79	6.81 10 <sup>-3</sup>
136	N Atlantic	30/06/11	9:05	-47.790	21.742	1.02	4.02 10 <sup>-3</sup>
138	N Atlantic	02/07/11	7:30	-41.912	23.736	1.24	7.80 10 <sup>-3</sup>
140	N Atlantic	04/07/11	7:35	-35.274	26.111	0.16	8.79 10 <sup>-4</sup>
142	N Atlantic	06/07/11	6:35	-29.673	27.983	0.46	2.71 10 <sup>-3</sup>
144	N Atlantic	08/07/11	6:45	-23.693	29.966	1.75	7.95 10 <sup>-3</sup>
146	N Atlantic	10/07/11	5:43	-17.260	32.088	1.26	6.78 10 <sup>-3</sup>
R	Southern*			-60.388	-62.657		
J	Southern*			-60.369	-62.659		

**Text S1. Materials and Methods**Particulate samples

Filters containing the particulate samples were freeze dried, weighted and soxhlet extracted overnight with DCIM/MeOH (2:1). The extract was concentrated on a rotary evaporator system and solvent changed to isooctane. Then, samples were further purified and fractionated over an alumina column (3 g, 3% deactivated alumina (with 90  $\mu$ L of chromatographical grade water) with a 1 cm sulfate top layer, packed with Hx). Fractioning was set with 6 mL Hx for the the first fraction of alifatic compounds, 12 mL Hx/DCIM (3:1) for the second fraction containing the aromatic compounds, 35 mL DCIM for organophosphate esters on a third fraction, and a last fraction of 15 mL DCIM/MeOH (2:1) for other products. Fractions 1, 2 and 3 were reduced under a gentle nitrogen stream and solvent changed to isooctane down to 100  $\mu$ L.

Plankton samples

Plankton filters were freeze dried, weighted and soxhlet extracted overnight with DCIM/Hex (1:1). Plankton samples were purified and fractionated over a combined silica and alumina column (top 1 cm sulphate, intermediate 5 g muffled neutral silica, and bottom 3 g, 3% deactivated alumina, packed with Hx). Fractioning was set with 25 mL Hex for the the first fraction of alifatic compounds, 40 mL Hex/DCIM (3:1) for the second fraction containing the aromatic compounds, 20 mL DCIM/Acetone (70:30) for organophosphate esters on a third fraction and a last fraction of 25 mL DCIM/MeOH (2:1) for other polar compounds. Fractions 1, 2 and 3 were reduced under a gentle nitrogen stream and solvent changed to isooctane down to 100  $\mu$ L.

**Table S3.** Blanks (total pg per sample) and surrogate recoveries (%) for particulate phase samples (All samples have been surrogate recovery corrected by Perylene D12).

	Mean laboratory blank ( <i>n</i> =7)	Mean field blank ( <i>n</i> =4)		Surrogate recovery ( <i>n</i> =69)
Naphthalene	0.154	0.165		
Dimethylnaphthalenes	0.057	0.053		
Methylnaphthalenes	0.000	0.000		
Acenaphthylene	0.038	0.045		
Acenaphthene	0.112	0.242		
Fluorene	0.095	0.295		
Dibenzothiophene	0.049	0.098		
Methyldibenzothiophenes	0.174	0.341		
Dimethyldibenzothiophenes	0.214	0.356		
Phenanthrene	0.433	1.016		
Methylphenanthrenes	0.303	0.345		
Dimethylphenanthrenes	0.222	0.248		
Anthracene	0.047	0.049		
Fluoranthene	0.336	0.370		
Pyrene	0.130	0.173		
Methylpyrene	0.051	0.068		
Dimethylpyrene	0.000	0.085		
Benzo[ <i>ghi</i> ]fluoranthene	0.069	0.070		
Benzo[ <i>a</i> ]anthracene	0.134	0.201		
Chrysene	0.069	0.079		
Methylchrysenes	0.000	0.056		
Benzo[ <i>b+k</i> ]fluoranthenes	0.164	0.165		
Benzo[ <i>e</i> ]pyrene	0.076	0.096		
Benzo[ <i>a</i> ]pyrene	0.011	0.080		
Perylene	0.097	0.101	Perylene D12	76.2
Indeno[1,2,3- <i>cd</i> ]pyrene	0.045	0.095		
Dibenzo[ <i>a,h</i> ]anthracene	0.062	0.089		
Benzo[ <i>ghi</i> ]perylene	0.058	0.095		



**Table S4.** Blanks (total pg per sample), breakthroughs and surrogate recoveries (%) for plankton samples. All samples have been surrogate recovery corrected by the indicated deuterated standard. Tropical oceans samples attend for the Malaspina 2010 campaign. Southern ocean attends for samples from the campaign at the Livingston Island, Antarctica, in 2014-2015 Antarctic summer.

	Mean laboratory blank (pg) (n=7)	Mean 1 <sup>st</sup> Breakthrough extraction (%) (n=5)	Mean field blank (pg)		Surrogate recovery (%)	
			Tropical oceans (n=4)	Southern ocean (n=5)	Tropical oceans (n=71)	Southern ocean (n= 26)
Naphthalene	0.006	81	0.19			
Methylnaphthalenes	0.027	85	0.84			
Dimethylnaphthalenes	0.012	96	0.94			
Acenaphthylene	0.0	91	0.03	0.002	<b>Acenaphthene D<sub>10</sub></b>	
Acenaphthene	0.013	99	0.42	0.047	25	52
Fluorene	0.004	92	0.069	0.028		
Dibenzothiophene	0.0	100	0.0			
Methyldibenzothiophenes	0.002	88	0.0	0.005		
Dimethyldibenzothiophenes	0.0	94	0.0	0.022	<b>Phenanthrene D<sub>10</sub></b>	
Phenanthrene	0.015	97	0.26	0.11	42	58
Methylphenanthrenes	0.004	97	0.20	0.013		
Dimethylphenanthrenes	0.007	99	0.0	0.007		
Anthracene	0.0	86	0.067	0.0		
Fluoranthene	0.036	97	0.13	0.015		
Pyrene	0.026	96	0.28	0.018		
Methylpyrenes	0.0	100	0.0	0.025		
Dimethylpyrenes	0.0	100	0.0	0.0		
Benzo[ghi]fluoranthene	0.0	100	0.037	0.0		
Benzo[a]anthracene	0.11	96	0.12	0.099	<b>Chrysene D<sub>12</sub></b>	
Chrysene	0.021	95	0.015	0.002	70	68
Methylchrysenes	0.0	100	0.0	0.49		
Benzo[b+k]fluoranthenes	0.12	94	0.0	0.054		
Benzo[e]pyrene	0.0	93	0.078	0.008		
Benzo[a]pyrene	0.0	100	0.0			
Perylene	0.0	100	0.0	0.027	<b>Perylene D<sub>12</sub></b>	
Indeno[1,2,3-cd]pyrene	0.071	100	0.0	0.0	102	82
Dibenzo[a,h]anthracene	0.28	100	0.0	0.0		
Benzo[ghi]perylene	0.15	100	0.0	0.0		

**Table S5.** Particulate organic carbon (POC,  $\mu\text{M}$ ) at surface (3 m depth). Averaged values between subsequent stations have been used when an intermediate value has been missing for the normalization calculations.

Station	POC	Station	POC
1	1.9	61	0.9
3	1.7	63	1.1
4	1.6	65	4.4
6	1.7	67	2.3
8	1.7	74	2.4
10	2.2	0	-
12	2.3	80	2.2
14	2.4	83	3.7
16	2.0	85	2.7
18	2.3	88	1.7
20	2.3	92	1.4
22	1.5	95	2.0
24	2.2	98	1.4
26	2.5	103	4.6
27	2.5	105	1.6
28	2.5	107	2.7
29	1.5	109	2.4
30	2.0	111	1.4
34	3.4	113	1.3
37	1.8	115	2.5
41	1.8	117	1.9
42	1.7	120	2.3
43	3.3	123	4.9
44	4.3	125	9.3
45	6.1	129	2.3
46	2.2	131	2.3
48	1.6	133	1.7
50	1.4	134	1.9-
51	1.3	136	2.0
52	1.2	138	1.6
53	2.4	140	1.7
55	0.9	142	1.3
57	0.9	144	1.8
59	1.0	146	4.5

**Table S6.** Carbon, Nitrogen and estimated trophic position for plankton samples. \* Biomass values represent the total biomass of plankton as the sum of values for all size-classes between 40 and 5000  $\mu\text{m}$ .  $\delta^{15}\text{N}$  and  $\delta^{13}\text{C}$  values are biomass-weighted average values for all size classes. Trophic position attends for the estimated TP of the plankton fraction 500-1000  $\mu\text{m}$  calculated by  $(\delta^{15}\text{N}_{500-1000} - \delta^{15}\text{N}_{40-200}/3.4)+1.5$ .

Station	N biomass ( $\text{mg N m}^{-3}$ )	C biomass ( $\text{mg C m}^{-3}$ )	C:N (molar)	$\delta^{15}\text{N}$ (‰)	$\delta^{13}\text{C}$ (‰)	Trophic position*
10	1.56	6.43	4.81	4.95	-19.57	1.58
29	2.78	11.66	4.88	1.92	-19.77	
35	1.09	4.30	4.60	5.87	-21.43	1.29
39	2.07	9.86	5.56	8.42	-18.34	1.57
45	2.77	10.89	4.58	6.55	-19.07	1.43
46	2.13	8.46	4.64	4.92	-20.09	1.70
48	1.11	5.65	5.94	4.38	-21.78	1.80
50	0.50	2.46	5.81	4.85	-17.75	1.41
52	1.90	7.19	4.43	4.68	-20.86	1.17
53	2.32	9.09	4.57	3.75	-20.87	1.27
55	1.47	5.50	4.37	4.76	-20.96	1.24
57	1.71	6.64	4.54	5.59	-21.08	1.46
59	1.07	4.39	4.78	8.86	-21.24	1.43
61	1.88	7.42	4.60	6.59	-20.93	1.55
63	1.54	6.14	4.64	8.19	-21.30	1.21
65	1.88	6.96	4.32	3.53	-22.29	1.20
67	1.40	5.86	4.88	3.92	-20.54	1.89
74	2.24	8.72	4.54	12.61	-20.30	1.64
79	1.96	7.13	4.25	6.88	-20.69	1.31
83	1.98	8.05	4.76	1.68	-19.88	1.66
85	1.29	5.11	4.61	2.27	-19.08	1.44
88	1.65	6.13	4.33	12.65	-19.33	1.72
92	2.13	8.10	4.44	3.57	-19.42	1.57
95	7.36	27.90	4.43	6.26	-19.83	1.70
98	0.86	3.86	5.25	8.11	-19.48	1.88
103	2.08	7.84	4.40	8.12	-20.36	1.42
105	2.04	8.07	4.61	4.45	-20.36	1.60
106	1.39	5.39	4.52	7.92	-20.81	1.45
107	1.79	6.88	4.49	8.76	-20.92	1.52
109	2.47	9.60	4.54	8.16	-20.40	1.65
111	2.56	10.21	4.65	10.25	-20.80	1.91
113	2.43	9.37	4.50	10.48	-20.91	1.68
115	3.13	12.09	4.51	10.38	-21.01	1.45
116	2.03	8.33	4.79	8.68	-21.76	2.12
117	2.30	9.18	4.66	9.68	-20.62	1.50
118	2.50	9.76	4.56	10.43	-20.59	1.76
120	3.54	15.30	5.05	9.49	-19.32	1.50
123	5.42	20.02	4.31	6.75	-21.45	1.63
125	6.28	24.29	4.51	5.10	-21.34	1.80
129	3.10	12.14	4.57	1.11	-18.50	1.73
131	1.38	5.40	4.58	1.87	-18.97	1.66
133	1.70	6.73	4.61	0.39	-19.25	1.49
134	1.99	7.97	4.67	0.30	-18.52	1.56
136	1.56	6.18	4.63	0.69	-19.36	1.32
138	1.48	6.21	4.90	1.04	-19.24	1.77
140	1.12	4.72	4.94	1.52	-20.41	1.64
142	1.08	4.16	4.51	2.59	-21.33	1.44
144	1.92	7.40	4.49	3.36	-21.44	1.66
145	1.97	7.72	4.58	3.21	-21.76	1.70

**Table S7.** Organic carbon export from the surface mixed layer due to phytoplankton ( $F_{OC-Phyto}$ ), zooplankton pellets ( $F_{OC-Fecal}$ ) and total fluxes ( $F_{OC}$ ) ( $\text{mgC m}^{-2}\text{day}^{-1}$ )

Station	$F_{OCPhyto}$	$F_{OCFecal}$	$F_{OC}$	Station	$F_{OCPhyto}$	$F_{OCFecal}$	$F_{OC}$
1	5.92	26.61	32.53	65	0.34	21.71	22.05
3	2.96	29.67	32.63	67	0.98	39.81	40.79
6	5.36	43.10	48.45	74	8.15	49.69	57.83
8	6.66	53.92	60.58	4b1	6.29	52.28	58.56
10	10.97	79.32	90.29	79	2.36	37.35	39.71
12	8.59	53.54	62.14	83	2.31	41.33	43.65
14	13.67	68.05	81.72	85	1.00	38.23	39.23
16	7.82	60.17	67.99	88	0.49	39.62	40.11
18	1.18	55.16	56.35	92	10.59	97.14	107.73
20	0.21	35.79	36.00	95	7.46	69.10	76.56
22	0.15	30.60	30.75	98	0.62	33.67	34.30
24	0.49	43.92	44.41	103	0.54	40.18	40.72
25	0.75	43.42	44.16	105	0.36	38.43	38.79
27	0.43	42.07	42.50	106	0.53	37.63	38.17
28	0.38	35.40	35.78	107	0.39	36.94	37.33
29	0.47	34.28	34.75	109	0.30	32.96	33.26
30	0.53	34.63	35.16	111	0.46	33.09	33.55
31	0.24	27.45	27.69	113	1.75	44.82	46.57
34	0.10	21.18	21.28	115	2.02	51.62	53.64
37	0.05	19.25	19.30	116	2.91	52.96	55.87
41	0.21	24.16	24.36	117	3.56	56.49	60.04
42	0.31	25.52	25.82	118	3.95	55.09	59.04
43	0.79	31.31	32.10	120	3.53	48.01	51.54
44	2.43	41.23	43.65	123	33.00	127.11	160.11
45	54.30	198.96	253.26	125	21.84	93.34	115.18
46	4.19	51.01	55.20	129	4.77	48.64	53.41
48	1.17	41.44	42.61	131	3.34	46.50	49.84
50	0.60	38.37	38.97	133	0.74	24.20	24.94
52	0.25	20.81	21.06	134	0.37	20.85	21.22
53	0.87	31.25	32.13	136	0.15	16.35	16.50
55	0.21	19.01	19.22	138	0.24	14.19	14.43
57	0.18	16.96	17.14	140	0.14	12.17	12.31
59	0.15	16.07	16.22	142	0.21	15.32	15.53
61	0.18	18.28	18.45	144	0.26	16.58	16.84
63	0.19	15.44	15.63	146	0.64	28.07	28.71

Table S8. Particulate phase average PAHs concentrations per oceanic subbasin (ng gdw<sup>-1</sup>)

	ng g <sup>-1</sup>	Naphthalene	Dimethyl naphthalene	Methyl naphthalene	Trimethyl naphthalene	Acenaphthylene	Acenaphthene	Fluorene	Dibenzo thioaphene	Methyl dibenzothioaphene	Dimethyl dibenzothioaphene	Phenanthrene	Methyl phenanthrenes	Dimethyl phenanthrenes	Anthracene	Fluoranthene	Pyrene	Methylpyrenes	Dimethylpyrenes	Benzo[ghi]fluoranthene	Benzo[a]anthracene	Chrysene	Methylchrysenes	Benzo[b]kfluoranthene	Benzo[e]pyrene	Benzo[a]pyrene	Perylene	Indeno[1,2,3-cd]pyrene	Dibenzo[a,h]anthracene	Benzo[ghi]perylene	Σ <sub>16</sub> PAHs
<b>North Atlantic</b>	median	1.1	0.42	n.d.	n.d.	0.32	1.6	1.8	3.1	17	20	11	16	13	0.73	3.4	3.6	0.27	0.99	0.66	1.1	0.89	0.87	2.0	1.1	0.90	1.0	1.3	0.49	1.5	140
	mean	23	20	n.d.	n.d.	0.37	1.8	2.1	3.1	24	46	15	22	20	1.0	4.2	6.0	0.34	1.3	1.6	1.1	0.90	1.8	2.3	1.5	0.92	1.0	2.2	0.52	1.5	210
	min	0.13	0.06	n.d.	n.d.	n.d.	0.52	0.84	0.37	1.3	1.6	3.1	2.2	1.7	0.19	1.9	2.2	0.15	0.53	n.d.	n.d.	0.48	0.23	0.70	0.53	0.30	n.d.	0.34	n.d.	0.30	30
	max	200	190	n.d.	n.d.	0.75	4.6	5.1	8.9	93	200	39	71	64	31	8.2	16	0.75	3.5	10	2.0	1.4	12	7.2	4.5	2.0	2.8	8.6	0.95	3.4	520
	SD	55	51	n.d.	n.d.	0.18	1.1	1.2	2.6	27	61	12	20	19	0.78	2.1	4.2	0.20	0.84	2.8	0.45	0.27	2.8	1.5	1.0	0.43	0.63	2.3	0.22	0.93	150
<b>South Atlantic</b>	median	1.6	0.28	n.d.	n.d.	0.43	1.4	2.1	0.60	1.8	2.7	4.3	4.7	5.3	0.69	2.3	2.7	0.26	0.67	0.51	0.99	0.70	0.56	1.9	1.3	1.1	0.83	0.69	0.57	1.3	55
	mean	3.4	2.5	n.d.	n.d.	0.85	4.0	9.3	1.6	5.8	7.3	6.4	5.4	6.1	0.95	2.5	2.8	0.66	2.2	1.7	0.95	0.61	0.82	2.2	1.6	1.1	1.4	1.6	0.60	1.6	76
	min	0.08	0.06	n.d.	n.d.	0.18	0.44	0.14	0.20	0.55	0.32	0.12	1.6	0.51	0.19	0.71	1.3	0.16	0.10	0.29	0.68	0.30	0.31	0.94	0.64	0.28	0.33	0.36	0.24	0.25	7.8
	max	15	38	n.d.	n.d.	6.5	11	120	12	39	42	23	16	15	4.2	5.3	6.2	6.9	2.4	19	2.3	1.6	4.1	4.9	5.1	2.9	10.3	6.8	1.9	4.8	410
	SD	4.2	9.0	n.d.	n.d.	1.5	3.8	28	3.1	11	12	5.6	3.7	4.2	0.93	1.4	1.5	1.6	5.6	4.6	0.73	0.49	0.99	1.1	1.2	0.67	2.3	1.8	0.41	1.4	89
<b>Indian</b>	median	3.0	3.9	n.d.	n.d.	0.69	1.9	3.6	5.2	16	15	12	13	9.6	2.1	2.5	5.1	0.20	0.92	0.46	1.3	1.1	0.54	3.0	0.76	1.8	1.4	2.5	0.41	2.4	190
	mean	46	99	n.d.	n.d.	6.3	19	25	54.3	75	73	40	49	49	10	18	14	7.8	7.2	14	10	4.9	22	13	12	8.2	5.2	4.3	13	720	
	min	0.26	0.14	n.d.	n.d.	0.14	0.40	0.84	0.33	1.1	2.1	1.0	1.7	1.3	0.34	1.5	1.0	0.14	0.43	0.24	0.52	0.30	0.44	1.1	0.41	0.47	0.54	0.71	0.27	0.48	26
	max	470	860	n.d.	n.d.	49	170	190	380	670	640	350	400	260	64	230	190	170	42	33	110	94	36	270	180	150	95	43	56	170	4700
	SD	120	230	n.d.	n.d.	13	44	48	110	170	160	89	100	79	18	58	49	43	13	12	30	24	11	70	46	39	24	11	14	42	1200
<b>South Pacific</b>	median	0.41	0.63	n.d.	n.d.	0.29	0.53	2.4	3.2	13	16	16	7.1	4.8	0.49	2.6	2.7	0.16	0.79	0.36	0.81	0.51	0.60	3.3	1.4	0.53	1.1	1.9	0.58	2.3	83
	mean	0.41	0.80	n.d.	n.d.	0.33	0.65	2.4	3.8	23	38	17	14	12	1.4	3.0	3.8	0.17	0.95	0.38	0.82	0.61	0.65	3.4	1.3	0.54	0.99	2.0	0.56	2.1	140
	min	0.09	0.51	n.d.	n.d.	0.18	0.28	1.4	0.42	1.4	2.9	3.6	3.2	2.0	0.37	2.0	1.9	0.14	0.53	0.32	0.62	0.39	0.44	1.1	0.49	0.36	0.53	1.1	0.28	0.35	40
	max	0.68	1.3	n.d.	n.d.	0.56	1.4	4.0	9.4	73	140	38	48	43	5.9	5.2	10	0.22	1.9	0.43	1.0	0.24	0.21	6.2	2.2	0.82	1.3	2.8	0.83	4.0	400
	SD	0.21	0.36	n.d.	n.d.	0.16	0.40	0.95	3.5	27	53	13	17	16	2.2	1.1	3.1	0.03	0.50	0.04	0.15	0.20	0.21	2.2	0.70	0.17	0.33	0.68	0.26	1.5	140
<b>North Pacific</b>	median	0.37	0.28	n.d.	n.d.	0.21	0.45	1.6	3.2	21	31	18	21	17	0.69	3.0	2.7	0.15	1.2	0.50	0.79	0.58	0.56	1.5	0.66	0.55	1.1	1.2	0.39	1.4	140
	mean	0.59	0.53	n.d.	n.d.	0.24	0.58	1.8	3.7	25	45	16	19	17	4.1	3.5	4.9	0.17	1.9	0.51	0.74	0.57	0.90	1.9	0.72	0.60	1.2	1.4	0.39	1.6	150
	min	0.02	n.d.	n.d.	n.d.	n.d.	n.d.	0.38	0.26	0.79	1.2	1.4	2.3	0.74	0.25	0.94	0.15	n.d.	0.46	0.29	0.29	0.26	0.32	0.30	n.d.	0.35	0.56	0.64	n.d.	0.37	25
	max	3.1	2.6	n.d.	n.d.	0.43	1.4	4.4	11	61	120	40	44	55	37	7.4	15	0.53	7.0	1.0	1.0	0.91	3.1	7.0	1.4	1.1	2.3	2.2	0.85	3.9	330
	SD	0.86	0.72	n.d.	n.d.	0.13	0.45	1.3	3.6	22	43	12	15	17	11	1.9	4.6	0.14	2.1	0.22	0.19	0.19	0.78	1.8	0.37	0.19	0.51	0.59	0.30	1.1	100

**Table S9.** Particulate phase average PAHs concentrations per oceanic subbasin (ng gC<sup>-1</sup>)

<b>North Atlantic</b>	mea	50	18	n.d.	n.d.	22	95	96	140	850	890	730	970	560	34	200	240	14	64	43	65	50	50	110	60	52	56	69	29	76	8100		
	an	1700	1600	n.d.	n.d.	24	110	120	170	1100	2000	760	1100	940	62	220	290	20	69	59	67	53	74	120	73	52	54	120	31	87	11000		
	n	2.5	3.0	n.d.	n.d.	n.d.	14.0	24	26	91	100	150	190	170	20	120	110	6.0	29	n.d.	n.d.	20	19	37	28	16	n.d.	21	n.d.	16	2400		
	max	1300	1200	0	n.d.	71	300	440	560	4500	9000	2500	3800	3200	230	530	690	55	160	270	110	95	250	230	170	92	87	380	63	250	28000		
	SD	4000	3700	n.d.	n.d.	16	76	92	140	1200	2600	600	1000	890	54	98	160	14	35	70	32	23	69	59	39	22	24	110	18	67	8300		
	mea	90	12	n.d.	n.d.	22	130	100	27	77	120	200	210	170	34	84	92	11	28	20	36	22	21	91	51	39	32	36	21	45	2200		
	an	200	220	n.d.	n.d.	57	210	730	100	340	420	350	240	310	53	120	130	48	160	130	42	27	40	130	86	56	9	n.d.	87	32	87	4500	
	n	2.4	1.8	n.d.	n.d.	6.1	22	16	n.d.	24	40	24	n.d.	96	14	n.d.	n.d.	16	n.d.	n.d.	n.d.	n.d.	n.d.	30	n.d.	9.4	n.d.	n.d.	n.d.	13	1100		
	max	1300	3400	n.d.	n.d.	590	900	1100	1100	3500	3800	2000	710	1400	380	320	350	620	2100	1800	140	99	260	330	460	180	930	430	170	350	37000		
	SD	330	820	n.d.	n.d.	140	240	2500	260	850	910	480	170	330	85	84	90	150	510	420	37	25	61	100	100	43	220	20	39	94	8400		
<b>South Atlantic</b>	mea	290	370	n.d.	n.d.	66	160	260	360	1500	810	820	850	790	170	180	200	14	66	38	91	87	35	200	54	130	130	180	28	170	15000		
	an	4900	7200	n.d.	n.d.	420	1100	1700	5000	4700	4600	2400	3100	4200	1100	840	1100	2100	680	670	860	560	470	1100	630	610	420	300	210	620	52000		
	n	6.1	18	n.d.	n.d.	5.1	n.d.	50	22	74	140	140	n.d.	n.d.	13	n.d.	n.d.	n.d.	n.d.	n.d.	n.d.	n.d.	n.d.	26	n.d.	12	n.d.	27	n.d.	1700			
	max	5700	4800	0	n.d.	2200	7000	7700	4600	2800	2600	1400	1600	2400	7700	9300	7900	2800	0	4500	4200	4700	3900	4900	1100	7400	6400	3900	1800	2300	6800	21000	
	SD	1500	1300	0	n.d.	720	2000	2300	1200	7700	7300	4300	4800	7000	2200	2400	2100	7200	1200	1300	1400	1000	1300	2800	1900	1600	1600	1000	420	580	1700	70000	
	mea	14	37	n.d.	n.d.	14	32	120	200	650	780	870	370	280	27	140	160	8.7	35	18	34	22	28	140	49	24	43	85	22	85	4200		
	an	18	40	n.d.	n.d.	18	30	120	1100	1700	860	640	500	56	130	170	7.8	39	18	38	25	31	180	62	25	43	84	84	22	76	6200		
	n	6.2	21	n.d.	n.d.	5.5	17	86	28	110	200	170	110	19	93	98	4.3	33	13	26	19	16	85	27	15	29	68	17	19	2300			
	max	37	65	n.d.	n.d.	31	47	160	340	2200	4200	1300	1400	1300	180	160	300	10	56	24	50	35	59	34	120	35	57	110	29	150	12000		
	SD	12	16	n.d.	n.d.	12	15	30	120	880	1700	420	520	490	68	24	84	2.8	9.4	4.9	11	6.5	16	100	36	8.0	11	17	4.9	53	4000		
<b>North Pacific</b>	mea	16	17	n.d.	n.d.	13	27	65	83	500	650	500	50	330	35	130	120	11	65	30	39	27	36	88	38	31	53	74	22	51	5800		
	an	32	18	n.d.	n.d.	14	31	89	210	1400	2500	860	960	910	230	180	260	10	84	28	41	31	39	110	37	31	61	79	21	72	8300		
	n	1.4	n.d.	n.d.	n.d.	n.d.	n.d.	23	15	47	71	88	140	44	11	56	8.8	n.d.	24	4.2	10	8.1	19	n.d.	10	22	8.3	n.d.	26	1800			
	max	180	35	n.d.	n.d.	30	84	260	750	4700	8300	2400	2600	3300	2200	440	900	31	260	62	69	54	78	480	58	54	140	160	44	140	23000		
	SD	51	9.9	n.d.	n.d.	8.3	24	74	250	1600	3000	800	900	1100	660	130	290	9.0	74	16	21	16	19	130	20	12	33	46	15	42	7500		
	<b>Indian</b>	mea	14	37	n.d.	n.d.	14	32	120	200	650	780	870	370	280	27	140	160	8.7	35	18	34	22	28	140	49	24	43	85	22	85	4200	
		an	18	40	n.d.	n.d.	18	30	120	1100	1700	860	640	500	56	130	170	7.8	39	18	38	25	31	180	62	25	43	84	84	22	76	6200	
		n	6.1	18	n.d.	n.d.	5.1	n.d.	50	22	74	140	140	n.d.	n.d.	13	n.d.	n.d.	n.d.	n.d.	n.d.	n.d.	n.d.	n.d.	26	n.d.	12	n.d.	27	n.d.	1700		
		max	5700	4800	0	n.d.	2200	7000	7700	4600	2800	2600	1400	1600	2400	7700	9300	7900	2800	0	4500	4200	4700	3900	4900	1100	7400	6400	3900	1800	2300	6800	21000
		SD	1500	1300	0	n.d.	720	2000	2300	1200	7700	7300	4300	4800	7000	2200	2400	2100	7200	1200	1300	1400	1000	1300	2800	1900	1600	1600	1000	420	580	1700	70000
<b>South Atlantic</b>		mea	14	37	n.d.	n.d.	14	32	120	200	650	780	870	370	280	27	140	160	8.7	35	18	34	22	28	140	49	24	43	85	22	85	4200	
		an	18	40	n.d.	n.d.	18	30	120	1100	1700	860	640	500	56	130	170	7.8	39	18	38	25	31	180	62	25	43	84	84	22	76	6200	
		n	6.2	21	n.d.	n.d.	5.5	17	86	28	110	200	170	110	19	93	98	4.3	33	13	26	19	16	85	27	15	29	68	17	19	2300		
		max	37	65	n.d.	n.d.	31	47	160	340	2200	4200	1300	1400	1300	180	160	300	10	56	24	50	35	59	34	120	35	57	110	29	150	12000	
		SD	12	16	n.d.	n.d.	12	15	30	120	880	1700	420	520	490	68	24	84	2.8	9.4	4.9	11	6.5	16	100	36	8.0	11	17	4.9	53	4000	
	<b>North Atlantic</b>	mea	16	17	n.d.	n.d.	13	27	65	83	500	650	500	50	330	35	130	120	11	65	30	39	27	36	88	38	31	53	74	22	51	5800	
		an	32	18	n.d.	n.d.	14	31	89	210	1400	2500	860	960	910	230	180	260	10	84	28	41	31	39	110	37	31	61	79	21	72	8300	
		n	1.4	n.d.	n.d.	n.d.	n.d.	n.d.	23	15	47	71	88	140	44	11	56	8.8	n.d.	24	4.2	10	8.1	19	n.d.	10	22	8.3	n.d.	26	1800		
		max	180	35	n.d.	n.d.	30	84	260	750	4700	8300	2400	2600	3300	2200	440	900	31	260	62	69	54	78	480	58	54	140	160	44	140	23000	
		SD	51	9.9	n.d.	n.d.	8.3	24	74	250	1600	3000	800	900	1100	660	130	290	9.0	74	16	21	16	19	130	20	12	33	46	15	42	7500	
<b>Indian</b>		mea	14	37	n.d.	n.d.	14	32	120	200	650	780	870	370	280	27	140	160	8.7	35	18	34	22	28	140	49	24	43	85	22	85	4200	
		an	18	40	n.d.	n.d.	18	30	120	1100	1700	860	640	500	56	130	170	7.8	39	18	38	25	31	180	62	25	43	84	84	22	76	6200	
		n	6.1	18	n.d.	n.d.	5.1	n.d.	50	22	74	140	140	n.d.	n.d.	13	n.d.	n.d.	n.d.	n.d.	n.d.	n.d.	n.d.	n.d.	26	n.d.	12	n.d.	27	n.d.	1700		
		max	5700	4800	0	n.d.	2200	7000	7700	4600	2800	2600	1400	1600	2400	7700	9300	7900	2800	0	4500	4200	4700	3900	4900	1100	7400	6400	3900	1800	2300	6800	21000
		SD	1500	1300	0	n.d.	720	2000	2300	1200	7700	7300	4300	4800	7000	2200	2400	2100	7200	1200	1300	1400	1000	1300	2800	190							

Table S10. Plankton phase measured PAHs concentrations (ng gdw<sup>-1</sup>)

	ng/gdw	Naphthalene	Dimethyl naphthalene	Methyl naphthalene	Trimethyl naphthalene	Acenaphthylene	Acenaphthene	Fluorene	Dibenzo thiophene	Methyl dibenzothioophene	Dimethyl dibenzothioophene	Phenanthrene	Methyl phenanthrenes	Dimethyl phenanthrenes	Anthracene	Fluoranthene	Pyrene	Methylpyrenes	Dimethylpyrenes	Benzol[ghi]perylene	Benzol[ghi]fluoranthene	Benzol[b+k]fluoranthene	Benzol[e]pyrene	Benzol[a]pyrene	Perylene	Indeno[1,2,3-cd]pyrene	Dibenzol[a,h]anthracene	Benzol[ghi]perylene	Σ <sub>6</sub> PAHs					
North Atlantic	median	2.4	6.8	3.2	1.4	0.41	10	3.4	n.d.	0.80	0.87	7.9	9.3	14	0.70	8.0	5.9	0.33	0.60	0.14	0.55	1.4	0.80	4.1	0.71	0.27	0.25	0.22	0.27	0.35	180			
	mean	6.2	15	13	4.6	5.7	21	11	0.44	6.7	9.0	30	43	28	6.1	13	7.5	1.2	2.4	0.41	5.2	6.7	2.2	6.3	2.7	0.84	0.63	0.99	0.46	1.4	250			
	min	0.18	0.15	0.29	0.09	0.12	2.2	1.0	0.03	0.08	0.03	2.2	1.2	1.3	0.18	0.96	0.39	0.18	0.19	0.11	0.17	0.22	0.24	0.86	0.23	0.17	0.13	0.18	0.17	0.05	18			
	max	35	65	87	20	51	140	50	3.8	33	77	120	260	190	69	51	41	9.7	19	1.8	51	52	13	30	9.8	4.1	2.6	4.9	2.0	6.5	790			
	SD	9.2	19	22	7.0	13	34	14	1.0	11	19	39	68	46	17	14	10	2.3	5.0	0.51	12	13	3.3	1.2	0.76	1.7	0.56	2.1	230					
South Atlantic	median	2.2	8.3	4.2	1.7	0.22	5.7	2.4	0.27	1.3	1.8	7.3	7.7	7.0	0.72	8.6	3.8	1.3	1.4	0.47	1.6	2.1	1.7	3.6	1.9	0.77	0.44	0.46	0.47	1.4	88			
	mean	30	27	33	23	0.69	21	11	0.85	4.4	11	18	17	31	1.7	9.3	6.2	2.3	4.9	0.81	2.3	3.5	3.9	5.4	2.7	1.6	0.85	1.6	0.89	2.2	280			
	min	0.15	0.98	0.22	0.15	0.08	0.99	0.61	0.08	0.03	0.02	0.98	0.88	1.1	0.12	0.77	0.21	0.09	0.25	0.05	0.11	0.20	0.22	0.63	0.21	0.12	0.10	0.09	0.13	0.15	13			
	max	180	140	180	140	3.9	120	91	8.6	40	110	120	94	280	7.6	32	23	15	44	2.3	16	15	21	20	11	9.7	2.8	12	3.5	8.7	1300			
	SD	5.7	39	56	44	1.1	35	22	2.0	9.7	27	28	23	68	1.9	7.0	6.6	3.6	11	0.76	3.7	3.9	5.3	5.8	2.9	2.3	0.84	2.8	1.1	2.4	390			
Indian	median	1.3	5.4	2.7	1.1	0.32	5.7	2.6	n.d.	0.29	0.19	6.3	4.9	5.8	0.53	1.4	0.90	0.34	0.57	0.21	0.40	0.64	0.74	2.0	0.70	0.42	0.34	0.05	0.33	0.51	45			
	mean	2.9	11	4.8	2.4	0.60	14	4.7	0.27	1.8	2.2	13	17	24	2.4	3.1	2.8	1.3	2.8	0.58	0.91	1.5	2.1	4.1	1.6	1.1	0.71	0.46	0.89	1.3	130			
	min	0.13	1.1	0.25	0.14	0.11	2.2	0.71	0.11	0.03	0.04	1.8	1.5	1.1	0.23	0.47	0.21	0.09	0.12	0.05	0.13	0.13	0.16	0.64	0.18	0.20	0.17	0.05	0.15	0.07	15			
	max	15	33	24	13	2.3	43	19	1.8	10	12	59	88	190	11	9.4	11	7.9	21	2.3	3.5	6.7	11	20	7.2	6.0	3.9	3.6	5.2	6.4	440			
	SD	4.4	11	6.3	3.6	0.64	16	5.3	0.54	3.0	3.8	15	25	49	3.2	3.2	3.7	2.1	5.5	0.71	1.0	2.0	3.0	5.2	2.0	1.6	1.0	0.97	1.4	1.9	130			
South Pacific	median	0.31	2.7	0.82	0.08	0.49	8.3	4.1	0.14	0.60	0.80	7.6	6.5	13	0.65	4.1	2.6	0.79	2.0	0.99	0.92	1.3	1.6	4.4	1.3	0.91	0.52	1.0	0.69	2.4	110			
	mean	0.60	3.9	1.1	0.31	0.78	8.6	8.6	0.15	0.81	1.2	11	17	34	2.0	5.2	5.5	1.7	4.6	1.7	1.3	2.6	3.7	7.0	1.7	0.93	1.2	0.98	0.63	2.1	140			
	min	n.d.	0.94	0.06	0.08	0.16	2.8	0.63	0.14	0.13	0.28	4.8	1.7	1.9	0.27	2.3	1.7	0.09	0.23	0.24	0.17	0.27	0.23	0.85	0.40	0.23	0.16	0.02	0.18	0.35	40			
	max	1.7	9.1	2.8	1.1	5.1	18	41	0.58	2.8	4.4	33	67	160	9.5	13	12	7.6	22	5.6	3.2	8.0	12	26	4.3	2.4	5.1	2.3	1.3	3.2	360			
	SD	0.69	3.5	1.1	0.43	1.9	6.3	14	0.21	0.95	1.5	11	24	57	3.4	3.9	4.3	2.7	7.8	1.8	1.2	2.9	4.4	8.8	1.5	0.77	1.8	0.89	0.49	1.1	120			
North Pacific	median	0.57	1.92	0.92	0.48	0.16	3.5	0.49	0.03	0.24	0.31	4.0	3.7	5.4	0.32	4.5	1.2	0.24	0.58	0.19	0.20	0.63	0.71	0.77	0.33	0.22	0.13	0.04	0.17	0.25	37			
	mean	1.78	5.28	3.10	1.35	0.50	36	31	2.7	4.3	2.6	78	21	16	8.9	93	62	12	50	5.2	37	36	8.5	34	19	18	5.1	20	6.2	16	590			
	min	0.17	0.64	0.26	0.14	0.05	1.1	0.16	0.0	0.03	0.01	0.66	0.66	0.97	0.09	0.81	0.17	0.04	0.13	0.04	0.05	0.08	0.17	0.32	0.09	0.06	0.06	n.d.	0.08	0.05	11			
	max	12.35	41.78	27.16	9.07	4.7	440	420	37	55	28	1035	240	140	120	1250	850	160	52	70	520	490	100	460	250	250	69	270	83	220	7700			
	SD	3.23	10.68	7.02	2.38	1.2	120	110	9.9	15	7.3	280	63	37	32	330	230	42	14	19	140	130	27	120	68	68	19	72	22	58	2000			
Southern Ocean	median																																	
	mean																																	
	min																																	
	max																																	
	SD																																	





ng m <sup>-3</sup> day	Flux <sup>Feed</sup>																Σ <sub>64</sub> PAHs															
	Naphthalene	Dimethyl naphthalene	Methyl naphthalene	Trimethyl naphthalene	Acenaphthylene	Acenaphthene	Fluorene	Dibenzothiophene	Methyl dibenzothiophene	Dimethyl dibenzothiophene	Phenanthrene	Methyl phenanthrenes	Dimethyl phenanthrenes	Anthracene	Fluoranthene	Pyrene		Methylpyrenes	Dimethylpyrenes	Benzofluoranthene	Benzofluoranthene	Fluoranthene	Benzofluoranthene	Benzofluoranthene	Benzofluoranthene	Perylene	Indeno[1,2,3-cd]pyrene	Dibenzofluoranthene	Benzofluoranthene	Benzo[ghi]perylene		
North Atlantic	median	0.08	0.42	0.19	0.06	0.05	1.6	0.52	0.0	0.11	0.05	0.69	1.2	1.4	0.13	0.27	0.22	0.07	0.21	0.04	0.14	0.20	0.21	0.21	0.20	0.07	0.03	0.07	0.06	0.08	14	
	mean	5.5	10	8.9	2.9	3.7	6.4	5.7	0.14	5.7	4.6	20	33	14	4.6	8.51	4.7	0.37	0.74	0.11	2.7	4.1	0.51	3.5	1.4	0.24	0.16	0.30	0.15	0.63	150	
	min	n.d.	0.02	n.d.	n.d.	0.01	0.09	0.04	n.d.	n.d.	n.d.	0.09	0.05	0.06	0.01	0.04	0.01	n.d.	n.d.	n.d.	n.d.	n.d.	n.d.	n.d.	0.03	n.d.	n.d.	n.d.	n.d.	n.d.	n.d.	0.77
	max	63	73	47	17	45	35	26	1.3	59	26	130	230	68	59	61	29	3.3	6.6	0.60	24	24	3.5	18	8.8	1.2	0.88	2.1	0.61	4.9	820	
	SD	15	20	15	6.1	11	10	9.6	0.38	15	8.9	41	68	24	15	16	8.0	0.79	1.6	0.16	6.2	7.8	0.86	5.4	2.8	0.35	0.25	0.58	0.19	1.3	250	
South Atlantic	median	0.94	4.4	2.7	0.73	0.13	3.2	1.7	0.08	0.38	0.57	3.6	4.0	4.4	0.32	2.9	1.1	0.39	0.64	0.14	0.35	0.59	0.57	1.1	0.51	0.25	0.21	0.26	0.19	0.43	43	
	mean	7.4	6.0	6.6	5.5	0.19	4.3	2.1	0.18	1.2	5.9	5.5	5.7	17	0.67	5.6	3.2	1.4	2.8	0.41	1.5	1.9	1.9	2.6	1.3	0.95	0.41	1.1	0.45	1.2	89	
	min	0.09	0.60	0.18	0.09	0.04	0.41	0.33	n.d.	0.02	n.d.	0.66	0.58	0.33	0.09	0.22	0.14	0.05	0.08	0.03	0.05	0.08	0.09	0.18	0.09	0.04	0.03	n.d.	n.d.	0.03	12	
	max	76	20	48	56	0.50	14	8.0	0.86	8.8	85	27	30	220	3.6	35	25	12	35	2.5	17	16	17	22	11	10	3.0	13	3.5	9.3	460	
	SD	19	5.5	12	14	0.16	3.7	2.0	0.26	2.2	20	6.8	7.2	53	0.92	8.3	5.9	3.0	8.2	0.65	4.1	3.9	4.0	5.1	2.6	2.5	0.70	3.0	0.84	2.2	120	
Indian	median	0.11	0.46	0.21	0.09	0.02	0.52	0.10	0.0	0.02	0.02	0.39	0.31	0.27	0.05	0.10	0.06	0.02	0.03	0.01	0.03	0.03	0.03	0.10	0.04	0.02	0.01	0.0	0.02	0.02	3.8	
	mean	0.64	1.0	0.65	0.48	0.06	1.2	0.53	0.06	0.33	0.46	1.6	2.7	4.8	0.29	0.59	0.67	0.29	0.59	0.14	0.21	0.41	0.46	0.50	0.28	0.17	0.07	0.20	0.08	0.36	19	
	min	0.01	0.06	0.01	0.01	0.01	0.07	0.03	n.d.	n.d.	n.d.	0.09	0.07	0.06	0.01	0.02	0.01	n.d.	n.d.	0.01	n.d.	0.01	0.01	0.05	0.01	0.01	0.01	n.d.	n.d.	0.01	n.d.	0.71
	max	7.3	5.6	6.0	5.3	0.41	4.6	3.2	0.66	3.3	4.6	13	19	32	1.8	6.1	7.1	2.5	4.4	1.5	2.3	4.4	4.0	4.7	3.0	1.7	0.47	2.4	0.61	4.2	150	
	SD	1.9	1.5	1.6	1.4	0.11	1.5	0.87	0.18	0.89	1.3	3.3	5.9	11	0.57	1.6	1.9	0.71	1.4	0.40	0.60	1.2	1.1	1.2	0.77	0.45	0.12	0.63	0.16	1.1	42	
South Pacific	median	0.05	0.29	0.09	0.01	0.05	0.80	0.42	0.01	0.07	0.11	0.91	1.3	2.1	0.10	0.53	0.51	0.12	0.23	0.15	0.10	0.20	0.26	0.48	0.14	0.08	0.07	0.07	0.04	0.15	12	
	mean	0.08	0.53	0.16	0.06	0.43	0.96	0.65	0.03	0.14	0.21	1.3	1.5	2.7	0.17	0.60	0.61	0.14	0.38	0.15	0.15	0.29	0.41	0.57	0.19	0.10	0.09	0.11	0.06	0.21	13	
	min	n.d.	n.d.	n.d.	n.d.	0.02	n.d.	0.08	0.0	n.d.	n.d.	n.d.	n.d.	n.d.	n.d.	0.11	0.12	n.d.	n.d.	0.04	n.d.	n.d.	n.d.	0.11	n.d.	n.d.	0.02	n.d.	n.d.	n.d.	0.05	5.1
	max	0.30	1.6	0.58	0.24	2.3	2.8	1.9	0.12	0.59	0.91	2.8	3.6	8.5	0.50	1.2	1.6	0.40	1.2	0.25	0.41	0.69	1.3	1.2	0.47	0.23	0.23	0.33	0.14	0.49	23	
	SD	0.11	0.58	0.21	0.09	0.94	0.97	0.65	0.05	0.22	0.34	1.1	1.4	3.2	0.19	0.46	0.52	0.16	0.45	0.07	0.16	0.30	0.50	0.44	0.18	0.10	0.08	0.13	0.06	0.16	81	
North Pacific	median	0.07	0.22	0.10	0.05	0.03	0.54	0.09	0.0	0.03	0.04	0.58	0.64	0.05	0.48	0.18	0.04	0.11	0.03	0.05	0.09	0.14	0.14	0.08	0.04	0.02	0.02	0.02	0.03	0.05	5.3	
	mean	0.22	0.60	0.35	0.17	0.06	3.5	2.8	0.24	0.39	0.25	7.2	2.0	1.8	0.81	8.4	5.6	1.1	0.51	0.48	3.3	3.2	0.82	3.1	1.7	1.6	0.47	1.8	0.56	1.5	54	
	min	n.d.	n.d.	n.d.	n.d.	n.d.	n.d.	n.d.	n.d.	n.d.	n.d.	n.d.	n.d.	n.d.	n.d.	n.d.	n.d.	n.d.	n.d.	n.d.	n.d.	n.d.	n.d.	n.d.	n.d.	n.d.	n.d.	n.d.	n.d.	n.d.	n.d.	0.0
	max	1.3	4.2	2.8	0.92	0.48	45	43	3.8	5.5	2.8	110	24	15	12	130	86	16	5.3	7.1	53	49	11	47	26	26	7.1	27	8.5	22	780	
	SD	0.35	1.0	0.70	0.27	0.12	11	11	0.94	1.4	0.69	26	5.9	3.5	3.0	32	22	4.0	1.3	1.8	13	12	2.6	12	6.4	6.4	1.8	6.8	2.1	5.5	190	

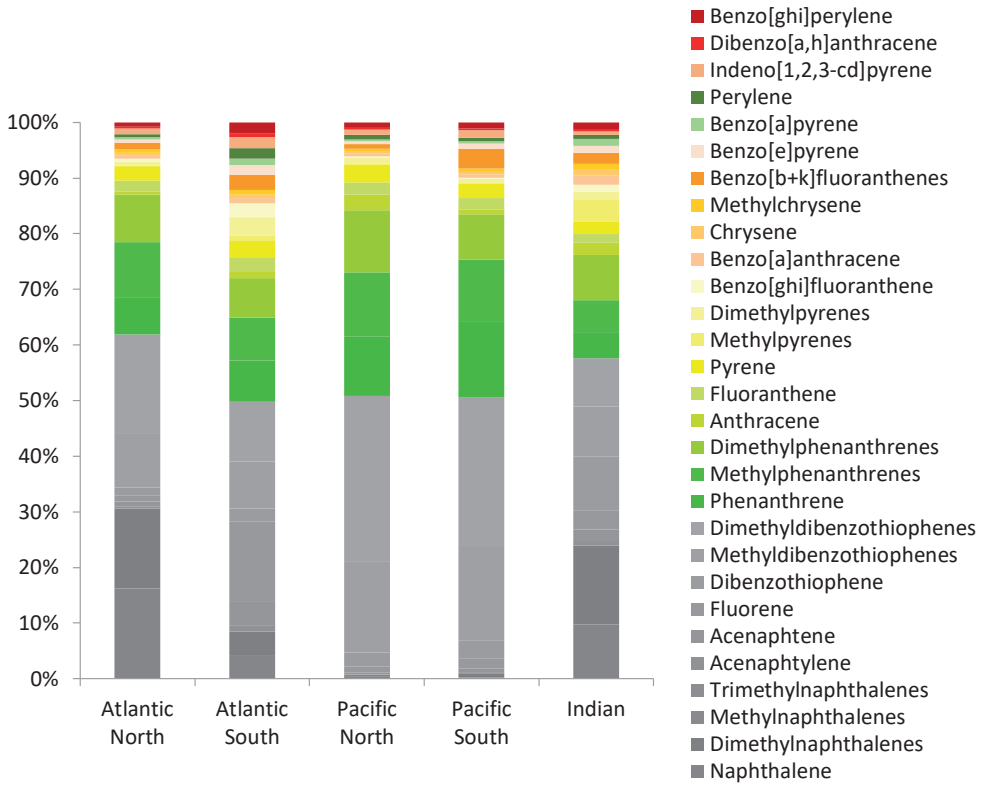
**Table S12.** Slopes fitted to the field data of  $C_{\text{Plankton}}$  versus Biomass

	<b>m</b>
<b>Naphthalene</b>	-0.97
<b>Methylnaphthalene</b>	-0.92
<b>Dimethylnaphthalenes</b>	-0.85
<b>Acenaphtylene</b>	-0.55
<b>Acenaphtene</b>	-0.70
<b>Fluorene</b>	-0.73
<b>Dibenzothiophene</b>	-1.35
<b>Methyldibenzothiophenes</b>	-0.97
<b>Dimethyldibenzothiopenes</b>	-0.96
<b>Phenanthrene</b>	-0.65
<b>Methylphenanthrenes</b>	-0.59
<b>Dimethylphenanthrenes</b>	-0.50
<b>Anthracene</b>	-0.63
<b>Fluoranthene</b>	-0.26
<b>Pyrene</b>	-0.46
<b>Methylpyrenes</b>	-0.61
<b>Dimethylpyrenes</b>	-0.50
<b>Benzo[ghi]fluoranthene</b>	-0.66
<b>Benzo[a]anthracene</b>	-0.49
<b>Chrysene</b>	-0.39
<b>Methylchrysenes</b>	-0.53
<b>Benzo[b+k]fluoranthenes</b>	-0.66
<b>Benzo[e]pyrene</b>	-0.61
<b>Benzo[a]pyrene</b>	-0.75
<b>Perylene</b>	-0.83
<b>Indeno[1,2,3-cd]pyrene</b>	-0.61
<b>Dibenzo[a,h]anthracene</b>	-0.81
<b>Benzo[ghi]perylene</b>	-0.50

**Table S13.** Relative abundance of alpha and beta subunits of RHD per ocean basin

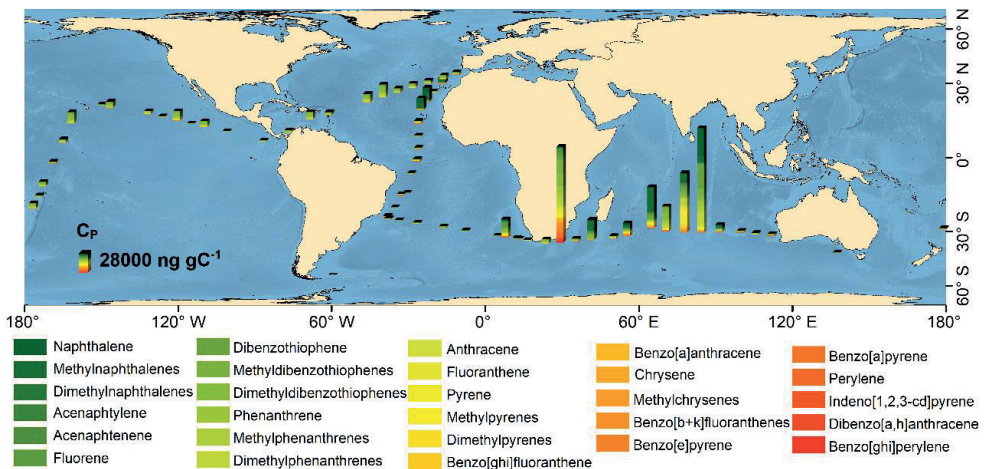
Subbasin		Subunit Alpha			Subunit Beta		
		DCM	Mixed layer	Surface	DCM	Mixed layer	Surface
Indian Ocean	mean	0.89		0.61	0.032		0.020
	max	1.13		0.95	0.053		0.026
	min	0.63		0.38	0.023		0.014
	sd	0.16		0.19	0.0092		0.0040
	n	9		12	9		12
3Mediterranean Sea	mean	0.86		0.63	0.039		0.026
	max	1.18		0.74	0.075		0.036
	min	0.59		0.50	0.020		0.0128
	sd	0.20		0.09	0.019		0.0095
	n	6		6	6		6
North Atlantic Ocean	mean	1.02	1.11	0.95	0.031	0.024	0.031
	max	1.15	1.11	1.21	0.039	0.024	0.051
	min	0.89	1.11	0.61	0.025	0.024	0.013
	sd	0.12		0.19	0.0066		0.013
	n	4	1	10	4	1	10
North Pacific Ocean	mean	0.90		0.56	0.034		0.016
	max	1.23		0.71	0.045		0.020
	min	0.59		0.43	0.023		0.010
	sd	0.29		0.10	0.0097		0.0041
	n	5		6	5		6
Red Sea	mean	1.23		0.70	0.12		0.027
	max	1.29		0.83	0.17		0.037
	min	1.18		0.57	0.075		0.021
	sd	0.07		0.13	0.070		0.0072
	n	2		4	2		4
South Atlantic Ocean	mean	0.99		0.80	0.043		0.027
	max	1.20		1.18	0.079		0.042
	min	0.73		0.50	0.024		0.015
	sd	0.16		0.27	0.022		0.0082
	n	6		8	6		8
Southern Ocean	mean	0.77		0.70	0.028		0.030
	max	0.77		0.73	0.028		0.036
	min	0.77		0.68	0.028		0.023
	sd			0.04			0.0091
	n	1		2	1		2
South Pacific Ocean	mean	0.82	1.02	0.60	0.036	0.11	0.020
	max	1.08	1.09	0.92	0.057	0.11	0.063
	min	0.63	0.96	0.41	0.020	0.09	0.0092
	sd	0.14	0.064	0.14	0.013	0.011	0.014
	n	9	3	15	9	3	15

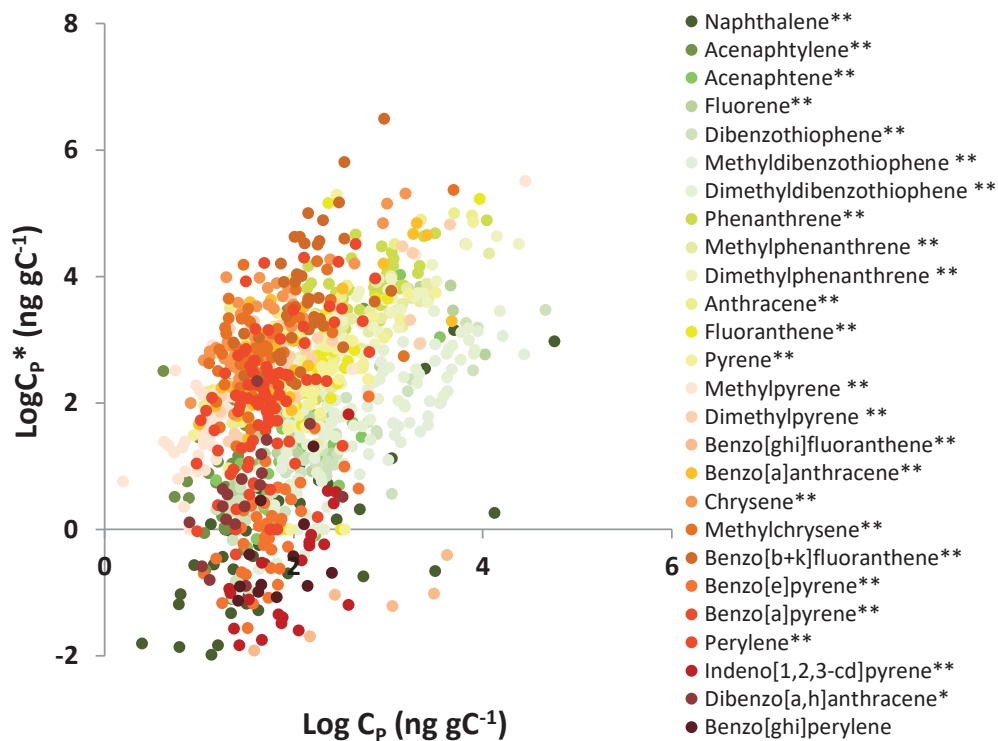
**Figure S1.** Relative abundance of PAHs in the particulate phase per subbasin.



**Figure S2.** Particulate phase measured PAHs concentrations map ( $\text{ng gC}^{-1}$ ).

64 PAHs  $C_p$  in  $\text{ng gC}^{-1}$  (POC corrected)



**Figure S3.** Correlation between measured and estimated CP ( $\text{ng gC}^{-1}$ ).

Correlation between the estimated  $C_p^*$  from the measured CG and the field measured  $C_p$  for the surface ocean. Statistical significance is noted per each individual PAH \*\* ( $p < 0.01$ ). \* ( $p < 0.05$ ). The ratio  $C_p^*/C_p$  equals the air-water fugacity ratio ( $f_A/f_W$ ), implying under-saturated surface water concentrations respect to atmospheric PAHs, driving a net air to water diffusive flux (González-Gaya et al., 2016).  $f_A/f_W$  is related to the relative kinetics of air-water exchange and the water column sinks depleting chemical concentration (Text S2, SI).

**Text S2.** Settling and degradation as drivers of air-water dis-equilibrium

As demonstrated in the companion work González-Gaya et al. 2016, there was an air-water disequilibrium which was evidenced with the air-water fugacity ratio ( $f_g/f_w$ ) (Figure S8 of González-Gaya et al. 2016). The  $f_g/f_w$  ratio depends on the relative kinetics of air-water exchange and removal processes in the surface ocean (Dachs et al. 2002, Jurado and Dachs 2008, Berrojalbiz et al., 2014). In the oligotrophic ocean, settling is much slower than air-water exchange, and for chemicals for which settling is the only sink, the residence times in the water column are very long (decades or even centuries).

In the case that settling is much slower than air-water exchange, as it happens in the oligotrophic ocean for chemicals with mid hydrophobicities ( $\log K_{ow} < 6$ ) (Dachs et al. 2002, Jurado & Dachs 2008, Berrojalbiz et al, 2014), then,

$$\frac{f_A}{f_w} = \frac{1}{1 - \frac{k_{DegW}}{k_{AW} + k_{DegW}}} \quad [1]$$

Where  $k_{AW}$  is the air-water mass transfer coefficient ( $m\ d^{-1}$ ) as estimated in Gonzalez-Gaya et al. 2016, and  $k_{DegW}$  ( $m\ d^{-1}$ ) is the mass transfer coefficient for degradation (all mechanisms) in the water column, and estimated as,

$$k_{DegW} = H r_{DegW} \quad [2]$$

Where  $H$  is the depth of the considered water layer (for example 200 m), and  $r_{DegW}$  is the reaction rate constant ( $d^{-1}$ ).

$f_g/f_w$  was higher than 3 for phenanthrene and methylphenanthrenes and other PAHs (see Figure S8 of supplementary material of González-Gaya et al. 2016). Furthermore, the value of  $k_{AW}$  was always lower than  $4\ m\ d^{-1}$ , in fact, it is generally much lower depending on the wind speed and chemical Henry's law constant. Then, for a water column of 200 m, the value  $r_{DegW}$  must be higher than  $0.03d^{-1}$ , or half-lives of 33 days. For air-water exchange velocities lower than  $4\ m\ d^{-1}$ , as usually observed, chemicals with longer half-live due to biodegradation could lead to the observed disequilibrium. As noted below, several studies have reported shorter half-lives than 33 days for degradation of 2-4 ring PAHs (see Table below). This modelling exercise proves that it is feasible that degradation (including biodegradation) of PAHs at surface waters induces the air-water gradient of concentrations, driving therefore the large inputs of aromatic hydrocarbons. Furthermore, the comparison with the settling fluxes, shows that biodegradation can explain the disappearance of most PAHs in the top ocean.

Table for text S2: Half-lives of low MW PAHs and/or high MW PAHs as reported in the literature.

Reference	Compound	Half-Life-time	Site
Bagi et al. 2014	Naphthalene	21-15 days	Temperate and Arctic
Bacosa et al. 2015	LMW+HMW	10-20 days	Gulf of Mexico
Stewart et al 1993	LMW+HMW	60 days	Seawater
Zahed et al 2011	LMW+HMW	28-75 days	Oil contaminated Perai area Butterworth, NW Malaysia
Aldrett et al 1997	LMW+HMW	28 days	Gulf of Mexico
Garneau et al 2016	LMW+HMW	12-15 days	Arctic sub-ice and sea-ice
Bagby et al. 2016	LMW	160 d (less 5% remaining, thus shorter half- lives)	Oil-particles from Deep- horizon oil spill

**Figure S4.** Median concentrations of PAHs in the plankton phase for the tropical and southern oceanic basins. Standard deviations have not been included in the graph to ease the bars analysis, though they are included in the table S10.

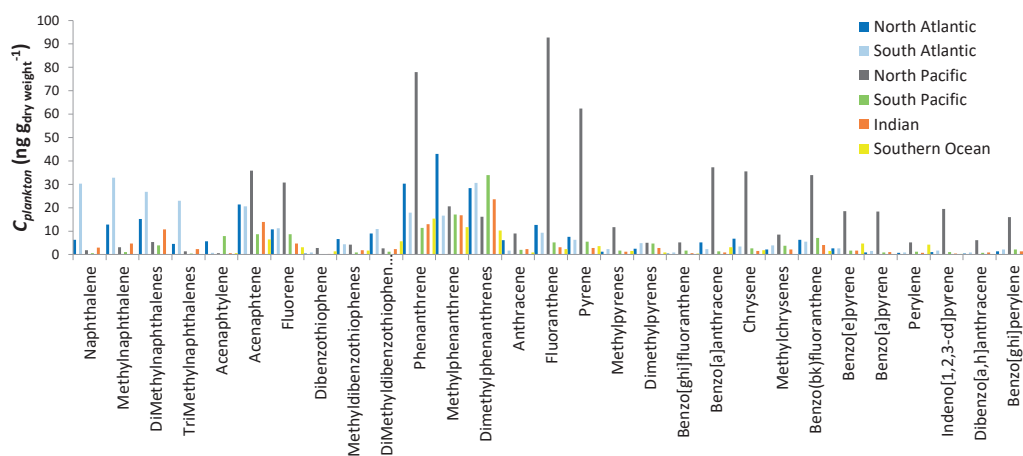


**Figure S5.** Relative occurrence of individual PAHs in plankton per subbasin

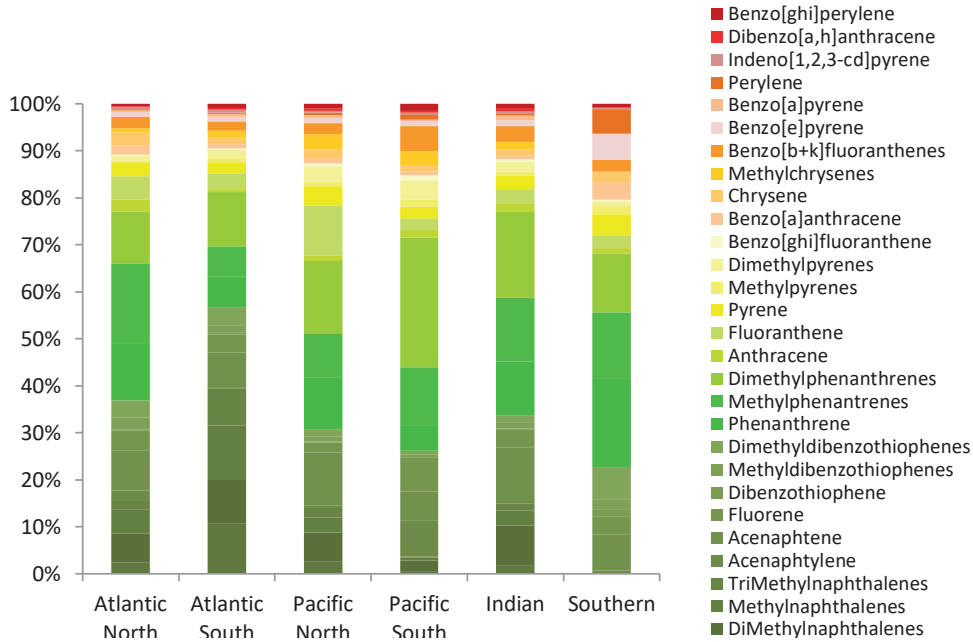


**Figure S6.** Diagnostic ratios for PAHs sources in plankton samples per subbasin. Axes of upper panel have been modified manually to exclude some outliers and to ease the observation of most of the data. Petrogenic and pyrolytic origin of the PAHs measured in the samples are classified according to the reference line proposed by Budzinsky et al. as suggested by Lima et al. in the upper panel (Lima et al., 2005). Results show mixed contributions of pyrolytic and petrogenic PAHs.

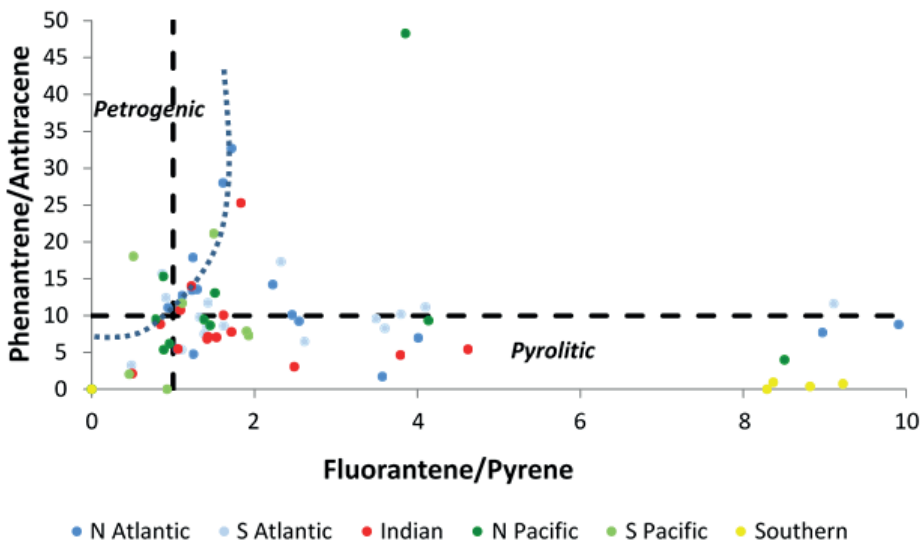




**Figure S7.** Biological pump fluxes; phytoplankton and fecal fluxes maps. Biological pump fluxes for the algal settling flux ( $F_{\text{Phyto}}$ ) (top panel), and the fecal settling flux ( $F_{\text{Fecal}}$ ) (bottom panel). Marked bars ( $\approx$ ) have been reduced by a factor of 10 in order to ease the global comparison of all the measurements.

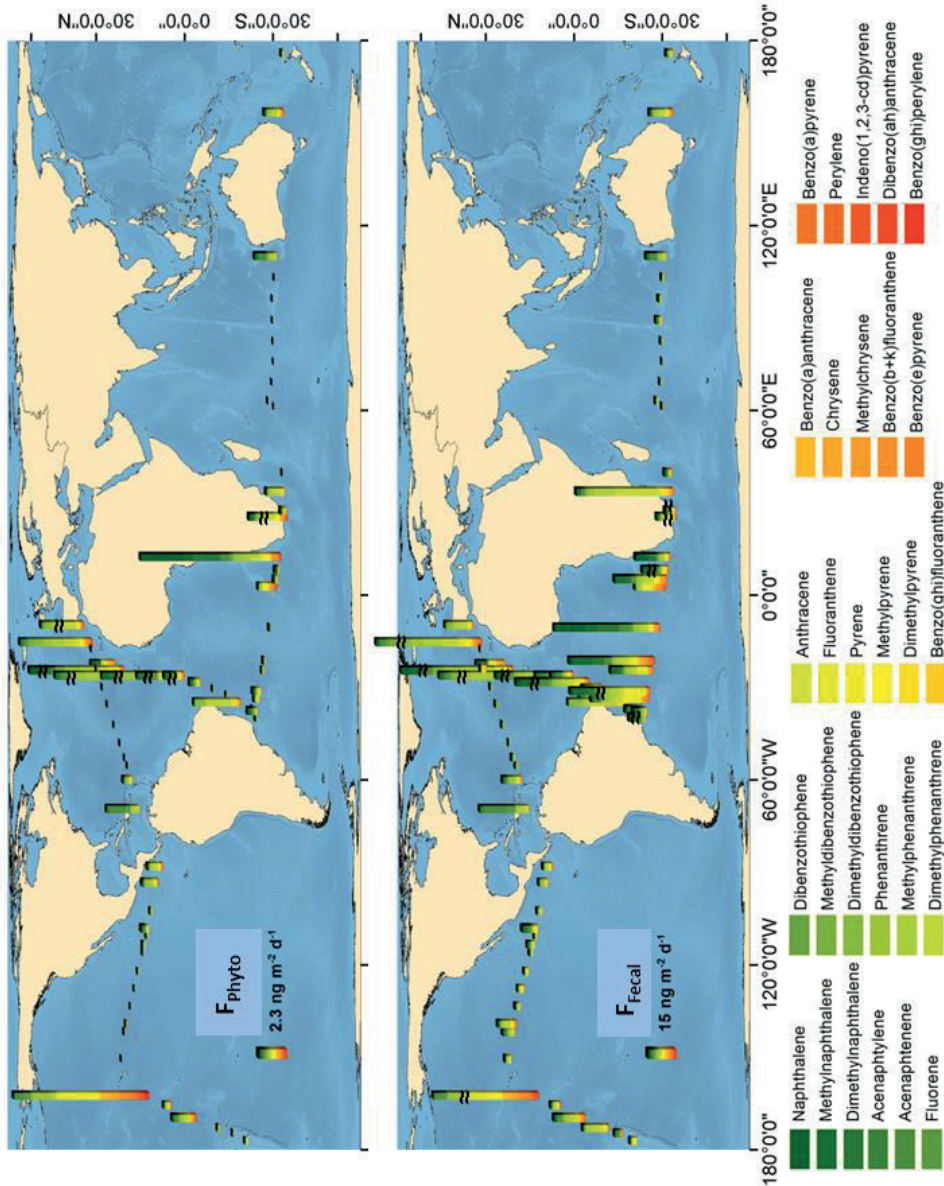


**Figure S8.** Surface Ocean Entrance/Exit fluxes ratio versus  $K_{ow}$ . Fluxes balance is calculated with the entrance fluxes, which correspond to the sum of net diffusive exchange plus dry deposition flux, divided by the export flux of the biological pump. Symbols correspond to the different oceanic subbasins samples:  $\diamond$ North Atlantic,  $\square$ South Atlantic,  $\bullet$ Indic,  $\times$ South Pacific and  $+$ North Pacific. Colors follow the same PAHs identification as in the rest of the figures, also indicated in the arrows.

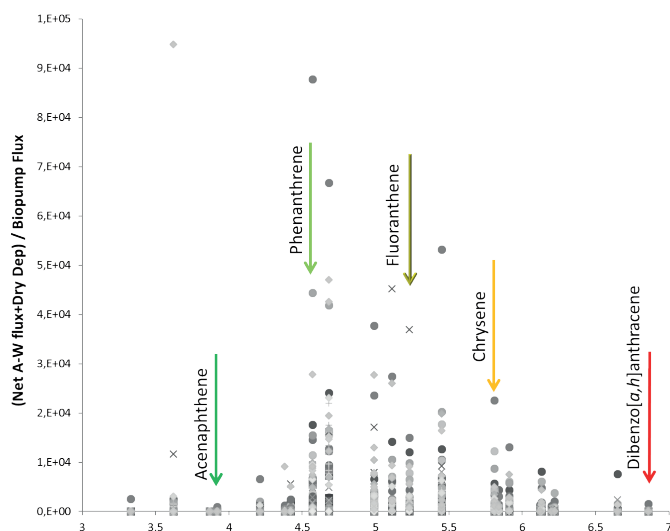


**Figure S9.** Methyl anthracene / Methyl phenanthrene ratios in dissolved samples. Diagnostic ratios in the dissolved water samples pointing a separation of heavy fuels oil versus crude oil as proposed by Zhang et al. 2016. According to this study ratios below 0.1 in both axes belong to crude oil, while over that value correspond to heavy fuels. Samples from the Malaspina cruise are influenced by heavy fuel oils, in particular those from the Atlantic Ocean.

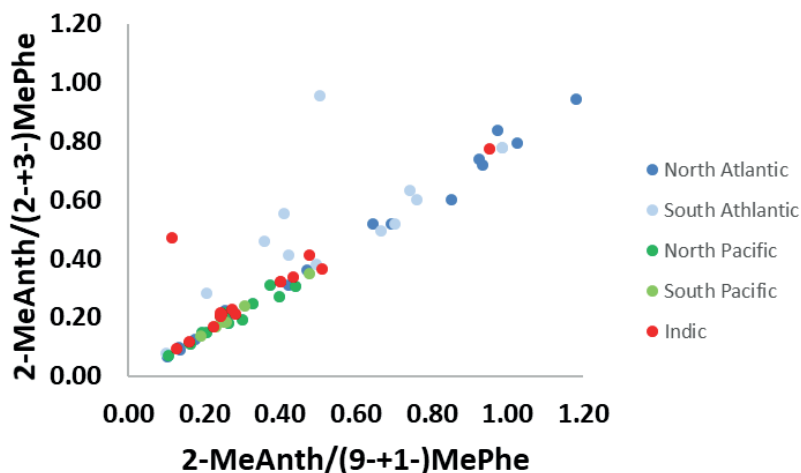


**Figure S10.** Relative abundance of alpha and beta subunits of RHD per ocean basin. Salmon and turquoise colors attend for the alpha and beta subunits, respectively as indicated in the top labels of the panel.

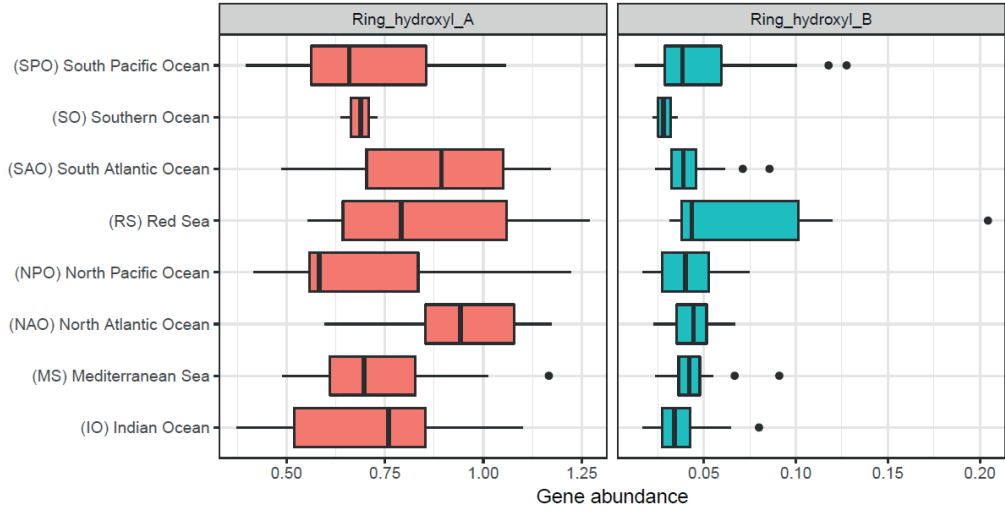
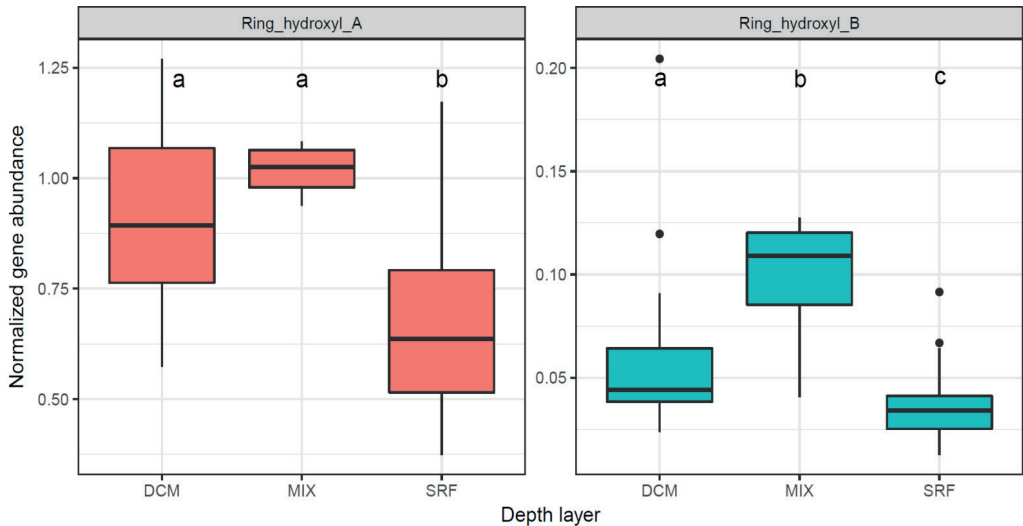


**Figure S11.** Relative abundance of alpha and beta subunits of RHD over depth.



## ADDITIONAL REFERENCES

Aldrett, Salvador, James S. Bonner, Marc A. Mills, Robin L. Autenrieth, and Frank L. Stephens. "Microbial degradation of crude oil in marine environments tested in a flask experiment." *Water Research* 31, 2840-2848 (1997).

Bacosa, H.P., Erdner, D.L. and Liu, Z. Differentiating the roles of photooxidation and biodegradation in the weathering of Light Louisiana Sweet crude oil in surface water from the Deepwater Horizon site. *Marine pollution bulletin* 95, 265-272 (2015).

Bagby, S.C, C.M. Reddy, C. Aeppli, G.B. Fisher, D.L. Valentine. Persistence and biodegradation of oil at the ocean floor following Deepwater Horizon. *PNAS* E9-E18 (2016).

Bagi, A., Pampanin, D. M., Brakstad, G., & Kommedal, R. (2014). Estimation of hydrocarbon biodegradation rates in marine environments: A critical review of the Q 10 approach. *Marine Environmental Research*. <https://doi.org/10.1016/j.marenvres.2013.05.005>.

Berrojalbiz, N. Biogeochemical and physical controls on the occurrence of persistent organic pollutants in the Mediterranean Sea atmosphere, seawater and biota. PhD thesis, Universitat Polytechnica de Catalunya, 2014.

Dachs, J. et al. Oceanic Biogeochemical controls on global dynamics of persistent organic pollutants. *Environ. Sci. Technol.* 36, 4229-4237, 2002.

Jurado, E., J. Dachs. Seasonality in the "grasshopping" and atmospheric residence times of persistent organic pollutants over the oceans. *Geophys. Res. Lett.* 35, L17805, 2008.

Lima, A. L. C., Farrington, J. W. & Reddy, C. M. Combustion-derived polycyclic aromatic hydrocarbons in the environment—a review. *Environmental Forensics* 6, 109-131 (2005).

Garneau, M.-È., Michel, C., Meisterhans, G., Fortin, N., King, T. L., Greer, C. W., & Lee, K. (2016). Hydrocarbon biodegradation by Arctic sea-ice and sub-ice microbial communities during microcosm experiments, Northwest Passage (Nunavut, Canada). *FEMS Microbiol. Ecol.* 92, fiw130.

Morales, L. et al. Oceanic Sink and Biogeochemical Controls on the Accumulation of Polychlorinated Dibenzo-p-dioxins, Dibenzofurans, and Biphenyls in Plankton. *Environ. Sci. Technol.* 49, 13853-13861, doi:10.1021/acs.est.5b01360 (2015).

Stewart P. S., Tedaldi D. J., Lewis A. R., Goldman E. (1993). Biodegradation rates of crude oil in seawater. *Water Environ. Res.* 65, 845–848. (1993)

Zahed, M. A., Abdul Aziz, H., Hasnain Isa, M., Mohajeri, L., Mohajeri, S., Rahman, S., & Kutty, M. Kinetic modeling and half life study on bioremediation of crude oil dispersed by Corexit 9500. *Journal of Hazardous Materials*, 185, 1027–1031 (2011).

Zhang, H. New diagnostic ratios based on phenanthrenes and anthracenes for effective distinguishing heavy fuels oils from crude oils. *Marine Pollution Bulletin* 106, 58-61 (2016).



## **Supporting information of Chapter 2**

**Table S1.** Biotic and abiotic features at initial conditions and over the course of the incubation for each experimental condition. (\* indicate significant differences between treatment and control in that time-point, paired t-test,  $p < 0.05$ )

	ANTARCTICA						MEDITERRANEAN								
	T3		T48		Initial conditions	PAH	T3		T48		Initial conditions	PAH	T48		
	Control	PAH	Control	PAH			Control	PAH	Control	PAH			Control	PAH	
Latitude	62.63 S						41.67 N								
Longitude	60.4 W						2.8 E								
Sea Surface Temperature (°C)	1.46														
Salinity (PSU)	33.49														
All BA (Cells mL <sup>-1</sup> )	338000 ± 95767.08	244750 ± 19050.37	181777.78 ± 111423.91	501750 ± 78321.23	498125 ± 97775.89	602250 ± 18661.46	638750 ± 8770.21	698625 ± 35387.40	805000 ± 38444.77	743500 ± 89061.78					
HNA (Cells mL <sup>-1</sup> )	243750 ± 73031.39	175750 ± 16839.93	111246.67 ± 97496.28	379875 ± 68861.01	364875 ± 74060.67	249750 ± 9810.71	328000 ± 4760.95	302500 ± 54542.25	545750 ± 16028.62	482625 ± 83718.81					
LNA (Cells mL <sup>-1</sup> )	94175 ± 25447.77	69450 ± 8306.82	70655.56 ± 20918.30	121875 ± 12040.85	132812.50 ± 47071.33	352500 ± 10279.43	310750 ± 6652.07	396250 ± 33648.39	259000 ± 26267.85	261000 ± 34570.84					
N-NH <sub>4</sub> <sup>+</sup> (μmol L <sup>-1</sup> )	7.43 ± 1.18	2.73 ± 2.47	2.40 ± 1.90	6.07 ± 3.08	8.02 ± 4.05	n.d.	0.17 ± 0.16	0.11 ± 0.02	2 ± 2.10	0.20 ± 0.20					
NO <sup>-3</sup> + NO <sup>-2</sup> (μmol L <sup>-1</sup> )	14.06 ± 0.72	23.93 ± 2.59	25.01 ± 1.46	24.75 ± 0.12	20.08 ± 4.43	n.d.	2.18 ± 0.01	0.39 ± 0.12 (*)	3.17 ± 0.08	0.82 ± 0.25 (*)					
PO <sub>4</sub> <sup>3-</sup> (μmol L <sup>-1</sup> )	1.11 ± 0.03	1.60 ± 0.14	1.68 ± 0.07	1.65 ± 0.02	1.45 ± 0.21	n.d.	0.12 ± 0.12	0.04 ± 0.01	0.02 ± 0	0.02 ± 0					
Shannon diversity index 16S ASV	1.20 ± 0.21	1.56 ± 0.30	2.30 ± 0.77	3.40 ± 0.01	3.44 ± 0.04	4.58	4.61 ± 0.10	4.66 ± 0.08	4.66 ± 0.01	4.77 ± 0.08					

**Table S2.** Community composition of microbial communities at initial time point (T3) measured by 16S rRNA gene amplicon sequencing (Relative abundances in % of total reads and variability expressed in standard deviation, HC : Hydrocarbonoclastic). Notice that counts of general taxonomical groups include HC bacteria.

	Antarctica		Mediterranean	
	Control	PAH	Control	PAH
Alphaproteobacteria	16.35 ± 1.70	17.67 ± 12.46	45.74 ± 0.85	45.32 ± 0.44
SAR11 clade	9.20 ± 4.26	11.76 ± 12.38	7.67 ± 0.95	11.80 ± 2.25
Rhodobacterales	4.67 ± 3.82	1.96 ± 0.99	3.75 ± 0.02	3.01 ± 0.08
Rickettsiales	1.67 ± 0.94	3.01 ± 0.84	18.22 ± 0.44	14.38 ± 1.22
Gammaproteobacteria	28.37 ± 0.37	25.70 ± 8.16	16.61 ± 0.04	19.20 ± 0.21
Alteromonadales	6.00 ± 3.99	3.21 ± 2.49	0.31 ± 0.07	0.72 ± 0.05
Cellvibrionales	4.65 ± 1.51	5.32 ± 1.36	6.37 ± 0.01	6.65 ± 0.56
Oceanospirillales	11.70 ± 3.08	11.84 ± 5.44	1.52 ± 0.20	1.66 ± 0.04
Pseudomonadales	0.31 ± 0.34	0.17 ± 0.09	0.05 ± 0.04	0.03
Thiotrichales	1.71 ± 0.07	1.49 ± 0.86	0	0
Bacteroidota	53.87 ± 0.48	54.54 ± 5.98	27.00 ± 0.27	26.45 ± 1.63
Sphingobacteriales	51.77 ± 0.59	52.95 ± 6.89	20.02 ± 0.47	19.54 ± 1.52
Flavobacteriales	0.09 ± 0.03	0.07 ± 0.06	0.63 ± 0.05	0.64 ± 0.02
Cyanobacteria	0	0	7.05 ± 0.97	5.90 ± 1.23
Other Bacterial groups	0.44 ± 0.26	0.42 ± 0.28	0.28 ± 0.08	0.22 ± 0.01
HC Actinobacteria	0.07	0.29 ± 0.30	0.17 ± 0.03	0.07 ± 0.01
<i>Arthrobacter</i>	0	0.18	0.17 ± 0.03	0.06 ± 0.00
<i>Nocardioides</i>	0.07	0.20 ± 0.17	0	0.02
HC Alphaproteobacteria	4.20 ± 3.24	7.30 ± 9.06	0.16 ± 0.00	0.46 ± 0.07
<i>Jannaschia</i>	0	0	0.15 ± 0.02	0.42 ± 0.09
HC Gammaproteobacteria	6.03 ± 4.25	3.23 ± 2.54	0.83 ± 0.21	2.49 ± 0.83
HC Alteromonadales	5.42 ± 3.79	2.86 ± 2.30	0.08 ± 0.04	0.30 ± 0.02
<i>Colwellia</i>	4.73 ± 3.19	2.51 ± 2.15	0	0
<i>Glaciecola</i>	0	0	0.03	0.07 ± 0.01
<i>Thalassotalea</i>	0.14	0.23	0.01	0.03
<i>Pseudoalteromonas</i>	0.62 ± 0.69	0.28 ± 0.18	0.06 ± 0.03	0.21 ± 0.00
HC Pseudomonadales	0.31 ± 0.34	0.17 ± 0.09	0.05 ± 0.04	0.03
<i>Pseudomonas</i>	0	0.08 ± 0.05	0	0
HC Vibrionales	0	0	0.68 ± 0.21	2.14 ± 0.88
HC Bacteroidia	0.24 ± 0.21	0.12 ± 0.12	0.04 ± 0.02	0
All HCB	10.50 ± 1.17	10.87 ± 7.60	1.21 ± 0.26	3.02 ± 0.88



**Table S3.** PAH dissolved and particulate phase concentrations time course in each experimental site, treatment and time-point (units are ng L-1 and variability is expressed as the standard error of mean) (Part: Particulate phase concentrations, Diss: Dissolved phase concentrations, FL: Fluorene, ANT: Anthracene, PHE: Phenantrene, PYR: Pyrene, FLT: Fluoranthene, CRY: Chrysene, BaA: Benz(a)anthracene, BbF : Benzo(b)fluoranthene, BkF: Benzo(k)fluoranthene, BaP: Benzo(a)pyrene; DBA: Dibenz(a,h)anthracene, IPY : Indeno(1,2,3-cd)pyrene, BghP: Benzo(ghi)perylene)

	T0												T48											
	Control						PAH						Control						PAH					
	Diss.	Part.	Total	Diss.	Part.	Total	Diss.	Part.	Total	Diss.	Part.	Total	Diss.	Part.	Total	Diss.	Part.	Total						
FL	2.38 ± 1.44	0.61 ± 0.15	2.99 ± 1.59	11.44 ± 3.43	0.06 ± 0.02	11.50 ± 3.45	0.85 ± 0.03	0.62 ± 0.29	1.47 ± 0.25	12.58 ± 0.17	0.42 ± 0.13	13.00 ± 0.29												
ANT	0.26 ± 0.05	0.37 ± 0.03	0.63 ± 0.08	47.27 ± 19.29	0.47 ± 0.19	47.74 ± 19.48	0.21 ± 0.00	0.67 ± 0.14	0.67 ± 0.14	58.31 ± 9.98	0.73 ± 0.23	59.05 ± 9.75												
PHE	2.21 ± 1.06	1.04 ± 0.07	3.25 ± 1.14	19.33 ± 3.90	0.20 ± 0.04	19.53 ± 3.94	1.05 ± 0.05	1.23 ± 0.41	2.28 ± 0.36	19.84 ± 0.05	1.15 ± 0.03	20.99 ± 0.02												
PYR	1.36 ± 0.35	1.83 ± 0.16	3.20 ± 0.50	163.82 ± 7.88	4.33 ± 0.21	168.15 ± 8.09	1.20 ± 0.15	2.38 ± 0.71	3.57 ± 0.56	149.73 ± 1.56	8.23 ± 0.47	157.96 ± 2.03												
FLT	1.51 ± 0.54	1.57 ± 0.13	3.08 ± 0.67	194.75 ± 6.68	9.75 ± 0.33	204.50 ± 7.01	1.25 ± 0.18	2.22 ± 0.98	3.47 ± 0.40	190.48 ± 9.75	8.36 ± 0.01	198.84 ± 9.74												
CRY	1.68 ± 0.41	1.17 ± 0.02	2.85 ± 0.43	12.08 ± 2.95	2.21 ± 0.54	14.29 ± 3.49	1.16 ± 0.09	1.76 ± 0.53	2.92 ± 0.45	24.46 ± 4.28	16.64 ± 8.28	41.11 ± 12.56												
BaA	1.75 ± 0.94	0.51 ± 0.12	2.27 ± 1.06	44.54 ± 9.11	8.74 ± 1.79	53.28 ± 10.89	0.74 ± 0.10	0.68 ± 0.10	1.42 ± 0.00	71.80 ± 9.64	25.02 ± 7.35	96.82 ± 16.99												
BbF	0.29 ± 0.29	0.23 ± 0.03	0.52 ± 0.38	10.46 ± 2.57	2.15 ± 0.53	12.61 ± 3.09	0.00 ± 0.00	0.13 ± 0.00	0.13 ± 0.00	14.26 ± 2.83	16.69 ± 6.11	30.95 ± 8.93												
BkF	0.38 ± 0.16	0.29 ± 0.04	0.67 ± 0.20	3.07 ± 0.91	1.33 ± 0.40	4.40 ± 1.31	0.00 ± 0.00	0.30 ± 0.06	0.30 ± 0.06	6.12 ± 1.10	13.21 ± 6.96	19.33 ± 8.06												
BaP	0.00 ± 0.00	0.13 ± 0.03	0.13 ± 0.03	9.07 ± 2.12	4.13 ± 0.96	13.20 ± 3.08	0.00 ± 0.00	0.09 ± 0.03	0.09 ± 0.03	15.99 ± 1.93	15.11 ± 4.83	31.10 ± 6.76												
DBA	0.19 ± 0.19	0.24 ± 0.11	0.42 ± 0.29	2.95 ± 1.43	3.12 ± 1.52	6.07 ± 2.95	0.00 ± 0.00	0.18 ± 0.06	0.18 ± 0.06	5.19 ± 0.90	28.56 ± 9.96	33.75 ± 10.87												
IPY	1.31 ± 0.30	1.19 ± 0.06	2.51 ± 0.36	5.45 ± 2.21	6.92 ± 2.81	12.38 ± 5.02	0.92 ± 0.02	1.48 ± 0.36	2.40 ± 0.35	11.25 ± 0.56	29.59 ± 8.14	40.84 ± 8.69												
BghP	0.64 ± 0.24	0.82 ± 0.10	1.46 ± 0.33	2.90 ± 0.99	4.13 ± 1.41	7.03 ± 2.41	0.33 ± 0.01	0.00 ± 0.00	0.33 ± 0.01	4.59 ± 0.37	18.96 ± 8.60	23.54 ± 8.97												
<b>TOTAL</b>	<b>13.97 ± 5.96</b>	<b>10.01 ± 1.11</b>	<b>23.98 ± 7.06</b>	<b>527.14 ± 63.47</b>	<b>47.55 ± 10.74</b>	<b>574.69 ± 74.21</b>	<b>7.72 ± 0.62</b>	<b>11.52 ± 3.10</b>	<b>19.24 ± 2.48</b>	<b>584.61 ± 19.61</b>	<b>182.67 ± 59.88</b>	<b>767.28 ± 79.49</b>												

Antarctica

	T10												T48														
	Control						PAH						Control						PAH								
	Diss.	Part.	Total	Diss.	Part.	Total	Diss.	Part.	Total	Diss.	Part.	Total	Diss.	Part.	Total	Diss.	Part.	Total									
FL	1.03 ± 0.08	0.10 ± 0.01	1.13 ± 0.09	198.85 ± 94.93	0.83 ± 0.40	199.68 ± 95.33	1.72 ± 0.29	0.14 ± 0.00	1.86 ± 0.29	0.00 ± 0.00	0.37 ± 0.20	0.37 ± 0.20	0.17 ± 0.03	0.01 ± 0.00	0.18 ± 0.03	104.94 ± 7.36	0.74 ± 0.05	105.28 ± 7.41	0.15 ± 0.05	0.01 ± 0.00	0.17 ± 0.04	22.06 ± 1.18	0.03 ± 0.01	0.03 ± 0.01	22.10 ± 1.19		
ANT	0.17 ± 0.03	0.01 ± 0.00	0.18 ± 0.03	104.94 ± 7.36	0.74 ± 0.05	105.28 ± 7.41	0.15 ± 0.05	0.01 ± 0.00	0.17 ± 0.04	22.06 ± 1.18	0.03 ± 0.01	22.10 ± 1.19	0.03 ± 0.01	0.00 ± 0.00	0.03 ± 0.01	3.10 ± 0.02	0.08 ± 0.02	3.18 ± 0.46	0.68 ± 0.02	0.21 ± 0.03	3.16 ± 0.28	8.89 ± 0.61	0.34 ± 0.17	9.23 ± 0.45			
PHE	3.10 ± 0.45	0.08 ± 0.02	3.18 ± 0.46	94.19 ± 2.58	0.68 ± 0.02	94.86 ± 2.60	2.95 ± 0.31	0.21 ± 0.03	3.16 ± 0.28	8.89 ± 0.61	0.34 ± 0.17	9.23 ± 0.45	0.08 ± 0.01	0.09 ± 0.01	0.92 ± 0.02	269.89 ± 1.05	4.35 ± 0.02	274.25 ± 1.07	0.85 ± 0.06	0.08 ± 0.00	0.93 ± 0.07	48.12 ± 7.92	0.56 ± 0.29	0.56 ± 0.29	48.68 ± 8.22		
PYR	0.88 ± 0.08	0.04 ± 0.01	0.92 ± 0.09	341.53 ± 9.94	4.35 ± 0.82	350.98 ± 10.76	0.78 ± 0.04	0.03 ± 0.00	0.81 ± 0.05	51.36 ± 10.27	0.30 ± 0.13	51.66 ± 10.39	0.04 ± 0.00	0.01 ± 0.00	0.05 ± 0.04	57.86 ± 9.94	4.80 ± 0.82	62.66 ± 10.76	0.12 ± 0.04	0.02 ± 0.00	0.15 ± 0.04	48.69 ± 1.07	2.32 ± 0.33	2.32 ± 0.33	51.02 ± 1.40		
FLT	0.74 ± 0.08	0.02 ± 0.00	0.76 ± 0.08	341.53 ± 9.94	4.35 ± 0.82	350.98 ± 10.76	0.78 ± 0.04	0.03 ± 0.00	0.81 ± 0.05	51.36 ± 10.27	0.30 ± 0.13	51.66 ± 10.39	0.04 ± 0.00	0.01 ± 0.00	0.05 ± 0.04	145.52 ± 16.80	12.80 ± 1.48	158.31 ± 18.28	0.32 ± 0.04	0.00 ± 0.00	0.32 ± 0.04	121.75 ± 0.85	2.10 ± 0.42	2.10 ± 0.42	123.85 ± 1.27		
CRY	0.09 ± 0.00	0.01 ± 0.00	0.10 ± 0.01	57.86 ± 9.94	4.80 ± 0.82	62.66 ± 10.76	0.12 ± 0.04	0.02 ± 0.00	0.15 ± 0.04	48.69 ± 1.07	2.32 ± 0.33	51.02 ± 1.40	0.00 ± 0.00	0.00 ± 0.00	0.00 ± 0.00	145.52 ± 16.80	12.80 ± 1.48	158.31 ± 18.28	0.32 ± 0.04	0.00 ± 0.00	0.32 ± 0.04	121.75 ± 0.85	2.10 ± 0.42	2.10 ± 0.42	123.85 ± 1.27		
BaA	0.29 ± 0.00	0.00 ± 0.00	0.29 ± 0.00	38.07 ± 4.50	3.48 ± 0.41	41.55 ± 4.91	0.00 ± 0.00	0.01 ± 0.01	0.01 ± 0.01	23.83 ± 1.12	5.89 ± 0.73	29.73 ± 1.84	0.00 ± 0.00	0.00 ± 0.00	0.00 ± 0.00	38.07 ± 4.50	3.48 ± 0.41	41.55 ± 4.91	0.00 ± 0.00	0.01 ± 0.01	0.01 ± 0.01	10.81 ± 1.12	2.91 ± 0.73	2.91 ± 0.73	13.72 ± 1.84		
BbF	0.00 ± 0.00	0.00 ± 0.00	0.00 ± 0.00	15.74 ± 2.99	2.72 ± 0.52	18.46 ± 3.50	0.00 ± 0.00	0.01 ± 0.01	0.01 ± 0.01	0.58 ± 0.01	0.47 ± 0.01	1.04 ± 0.01	0.00 ± 0.00	0.00 ± 0.00	0.00 ± 0.00	15.74 ± 2.99	2.72 ± 0.52	18.46 ± 3.50	0.00 ± 0.00	0.01 ± 0.01	0.01 ± 0.01	23.83 ± 1.12	5.89 ± 0.73	5.89 ± 0.73	29.73 ± 1.84		
BkF	0.00 ± 0.00	0.00 ± 0.00	0.00 ± 0.00	35.69 ± 4.25	6.40 ± 0.76	42.09 ± 5.01	0.00 ± 0.00	0.01 ± 0.01	0.01 ± 0.01	0.58 ± 0.01	0.47 ± 0.01	1.04 ± 0.01	0.00 ± 0.00	0.00 ± 0.00	0.00 ± 0.00	35.69 ± 4.25	6.40 ± 0.76	42.09 ± 5.01	0.00 ± 0.00	0.01 ± 0.01	0.01 ± 0.01	23.83 ± 1.12	5.89 ± 0.73	5.89 ± 0.73	29.73 ± 1.84		
BaP	0.00 ± 0.00	0.00 ± 0.00	0.00 ± 0.00	9.29 ± 1.05	3.40 ± 0.39	12.70 ± 1.44	0.00 ± 0.00	0.00 ± 0.00	0.00 ± 0.00	4.71 ± 1.05	0.00 ± 0.00	4.71 ± 1.05	0.00 ± 0.00	0.00 ± 0.00	0.00 ± 0.00	9.29 ± 1.05	3.40 ± 0.39	12.70 ± 1.44	0.00 ± 0.00	0.00 ± 0.00	0.00 ± 0.00	4.71 ± 1.05	0.00 ± 0.00	0.00 ± 0.00	4.71 ± 1.05		
DBA	0.00 ± 0.00	0.01 ± 0.01	0.03 ± 0.02	25.22 ± 4.28	10.77 ± 1.83	36.00 ± 6.11	0.01 ± 0.01	0.02 ± 0.01	0.03 ± 0.01	19.50 ± 0.92	9.53 ± 1.28	29.03 ± 2.20	0.00 ± 0.00	0.02 ± 0.00	0.02 ± 0.00	25.22 ± 4.28	10.77 ± 1.83	36.00 ± 6.11	0.01 ± 0.01	0.02 ± 0.01	0.03 ± 0.01	19.50 ± 0.92	9.53 ± 1.28	9.53 ± 1.28	29.03 ± 2.20		
IPY	0.02 ± 0.00	0.02 ± 0.00	0.04 ± 0.00	8.29 ± 0.89	3.90 ± 0.42	12.20 ± 1.30	0.00 ± 0.00	0.02 ± 0.00	0.02 ± 0.00	4.37 ± 0.71	2.21 ± 0.38	6.58 ± 1.09	0.00 ± 0.00	0.00 ± 0.00	0.00 ± 0.00	8.29 ± 0.89	3.90 ± 0.42	12.20 ± 1.30	0.00 ± 0.00	0.02 ± 0.00	0.02 ± 0.00	4.37 ± 0.71	2.21 ± 0.38	2.21 ± 0.38	6.58 ± 1.09		
Bghp	0.00 ± 0.00	0.02 ± 0.00	0.02 ± 0.00	8.29 ± 0.89	3.90 ± 0.42	12.20 ± 1.30	0.00 ± 0.00	0.02 ± 0.00	0.02 ± 0.00	4.37 ± 0.71	2.21 ± 0.38	6.58 ± 1.09	0.00 ± 0.00	0.00 ± 0.00	0.00 ± 0.00	8.29 ± 0.89	3.90 ± 0.42	12.20 ± 1.30	0.00 ± 0.00	0.02 ± 0.00	0.02 ± 0.00	4.37 ± 0.71	2.21 ± 0.38	2.21 ± 0.38	6.58 ± 1.09		
<b>TOTAL</b>	<b>6.31 ± 0.72</b>	<b>0.30 ± 0.04</b>	<b>6.61 ± 0.76</b>	<b>1344.69 ± 45.78</b>	<b>64.32 ± 6.26</b>	<b>1409.01 ± 39.52</b>	<b>6.91 ± 0.67</b>	<b>0.54 ± 0.06</b>	<b>7.45 ± 0.61</b>	<b>387.93 ± 24.91</b>	<b>27.76 ± 4.71</b>	<b>410.59 ± 28.58</b>															

**Table S4.** Pfam profiles of proteins involved in PAH degradation and horizontal gene transfer. (Pfam: The protein families database number)

Pfam	Function	Name
PF00848	Upstream PAH degradation pathway	Ring-hydroxylating dioxygenase
PF00171		Salicylaldehyde dehydrogenase
PF00596		3,4-dihydroxyphthalate decarboxylase
PF00701		Dihydrodipicolinate synthetase
PF00775		Protocatechuate 3,4-dioxygenase beta chain
PF00106		1,6-dihydroxycyclohexa-2,4-diene-1-carboxylate dehydrogenase
PF00903		Glyoxalase dioxygenase
PF01323		2-hydroxychromene-2-carboxylate isomerase
PF01494		Salicylate hydroxylase
PF09084		4,5-dihydroxyphthalate decarboxylase
PF00561	Catechol degradation pathway	2-hydroxymuconate semialdehyde hydrolase
PF00903		Metapyrocatechase
PF02746		Muconate cycloisomerase 1
PF04444		Catechol 1,2-dioxygenase
PF07836		4-hydroxy-2-oxovalerate aldolase
PF02426		Muconolactone Delta-isomerase
PF00206	Benzoate and protocatechuate degradation pathway	3-carboxy-cis,cis-muconate cycloisomerase
PF00561		3-oxoadipate enol-lactonase
PF01144		Coenzyme A transferase
PF02627		4-carboxymuconolactone decarboxylase
PF00665	DNA transposons	Retroviral integrase (rve)
PF01609		Transposase 11 superfamily (DDE_Tnp_1)
PF00589		Phage integrase
PF01797		Transposase 17 (Y1_Tnp)
PF05717		Transposase 34 (TnpB_IS66)
PF04986		Transposase 32 (Y2_Tnp)

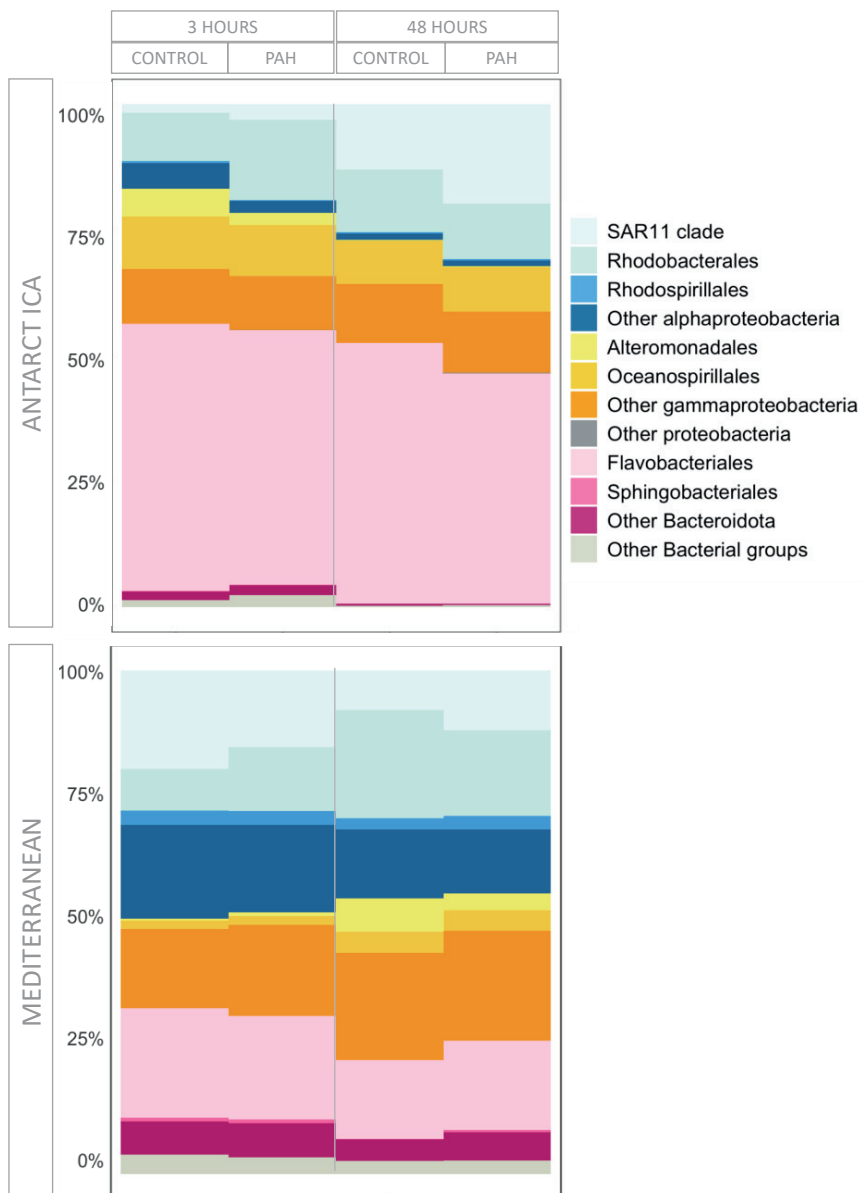
**Table S5.** Community composition of microbial communities at final time point (T48) measured by 16S rRNA gene amplicon sequencing (Relative abundances in % of total reads and variability expressed in standard deviation, HC : Hydrocarbonoclastic). Notice that counts of general taxonomical groups include HC bacteria.

	Antarctica		Mediterranean	
	Control	PAH	Control	PAH
Alphaproteobacteria	26.96 ± 2.74	32.23 ± 0.41	44.50 ± 0.63	43.22 ± 2.47
SAR11 clade	12.97 ± 4.09	19.61 ± 2.70	7.82 ± 0.67	11.61 ± 1.07
Rhodobacterales	12.53 ± 7.05	11.20 ± 2.62	21.14 ± 1.72	16.50 ± 1.23
Rickettsiales	0.58 ± 0.08	0.31 ± 0.08	2.39 ± 0.41	2.49 ± 0.21
Gammaproteobacteria	20.55 ± 1.09	21.41 ± 1.78	31.55 ± 0.92	28.64 ± 2.27
Alteromonadales	0.08 ± 0.06	0.08 ± 0.04	6.44 ± 1.31	3.16 ± 0.46
Cellvibrionales	4.75 ± 0.92	4.45 ± 0.41	8.69 ± 0.33	6.71 ± 0.70
Oceanospirillales	8.59 ± 0.61	8.95 ± 1.29	4.12 ± 0.34	3.97 ± 0.68
Pseudomonadales	0.03 ± 0.02	0.10 ± 0.04	0	0
Thiotrichales	0.54 ± 0.05	0.59 ± 0.03	0	0
Bacteroidota	52.21 ± 3.74	45.98 ± 2.16	19.72 ± 0.41	23.28 ± 0.11
Sphingobacteriales	0	0.01 ± 0.00	0.12 ± 0.04	0.41 ± 0.09
Flavobacteriales	51.84 ± 3.75	45.63 ± 2.15	15.44 ± 0.67	17.35 ± 0.11
Cyanobacteria	0	0	1.63 ± 0.15	2.19 ± 0.15
Other Bacterial groups	0.03 ± 0.03	0.06 ± 0.02	0.15 ± 0.01	0.42 ± 0.06
HC Actinobacteria	0.05	0.01 ± 0.00	0.22 ± 0.11	0.04 ± 0.01
<i>Arthrobacter</i>	0.05	0.02	0.22 ± 0.11	0.03
HC Alphaproteobacteria	7.17 ± 6.14	5.89 ± 2.74	2.85 ± 0.25	2.14 ± 0.24
<i>Jannaschia</i>	0	0	2.68 ± 0.16	2.05 ± 0.26
HC Gammaproteobacteria	0.09 ± 0.04	0.15 ± 0.05	11.32 ± 0.73	10.67 ± 2.28
HC Alteromonadales	0.06 ± 0.03	0.05 ± 0.05	4.41 ± 0.98	2.13 ± 0.26
<i>Colwellia</i>	0.05 ± 0.01	0.04 ± 0.03	0	0
<i>Glaciecola</i>	0	0.01	1.50 ± 0.52	0.53 ± 0.22
<i>Thalassotalea</i>	0	0.01	0.45 ± 0.17	0.13 ± 0.04
<i>Pseudoalteromonas</i>	0.02	0.04	1.28 ± 0.07	0.89 ± 0.12
HC Pseudomonadales	0.03 ± 0.02	0.10 ± 0.04	0	0
<i>Pseudomonas</i>	0	0.04 ± 0.03	0	0
HC Vibrionales	0	0	6.16 ± 0.56	7.51 ± 1.77
HC Bacteroidia	0.03 ± 0.02	0.03 ± 0.03	0	0
All HCB	7.31 ± 6.13	6.06 ± 2.71	14.39 ± 1.09	12.85 ± 2.13

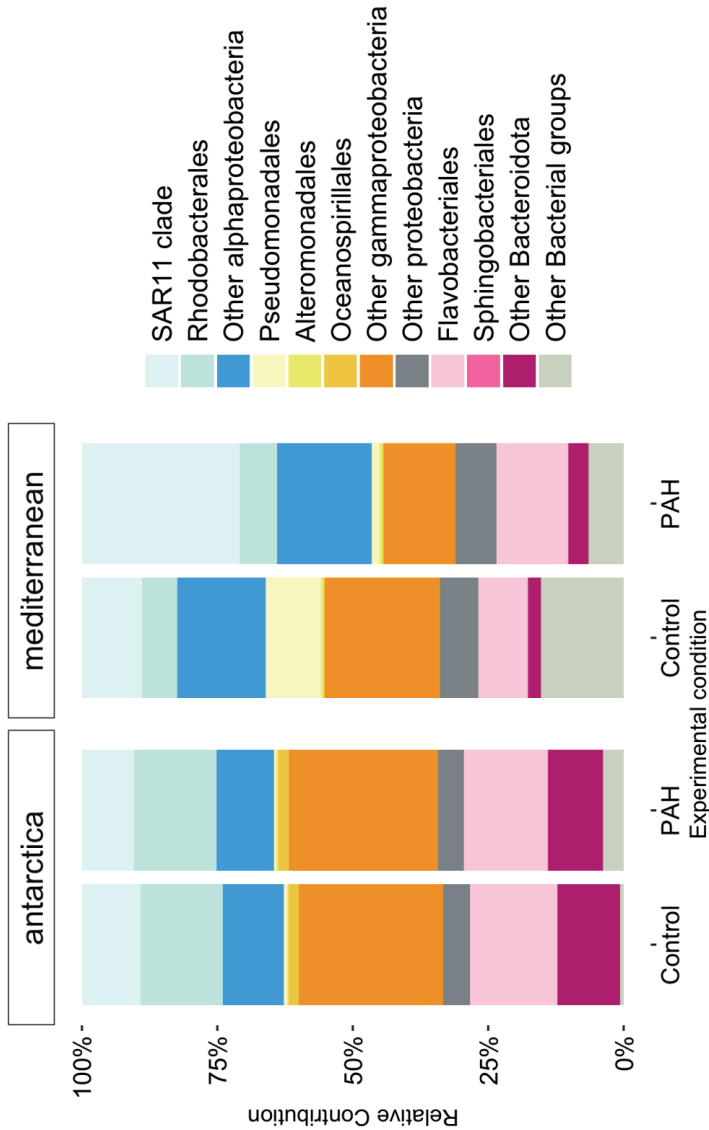
**Table S6.** Subset of genera including previously reported hydrocarbonoclastic bacterial strains or strains found in oil polluted marine environments (Karthikeyan et al., 2020, Lozada et al., 2014, Takahashi et al., 2013) detected in the experimental dataset of both sites. Grey boxes indicate presence of that strain in that site. (HC : Hydrocarbonoclastic, Ant: Antarctica, Med: Mediterranean)

Label	Genera	Ant	Med
HC Actinobacteria	<i>Arthrobacter</i>		
	<i>Nocardioides</i>		
HC Alphaproteobacteria	<i>Jannaschia</i>		
	<i>Roseovarius</i>		
	<i>Sphingomonas</i>		
	<i>Sulfitobacter</i>		
	<i>Tropicibacter</i>		
HC Bacilli	<i>Bacillus</i>		
HC Bacteroidia	<i>Flavobacterium</i>		
	<i>Nonlabens</i>		
	<i>Paludibacter</i>		
HC Bdellovibrionia	<i>Bdellovibrio</i>		
	<i>Halobacteriovorax</i>		
HC Fusobacteriia	<i>Psychrilyobacter</i>		
HC Gammaproteobacteria	<i>Acinetobacter</i>		
	<i>Alkanindiges</i>		
	<i>Alteromonas</i>		
	<i>Bermanella</i>		
	<i>Colwellia</i>		
	<i>Delftia</i>		
	<i>Glaciecola</i>		
	<i>Kangiella</i>		
	<i>Marinobacter</i>		
	<i>Marinomonas</i>		
	<i>Neptuniibacter</i>		
	<i>Neptunomonas</i>		
	<i>Oleibacter</i>		
	<i>Oleiphilus</i>		
	<i>Oleispira</i>		
	<i>Pseudoalteromonas</i>		
	<i>Pseudomonas</i>		
	<i>Psychrobacter</i>		
	<i>Shewanella</i>		
	<i>Thalassolituus</i>		
<i>Thalassotalea</i>			
<i>Vibrio</i>			
<i>Woeseia</i>			

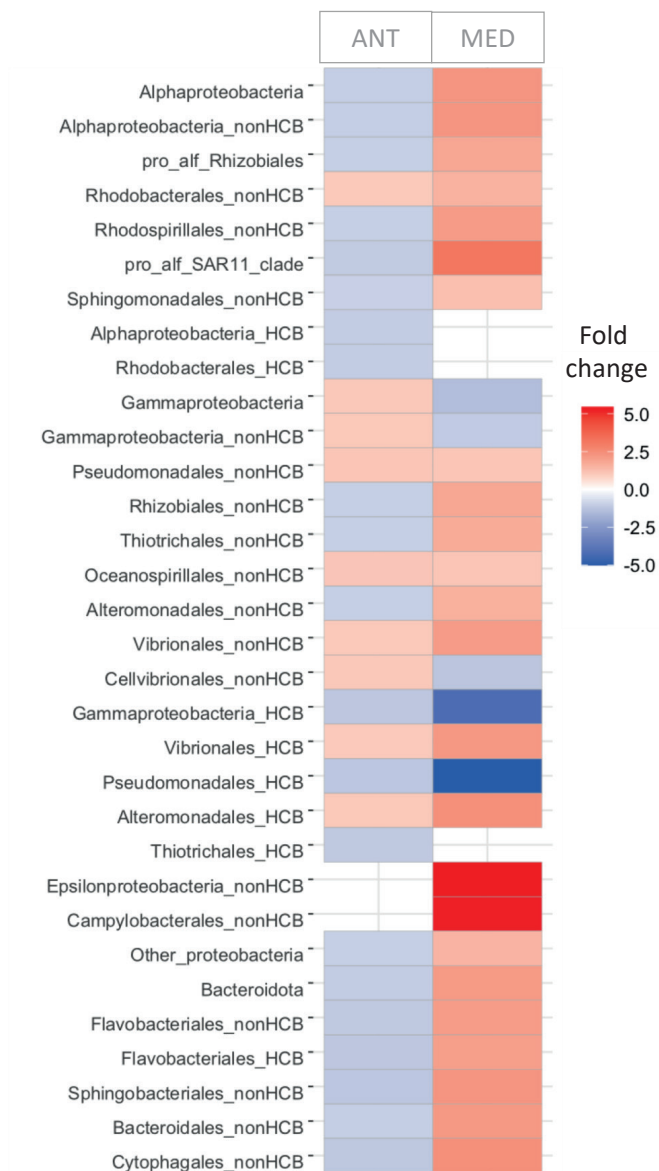
**Figure S1.** Taxonomical composition of free living bacteria for each experimental site and sampling time point for PAH exposure and control samples.



**Figure S2.** Metatranscripts taxonomical assignment 3 h after PAH exposure. (\*PERMANOVA shows no differences in ORFs between treatment and control)

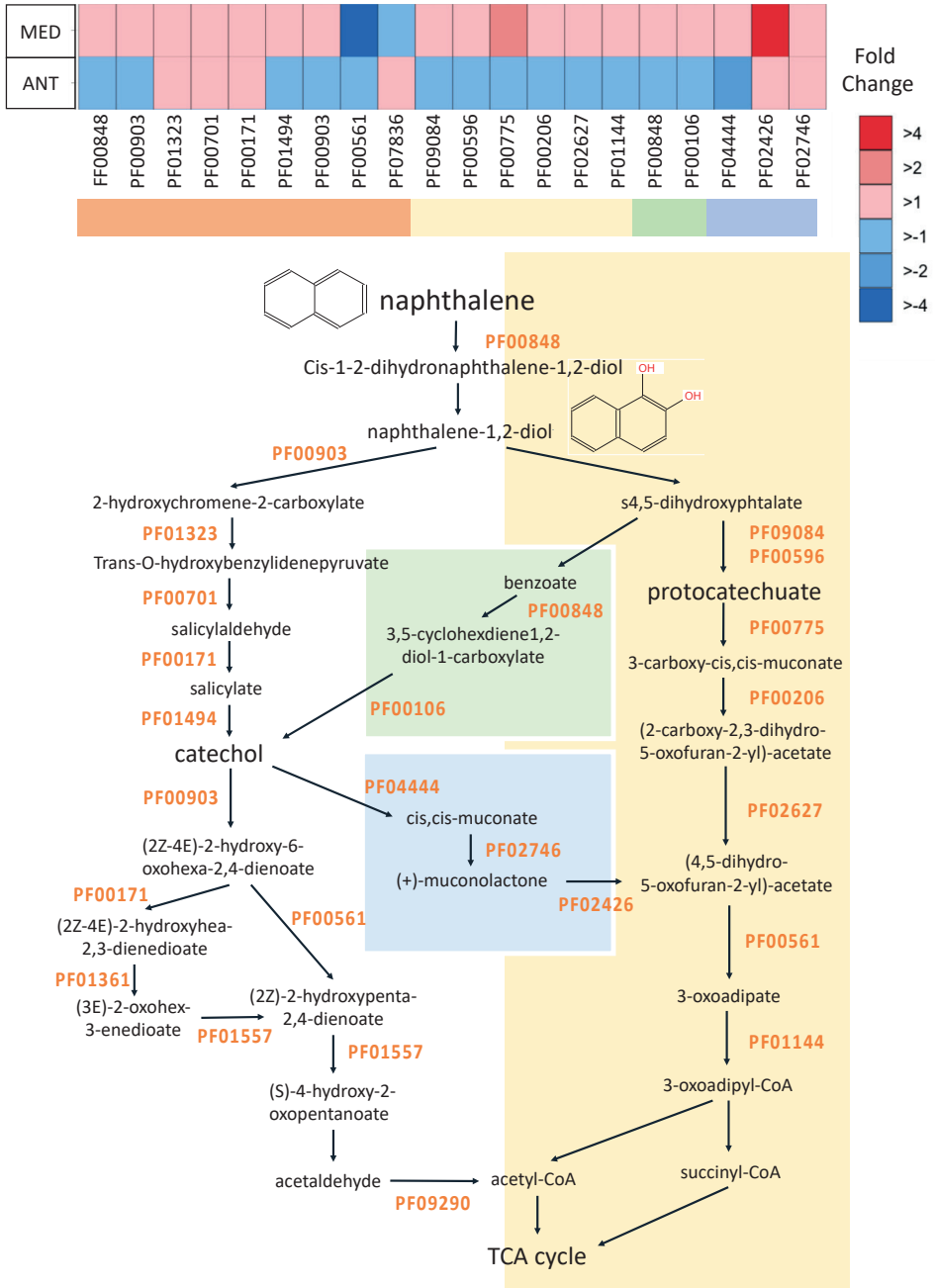


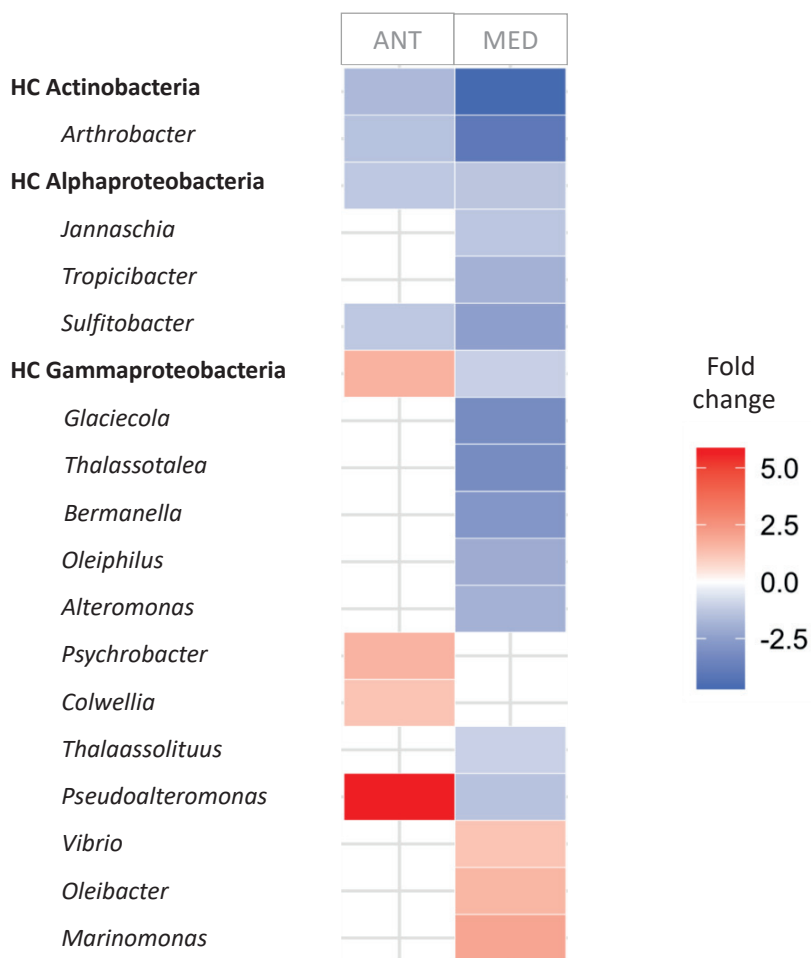
**Figure S3.** Metatranscriptomes taxonomic affiliation fold changes between PAH and control treatments after 3 h of PAH exposure. (HCB includes only HCB strains, nonHCB exclude all HCB strains within that group) (no taxonomic significant differences in relative transcript contribution between control and treatments)



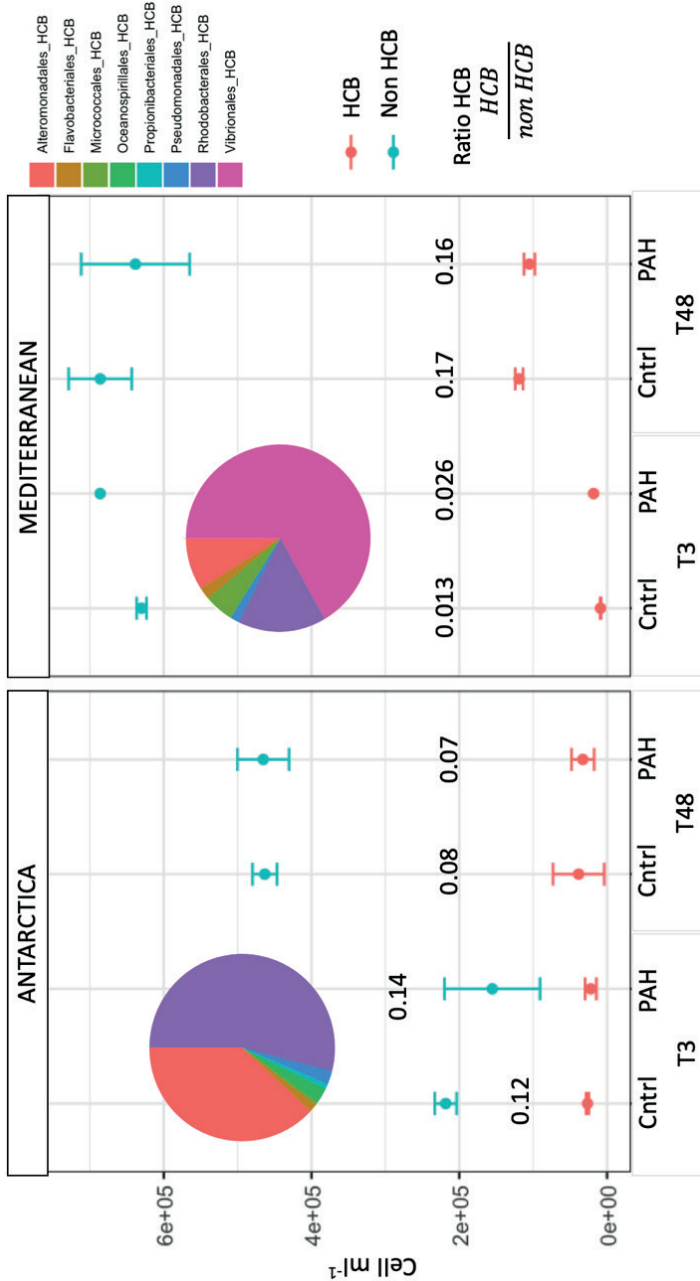


**Figure S4.** Fold-change in expression of genes involved in PAH degradation between PAH treatments and controls measured by metatranscriptomics. PAH degradation pathway is represented for the naphthalene (model and simplest PAH compound). The list of the specific Pfam profiles involved in PAH degradation is listed in Table S4.



**Figure S5.** Fold change 16S HCB at time 48 between control and PAH exposed community.

**Figure S6.** Contribution of ASV corresponding to hydrocarbonoclastic bacteria (HCB) over the ASV assigned to non hydrocarbonoclastic bacteria, normalized by bacterial abundance counts. Color plots shows the averaged HCB population composition 3 hours after the beginning of the incubation.



## ADDITIONAL REFERENCES

Karhikeyan, S., Rodriguez-R, L.M., Heritier-Robbins, P., Hatt, J.K., Huettel, M., Kostka, J.E., and Konstantinidis, K.T. (2020) Genome repository of oil systems: An interactive and searchable database that expands the catalogued diversity of crude oil-associated microbes. *Environ Microbiol* 22: 2094–2106.

Lozada, M., Marcos, M.S., Commendatore, M.G., Gil, M.N., and Dionisi, H.M. (2014) The bacterial community structure of hydrocarbon-polluted marine environments as the basis for the definition of an ecological index of hydrocarbon exposure. *Microbes Environ* 29: 269–76.

Takahashi, S., Abe, K., and Ker, Y. (2013) Microbial Degradation of Persistent Organophosphorus Flame Retardants. In *Environmental Biotechnology - New Approaches and Prospective Applications*. InTech.



## **Supporting information of Chapter 3**

**Table S1.** Coordinates of the sampling stations from South Bay, Livingston Island.

Station	Coordinates	
	S	W
St-1	62°38.792'	60°38.411'
St-2	62°38.346'	60°23.912'
St-3	62°39.425'	60°23.277'
St-4	62° 39.556'	60° 22.132'
St-5	62°37.718'	060°21.40'

**Table S2.** Ancillary data for the seawater sampling sites.

Date	Sampling station	Fluorescence (RFU)	Salinity (PSU)	Temperature (°C)	Turbidity (FTU)
08/01/2018	St-4	n.d	n.d	n.d	n.d
16/01/2018	St-4	n.d	n.d	n.d	n.d
18/01/2018	St-3	0.27	33.49	1.56	10.11
19/01/2018	St-4	0.27	33.49	1.56	10.11
20/01/2018	St-2	0.66	34.14	1.60	3.56
22/01/2018	St-4	0.40	33.30	1.42	7.84
24/01/2018	St-2	0.88	33.94	2.23	3.66
25/01/2018	St-4	0.27	33.46	1.71	5.85
27/01/2018	St-2	0.31	33.68	2.43	4.86
29/01/2018	St-4	0.58	33.49	1.87	6.04
03/02/2018	St-2	0.15	34.75	1.59	3.55
05/02/2018	St-4	0.44	33.61	1.47	6.41
08/02/2018	St-1	n.d	n.d	n.d	n.d
12/02/2018	St-2	0.18	33.67	1.76	7.11
16/02/2018	St-4	0.23	33.26	1.78	7.44
20/02/2018	St-2	0.23	33.86	2.93	3.87
23/02/2018	St-4	0.19	33.16	1.82	9.83
28/02/2018	St-5	0.28	33.63	1.14	5.44
01/03/2018	St-1	n.d	n.d	n.d	n.d
<i>Averaged by station</i>					
	St-1	n.d	n.d	n.d	n.d
	St-2	0.4±0.3	34.01±0.41	2.09±0.54	4.43±1.4
	St-3	0.27	33.49	1.56	10.11
	St-4	0.32±0.14	33.38±0.15	1.67±0.17	7.62±1.62
	St-5	0.28	33.63	1.14	5.44

**Table S3.** Meteorological conditions for each sampling event. The values were averaged coinciding the sampling hours (From 9 am to 11.30 am).

Date	Wind speed (m/s)	Wind direction (°)	Temperature (°C)	Minimum temp. (°C)	Maximum temp. (°C)	Relative humidity (%)	Precipitation (mm)	Atmospheric pressure (hPa)	Radiation (Wm <sup>-2</sup> )
08/01/2018	1.2	250.4	1.9	1.8	2.0	88.6	0.0	1000.9	137.5
11/01/2018	2.0	203.4	2.4	2.2	2.6	95.9	0.0	980.4	86.1
16/01/2018	3.7	56.3	2.7	2.6	2.8	89.9	0.0	978.3	107.4
17/01/2018	0.7	197.3	2.3	2.2	2.5	93.2	0.0	978.8	67.4
18/01/2018	1.3	160.9	1.3	1.1	1.4	88.5	0.0	989.3	98.0
19/01/2018	1.1	156.8	3.0	2.9	3.2	90.9	0.0	978.2	6.7
20/01/2018	n.d.	n.d.	n.d.	n.d.	n.d.	n.d.	n.d.	n.d.	n.d.
22/01/2018	3.1	0.0	1.9	1.8	2.0	92.8	0.0	973.8	29.2
24/01/2018	3.6	18.6	1.8	1.8	1.9	93.9	0.0	985.8	50.7
25/01/2018	1.4	102.5	2.7	2.6	2.8	92.5	0.0	984.5	33.8
27/01/2018	1.5	65.7	2.7	2.6	2.8	75.9	0.0	990.6	153.8
29/01/2018	4.6	53.9	5.6	5.4	5.7	74.3	0.0	979.1	136.6
03/02/2018	1.6	50.8	3.0	3.1	3.0	92.9	0.0	977.2	18.0
05/02/2018	1.0	188.3	2.4	2.3	2.6	88.4	0.0	987	126.8
06/02/2018	6.5	0.0	3.0	2.9	3.5	95.4	0.1	980.9	14.5
08/02/2018	3.9	32.7	2.5	2.4	4.2	93.0	0.0	973.4	23.9
12/02/2018	0.4	131.8	3.4	1.4	3.2	91.1	0.0	974.3	39.1
16/02/2018	4.0	33.5	4.1	3.4	4.0	88.0	0.0	986.4	21.4
20/02/2018	6.7	22	1.4	1.3	1.3	88.4	0.0	997.7	41.8
23/02/2018	1.8	74.4	3.3	3.2	3.2	94.6	0.0	992.0	22.5
28/02/2018	2.8	155.8	0.6	0.6	0.7	84.3	0.0	991.4	38
01/03/2018	1.5	52.1	3.1	3.0	3.3	91.1	0.0	970.1	19.5



**Table S4.** Inorganic nutrient concentrations and PFOS concentrations for the SML and SSL and for each sampling event. PFOS is taken as surrogate of ADOC and SML occurrence.

Date	Sampling Station	sea layer	Inorganic nutrients			Proxy of ADOC and SML stability
			N-NH <sub>4</sub> <sup>+</sup> (µmol L <sup>-1</sup> )	NO <sub>3</sub> + NO <sub>2</sub> (µmol L <sup>-1</sup> )	-PO <sub>4</sub> <sup>3-</sup> (µmol L <sup>-1</sup> )	PFOS (µg L <sup>-1</sup> )
08/01/2018	St-4	sml	n.d	n.d	n.d	n.d
		ssl	7.65±7.42	9.56±1.08	1.06±0.1	n.d
16/01/2018	St-4	sml	2.43	22.21	1.71	85
		ssl	10.8±9.23	19.83±2.87	2.12±0.1	32.5
18/01/2018	St-3	sml	n.d	n.d	n.d	55
		ssl	5.43	14.6	1.26	17.5
19/01/2018	St-4	sml	6.89	14.52	1.68	40
		ssl	n.d	n.d	n.d	17.5
20/01/2018	St-2	sml	1.9	27.04	1.78	15
		ssl	1.97±0.27	26.15±1.39	1.69±0.09	16.25
22/01/2018	St-4	sml	5.24	21.36	1.78	15
		ssl	20.91±20.34	19.37±2.19	1.535±0.19	8.75
24/01/2018	St-2	sml	2.98	26.39	1.52	25
		ssl	2.65±1.14	26.83±0.13	1.87±0.13	8.75
25/01/2018	St-4	sml	n.d	n.d	n.d	60
		ssl	2.84±0.0	18.31±3.41	1.42±0.14	8.75
27/01/2018	St-2	sml	n.d	n.d	n.d	230
		ssl	2.52±1.81	23.27±7.12	1.4±0.06	8.75
29/01/2018	St-4	sml	3.04	24.3	1.87	35
		ssl	3.05±0.49	20.47±3.73	1.59±0.16	10
03/02/2018	St-2	sml	13.39	19.7	1.39	30
		ssl	10.44	16.4	1.68	17.5
05/02/2018	St-4	sml	11.29	18.6	1.89	n.d
		ssl	5.08±1.69	15.32±4.31	1.46±0.11	n.d
08/02/2018	St-1	sml	1.74	27.37	1.93	15
		ssl	3.07±1.48	23.36±3.43	1.62±0.18	12.5
12/02/2018	St-2	sml	1.31	23.08	1.55	20
		ssl	13.05±0.62	20.7±1.5	1.35±0.13	10
16/02/2018	St-4	sml	2.73	19.23	1.52	35
		ssl	9.76±0.58	17.75±1.35	1.32	33.75
20/02/2018	St-2	sml	n.d	n.d	n.d	25
		ssl	6.975±6.47	20.78±2.94	1.38±0.144	7.5
23/02/2018	St-4	sml	7.6±1.84	16.92±0.76	1.40±0.20	n.d
		ssl	8.51±5.34	14.53±3.26	1.26±0.11	n.d
28/02/2018	St-5	sml	n.d	n.d	n.d	n.d
		ssl	5.32±2.34	24.25±0.63	1.39±0.01	n.d
01/03/2018	St-1	sml	n.d	n.d	n.d	70
		ssl	1.12±0.02	10.6±0.75	1.16±0.1	22.5
<i>Averaged by station</i>						
St-1	sml		1.72±0.02	25.4±2.28	1.75±0.2	42.5±38.8
		ssl	2.09±1.43	16.98±7.2	1.39±0.28	17.5± 7.1
St-2	sml		4.08±4.96	24.2±2.78	1.65±0.24	64±93
		ssl	5.89±5.07	22.9±4.45	1.55±0.23	12.3±4.2
St-3	sml		2.83	26.79	1.8	55
		ssl	5.43	14.61	1.26	17.5
St-4	sml		5.61±2.99	18.95±3.07	1.64±0.2	43.8±21.9
		ssl	8.57±9.33	16.9±4.32	1.47±0.31	18.5± 11.1
St-5	ssl		5.32±2.34	24.25±0.63	1.39±0.01	n.d
TOTAL AVERAGED	sml		4.3 ± 3.7	22 ± 4.1	1.7 ± 0.2*	50.3±50.8
		ssl	6.3 ± 7	19.1 ± 5.4	1.4 ± 0.3*	16.5±8.7

**Table S5.** Subset of taxa, previously reported as bacterial ADOC degraders (AD) (Takahashi et al., 2013; Lozada et al., 2014), detected in our dataset from the maritime Antarctica. As these taxa have also been reported to exudate biosurfactants, the type of surfactants and citation is also given. In bold, marine biosurfactant-producing bacterial strains.

Label	Phylum/Class	Genus	Biosurfactant-producing bacteria	
Actinobacteria AD	Phylum: Actinobacteria	<i>Mycobacterium</i>	Polymeric surfactants	Vijayakumar and Saravanan, 2015
		<i>Nocardioides</i>		
		<i>Rhodococcus</i>	<b>Exopolysaccharides/complex surface active polymer producer</b>	Peng et al., 2007
		<i>Arthrobacter</i>	<b>Glycolipid surface active molecules</b>	Schulz et al., 1991
		<i>Gordonia</i>	Extracellular bioemulsifiers, and cell-bound glycolipid biosurfactants (isolated from hydrocarbon polluted site)	Franzetti et al., 2009
		<i>Microbacterium</i>	Biosurfactant (long chain fatty acid lipid type) (isolated from Amazonas river)	Silva Lima et al., 2017
		<i>Dietzia</i>	<b>Rhamnolipid</b>	Wang et al., 2014
		<i>Micrococcus</i>	Biosurfactant (isolated from waste water sludge)	Yilmaz et al., 2009
Alphaproteobacteria AD	Phylum: Proteobacteria Class: Alphaproteobacteria	<i>Sulfitobacter</i>		
		<i>Sphingopyxis</i>	Biosurfactant (Contaminated soil)	Saisa-ard et al., 2013
		<i>Sphingomonas</i>	Polymeric surfactant	Santos et al., 2016
		<i>Roseovarius</i>	<b>Biosurfactant</b>	Antoniou et al., 2015
		<i>Roseobacter</i>		
		<i>Sphingobium</i>	Biourfactant (Contaminated soil)	Saisa-ard et al., 2013
		<i>Tropicibacter</i>		
		<i>Novosphingobium</i>		
		<i>Jannaschia</i>		
		<i>Ochrobactrum</i>	Biosurfactant	Zarinviarsagh et al., 2017 Domingues et al., 2020
		<i>Thalassospira</i>	<b>Biosurfactant</b>	Antoniou et al., 2015
<i>Kordiimonas</i>				
Bacilli AD	Phylum: Firmicutes Class: Bacilli	<i>Bacillus</i>	<b>Exopolysaccharide, complex surface active polymer/polymeric surfactants</b>	Das et al., 2008
Betaproteobacteria AD	Phylum: Proteobacteria Class: Betaproteobacteria	<i>Acidovorax</i>		
		<i>Comamonas</i>	Biosurfactant (From agricultural soil)	Sun et al., 2013
		<i>Polaromonas</i>		
		<i>Ralstonia</i>	Biosurfactant (from Petroleum waste)	Plaza et al., 2007
		<i>Delftia</i>	glycolipids Surfactant (from Oilfield water injection)	Lenchi et al., 2020
		<i>Alcaligenes</i>	Biosurfactant (from Petroleum waste)	Plaza et al., 2007

Label	Phylum/Class	Genus	Biosurfactant-producing bacteria	
Cytophagia AD	Phylum: Bacteroidetes Class: Cytophagia	<i>Cytophaga</i>		
Deltaproteobacteria AD	Phylum: Proteobacteria Class: Deltaproteobacteria	<i>Desulfatiferula</i>		
		<i>Desulfococcus</i>		
		<i>Desulfatibacillum</i>		
		<i>Desulfobacterium</i>		
Flavobacteriia AD	Phylum: Bacteroidetes Class: Flavobacteriia	<i>Flavobacterium</i>	Biosurfactant (From contaminated arid soils)	Bodour <i>et al.</i> , 2003
Gammaproteobacteria AD	Phylum: Proteobacteria Class: Gammaproteobacteria	<i>Pseudoalteromonas</i>	<b>Exopolysaccharides/complex Surface active polymer</b>	Roca <i>et al.</i> , 2016
		<i>Pseudomonas</i>	<b>Polymeric biosurfactant/bioemulsifier, lipopeptides, glycolipids and particulate surfactant</b>	Wittgens <i>et al.</i> , 2017
		<i>Colwellia</i>	<b>Biosurfactant</b>	Mapelli <i>et al.</i> , 2017
		<i>Cycloclasticus</i>	<b>Biosurfactant</b>	Mapelli <i>et al.</i> , 2017
		<i>Alkanindiges</i>		
		<i>Acinetobacter</i>	<b>Polymeric biosurfactant/bioemulsifier</b>	Rosenberg <i>et al.</i> , 1988
		<i>Oleispira</i>		
		<i>Shewanella</i>	<b>Biosurfactant</b>	Antoniou <i>et al.</i> , 2015
		<i>Halomonas</i>	<b>Polymeric biosurfactant/bioemulsifier, glycolipid surface active molecules and Exopolysaccharides (complex Surface active polymer)</b>	Gutiérrez <i>et al.</i> , 2007
		<i>Vibrio</i>	<b>Exopolysaccharides (complex Surface active polymer )</b>	Satpute <i>et al.</i> , 2010
		<i>Oleibacter</i>		
		<i>Alteromonas</i>	<b>Biosurfactant</b>	Satpute <i>et al.</i> , 2010
		<i>Microbulbifer</i>		
		<i>Neptunomonas</i>		
		<i>Thalassolituus</i>		
<i>Marinobacter</i>	<b>Polymeric biosurfactant/bioemulsifier</b>	Domingues <i>et al.</i> 2020		
<i>Alcanivorax</i>	<b>Glycolipid surface active molecules (rhamnolipid and sophorolipid)</b>	Abraham <i>et al.</i> , 1998		
All AD		*Includes all listed above		

**Figure S1.** Nutrient and PFOS concentrations in the SML and SSL during the austral summer. Gray background indicates those days with SML disruption. Average wind speed and solar radiation measurements are also shown.

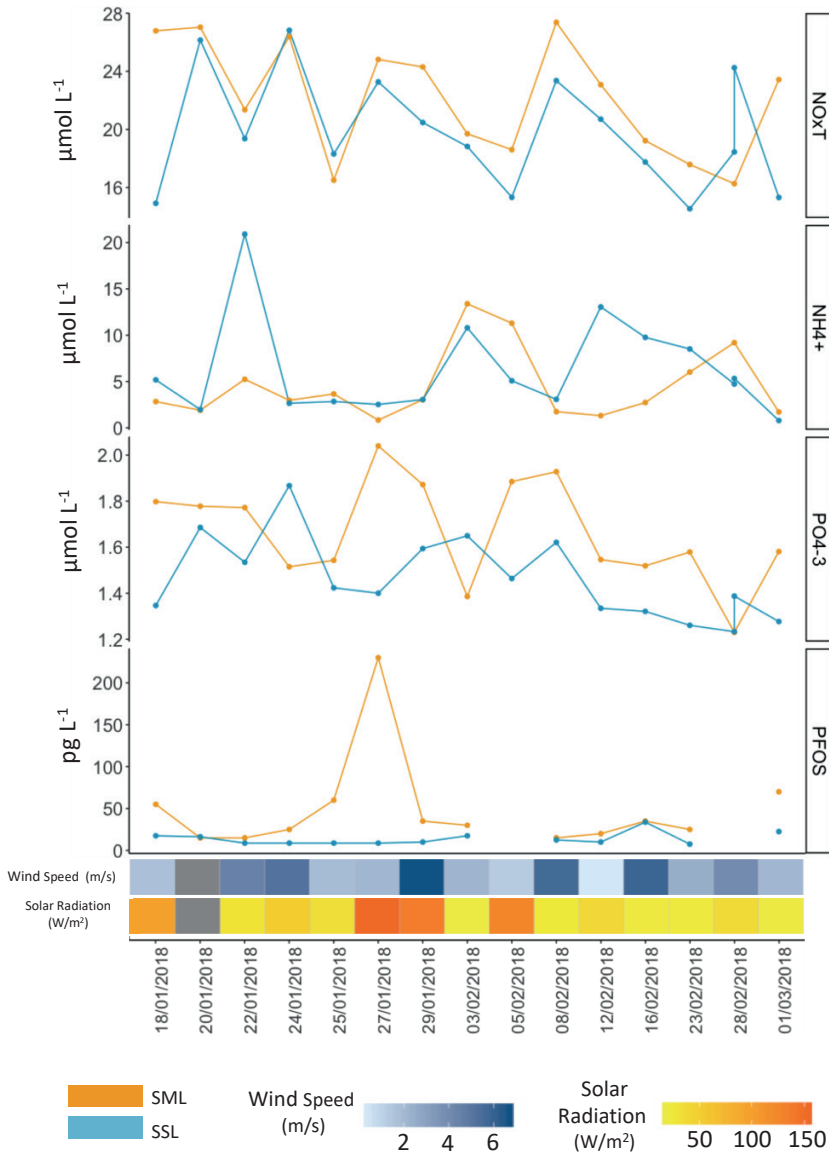


**Figure S2.** Relative abundances of the dominant taxonomical groups at the SML and in SSL for each sampling station.

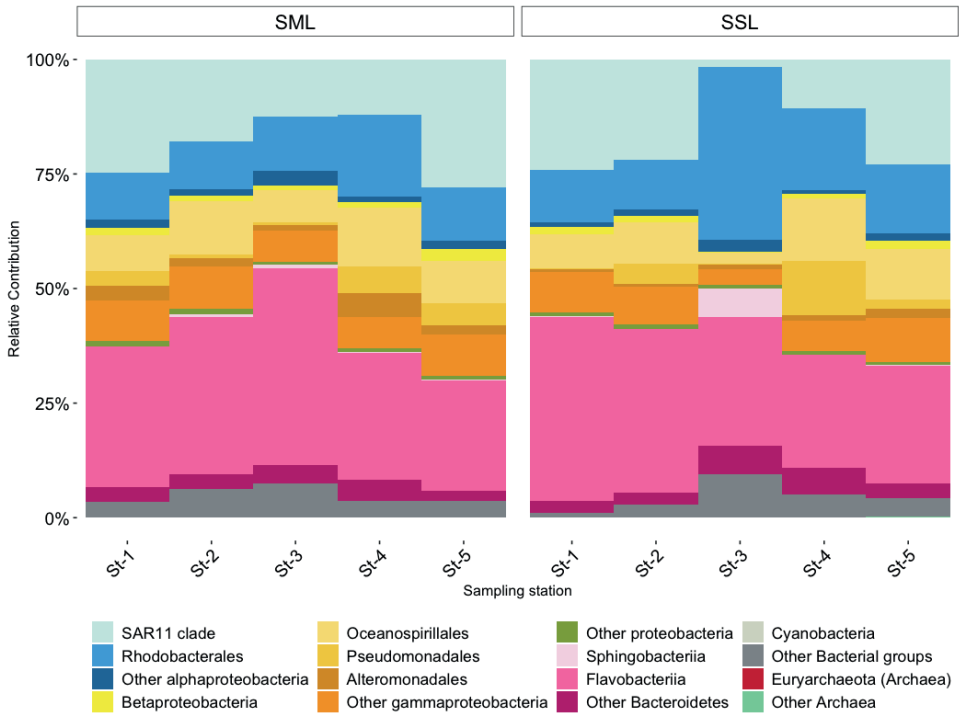


**Figure S3.** Relative abundance of the dominant taxonomical groups in the SML and SSL during the austral summer. Average wind speed and solar radiation measurements are also shown.

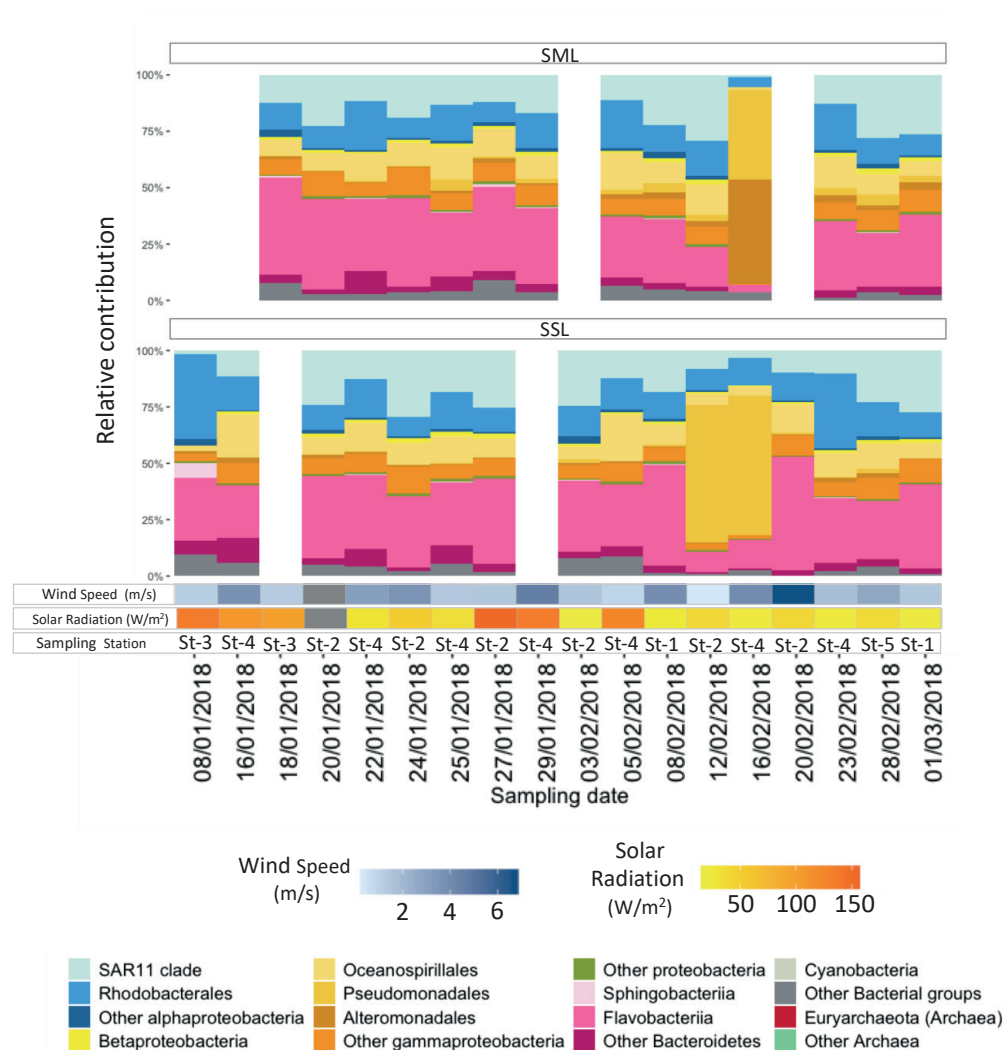
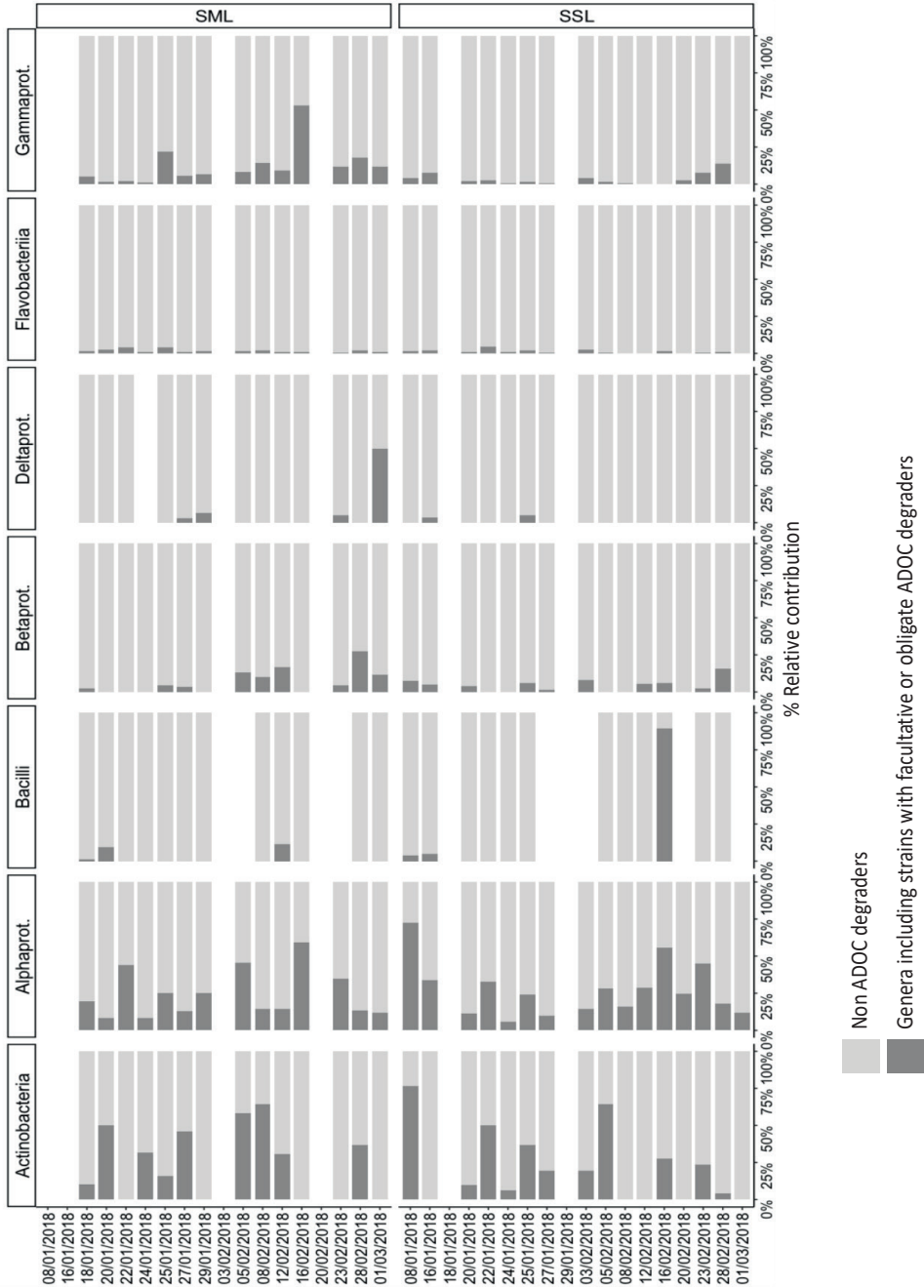


**Figure S4.** ADOC degraders relative abundance for each layer during the austral summer and corresponding taxonomical class.



## ADDITIONAL REFERENCES

- Abraham, W.R., Meyer, H., and Yakimov, M. (1998) Novel glycine containing glucolipids from the alkane using bacterium *Alcanivorax borkumensis*. *Biochim Biophys Acta - Lipids Lipid Metab* 1393: 57–62.
- Antoniou, E., Fodelianakis, S., Korkakaki, E., and Kalogerakis, N. (2015) Biosurfactant production from marine hydrocarbon-degrading consortia and pure bacterial strains using crude oil as carbon source. *Front Microbiol* 6: 274.
- Bodour, A.A., Drees, K.P., and Maier, R.M. (2003) Distribution of biosurfactant-producing bacteria in undisturbed and contaminated arid southwestern soils. *Appl Environ Microbiol* 69: 3280–3287.
- Das, P., Mukherjee, S., and Sen, R. (2008) Improved bioavailability and biodegradation of a model polyaromatic hydrocarbon by a biosurfactant producing bacterium of marine origin. *Chemosphere* 72: 1229–1234.
- Domingues, P.M., Oliveira, V., Serafim, L.S., Gomes, N.C.M., and Cunha, Â. (2020) Biosurfactant production in sub-oxic conditions detected in hydrocarbon-degrading isolates from marine and estuarine sediments. *Int J Environ Res Public Health* 17:.
- Franzetti, A., Caredda, P., La Colla, P., Pintus, M., Tamburini, E., Papacchini, M., and Bestetti, G. (2009) Cultural factors affecting biosurfactant production by *Gordonia* sp. BS29. *Int Biodeterior Biodegrad* 63: 943–947.
- Gutiérrez, T., Mulloy, B., Black, K., and Green, D.H. (2007) Glycoprotein emulsifiers from two marine *Halomonas* species: Chemical and physical characterization. *J Appl Microbiol* 103: 1716–1727.
- Lenchi, N., Kebbouche-Gana, S., Servais, P., Gana, M.L., and Lliros, M. (2020) Diesel Biodegradation Capacities and Biosurfactant Production in Saline-Alkaline Conditions by *Delftia* sp NL1, Isolated from an Algerian Oilfield. *Geomicrobiol J.* 37: 454-466.
- Lozada, M., Marcos, M.S., Commendatore, M.G., Gil, M.N., and Dionisi, H.M. (2014) The bacterial community structure of hydrocarbon-polluted marine environments as the basis for the definition of an ecological index of hydrocarbon exposure. *Microbes Environ* 29: 269–76.
- Peng, F., Liu, Z., Wang, L., and Shao, Z. (2007) An oil-degrading bacterium: *Rhodococcus erythropolis* strain 3C-9 and its biosurfactants. *J Appl Microbiol* 102: 1603–1611.
- Płaza, G.A., Jangid, K., Łukasik, K., Nałęcz-Jawecki, G., Berry, C., and Brigmon, R.L. (2007) Biodegradation of petroleum-waste by biosurfactant-producing bacteria, Savannah River Site (S.C.).
- Roca, C., Lehmann, M., Torres, C.A.V., Baptista, S., Gaudêncio, S.P., Freitas, F., and Reis, M.A.M. (2016) Exopolysaccharide production by a marine *Pseudoalteromonas* sp. strain isolated from Madeira Archipelago ocean sediments. *N Biotechnol* 33: 460–466.
- Rosenberg, E., Rubinovitz, C., Legmann, R., and Ron, E. (1988) Purification and chemical properties of *Acinetobacter calcoaceticus* A2 biosurfactant. *Appl Environ Microbiol.* 54 : 323-326.
- Saisa-Ard, K., Saimmai, A., and Maneerat, S. (2013) Characterization and phylogenetic analysis of biosurfactant-producing bacteria isolated from palm oil contaminated soils. *Songklanakarin Journal of Science & Technology*, 36.
- Santos, D.K.F., Rufino, R.D., Luna, J.M., Santos, V.A., and Sarubbo, L.A. (2016) Biosurfactants: multifunctional biomolecules of the 21st century. *Int J Mol Sci* 17: 401.
- Satpute, S.K., Banat, I.M., Dhakephalkar, P.K., Banpurkar, A.G., and Chopade, B.A. (2010) Biosurfactants, bioemulsifiers and exopolysaccharides from marine microorganisms. *Biotechnol Adv* 28: 436–450.
- Schulz, D., Passeri, A., Schmidt, M., Lang, S., Wagner, F., Wray, V., and Gunkel, W. (1991) Marine biosurfactants. I. Screening for biosurfactants among crude oil degrading marine microorganisms from the North Sea. *Z Naturforsch* 46: 197-203.
- Silva Lima, J.M., Pereira, J.O., Batista, I.H., Pereira Junior, R.C., Barroso, H. dos S., Neto, P. de Q.C., et al. (2017) Biosurfactantes produzidos por *Microbacterium* sp., isolada de macrófita aquática em área impactada por hidrocarbonetos no Rio Negro, Manaus, Amazonas. *Acta Sci - Biol Sci* 39: 13–20.
- Sun, L.N., Zhang, J., Chen, Q., He, J., Li, Q.F., and Li, S.P. (2013) *Comamonas jiangduensis* sp. nov., a biosurfactant-producing bacterium isolated from agricultural soil. *Int J Syst Evol Microbiol* 63: 2168–2173.
- Takahashi, S., Abe, K., and Ker, Y. (2013) Microbial Degradation of Persistent Organophosphorus Flame Retardants. In *Environmental Biotechnology - New Approaches and Prospective Applications*. InTech. Edited by Marian Petre: 91.



Vijayakumar, S. and Saravanan, V. (2015) Biosurfactants-Types, Sources and Applications. *Res J Microbiol* 10: 181–192.

Wang, W., Cai, B., and Shao, Z. (2014) Oil degradation and biosurfactant production by the deep sea bacterium *Dietzia maris* As-13-3. *Front Microbiol* 5: 711.

Wittgens, A., Kovacic, F., Müller, M.M., Gerlitzki, M., Santiago-Schübel, B., Hofmann, D., et al. (2017) Novel insights into biosynthesis and uptake of rhamnolipids and their precursors. *Appl Microbiol Biotechnol* 101: 2865–2878.

Yilmaz, F., Ergene, A., Yalcin, E., and Tan, S. (2009) Production and characterization of biosurfactants produced by microorganisms isolated from milk factory wastewaters. *Environ Technol* 30: 1397–1404.

Zarinviarsagh, M., Ebrahimipour, G., and Sadeghi, H. (2017) Lipase and biosurfactant from *Ochrobactrum intermedium* strain MZV101 isolated by washing powder for detergent application. *Lipids Health Dis* 16: 177.

## **Supporting information of Chapter 4**

**Table S1.** Abiotic and meteorological parameters at initial conditions. a) Ancillary data for the seawater sampling site on 21/02/2018 at 62°38.346' S, 60°23.912' W (Figure S1). b) Meteorological conditions during the sampling event. The values were averaged coinciding the sampling hours (From 8 am to 11.00 am).

<b>a) Ancillary data for the seawater sampling site:</b>	
Surface Sea Temperature (°C)	1.9
Salinity (PSU)	33.9
Conductivity	3.0
Fluorescence (RFU)	0.5
PAR/Irradiance, Biospherical/Licor	0.3
Turbidity (FTU)	3.8
Density	27.2
<b>b) Meteorological conditions during the sampling event:</b>	
Wind speed (ms <sup>-1</sup> )	2.4
Wind direction (°)	42.5
Temperature (°C)	3.5
Minimum temp. (°C)	3.5
Maximum temp. (°C)	3.6
Relative humidity (%)	95.1
Precipitation (mm)	0.0
Atmospheric pressure (hPa)	993.0
Radiation (Wm <sup>-2</sup> )	5.7

**Table S2.** PAH dissolved phase concentrations time course in each condition, layer and time-point (units are ng L<sup>-1</sup> and variability is expressed as the standard error of mean).

	<b>ABIOTIC CONTROL</b>	
	<b>T0</b>	<b>T24</b>
Fluorene	20.43 ± 2.55	34.25 ± 1.77
Anthracene	24.48 ± 3.22	40.68 ± 2.18
Phenanthrene	29.98 ± 3.53	41.39 ± 1.71
Pyrene	41.91 ± 3.88	53.12 ± 1.43
Fluoranthene	47.93 ± 4.9	59.92 ± 1.78
Crysene	7.42 ± 0.13	9.38 ± 1.74
Benzo(a)anthracene	23.05 ± 0.32	29.07 ± 3.63
Benzo(b)fluoranthene	41.82 ± 0.33	59.85 ± 7.94
Benzo(k)fluoranthene	24.68 ± 0.37	22.68 ± 7.25
Benzo(a)pyrene	59.55 ± 1.23	58.89 ± 14.62
Dibenzo(a,h)anthracene	35.42 ± 0.03	20.26 ± 14.5
Indeno(1,2,3-cd)pyrene	48.11 ± 0.27	34.45 ± 15.62
Benzo(ghi)perylene	27.38 ± 0.03	17 ± 10.5
Σ LMW PAHs	74.9 ± 9.29	116.32 ± 5.66
Σ HMW PAHs	357.27 ± 7.47	364.61 ± 79.01
Σ total PAHs	432.17 ± 16.76	480.93 ± 84.68

	SML CONTROL		SML PAH TREATMENT		SSL CONTROL		SSL PAH TREATMENT	
	T0	T24	T0	T24	T0	T24	T0	T24
Fluorene	0.12 ± 0.02	0.34 ± 0.1	13.65 ± 0.32	12.92 ± 1.76	0.88 ± 0.03	0.07 ± 0.07	10.73 ± 1.95	5.97 ± 0.75
Anthracene	0.02 ± 0.01	0.04 ± 0	15.07 ± 2.36	9.13 ± 1.49	0.11 ± 0.01	0.02 ± 0	6.52 ± 0.98	3.88 ± 1.59
Phenanthrene	0.27 ± 0.09	0.83 ± 0.09	17.7 ± 1.42	13.92 ± 0.89	2.26 ± 0.12	0.38 ± 0.06	12.34 ± 2.91	7.26 ± 1.52
Pyrene	0.03 ± 0	0.05 ± 0.02	18.85 ± 3.12	11.95 ± 0.32	0.1 ± 0	0.06 ± 0.01	12.23 ± 5.39	5.15 ± 1.71
Fluoranthene	0.03 ± 0	0.04 ± 0	22.5 ± 3.84	13.84 ± 0.37	0.09 ± 0	0.04 ± 0	13.65 ± 5.98	6.4 ± 2.15
Crysene	0.03 ± 0.01	0 ± 0	15.16 ± 5.03	5.56 ± 1.49	0.01 ± 0.01	0 ± 0	1.87 ± 0.08	1.98 ± 0.97
Benzo(a)anthracene	0 ± 0	0 ± 0	28.63 ± 7.84	12.88 ± 2.72	0 ± 0	0 ± 0	5.92 ± 0.02	5.52 ± 2.42
Benzo(b)fluoranthene	0 ± 0	0 ± 0	70.53 ± 26.91	26.73 ± 7.64	0 ± 0	0 ± 0	11.6 ± 0.28	10.76 ± 3.58
Benzo(k)fluoranthene	0 ± 0	0 ± 0	61.58 ± 24.34	21.63 ± 7.79	0 ± 0	0 ± 0	6.52 ± 0.34	6.63 ± 2.46
Benzo(a)pyrene	0 ± 0	0 ± 0	113.61 ± 36.57	46.59 ± 14.13	0 ± 0	0 ± 0	18.09 ± 0.18	17.28 ± 6.55
Dibenzo(a,h)anthracene	0 ± 0	0 ± 0	106.09 ± 41.28	37.15 ± 17.69	0 ± 0	0 ± 0	8.29 ± 1.08	7.8 ± 2.81
Indeno (1,2,3-cd)pyrene	0.14 ± 0.01	0.03 ± 0.03	118.19 ± 46	44.31 ± 17.5	0.11 ± 0.02	0.02 ± 0.02	13.05 ± 0.01	12.89 ± 4.6
Benzo(ghi)perylene	0.09 ± 0	0.02 ± 0.02	78.92 ± 33.68	12.77 ± 28.63 ± 35.96 ±	0.07 ± 0	0.02 ± 0.02	6.84 ± 0.42	6.51 ± 2.08
Σ LMW PAHS	0.41 ± 0.11	1.21 ± 0.19	46.42 ± 4.1	4.14 ± 249.27 ±	3.25 ± 0.16	0.47 ± 0.01	29.59 ± 5.84	17.11 ± 3.87
Σ HMW PAHS	0.32 ± 0.03	0.14 ± 0.06	634.06 ± 228.61	82.41 ± 285.23 ±	0.38 ± 0.03	0.13 ± 0.02	12.55 ± 127.65 ±	29.33 ± 98.02 ±
Σ total PAHS	0.74 ± 0.14	1.36 ± 0.26	680.48 ± 232.7	86.55 ± 3.63 ± 0.19	0.6 ± 0.03		18.38 ± 33.2	

**Table S3.** Summary of experimental conditions and analyses performed.

Bottle	Time point	Layer/ water	Treatment	Replicate	PAH concentrations	16S rRNA	MetaT
BOT1	T0	SML	PAH	A	X	X	X
BOT2	T0	SML	PAH	B	X	X	X
BOT3	T0	SSL	PAH	A	X	X	X
BOT4	T0	SSL	PAH	B	X	X	X
BOT5	T0	SML	control	A	X	X	X
BOT6	T0	SML	control	B	X	X	X
BOT7	T0	SSL	control	A	X	X	X
BOT8	T0	SSL	control	B	X	X	X
BOT9	T24	SML	PAH	A	X	X	X
BOT10	T24	SML	PAH	B	X	X	X
BOT11	T24	SSL	PAH	A	X	X	X
BOT12	T24	SSL	PAH	B	X	X	X
BOT13	T24	SML	control	A	X	X	X
BOT14	T24	SML	control	B	X	X	X
BOT15	T24	SSL	control	A	X	X	X
BOT16	T24	SSL	control	B	X	X	X
BOT17	T0	HPLC	PAH	A	X		
BOT18	T0	HPLC	PAH	B	X		
BOT19	T24	HPLC	PAH	A	X		
BOT20	T24	HPLC	PAH	B	X		

**Table S4.** Sequencing depths for the 16S rDNA amplicon sequences (SML: sea surface microlayer; SSL: subsurface layer; FL: Free Living, PA: Particle-Associated)

Sample ID SRA	Seq. depth	Unique ASV	Cohort	Time point	Layer	Treatment	Replicate
U1	137739	237	FL	T0	SML	PAH	A
U10	53255	155	FL	T24	SML	PAH	B
U11	19174	137	FL	T24	SSL	PAH	A
U12	17240	127	FL	T24	SSL	PAH	B
U13	37126	143	FL	T24	SML	control	A
U14	51696	154	FL	T24	SML	control	B
U15	73586	220	FL	T24	SSL	control	A
U16	87079	202	FL	T24	SSL	control	B
U3	61661	190	FL	T0	SSL	PAH	A
U33	40456	161	PA	T0	SML	PAH	A
U35	46465	196	PA	T0	SSL	PAH	A
U37	29167	154	PA	T0	SML	control	A
U39	33197	93	PA	T0	SSL	control	A
U41	28337	158	PA	T24	SML	PAH	A
U42	25367	132	PA	T24	SML	PAH	B
U43	22141	83	PA	T24	SSL	PAH	A
U44	11664	68	PA	T24	SSL	PAH	B
U45	30736	156	PA	T24	SML	control	A
U46	40818	127	PA	T24	SSL	control	A
U47	21916	87	PA	T24	SSL	control	B
U5	44108	159	FL	T0	SML	control	A
U7	72715	179	FL	T0	SSL	control	A
U9	19202	72	FL	T24	SML	PAH	A

**Table S5.** Metatranscriptome library sizes (SML: sea surface microlayer; SSL: subsurface layer; FL: Free Living, PA: Particle-Associated)

Sample ID SRA	Library size	Cohort	Time point	Layer	Treatment	Replicate
S1_126UDI	21222581	PA	T24	SML	control	A
S1_138UDI	4567076	PA	T24	SSL	control	A
S2_115UDI	8280899	FL	T0	SML	control	A
S2_139UDI	8111315	PA	T24	SML	PAH	A
S2_19UDI	5331503	FL	T0	SSL	control	A
S2_31UDI	4484565	FL	T24	SML	control	A
S2_43UDI	5784411	PA	T0	SML	control	A
S2_7UDI	3646155	PA	T24	SSL	control	B
S3_100UDI	6269886	FL	T0	SML	control	B
S3_112UDI	10768454	FL	T0	SSL	control	B
S3_124UDI	5849038	FL	T24	SML	PAH	A
S3_136UDI	6173900	FL	T24	SML	PAH	B
S3_16UDI	7988369	FL	T0	SML	PAH	B
S3_17UDI	6779729	FL	T24	SSL	PAH	B
S3_28UDI	5611156	FL	T0	SSL	PAH	A
S3_40UDI	10205518	FL	T0	SSL	PAH	B
S3_4UDI	5294704	FL	T0	SML	PAH	A
S3_5UDI	9107911	FL	T24	SSL	PAH	A
S4_101UDI	9715689	FL	T24	SSL	control	B
S4_102UDI	5138788	PA	T24	SSL	PAH	A
S4_113UDI	5716160	PA	T0	SML	PAH	A
S4_114UDI	3082398	PA	T24	SSL	PAH	B
S4_125UDI	27028349	PA	T0	SML	PAH	B
S4_137UDI	7594777	PA	T0	SSL	PAH	A
S4_18UDI	6513608	PA	T0	SSL	control	A
S4_30UDI	7222310	PA	T0	SSL	control	B
S4_41UDI	7748495	FL	T24	SSL	control	A
S4_42UDI	6187946	PA	T24	SML	PAH	B
S4_6UDI	7096732	PA	T0	SML	control	B
S7_103UDI	2970296	PA	T24	SML	control	B
S7_31UDI	2825865	FL	T24	SML	control	B

**Table S6.** Pfam profiles of proteins involved in PAH degradation. In bold, the initiating PAH degrading enzyme, catalyzing the hydroxylation of the aromatic ring. (Pfam: The protein families database number; EC: Enzyme Commission number)

Pfam	Pathway	Name	gene	E.C. no.
<b>PF00848</b>		<b>Ring-hydroxylating dioxygenase</b>	<b>nahA</b>	<b>1.14.12.12</b>
PF00171		Salicylaldehyde dehydrogenase	nahF	1.2.1.65
PF00596		3,4-dihydroxyphthalate decarboxylase	padC	4.1.1.69
PF00701		Dihydrodipicolinate synthetase	nahE	4.1.2.45
PF00775	Upstream PAH degradation	Protocatechuate 3,4-dioxygenase beta chain	pcaH	1.13.11.3
PF00106		1,6-dihydroxycyclohexa-2,4-diene-1-carboxylate dehydrogenase	benD	1.3.1.25
PF00903		Glyoxalase dioxygenase	nahC	1.13.11.56
PF01323		2-hydroxychromene-2-carboxylate isomerase	nahD	5.99.1.4
PF01494		Salicylate hydroxylase	nahG	1.14.13.1
PF09084		4,5-dihydroxyphthalate decarboxylase	pht5	4.1.1.55
PF00561	Catechol degradation	2-hydroxymuconate semialdehyde hydrolase	xylF	3.7.1.9
PF00903		Metapyrocatechase	xylE	1.13.11.2
PF02746		Muconate cycloisomerase 1	catB	5.5.1.1
PF04444		Catechol 1,2-dioxygenase	catA	1.13.11.1
PF07836		4-hydroxy-2-oxovalerate aldolase	xylK	4.1.3.39
PF02426		Muconolactone Delta-isomerase	catC	5.3.3.4
PF00206	Benzoate and protocatechuate degradation	3-carboxy-cis,cis-muconate cycloisomerase	pcaB	5.5.1.2
PF00561		3-oxoadipate enol-lactonase	pcaD	3.1.1.24
PF01144		Coenzyme A transferase	pcaI	2.8.3.6
PF02627		4-carboxymuconolactone decarboxylase	pcaC	4.1.1.44



**Table S7.** Subset of genera including previously reported hydrocarbonoclastic bacterial strains and metagenome-assembled genome (MAG) genera retrieved from oil polluted marine environments (Lozada et al., 2014; Karthikeyan et al., 2020) and detected in our experimental dataset. As some of these taxa have also been reported to exudate biosurfactants or form biofilms, the type and citation is also given. In bold, marine biosurfactant-producing bacterial strains within the genera (HC : Hydrocarbonoclastic).

Label	Phylum/Class	Genus	Biosurfactant-producing bacteria
HC	Phylum:	<i>Arthrobacter</i>	<b>Glycolipid</b> (Schulz <i>et al.</i> , 1991)
Actinobacteria	Actinobacteria	<i>Nocardioiodes</i>	Glycolipid (Vasileva-Tonkova and Gesheva, 2005)
HC Alphaprot.	Phylum:	<i>Sulfitobacter</i>	
	Proteobacteria	<i>Sphingomonas</i>	Polymeric surfactant (Santos <i>et al.</i> , 2016)
	Class: Alphaprot.	<i>Roseobacter</i>	Biofilm formation (high temperature adaptation) (Kent <i>et al.</i> , 2018)
HC Bacteroidia	Phylum:	<i>Flavobacterium</i>	Biosurfactant (From contaminated arid soils) (Bodour <i>et al.</i> , 2003)
	Bacteroidetes		
	Class:		
	Flavobacteriia		
HC Gammaprot.	Phylum:	<i>Acinetobacter</i>	<b>Polymeric biosurfactant/</b>
	Proteobacteria		<b>Bioemulsifier</b> (Rosenberg <i>et al.</i> , 1988)
	Class:	<i>Arenimonas</i>	
	Gammaprot.	<i>Colwellia</i>	<b>Biosurfactant</b> (Mapelli <i>et al.</i> , 2017)
		<i>Glaciicola</i>	<b>Biosurfactant/ bioemulsifier</b> (Dang <i>et al.</i> , 2016)
		<i>Halomonas</i>	<b>Polymeric biosurfactant/</b> <b>bioemulsifier, glycolipid and Exopolysaccharides</b> (Isolated from Surface waters affected by Deep Horizon Oil spill in the Gulf of Mexico) (Gutiérrez <i>et al.</i> , 2007; Gutiérrez <i>et al.</i> , 2013)
		<i>Marinomonas</i>	<b>Biosurfactant</b> (Dang <i>et al.</i> , 2016)
		<i>Oleiphilus</i>	
		<i>Oleispira</i>	
		<i>Pseudoalteromonas</i>	<b>Exopolysaccharides (complex Surface active polymer )</b> (Malavenda <i>et al.</i> , 2015; Roca <i>et al.</i> , 2016)
		<i>Pseudomonas</i>	<b>Polymeric biosurfactant/</b> <b>bioemulsifier, lipopeptides, glycolipids and particulate surfactant</b> (Wittgens <i>et al.</i> , 2017; Domingues <i>et al.</i> , 2020)
		<i>Pshychrobacter</i>	<b>Biosurfactant</b> (Domingues <i>et al.</i> , 2020; Trudgeon <i>et al.</i> , 2020)
		<i>Shewanella</i>	<b>Biosurfactant</b> (Antonioni <i>et al.</i> , 2015)
		<i>Vibrio</i>	<b>Exopolysaccharides (complex Surface active polymer )</b>
		<i>Woeseia</i>	
All HCB		*Includes all the above	

**Table S8.** Inorganic nutrient concentrations and bacterial abundance measurements for the SML and SSL over the time course of the incubation. Variability is expressed with standard deviation. (SML: sea surface microlayer; SSL: subsurface layer; LNA: Low Nucleic Acid; HNA: High Nucleic Acid; All BA : All Bacterial Abundance; FL: Free living, PA: Particle-associated)

	T0				T24			
	SML		SSL		SML		SSL	
		Control		Control		Control		Control
N-NH <sub>4</sub> <sup>+</sup> (μmol L <sup>-1</sup> )	4.9 ± 5.3	4.3 ± 2.6	5.1 ± 3.3	2.9 ± 0.3	9.2 ± 7.1	2.5 ± 0.6		
NO <sub>3</sub> + NO <sub>2</sub> (μmol L <sup>-1</sup> )	23.2 ± 2.6	18 ± 6.3	22.6 ± 4	24 ± 0.4	16.6 ± 6.5	23.1 ± 1.5		
-PO <sub>4</sub> <sup>3-</sup> (μmol L <sup>-1</sup> )	1.6 ± 0.2	1.4 ± 0.2	1.4 ± 0.1	1.4 ± 0	1.3 ± 0.2	1.5 ± 0.1		
LNA (Cells mL <sup>-1</sup> )	131408.1±	157930.8±	165009.0±	153743±	132735.1±	163931.7±		
	60065.5	41564.9	19286.8	64633.4	34322.9	19980.9		
HNA (Cells mL <sup>-1</sup> )	428419.8 ±	498016.0 ±	588590.6±	338282 ±	446875.6±	474584.1±		
	187039.5	157063.5	107145.4	242176.2	138310.3	93771		
All BA (Cells mL <sup>-1</sup> )	559827.9 ±	655946.8 ±	753599.7±	492025±	579610.7±	638515.7±		
	245034.8	195410.2	126070.3	239429.3	172019	112373		
Bacterial abundance yields (Cells mL <sup>-1</sup> h <sup>-1</sup> )			0.01±0.06	0.00±0.03	-0.002±0.008	-0.004±0.01		

**Table S9.** Community composition of microbial communities at initial time point measured by 16S rRNA gene amplicon sequencing (Relative abundances in % of total reads and variability expressed in standard deviation, SML: sea surface microlayer; SSL: subsurface layer; FL: Free Living, PA: Particle Associated; HC : Hydrocarbonoclastic). Notice that counts of general taxonomical groups include HC bacteria.

	SML		SSL	
	FL	PA	FL	PA
Actinobacteriota	0.05 ± 0.04	0.29 ± 0.37	0.03 ± 0	0.56 ± 0.38
Alphaproteobacteria	21.74 ± 1.13	15.06 ± 2.28	21.3 ± 0.46	19.36 ± 4.75
SAR11 clade	8 ± 0.63	2.64 ± 0.1	6.99 ± 0.1	2.36 ± 0.35
Caulobacterales	0	0.05 ± 0.03	0	0.13 ± 0
Rhodobacterales	11.91 ± 0.51	6.62 ± 0.58	12.74 ± 0.61	7.87 ± 0.14
Rhodospirillales	0.55 ± 0.01	0.45 ± 0.16	0.56 ± 0.07	0.54 ± 0.08
Sphingomonadales	0	0.05 ± 0	0	0.11 ± 0.03
Rickettsiales	0.38 ± 0.04	4.94 ± 1.82	0.23 ± 0.1	8.15 ± 5.42
Gammaproteobacteria	36.04 ± 0.29	33.39 ± 4.62	34.66 ± 0.67	26.42 ± 2.77
Alteromonadales	1.97 ± 1.66	7.2 ± 4.99	0.15 ± 0.06	8.09 ± 1.71
Burkholderiales	0.68 ± 0.06	0.14 ± 0	0.71 ± 0.25	0.13 ± 0.05
Cellvibrionales	6.61 ± 0.19	3.62 ± 1.05	7.45 ± 0.34	3.05 ± 1.19
Oceanospirillales	19.08 ± 0.83	12.6 ± 0.63	20.11 ± 0.69	11.73 ± 2.25
Pseudomonadales	1.02 ± 0.17	7.51 ± 2.61	0.09 ± 0.04	0.16 ± 0
SAR86 clade	2.54 ± 0.2	0.63 ± 0.15	2.1 ± 0.47	0.44 ± 0.22
Thiotrichales	0.27 ± 0.02	0.49 ± 0	0.21 ± 0.02	0.37 ± 0.02
Other gammaproteobacteria	3.87 ± 0.28	1.43 ± 0.06	3.85 ± 0.09	2.53 ± 0.36
Bacteroidota	41.8 ± 0.91	50.22 ± 6.71	43.66 ± 0.27	52.88 ± 6.71
Cytophagales	0.87 ± 0.02	4.19 ± 1.3	0.86 ± 0.08	4.94 ± 0.47
Flavobacteriales	40.92 ± 0.91	45.52 ± 5.42	42.8 ± 0.36	47.35 ± 7.03
Verrucomicrobiota	0.08 ± 0.04	0.23 ± 0.02	0.08 ± 0.01	0.26 ± 0
Other Bacterial groups	0.05 ± 0	0.33 ± 0.03	0.08 ± 0.03	0.54 ± 0.08
All HCB	7.72 ± 1.92	18.18 ± 2.1	5.95 ± 0.55	12.74 ± 0.69
HC Actinobacteria	0	0.04 ± 0	0.02 ± 0	0.56 ± 0.38
HC Bacteroidia	0.03 ± 0	0.16 ± 0.02	0.04 ± 0	0.3 ± 0
HC Alphaproteobacteria	4.74 ± 0.08	3.38 ± 0.45	5.69 ± 0.57	3.9 ± 0.5
<i>Sulfitobacter</i>	4.74 ± 0.08	3.36 ± 0.43	5.69 ± 0.57	3.9 ± 0.5
HC Gammaproteobacteria	2.96 ± 1.82	14.62 ± 2.5	0.22 ± 0.04	8.14 ± 1.78
<i>Colwellia</i>	0.03 ± 0	0.05 ± 0	0.1 ± 0.04	7.62 ± 1.83
<i>Pseudoalteromonas</i>	1.91 ± 1.61	6.92 ± 5.28	0.06 ± 0	0.11 ± 0.11
<i>Psychrobacter</i>	1.02 ± 0.17	7.47 ± 2.56	0.09 ± 0.04	0.16 ± 0

**Table S10.** Community composition of microbial communities at final time point (24 h) measured by 16S rRNA gene amplicon sequencing. (Relative abundances in % of total reads and variability expressed in standard deviation, SML: sea surface microlayer; SSL: subsurface layer; FL: Free Living, PA: Particle-Associated; HC : Hydrocarbonoclastic). Notice that counts of general taxonomical groups include HC bacteria.

	SML				PA				SSL			
	FL	PAH	ENTRL	PAH	FL	PAH	ENTRL	PAH	FL	PAH	ENTRL	PAH
Actinobacteriota	0.03 ± 0.01	0.01 ± 0	0.11	0.05 ± 0	0.05 ± 0.01	0.05 ± 0.02	0.05 ± 0.01	0.05 ± 0.02	0.7 ± 0.41	ENTRL	PAH	0.68 ± 0
Alphaproteobacteria	26.02 ± 1.18	25.34 ± 0.28	14.17	12.11 ± 0.22	24.5 ± 0.37	25.38 ± 1.2	19.77 ± 0.23	20.63 ± 1.55				
SAR11 clade	7.64 ± 0.32	7.34 ± 1.39	1.64	2 ± 0.5	7.64 ± 0.12	7.33 ± 0.28	1.62 ± 0.65	1.85 ± 0.15				
Rhodobacterales	16.6 ± 0.52	16.48 ± 1.08	7.62	5.39 ± 0.67	15.1 ± 0.47	15.95 ± 0.9	8.87 ± 1.32	8.39 ± 0.21				
Rhodospirillales	0.5 ± 0.01	0.44 ± 0.04	0.35	0.27 ± 0.07	0.41 ± 0.01	0.57 ± 0.04	0.17 ± 0	0.54 ± 0.08				
Rickettsiales	0.6 ± 0.27	0.26 ± 0.04	4.17	4.13 ± 0.94	0.56 ± 0.07	0.63 ± 0	8.49 ± 1.91	9.02 ± 2.06				
Gammaproteobacteria	36.85 ± 0.38	39.27 ± 0.26	43.95	53.09 ± 0.37	35.56 ± 0.64	34.94 ± 0.4	29.01 ± 3.37	28.43 ± 1.12				
Alteromonadales	0.84 ± 0.29	5.86 ± 0.96	4.26	26.39 ± 0.55	0.21 ± 0.01	0.22 ± 0.06	13.31 ± 3.97	15.44 ± 0.8				
Burkholderiales	0.63 ± 0.11	0.76 ± 0.08	0	0.18 ± 0	0.72 ± 0.06	0.7 ± 0.08	0	0.1 ± 0				
Cellvibrionales	7.78 ± 0.08	7.59 ± 1.73	4.17	2.8 ± 0.28	7.63 ± 0.21	7.58 ± 0.17	2.24 ± 0.24	1.77 ± 0.99				
Oceanospirillales	20.65 ± 0.15	17.87 ± 2.39	13.01	7.39 ± 0.24	19.97 ± 0.57	19.69 ± 0.38	9.82 ± 0.38	8.24 ± 1.09				
Pseudomonadales	1.26 ± 1.31	1.12 ± 0.08	20.71	15.05 ± 0.88	0.07 ± 0.01	0.04 ± 0	0.17 ± 0	0.29 ± 0				
SAR86 clade	2.39 ± 0.52	2.44 ± 0.15	0.13	0.36 ± 0	2.87 ± 0.08	2.48 ± 0.32	0.66 ± 0	0.45 ± 0.09				
Thiotrichales	0.13 ± 0.02	0.1 ± 0.07	0.3	0.41 ± 0.2	0.14 ± 0.05	0.18 ± 0.01	0.7 ± 0.06	0.23 ± 0.09				
Other gammaproteobacteria	3.19 ± 0.96	3.52 ± 0.26	1.37	0.78 ± 0.07	3.96 ± 0.17	4.07 ± 0.15	2.53 ± 0.87	2.12 ± 0.12				
Other proteobacteria	0.14 ± 0.04	0.1 ± 0.04	0.43	0.15 ± 0.03	0.21 ± 0.02	0.13 ± 0.04	0.17 ± 0	0				
Bacteroidota	36.77 ± 0.89	35.17 ± 0.66	40.59	34.16 ± 0.47	39.33 ± 0.96	39.19 ± 1.72	49.48 ± 2.43	49.51 ± 0.88				
Cytophagales	0.75 ± 0.05	0.49 ± 0.22	3.04	2.54 ± 0.17	1.02 ± 0.09	0.89 ± 0.15	5.06 ± 0.37	4.28 ± 0.56				
Flavobacteriales	36 ± 0.91	34.65 ± 0.91	37.19	31.08 ± 0.99	38.28 ± 0.85	38.3 ± 1.56	43.64 ± 2.39	44.5 ± 0.45				
Other Bacterial groups	0.03 ± 0.01	0.03 ± 0	0.3	0.1 ± 0.08	0.14 ± 0.09	0.11 ± 0.01	0.79 ± 0.41	0.79 ± 0.39				
All HCB	10.97 ± 0.54	15.97 ± 0.12	29.81	45.33 ± 1	8.68 ± 0.14	9.05 ± 0.11	18.9 ± 3.69	21.27 ± 0.52				
HC Actinobacteria	0	0	0	0	0.03 ± 0.01	0.05 ± 0.02	0.7 ± 0.41	0.68 ± 0				
HC Alphaproteobacteria	8.83 ± 0.53	9.02 ± 0.88	4.42	3.55 ± 0.26	8.4 ± 0.13	8.79 ± 0.06	4.85 ± 1.01	4.96 ± 1.52				
Sphingomonas	0	0	0	0.02 ± 0	0	0	0	0				
Sulfifobacter	8.83 ± 0.53	9.02 ± 0.88	4.42	3.53 ± 0.25	8.4 ± 0.13	8.79 ± 0.06	4.85 ± 1.01	4.96 ± 1.52				
HC Gammaproteobacteria	2.13 ± 1.06	6.95 ± 1.01	25.15	41.54 ± 0.54	0.25 ± 0.02	0.21 ± 0.14	13.35 ± 3.09	15.97 ± 1.56				
Colwellia	0.02 ± 0.02	0.03 ± 0	0.3	0.61 ± 0.24	0.17 ± 0.01	0.11 ± 0.01	12.69 ± 4.02	14.98 ± 0.76				
Marinomonas	0.06 ± 0	0.02 ± 0	0.43	0.22 ± 0	0	0	0	0				
Oleispira	0	0	0	0	0.01 ± 0	0	0.58 ± 0	0.78 ± 0				
Pseudalteromonas	0.82 ± 0.27	5.81 ± 0.9	3.72	25.67 ± 0.28	0.01 ± 0	0.14 ± 0	0	0				
Psychrobacter	1.24 ± 1.29	1.12 ± 0.08	18.29	15.05 ± 0.88	0.07 ± 0.01	0.04 ± 0	0.17 ± 0	0.29 ± 0				
HC Bacteroidia	0.02 ± 0	0	0.19	0.25 ± 0.2	0.01 ± 0	0	0	0				

**Figure S1.** Map of the sampled sea water (sea surface microlayer and subsurface water) for the incubation experiment. Coordinates: 62°38.346' S, 60°23.912'W.



**Figure S2.** PAH degradation rates in the sea surface microlayer (SML) and the subsurface layer (SSL) for treatments and controls using concentrations corrected by benchmarking approach using phenanthrene (PHE). Significant differences between layers (Mann-Whitney test,  $p < 0.05$ ) are labeled with an asterisk at the SML panel only.

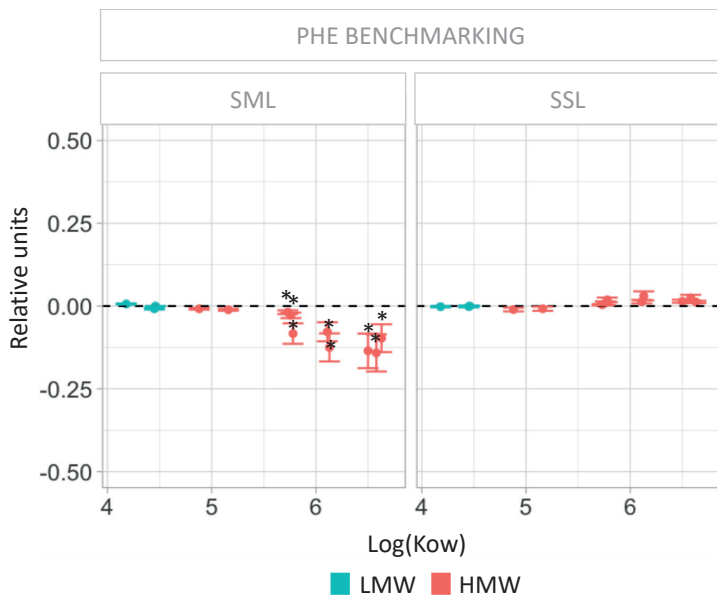


**Figure S3.** Comparison of relative abundance of genes and transcripts between bacterial layers (SML vs SSL) for each bacterial fraction in the rRNA 16S gene pool and the taxonomical assignment of the metatranscriptome at initial conditions. Significant statistical differences in the relative abundances between layers were detected by t-test (labeled with an \*). (SML: sea surface microlayer; SSL: subsurface layer).

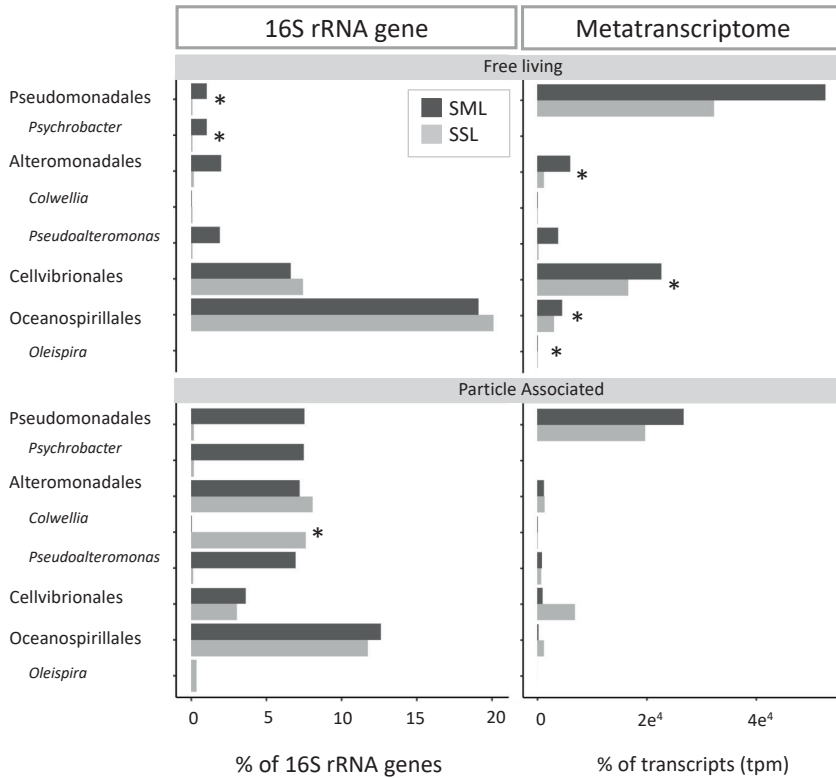


**Figure S4.** Principal component analysis (PCA) plot showing 16S of rRNA gene at initial conditions from the different sampled communities. (SML: sea surface microlayer; SSL: subsurface layer)

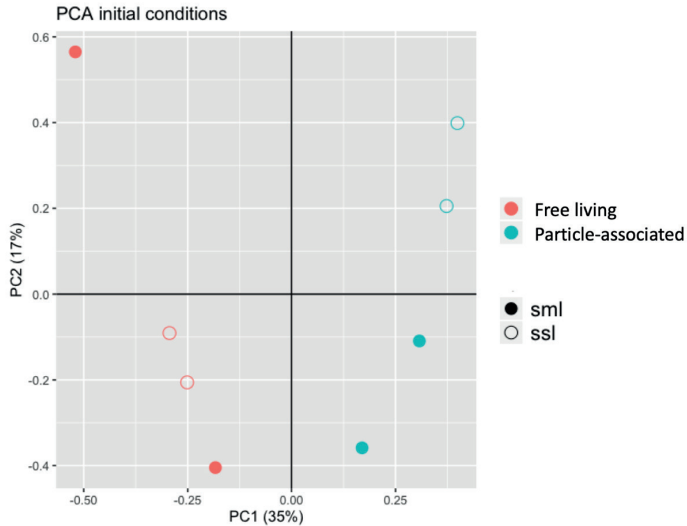


**Figure S5.** Relative abundances of hydrocarbonoclastic bacterial strains based on the 16S rRNA gene amplicon sequencing at initial conditions. Taxonomical affiliations are based on Table S6.

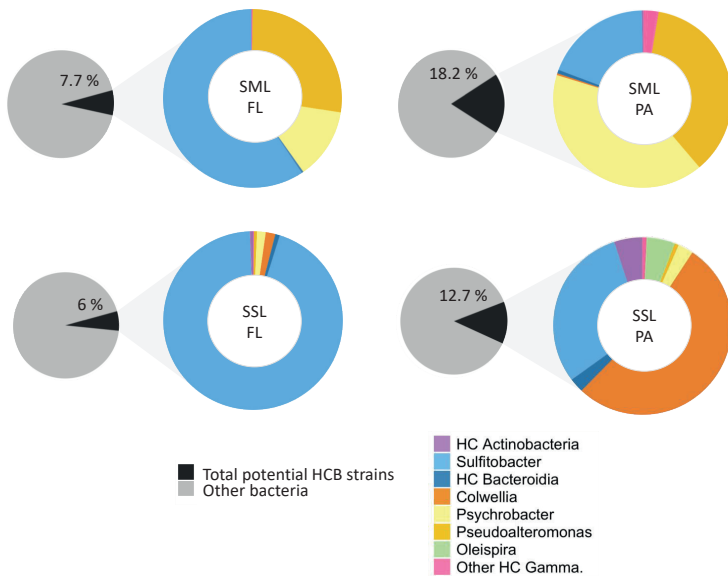


**Figure S6.** Relative contributions of taxa to the community composition and transcripts pool measured by 16S rRNA gene amplicon sequencing and metatranscriptomics at initial conditions and after 24 hours. The particle associated community are those bacterial cells sizing >3.0  $\mu\text{m}$ , the free living fraction correspond to cells ranging from 0.2–3.0  $\mu\text{m}$ . (SML: sea surface microlayer; SSL: subsurface layer; Ctrl: Control).

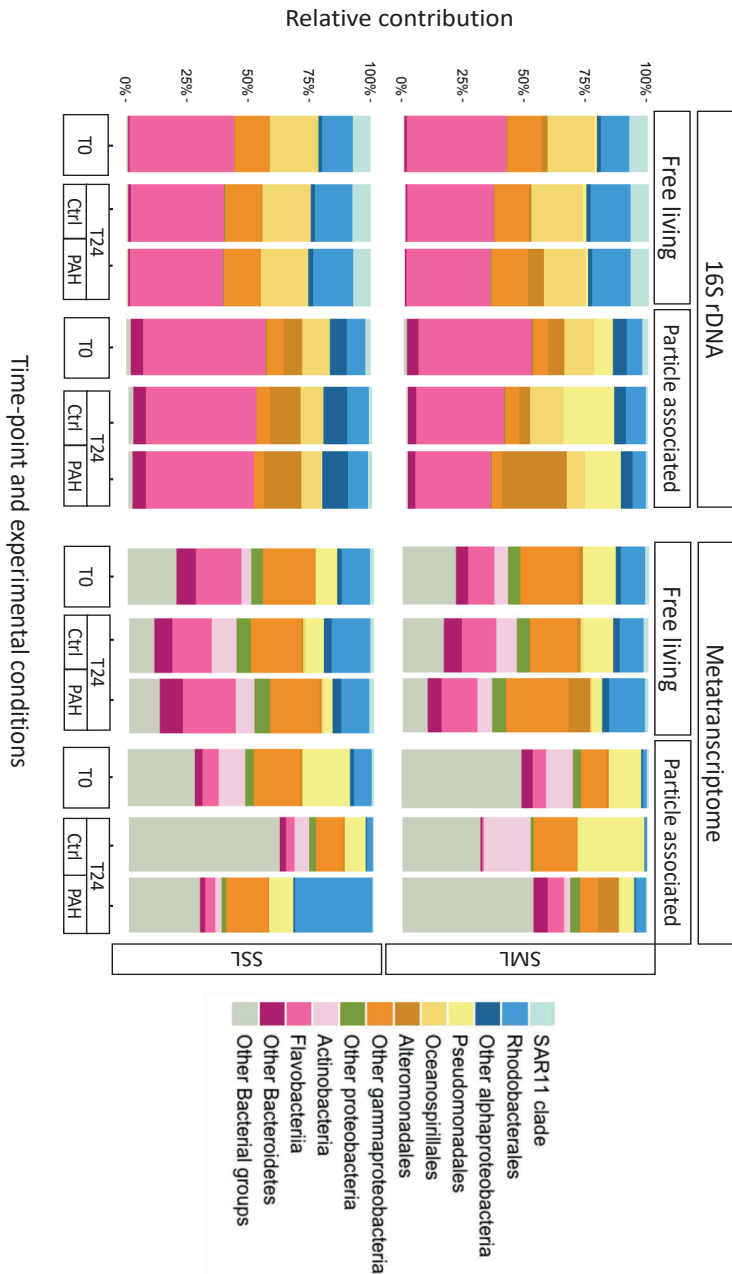
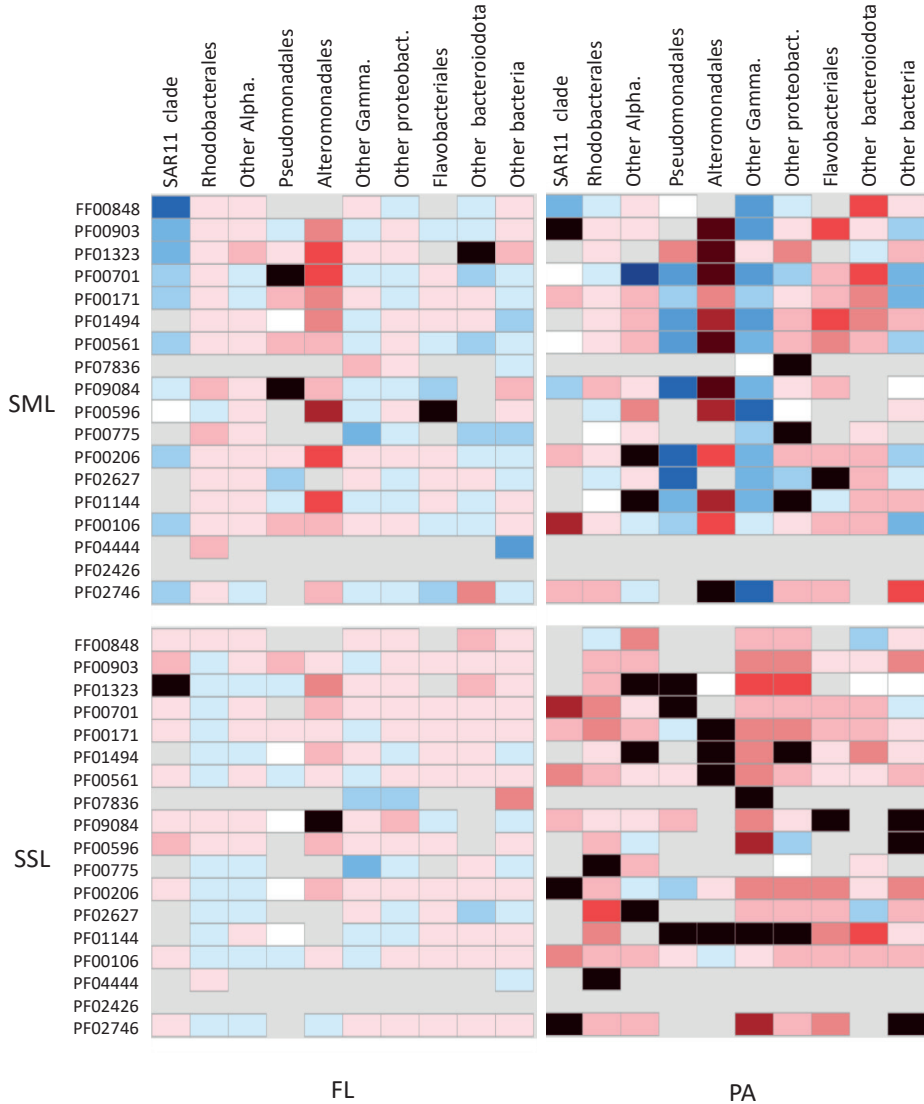




**Figure S7.** Fold-change in expression of genes involved in PAH degradation between PAH treatments and controls and their taxonomic affiliation.





## ADDITIONAL REFERENCES

- Antoniou, E., Fodelianakis, S., Korkakaki, E., and Kalogerakis, N. (2015) Biosurfactant production from marine hydrocarbon-degrading consortia and pure bacterial strains using crude oil as carbon source. *Front Microbiol* 6.
- Bodour, A.A., Drees, K.P., and Maier, R.M. (2003) Distribution of biosurfactant-producing bacteria in undisturbed and contaminated arid southwestern soils. *Appl Environ Microbiol* 69: 3280–3287.
- Dang, N.P., Landfald, B., and Willassen, N.P. (2016) Biological surface-active compounds from marine bacteria. *Environ Technol (United Kingdom)* 37: 1151–1158.
- Domingues, P.M., Oliveira, V., Serafim, L.S., Gomes, N.C.M., and Cunha, Â. (2020) Biosurfactant production in sub-oxic conditions detected in hydrocarbon-degrading isolates from marine and estuarine sediments. *Int J Environ Res Public Health* 17: 1746.
- Gutierrez, T., Berry, D., Yang, T., Mishamandani, S., McKay, L., Teske, A., and Aitken, M.D. (2013) Role of Bacterial Exopolysaccharides (EPS) in the Fate of the Oil Released during the Deepwater Horizon Oil Spill. *PLoS One* 8: :e67717.
- Gutiérrez, T., Mulloy, B., Black, K., and Green, D.H. (2007) Glycoprotein emulsifiers from two marine *Halo*monas species: Chemical and physical characterization. *J Appl Microbiol* 103: 1716–1727.
- Karthikeyan, S., Rodriguez-R, L.M., Heritier-Robbins, P., Hatt, J.K., Huettel, M., Kostka, J.E., and Konstantinidis, K.T. (2020) Genome repository of oil systems: An interactive and searchable database that expands the catalogued diversity of crude oil-associated microbes. *Environ Microbiol* 22: 2094–2106.
- Kent, A.G., Garcia, C.A., and Martiny, A.C. (2018) Increased biofilm formation due to high-temperature adaptation in marine *Roseobacter*. *Nat Microbiol* 3: 989–995.
- Lozada, M., Marcos, M.S., Commendatore, M.G., Gil, M.N., and Dionisi, H.M. (2014) The bacterial community structure of hydrocarbon-polluted marine environments as the basis for the definition of an ecological index of hydrocarbon exposure. *Microbes Environ* 29: 269–76.
- Malavenda, R., Rizzo, C., Michaud, L., Gerçe, B., Bruni, V., Sylđatk, C., et al. (2015) Biosurfactant production by Arctic and Antarctic bacteria growing on hydrocarbons. *Polar Biol* 38: 1565–1574.
- Mapelli, F., Scoma, A., Michoud, G., Aulenta, F., Boon, N., Borin, S., et al. (2017) Biotechnologies for Marine Oil Spill Cleanup: Indissoluble Ties with Microorganisms. *Trends Biotechnol* 35: 860–870.
- Roca, C., Lehmann, M., Torres, C.A.V., Baptista, S., Gaudêncio, S.P., Freitas, F., and Reis, M.A.M. (2016) Exopolysaccharide production by a marine *Pseudoalteromonas* sp. strain isolated from Madeira Archipelago ocean sediments. *N Biotechnol* 33: 460–466.
- Rosenberg, E., Rubinovitz, C., Legmann, R., and Ron, E. (1988) Purification and Chemical Properties of *Acinetobacter calcoaceticus* A2 Biodispersan. *Appl Env Microbiol* 54: 323–6.
- Santos, D.K.F., Rufino, R.D., Luna, J.M., Santos, V.A., and Sarubbo, L.A. (2016) Biosurfactants: Multifunctional biomolecules of the 21st century. *Int J Mol Sci* 17: 401.
- Satpute, S.K., Banat, I.M., Dhakephalkar, P.K., Banpurkar, A.G., and Chopade, B.A. (2010) Biosurfactants, bioemulsifiers and exopolysaccharides from marine microorganisms. *Biotechnol Adv* 28: 436–450.
- Schulz, D., Passeri, A., Schmidt, M., Lang, S., Wagner, F., Wray, V., and Gunkel, W. (1991) Marine biosurfactants, I. Screening for biosurfactants among crude oil degrading marine microorganisms from the North Sea. *Z Naturforsch C J Biosci* 46: 197–203.
- Trudgeon, B., Diesler, M., Balasubramanian, N., Messmer, M., and Foreman, C.M. (2020) Low-temperature biosurfactants from polar microbes. *Microorganisms* 8: 1–14.
- Vasileva-Tonkova, E. and Gesheva, V. (2005) Glycolipids produced by Antarctic *Nocardioides* sp. during growth on n-paraffin. *Process Biochem* 40: 2387–2391.
- Wittgens, A., Kovacic, F., Müller, M.M., Gerlitzki, M., Santiago-Schübel, B., Hofmann, D., et al. (2017) Novel insights into biosynthesis and uptake of rhamnolipids and their precursors. *Appl Microbiol Biotechnol* 101: 2865–2878.

## **Supporting information of Chapter 5**

**Table S1.** Coordinates and physical variables of the sampling sites.

	NORTH	CENTRAL	SOUTH
<b>Coordinates</b>	55.0 N 138.6 W	52.6 N 130.3 W	48.7 N 126.7 W
<b>PAR (<math>\mu\text{Em}^{-2}\text{s}^{-1}</math>)</b>	16.7	2.7	39.8
<b>Pressure (db)</b>	4.5	10.5	4.5
<b>Temperature (<math>^{\circ}\text{C}</math>)</b>	13.6	13.7	15.9
<b>Transparency (%)</b>	91.9	90.8	96.9
<b>Conductivity</b>	3.9	3.8	4

**Table S2.** Biological parameters of the three sampled sites at initial conditions. Statistical differences between sites were detected by ANOVA (labeled with an \*) followed by a post-hoc Tukey test (labeled with a letter next to the values), ( $p \leq 0.05$ ).

	North	Central	South	
<b>Microbial abundance</b>				
Low DNA	294500 $\pm$ 707.1 (a)	615500 $\pm$ 9192.4 (b)	462000 $\pm$ 7071.1 (c)	*
High DNA	386000 $\pm$ 16970.6 (a)	691500 $\pm$ 7778.2 (b)	521000 $\pm$ 5656.9 (c)	*
All Bacteria	680500 $\pm$ 17677.7(a)	1305000 $\pm$ 21213 (b)	982500 $\pm$ 13435 (c)	*
Prochlorococcus	68 $\pm$ 14.1(a)	150.5 $\pm$ 13.4 (b)	203.5 $\pm$ 7.8 (c)	*
Synechococcus	4925 $\pm$ 171.1 (a)	31150 $\pm$ 223.5 (b)	21900 $\pm$ 936.2 (c)	*
PicoEUK	2575 $\pm$ 6.4 (a)	5165 $\pm$ 49.5 (b)	2095 $\pm$ 32.5 (c)	*
NanoEUK	1210 $\pm$ 15.6 (a)	2120 $\pm$ 41 (b)	673 $\pm$ 16.9 (c)	*
All_phyto	8775 $\pm$ 176.1 (a)	38650 $\pm$ 228.4 (b)	24850 $\pm$ 928.4 (c)	*
<b>Bioorthogonal non-canonical amino acid tagging of active prokaryotes (Boncat - %)</b>				
	8.07	12.06 $\pm$ 6.9	7.45 $\pm$ 2.8	
<b>Bacterial Production (nM Leucine uptake <math>\text{d}^{-1}</math>)</b>				
	1.245	1.494	0.7	
<b>Chlorophyll (<math>\mu\text{g L}^{-1}</math>)</b>				
	1.7	1.7	0.2	
<b>Sulfur model molecule cycle</b>				
DMSPd_turnover_flux (nM $\text{d}^{-1}$ )	7.7	98	40.7	
k_DMS_loss_( $\text{d}^{-1}$ )	0.1	1.3	2.7	
kDMSPd_loss_( $\text{d}^{-1}$ )	2.3	49.5	38.6	
[DMS]_(nM)	12.7	1.2	0.7	
[DMSPd]_(nM)	3.36	2	1.1	
[DMSPt]_(nM)	83.6	46.1	19.3	
BDMSC_(nM $\text{d}^{-1}$ )	1.44	1.59	1.89	
$\Delta^{\text{''}}\text{DMS}_\text{(d)}$	8.8	0.8	0.4	
$\Delta^{\text{''}}\text{DMSPt}_\text{via}_\text{DMSPd}_\text{(d)}$	10.9	0.5	0.5	

**Table S3.** Environmental concentrations of selected pollutants from the ADOC pool at the three sites.

	North	Central	South
<b>Polycyclic aromatic hydrocarbons (ng L<sup>-1</sup>)</b>			
Naphthalene	1.86	0.82	1.69
Methylnaphthalene	0.62	0.72	0.80
Dimethylnaphthalene	1.06	1.17	0.84
Trimethylnaphthalene	0.50	0.38	0.56
Acenaphthylene	0.04	0.03	0.04
Acenaphthene	0.07	0.05	0.04
Fluorene	0.23	0.22	0.14
Dibenzothiophene	0.01	0.06	0.17
Methyldibenzothiophenes	0.18	0.23	0.36
Dimethyldibenzothiophenes	0.29	0.63	1.08
Phenanthrene	0.78	0.70	1.04
Methylphenanthrenes	1.16	1.6	2.15
Dimethylphenanthrenes	0.67	1.07	2.27
Trimethylphenanthrene	0.87	0.41	1.63
Anthracene	0.04	0.06	0.07
Fluoranthene	0.66	0.92	3.28
Pyrene	0.39	0.68	2.64
Methylpyrenes	0.1	0.14	0.43
Dimethylpyrenes	0.02	0.01	0.14
Benzo(a)anthracene	0.08	0.06	0.04
Chrysene	0.02	0.02	0.14
1,2-Methylchrysene	0.02	0.02	0.18
Benzo(a)pyrene	0.17	0.18	0.10
Triphenylene	0.22	0.29	1.51
Rethene	0.01	0.00	0.01
Benzonaphthothiophene	0.06	0.09	0.42
<b>Low molecular weight PAHs</b>	<b>8.47</b>	<b>8.24</b>	<b>13.28</b>
<b>High molecular weight PAHs</b>	<b>1.69</b>	<b>2.32</b>	<b>8.46</b>
<b>∑<sub>64</sub>PAHs</b>	<b>10.15</b>	<b>10.57</b>	<b>21.74</b>
<b>Organophosphate esters flame retardants &amp; pasticizers (ng L<sup>-1</sup>)</b>			
TIBP	2.03	2.13	1.40
TnBP	5.05	5.46	3.48
TCEP	9.23	9.74	6.82
EHDPP	0.00	0.00	4.36
TEHP	0.00	0.00	2.52
<b>∑ OPE</b>	<b>16.31</b>	<b>17.33</b>	<b>18.58</b>

	North	Central	South
<b>n-Alkanes (ng L<sup>-1</sup>)</b>			
Dodecane	0.09	0.14	0.09
Tridecane	0.33	0.43	0.30
Tetradecane	1.36	1.80	1.88
Pentadecane	7.28	8.11	7.19
Hexadecane	4.02	4.10	3.84
Heptadecane	2.22	2.49	3.59
Octadecane	9.52	11.60	10.36
Nonadecane	2.10	4.62	3.94
Eicosane	15.12	19.80	19.28
Heneicosane	2.18	5.51	11.13
Docosane	7.17	13.92	25.28
Tricosane	4.72	15.76	36.31
Tetracosane	11.99	27.23	57.18
Pentacosane	2.25	13.72	56.74
Hexacosane	8.17	15.63	71.32
Heptacosane	7.02	9.11	63.54
Octacosane	18.13	13.25	63.20
Nonacosane	26.83	7.98	60.58
Triacontane	45.33	12.04	66.12
Hentriacontane	47.52	7.06	60.85
Dotriacontane	63.38	11.73	67.32
Tritriacontane	54.80	4.32	55.20
Tetratriacontane	68.75	2.30	53.35
Pentatriacontane	54.65	0.60	49.39
<b>Medium chain alkanes (C<sub>12</sub>-C<sub>20</sub>)</b>	<b>42.05</b>	<b>53.08</b>	<b>50.47</b>
<b>Long chain alkanes (&gt; C<sub>20</sub>)</b>	<b>422.91</b>	<b>160.17</b>	<b>797.51</b>
<b>∑ n-alkanes</b>	<b>464.96</b>	<b>213.25</b>	<b>847.99</b>

**Table S4.** Subset of taxa, previously reported as being associated to the presence of ADOC (ADOC-A) (Takahashi et al., 2013; Lozada et al., 2014; Karthikeyan et al., 2020), detected in our dataset from the NESAP region.

Label	Phylum/Class	Genus
Alphaproteobacteria ADOC-A	Phylum: Proteobacteria Class: Alphaproteobacteria	<i>Sphingomonas</i> <i>Sulfitobacter</i> <i>Sphingobium</i> <i>Thalassospira</i> <i>Jannaschia</i> <i>Roseobacter</i>
Betaproteobacteria ADOC-A		<i>Comamonas</i> <i>Polaromonas</i>
Bacilli ADOC-A	Phylum: Firmicutes Class: Bacilli	<i>Bacillus</i>
Bacteroidia ADOC-A	Phylum: Bacteroidota Class: Bacteroidia	<i>Nonlabens</i> <i>Flavobacterium</i> <i>Salegentibacter</i> <i>Bacteroides</i>
Gammaproteobacteria ADOC-A	Phylum: Proteobacteria Class: Gammaproteobacteria	<i>Acinetobacter</i> <i>Pseudoalteromonas</i> <i>Pseudomonas</i> <i>Polycyclovorans</i> <i>Woeseia</i> <i>Psychrobacter</i> <i>Alteromonas</i> <i>Colwellia</i> <i>Alcanivorax</i> <i>Alkanindiges</i> <i>Thalassolituus</i> <i>Idiomarina</i> <i>Halomonas</i> <i>Methylophaga</i> <i>Marinomonas</i> <i>Oleibacter</i>
All ADOC-A		*Includes all listed above



**Table S5.** Relative abundances of taxonomical groups associated to ADOC at initial conditions (in % of total 16S rDNA pool).

	DNA			RNA		
	North	Central	South	North	Central	South
	Alphaproteobacteria					
ADOC-A <sup>1</sup>	0.20±0.00	0.06±0.04	0.02±0.01	0.21±0.00	0.00±0.00	0.01±0.00
Gammaproteobacteria						
ADOC-A <sup>1</sup>	0.05±0.00	0.12±0.01	0.15±0.01	0.05±0.02	0.15±0.03	0.85±0.11
Bacilli ADOC-A <sup>1</sup>	0.00±0.00	0.00±0.00	0.00±0.00	0.09±0.07	0.00±0.00	0.00±0.00
Total ADOC-A genera <sup>1</sup>	0.25±0.00	0.18±0.02	0.17±0.01	0.26±0.02	0.15±0.03	0.86±0.01
Caulobacterales <sup>2</sup>	0.00±0.00	0.02±0.01	0.01±0.01	0.00±0.00	0.01±0.00	0.02±0.00
Rhizobiales <sup>2</sup>	0.11±0.00	0.03±0.00	0.04±0.00	0.00±0.00	0.19±0.00	0.23±0.04
Rhodobacterales <sup>2</sup>	10.62±0.00	8.24±1.08	3.53±0.15	20.77±1.44	4.14±3.27	2.47±0.50
Rhodospirillales <sup>2</sup>	3.81±0.00	0.69±0.09	0.93±0.16	3.57±1.20	1.08±0.34	2.19±0.59
Rickettsiales <sup>2</sup>	0.03±0.00	0.46±0.10	0.29±0.02	0.06±0.04	0.88±0.21	0.71±0.01
Sphingomonadales <sup>2</sup>	0.20±0.00	0.05±0.04	0.02±0.01	0.21±0.00	0.00±0.00	0.01±0.00
Alteromonadales <sup>2</sup>	0.00±0.00	0.00±0.01	0.00±0.00	0.00±0.00	0.04±0.04	0.12±0.07
Burkholderiales <sup>2</sup>	1.34±0.00	1.43±0.06	1.03±0.07	0.99±0.15	1.71±0.13	1.38±0.09
Oceanospirillales <sup>2</sup>	0.00±0.00	0.05±0.02	0.47±0.25	0.24±0.28	0.18±0.10	1.13±0.12
Pseudomonadales <sup>2</sup>	0.00±0.00	0.04±0.00	0.05±0.06	0.00±0.00	0.02±0.00	0.14±0.00
Thiotrichales <sup>2</sup>	0.70±0.00	0.62±0.09	1.03±0.05	0.45±0.11	0.78±0.48	1.54±0.11

<sup>1</sup>Bacterial genera associated to ADOC presence described in Table S4.

<sup>2</sup>Taxonomical groups with representatives that degrade hydrocarbons or have been observed to be stimulated by the presence of oil (Hazen et al., 2010; Neethu et al., 2019; Takahashi et al., 2013; Krollicka et al., 2017; Lozada et al., 2014; Garneau et al., 2016; Joye et al., 2016; Karthikeyan et al., 2020).

**Table S6.** ADOC amendment enrichment factors in the experiments, defined as the ratio of spiked ADOC concentrations over the in situ ADOC concentrations at each experiment site. The ADOC individual compounds amended in the incubations are indicated below the table.

Experiment	ADOC compound	Low dose	High dose
North	n-alkanes	6.6	168.8
	OPE	28.6	828.7
	PAH	48.3	1419.1
	<b>Σ ADOC</b>	8.2	216.5
Central	n-alkanes	13.19	366.8
	OPE	10.5	285
	PAH	46.4	1363.7
	<b>Σ ADOC</b>	14	391.2
South	n-alkanes	4.1	93
	OPE	3.4	71.5
	PAH	23.1	663.3
	<b>Σ ADOC</b>	4.3	100.8

**n-alkanes** : Decane, Docosane, Dodecane, Dotriacontane, Dotriacontane, Eicosane, Heneicosane, Hentriacontane, Heptacosane, Heptadecane, Hexacosane, Hexadecane, Hexatriacontane, nonacosane, Nonadecane, Octadecane, Octane, Octatriacontane, Pentacosane, Pentadecane, Pentatriacontane, Tetradecane, Tetratriacontane, Tricosane, Tridecane, Tritriacontane, Undecane, Octacosane, Tetracontane, Tetracosane, Triacontane.

**PAH** : Acenaphthene, Acenaphthylene, Anthracene, Benz[a]anthracene, Benzo[a]pyrenem, Benzo[b]fluoranthene, Benzo[ghi]perylene, Chrysene, Dibenzo(a,h)anthracene, Fluoranthene, Fluorene, Indeno[1,2,3-cd]pyrene, Naphthalene, Phenanthrene, Pyrene

**OPE**: Tri-n-butyl phosphate (TnBP), Tris(2-chloroethyl)phosphate (TCEP), Tris(1-chloro-2-propyl)phosphate (TCPP), Tris(dichlorisopropyl)phosphate (TDCP), Triphenyl phosphate (TPhP), Tributoxyethyl phosphate (TBEP), 2-Ethylhexyl diphenyl phosphate (EHDPP), Tri(2-ethylhexyl) phosphate (TEHP) , Tricresyl phosphate / Tritolyl phosphate (TCrP).

**Table S7.** Relative abundances of ADOC associated taxa in community composition (% of 16S rDNA pool) and community activities (% of 16S rRNA pool) after 24h of ADOC exposure. This table continues in the next page.

	16S rDNA											
	North				Central				South			
	Control	Low	High	Control	Low	High	Control	Low	High	Control	Low	High
Alphaproteobacteria	0.14±0.03	0.03±0.03	0.11±0.07	0.02±0.00	0.03±0.02	0.03±0.02	0.05±0.02	0.10±0.01	0.07±0.00	0.05±0.02	0.04±0.00	0.07±0.00
ADOC-A <sup>1</sup>	0.11±0.00	0.00±0.00	0.01±0.00	0.01±0.00	0.00±0.00	0.02±0.00	0.00±0.00	0.04±0.00	0.00±0.00	0.00±0.00	0.04±0.00	0.00±0.00
Sphingobium <sup>1</sup>	0.05±0.00	0.00±0.00	0.00±0.00	0.00±0.00	0.01±0.00	0.00±0.00	0.00±0.00	0.02±0.01	0.01±0.00	0.00±0.00	0.02±0.01	0.01±0.00
Sphingomonas <sup>1</sup>	0.05±0.03	0.05±0.00	0.10±0.06	0.01±0.00	0.02±0.03	0.04±0.00	0.02±0.01	0.02±0.00	0.02±0.01	0.02±0.01	0.02±0.00	0.02±0.01
Sulfobacter <sup>1</sup>	0.00±0.00	0.00±0.00	0.00±0.00	0.00±0.00	0.00±0.00	0.00±0.00	0.02±0.01	0.06±0.01	0.04±0.01	0.02±0.01	0.06±0.01	0.04±0.01
Thalassospira <sup>1</sup>	0.04±0.00	0.00±0.00	0.03±0.00	0.00±0.00	0.00±0.00	0.00±0.00	0.00±0.00	0.00±0.00	0.00±0.00	0.00±0.00	0.00±0.00	0.00±0.00
Bacteroidia ADOC-A <sup>1</sup>	0.76±0.16	0.57±0.00	1.73±0.68	0.12±0.04	0.26±0.06	0.14±0.13	0.30±0.07	0.42±0.06	0.34±0.19	0.30±0.07	0.42±0.06	0.34±0.19
Gammaaproteobacteria	0.00±0.00	0.00±0.00	0.03±0.00	0.00±0.00	0.00±0.00	0.00±0.00	0.00±0.00	0.00±0.00	0.00±0.00	0.00±0.00	0.00±0.00	0.00±0.00
ADOC-A <sup>1</sup>	0.03±0.02	0.02±0.00	0.05±0.02	0.00±0.00	0.00±0.00	0.00±0.00	0.02±0.00	0.01±0.00	0.01±0.00	0.02±0.00	0.01±0.00	0.01±0.00
Alcanivorax <sup>1</sup>	0.00±0.00	0.00±0.00	0.00±0.00	0.00±0.00	0.00±0.00	0.05±0.00	0.02±0.00	0.00±0.00	0.00±0.00	0.02±0.00	0.00±0.00	0.00±0.00
Alteromonas <sup>1</sup>	0.70±0.10	0.45±0.07	1.56±0.75	0.00±0.00	0.12±0.01	0.05±0.00	0.11±0.04	0.11±0.01	0.11±0.03	0.11±0.04	0.11±0.01	0.11±0.03
Colwellia <sup>1</sup>	0.00±0.00	0.09±0.00	0.06±0.00	0.00±0.00	0.07±0.00	0.00±0.00	0.00±0.00	0.00±0.00	0.02±0.00	0.00±0.00	0.00±0.00	0.02±0.00
Pseudoalteromonas <sup>1</sup>	0.00±0.00	0.00±0.00	0.00±0.00	0.10±0.06	0.01±0.01	0.05±0.04	0.03±0.01	0.05±0.07	0.06±0.09	0.03±0.01	0.05±0.07	0.06±0.09
Pseudomonas <sup>1</sup>	0.81±0.20	0.63±0.12	1.85±0.87	0.18±0.06	0.32±0.06	0.18±0.10	0.29±0.06	0.53±0.16	0.37±0.09	0.29±0.06	0.53±0.16	0.37±0.09
Acinetobacter <sup>1</sup>	0.00±0.00	0.00±0.00	0.00±0.00	0.02±0.00	0.20±0.26	0.04±0.01	0.07±0.06	0.05±0.02	0.05±0.03	0.07±0.06	0.05±0.02	0.05±0.03
Total ADOC-A genera <sup>1</sup>	0.16±0.06	0.13±0.00	0.22±0.02	0.04±0.01	0.06±0.03	0.04±0.02	0.05±0.03	0.04±0.01	0.06±0.01	0.05±0.03	0.04±0.01	0.06±0.01
Caulobacteriales	0.30±0.05	0.28±0.16	0.25±0.01	1.30±0.07	1.43±0.06	1.25±0.15	1.11±0.01	1.04±0.06	0.92±0.04	1.11±0.01	1.04±0.06	0.92±0.04
Rhizobiales	10.78±0.37	11.49±0.66	11.89±0.34	10.81±0.12	10.18±1.51	9.67±2.45	4.79±1.07	4.48±0.28	4.58±0.08	4.79±1.07	4.48±0.28	4.58±0.08
Burkholderiales	0.49±0.03	0.64±0.22	1.14±0.06	0.61±0.30	0.82±0.23	0.83±0.20	1.09±0.30	0.76±0.10	0.90±0.14	1.09±0.30	0.76±0.10	0.90±0.14
Rhodobacteriales	1.51±0.13	1.06±0.08	1.35±0.09	0.44±0.25	0.41±0.02	0.47±0.03	0.39±0.01	0.37±0.00	0.42±0.06	0.39±0.01	0.37±0.00	0.42±0.06
Rickettsiales	0.08±0.04	0.00±0.00	0.03±0.03	0.02±0.01	0.02±0.00	0.05±0.02	0.04±0.02	0.10±0.01	0.06±0.00	0.04±0.02	0.10±0.01	0.06±0.00
Sphingomonadales	0.73±0.12	0.47±0.05	1.60±0.77	0.00±0.00	0.15±0.02	0.07±0.00	0.12±0.05	0.13±0.01	0.12±0.04	0.12±0.05	0.13±0.01	0.12±0.04
Alteromonadales	0.06±0.00	0.00±0.00	0.35±0.05	0.56±0.25	0.88±0.02	0.85±0.21	0.74±0.19	0.56±0.04	0.60±0.10	0.74±0.19	0.56±0.04	0.60±0.10
Oceanospirillales	0.00±0.00	0.11±0.05	0.12±0.00	0.08±0.04	0.08±0.00	0.05±0.05	0.05±0.00	0.27±0.13	0.29±0.00	0.05±0.00	0.27±0.13	0.29±0.00
Pseudomonadales	0.15±0.00	0.15±0.00	0.14±0.02	0.27±0.07	0.28±0.08	0.27±0.03	0.51±0.09	0.49±0.00	0.48±0.06	0.51±0.09	0.49±0.00	0.48±0.06
Thiotrichales												

	16S rRNA								
	North			Central			South		
	Control	Low	High	Control	Low	High	Control	Low	High
Alphaproteobacteria									
ADOC-A <sup>1</sup>	0.20±0.06	0.04±0.00	0.01±0.00	0.06±0.01	0.00±0.00	0.00±0.00	0.09±0.09	0.06±0.03	0.02±0.00
<i>Sphingobium</i> <sup>1</sup>	0.10±0.00	0.00±0.00	0.00±0.00	0.04±0.02	0.00±0.00	0.00±0.00	0.03±0.01	0.00±0.00	0.00±0.00
<i>Sphingomonas</i> <sup>1</sup>	0.00±0.00	0.03±0.00	0.00±0.00	0.04±0.00	0.00±0.00	0.00±0.00	0.00±0.00	0.02±0.01	0.00±0.00
<i>Sulfobacter</i> <sup>1</sup>	0.15±0.00	0.00±0.00	0.00±0.00	0.00±0.00	0.00±0.00	0.00±0.00	0.00±0.00	0.03±0.00	0.02±0.00
<i>Thalassospira</i> <sup>1</sup>	0.00±0.00	0.00±0.00	0.00±0.00	0.00±0.00	0.00±0.00	0.00±0.00	0.11±0.00	0.06±0.00	0.00±0.00
Bacteroidia ADOC-A <sup>1</sup>	0.04±0.00	0.00±0.00	0.01±0.00	0.02±0.00	0.00±0.00	0.00±0.00	0.00±0.00	0.00±0.00	0.00±0.00
Gammaproteobacteria									
ADOC-A <sup>1</sup>	1.57±1.05	1.12±0.04	6.05±0.40	0.34±0.14	0.22±0.04	0.28±0.09	0.65±0.12	0.81±0.08	1.00±0.12
<i>Alcanivorax</i> <sup>1</sup>	0.00±0.00	0.00±0.00	0.03±0.00	0.00±0.00	0.00±0.00	0.00±0.00	0.00±0.00	0.00±0.00	0.00±0.00
<i>Alteromonas</i> <sup>1</sup>	0.03±0.02	0.02±0.00	0.05±0.02	0.00±0.00	0.00±0.00	0.00±0.00	0.02±0.00	0.01±0.00	0.01±0.00
<i>Colwellia</i> <sup>1</sup>	0.00±0.00	0.00±0.00	0.00±0.00	0.00±0.00	0.00±0.00	0.05±0.00	0.02±0.00	0.00±0.00	0.00±0.00
<i>Pseudoalteromonas</i> <sup>1</sup>	1.19±0.62	0.91±0.27	5.23±0.52	0.03±0.00	0.14±0.00	0.11±0.02	0.28±0.03	0.32±0.06	0.51±0.11
<i>Pseudomonas</i> <sup>1</sup>	0.49±0.00	0.22±0.00	0.22±0.02	0.05±0.04	0.07±0.00	0.00±0.00	0.06±0.00	0.10±0.00	0.00±0.00
<i>Acinetobacter</i> <sup>1</sup>	0.00±0.00	0.00±0.00	0.00±0.00	0.14±0.11	0.00±0.00	0.11±0.00	0.09±0.06	0.07±0.02	0.25±0.00
Total ADOC-A general <sup>1</sup>	1.63±1.01	1.06±0.07	6.09±0.42	0.39±0.13	0.21±0.03	0.26±0.09	0.74±0.26	0.78±0.09	0.98±0.13
Caulobacteriales	0.00±0.00	0.00±0.00	0.00±0.00	0.09±0.01	0.17±0.18	0.07±0.01	0.07±0.03	0.10±0.10	0.05±0.00
Rhizobiales	0.81±0.07	0.58±0.11	0.57±0.03	0.30±0.04	0.22±0.07	0.28±0.06	0.33±0.08	0.23±0.08	0.23±0.01
Rhodobacterales	21.79±2.35	23.00±1.44	11.61±4.17	9.24±1.33	6.69±0.49	6.77±0.83	5.02±2.29	4.20±2.75	4.28±1.30
Rhodospirillales	2.03±0.34	2.03±0.02	1.96±0.40	2.77±0.02	2.20±0.08	2.44±0.05	2.65±0.86	2.27±1.30	2.31±0.99
Rickettsiales	1.51±0.13	1.06±0.08	1.35±0.09	0.44±0.25	0.41±0.02	0.47±0.03	0.39±0.01	0.37±0.00	0.42±0.06
Sphingomomadales	0.10±0.00	0.03±0.00	0.00±0.00	0.06±0.01	0.00±0.00	0.02±0.00	0.04±0.02	0.02±0.01	0.02±0.00
Alteromonadales	1.31±0.68	0.98±0.16	5.70±0.47	0.03±0.00	0.15±0.01	0.13±0.00	0.35±0.05	0.44±0.01	0.62±0.23
Burkholderiales	0.43±0.09	0.37±0.10	0.39±0.08	2.79±0.96	4.09±0.40	1.94±0.04	2.36±1.37	2.96±1.49	2.96±0.80
Oceanospirillales	0.19±0.00	0.18±0.01	0.23±0.02	1.17±0.13	0.64±0.04	0.86±0.22	0.96±0.12	0.92±0.24	1.10±0.41
Pseudomonadales	0.49±0.00	0.22±0.00	0.22±0.02	0.22±0.11	0.07±0.00	0.17±0.00	0.15±0.03	0.22±0.11	0.16±0.13
Thiotrichales	0.13±0.00	0.00±0.00	0.15±0.02	0.21±0.02	0.60±0.12	0.56±0.12	0.48±0.06	0.46±0.03	0.52±0.02

<sup>1</sup> Bacterial genera associated to ADOC presence described in Table S4.

<sup>2</sup> Taxonomical groups with representatives that degrade hydrocarbons or have been observed to be stimulated by the presence of oil (Hazen et al., 2010; Neethu et al., 2019; Takahashi et al., 2013; Krollicka et al., 2017; Lozada et al., 2014; Garneau et al., 2016; Joye et al., 2016; Karthikeyan et al., 2020).

**Table S8.** List of ADOC model families, degradation pathway genes and half-life times.

Compound	Gene name	Protein name	Enzymatic function	Ref.	Half-life	Ref.
<b>n-Alkanes</b>						
alkanes >C12	almA	Probable FAD-binding monoxygenase AlmA	Hydroxylating	Throne-Holst <i>et al.</i> , 2007		
alkanes C5-C11	alkB	Alkane 1-monoxygenase	oxyreductase activity	Van Beilen <i>et al.</i> , 2003		
alkanes <C4	pMMO and sMMO	Methane monoxygenase regulatory protein		McDonald <i>et al.</i> , 2006		
<b>PAH</b>						
Polycyclic aromatic hydrocarbon	RHO/RHD	Ring hydroxylating oxygenase/dioxygenase			LMW 15-60 days	Gonzalez-Gaya <i>et al.</i> , 2019
Benzoate	benA and benB	Benzoate 1,2-dioxygenase (alpha&beta subunits)		Kweon <i>et al.</i> , 2008 Hazen <i>et al.</i> , 2010 Dombrowski <i>et al.</i> , 2016 Wang <i>et al.</i> , 2008	HMW > 100 days	Louvado <i>et al.</i> , 2015
Catechol	catA	Catechol dioxygenase	Hydroxylating oxyreductase activity			
Xylene	catB	Muconate cycloisomerase				
Biphenil	bphA and bphC	Biphenyl and dihydroxybiphenyl dioxygenase				
Protocatechuate	pcaG and pcaH	Protocatechuate dioxygenase (alpha&beta subunits)				
<b>OPE</b>						
Phosphate triester	PTE and PTE-LL	Phosphotriesterase and Phosphotriesterase like lactamase		Singh and Walker, 2006 Afrati-Jurnou <i>et al.</i> , 2012		Singh and Walker, 2006
Phosphate diester	PDE	Phosphodiesterase	Phosphate ester bonds hydrolyzing activity	Mabanglo <i>et al.</i> , 2016 Abe <i>et al.</i> , 2014 Abe <i>et al.</i> , 2017	30-180 days	
Phosphate monoester	PMO	Phosphomonoesterase				

**Table S9.** Sequencing depth for each library.

Sample ID (SRA)	Library size	Site	Material	Time point	Treatment	Replicate
101	151354	NORTH	DNA	24	Control	A
102	147677	NORTH	DNA	24	Control	B
119	218885	NORTH	DNA	0	Control	A
12	77149	NORTH	RNA	0	Control	A
13	92181	NORTH	RNA	0	Control	B
1	87471	NORTH	RNA	24	Control	A
2	96912	NORTH	RNA	24	Control	B
107b	229654	NORTH	DNA	24	High	A
108b	228209	NORTH	DNA	24	High	B
7	128984	NORTH	RNA	24	High	A
8	100782	NORTH	RNA	24	High	B
103	92651	NORTH	DNA	24	Low	A
104	169877	NORTH	DNA	24	Low	B
3	76350	NORTH	RNA	24	Low	A
4	98450	NORTH	RNA	24	Low	B
111	262329	CENTRAL	DNA	24	Control	A
112b	306093	CENTRAL	DNA	24	Control	B
126	222820	CENTRAL	DNA	0	Control	A
127b	230890	CENTRAL	DNA	0	Control	B
146	242835	CENTRAL	DNA	24	Control	A
20	201338	CENTRAL	RNA	0	Control	A
21	170415	CENTRAL	RNA	0	Control	B
239	32257	CENTRAL	RNA	24	Control	A
240	22035	CENTRAL	RNA	24	Control	B
217	22711	CENTRAL	RNA	24	High	A
218	33260	CENTRAL	RNA	24	High	B
249	36853	CENTRAL	DNA	24	High	B
485	80420	CENTRAL	DNA	24	High	A
215	29516	CENTRAL	RNA	24	Low	A
216	40372	CENTRAL	RNA	24	Low	B
248	72226	CENTRAL	DNA	24	Low	B
483	81633	CENTRAL	DNA	24	Low	A
130	249760	SOUTH	DNA	0	Control	A
131	152498	SOUTH	DNA	0	Control	B
24	132461	SOUTH	RNA	0	Control	A
25	74204	SOUTH	RNA	0	Control	B
219	35650	SOUTH	RNA	24	Control	A
220	42269	SOUTH	RNA	24	Control	B
250	41068	SOUTH	DNA	24	Control	B
487	104933	SOUTH	DNA	24	Control	A
235	31639	SOUTH	RNA	24	High	A
236	32964	SOUTH	RNA	24	High	B
493	63269	SOUTH	DNA	24	High	A
494	56160	SOUTH	DNA	24	High	B
221	41863	SOUTH	RNA	24	Low	A
222	36158	SOUTH	RNA	24	Low	B
489	78306	SOUTH	DNA	24	Low	A
490	67924	SOUTH	DNA	24	Low	B

**Table S10.** Average identity match of ASVs from our data set assigned to genera previously reported as being associated to the presence of ADOC (ADOC-A) (Takahashi et al., 2013; Lozada et al., 2014; Karthikeyan et al., 2020), against isolates genomes from the same genera reported to be found in ADOC polluted sites and/or with metabolic capabilities to consume ADOC. This table continues in the following pages.

Genus keyword	ASV name	Genome	Query cover	Average Identity	Reference	
Alcanivorax	asv.1	Alcanivorax sp. TH11	99%	99.22%	Submitted by Oka et al., 2019, from Manabu Hori Yamaguchi University Acc. No. LC498508.1	
Alcanivorax	asv.2	Alcanivorax sp. TH11	99%	99.22%		
Alcanivorax	asv.1	Alcanivorax sp. AU7AG3	99%	99.22%	Catania et al., 2015	
Alcanivorax	asv.2	Alcanivorax sp. AU7AG3	99%	99.22%		
Alcanivorax	asv.1	Alcanivorax sp. AU4SA4	99%	99.22%		
Alcanivorax	asv.2	Alcanivorax sp. AU4SA4	99%	99.22%		
Alcanivorax	asv.1	Alcanivorax borkumensis SK2	99%	100.00%		Sabirova et al., 2008
Alcanivorax	asv.2	Alcanivorax borkumensis SK2	99%	100.00%		
Alteromonas	asv.3	Alteromonas naphthalenivorans	99%	99.22%	Jin et al., 2015	
Alteromonas	asv.4	Alteromonas naphthalenivorans	99%	99.22%		
Alteromonas	asv.5	Alteromonas naphthalenivorans	99%	99.22%		
Alteromonas	asv.6	Alteromonas naphthalenivorans	99%	99.22%		
Alteromonas	asv.7	Alteromonas naphthalenivorans	99%	99.22%		
Alteromonas	asv.8	Alteromonas naphthalenivorans	99%	99.22%		
Alteromonas	asv.9	Alteromonas naphthalenivorans	99%	99.22%		
Alteromonas	asv.10	Alteromonas naphthalenivorans	99%	99.22%		
Alteromonas	asv.11	Alteromonas naphthalenivorans	99%	99.22%		
Colwellia	asv.12	Colwellia psycherythraea strain 34H	99%	97.14%		Mason et al., 2014; Peña-Montenegro et al., 2020
Colwellia	asv.13	Colwellia psycherythraea strain 34H	99%	97.14%		
Colwellia	asv.14	Colwellia psycherythraea strain 34H	99%	97.14%		
Colwellia	asv.15	Colwellia psycherythraea strain 34H	99%	97.14%		
Colwellia	asv.16	Colwellia psycherythraea strain 34H	99%	97.14%		
Colwellia	asv.17	Colwellia psycherythraea strain 34H	99%	97.14%		
Colwellia	asv.18	Colwellia psycherythraea strain 34H	99%	97.14%		
Colwellia	asv.19	Colwellia psycherythraea strain 34H	99%	97.14%		
Colwellia	asv.20	Colwellia psycherythraea strain 34H	99%	97.14%		
Colwellia	asv.21	Colwellia psycherythraea strain 34H	99%	97.14%		
Colwellia	asv.22	Colwellia psycherythraea strain 34H	99%	97.14%		
Colwellia	asv.23	Colwellia psycherythraea strain 34H	99%	97.14%		
Pseudoalteromonas	asv.24	Pseudoalteromonas gelatinilytica strain 2216E-X-23	98%	98.18%	GROS ; Karthikeyan et al., 2020	
Pseudoalteromonas	asv.25	Pseudoalteromonas gelatinilytica strain 2216E-X-23	98%	98.18%		
Pseudoalteromonas	asv.26	Pseudoalteromonas gelatinilytica strain 2216E-X-23	98%	98.18%		
Pseudoalteromonas	asv.27	Pseudoalteromonas gelatinilytica strain 2216E-X-23	98%	98.18%		

Genus keyword	ASV name	Genome	Query cover	Average Identity	Reference
Pseudoalteromonas	asv.28	Pseudoalteromonas gelatinilytica strain 2216F-X-23	98%	98.18%	
Pseudoalteromonas	asv.29	Pseudoalteromonas gelatinilytica strain 2216F-X-23	98%	98.18%	
Pseudoalteromonas	asv.30	Pseudoalteromonas gelatinilytica strain 2216F-X-23	98%	98.18%	
Pseudoalteromonas	asv.31	Pseudoalteromonas gelatinilytica strain 2216F-X-23	98%	98.18%	
Pseudoalteromonas	asv.32	Pseudoalteromonas gelatinilytica strain 2216F-X-23	98%	98.18%	
Pseudoalteromonas	asv.24	Pseudoalteromonas Strain ND6B	99%	99.73%	Harris et al., 2014
Pseudoalteromonas	asv.25	Pseudoalteromonas Strain ND6B	99%	99.73%	
Pseudoalteromonas	asv.26	Pseudoalteromonas Strain ND6B	99%	99.73%	
Pseudoalteromonas	asv.27	Pseudoalteromonas Strain ND6B	99%	99.73%	
Pseudoalteromonas	asv.28	Pseudoalteromonas Strain ND6B	99%	99.73%	
Pseudoalteromonas	asv.29	Pseudoalteromonas Strain ND6B	99%	99.73%	
Pseudoalteromonas	asv.30	Pseudoalteromonas Strain ND6B	99%	99.73%	
Pseudoalteromonas	asv.31	Pseudoalteromonas Strain ND6B	99%	99.73%	
Pseudoalteromonas	asv.32	Pseudoalteromonas Strain ND6B	99%	99.73%	
Pseudoalteromonas	asv.24	Pseudoalteromonas strain 13-15	95%	99.22%	Duhaine et al., 2016
Pseudoalteromonas	asv.25	Pseudoalteromonas strain 13-15	95%	99.22%	
Pseudoalteromonas	asv.26	Pseudoalteromonas strain 13-15	95%	99.22%	
Pseudoalteromonas	asv.27	Pseudoalteromonas strain 13-15	95%	99.22%	
Pseudoalteromonas	asv.28	Pseudoalteromonas strain 13-15	95%	99.22%	
Pseudoalteromonas	asv.29	Pseudoalteromonas strain 13-15	95%	99.22%	
Pseudoalteromonas	asv.30	Pseudoalteromonas strain 13-15	95%	99.22%	
Pseudoalteromonas	asv.31	Pseudoalteromonas strain 13-15	95%	99.22%	
Pseudoalteromonas	asv.32	Pseudoalteromonas strain 13-15	95%	99.22%	
Pseudoalteromonas	asv.24	Pseudoalteromonas atlantica	99%	98.96%	Chromopoulou et al., 2015
Pseudoalteromonas	asv.25	Pseudoalteromonas atlantica	99%	98.96%	
Pseudoalteromonas	asv.26	Pseudoalteromonas atlantica	99%	98.96%	
Pseudoalteromonas	asv.27	Pseudoalteromonas atlantica	99%	98.96%	
Pseudoalteromonas	asv.28	Pseudoalteromonas atlantica	99%	98.96%	
Pseudoalteromonas	asv.29	Pseudoalteromonas atlantica	99%	98.96%	
Pseudoalteromonas	asv.30	Pseudoalteromonas atlantica	99%	98.96%	
Pseudoalteromonas	asv.31	Pseudoalteromonas atlantica	99%	98.96%	
Pseudoalteromonas	asv.32	Pseudoalteromonas atlantica	99%	98.96%	
Pseudoalteromonas	asv.24	Pseudoalteromonas strain H103	99%	99.73%	Duhaine et al., 2016
Pseudoalteromonas	asv.25	Pseudoalteromonas strain H103	99%	99.73%	
Pseudoalteromonas	asv.26	Pseudoalteromonas strain H103	99%	99.73%	



Genus keyword	ASV name	Genome	Query cover	Average Identity	Reference
Pseudoalteromonas	asv.27	Pseudoalteromonas strain H103	99%	99.73%	
Pseudoalteromonas	asv.28	Pseudoalteromonas strain H103	99%	99.73%	
Pseudoalteromonas	asv.29	Pseudoalteromonas strain H103	99%	99.73%	
Pseudoalteromonas	asv.30	Pseudoalteromonas strain H103	99%	99.73%	
Pseudoalteromonas	asv.31	Pseudoalteromonas strain H103	99%	99.73%	
Pseudoalteromonas	asv.32	Pseudoalteromonas strain H103	99%	99.73%	
Pseudoalteromonas	asv.24	Pseudoalteromonas strain H71	99%	99.73%	
Pseudoalteromonas	asv.25	Pseudoalteromonas strain H71	99%	99.73%	Duhaime et al., 2016
Pseudoalteromonas	asv.26	Pseudoalteromonas strain H71	99%	99.73%	
Pseudoalteromonas	asv.27	Pseudoalteromonas strain H71	99%	99.73%	
Pseudoalteromonas	asv.28	Pseudoalteromonas strain H71	99%	99.73%	
Pseudoalteromonas	asv.29	Pseudoalteromonas strain H71	99%	99.73%	
Pseudoalteromonas	asv.30	Pseudoalteromonas strain H71	99%	99.73%	
Pseudoalteromonas	asv.31	Pseudoalteromonas strain H71	99%	99.73%	
Pseudoalteromonas	asv.32	Pseudoalteromonas strain H71	99%	99.73%	
Sphingobium	asv.33	Sphingobium yanoikuyae strain SAFY	99%	97.59%	Guo et al., 2011
Sphingobium	asv.33	Sphingobium yanoikuyae sp.	99%	98.93%	Borde et al., 2003
Sphingomonas	asv.34	Sphingomonas paucimobilis strain AIMST S2	99%	98.44%	Ravintharan et al., 2019
Sphingomonas	asv.35	Sphingomonas paucimobilis strain AIMST S2	99%	98.44%	
Sphingomonas	asv.36	Sphingomonas paucimobilis strain AIMST S2	99%	98.44%	
Sphingomonas	asv.37	Sphingomonas paucimobilis strain AIMST S2	99%	98.44%	
Thalassospira	asv.38	Thalassospira xiamenensis strain M-5	99%	98.92%	Liu et al., 2007
Thalassospira	asv.38	Thalassospira tepidiphila sp	99%	99.46%	Kodama et al., 2008
Thalassospira	asv.38	Thalassospira sp. EM202	99%	100.00%	Submitted by Lee,D.-H. in 2013 from Department of Biology, Jeju National University
Thalassospira	asv.38	Thalassospira tepidiphila strain DIFJ7-5	99%	99.46%	Acc.no. KC469107.1 Wang et al., 2014

\* The ASV sequences assigned to each ASV name can be found in Table S11 in the SI of the publication.

**Figure S1.** 16S rRNA gene ASV sequences dendrogram at initial conditions.

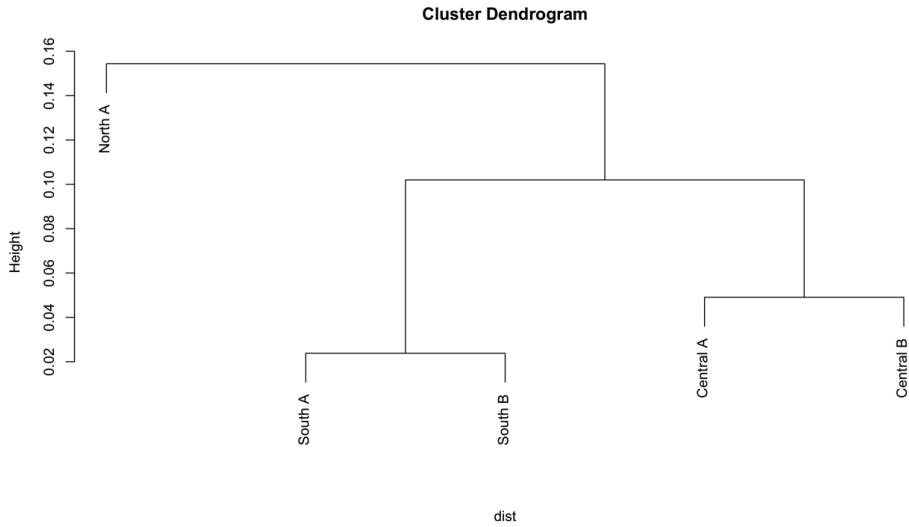


**Figure S2.** Contribution of the dominant groups to the total 16S rDNA and rRNA pool at the three NESAP sites.

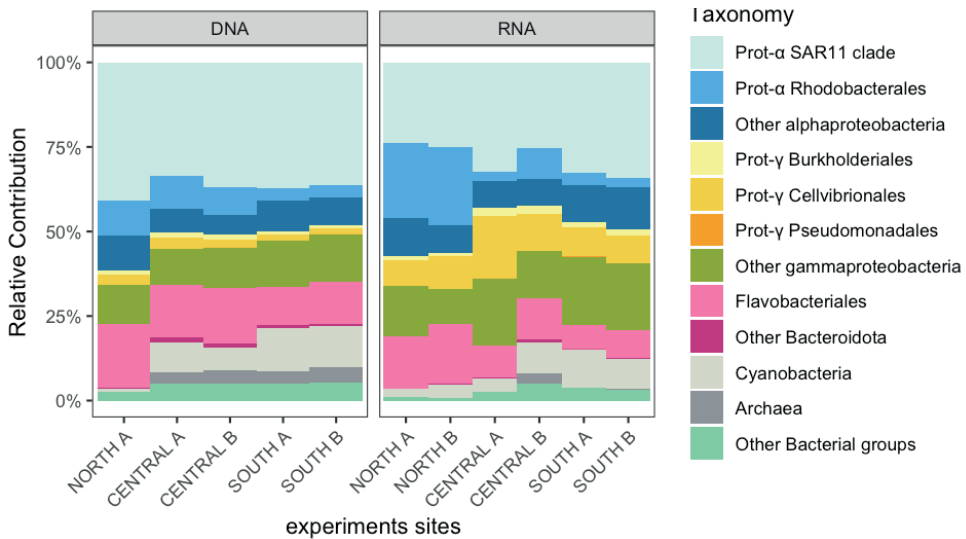


Figure S3. 16S rRNA gene ASV sequences dendrogram at initial conditions.

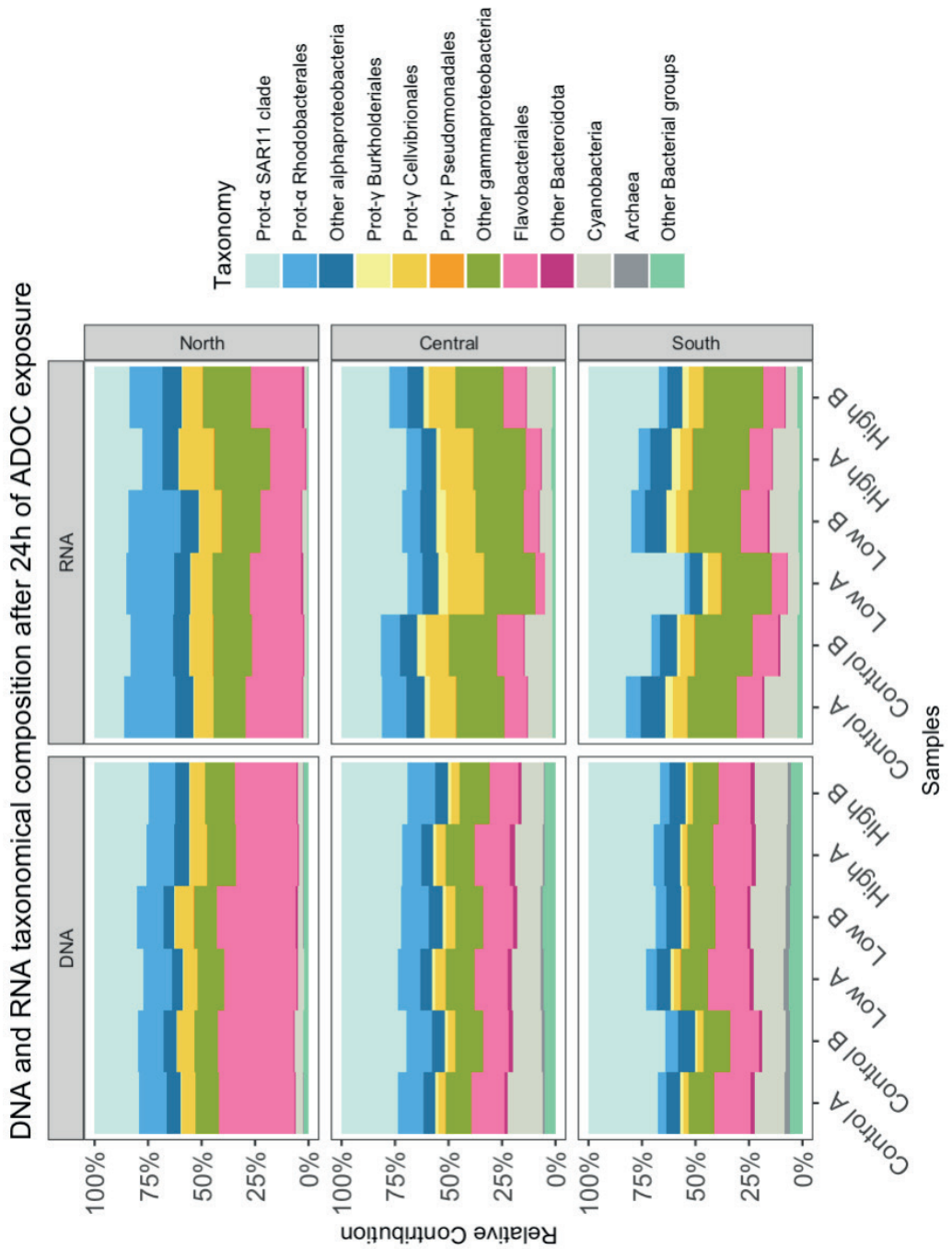
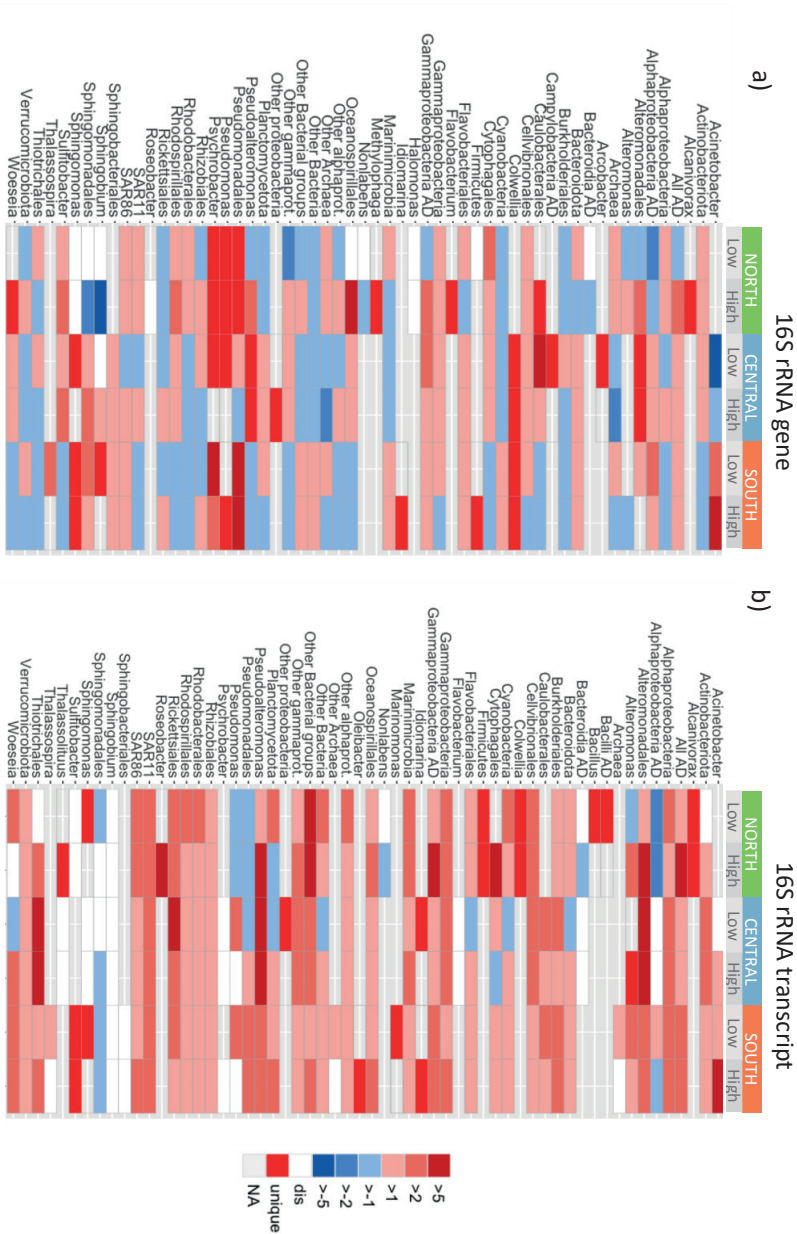
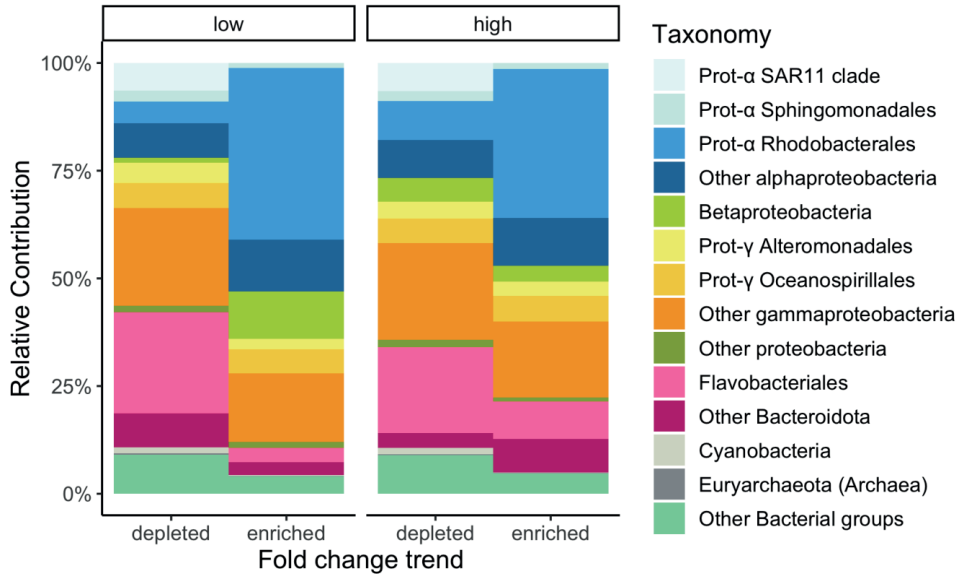


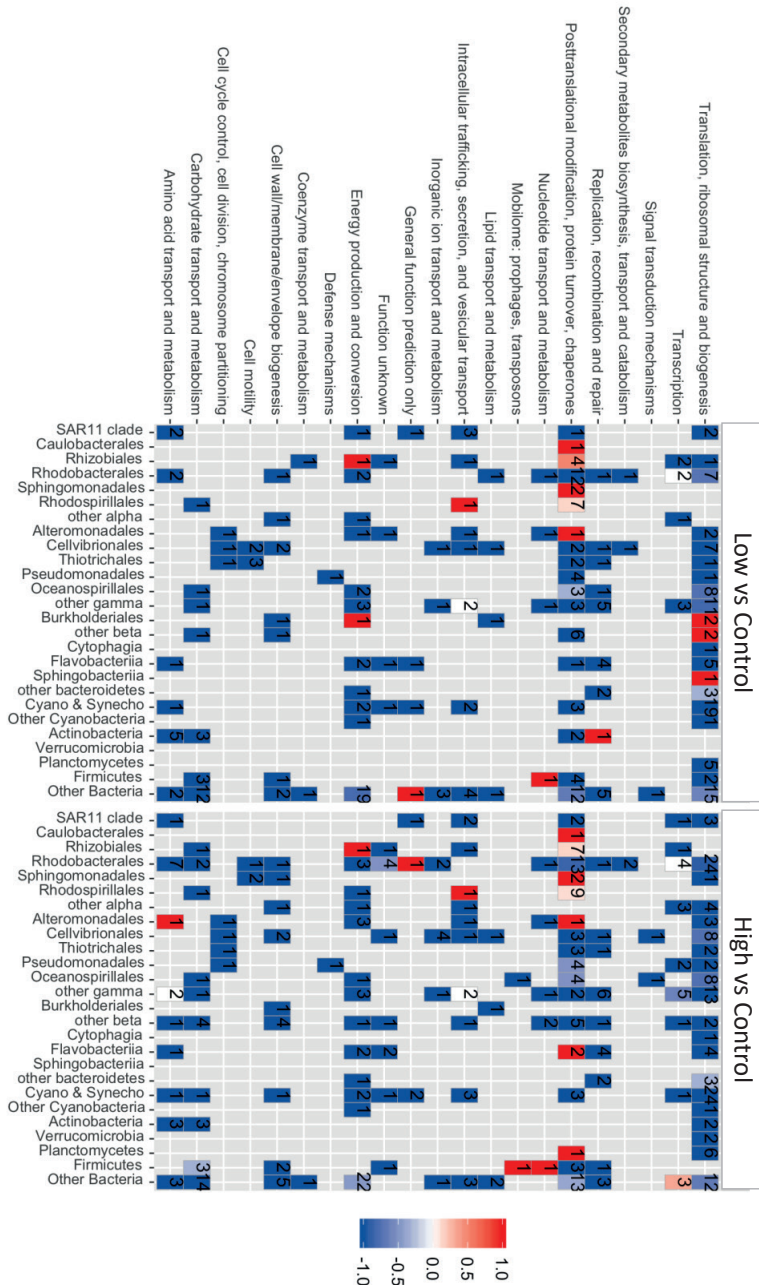
Figure S4. 16S rRNA gene ASV sequences dendrogram at initial conditions.



**Figure S5.** Contribution of dominant groups to the pool of transcripts enriched (positive) and depleted (negative) in ADOC treatments (high and low concentrations) compared to controls after 24 hours at Central.



**Figure S6.** Edge-R significant taxonomy-specific changes in transcriptome regulation. Numbers indicate total of significant changes within that category and assigned to that taxon (FDR < 0.05).



## ADDITIONAL REFERENCES

- Abe, K., Mukai, N., Morooka, Y., Makino, T., Oshima, K., Takahashi, S., and Kera, Y. (2017) An atypical phosphodiesterase capable of degrading haloalkyl phosphate diesters from *Sphingobium* sp. strain TCM1. *Sci Rep* 7:.
- Abe, K., Yoshida, S., Suzuki, Y., Mori, J., Doi, Y., Takahashi, S., and Kera, Y. (2014) Haloalkylphosphorus hydrolases purified from *Sphingomonas* sp. strain TDK1 and *Sphingobium* sp. strain TCM1. *Appl Environ Microbiol* 80: 5866–73.
- Afriat-Jurnou, L., Jackson, C.J., and Tawfik, D.S. (2012) Reconstructing a missing link in the evolution of a recently diverged phosphotriesterase by active-site loop remodeling. *Biochemistry* 51: 6047–6055.
- Van Beilen, J.B., Li, Z., Duetz, W.A., Smits, T.H.M., and Witholt, B. (2003) Diversity of Alkane Hydroxylase Systems in the Environment.
- Borde, X., Guieysse, B., Delgado, O., Muñoz, R., Hatti-Kaul, R., Nugier-Chauvin, C., et al. (2003) Synergistic relationships in algal–bacterial microcosms for the treatment of aromatic pollutants. *Bioresour Technol* 86: 293–300.
- Catania, V., Santisi, S., Signa, G., Vizzini, S., Mazzola, A., Cappello, S., et al. (2015) Intrinsic bioremediation potential of a chronically polluted marine coastal area. *Mar Pollut Bull* 99: 138–149.
- Chronopoulou, P.M., Sanni, G.O., Silas-Olu, D.I., van der Meer, J.R., Timmis, K.N., Brussaard, C.P.D., and McGenity, T.J. (2015) Generalist hydrocarbon-degrading bacterial communities in the oil-polluted water column of the North Sea. *Microb Biotechnol* 8: 434–447.
- Dombrowski, N., Donaho, J.A., Gutierrez, T., Seitz, K.W., Teske, A.P., and Baker, B.J. (2016) Reconstructing metabolic pathways of hydrocarbon-degrading bacteria from the Deepwater Horizon oil spill. *Nat Microbiol* 1: 16057.
- Duhaime, M.B., Wichels, A., and Sullivan, M.B. (2016) Six *Pseudoalteromonas* strains isolated from surface waters of Kabeltonne, offshore Helgoland, North Sea. *Genome Announc* 4: 1697–1712.
- Garneau, M.-È., Michel, C., Meisterhans, G., Fortin, N., King, T.L., Greer, C.W., and Lee, K. (2016) Hydrocarbon biodegradation by Arctic sea-ice and sub-ice microbial communities during microcosm experiments, Northwest Passage (Nunavut, Canada). *FEMS Microbiol Ecol* 92: fiw130.
- González-Gaya, B., Martínez-Varela, A., Vila-Costa, M., Casal, P., Cerro-Gálvez, E., Berrojalbiz, N., et al. (2019) Biodegradation as an important sink of aromatic hydrocarbons in the oceans. *Nat Geosci* 12:.
- Guo, C., Ke, L., Dang, Z., and Tam, N.F. (2011) Temporal changes in *Sphingomonas* and *Mycobacterium* populations in mangrove sediments contaminated with different concentrations of polycyclic aromatic hydrocarbons (PAHs). *Mar Pollut Bull* 62: 133–139.
- Harris, A.P., Techtmann, S.M., Stelling, S.C., Utturkar, S.M., Alshibli, N.K., Brown, S.D., and Hazen, T.C. (2014) Draft genome sequence of *Pseudoalteromonas* sp. strain ND6B, an oildegrading isolate from eastern Mediterranean Sea water collected at a depth of 1,210 meters. *Genome Announc* 2:.
- Hazen, T.C., Dubinsky, E.A., DeSantis, T.Z., Andersen, G.L., Piceno, Y.M., Singh, N., et al. (2010) Deep-sea oil plume enriches indigenous oil-degrading bacteria. *Science* (80- ) 330: 204–208.
- Karthikeyan, S., Rodriguez-R, L.M., Heritier-Robbins, P., Hatt, J.K., Huettel, M., Kostka, J.E., and Konstantinidis, K.T. (2020) Genome repository of oil systems: An interactive and searchable database that expands the catalogued diversity of crude oil-associated microbes. *Environ Microbiol* 22: 2094–2106.
- Kleindienst, S., Grim, S., Sogin, M., Bracco, A., Crespo-Medina, M., and Joye, S.B. (2016) Diverse, rare microbial taxa responded to the Deepwater Horizon deep-sea hydrocarbon plume. *ISME J* 10: 400–415.
- Kodama, Y., Stiknowati, L.I., Ueki, A., and Ueki, K. (2017) *Thalassospira tepidiphila* sp. nov., a polycyclic aromatic hydrocarbon-degrading bacterium isolated from seawater. 711–715.
- Krolicka, A., Boccadoro, C., Nilsen, M.M., and Baussant, T. (2017) Capturing Early Changes in the Marine Bacterial Community as a Result of Crude Oil Pollution in a Mesocosm Experiment. *Microbes Environ* 32: 358–366.
- Kweon, O., Kim, S.-J., Baek, S., Chae, J.-C., Adjei, M.D., Baek, D.-H., et al. (2008) A new classification system for bacterial Rieske non-heme iron aromatic ring-hydroxylating oxygenases. *BMC Biochem* 9: 11.
- Liu, C., Wu, Y., Li, L., Yingfei, M., and Shao, Z. (2007) *Thalassospira xiamenensis* sp. nov. and *Thalassospira profundimaris* sp. nov. *Int J Syst Evol Microbiol* 57: 316–320.

Louvado, A., Gomes, N.C.M., Simões, M.M.Q., Almeida, A., Cleary, D.F.R., and Cunha, A. (2015) Polycyclic aromatic hydrocarbons in deep sea sediments: Microbe–pollutant interactions in a remote environment. *Sci Total Environ* 526: 312–328.

Mabanglo, M.F., Xiang, D.F., Bigley, A.N., and Raushel, F.M. (2016) Structure of a Novel Phosphotriesterase from *Sphingobium* sp. TCM1: A Familiar Binuclear Metal Center Embedded in a Seven-Bladed  $\beta$ -Propeller Protein Fold. *Biochemistry* 55: 3963–3974.

Mason, O.U., Scott, N.M., Gonzalez, A., Robbins-Pianka, A., Bælum, J., Kimbrel, J., et al. (2014) Metagenomics reveals sediment microbial community response to Deepwater Horizon oil spill. *ISME J* 8: 1464–1475.

McDonald, I.R., Miguez, C.B., Rogge, G., Bourque, D., Wendlandt, K.D., Groleau, D., and Murrell, J.C. (2006) Diversity of soluble methane monooxygenase-containing methanotrophs isolated from polluted environments. *FEMS Microbiol Lett* 255: 225–232.

Neethu, C.S., Saravanakumar, C., Purvaja, R., Robin, R.S., and Ramesh, R. (2019) Oil-Spill Triggered Shift in Indigenous Microbial Structure and Functional Dynamics in Different Marine Environmental Matrices. *Sci Rep*.

Peña-Montenegro, T.D., Kleindienst, S., Allen, A.E., Eren, A.M., McCrow, J.P., Sánchez-Calderón, J.D., et al. (2020) *Colwellia* and *Marinobacter* metapangenomes reveal species-specific responses to oil and dispersant exposure in deepsea microbial communities. *bioRxiv* 2020.09.28.317438.

Ravintheran, S.K., Sivaprakasam, S., Loke, S., Lee, S.Y., Manickam, R., Yahya, A., et al. (2019) Complete genome sequence of *Sphingomonas paucimobilis* AIMST S2, a xenobiotic-degrading bacterium. *Sci Data* 6: 1–6.

Sabirova, J.S., Chernikova, T.N., Timmis, K.N., and Golyshin, P.N. (2008) Niche-specificity factors of a marine oil-degrading bacterium *Alcanivorax borkumensis* SK2. *FEMS Microbiol Lett* 285: 89–96.

Singh, B.K. and Walker, A. (2006) Microbial degradation of organophosphorus compounds. *FEMS Microbiol Rev* 30: 428–471.

Throne-Holst, M., Wentzel, A., Ellingsen, T.E., Kotlar, H.K., and Zotchev, S.B. (2007) Identification of novel genes involved in long-chain n-alkane degradation by *Acinetobacter* sp. strain DSM 17874. *Appl Environ Microbiol* 73: 3327–3332.

Wang, B., Lai, Q., Cui, Z., Tan, T., and Shao, Z. (2008) A pyrene-degrading consortium from deep-sea sediment of the West Pacific and its key member *Cycloclasticus* sp. P1. *Environ Microbiol* 10: 1948–1963.

Wang, W., Zhong, R., Shan, D., and Shao, Z. (2014) Indigenous oil-degrading bacteria in crude oil-contaminated seawater of the Yellow sea, China. *Appl Microbiol Biotechnol* 98: 7253–7269.





## **Aknowledgements**



# GRÀCIES · THANKS · GRACIAS ·

For the last part of this journey I have thought of this academic period as a mountain summit hike. You start with a map, probably a decent map, but soon you realize that it is either outdated because the landslides and forest have changed the trail, or it is cropped or blurry in those areas that you would have liked to have some geographic guidance. With no useful map the landscape speaks: the trodden grassy path seems to take you to the right direction, maybe it isn't the shortest way, but surely the one with the best views. Streams of water, berry bushes and hazelnut tree shades await for the hiker to rest, feed and hydrate. With altitude the grass recedes, and the birches and then the screes take over. Milestones left by the ones that walked the path before seem to be outstandingly helpful and easy to follow. Some milestones take you a bit further your original trail, but hey: "I took the trail less traveled by, as it made all the difference". Sometimes you might lose the trail, and just look at the rocky slope with uncertainty until finding the right direction. Wind, marmots and water have disassembled some milestones to which you add new stones, to make sure the ones that follow will not get lost as you did. Even at some spots you decide to set new milestones from scratch. Although you feel tired, cold and sweaty, you devise afar the hull that will take you to the summit. It is then you are thankful that all the way up you were not alone, not one minute, as family, friends, mentors and colleagues walked along, telling stories and jokes to ease the hike, questioning whether that was the right track, putting you a wound bandage after you fell, advising you on what berries to eat and what mushrooms should stay away, sharing walking sticks when you thought your knees had had enough and giving you snacks when you had already eaten yours.

**Thank you all to walk along.**

Maria, gràcies per compartir l'entusiasme per la ciència, una ciència feminista! Gràcies per ensenyar-me a fer-me preguntes, i que equivocar-se moltes vegades és part del procés. Gràcies per fer-me viatjar, i convidar-me a veure món, i sobretot fer-me treballar en equips internacionals on a banda de compartir ciència amb grans equips científics, també eren unes bellíssimes persones.

Gràcies a l'Elna i l'Arnau per deixar-me temps de la vostra mama durant el confinament, quan erem tots a casa tancats i haguéssiu preferit estar jugant o pintant amb ella.

En Benjamí, que sempre té la porta del despatx oberta, convidant a tothom a entrar, fer preguntes i sortir amb respostes... o amb més preguntes! Gràcies per facilitar-me eines estadístiques i corregir-em la feina amb tanta precisió lingüística.

Gràcies a en Jordi Dachs per les discussions científiques a primera hora del matí, al despatx o a bord del Sarmiento. Gràcies per les correccions i observacions sobre les publicacions, i sobretot per la confiança i les converses sobre la vida (i perquè no dir-ho: pels vins i els formatges!).

# KIITOS · TACK · TODA · GRÀCIES

Gràcies als meus pares, que han encoixinat el camí perquè arribés fins aquí, facilitant un ambient estimulador intel·lectualment des de ben petita, encoratjant la meva curiositat i fent-me creure sempre que podia fer el que jo volgués. Al tiet Pau, qui va encantar el meló dels doctors Martínez. Encara recordo la seva celebració de doctorat quan jo era petita. Gràcies per insistir en que no ho deixés estar. A la Susi, a en Sergi, a la Cristina i a la Gemma, gràcies per ser-hi i haver-me escoltat o compartit estones amb mi, i sempre mostrar interès pel que faig. Als padrins, perquè m'hagués agradat molt que hi fossin els dos. Gràcies padrina per estimar-nos i dedicar-nos la teua vida, gràcies pels consells i... la recepta de croquetes de bacallà, perquè la ciència es fa ben alimentat.

Thanks to the overseas family, that took me into their homes over the Christmas of 2018 making me feel as one more. Thank you Cooper, Matthew, Richard, Davis, Liza and Juanita, I love you and miss you. To Pepita, estás donde estás, I send a big kiss to you too, Guapa!

Gràcies a les gallines del Gallinero, l'Elena i en Paulo, que durant els dos primers anys de tesi van fer un excel·lent traspàs de coneixements, tot fent que el dia dia fos lleuger, alegre i emocionant. Gràcies a la Gemma, amb qui he tingut una traça paral·lela, compartint laboratori, ploreres, caminates pels Andes i relliscades a pingüïneres... i alguns papers! Gràcies pels ànims, per escoltar, per ajudar-me tantíssim al laboratori, per ser tant brillant i saber-ne tant!

Eskerrikasko Naiara, que simplement és una crac però ella no ho vol reconèixer. Pertsona zoragarria zara, eskerrik asko PAHen bitzta eta mirariak behin eta berriro azaltzeko pазientzia izateagatik.

I als pollets que s'han incorporat els darrers anys, la Núria i en Jon, que han amanit la festa i de qui he après també una altra manera de fer i veure la ciència. Ah! i a la gallina adoptada, la Berta Sala, sens dubte una peça clau, sempre disposada a escoltar, a riure i anar d'aventures.

Gràcies a l'equip tècnic que m'ha ajudat en diferents passos de la recerca, en especial a la Mariana i a la Marta Casado, dues cracs de les seves disciplines amb molta paciència per aguantar als pollitos que no sabem què és una pipeta pasteur o una mufla.

Gràcies a l'Adrià, almost-Dr Auladell! Moltes gràcies pels ànims, les converses i tanta ajuda en aquest món de la bionfinformàtica on tan bé et navegues.

Equipo cuevita, la Marta i l'Andrea (i... Dunita), científiques brillants i incansables, però sobretot bones amigues. Gràcies per cuidar-me quan jo no podia caminar, per animar-me en aquest darrer tram, i per fer-me riure i gaudir de la vostra companyia!

A la Claudichi, que ha estat el descobriment del 2020, un regal després d'un any que ens va fer patir tant a tots. El mestre shaoli, la psicòloga d'abord, l'artista i creadora de ten-

dències eclèctiques de roba (pa que veas).

A les Safaregistes del Figueró, un equipàs de dones combatives, que em posen a lloc i m'aguanten mentres rondino perquè vaig atavalada. Gràcies pels dinars infinits, pels teatres i per ser-hi. Gràcies per compartir.

A la Montse i la Jana, que em cuiden i m'estimen, i són la nostra família de la Vall!

Gràcies a la colla, als que fan d'àncora, als que sempre hi són encara que visquin lluny. Gràcies a la Laura, a en Michele, a la Lídia, a en Dudu, a la Miri, a la Nerea, a l'Alexandra, a l'Edu, a la Caterina d'Altron, a l'Alba de Bèlgica, a en Joanmas... Perquè ja sigui per anar a treure el gos, per xerrar sobre la vida amb una infusió, per fer un puzzle, anar a un concert, per demanar consell, per cuinar una paella, per anar a esquiar, de viatge o a fer una ruta per la muntanya... Saber que sempre puc comptar amb vosaltres és el millor tresor. Us estimo molt.

Special thanks to all those international friends, that have certainly enriched my thinking by teaching me the multiple (probably infinite) ways of living, existing, loving and doing science.

Thanks to Dr. Daniel Lundin! The Swedish R Boss, who introduced me to R and guided me through it! Thanks for being so patient and available to solve our doubts! It has been a pleasure to share this trip with you.

Thank you to Dr. Kristinan Spilling and the gang, Dr. Teresita and Dr. Tobito, for the first oceanographic campaigns and scientific experiences. Honestly... how did you trust me? I enjoyed so much learning by your side, and I am so proud of all of your scientific careers. I am sure I'll see you soon!

Thank you Mary Ann Moran to open the doors to your lab at UGA. Brent, Frank and Jeremy, from the second I landed to the second I left, you took me into your barrow. Climbing, eating and ... laughing, laughing a lot. To be honest: I won't ever forget your bravery of eating vacuum sealed snails from a vending machine in Barcelona. You brave men!

Thank you to the team of Dr. Dan Tawfik from Weizmann Institute. Who left us in 2020, leaving behind a tremendous heritage to his phd students, postdocs and technical team. Not only scientifically speaking, but a way of doing science with care, with passion.

I les darreres gràcies les envio a casa.

A en Cep, que durant dos anys m'ha fet sortir de casa a passejar plegats, airejant les idees tants i tants dies.

Gràcies Pau. Que sempre hi ets. Gràcies per es dosis de serenor quan jo l'he perdut.

Gràcies per alimentar-me amb menjar que brota al costat de les finestres, per ensenyar-me una altra manera de viure. Gràcies per estimar-me tant.

Gràcies a tots i totes!

These pages are dedicated to all women that have pursued a scientific career, and specially to those female scientist names which have not been included in the written history of science. I want to highlight the relevance of their work and persistence in helping to break the barrier of gender in science.

Below these lines a timeline with a brief biographic note of those women whose contributions are relevant to this thesis.



Angelina Fanny Hesse (1850 – 1934)  
Microbiologist. Proposed agar media for cultures. Dr. Robert Koch was recognized for her innovation.

Dr. Barbara McClintock (1902 – 1992)  
Awarded in 1983 with the Nobel Prize in Physiology or Medicine for discovering transposition and demonstrating that genes are responsible for turning physical characteristics on and off.



## Women in Science

Caroline Herschel (1750-1848)  
Astronomer. First woman to receive a salary for her scientific research.



Rachel Carson (1907 – 1964)  
Marine biologist and environmental activist. Author of "Silent Spring", among other books.

Dr. Marjory Stephenson (1885 – 1948)  
Bacterial metabolisms. First scientist to isolate a bacterial enzyme from the cell in 1928, the enzyme was lactic dehydrogenase from *Escherichia coli*.







**Dr. Esther Lederberg**  
(1922 – 2006)  
Replica plating technique. Lederberg also identified the transfer of genes between bacteria (Horizontal Gene Transfer, HGT) through a process called “specialized transduction”.



**Dr. Josefina Castellví**  
(1935)  
Catalan marine microbiologist. She was the first Spanish woman to participate in an Antarctic expedition. She led the civilian Spanish Antarctic Base from year 1989 to 1997.

**Lynn Margulis**  
(1938 – 2011)  
Endosymbiosis theory. She proposed symbiosis and cooperative relationships between species as an evolutionary force.



**Dr. Rosalind Franklin**  
(1920 – 1958)  
Used X-ray crystallography to deduce the basic dimensions of DNA and identified that phosphates were located on the outside of what looked like a helical structure. Her images were used by Watson and Crick, to support their 1953 publication on the theoretical structure of DNA, for which they received the Nobel Prize in 1962.



**Dr. Jo Handelsman**  
(1959)  
Coined the term “metagenomics”, which refers to the practice of using genetic sequencing to characterize all of the different genes found in a sample, such as a sea water sample.









